OTITIS MEDIA GENOMICS AND THE MIDDLE EAR MICROBIOME

EDITED BY: Regie Santos-Cortez, Allen Frederic Ryan and Garth D. Ehrlich
PUBLISHED IN: Frontiers in Genetics and
Frontiers in Cellular and Infection Microbiology

frontiers Research Topics

ISSN 1664-8714
ISBN 978-2-88971-810-8
DOI 10.3389/978-2-88971-810-8

About Frontiers

Frontiers is more than just an open-access publisher of scholarly articles: it is a pioneering approach to the world of academia, radically improving the way scholarly research is managed. The grand vision of Frontiers is a world where all people have an equal opportunity to seek, share and generate knowledge. Frontiers provides immediate and permanent online open access to all its publications, but this alone is not enough to realize our grand goals.

Frontiers Journal Series

The Frontiers Journal Series is a multi-tier and interdisciplinary set of open-access, online journals, promising a paradigm shift from the current review, selection and dissemination processes in academic publishing. All Frontiers journals are driven by researchers for researchers; therefore, they constitute a service to the scholarly community. At the same time, the Frontiers Journal Series operates on a revolutionary invention, the tiered publishing system, initially addressing specific communities of scholars, and gradually climbing up to broader public understanding, thus serving the interests of the lay society, too.

Dedication to Quality

Each Frontiers article is a landmark of the highest quality, thanks to genuinely collaborative interactions between authors and review editors, who include some of the world's best academicians. Research must be certified by peers before entering a stream of knowledge that may eventually reach the public - and shape society; therefore, Frontiers only applies the most rigorous and unbiased reviews.
Frontiers revolutionizes research publishing by freely delivering the most outstanding research, evaluated with no bias from both the academic and social point of view. By applying the most advanced information technologies, Frontiers is catapulting scholarly publishing into a new generation.

What are Frontiers Research Topics?

Frontiers Research Topics are very popular trademarks of the Frontiers Journals Series: they are collections of at least ten articles, all centered on a particular subject. With their unique mix of varied contributions from Original Research to Review Articles, Frontiers Research Topics unify the most influential researchers, the latest key findings and historical advances in a hot research area! Find out more on how to host your own Frontiers Research Topic or contribute to one as an author by contacting the Frontiers Editorial Office: frontiersin.org/about/contact

OTITIS MEDIA GENOMICS AND THE MIDDLE EAR MICROBIOME

Topic Editors:
Regie Santos-Cortez, University of Colorado, United States
Allen Frederic Ryan, University of California, San Diego, United States
Garth D. Ehrlich, Drexel University, United States

Citation: Santos-Cortez, R., Ryan, A. F., Ehrlich, G. D., eds. (2021). Otitis Media Genomics and the Middle Ear Microbiome. Lausanne: Frontiers Media SA.
doi: 10.3389/978-2-88971-810-8

Table of Contents

frontiers in Genetics

EDITORIAL
published: 12 October 2021
doi: 10.3389/fgene.2021.763688

Editorial: Otitis Media Genomics and the Middle Ear Microbiome

Regie Lyn P. Santos-Cortez[1,2]*, *Garth D. Ehrlich*[3,4]* and *Allen F. Ryan*[5,6]*

[1]Department of Otolaryngology-Head and Neck Surgery, School of Medicine, University of Colorado Anschutz Medical Campus, Aurora, CO, United States, [2]Center for Children's Surgery, Children's Hospital Colorado, Aurora, CO, United States, [3]Institute for Molecular Medicine and Infectious Disease, Drexel University College of Medicine, Philadelphia, PA, United States, [4]Departments of Otolaryngology-Head and Neck Surgery, and Microbiology and Immunology, Drexel University College of Medicine, Philadelphia, PA, United States, [5]Division of Otolaryngology, Department of Surgery, University of California San Diego School of Medicine, La Jolla, CA, United States, [6]Veterans Affairs Medical Center, La Jolla, CA, United States

Keywords: gene, microbiome, middle ear, nasopharynx, otitis media (OM), sequencing

Editorial on the Research Topic

Otitis Media Genomics and the Middle Ear Microbiome

OPEN ACCESS

Edited and reviewed by:
Jordi Pérez-Tur,
Instituto de Biomedicina de Valencia (CSIC), Spain

***Correspondence:**
Regie Lyn P. Santos-Cortez
regie.santos-cortez@cuanschutz.edu
Garth D. Ehrlich
ge33@drexel.edu
Allen F. Ryan
afryan@health.ucsd.edu

Specialty section:
This article was submitted to Genetics of Common and Rare Diseases, a section of the journal Frontiers in Genetics

Received: *24 August 2021*
Accepted: *22 September 2021*
Published: *12 October 2021*

Citation:
Santos-Cortez RLP, Ehrlich GD and Ryan AF (2021) Editorial: Otitis Media Genomics and the Middle Ear Microbiome. Front. Genet. 12:763688. doi: 10.3389/fgene.2021.763688

OTITIS MEDIA AS A CLINICAL DISEASE AND A PUBLIC HEALTH ISSUE

Otitis media (OM), defined as inflammation of the middle ear (ME), usually occurs after ME infection and may cause hearing loss (HL) at any age, but most frequently in early childhood when development of speech and cognition occurs (Davis and Hind, 1999; Chonmaitree et al., 2016; Singer et al., 2018). Globally in 2019, 64% of children 1–5 years have HL due to OM (GBD, 2021). Antibiotics are prescribed for 67–98% of children with OM (Hersh et al., 2016; Frost et al., 2020), which contributes to antibiotic resistance and drug-specific adverse effects, even if administered appropriately (Fleming-Dutra et al., 2016; DeMuri et al., 2017; Islam et al., 2020). 4–10% of children require surgery due to recurrent acute (RA) OM or chronic OM with effusion (COME) (Beyea et al., 1999; Bhattacharyya and Shay, 2020). RAOM is diagnosed in children with ≥3 OM episodes in 6 months or ≥4 in 12 months, and COME if ME effusion behind the intact eardrum persists for >2 months (Rosenfeld et al., 2016). Combined, these OM types and surgery are associated with 4–11× risk of permanent HL (Rach et al., 1988; Beyea et al., 1999). RAOM/COME cause defects in language ability, auditory perception, sound localization and auditory processing in 5–11% of school-age children, which impedes academic progress (Morrongiello, 1989; Zargi and Boltezar, 1992; Moore, 2007; Hind et al., 2011; Skarzynski et al., 2015; Graydon et al., 2017; Cordeiro et al., 2018; Leach et al., 2020). In 10–24% of chronic OM cases a highly destructive, cyst-like ME lesion, cholesteatoma, can later grow and erode functionally critical bony and neural structures (Schmidt Rosito et al., 2017). Complications of OM/cholesteatoma besides HL include balance disorders, facial nerve paralysis, soft tissue abscess, or intracranial infection (O'Connor et al., 2009). Cholesteatoma is treated surgically, but often recurs (Kuo et al., 2012; Nardone et al., 2012). Novel strategies for prevention and early treatment of OM are needed to decrease the health burden worldwide due to OM and HL. Unfortunately, OM and its comorbidities remain severely understudied compared to other common diseases.

OM phenotypes (acute OM, RAOM, COME, chronic OM, cholesteatoma) are not distinct entities but fall within a spectrum. However, the mechanisms by which common acute OM progresses in severity despite treatment are poorly understood. Elucidation of molecular mechanisms of genetic susceptibility in humans, and of host-microbiota interactions are key to understanding OM progression and improving current protocols for prevention, diagnosis and treatment (Marsh et al., 2020; Santos-Cortez et al., 2020; Thornton et al., 2020).

WHAT THIS RESEARCH TOPIC CONTRIBUTES TO SCIENTIFIC KNOWLEDGE ON OTITIS MEDIA

Three reviews in this research topic (Mittal et al.; Geng et al.; Giese et al.) provide comprehensive overviews of the current knowledge on the genomics of host-microbial interactions within the context of OM. They enumerate the genes that have been identified in humans and animal models as predisposing to OM, as well as their effects on the nasopharyngeal and ME microbiotas. Additionally, Lappan et al. summarized what is known about two bacterial species *Alloiococcus otitidis* and *Turicella otitidis* that are identified by sequencing in the ME and/or external ear. They suggested studies to delineate the role of these two bacteria in the ME, including microbiota, transcriptomic and animal model studies to aid understanding metabolic functions, strain heterogeneity, inflammatory effects and changes in OM severity due to *A. otitidis* or *T. otitidis* alone, or in concert with other otopathogens.

The Otitis Media-Related Microbiotas of the Pediatric Middle Ear and Nasopharynx (NP)

Three microbiota studies were performed using ME and NP samples from children with OM. Brugger et al. showed that the NP microbiota increased in richness but decreased in evenness with age, suggesting a personalized microbiota becoming more similar to adults with time; e.g., increased relative abundance of *Staphylococcus* and *Corynebacterium*. Xu et al. determined that microbiota from nasal washes or ME fluid at onset of acute OM were similar, but lower in biodiversity than the healthy state in the same children 3 weeks prior. These findings highlight the importance of temporal specificity when collecting paired NP and ME samples for OM studies. On a different note, Kolbe et al. found that in children with COME, the ME had less microbial biodiversity if the child had lower respiratory tract (LRT) disease i.e., asthma, bronchiolitis. Children with both COME and LRT disease also had greater relative abundances for *Haemophilus, Staphylococcus* and *Moraxella* but less *Turicella* or *Alloiococcus* in ME fluid. Altogether these ME and NP microbiota findings will be useful as guide in the design and interpretation of future microbial profiling and metagenomic studies.

The Middle Ear Transcriptome in Health and Otitis Media

Among five studies on ME gene expression, two were performed on human samples while three studies included rodent ME tissues. Microarray profiling of leukocytes from ME fluid of children with COME revealed enriched hypoxia signaling pathways and increased VEGF (compared to blood or plasma) that decreased with age (Bhutta et al.). This was concurrent with upregulation of inflammatory networks and increased myeloid cell signature and neutrophil counts in mucoid ME effusions; in contrast, lymphocytes and eosinophils were higher in serous ME fluid. Baschal et al. performed bulk mRNA-sequencing on human cholesteatoma and ME mucosal tissues from chronic OM patients, compared to published datasets from sinus and LRT. Their main findings include 1,806 differentially expressed genes (DEGs) and 68 enriched pathways in cholesteatoma compared to ME mucosa, as well as DEGs (including novel genes *CR1* and *SAA1*) and pathways that overlap among the ME, upper and lower airways.

Ryan et al. performed the first single-cell RNA-sequencing study of ME tissue, using wildtype, non-infected mice. They extensively described transcriptomic profiles across 22 ME cell types, including genes involved in innate immunity and basic cellular pathways related to infection responses. Zhao et al. studied the endoplasmic reticulum (ER) stress pathway, characterizing histologic, hearing, multi-gene expression and oxidative stress responses in inflamed mouse MEs with or without an ER stress inhibitor. The ME inflammatory responses were reduced by administration of ER stress inhibitor, suggesting ER stress pathways as a potential target for treatment of OM. Similarly, Yadav et al. demonstrated in rat ME that Asian sand dust, in concert with pneumococcal infection, promoted bacterial colonization, biofilm growth, cell apoptosis, ROS production, pro-inflammatory responses, and differential expression of host genes in multiple pathways such as immune defence, cell differentiation and neurogenesis. Expression of microbial genes involved with competence, biofilm and toxin production was also increased. These transcriptome studies serve as seminal references for future identification of novel genes, pathways and responses to various agents contributing to OM.

Genetic or Environmental Mouse Models and the Otitis Media Phenotype

Three mouse models were reported within this topic. Double-mutant *Id1-Id3* mice had hearing loss, and ME fluid depending on genotype (Zheng et al.). Histologic analysis confirmed ME polymorphonuclear cell infiltration, fibrosis and mucosal thickening, likely due to immune effects of *Id* gene knockout (KO). In a study of *Fbxo11* variants, the *Jeff* mouse which has an *Fbxo11* missense variant developed chronic OM and HL while the KO-mouse only had a milder craniofacial defect and ME mucosal thickening but no ME fluid or auditory phenotype (Kubinyecz et al.). Profile differences in cytokine levels and cell populations for innate or adaptive immunity were also stronger in the *Jeff* mouse than the KO (Vikhe et al.). These disparate phenotypes suggest a gain-of-function effect of the *Jeff* missense mutation. In summary, these mouse models demonstrate downstream effects of changes in the immune and TGF-beta pathways that aid understanding of the OM phenotype.

FUTURE PERSPECTIVES

Overall, the findings in the articles included in this topic suggest that: (A) dysbiosis in the ME and NP microbiotas according to age, temporality with OM onset, and occurrence of LRT disease contribute to OM susceptibility; (B) although transcriptome studies identified novel genes and pathways that are involved

in OM susceptibility, many more genes and pathways that are potential targets for novel therapies need to be validated or identified; and (C) animal models remain useful in elucidating mechanisms for OM susceptibility. Future *meta*-omic analyses will help in further understanding the metabolic functions and strain heterogeneity of bacteria in the ME and NP, and will enable detection of microbial factors (e.g., microbial genetic variants, serotypes) that favor resistance to antibiotics or antivirals, biofilm formation, immune evasion, metabolic efficiency, and virulence (Pettigrew et al., 2002; Ecevit et al., 2004; Ehrlich et al., 2005; Shen et al., 2005; Pettigrew et al., 2006; Buchinsky et al., 2007; Hiller et al., 2011; Pettigrew et al., 2011; Thomas et al., 2011; Pettigrew et al., 2012; Lewnard et al., 2016; Hu et al., 2019; Hammond et al., 2020; Harrison et al., 2020). Virulence factors of otopathogens may also identify candidate antigens for novel vaccines (Mottram et al., 2019). The continued study of the confluence of clinical, environmental, genetic, microbiota and immune profiles of patients and animal models with OM will also help identify OM sub-phenotypes that can be useful in personalizing OM treatments.

AUTHOR CONTRIBUTIONS

RS-C, GE and AR edited this research topic and wrote the editorial.

FUNDING

RS-C is funded by NIH-NIDCD R01 DC015004. GE is supported by NIH-NIDCD R01 002148. AR is supported by Grants NIH-NIDCD R01 DC000129 and R01 DC012595.

REFERENCES

Beyea, J. A., Cooke, B., Rosen, E., and Nguyen, P. (1999). Association of tympanostomy tubes with future assistive hearing devices-a population based study. *BMC Pediatr.* 20, 76. doi:10.1186/s12887-020-1977-6

Bhattacharyya, N., and Shay, S. G. (2020). Epidemiology of pediatric tympanostomy tube placement in the United States. *Otolaryngol. Head Neck Surg.* 163, 600–602. doi:10.1177/0194599820917397

Buchinsky, F. J., Forbes, M. L., Hayes, J. D., Shen, K., Ezzo, S., Compliment, J., et al. (2007). Virulence phenotypes of low-passage clinical isolates of nontypeable Haemophilus influenzae assessed using the chinchilla laniger model of otitis media. *BMC Microbiol.* 7, 56. doi:10.1186/1471-2180-7-56

Chonmaitree, T., Trujillo, R., Jennings, K., Alvarez-Fernandez, P., Patel, J. A., Loeffelholz, M. J., et al. (2016). Acute otitis media and other complications of viral respiratory infection. *Pediatrics* 137, e20153555. doi:10.1542/peds.2015-3555

Cordeiro, F. P., da Costa Monsanto, R., Kasemodel, A. L. P., de Almeida Gondra, L., and de Oliveira Penido, N. (2018). Extended high-frequency hearing loss following the first episode of otitis media. *The Laryngoscope* 128, 2879–2884. doi:10.1002/lary.27309

Davis, A., and Hind, S. (1999). The impact of hearing impairment: a global health problem. *Int. J. Pediatr. Otorhinolaryngol.* 49 (Suppl. 1), S51–S54. doi:10.1016/s0165-5876(99)00213-x

DeMuri, G. P., Sterkel, A. K., Kubica, P. A., Duster, M. N., Reed, K. D., and Wald, E. R. (2017). Macrolide and clindamycin resistance in Group A Streptococci isolated from children with pharyngitis. *Pediatr. Infect. Dis. J.* 36, 342–344. doi:10.1097/inf.0000000000001442

Ecevit, I. Z., McCrea, K. W., Pettigrew, M. M., Sen, A., Marrs, C. F., and Gilsdorf, J. R. (2004). Prevalence of the hifBC , hmw1A , hmw2A , hmwC , and hia Genes in Haemophilus influenzae Isolates. *J. Clin. Microbiol.* 42, 3065–3072. doi:10.1128/jcm.42.7.3065-3072.2004

Ehrlich, G. D., Hu, F. Z., Shen, K., Stoodley, P., and Post, J. C. (2005). Bacterial plurality as a general mechanism driving persistence in chronic infections. *Clin. Orthopaedics Relat. Res.* &NA;, 20–24. doi:10.1097/00003086-200508000-00005

Fleming-Dutra, K. E., Hersh, A. L., Shapiro, D. J., Bartoces, M., Enns, E. A., File, T. M., Jr., et al. (2016). Prevalence of inappropriate antibiotic prescriptions among US ambulatory care visits, 2010-2011. *JAMA* 315, 1864–1867. doi:10.1001/jama.2016.4151

Frost, H. M., Becker, L. F., Knepper, B. C., Shihadeh, K. C., and Jenkins, T. C. (2020). Antibiotic prescribing patterns for acute otitis media for children 2 years and older. *J. Pediatr.* 220, 109–115. doi:10.1016/j.jpeds.2020.01.045

GBD Hearing Loss Collaborators (2021). Hearing loss prevalence and years lived with disability, 1990-2019: findings from the Global Burden of Disease Study 2019. *Lancet* 397, 996–1009.

Graydon, K., Rance, G., Dowell, R., and Van Dun, B. (2017). Consequences of early conductive hearing loss on long-term binaural processing. *Ear Hear* 38, 621–627. doi:10.1097/aud.0000000000000431

Hammond, J. A., Gordon, E. A., Socarras, K. M., Chang Mell, J., and Ehrlich, G. D. (2020). Beyond the pan-genome: current perspectives on the functional and practical outcomes of the distributed genome hypothesis. *Biochem. Soc. Trans.* 48, 2437–2455. doi:10.1042/bst20190713

Harrison, A., Hardison, R. L., Fullen, A. R., Wallace, R. M., Gordon, D. M., White, P., et al. (2020). Continuous microevolution accelerates disease progression during sequential episodes of infection. *Cel Rep.* 30, 2978–2988e3. doi:10.1016/j.celrep.2020.02.019

Hersh, A. L., Fleming-Dutra, K. E., Shapiro, D. J., Hyun, D. Y., and Hicks, L. A. (2016). Outpatient Antibiotic Use Target-Setting WorkgroupFrequency of first-line antibiotic selection among US ambulatory care visits for otitis media, sinusitis, and pharyngitis. *JAMA Intern. Med.* 176, 1870–1872. doi:10.1001/jamainternmed.2016.6625

Hiller, N. L., Eutsey, R. A., Powell, E., Earl, J. P., Janto, B., Martin, D. P., et al. (2011). Differences in genotype and virulence among four multidrug-resistant Streptococcus pneumoniae isolates belonging to the PMEN1 clone. *PLoS One* 6, e28850. doi:10.1371/journal.pone.0028850

Hind, S. E., Haines-Bazrafshan, R., Benton, C. L., Brassington, W., Towle, B., and Moore, D. R. (2011). Prevalence of clinical referrals having hearing thresholds within normal limits. *Int. J. Audiol.* 50, 708–716. doi:10.3109/14992027.2011.582049

Hu, F. Z., Król, J. E., Tsai, C. H. S., Eutsey, R. A., Hiller, L. N., Sen, B., et al. (2019). Deletion of genes involved in the ketogluconate metabolism, Entner-Doudoroff pathway, and glucose dehydrogenase increase local and invasive virulence phenotypes in Streptococcus pneumoniae. *PLoS One* 14, e0209688. doi:10.1371/journal.pone.0209688

Islam, S., Mannix, M. K., Breuer, R. K., and Hassinger, A. B. (2020). Guideline adherence and antibiotic utilization by community pediatricians, private urgent care centers, and a pediatric emergency department. *Clin. Pediatr. (Phila)* 59, 21–30. doi:10.1177/0009922819879462

Kuo, C.-L., Shiao, A.-S., Liao, W.-H., Ho, C.-Y., and Lien, C.-F. (2012). How long is long enough to follow up children after cholesteatoma surgery? A 29-year study. *The Laryngoscope* 122, 2568–2573. doi:10.1002/lary.23510

Leach, A. J., Homøe, P., Chidziva, C., Gunasekera, H., Kong, K., Bhutta, M. F., et al. (2020). Panel 6: Otitis media and associated hearing loss among disadvantaged populations and low to middle-income countries. *Int. J. Pediatr. Otorhinolaryngol.* 130 (Suppl. 1), 109857. doi:10.1016/j.ijporl.2019.109857

Lewnard, J. A., Huppert, A., Givon-Lavi, N., Pettigrew, M. M., Regev-Yochay, G., Dagan, R., et al. (2016). Density, Serotype Diversity, and Fitness ofStreptococcus pneumoniaein Upper Respiratory Tract Cocolonization with NontypeableHaemophilus influenzae. *J. Infect. Dis.* 214, 1411–1420. doi:10.1093/infdis/jiw381

Marsh, R. L., Aho, C., Beissbarth, J., Bialasiewicz, S., Binks, M., Cervin, A., et al. (2020). Panel 4: Recent advances in understanding the natural history of the

otitis media microbiome and its response to environmental pressures. *Int. J. Pediatr. Otorhinolaryngol.* 130 (Suppl. 1), 109836. doi:10.1016/j.ijporl.2019.109836

Moore, D. R. (2007). Auditory processing disorders: acquisition and treatment. *J. Commun. Disord.* 40, 295–304. doi:10.1016/j.jcomdis.2007.03.005

Morrongiello, B. A. (1989). Infants' monaural localization of sounds: Effects of unilateral ear infection. *The J. Acoust. Soc. America* 86, 597–602. doi:10.1121/1.398749

Mottram, L., Chakraborty, S., Cox, E., and Fleckenstein, J. (2019). How genomics can be used to understand host susceptibility to enteric infection, aiding in the development of vaccines and immunotherapeutic interventions. *Vaccine* 37, 4805–4810. doi:10.1016/j.vaccine.2019.01.016

Nardone, M., Sommerville, R., Bowman, J., and Danesi, G. (2012). Myringoplasty in Simple Chronic Otitis Media. *Otol Neurotol* 33, 48–53. doi:10.1097/mao.0b013e31823dbc26

O'Connor, T. E., Perry, C. F., and Lannigan, F. J. (2009). Complications of otitis media in Indigenous and non-indigenous children. *Med. J. Aust.* 191, S60–S64.

Pettigrew, M. M., Fennie, K. P., York, M. P., Daniels, J., and Ghaffar, F. (2006). Variation in the presence of neuraminidase genes among Streptococcus pneumoniae isolates with identical sequence types. *Infect. Immun.* 74, 3360–3365. doi:10.1128/iai.01442-05

Pettigrew, M. M., Foxman, B., Marrs, C. F., and Gilsdorf, J. R. (2002). Identification of the lipooligosaccharide biosynthesis gene lic2B as a putative virulence factor in strains of nontypeable Haemophilus influenzae that cause otitis media. *Infect. Immun.* 70, 3551–3556. doi:10.1128/iai.70.7.3551-3556.2002

Pettigrew, M. M., Gent, J. F., Pyles, R. B., Miller, A. L., Nokso-Koivisto, J., and Chonmaitree, T. (2011). Viral-bacterial interactions and risk of acute otitis media complicating upper respiratory tract infection. *J. Clin. Microbiol.* 49, 3750–3755. doi:10.1128/jcm.01186-11

Pettigrew, M. M., Laufer, A. S., Gent, J. F., Kong, Y., Fennie, K. P., and Metlay, J. P. (2012). Upper respiratory tract microbial communities, acute otitis media pathogens, and antibiotic use in healthy and sick children. *Appl. Environ. Microbiol.* 78, 6262–6270. doi:10.1128/aem.01051-12

Rach, G. H., Zielhuis, G. A., and van den Broek, P. (1988). The influence of chronic persistent otitis media with effusion on language development of 2- to 4-year-olds. *Int. J. Pediatr. Otorhinolaryngol.* 15, 253–261. doi:10.1016/0165-5876(88)90080-8

Rosenfeld, R. M., Shin, J. J., Schwartz, S. R., Coggins, R., Gagnon, L., Hackell, J. M., et al. (2016). Clinical Practice Guideline: Otitis Media with Effusion (Update). *Otolaryngol. Head Neck Surg.* 154, S1–S41. doi:10.1177/0194599815623467

Rosito, L. P. S., da Silva, M. N. L., Selaimen, F. A., Jung, Y. P., Pauletti, M. G. T., Jung, L. P., et al. (2017). Characteristics of 419 patients with acquired middle ear cholesteatoma. *Braz. J. Otorhinolaryngol.* 83, 126–131. doi:10.1016/j.bjorl.2016.02.013

Santos-Cortez, R. L. P., Bhutta, M. F., Earl, J. P., Hafrén, L., Jennings, M., Mell, J. C., et al. (2020). Panel 3: Genomics, precision medicine and targeted therapies. *Int. J. Pediatr. Otorhinolaryngol.* 130 (Suppl. 1), 109835. doi:10.1016/j.ijporl.2019.109835

Shen, K., Antalis, P., Gladitz, J., Sayeed, S., Ahmed, A., Yu, S., et al. (2005). Identification, distribution, and expression of novel genes in 10 clinical isolates of nontypeable *Haemophilus influenzae*. *Infect. Immun.* 73, 3479–3491. doi:10.1128/iai.73.6.3479-3491.2005

Singer, A. E. A., Abdel-Naby Awad, O. G., El-Kader, R. M. A., and Mohamed, A. R. (2018). Risk factors of sensorineural hearing loss in patients with unilateral safe chronic suppurative otitis media. *Am. J. Otolaryngol.* 39, 88–93. doi:10.1016/j.amjoto.2018.01.002

Skarzynski, P. H., Wlodarczyk, A. W., Kochanek, K., Pilka, A., Jedrzejczak, W., Olszewski, L., et al. (2015). Central auditory processing disorder (CAPD) tests in a school-age hearing screening programme - analysis of 76,429 children. *Ann. Agric. Environ. Med.* 22, 90–95. doi:10.5604/12321966.1141375

Thomas, J. C., Figueira, M., Fennie, K. P., Laufer, A. S., Kong, Y., Pichichero, M. E., et al. (2011). Streptococcus pneumoniae clonal complex 199: genetic diversity and tissue-specific virulence. *PLoS One* 6, e18649. doi:10.1371/journal.pone.0018649

Thornton, R. B., Hakansson, A., Hood, D. W., Nokso-Koivisto, J., Preciado, D., Riesbeck, K., et al. (2020). Panel 7 - Pathogenesis of otitis media - a review of the literature between 2015 and 2019. *Int. J. Pediatr. Otorhinolaryngol.* 130 (Suppl. 1), 109838. doi:10.1016/j.ijporl.2019.109838

Zargi, M., and Boltezar, I. H. (1992). Effects of recurrent otitis media in infancy on auditory perception and speech. *Am. J. Otolaryngol.* 13, 366–372. doi:10.1016/0196-0709(92)90078-8

Conflict of Interest: The authors declare that the research was conducted in the absence of any commercial or financial relationships that could be construed as a potential conflict of interest.

Publisher's Note: All claims expressed in this article are solely those of the authors and do not necessarily represent those of their affiliated organizations, or those of the publisher, the editors and the reviewers. Any product that may be evaluated in this article, or claim that may be made by its manufacturer, is not guaranteed or endorsed by the publisher.

frontiers in Genetics

ORIGINAL RESEARCH
published: 19 June 2019
doi: 10.3389/fgene.2019.00555

Age-Dependent Dissimilarity of the Nasopharyngeal and Middle Ear Microbiota in Children With Acute Otitis Media

*Silvio D. Brugger[1,2,3†], Julia G. Kraemer[1,4†], Weihong Qi[5], Lindsey Bomar[2,6], Anne Oppliger[4] and Markus Hilty[1]**

[1] *Institute for Infectious Diseases, Faculty of Medicine, University of Bern, Bern, Switzerland,* [2] *Department of Oral Medicine, Infection and Immunity, Harvard School of Dental Medicine, Boston, MA, United States,* [3] *Department of Infectious Diseases and Hospital Epidemiology, University Hospital Zurich – University of Zurich, Zurich, Switzerland,* [4] *Institute for Work and Health, University of Lausanne, University of Geneva, Épalinges, Switzerland,* [5] *Functional Genomics Center Zurich, Swiss Federal Institute of Technology Zurich, University of Zurich, Zurich, Switzerland,* [6] *Department of Microbiology, The Forsyth Institute, Cambridge, MA, United States*

OPEN ACCESS

Edited by:
Regie Santos-Cortez, University of Colorado Denver, United States

Reviewed by:
Paola Marchisio, University of Milan, Italy
Theodora Katsila, National Hellenic Research Foundation, Greece

***Correspondence:**
Markus Hilty
Markus.Hilty@ifik.unibe.ch

† These authors have contributed equally to this work

Specialty section:
This article was submitted to Genetic Disorders, a section of the journal Frontiers in Genetics

Received: *21 March 2019*
Accepted: *24 May 2019*
Published: *19 June 2019*

Citation:
Brugger SD, Kraemer JG, Qi W, Bomar L, Oppliger A and Hilty M (2019) Age-Dependent Dissimilarity of the Nasopharyngeal and Middle Ear Microbiota in Children With Acute Otitis Media. Front. Genet. 10:555. doi: 10.3389/fgene.2019.00555

Acute bacterial otitis media is usually caused by otopathogens ascending to the middle ear from the nasopharynx (NP). However, it is unknown if the nasopharyngeal microbiota of children with acute otitis media (AOM) can serve as an age-dependent or independent proxy for the microbial communities of the middle ear fluid (MEF) as there is a lack of 16S rRNA amplicon sequencing studies simultaneously analyzing the microbial communities of the two sites. Within this study, we performed 16S rRNA next generation sequencing on a total of 286 nasopharyngeal swabs (NPSs) collected between 2004 and 2013 within a Swiss national AOM surveillance program from children (0–6 years) with AOM. In addition, 42/286 children had spontaneous tympanic membrane perforation and, therefore, those MEF could also be analyzed. We found that alpha [Richness, Shannon diversity index (SDI) and Evenness] and beta diversity measurements of the nasopharyngeal bacterial microbiota showed a clear dependency of the increasing age of the children. In more detail, bacterial richness and personalized profiles (measured by beta dispersion) were higher and more frequent in older children, respectively. Dissimilarity values based on the binary distance matrix of the microbiota patterns of the NP and the MEF also correlated with increasing age. In general, positive (PPV) and negative predictive values (NPV) of the most abundant operational taxonomic units (OTUs) in the NP were moderately and well predictive for their presence in the MEF, respectively. This data is crucial to better understand polymicrobial infections and therefore AOM pathogenesis.

Keywords: nasopharyngeal microbiota, bacterial families, toddlers, acute otitis media, middle ear fluid, age

Abbreviations: CI, confidence interval; MEF, middle ear fluid; MID, multiplex identifier; nMDS, non-metric multidimensional scaling; NP, nasopharynx; NPS, nasopharyngeal swab; OTU, operational taxonomic unit; PCV, pneumococcal conjugate vaccine; rRNA, ribosomal RNA; SD, standard deviation; SDI, shannon diversity index.

INTRODUCTION

Acute otitis media (AOM) is one of the most frequent pediatric diseases with a peak incidence at 6–12 months of age and is still responsible for high rates of antibiotic prescription (Lieberthal et al., 2013). Conventionally, bacterial or viral culturing of the MEF has been used as the gold standard for establishing microbial etiology of AOM (Yatsyshina et al., 2016). Traditionally, *Streptococcus pneumoniae*, non-typeable *Haemophilus influenzae* and *Moraxella catarrhalis* have been reported as the most common bacterial causes of AOM (Post et al., 1995; Kilpi et al., 2001; van Dongen et al., 2013; Kaur et al., 2014, 2017). However, the incidences of the pathogens causing AOM seem to be age-dependent, e.g., it has been reported that the incidence of pneumococcal AOM peaks around 12 months of age, whereas the incidence of *M. catarrhalis* AOM first peaks at 6 months and *H. influenzae* AOM at 20 months (Kilpi et al., 2001; Kaur et al., 2014).

A clinically important question to address, is whether sampling the NP provides an accurate estimate of the presence of the various microorganisms involved in otitis media as access to the NP is much less invasive than that to the middle ear (tympanocentesis) (van Dongen et al., 2013). Furthermore, it is hypothesized that bacterial AOM is caused by otopathogens residing in the nasal passages by ascension through the Eustachian tube under disturbance of the normal homeostasis (Coticchia et al., 2013). It has been described that nasopharyngeal colonization with the bacterial species most known to cause AOM is associated with middle ear disease with odds ratios (ORs) of approximately 2 (Faden et al., 1997; Revai et al., 2008). However, all of these studies are culture based or used specific PCR protocols targeting distinct species (Yatsyshina et al., 2016). There is a lack of 16S rRNA next generation sequencing studies characterizing the whole bacterial microbiota, rather than single species, with paired samples of NPSs and MEF of patients with AOM as well as of studies investigating the nasopharyngeal microbiota in toddlers and prepubertal children. Some very recent studies by us and others analyzing either the middle ear (Sillanpaa et al., 2017) and/or the NP (Hilty et al., 2012; Chonmaitree et al., 2017; Lappan et al., 2018) have already shown that a broader, sequencing-based survey of the bacterial microbiota provides additional important information which cannot be derived by bacterial cultures. Therefore, the overarching aim of this study was to characterize the bacterial, nasopharyngeal microbiota in Swiss children with AOM and to simultaneously characterize the bacterial microbiota of MEF and NPS in patients with AOM who also had a perforated tympanic membrane, at different ages. In more detail we aimed at (a) characterizing the nasopharyngeal microbiota of children with AOM aged <7 years and at (b) simultaneously characterizing the microbiota of NP and MEF of 42 children with spontaneous tympanic membrane perforation in different age groups in order to predict if and to what extend the microbiota of NPS may serve as proxy for the microbiota of MEF.

MATERIALS AND METHODS

Study Design

This study included outpatients with AOM between 2004 and 2013. All children aged less than 7 years were included. Children were observed within a Swiss nationwide prospective surveillance system for various diseases, which is ongoing since 1998 and has been explained previously (Muhlemann et al., 2003; Allemann et al., 2017). The diagnosis of AOM episodes was done according to Centers for Disease Control and Prevention definitions which included two or more of the following symptoms: fever (>38°C), inflamed or painful or retracted tympanic membrane, reduced mobility of the tympanic membrane or fluid behind the tympanic membrane on otoscopy. Patients were eligible to be signed up repeatedly for each new episode of AOM (Muhlemann et al., 2003; Allemann et al., 2017). Participating physicians seeing AOM patients sampled the NP and provided a sample of the MEF in case of spontaneous rupture of the tympanic membrane. In total, 42/286 of participants provided both, MEF and a NPS. Tympanocentesis for routine surveillance was not intended in the surveillance system and was fully up to the decision of the treating physician. Participating physicians were only asked to swab MEF of spontaneously ruptured tympanic membranes. Nasopharyngeal samples analysis included the data from a previous study for children age 0–1 years (Hilty et al., 2012). NPS samples from the other age groups (>1 year but <7 years) and MEF samples are presented for the first time in this study. The overall AOM surveillance program is part of the governmental public health surveillance and is therefore exempted from approval by Institutional Review Boards. Informed consent was received from the parents.

Sample Collection

Nasopharyngeal swabs were obtained through the nose reaching the NP using twisted wire rayon tipped applicators (Copan Ventury Transystem; Copan, Italy), and MEF were gained using the identical or cotton tip swabs (Allemann et al., 2017). Concerning the latter, the amount of time between spontaneous perforation and collection of samples was not recorded. With each sample, practitioners submitted a standardized questionnaire comprising the following patient data: age, gender, vaccination status, preceding antibiotic therapy, day care attendance, AOM history (number of otitis media episodes within the last 12 months) and place of residence. Culture and subsequent serotyping for *S. pneumoniae* was done for all NPS and MEF as described (Allemann et al., 2017).

PCR Amplification and Amplicon Sequencing of 16S rRNA Genes

Amplification by PCR and amplicon sequencing has been described elsewhere (Hilty et al., 2012). In brief, DNA was extracted using 200 μl of transport medium, followed by amplification of bacterial 16S rRNA variable regions V3-V5

by MID tagged primer pair 341F/907R (*Escherichia coli* numbering). The final primer sequences including MID and adaptor sequences were A-341F, 5′-cgtatcgcctccctcgcgccatcag-[NNNNNNNNNN]-*ACTCCTACGGGAGGCAGCAG*-3′ and B-926R, 5′-ctatgcgccttgccagcccgctcag-[NNNNNNNNNN]-*CCGTCAATTCMTTTGAGTTT*-3′. PCR reactions were eluted by 40 µl double distilled water and the eluate was measured by Agilent 2100 Bioanalyzer (Agilent Technologies, Basel, Switzerland). PCR products with a concentration <1.0 ng/µl were excluded from the study. This corresponds to <1 pg/µl bacterial DNA as evaluated by quantitative PCR of pneumococcal DNA at different dilutions (Mika et al., 2015). A minimum of 1 pg/µl of bacterial DNA has been suggested as the cut-off when dealing with low density sample material (Biesbroek et al., 2012). Resulting PCR products were evenly pooled (40 ng), whereas every MID was used once, resulting in eight amplicon pools (Hilty et al., 2012). The amplicon pools were sequenced using the 454 sequencing platform. The resulting reads were submitted to the National Center for Biotechnology Information Sequence Read Archive (accession numbers SRR077426, SRR086165, SRR086166, and PRJEB23228).

Analysis of Sequence Reads

Several quality control steps were performed for the "raw" 454 sequence reads to circumvent artificial inflation of diversity estimates (Kunin et al., 2010). First, forward reads were trimmed to 230 base pairs (bp) with shorter reads being rejected. The length of 230 bp was selected because the quality scores generally dropped for bases after this cut off as we have already previously shown (Hilty et al., 2012). After the additional trimming of MID and primer sequences, the actual sequences subjected to microbial diversity analysis were 200 bp long. It has been previously hypothesized that the 200 bp long forward reads are appropriate for accurate microbial community analysis (Liu et al., 2007). Second, reads having any unresolved bases ("N"s) or homopolymers longer than 8 bp were excluded, as well as singleton reads (reads, which appear only once in all samples and are therefore likely to be the product of polymerase errors). Finally, trimmed reads were filtered with a modified version of

TABLE 1 | Overview of study population/samples.

		Age of patients with episodes of AOM						
		0–1 years	**1–2 years**	**2–3 years**	**3–4 years**	**4–5 years**	**5–6 years**	**6–7 years**
Total number of NPS		65	108	8	36	33	21	15
Year								
	2004–2006	30	27	2	11	14	11	9
	2007–2009	30	76	3	20	16	8	5
	2010–2012	5	5	3	5	3	2	1
Day care visits								
	Yes	24	40	3	18	11	4	1
	No	40	59	5	18	21	16	13
	NA							
Region								
	East	25	41	1	18	23	9	7
	West	39	67	7	18	8	12	8
	NA							
Gender								
	Female	35	51	4	17	10	10	6
	Male	30	56	4	19	23	11	9
	NA	0	1	0	0	0	0	0
Vaccination status								
PCV7/PCV13	yes	31	68	5	14	4	1	0
	no	30	35	3	21	29	20	14
	NA	4	5	0	1	0	0	1
Antibiotics during the last 8 weeks								
	No	42	74	5	34	31	21	15
	Yes	15	26	3	2	1	0	0
	NA	8	8	0	0	1	0	0
AOM history								
	No	36	49	0	20	23	16	9
	≥1 previous episode	26	50	7	14	7	1	2
	NA	3	7	1	2	3	4	4

AOM, acute otitis media; NPS, nasopharyngeal swabs; PCV, pneumococcal conjugate vaccine.

the quality filtering script in Pyrotagger (Kunin and Hugenholtz, 2010). The script removes first reads containing sequence error(s) in its MID and/or primer, and then discards reads in which over 15% of bases show a quality score lower than 20.

Taxonomic Assignments and Calculation of Relative Bacterial Abundances of Operational Taxonomic Units (OTUs) and Bacterial Families

Pyrotagger was also used for the definition of OTUs, estimation of chimeras, and taxonomy assignments as previously described (Hilty et al., 2012). In brief, reads were clustered at a 97% sequence identity threshold using the Pyroclust algorithm. Putative chimera clusters flagged by Pyrotagger were discarded. The most abundant unique sequence was then chosen as a cluster representative and classified by comparison to Phylodb, which contains reference sequences exported from Greengene and SILVA databases (Kunin and Hugenholtz, 2010). An in house perl script was additionally used to collate family level taxonomic abundance for each sample by summing the number of reads belonging to a given family.

Within this study, the five most abundant families were analyzed separately, whereas all the remaining families were grouped as "others." These analyses included the calculations of mean values and SEM (standard error of the mean) of the

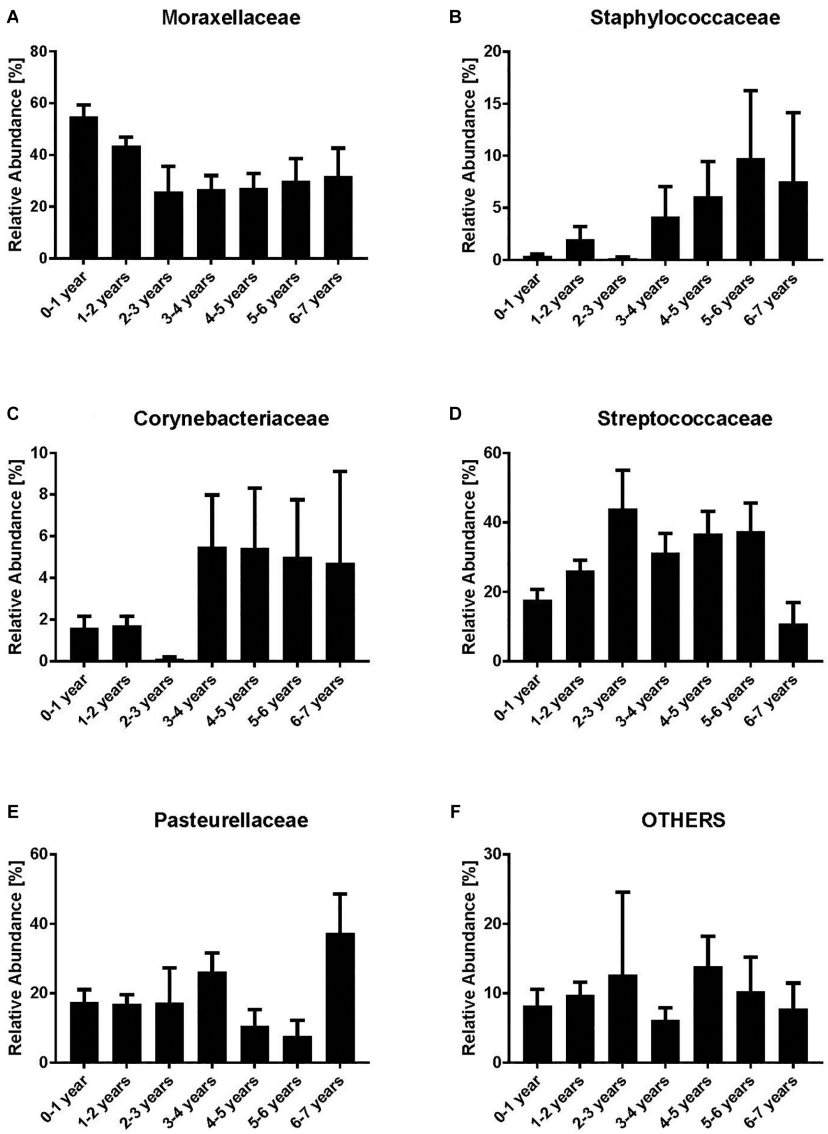

FIGURE 1 | Relative abundances of bacterial families [Moraxellaceae **(A)**, Staphylococcaceae **(B)**, Corynebacteriaceae **(C)**, Streptococcaceae **(D)**, Pasteurellaceae **(E)** and Others **(F)**]. Indicated are the most abundant bacterial families while all the remaining are grouped as "others." Bars represent mean values according to the age of the children with acute otitis media on the *x*-axis (in years). Moraxellaceae is the most abundant family within the younger age groups, whereas in older age groups Corynebacteriaceae and Staphylococcaceae are most abundant.

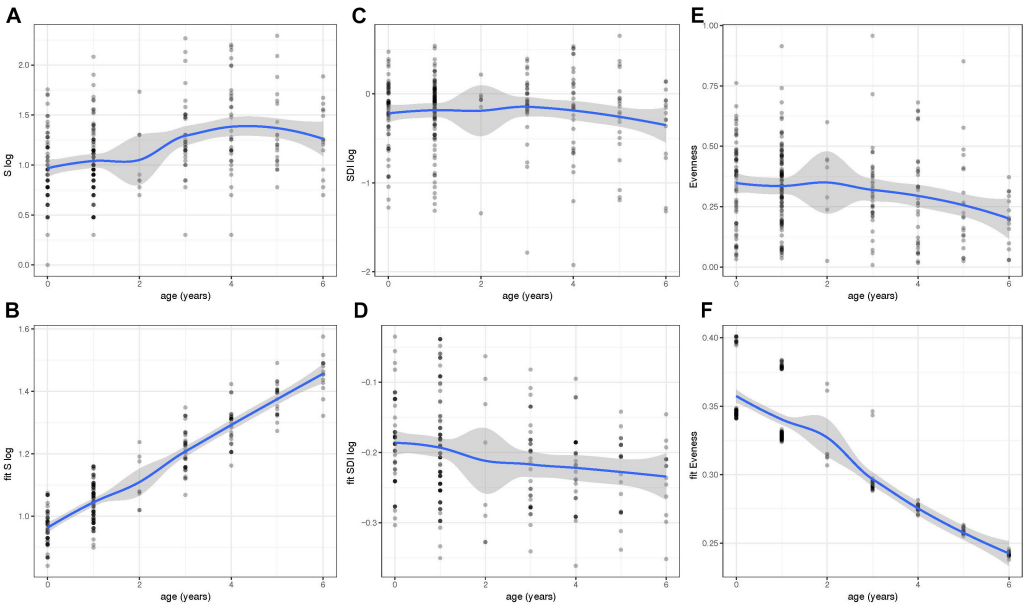

FIGURE 2 | Within-community diversity [Richness (S), Shannon Diversity Index (SDI) and Evenness] analysis in different age groups. Values of S **(A)**, SDI **(C)**, and Evenness **(E)** were obtained at different ages (0–6 years of age). However, the residuals of the models for S and SDI were not normally distributed and, therefore, were log transformed **(A–D)**. To correct for the dependency nature of the study, linear mixed models including fixed effects were also done and fitted values of S **(B)**, SDI **(D)**, and evenness **(F)** were plotted throughout time. Richness and Evenness values reveal an increase and decrease in older children, respectively. Fitted values were obtained using the lme4 R package and plots were generated using ggplot2.

relative abundances per age group (0–1, 1–2, 2–3, 3–4, 4–5, 5–6, and 6–7 years).

Alpha Diversity Calculations of NPS

Alpha diversity [Richness (S), SDI, and Evenness], referred to as within-community diversity (Lemon et al., 2012), was assessed for OTUs based on 97% sequencing identity.

Richness is defined by the total number of OTUs while evenness refers to the similarity in OTU relative abundance in a bacterial community. Shannon's index accounts for both abundance and evenness of the species present. Values were calculated in R[1], using the respective function of the *vegan* package. SDI and Richness values were log-transformed to achieve normally distributed residuals. Values of log-transformed Richness (S), log-transformed SDI, and Evenness were grouped according to the age of the study participant and regression analysis was performed. Shannon or Shannon–Weaver (or Shannon–Wiener) index is defined as $H = -sum\ p\_i\ log(b)\ p\_i$, where p_i is the proportional abundance of species i and b is the base of the logarithm.

Evenness index is defined as $J' = H'/H'_{max}$, where H' is the number derived from the SDI and H'_{max} is the maximum possible value of H'. To correct for the dependency nature of the study, a linear mixed model including fixed effects [different age groups, the year of sampling, previous antibiotic treatment of the patient (yes or no), region of origin (West or East of Switzerland) and day care attendance (yes or no)] was done using the package lme4 in R (lm command). SDI and Richness values were log-transformed to achieve normally distributed residuals and outcomes were visualized according to the different age groups [e.g., for SDI: model.sdilog < −lm(df.SDI$SDIlog∼df.SDI$age + df.SDI$year + df.SDI$antibiotic + df.SDI$Region + df.SDI$day_care, na.action = na.exclude)].

Beta Diversity Analyses of NPS

Beta-diversity (between-sample diversity) was measured by the weighted Ružička index (abundance-based) and the unweighted Jaccard index (presence/absence-based) of dissimilarity. Jaccard index is computed as 2B/(1+B), where B is Bray–Curtis *(d[jk] = (sum abs(x[ij]-x[ik])/(sum (x[ij]+x[ik])))* dissimilarity using the binary = TRUE flag. Ružička index is calculated identical to the Jaccard index but binary = FALSE. Pairwise distances between samples were received by the *vegdist* function and the resulting matrices were included to create NMDS plots (*metaMDS* function). Significant groupings between samples were assessed by a permutational multivariate analysis of variance using 1000 Monte Carlo permutation tests (PERMANOVA; *adonis* function). The multivariate dispersion of each sample group was determined by calculating the average distance (based on Jaccard and Ružička indices) to the sample type's centroid using the *betadisper* function, and significant differences were assessed with Tukey's Honest Significant Difference Test (TukeyHSD function). Boxplots and NMDS plots were generated in R utilizing the ggplot2 package.

[1]http://www.R-project.org

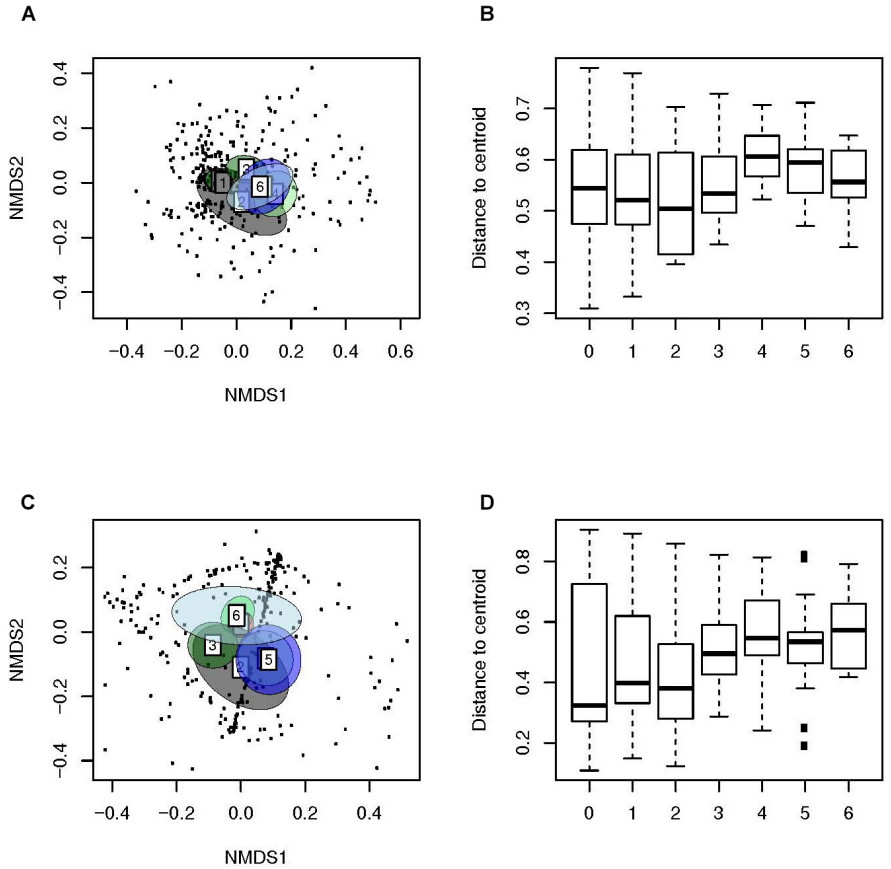

FIGURE 3 | Beta-diversity analyses of samples of children with AOM suggest a more personalized bacterial microbiota with age. Illustrated are **(A)** Weighted (Ružička) and **(C)** unweighted (Jaccard) distances in microbiota composition, reduced in a 2D-space by using NMDS, 95% confidence ellipse for the group centroid shown. In addition, shown are the beta-dispersion based on **(B)** Ružička and **(D)** Jaccard dissimilarity indices in each sample type. The boxplots represent median (midline), interquartile ranges (shaded boxes), and ranges (whiskers). Data is shown according to the age (years) of the children with AOM.

Analyses of Paired Samples (NPS and MEF)

Heat maps of the most abundant OTUs were plotted using the *ComplexHeatmap* function in R. Dissimilarity values between paired NP and MEF samples were derived by the weighted Ružička (abundance-based) and the unweighted Jaccard (presence/absence-based) distance matrices. Sensitivity/specificity and PPV/NPV including 95% CIs for the most abundant OTUs and pneumococcal serotypes were calculated. Linear correlation of weighted (Ružička) or unweighted (Jaccard) paired dissimilarity values and age (in months) of the patients with AOM were calculated using Graph pad prism.

RESULTS

Study Population and Sample Processing

A total of 286 NPS from children (<7 years) with AOM were collected from 2004–2013. Samples were roughly equally distributed for sex and region of origin (i.e., west as compared to east). Very young children (0–3 years of age) were more likely to attend a day care and were more likely to be vaccinated with either PCV7 or PCV13. Detailed information on the study population, including previous antibiotic exposure and previous otitis media episodes, is listed in **Table 1**. In addition, 42/286 children were reported having tympanic membrane perforation and, therefore, provided both, MEF and a NPS. The microbiota of all samples was analyzed. After exclusion of low-quality reads, this resulted in 299'966 (mean, 1048.8; SD), ±940) and 39'726 (mean, 945.9; SD, ±580.9) high quality sequence reads for the NPS and MEF samples, respectively. Comparing the values for extrapolated true richness and extrapolated estimated richness indices revealed a coverage of 66.8 and 65.4% for the NPS (**Supplementary Figure 1**) and MEF (**Supplementary Figure 2**), respectively.

Dynamics of Bacterial Families Within NPS

We analyzed the dynamics of the five most abundant bacterial families (Moraxellaceae, Streptococcaceae, Corynebacteriaceae, Pasteurellaceae, and Staphylococcaceae) and all remaining

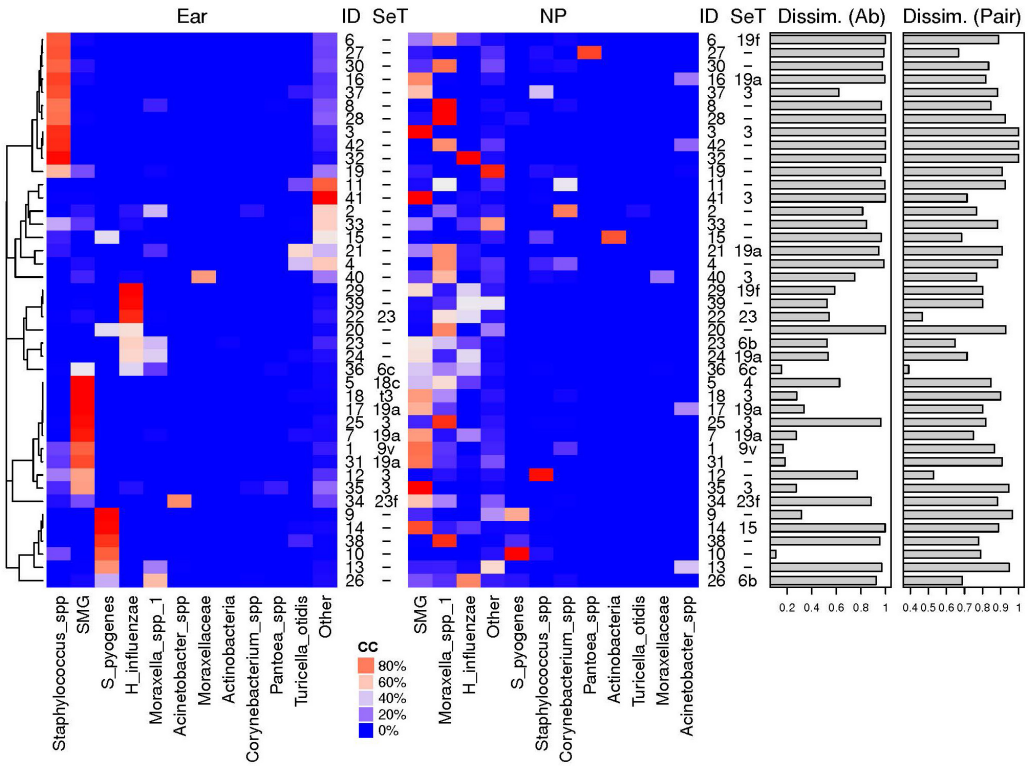

FIGURE 4 | Relative abundances of most abundant OTUs in MEF from ear and NP. Shown are the heat maps of the relative abundances of the most abundant OTUs in % [illustrated by a distinct color code (CC)]. The pneumococcal serotpyes (SeT) are indicated. Dissimilarly values based on abundance based Ružička (Dissim. Ab) and presence-absence based Jaccard (Dissim. Pair) distance values between the two different sample types of the same individual (ID) are shown as bar plots. High similarity of the bacterial microbiota of NPS and MEF when *S. pyogenes*, *H. influenzae* or *S. pneumoniae* were the predominant OTUs and overall high negative predictive values for NPS based prediction of MEF (see **Table 2** and text for more details). SMG, *Streptococcus mitis* group members (including *Streptococcus pneumoniae*).

families ("others"). Moraxellaceae was the most abundant bacterial family with a maximum relative abundance within the first year of life (mean 54.7%) (**Figure 1A**). However, a clear decrease of Moraxellaceae from the 3rd to the 6th year of life was noted. In contrast, we observed an increase of Staphylococcaceae and Corynebacteriaceae with increasing age (**Figures 1B,C**). No clear monotonic changes were noted for Streptococcaceae, Pasteurellaceae and others (**Figures 1D–F**) though the relative abundance of Staphylococcaceae and Corynebacteriacecae decreased at age 2–3 and increased between 3–4 years, and, the relative abundance of Streptococcaceae slightly decreased between 3–4 years. Due to the low number of NP samples at age 2–3 ($n = 8$), the observed non-monotonic changes might be coincidental.

Bacterial Richness of the Nasopharyngeal Microbiota Increases With Age in Children With AOM

We next determined the values for the alpha diversity indices of richness (S), SDI, and evenness based on 97% OTUs (**Figures 2A–F**). The residuals of the models for S and SDI were not normally distributed and, therefore, were log transformed (**Figures 2A–D**). To correct for the dependency nature of the study, linear mixed models including fixed effects were done (**Figures 2B,D,F**). Results showed that the bacterial richness (S) based on OTUs with 97% sequence identity, increased with age and was highest in children with 6 years of age (**Figures 2A,B**). Increase was significant using a linear mixed effect (LM) model with fixed effects age, year of sample collection, previous antibiotic usage, day care attendance and geographical origin (**Figure 2B**) ($P < 0.001$). In contrast, there was no such trend for SDI (**Figures 2C,D**), whereas for evenness, we observed a significant decrease between younger and older age groups ($P < 0.001$) and values were lowest at 6 years of age (**Figures 2E,F**).

Beta Diversity Analyses Revealed Clustering of NPS According to Age

We then used weighted (**Figures 3A,B**) and unweighted distance matrices (**Figures 3C,D**) to create ordination method based NMDS (**Figures 3A,C**) and multivariate dispersion plots (**Figures 3B,D**) for the analysis of Beta diversity. The ordination method based NMDS plots (**Figures 3A,C**) showed a distinct clustering of the microbiota of the NP of children with AOM according to age (PERMANOVA, unweighted: F-value: 6.6, $P < 0.01$, weighted: F-value: 6.3, $P < 0.01$). This indicates a

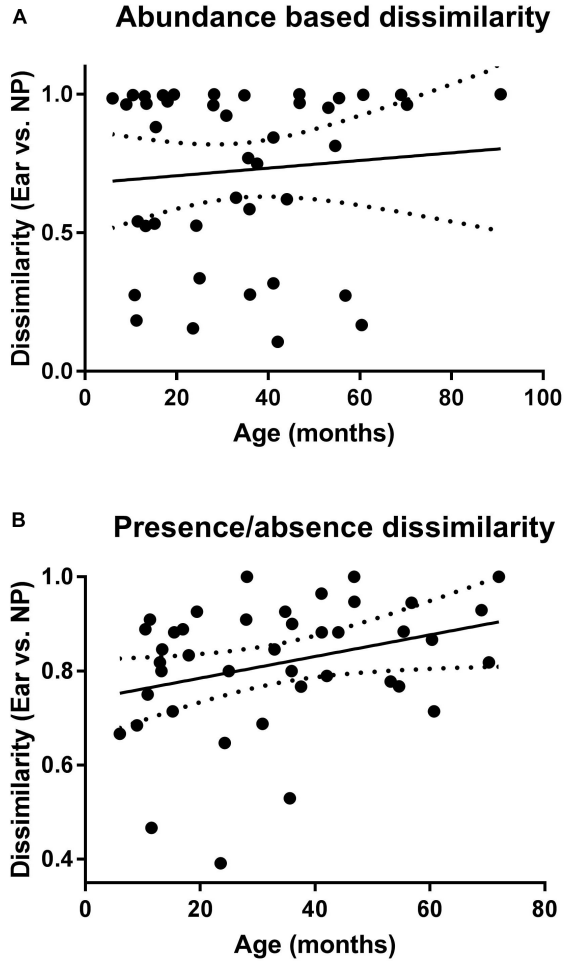

FIGURE 5 | Correlation of the microbiota of NP and MEF according to age. Shown are the abundance **(A)** and presence/absence **(B)** based dissimilarity values (for NP and MEF) for the children with AOM at different ages. Linear regression lines are indicated. *P*-value is significant for the presence/absence based dissimilarities ($P = 0.04$).

very strong effect of age on the human bacterial microbiota of the NP. Interestingly, children at a very young age seemed to display a significantly lower dispersion as compared to older children (unweighted distances from the centroid; Tukey's HSD test; $P < 0.001$; **Figure 3D**), indicating that an increase in age leads to a more heterogeneous microbial community structure. In contrast, all comparisons of weighted distances from the centroid were non-significant (**Figure 3B**), suggesting a stronger effect of community structure compared to community composition on multivariate dispersion across groups.

Microbiota of NP and MEF Show Highest Similarity When *S. pyogenes*, *H. influenzae* or *S. pneumoniae* Are the Predominant OTUs

We then compared the NPS microbiota profiles with the corresponding MEF profiles from 42 children. The 11 most abundant OTUs are illustrated (**Figure 4**) while all others were grouped ("others"). High dissimilarity values between the microbiota profiles of the NPS and the MEF were received if *Staphylococcus* spp. and "others" were the predominate OTUs within the MEF. Increased similarity was seen if the predominate OTUs within the MEF were *S. pyogenes*, *Streptococcus mitis* group (includes *S. pneumoniae)* and *H. influenzae*.

Calculation of the correlation between dissimilarity values and age of the children with AOM (**Figures 5A,B**) revealed a significant positive correlation for the presence/absence-based dissimilarity values (**Figure 5B**), which was not the case for the abundance-based values (**Figure 5A**).

Finally, we determined the sensitivity/specificity of individual OTUs and the pneumococcal serotypes for the prediction of corresponding MEF results (**Table 2**). Highest sensitivity/specificity values were achieved for *S. pyogenes* and the pneumococcal serotypes. For one patient, the serotyping results were discordant which might be due to multiple colonization of different *S. pneumoniae* (Brugger et al., 2009, 2010). Concerning the other OTUs, some were more often found in the MEF (especially *Turicella* spp.) while the opposite was true for e.g., *Corynebacterium* spp., *Moraxella* spp. and *H. influenzae*. In general, positive predictive values (PPV) revealed a considerable, pathogen-dependent variability while the negative predictive values (NPV) were found to be consistently high for most of the OTUs (**Table 2**).

DISCUSSION

This study analyzed the bacterial microbiota profiles from 286 children with AOM (286 NPS and 42 MEF). In the NP, we noted an increase in bacterial richness and beta dispersion with age and a decrease in evenness (**Figures 2**, **3**). This indicates the development of a more distinct bacterial microbiota profile toward the end of the sixth year of life. In addition, we found high similarity of the bacterial microbiota of NPS with MEF if the predominant OTU within the MEF was *S. pyogenes*, *H. influenzae*, or *S. pneumoniae*. The opposite was true for *Staphylococcus* spp. and others (**Figure 4** and **Table 2**).

We performed 454 sequencing in our study, a technique which has been replaced by more high-throughput platforms, e.g., Illumina. However, the nasal microbiota has a rather simple, low-diversity profile (Escapa et al., 2018) and in order to achieve an approximate OTU coverage of 70% (which is mainly recommended) there is no need for a large amount of sequencing reads (Hilty et al., 2012). In addition, 454 sequencing produced longer reads (as compared to Illumina) which increased the resolution for OTUs. Most importantly, our protocols have been systematically investigated as we have previously done validation work on mock communities using a similar design (Brugger et al., 2012). This included using different primers [i.e., 8F (for V1–V5) versus 341 F (for V3–V5)] and investigating the detection limit of bacteria (i.e., mock communities) which are very well known to be present in the NP of children. Using the

TABLE 2 | Sensitivity and specificity MEF/NP based on pneumococcal culture and presence and absence of the eight most frequent OTUs in the NPS and ears, respectively.

	NP+MEF+	NP−MEF−	NP−MEF+	NP+MEF−	Sensitivity (95% CI)	Specificity (95% CI)	PPV, % (95% CI)	NPV, % (95% CI)
Pneumococcal culture	10*	18	2	12	83 (52 – 98)	60 (41 – 77)	45 (33 – 58)	90 (71 – 97)
OTU name								
SMG	23	3	2	14	92 (74 – 99)	18 (4 – 43)	62 (56 – 68)	60 (22 – 89)
Moraxella spp.	10	9	1	22	91 (59 – 100)	29.0 (14 – 48)	31 (25 – 38)	90 (56 – 98)
H. influenzae	8	18	3	13	73 (40 – 94)	58.1 (39 – 75)	38 (26 – 52)	86 (69 – 94)
Staphylococcus spp.	10	13	14	5	42 (22 – 63)	72.2 (47 – 90)	67 (45 – 83)	48 (37 – 59)
S. pyogenes	6	33	2	1	75 (35 – 97)	97 (85 – 100)	86 (46 – 98)	94 (83 – 98)
Corynebacterium spp.	2	28	1	11	67 (9 – 99)	72 (55 – 85)	15 (7 – 32)	97 (85 – 99)
Acinetobacter spp.	1	36	1	4	50 (1 – 99)	90 (76 – 97)	20 (5 – 57)	97 (90 – 99)
Turicella otitidis	0	31	10	1	0 (0 – 31)	97 (84 – 100)	0	76 (74 – 77)

**Serotyping revealed that in 9 of 10 isolates, the serotype was identical in the middle ear fluid (MEF) as compared to the nasopharynx (NP). SMG, Streptococcus mitis group; OTU, operational taxonomic unit; PPV, positive predictive value; NPV, negative predictive value; CI, confidence interval.*

primer 8F, the detection limit was about 30 genome copies μl^{-1} with the exception of *H. influenzae* and *M. catarrhalis* (100 copies μl^{-1}). As for the observed difference of the detection limit, this is probably due to a SNP present in the conserved region of the forward primer 8F and therefore suboptimal PCR efficiency. There are no SNPs in the primer regions of 341F and 907R for the bacteria mentioned above and we therefore concluded this primer pair being appropriate for the study of the bacterial microbiota of the NP. Using Illumina MiSeq, the same primer design cannot be used as the reads are not long enough.

There is a lack of studies like ours describing the nasopharyngeal bacterial microbiota in children with AOM up to 7 years of age. However, data exists for infants at a younger age describing a distinct profile for the first 3 months of life with increased relative abundances of Staphylococcaceae and Corynebacteriaceae (Laufer et al., 2011; Biesbroek et al., 2014a,b; Mika et al., 2015; Teo et al., 2015; Bomar et al., 2017; Salter et al., 2017). In our study we found an increase of Staphylococcaceae and Corynebacteriaceae in children older than 3 years. This may indicate the transition toward a more "adult"-like composition of the microbiota as these two families are very often identified within the adult microbiome (Frank et al., 2010; Camarinha-Silva et al., 2014; Bomar et al., 2017). This transition may take place due to a more mature immune response resulting in less episodes of AOM in older children. In addition, common to our and other studies using molecular or conventional culture methods are the high (relative) abundances of Moraxellaceae and Streptococcaceae within the first 2 years of life (Faden et al., 1994, 1997; Bogaert et al., 2004, 2011; Hilty et al., 2012). However, in our study, we show that the abundance of Moraxellaceae drastically decreases in children aged more than 2 years.

A further major finding of our study was the discovery of a significant increasing correlation of age and dissimilarly of the microbiota of NP as compared to the MEF. Based on bacterial cultures, a recent study has observed that *S. pneumoniae* and non-typeable *Haemophilus influenzae* nasopharyngeal colonization increases significantly between 6 and 30–36 months of age, but as children get older the relationship between potential otopathogen in the NP with detection in MEF is weakened (Kaur et al., 2014). Similarly, a high prevalence of nasopharyngeal colonization but low frequency of *S. pneumoniae* as an etiology of AOM with age, especially after children became >18 months of age has been reported (Syrjanen et al., 2005). Our bacterial microbiota-based analyses showed similar findings as compared to culture-based studies. However, NP microbiota patterns from children below 2 years of age are still not very good surrogates of MEF cultures in children as dissimilarity values were quite high.

A recent systematic review of the literature reported the concordance between culture test results of the NP and MEF samples for the most prevalent microorganisms in children with otitis media (van Dongen et al., 2013). Culture-based AOM studies revealed higher PPVs (for *H. influenzae* and *S. aureus*) and lower PPVs (for *M. catarrhalis*) as compared to our study, respectively (van Dongen et al., 2013). As for *S. aureus*, this might be in part due to the fact that all MEF in this study were derived from cases with spontaneous tympanic membrane perforation which have been reported to contain a higher proportion of *S. aureus* (Brook and Gober, 2009).

However, with the exception of *S. aureus*, we received much higher NPVs as compared to culture-based studies. Our NPVs were also higher if compared to a study which was using a series of polymerase chain reactions in order to detect bacteria (Yatsyshina et al., 2016). This means that high-throughput sequencing of the bacterial microbiota of the NP results in decent NPVs for finding the pathogens within the MEF while this is not the case for the PPVs (with the exception of *S. pyogenes*).

Recently, Man et al. (2018) compared the microbiota of NP and MEF in almost 100 Dutch children under 5 years of age with AOM in children with tympanostomy tubes and also reported a high overall NPV (on OTU level) suggesting that the NP might be the main source of MEF bacteria in otitis media. The overall PPV was 0.4 (95%CI 0.39 – 0.42) which is in line with our results. However, significant quantitative correlations between NP and tympanostomy tube otorrhea (TTO) samples for *Haemophilus influenzae*, *S. aureus*, and *P. aeruginosa* abundance were reported (Man et al., 2018). In agreement with our results, *T. otitis* was

associated with MEF supporting its role as an otopathogen (Man et al., 2018).

This study has some major strengths. First, we have included a large number of NPS (n = 286) from children with AOM at different ages (up to <7 years of age). Patients were recruited from different outpatient settings from a well-defined sentinel network and medical diagnosis was done based on CDC case definition. In addition, we have included 42 paired samples of NPS and MEF allowing the investigation of the appropriateness of the NP as a proxy for the microbiota of the MEF. Apart from 16S rRNA sequencing, we also performed culturing for *S. pneumoniae* and subsequent serotyping for all positive samples.

This study has also some major limitations. Within our study, we did not investigate homogeneity of nasopharyngeal microbiota at the different locations of the nose of children with AOM. However, results from a recent study suggest that the microbiota at the different locations of the nose of children with AOM is almost homogeneous, irrespective of the clinical signs (Kaieda et al., 2005). We also only analyzed the bacterial microbiota and did not include virus detection in this study (e.g., by shotgun metagenomics sequencing). In addition, MEF collection was biased toward aggressive forms of AOM as only material of spontaneous perforations was collected which resulted in only 48 NP/MEF paired analyses. Also, based on the design of the surveillance program the information about the exact duration of the AOM episode as well as the time of tympanic membrane perforation was not recorded. Furthermore, sample acquisition was not standardized (i.e., no tympanocentesis samples) which could have resulted in contamination with skin flora. Thus, we cannot rule out that otitis externa might have been diagnosed as AOM in some cases (this could be reflected by the higher relative abundance of Staphylococcaceae in MEF compared to NPS, however, the pneumococcal isolation from NPS highly matched with pneumococcal isolation in MEF).

Further studies investigating the development of the bacterial microbiome including AOM should follow a prospective design (using a power calculation based on our results) to reduce the risk of unmeasured confounders.

CONCLUSION

In conclusion, this study revealed varying nasopharyngeal bacterial microbiota patterns according to age and moderate to high NPVs for the prediction of MEF OTUs based on analyses from the NP in a subset of children with spontaneous tympanic membrane rupture where we simultaneously characterized the bacterial microbiota of NPS and MEF. The NP of children with AOM serves as a moderate and insufficient proxy for the bacterial communities of the MEF at a very young and more advanced age, respectively. Given these results as well as previous culture (or species-specific PCR) based studies, the nasopharyngeal bacterial microbiota does not necessarily reflect the one of the middle ear in AOM and should only be used with caution for clinical decision decision-making. This might be in part due to the complex disease pathology in AOM, which also involves viruses and biofilms.

DATA AVAILABILITY

The datasets generated for this study can be found in National Center for Biotechnology Information Sequence Read Archive, SRR077426, SRR086165, SRR086166, and PRJEB23228.

ETHICS STATEMENT

The overall AOM surveillance program has been part of the governmental public health surveillance and has therefore been exempted from approval by Institutional Review Boards and the need for written consent from parents. Informed oral consent was received from the parents.

AUTHOR CONTRIBUTIONS

SB and MH were investigators in this study and contributed to the study design. SB, JK, WQ, LB, AO, and MH contributed to data collection and analysis. SB, JK, and MH contributed to data interpretation. All authors contributed to the writing, review of the report, and approved the final version of the manuscript.

FUNDING

The prospective surveillance study on the surveillance of acute otitis media within Sentinella including the investigations of MEF and NPS has been supported by the Federal Office of Public Health (FOPH). SB was supported by a grant (P3SMP3_155315) from the Swiss National Science Foundation (SNSF) and the Swiss Foundation for Grants in Biology and Medicine (SFGBM). This work was also partly supported by Swiss National Science Foundation (SNF) grant 320030_159791 to MH.

ACKNOWLEDGMENTS

We acknowledge Marianne Küffer and Chantal Studer for their extraordinary assistance. We are also very thankful to all the physicians who actively take and took part in the Sentinella surveillance system and who provided non-invasive MEF and NPS.

SUPPLEMENTARY MATERIAL

The Supplementary Material for this article can be found online at: https://www.frontiersin.org/articles/10.3389/fgene.2019.00555/full#supplementary-material

REFERENCES

Allemann, A., Frey, P. M., Brugger, S. D., and Hilty, M. (2017). Pneumococcal carriage and serotype variation before and after introduction of pneumococcal conjugate vaccines in patients with acute otitis media in Switzerland. *Vaccine* 35, 1946–1953. doi: 10.1016/j.vaccine.2017.02.010

Biesbroek, G., Bosch, A. A., Wang, X., Keijser, B. J., Veenhoven, R. H., Sanders, E. A., et al. (2014a). The impact of breastfeeding on nasopharyngeal microbial communities in infants. *Am. J. Respir. Crit. Care Med.* 190, 298–308. doi: 10.1164/rccm.201401-0073OC

Biesbroek, G., Tsivtsivadze, E., Sanders, E. A., Montijn, R., Veenhoven, R. H., Keijser, B. J., et al. (2014b). Early respiratory microbiota composition determines bacterial succession patterns and respiratory health in children. *Am. J. Respir. Crit. Care Med.* 190, 1283–1292. doi: 10.1164/rccm.201407-1240oc

Biesbroek, G., Sanders, E. A., Roeselers, G., Wang, X., Caspers, M. P., Trzcinski, K., et al. (2012). Deep sequencing analyses of low density microbial communities: working at the boundary of accurate microbiota detection. *PLoS One* 7:e32942. doi: 10.1371/journal.pone.0032942

Bogaert, D., Keijser, B., Huse, S., Rossen, J., Veenhoven, R., van Gils, E., et al. (2011). Variability and diversity of nasopharyngeal microbiota in children: a metagenomic analysis. *PLoS One* 6:e17035. doi: 10.1371/journal.pone.0017035

Bogaert, D., van Belkum, A., Sluijter, M., Luijendijk, A., de Groot, R., Rumke, H. C., et al. (2004). Colonisation by Streptococcus pneumoniae and *Staphylococcus aureus* in healthy children. *Lancet* 363, 1871–1872. doi: 10.1016/s0140-6736(04)16357-5

Bomar, L., Brugger, S. D., and Lemon, K. P. (2017). Bacterial microbiota of the nasal passages across the span of human life. *Curr. Opin. Microbiol.* 41, 8–14. doi: 10.1016/j.mib.2017.10.023

Brook, I., and Gober, A. E. (2009). Bacteriology of spontaneously draining acute otitis media in children before and after the introduction of pneumococcal vaccination. *Pediatr. Infect. Dis. J.* 28, 640–642. doi: 10.1097/INF.0b013e3181975221

Brugger, S. D., Frei, L., Frey, P. M., Aebi, S., Muhlemann, K., and Hilty, M. (2012). 16S rRNA terminal restriction fragment length polymorphism for the characterization of the nasopharyngeal microbiota. *PLoS One* 7:e52241. doi: 10.1371/journal.pone.0052241

Brugger, S. D., Frey, P., Aebi, S., Hinds, J., and Muhlemann, K. (2010). Multiple colonization with *S. pneumoniae* before and after introduction of the seven-valent conjugated pneumococcal polysaccharide vaccine. *PLoS One* 5:e11638. doi: 10.1371/journal.pone.0011638

Brugger, S. D., Hathaway, L. J., and Muhlemann, K. (2009). Detection of *Streptococcus pneumoniae* strain cocolonization in the nasopharynx. *J. Clin. Microbiol.* 47, 1750–1756. doi: 10.1128/JCM.01877-08

Camarinha-Silva, A., Jauregui, R., Chaves-Moreno, D., Oxley, A. P., Schaumburg, F., Becker, K., et al. (2014). Comparing the anterior nare bacterial community of two discrete human populations using illumina amplicon sequencing. *Environ. Microbiol.* 16, 2939–2952. doi: 10.1111/1462-2920.12362

Chonmaitree, T., Jennings, K., Golovko, G., Khanipov, K., Pimenova, M., Patel, J. A., et al. (2017). Nasopharyngeal microbiota in infants and changes during viral upper respiratory tract infection and acute otitis media. *PLoS One* 12:e0180630. doi: 10.1371/journal.pone.0180630

Coticchia, J. M., Chen, M., Sachdeva, L., and Mutchnick, S. (2013). New paradigms in the pathogenesis of otitis media in children. *Front. Pediatr.* 1:52. doi: 10.3389/fped.2013.00052

Escapa, I. F., Chen, T., Huang, Y., Gajare, P., Dewhirst, F. E., and Lemon, K. P. (2018). New insights into human nostril microbiome from the expanded human oral microbiome database (eHOMD): a resource for the microbiome of the human aerodigestive tract. *mSystems* 3:e187-18. doi: 10.1128/mSystems.00187-18

Faden, H., Duffy, L., Wasielewski, R., Wolf, J., Krystofik, D., and Tung, Y. (1997). Relationship between nasopharyngeal colonization and the development of otitis media in children. *J. Infect. Dis.* 175, 1440–1445. doi: 10.1086/516477

Faden, H., Harabuchi, Y., and Hong, J. J. (1994). Epidemiology of *Moraxella catarrhalis* in children during the first 2 years of life: relationship to otitis media. *J. Infect. Dis.* 169, 1312–1317. doi: 10.1093/infdis/169.6.1312

Frank, D. N., Feazel, L. M., Bessesen, M. T., Price, C. S., Janoff, E. N., and Pace, N. R. (2010). The human nasal microbiota and *Staphylococcus aureus* carriage. *PLoS One* 5:e10598. doi: 10.1371/journal.pone.0010598

Hilty, M., Qi, W., Brugger, S. D., Frei, L., Agyeman, P., Frey, P. M., et al. (2012). Nasopharyngeal microbiota in infants with acute otitis media. *J. Infect. Dis.* 205, 1048–1055. doi: 10.1093/infdis/jis024

Kaieda, S., Yano, H., Okitsu, N., Hosaka, Y., Okamoto, R., and Inoue, M. (2005). Investigation about the homogeneity of nasopharyngeal microflora at the different location of nasopharynx of children with acute otitis media. *Int. J. Pediatr. Otorhinolaryngol.* 69, 959–963. doi: 10.1016/j.ijporl.2005.01.036

Kaur, R., Czup, K., Casey, J. R., and Pichichero, M. E. (2014). Correlation of nasopharyngeal cultures prior to and at onset of acute otitis media with middle ear fluid cultures. *BMC Infect. Dis.* 14:640. doi: 10.1186/s12879-014-0640-y

Kaur, R., Morris, M., and Pichichero, M. E. (2017). Epidemiology of acute otitis media in the postpneumococcal conjugate vaccine era. *Pediatrics* 140:e20170181. doi: 10.1542/peds.2017-0181

Kilpi, T., Herva, E., Kaijalainen, T., Syrjanen, R., and Takala, A. K. (2001). Bacteriology of acute otitis media in a cohort of finnish children followed for the first two years of life. *Pediatr. Infect. Dis. J.* 20, 654–662. doi: 10.1097/00006454-200107000-00004

Kunin, V., Engelbrektson, A., Ochman, H., and Hugenholtz, P. (2010). Wrinkles in the rare biosphere: pyrosequencing errors can lead to artificial inflation of diversity estimates. *Environ. Microbiol.* 12, 118–123. doi: 10.1111/j.1462-2920.2009.02051.x

Kunin, V., and Hugenholtz, P. (2010). PyroTagger : a fast, accurate pipeline for analysis of rRNA amplicon pyrosequence data. *Open J.* 1, 1–8.

Lappan, R., Imbrogno, K., Sikazwe, C., Anderson, D., Mok, D., Coates, H., et al. (2018). A microbiome case-control study of recurrent acute otitis media identified potentially protective bacterial genera. *BMC Microbiol.* 18:13. doi: 10.1186/s12866-018-1154-3

Laufer, A. S., Metlay, J. P., Gent, J. F., Fennie, K. P., Kong, Y., Pettigrew, M. M., et al. (2011). Microbial communities of the upper respiratory tract and otitis media in children. *mBio* 2:e245-210. doi: 10.1128/mBio.00245-10

Lemon, K. P., Armitage, G. C., Relman, D. A., and Fischbach, M. A. (2012). Microbiota-targeted therapies: an ecological perspective. *Sci. Transl. Med.* 4:137rv5. doi: 10.1126/scitranslmed.3004183

Lieberthal, A. S., Carroll, A. E., Chonmaitree, T., Ganiats, T. G., Hoberman, A., Jackson, M. A., et al. (2013). The diagnosis and management of acute otitis media. *Pediatrics* 131, e964–e999. doi: 10.1542/peds.2012-3488

Liu, Z., Lozupone, C., Hamady, M., Bushman, F. D., and Knight, R. (2007). Short pyrosequencing reads suffice for accurate microbial community analysis. *Nucleic Acids Res.* 35:e120. doi: 10.1093/nar/gkm541

Man, W. H., van Dongen, T. M. A., Venekamp, R. P., Pluimakers, V. G., Chu, M., van, Houten MA, et al. (2018). Respiratory microbiota predicts clinical disease course of acute otorrhea in children with tympanostomy tubes. *Pediatr. Infect. Dis. J.* 38, e116–e125. doi: 10.1097/INF.0000000000002215

Mika, M., Mack, I., Korten, I., Qi, W., Aebi, S., Frey, U., et al. (2015). Dynamics of the nasal microbiota in infancy: a prospective cohort study. *J. Allergy Clin. Immunol.* 135, 905.e11–912.e11. doi: 10.1016/j.jaci.2014.12.1909

Muhlemann, K., Matter, H. C., Tauber, M. G., and Bodmer, T. (2003). Nationwide surveillance of nasopharyngeal *Streptococcus pneumoniae* isolates from children with respiratory infection, Switzerland, 1998-1999. *J. Infect. Dis.* 187, 589–596. doi: 10.1086/367994

Post, J. C., Preston, R. A., Aul, J. J., Larkins-Pettigrew, M., Rydquist-White, J., Anderson, K. W., et al. (1995). Molecular analysis of bacterial pathogens in otitis media with effusion. *JAMA* 273, 1598–1604. doi: 10.1001/jama.273.20.1598

Revai, K., Mamidi, D., and Chonmaitree, T. (2008). Association of nasopharyngeal bacterial colonization during upper respiratory tract infection and the development of acute otitis media. *Clin. Infect. Dis.* 46, e34–e37. doi: 10.1086/525856

Salter, S. J., Turner, C., Watthanaworawit, W., de, Goffau MC, Wagner, J., Parkhill, J., et al. (2017). A longitudinal study of the infant nasopharyngeal microbiota: the effects of age, illness and antibiotic use in a cohort of South East Asian children. *PLoS Negl. Trop. Dis.* 11:e0005975. doi: 10.1371/journal.pntd.0005975

Sillanpaa, S., Kramna, L., Oikarinen, S., Sipila, M., Rautiainen, M., Aittoniemi, J., et al. (2017). Next-generation sequencing combined with specific PCR assays to determine the bacterial 16S rRNA gene profiles of middle ear fluid collected

from children with acute otitis media. *mSphere* 2:e00006-17. doi: 10.1128/mSphere.00006-17

Syrjanen, R. K., Auranen, K. J., Leino, T. M., Kilpi, T. M., and Makela, P. H. (2005). Pneumococcal acute otitis media in relation to pneumococcal nasopharyngeal carriage. *Pediatr. Infect. Dis. J.* 24, 801–806. doi: 10.1097/01.inf.0000178072.83531.4f

Teo, S. M., Mok, D., Pham, K., Kusel, M., Serralha, M., Troy, N., et al. (2015). The infant nasopharyngeal microbiome impacts severity of lower respiratory infection and risk of asthma development. *Cell Host Microbe* 17, 704–715. doi: 10.1016/j.chom.2015.03.008

van Dongen, T. M., van der Heijden, G. J., van Zon, A., Bogaert, D., Sanders, E. A., Schilder, A. G., et al. (2013). Evaluation of concordance between the microorganisms detected in the nasopharynx and middle ear of children with otitis media. *Pediatr. Infect. Dis. J.* 32, 549–552. doi: 10.1097/INF.0b013e318280ab45

Yatsyshina, S., Mayanskiy, N., Shipulina, O., Kulichenko, T., Alyabieva, N., Katosova, L., et al. (2016). Detection of respiratory pathogens in pediatric acute otitis media by PCR and comparison of findings in the middle ear and nasopharynx. *Diagn. Microbiol. Infect. Dis.* 85, 125–130. doi: 10.1016/j.diagmicrobio.2016.02.010

Conflict of Interest Statement: MH received an educational grant from Pfizer AG for partial support of this project. However, Pfizer AG had no role in the data analysis and content of the manuscript.

The remaining authors declare that the research was conducted in the absence of any commercial or financial relationships that could be construed as a potential conflict of interest.

frontiers in Cellular and Infection Microbiology

ORIGINAL RESEARCH
published: 04 October 2019
doi: 10.3389/fcimb.2019.00339

Altered Middle Ear Microbiome in Children With Chronic Otitis Media With Effusion and Respiratory Illnesses

Allison R. Kolbe[1]*, *Eduardo Castro-Nallar*[2], *Diego Preciado*[3] and *Marcos Pérez-Losada*[1,4]

[1] Department of Biostatistics and Bioinformatics, Milken Institute School of Public Health, Computational Biology Institute, The George Washington University, Washington, DC, United States, [2] Facultad de Ciencias de la Vida, Center for Bioinformatics and Integrative Biology, Universidad Andrés Bello, Santiago, Chile, [3] Division of Pediatric Otolaryngology, Sheikh Zayed Institute, Children's National Health System, Washington, DC, United States, [4] CIBIO-InBIO, Centro de Investigação em Biodiversidade e Recursos Genéticos, Universidade Do Porto, Vairão, Portugal

OPEN ACCESS

Edited by:
Regie Santos-Cortez, University of Colorado Denver School of Medicine, United States

Reviewed by:
W. Edward Swords, University of Alabama at Birmingham, United States
Shujiro Minami, Tokyo Medical Center (NHO), Japan
Rebecca E. Walker, The University of Auckland, New Zealand

***Correspondence:**
Allison R. Kolbe
akolbe@gwu.edu

Specialty section:
This article was submitted to Microbiome in Health and Disease, a section of the journal Frontiers in Cellular and Infection Microbiology

Received: *23 July 2019*
Accepted: *18 September 2019*
Published: *04 October 2019*

Citation:
Kolbe AR, Castro-Nallar E, Preciado D and Pérez-Losada M (2019) Altered Middle Ear Microbiome in Children With Chronic Otitis Media With Effusion and Respiratory Illnesses. Front. Cell. Infect. Microbiol. 9:339. doi: 10.3389/fcimb.2019.00339

Chronic otitis media with effusion (COME) is a common childhood disease characterized by an accumulation of fluid behind the eardrum. COME often requires surgical intervention and can also lead to significant hearing loss and subsequent learning disabilities. Recent characterization of the middle ear fluid (MEF) microbiome in pediatric patients has led to an improved understanding of the microbiota present in the middle ear during COME. However, it is not currently known how the MEF microbiome might vary due to other conditions, particularly respiratory disorders. Here, we apply an amplicon sequence variant (ASV) pipeline to MEF 16S rRNA high-throughput sequencing data from 50 children with COME (ages 3–176 months) undergoing tube placement. We achieve a more detailed taxonomic resolution than previously reported, including species and genus level resolution. Additionally, we provide the first report of the functional roles of the MEF microbiome and demonstrate that despite high taxonomic diversity, the functional capacity of the MEF microbiome remains uniform between patients. Furthermore, we analyze microbiome differences between children with COME with and without a history of lower airway disease (i.e., asthma or bronchiolitis). The MEF microbiome was less diverse in participants with lower airway disease than in patients without, and phylogenetic β-diversity (weighted UniFrac) was significantly different based on lower airway disease status. Differential abundance between patients with lower airway disease and those without was observed for the genera *Haemophilus, Moraxella, Staphylococcus, Alloiococcus,* and *Turicella*. These findings support previous suggestions of a link between COME and respiratory illnesses and emphasize the need for future study of the middle ear and respiratory tract microbiomes in diseases such as asthma and bronchiolitis.

Keywords: otitis media, asthma, bronchiolitis, middle ear microbiome, amplicon sequence variants

INTRODUCTION

Chronic otitis media with effusion (COME) is characterized by an accumulation of fluid behind the eardrum which persists for 3 months or more, typically without signs of inflammation (Minovi and Dazert, 2014). COME is a leading cause of hearing loss in children, especially in developing countries (Monasta et al., 2012), and can result in learning disabilities and educational problems (Williams and Jacobs, 2009). Approximately 80% of children worldwide will have experienced an episode of COME by age 10 (Minovi and Dazert, 2014).

More than half of COME cases are preceded by acute otitis media (AOM), which are most commonly caused by bacterial infection with *Streptococcus pneumoniae*, *Moraxella catarrhalis*, and *Haemophilus influenzae* (Minovi and Dazert, 2014; Qureishi et al., 2014). However, the role of these pathogens or other components of the middle ear microbiome in COME is less well-understood. All three of these pathogens have been identified in middle ear fluid (MEF), as well as *Alloiococcus otitis*, *Turicella otitidis*, and *Staphylococcus* sp. (Harimaya et al., 2006; Guvenc et al., 2010; Jervis-Bardy et al., 2015; Chan et al., 2016; Lappan et al., 2018). Interestingly, several of these same species have been linked to the development of asthma and the asthma microbiome, particularly *M. catarrhalis* and *H. influenzae* (Bisgaard et al., 2007; Castro-Nallar et al., 2015; Pérez-Losada et al., 2015). However, the relationship between asthma and the middle ear microbiome, particularly in the context of COME, is not known.

Several studies have observed a relationship between otitis media (OM) and respiratory illnesses such as asthma and bronchiolitis. Bronchiolitis is a lung infection that most commonly affects young children at the same age as typical AOM incidence and is associated with airway inflammation and congestion. Asthma is a chronic condition characterized by airway inflammation and increased mucus production, and can result in shortness of breath, coughing, and wheezing, typically at an older age. Bacterial AOM is a common complication associated with bronchiolitis (Andrade et al., 1998; Gomaa et al., 2012). Similarly, large-scale studies in Germany and Mexico have observed that AOM episodes in infancy increases the risk of asthma development later in life (Eldeirawi et al., 2010; MacIntyre et al., 2010). Similar relationships have been observed between COME and asthma. A retrospective study of tube placement patients with COME found a significantly higher rate of asthma diagnosis at follow-up compared to children of the same age, as well as different clinical presentations of COME including mucoid effusion and a higher rate of multiple tube placements (Gamble et al., 1992). Interestingly, COME has also been associated with other atopic diseases such as allergic rhinitis (Alles et al., 2001; Luong and Roland, 2008; Kreiner-Moller et al., 2012). Although the directionality of this relationship is unclear, some have hypothesized that chronic inflammation due to asthma or other atopic diseases can reduce eustachian tube opening and impair mucociliary function (Alles et al., 2001; MacIntyre and Heinrich, 2012). Gamble et al. (1992) suggested that COME in asthmatics is not an isolated disease, but rather the result of atopic disease affecting the mucociliary system of the entire respiratory tract. While the link between bronchiolitis and COME has not been explored as extensively, it is possible that inflammation due to bronchiolitis could have a similar effect. At present, however, the nature of the relationship between COME and respiratory illnesses is poorly understood.

Microbiome dysbiosis has been well-characterized in the respiratory tract associated with asthma and bronchiolitis (Hilty et al., 2010; Huang et al., 2011; Marri et al., 2013; Castro-Nallar et al., 2015; Pérez-Losada et al., 2015; Hasegawa et al., 2016; Mansbach et al., 2016; Kozik and Huang, 2018), but it is not currently known whether this dysbiosis extends to the middle ear, particularly when associated with COME. In this study, we sought to characterize the MEF microbiome associated with COME in patients with and without asthma or bronchiolitis. To accomplish this goal, we re-analyzed the 16S rRNA high-throughput sequencing data previously published by Krueger et al. (2017), incorporating new metadata relating to lower airway disease diagnosis as well as analyzing the metabolic function of the microbial communities. Furthermore, we built upon the previous study by utilizing an amplicon sequence variant (ASV) approach which enhances taxonomic classification and reproducibility (Callahan et al., 2017). This study provides new insight into the MEF microbiome in COME, as well as MEF microbiome changes associated with asthma or bronchiolitis.

MATERIALS AND METHODS

Sample collection and DNA sequencing methodology for this study were previously described (Krueger et al., 2017). Briefly, middle ear effusion samples were collected from 50 children with chronic otitis media undergoing myringotomy with tympanostomy tube placement at Children's National Health System in Washington, D.C. The cohort ranged from 3 to 176 months of age, with 34 boys and 16 girls. Out of the 50 children, nearly three-fourths suffered from significant hearing loss (36/50). None of these children were treated with antibiotics for 2 weeks prior to sampling. Other (non-antibiotic) medication use was not recorded for this study. Thirteen of the children were diagnosed with lower airway disease such as asthma or bronchiolitis. To fit the categorization of being positive for these, the children needed to meet any of the following criteria: (1) history of pulmonary physician-diagnosed asthma; (2) documented chronic wheezing being treated with a daily respiratory inhaler; or (3) PCR (+) for rhinovirus bronchiolitis diagnosis. Although asthma and bronchiolitis are considered different respiratory illnesses, there often is a spectrum of disease over time and they cannot be reliably distinguished in young children. Therefore, we evaluated them together as lower airway disease in this study.

DNA purification from MEF was performed using the QiaAmp mini kit (Qiagen) and extracted following the MiSeq SOP protocol described in Kozich et al. (2013). The V4 region of the 16S rRNA gene was amplified and libraries were sequenced using the Illumina MiSeq at University of Michigan. Negative controls did not amplify, indicating that bacterial DNA was not present in the reagents, and therefore were not sequenced.

Abbreviations: AOM, acute otitis media; ASV, amplicon sequence variant; COME, chronic otitis media with effusion; OM, otitis media.

Raw fastq files from Krueger et al. (2017) were re-processed using dada2 version 1.12 (Callahan et al., 2016). This pipeline offers improved taxonomic resolution and reproducibility compared to OTU-based methods (Callahan et al., 2017). Reads were filtered using standard parameters, with no uncalled bases, maximum of two expected errors, and truncating reads at a quality score of two or less. Forward and reverse reads were truncated after 240 and 225 bases, respectively. The standard dada2 pipeline was then applied to perform amplicon sequence variant (ASV) inference, merge paired reads, and identify chimeras. Singleton ASVs are discarded in the dada2 pipeline (Callahan et al., 2017). Taxonomic assignment was performed against the Silva v132 database (Quast et al., 2013) using the dada2-formatted training files for taxonomy and species-level assignment (Callahan, 2018). ASV sequences were aligned using MAFFT (Katoh and Standley, 2013) and used to build a tree with FastTree (Price et al., 2010). The resulting ASV tables and phylogenetic tree were imported into phyloseq (McMurdie and Holmes, 2013) for further analysis.

Functional analysis of microbial communities was performed with PICRUSt2 (Douglas et al., 2019), following the standard pipeline. First, ASVs were aligned to reference sequences using HHMER (Howard Hughes Medical Institute, 2018) and placed into a reference tree with EPA-NG (Barbera et al., 2019) and GAPPA (Czech and Stamatakis, 2019). Hidden-state prediction was performed using castor (Louca and Doebeli, 2018), and along with the ASV abundance table generated by dada2, used to generate metagenome predictions. Finally, KEGG pathway level predictions were performed with MinPath (Ye and Doak, 2009). Exploratory analysis of functional abundances was performed in STAMP (Parks et al., 2014), and visualized with BURRITO (McNally et al., 2018). For visualization purposes, ASVs with <0.1% relative abundance were removed. To test for significant associations between functional profiles and clinical variables, general linear models implemented using MaAsLin, with significance considered at $q < 0.25$ as recommended by the authors (Morgan et al., 2012).

Alpha diversity indices (ASV richness and Shannon diversity) were calculated on raw counts using the *estimate_richness*() function in phyloseq and plotted with ggplot2 (Wickham, 2016). Significant differences based on asthma/bronchiolitis status were identified using linear models with clinical metadata (Muc5B +/−, Muc5AC +/−, significant hearing loss +/−, gender, over/under 24 months of age, mucoid/serous fluid) from Krueger et al. (2017) as covariables.

Prior to calculating beta diversity, read counts were normalized for with DESeq2 (Love et al., 2014), using the modified geometric mean ("poscounts") as implemented in the function *estimateSizeFactors*(). Beta diversity was calculated using the weighted and unweighted UniFrac distances implemented in the phyloseq package. Significance was determined by PERMANOVA using the R package vegan (Oksanen et al., 2019) with clinical metadata as covariables.

Differential abundance testing was performed with DESeq2 (Love et al., 2014) on normalized data as described before (McMurdie and Holmes, 2013). Using the negative binomial model implemented in DESeq2 accounts for library size differences and biological variability more appropriately than rarefying or using simple proportions (McMurdie and Holmes, 2013). The same variables and covariables listed above were used in the model formula. Significance was determined at $\alpha < 0.05$. All analyses were performed in R version 3.6 (R Core Team, 2019).

RESULTS

Taxonomic Composition of the Ear Microbiome During Chronic Infection

On average, 98% of sequences were assigned at the genus level (**Figure 1**), compared to ∼84% in Krueger et al. (2017). These included two previously unidentified genera, *Achromobacter* and *Pseudoflavitalea*. Furthermore, species level resolution was achieved for some ASVs. These included *Turicella otitidis* (6.9 ± 2.2%), *Alloiococcus otitis* (6.0 ± 1.7%), and *Stenotrophomonas*

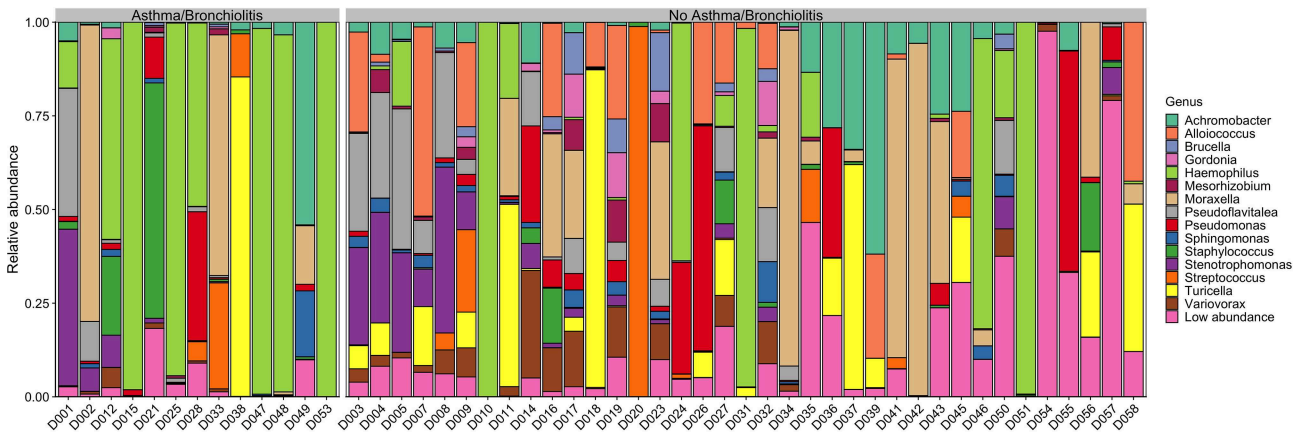

FIGURE 1 | Genus-level relative abundance in patients with or without asthma/bronchiolitis. Genera with mean relative abundance <1% across all samples are plotted as "Low abundance".

maltophilia (4.6 ± 1.4%), as well as several low abundance (<1%) ASVs (**Supplementary Table 1**).

The taxonomic composition of the middle ear effusion is quite diverse, with no core microbiome. Although *Haemophilus*, *Moraxella*, and *Turicella* were the largest genera by mean relative abundance, these genera were only present in approximately half of the studied samples (27/50, 26/50, and 26/50, respectively). *Achromobacter* and *Pseudomonas* were the most prevalent genera, present in 39/50 and 38/50 samples, respectively (**Supplementary Table 2**).

Metabolic Function of the Ear Microbiome During Chronic Infection

The functional roles of the middle ear microbiome were primarily classified into four groups: cellular processes (4.7 ± 0.2%), environmental information processing (20.4 ± 0.3%), genetic information processing (24.8 ± 0.5%), and metabolism (33.8 ± 0.3%). Approximately 16% were unclassified. The sub-pathways with the largest relative abundance were Membrane Transport (19.4 ± 0.3%), Translation (13.4 ± 0.4%), Amino acid metabolism (7.6 ± 0.2%), and Carbohydrate Metabolism (6.3 ± 0.1%). Functional profiles were similar across all patients (**Figure 2**). No significant associations were identified between the functional profiles and clinical variables using MaAsLin or principal component analysis.

Variation of Ear Microbiome Composition and Function During Chronic Infection

The α-diversity of the middle ear microbiome estimated by ASV richness and Shannon diversity indices was significantly

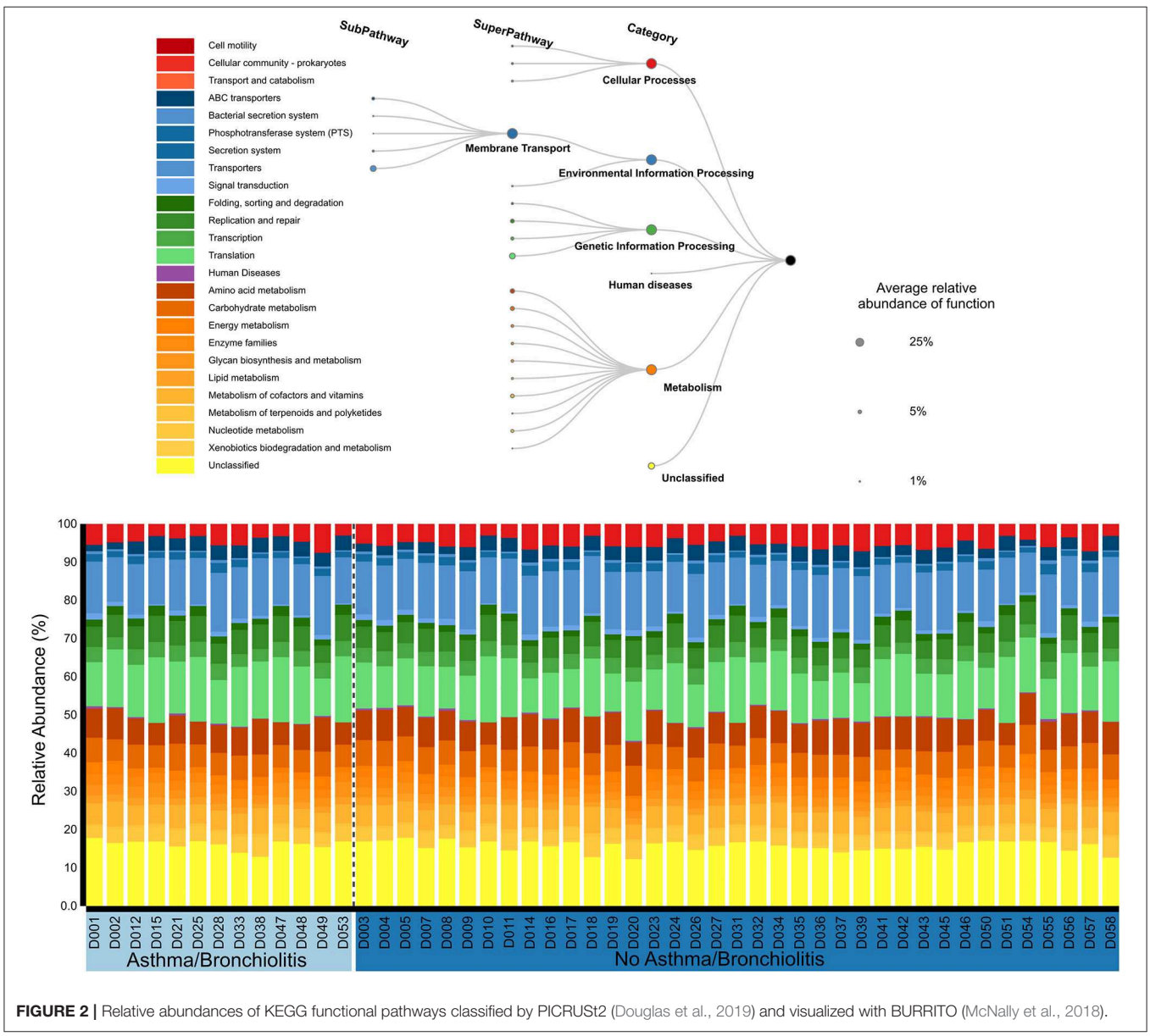

FIGURE 2 | Relative abundances of KEGG functional pathways classified by PICRUSt2 (Douglas et al., 2019) and visualized with BURRITO (McNally et al., 2018).

lower in patients with asthma or bronchiolitis than in patients without (**Figure 3**; $p < 0.05$). Mean ASV richness in patients with asthma/bronchiolitis was 16.4 compared to 31.1 in patients without; similarly, mean Shannon diversity in patients with asthma/bronchiolitis was 0.96 compared to 1.72 in patients without. α-diversity did not vary significantly between other clinical variables, including age, gender, significant hearing loss, mucoid/serous effusion, and presence of Muc5B and/or Muc5AC.

In contrast, principle coordinate analysis with weighted UniFrac distances and analysis with PERMANOVA indicated significant differences in β-diversity between patients with/without significant hearing loss and asthma/bronchiolitis status (**Figure 4A**). These variables were not significant in principle coordinate analysis with unweighted UniFrac distances (**Figure 4B**).

Differential abundance testing with DESeq2 identified several ASVs that varied significantly in the relative mean proportions with respect to asthma/bronchiolitis status, after accounting for variation in other clinical and demographic variables. *Haemophilus*, *Staphylococcus,* and *Moraxella* were significantly higher in children with asthma or bronchiolitis, whereas *Turicella* and *Alloiococcus* were significantly lower (**Figure 5**).

DISCUSSION

Chronic otitis media with effusion (COME) is the leading cause of hearing loss among children and affects as many as 80% of children by age 10 (Minovi and Dazert, 2014). Here, we present novel insights from the 16S data presented in Krueger et al. (2017), using amplicon sequence variants (ASVs) instead of OTUs, as well as evaluating links to diagnosed lower airway disease.

Using exact sequence variants instead of OTUs allows for greater precision and reproducibility in taxonomic assignment (Callahan et al., 2017, 2019; Edgar, 2018; Knight et al., 2018; Xue et al., 2018). Previous OTU-based approaches typically functioned by clustering sequences based on a 97% similarity threshold, and then assigning these clusters to reference tree-based OTUs. These approaches did not incorporate sequence quality information or statistical information about the reads into taxonomic assignments, and were therefore losing valuable information (Callahan et al., 2017). Using exact sequence variants improves estimations of diversity and taxonomic predictions, especially for communities which have not been studied extensively (Callahan et al., 2017; Caruso et al., 2019). With the approach implemented in dada2 (Callahan et al., 2016), we were able to achieve species level classifications

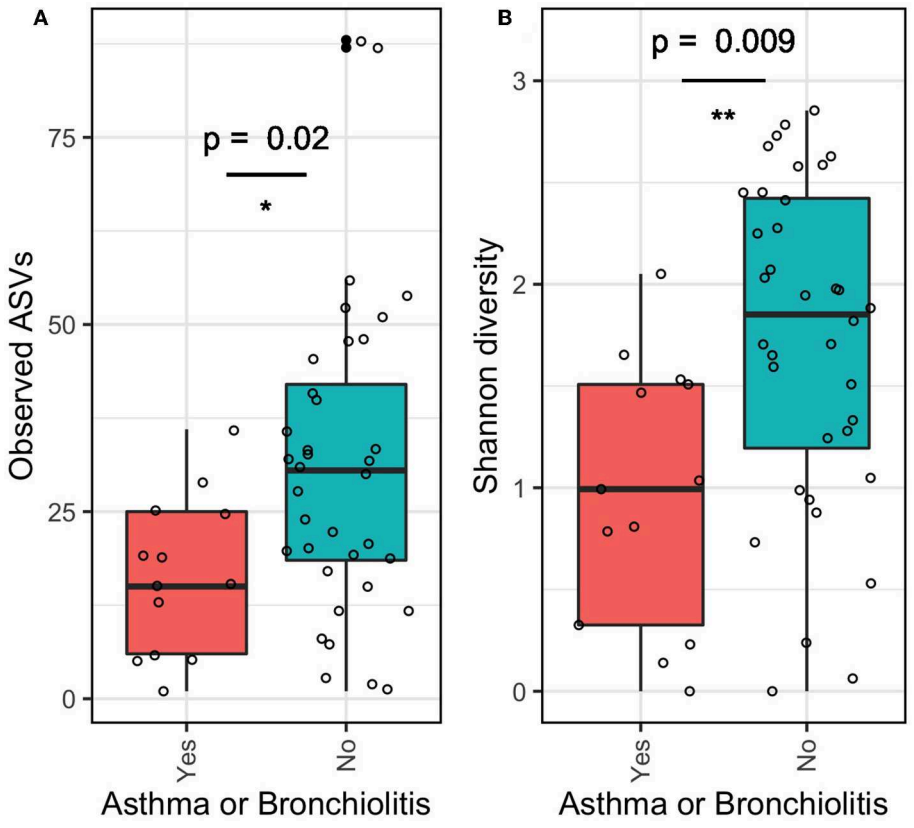

FIGURE 3 | α-diversity of middle ear fluid in patients with asthma or bronchiolitis. Estimates of richness (**A**; number of observed ASVs) and evenness (**B**; Shannon diversity) were significantly lower in patients with asthma or bronchiolitis. *$p < 0.05$, **$p < 0.01$.

for multiple ASVs, three of which were present at a mean relative abundance >1%. Of these, *Alloiococcus otitis* and *Turicella otiditis* have been previously identified as typical components of the OM microbiome (Tano et al., 2008; von Graevenitz and Funke, 2014; Lappan et al., 2018). In contrast, *Stenotrophomonas maltophilia* has not been described in many middle ear microbiomes, despite being identified as the source of numerous human diseases including respiratory infections (Brooke, 2012). However, recent work by Kalcioglu et al. (2018) identified *S. maltophilia* in tympanosclerotic plaques isolated from an individual undergoing surgery due to COME. Therefore, *S. maltophilia* may be found in a subset of COME patients, particularly those who have developed tympanosclerosis. Interestingly, *S. maltophilia* was not found in cholesteatomas in the same study, indicating it may serve a specialized role (Kalcioglu et al., 2018).

Furthermore, OTUs that had been previously classified at the family level only were able to be defined at the genus level now using dada2. These were *Achromobacter* (relative abundance: 6.6%, family: Alcaligenaceae) and *Pseudoflavitalea* (relative abundance: 5.3%, family: Chitinophagaceae). *Pseudoflavitalea* is a newly described genus that currently has only been isolated from soil samples (Kim et al., 2016); its potential role in human disease is unknown. On the other hand, *Achromobacter xylosoxidans* was initially isolated from ear discharge from OM patients (Yabuuchi and Ohyama, 1971) and was recently identified in cholesteatomas of multiple individuals with COME (Kalcioglu et al., 2018). Members of the *Achromobacter* genus, specifically *Achromobacter xylosidans*, have been shown to be opportunistic respiratory pathogens, particularly in patients with cystic fibrosis or immune deficiencies (Swenson and Sadikot, 2015). Given that *Achromobacter* was the most prevalent genus identified (present in 39/50 samples), with a mean relative abundance of 6.6%, further work on the role of *Achromobacter* in COME is warranted.

The high inter-patient variation and lack of core microbiome indicates that there is no typical middle ear microbiome associated with COME (**Figure 1**). In contrast to previous reports that found the middle ear microbiome to be dominated by a single genus, typically from *Alloicoccus, Moraxella, or Haemophilus* (Guvenc et al., 2010; Jervis-Bardy et al., 2015), the middle ear microbiome in this study was highly variable, generally compromising at least two high-abundance genera. This difference may be due to the finer resolution of the ASV pipeline implemented in dada2, and the larger quantity of data retained by not rarefying the counts. Furthermore, even the "typical" agents associated with AOM—namely, *Haemophilus, Moraxella,* and *Streptococcus*—were absent in ∼50% of the samples from our COME patients. These results highlight the complexity of the middle ear microbiome associated with COME, which is perhaps expected given that a multitude of risk factors and potential etiologies have been identified for COME.

To our knowledge, we present here the first characterization of microbiome function in the middle ear. Although taxonomic composition varied dramatically between patients, microbiome function was remarkably similar across all patients (**Figure 2**). This supports the idea that microbial community functions often converge despite different taxonomic compositions (Human Microbiome Project, 2012; Louca et al., 2018). These will include core functions that are essential for microbial life, such as translation (Human Microbiome Project, 2012), which was highly abundant in our analysis. Interestingly, one of the top functions of the middle ear microbial community was "Membrane Transport," which includes a wide range of genes such as transporters, the phosphotransferase system, and the bacterial secretion system. In our case, the majority of genes were subcategorized in the general category "Transporters." In previous human microbiome studies, membrane transport has been identified as an abundant component of the healthy laryngeal microbiome (Jette et al., 2016) and associated with gut microbiome dysbiosis in irritable bowel disease and obesity (Greenblum et al., 2012). Further work is necessary to understand if these functions represent unique roles of the microbial community during COME, or if overlapping functions are present in AOM and healthy MEF microbiome.

Microbial diversity varied significantly between COME patients with and without asthma/bronchiolitis (**Figures 3–5**). Measures of α-diversity indicated that both richness and evenness were lower in COME patients with asthma or bronchiolitis. Although α-diversity of the lower respiratory tract has been shown to be higher (Huang et al., 2011; Marri et al., 2013) or unchanged (Goleva et al., 2013) in asthma patients, Castro-Nallar et al. (2015) showed decreased α-diversity in the nasal cavities of asthma patients compared to healthy patients. Decreased α-diversity has also been observed in microbiome profiles associated with increased risk of bronchiolitis (Hasegawa et al., 2017). Therefore, it is possible that the upper and lower respiratory tracts exhibit distinct trends in asthma patients, with decreased α-diversity in the upper respiratory tract extending to the middle ear and increased α-diversity in the lower respiratory tract. This would lend credence to the theory of a unified airway, which suggests that upper and lower airway disease share a pathophysiologic origin, being induced by a commonality in allergic or non-allergic reproducible mechanisms (Giavina-Bianchi et al., 2016). To this point, it is noteworthy that in patients with an allergic asthmatic etiology, a parallel type of allergic inflammatory response is noted in the middle ear (Nguyen et al., 2004). Moreover, patients with asthma are well-known to present with comorbid conditions which contribute to respiratory symptoms, including allergic rhinitis and chronic rhinosinusitis. Epidemiological and pathophysiological links have been described between these conditions (Massoth et al., 2019). This study's microbiome data builds on this point, suggesting an association between asthma and otitis media. However, due to potential bias between different methodologies, further work using paired samples would be necessary to confirm this hypothesis.

Using the weighted UniFrac distance method, we observed significant differences in β-diversity based on two clinical variables: significant hearing loss and asthma/bronchiolitis diagnosis (**Figure 4**). The association with significant hearing loss was previously observed in Krueger et al. (2017) and was also confirmed here with the present methods; however, the relationship with lower airway disease status was not

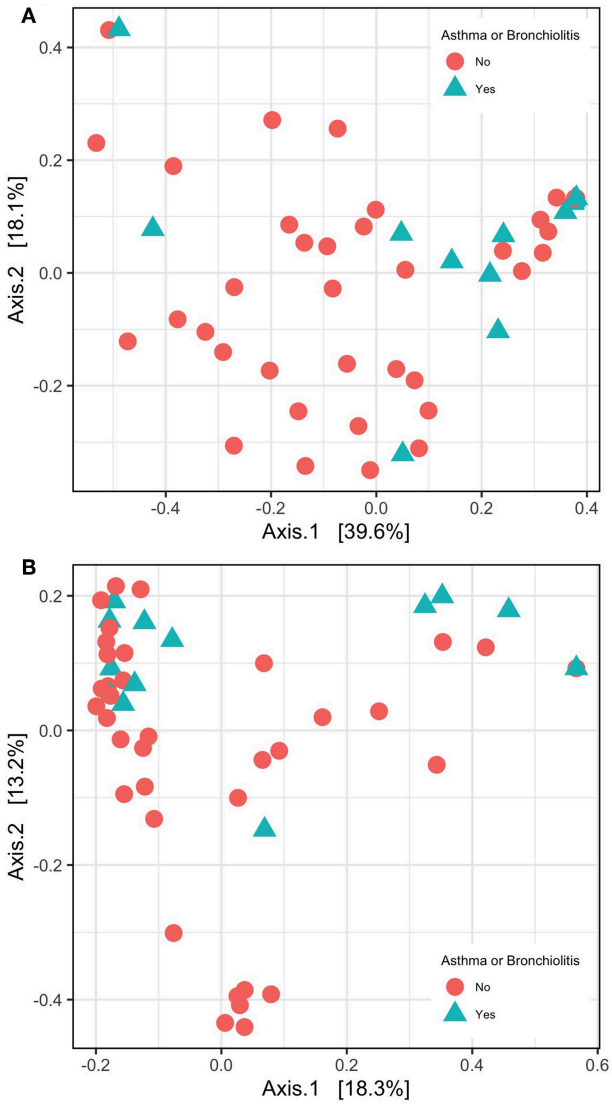

FIGURE 4 | β-diversity shown with principle coordinate analysis of weighted UniFrac distances **(A)** and unweighted UniFrac distance **(B)**.

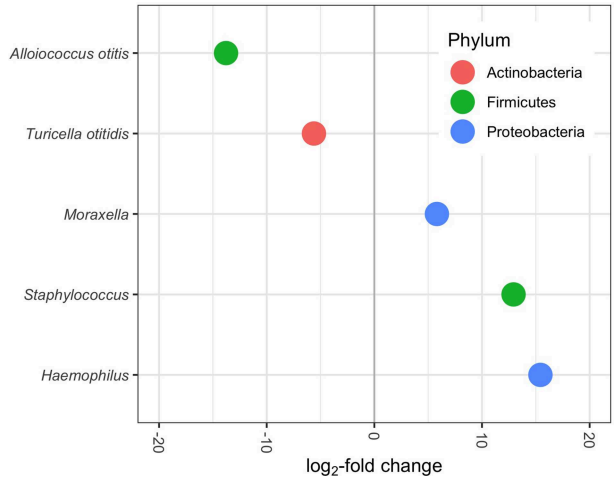

FIGURE 5 | Differentially abundant genera/species (*p-adjusted* < 0.05) in MEF of patients with lower airway disease diagnosis. Positive log_2-fold change indicates increased abundance in patients with asthma or bronchiolitis; negative log_2-fold change indicates decreased abundance. Each dot represents one ASV.

previously tested. In contrast to other β-diversity methods, UniFrac distances take into account the phylogenetic distance between ASVs. The weighted UniFrac distance additionally considers the abundance of ASVs, whereas the unweighted UniFrac only considers presence/absence (Lozupone et al., 2007). Interestingly, the unweighted UniFrac distance was not significant for any of these three variables. This indicates that similar patterns of presence/absence were evident but ASV abundance varied between patients with asthma/bronchiolitis and significant hearing loss.

Differential abundance analysis with DESeq2 (Love et al., 2014) indicated that four of the five most abundant genera, *Haemophilus, Turicella*, *Alloiococcus*, and *Moraxella,* were differentially abundant between patients with and without asthma/bronchiolitis (**Figure 5**). *Staphylococcus* was also significantly higher in patients with lower airway disease. These results highlight a potentially significant difference in the microbiome of COME patients with asthma or bronchiolitis. Both *Haemophilus* and *Moraxella* have been studied extensively in the asthma and bronchiolitis-related microbiome (Hilty et al., 2010; Vissing et al., 2013; Castro-Nallar et al., 2015; Pérez-Losada et al., 2015, 2017, 2018; Hasegawa et al., 2016; Mansbach et al., 2016); therefore, it is particularly interesting that these genera were found in greater abundance in asthma patients with COME. Early airway colonization with *Haemophilus* and *Moraxella* has been associated with asthma or bronchiolitis development later in childhood (Bisgaard et al., 2007; Vissing et al., 2013), and both have been found in higher abundance in patients with asthma or bronchiolitis (Hilty et al., 2010; Vissing et al., 2013; Castro-Nallar et al., 2015). *Staphylococcus*-dominated airway microbiomes has also been associated with an increased risk of bronchiolitis (Hasegawa et al., 2017). In contrast, *Turicella otiditis* and *Alloiococcus otitis* have been isolated almost exclusively from the human ear and have frequently been attributed to OM (Tano et al., 2008; von Graevenitz and Funke, 2014; Boers et al., 2018). The absence of these species from other parts of the upper respiratory tract has led to a debate about whether they are OM pathogens or part of commensal microbiota. However, it is striking that pathogens associated with asthma and bronchiolitis are increased in COME with lower airway disease, whereas pathogens typically associated with OM are decreased. These results suggest a potential link between the microbiome of the respiratory tract in children with lower airway disease and the microbiome associated with COME. Alternatively, the different microbial communities in patients with comorbid respiratory illnesses could be reflective of disease severity and increased pathogen load in the middle ear. In this study, significant hearing loss served as a proxy for symptom severity and was

included in models for differential abundance in DESeq2. It is also possible that medications commonly prescribed for patients with lower airway disease such as corticosteroids could influence the microbiota present in both the lower and upper airways. Denner et al. (2016) showed that corticoid steroid use affects microbiome composition in the lower airways; however, it is not currently known whether this effect would extend to the upper airways. Future work should consider additional metrics of disease severity as well as medication use when evaluating this potential link between the middle ear and respiratory illnesses.

A large body of work suggests a link between atopic disease and OM, and particularly COME. These associated atopic diseases include allergic rhinitis (Alles et al., 2001; Kreiner-Moller et al., 2012; Roditi et al., 2016), eczema (MacIntyre et al., 2010), and asthma (Gamble et al., 1992; Eldeirawi et al., 2010; MacIntyre et al., 2010; Bjur et al., 2012), but the same associations are not always reproduced between studies, leading to significant debate about the nature of these associations (Zernotti et al., 2017). Gamble et al. (1992) hypothesized that COME in asthmatics is not an isolated disease, but instead represents an atopic disease affecting the mucociliary system of entire respiratory tract. Similarly, inflammation from bronchiolitis could result in impaired mucociliary clearance and make the middle ear more susceptible to pathogens. The interesting decrease in specific ear-trophic OM pathogens (*Alloiococcus* and *Turicella*) accompanied by an increase in asthma- and bronchiolitis-associated pathogens (*Haemophilus, Moraxella, Staphylococcus*) in asthma and bronchiolitis patients supports the theory that respiratory disease-associated COME may have a distinct etiology than COME in children without respiratory illnesses (Gamble et al., 1992; Zernotti et al., 2017). Although the directionality of this relationship is unknown, our findings show that COME in children with lower airway disease is characterized by a distinct microbiome, which may also explain the higher frequency of COME complications such as mucoid effusion and COME recurrence observed in asthma patients (Gamble et al., 1992). The relationship between these diseases and their respective microbiomes should be further investigated in future work.

CONCLUSIONS

In this study, we performed a detailed characterization of the composition and function of the middle ear microbiome in children with COME. Using an ASV pipeline, we achieved greater resolution at the species and genus levels than using OTUs. Taxonomic profiles varied significantly between children, while microbiome function was remarkably similar across all patients. Furthermore, we identified significant differences in the middle ear microbiome associated with a lower airway disease diagnosis, including α- and β-diversity and relative abundance of *Haemophilus, Moraxella, Staphylococcus, Alloiococcus,* and *Turicella.* These results provide novel evidence linking the microbiome of respiratory illnesses with COME and warrant additional work on the link between these important childhood diseases.

DATA AVAILABILITY STATEMENT

Raw data files are available in the NCBI SRA under accession PRJNA555884.

ETHICS STATEMENT

The studies involving human participants were reviewed and approved by Institutional Review Board, Children's National Health System. Written informed consent to participate in this study was provided by the participants' legal guardian/next of kin.

AUTHOR CONTRIBUTIONS

AK, EC-N, DP, and MP-L conceived and designed this study. AK analyzed the data and wrote the manuscript with contributions of all the authors. All authors read and approved this manuscript.

FUNDING

This study was partially funded the Milken Institute School of Public Health Pilot Fund Program, the Margaret Q. Landenberger Research Foundation and the Fundação para a Ciência e a Tegnologia (T495756868-00032862).

SUPPLEMENTARY MATERIAL

The Supplementary Material for this article can be found online at: https://www.frontiersin.org/articles/10.3389/fcimb.2019.00339/full#supplementary-material

REFERENCES

Alles, R., Parikh, A., Hawk, L., Darby, Y., Romer, J. N., and Scadding, G. (2001). The prevalence of atopic disorders in children with chronic otitis media with effusion. *Pediatr. Allergy Immunol.* 12, 102–106. doi: 10.1046/j.0905-6157.2000.00008.x

Andrade, M. A., Hoberman, A., Glustein, J., Paradise, J. L., and Wald, E. R. (1998). Acute otitis media in children with bronchiolitis. *Pedatrics.* 101, 617–619. doi: 10.1542/peds.101.4.617

Barbera, P., Kozlov, A., Czech, L., Morel, B., Darriba, D., Flouri, T., et al. (2019). EPA-ng: massively parallel evolutionary placement of genetic sequences. *Syst. Biol.* 68, 365–369. doi: 10.1093/sysbio/syy054

Bisgaard, H., Northman Hermansen, M., Buchvald, F., Loland, L., Brydensholt Halkjaer, L., Bonnelykke, K., et al. (2007). Childhood asthma after bacterial colonization of the airway in neonates. *N. Engl. J. Med.* 357, 1487–1495. doi: 10.1056/NEJMoa052632

Bjur, K. A., Lynch, R. L., Fenta, Y. A., Yoo, K. H., Jacobson, R. M., Li, X., et al. (2012). Assessment of the association between atopic conditions and tympanostomy tube placement in children. *Allergy Asthma Proc.* 33, 289–296. doi: 10.2500/aap.2012.33.3529

Boers, S. A., de Zeeuw, M., Jansen, R., van der Schroeff, M. P., van Rossum, A. M. C., Hays, J. P., et al. (2018). Characterization of the nasopharyngeal and middle ear microbiota in gastroesophageal reflux-prone versus gastroesophageal reflux non-prone children. *Eur. J. Clin. Microbiol. Infect. Dis.* 37, 851–857. doi: 10.1007/s10096-017-3178-2

Brooke, J. S. (2012). *Stenotrophomonas maltophilia*: an emerging global opportunistic pathogen. *Clin. Microbiol. Rev.* 25, 2–41. doi: 10.1128/CMR.00019-11

Callahan, B. J. (2018). *Silva Taxonomic Training Data Formatted for DADA2*. Silva version 132. doi: 10.5281/zenodo.1172783

Callahan, B. J., McMurdie, P. J., and Holmes, S. P. (2017). Exact sequence variants should replace operational taxonomic units in marker-gene data analysis. *ISME J.* 11, 2639–2643. doi: 10.1038/ismej.2017.119

Callahan, B. J., McMurdie, P. J., Rosen, M. J., Han, A. W., Johnson, A. J., and Holmes, S. P. (2016). DADA2: high-resolution sample inference from Illumina amplicon data. *Nat. Methods* 13, 581–583. doi: 10.1038/nmeth.3869

Callahan, B. J., Wong, J., Heiner, C., Oh, S., Theriot, C. M., Gulati, A. S., et al. (2019). High-throughput amplicon sequencing of the full-length 16S rRNA gene with single-nucleotide resolution. *Nucleic Acids Res.* 47:e103. doi: 10.1093/nar/gkz569

Caruso, V., Song, X., Asquith, M., and Karstens, L. (2019). Performance of microbiome sequence inference methods in environments with varying biomass. *mSystems* 4:e00163–18. doi: 10.1128/mSystems.00163-18

Castro-Nallar, E., Shen, Y., Freishtat, R. J., Perez-Losada, M., Manimaran, S., Liu, G., et al. (2015). Integrating microbial and host transcriptomics to characterize asthma-associated microbial communities. *BMC Med Genomics* 8:50. doi: 10.1186/s12920-015-0121-1

Chan, C. L., Wabnitz, D., Bardy, J. J., Bassiouni, A., Wormald, P. J., Vreugde, S., et al. (2016). The microbiome of otitis media with effusion. *Laryngoscope* 126, 2844–2851. doi: 10.1002/lary.26128

Czech, L., and Stamatakis, A. (2019). Scalable methods for analyzing and visualizing phylogenetic placement of metagenomic samples. *PLoS ONE* 14:e0217050. doi: 10.1371/journal.pone.0217050

Denner, D. R., Sangwan, N., Becker, J. B., Hogarth, D. K., Oldham, J., Castillo, J., et al. (2016). Corticosteroid therapy and airflow obstruction influence the bronchial microbiome, which is distinct from that of bronchoalveolar lavage in asthmatic airways. *J. Allergy Clin. Immunol.* 137, 1398–1405 e1393. doi: 10.1016/j.jaci.2015.10.017

Douglas, G. M., Maffei, V. J., Zaneveld, J., Yurgel, S. N., Brown, J. R., Taylor, C. M., et al. (2019). PICRUSt2: an improved and extensible approach for metagenome inference. *bioRxiv*. doi: 10.1101/672295

Edgar, R. C. (2018). Updating the 97% identity threshold for 16S ribosomal RNA OTUs. *Bioinformatics* 34, 2371–2375. doi: 10.1093/bioinformatics/bty113

Eldeirawi, K., McConnell, R., Furner, S., Freels, S., Stayner, L., Hernandez, E., et al. (2010). Frequent ear infections in infancy and the risk of asthma in Mexican American children. *J. Asthma* 47, 473–477. doi: 10.3109/02770901003759428

Gamble, J. E., Bizal, J. A., and Daetwyler, E. P. (1992). Otitis media and chronic middle ear effusion in the asthmatic pediatric patient. *Ear Nose Throat J.* 71, 397–399. doi: 10.1177/014556139207100908

Giavina-Bianchi, P., Aun, M. V., Takejima, P., Kalil, J., and Agondi, R. C. (2016). United airway disease: current perspectives. *J. Asthma Allergy* 9, 93–100. doi: 10.2147/JAA.S81541

Goleva, E., Jackson, L. P., Harris, J. K., Robertson, C. E., Sutherland, E. R., Hall, C. F., et al. (2013). The effects of airway microbiome on corticosteroid responsiveness in asthma. *Am. J. Respir. Crit. Care Med.* 188, 1193–1201. doi: 10.1164/rccm.201304-0775OC

Gomaa, M. A., Galal, O., and Mahmoud, M. S. (2012). Risk of acute otitis media in relation to acute bronchiolitis in children. *Int. J. Pediatr. Otorhinolaryngol.* 76, 49–51. doi: 10.1016/j.ijporl.2011.09.029

Greenblum, S., Turnbaugh, P. J., and Borenstein, E. (2012). Metagenomic systems biology of the human gut microbiome reveals topological shifts associated with obesity and inflammatory bowel disease. *Proc. Natl. Acad. Sci. U.S.A.* 109, 594–599. doi: 10.1073/pnas.1116053109

Guvenc, M. G., Midilli, K., Inci, E., Kuskucu, M., Tahamiler, R., Ozergil, E., et al. (2010). Lack of *Chlamydophila pneumoniae* and predominance of *Alloiococcus otitidis* in middle ear fluids of children with otitis media with effusion. *Auris Nasus Larynx* 37, 269–273. doi: 10.1016/j.anl.2009.09.002

Harimaya, A., Takada, R., Hendolin, P. H., Fujii, N., Ylikoski, J., and Himi, T. (2006). High incidence of *Alloiococcus otitidis* in children with otitis media, despite treatment with antibiotics. *J. Clin. Microbiol.* 44, 946–949. doi: 10.1128/JCM.44.3.946-949.2006

Hasegawa, K., Linnemann, R. W., Mansbach, J. M., Ajami, N. J., Espinola, J. A., Petrosino, J. F., et al. (2017). Nasal airway microbiota profile and severe bronchiolitis in infants: a case-control study. *Pediatr. Infect. Dis. J.* 36, 1044–1051. doi: 10.1097/INF.0000000000001500

Hasegawa, K., Mansbach, J. M., Ajami, N. J., Espinola, J. A., Henke, D. M., Petrosino, J. F., et al. (2016). Association of nasopharyngeal microbiota profiles with bronchiolitis severity in infants hospitalised for bronchiolitis. *Eur. Respir. J.* 48, 1329–1339. doi: 10.1183/13993003.00152-2016

Hilty, M., Burke, C., Pedro, H., Cardenas, P., Bush, A., Bossley, C., et al. (2010). Disordered microbial communities in asthmatic airways. *PLoS ONE* 5:e8578. doi: 10.1371/journal.pone.0008578

Howard Hughes Medical Institute (2018). *HMMER 3.2.1*. Available online at: www.hmmer.org (accessed July 8, 2019).

Huang, Y. J., Nelson, C. E., Brodie, E. L., Desantis, T. Z., Baek, M. S., Liu, J., et al. (2011). Airway microbiota and bronchial hyperresponsiveness in patients with suboptimally controlled asthma. *J. Allergy Clin. Immunol.* 127, 372–381 e371–373. doi: 10.1016/j.jaci.2010.10.048

Human Microbiome Project, C. (2012). Structure, function and diversity of the healthy human microbiome. *Nature* 486, 207–214. doi: 10.1038/nature11234

Jervis-Bardy, J., Rogers, G. B., Morris, P. S., Smith-Vaughan, H. C., Nosworthy, E., Leong, L. E., et al. (2015). The microbiome of otitis media with effusion in Indigenous Australian children. *Int. J. Pediatr. Otorhinolaryngol.* 79, 1548–1555. doi: 10.1016/j.ijporl.2015.07.013

Jette, M. E., Dill-McFarland, K. A., Hanshew, A. S., Suen, G., and Thibeault, S. L. (2016). The human laryngeal microbiome: effects of cigarette smoke and reflux. *Sci. Rep.* 6:35882. doi: 10.1038/srep35882

Kalcioglu, M. T., Guldemir, D., Unaldi, O., Egilmez, O. K., Celebi, B., and Durmaz, R. (2018). Metagenomics analysis of bacterial population of tympanosclerotic plaques and cholesteatomas. *Otolaryngol. Head Neck Surg.* 159, 724–732. doi: 10.1177/0194599818772039

Katoh, K., and Standley, D. M. (2013). MAFFT multiple sequence alignment software version 7: improvements in performance and usability. *Mol. Biol. Evol.* 30, 772–780. doi: 10.1093/molbev/mst010

Kim, S. J., Cho, H., Ahn, J. H., Weon, H. Y., Seok, S. J., Kim, J. S., et al. (2016). Pseudoflavitalea rhizosphaerae gen. nov., sp. nov., isolated from rhizosphere of tomato, and proposal to reclassify *Flavitalea soli* as Pseudoflavitalea soli comb. *nov. Int. J. Syst. Evol. Microbiol.* 66, 4167–4171. doi: 10.1099/ijsem.0.001330

Knight, R., Vrbanac, A., Taylor, B. C., Aksenov, A., Callewaert, C., Debelius, J., et al. (2018). Best practices for analysing microbiomes. *Nat. Rev. Microbiol.* 16, 410–422. doi: 10.1038/s41579-018-0029-9

Kozich, J. J., Westcott, S. L., Baxter, N. T., Highlander, S. K., and Schloss, P. D. (2013). Development of a dual-index sequencing strategy and curation pipeline for analyzing amplicon sequence data on the MiSeq Illumina sequencing platform. *Appl. Environ. Microbiol.* 79, 5112–5120. doi: 10.1128/AEM.01043-13

Kozik, A. J., and Huang, Y. J. (2018). The microbiome in asthma: role in pathogenesis, phenotype, and response to treatment. *Ann. Allergy Asthma Immunol.* 122, 270–275. doi: 10.1016/j.anai.2018.12.005.

Kreiner-Moller, E., Chawes, B. L., Caye-Thomasen, P., Bonnelykke, K., and Bisgaard, H. (2012). Allergic rhinitis is associated with otitis media with effusion: a birth cohort study. *Clin. Exp. Allergy* 42, 1615–1620. doi: 10.1111/j.1365-2222.2012.04038.x

Krueger, A., Val, S., Perez-Losada, M., Panchapakesan, K., Devaney, J., Duah, V., et al. (2017). Relationship of the middle ear effusion microbiome to secretory mucin production in pediatric patients with chronic otitis media. *Pediatr. Infect. Dis. J.* 36, 635–640. doi: 10.1097/INF.0000000000001493

Lappan, R., Imbrogno, K., Sikazwe, C., Anderson, D., Mok, D., Coates, H., et al. (2018). A microbiome case-control study of recurrent acute otitis media identified potentially protective bacterial genera. *BMC Microbiol.* 18:13. doi: 10.1186/s12866-018-1154-3

Louca, S., and Doebeli, M. (2018). Efficient comparative phylogenetics on large trees. *Bioinformatics* 34, 1053–1055. doi: 10.1093/bioinformatics/btx701

Louca, S., Polz, M. F., Mazel, F., Albright, M. B. N., Huber, J. A., O'Connor, M. I., et al. (2018). Function and functional redundancy in microbial systems. *Nat. Ecol. Evol.* 2, 936–943. doi: 10.1038/s41559-018-0519-1

Love, M. I., Huber, W., and Anders, S. (2014). Moderated estimation of fold change and dispersion for RNA-seq data with DESeq2. *Genome Biol.* 15:550. doi: 10.1186/s13059-014-0550-8

Lozupone, C. A., Hamady, M., Kelley, S. T., and Knight, R. (2007). Quantitative and qualitative beta diversity measures lead to different insights into factors that structure microbial communities. *Appl. Environ. Microbiol.* 73, 1576–1585. doi: 10.1128/AEM.01996-06

Luong, A., and Roland, P. S. (2008). The link between allergic rhinitis and chronic otitis media with effusion in atopic patients. *Otolaryngol. Clin. North. Am.* 41, 311–323, vi. doi: 10.1016/j.otc.2007.11.004

MacIntyre, E. A., Chen, C.-M., Herbarth, O., Borte, M., Schaaf, B., Krämer, U., et al. (2010). Early-life otitis media and incident atopic disease at school age in a birth Cohort. *Pediatr. Infect. Dis. J.* 29, e96–e99. doi: 10.1097/INF.0b013e3181fcd9e8

MacIntyre, E. A., and Heinrich, J. (2012). Otitis media in infancy and the development of asthma and atopic disease. *Curr. Allergy Asthma Rep.* 12, 547–550. doi: 10.1007/s11882-012-0308-x

Mansbach, J. M., Hasegawa, K., Henke, D. M., Ajami, N. J., Petrosino, J. F., Shaw, C. A., et al. (2016). Respiratory syncytial virus and rhinovirus severe bronchiolitis are associated with distinct nasopharyngeal microbiota. *J. Allergy Clin. Immunol.* 137, 1909–1913 e1904. doi: 10.1016/j.jaci.2016.01.036

Marri, P. R., Stern, D. A., Wright, A. L., Billheimer, D., and Martinez, F. D. (2013). Asthma-associated differences in microbial composition of induced sputum. *J. Allergy Clin. Immunol.* 131, 346-352 e341–343. doi: 10.1016/j.jaci.2012.11.013

Massoth, L., Anderson, C., and McKinney, K. A. (2019). Asthma and chronic rhinosinusitis: diagnosis and medical management. *Med. Sci.* 7:E53. doi: 10.3390/medsci7040053

McMurdie, P. J., and Holmes, S. (2013). phyloseq: an R package for reproducible interactive analysis and graphics of microbiome census data. *PLoS ONE* 8:e61217. doi: 10.1371/journal.pone.0061217

McNally, C. P., Eng, A., Noecker, C., Gagne-Maynard, W. C., and Borenstein, E. (2018). BURRITO: an interactive multi-omic tool for visualizing taxa-function relationships in microbiome data. *Front. Microbiol.* 9:365. doi: 10.3389/fmicb.2018.00365

Minovi, A., and Dazert, S. (2014). Diseases of the middle ear in childhood. *GMS Curr. Top. Otorhinolaryngol. Head Neck Surg.* 13:Doc11. doi: 10.3205/cto000114

Monasta, L., Ronfani, L., Marchetti, F., Montico, M., Brumatti, L., Bavcar, A., et al. (2012). Burden of disease caused by otitis media: systematic review and global estimates. *PLoS ONE* 7:e36226. doi: 10.1371/journal.pone.0036226

Morgan, X. C., Tickle, T. L., Sokol, H., Gevers, D., Devaney, K. L., Ward, D. V., et al. (2012). Dysfunction of the intestinal microbiome in inflammatory bowel disease and treatment. *Genome Biol.* 13:R79. doi: 10.1186/gb-2012-13-9-r79

Nguyen, L. H., Manoukian, J. J., Sobol, S. E., Tewfik, T. L., Mazer, B. D., Schloss, M. D., et al. (2004). Similar allergic inflammation in the middle ear and the upper airway: evidence linking otitis media with effusion to the united airways concept. *J. Allergy Clin. Immunol.* 114, 1110–1115. doi: 10.1016/j.jaci.2004.07.061

Oksanen, J., Blanchet, F. G., Friendly, M., Kindt, R., Legendre, P., McGlinn, D., et al. (2019). "*vegan: Community Ecology Package*". *R Package Version* 2.5–5. Available online at: https://CRAN.R-project.org/package=vegan

Parks, D. H., Tyson, G. W., Hugenholtz, P., and Beiko, R. G. (2014). STAMP: statistical analysis of taxonomic and functional profiles. *Bioinformatics* 30, 3123–3124. doi: 10.1093/bioinformatics/btu494

Pérez-Losada, M., Alamri, L., Crandall, K. A., and Freishtat, R. J. (2017). Nasopharyngeal microbiome diversity changes over time in children with asthma. *PLoS ONE* 12:e0170543. doi: 10.1371/journal.pone.0170543

Pérez-Losada, M., Authelet, K. J., Hoptay, C. E., Kwak, C., Crandall, K. A., and Freishtat, R. J. (2018). Pediatric asthma comprises different phenotypic clusters with unique nasal microbiotas. *Microbiome* 6:179. doi: 10.1186/s40168-018-0564-7

Pérez-Losada, M., Castro-Nallar, E., Bendall, M. L., Freishtat, R. J., and Crandall, K. A. (2015). Dual transcriptomic profiling of host and microbiota during health and disease in pediatric asthma. *PLoS ONE* 10:e0131819. doi: 10.1371/journal.pone.0131819

Price, M. N., Dehal, P. S., and Arkin, A. P. (2010). FastTree 2 - approximately maximum-likelihood trees for large alignments. *PLoS ONE* 5:e9490. doi: 10.1371/journal.pone.0009490

Quast, C., Pruesse, E., Yilmaz, P., Gerken, J., Schweer, T., Yarza, P., et al. (2013). The SILVA ribosomal RNA gene database project: improved data processing and web-based tools. *Nucleic Acids Res.* 41, D590–596. doi: 10.1093/nar/gks1219

Qureishi, A., Lee, Y., Belfield, K., Birchall, J. P., and Daniel, M. (2014). Update on otitis media - prevention and treatment. *Infect. Drug Resist.* 7, 15–24. doi: 10.2147/IDR.S39637

R Core Team (2019). "*R: A Language and Environment for Statistical Computing*" (Vienna).

Roditi, R. E., Veling, M., and Shin, J. J. (2016). Age: An effect modifier of the association between allergic rhinitis and otitis media with effusion. *Laryngoscope* 126, 1687–1692. doi: 10.1002/lary.25682

Swenson, C. E., and Sadikot, R. T. (2015). *Achromobacter* respiratory infections. *Ann. Am. Thorac. Soc.* 12, 252–258. doi: 10.1513/AnnalsATS.201406-288FR

Tano, K., von Essen, R., Eriksson, P.-O., and Sjöstedt, A. (2008). *Alloiococcus otitidis* - otitis media pathogen or normal bacterial flora? *APMIS* 116, 785–790. doi: 10.1111/j.1600-0463.2008.01003.x

Vissing, N. H., Chawes, B. L., and Bisgaard, H. (2013). Increased risk of pneumonia and bronchiolitis after bacterial colonization of the airways as neonates. *Am. J. Respir. Crit. Care Med.* 188, 1246–1252. doi: 10.1164/rccm.201302-0215OC

von Graevenitz, A., and Funke, G. (2014). *Turicella otitidis* and *Corynebacterium auris*: 20 years on. *Infection.* 42, 1–4. doi: 10.1007/s15010-013-0488-x

Wickham, H. (2016). *ggplot2: Elegant Graphics for Data Analysis.* New York, NY: Springer-Verlag. doi: 10.1007/978-3-319-24277-4

Williams, C. J., and Jacobs, A. M. (2009). The impact of otitis media on cognitive and educational outcomes. *Med. J. Austr.* 191, S69–S72. doi: 10.5694/j.1326-5377.2009.tb02931.x

Xue, Z., Kable, M. E., and Marco, M. L. (2018). Impact of DNA sequencing and analysis methods on 16S rRNA gene bacterial community analysis of dairy products. *mSphere* 3, e00410–00418. doi: 10.1128/mSphere.00410-18

Yabuuchi, E., and Ohyama, A. (1971). Achromobacter xylosoxidans n. sp. from human ear discharge. *Japan. J. Microbiol.* 15, 477–481. doi: 10.1111/j.1348-0421.1971.tb00607.x

Ye, Y., and Doak, T. G. (2009). A parsimony approach to biological pathway reconstruction/inference for genomes and metagenomes. *PLoS Comput. Biol.* 5:e1000465. doi: 10.1371/journal.pcbi.1000465

Zernotti, M. E., Pawankar, R., Ansotegui, I., Badellino, H., Croce, J. S., Hossny, E., et al. (2017). Otitis media with effusion and atopy: is there a causal relationship? *World Allergy Organ. J.* 10:37. doi: 10.1186/s40413-017-0168-x

Conflict of Interest: The authors declare that the research was conducted in the absence of any commercial or financial relationships that could be construed as a potential conflict of interest.

frontiers in Genetics

BRIEF RESEARCH REPORT
published: 19 November 2019
doi: 10.3389/fgene.2019.01176

Comparative Analysis of Microbiome in Nasopharynx and Middle Ear in Young Children With Acute Otitis Media

Qingfu Xu[1†], Steve Gill[2], Lei Xu[1], Eduardo Gonzalez[1] and Michael E. Pichichero[1]*

[1] Center for Infectious Disease and Immunology, Rochester General Hospital Research Institute, Rochester, NY, United States,
[2] Department of Microbiology and Immunology, University of Rochester Medical Center, Rochester, NY, United States

OPEN ACCESS

Edited by:
Garth D. Ehrlich,
Drexel University,
United States

Reviewed by:
Prithvi Raj,
UT Southwestern Medical Center,
United States
Tal Marom,
Assuta Ashdod University Hospital,
Israel

***Correspondence:**
Michael E. Pichichero
Michael.Pichichero@rochesterregional.org

†Present address:
Qingfu Xu,
Cantel Medical, Rush, NY,
United States

Specialty section:
This article was submitted to Genetic Disorders, a section of the journal Frontiers in Genetics

Received: 16 July 2019
Accepted: 24 October 2019
Published: 19 November 2019

Citation:
Xu Q, Gill S, Xu L, Gonzalez E and Pichichero ME (2019) Comparative Analysis of Microbiome in Nasopharynx and Middle Ear in Young Children With Acute Otitis Media. Front. Genet. 10:1176. doi: 10.3389/fgene.2019.01176

Acute otitis media (AOM) is the most common pediatric infection for which antibiotics are prescribed in the United States. The role of the respiratory tract microbiome in pathogenesis and immune modulation of AOM remains unexplored. We sought to compare the nasopharyngeal (NP) microbiome of children 1 to 3 weeks prior to onset of AOM vs. at onset of AOM, and the NP microbiome with the microbiome in middle ear (ME). Six children age 6 to 24 months old were studied. Nasal washes (NW) were collected at healthy visits 1 to 3 weeks prior to AOM and at onset of AOM. The middle ear fluids (MEF) were collected by tympanocentesis at onset of AOM. Samples were stored in Trizol reagents or phosphate-buffered saline (PBS) at –80°C until use. The microbiome was characterized by 16S rRNA gene sequencing. Taxonomic designations and relative abundance of bacteria were determined using the RDP classifier tool through QIIME. Cumulative sum scaling normalization was applied before determining bacterial diversity and abundance. Shannon diversity index was calculated in Microsoft excel. The relative abundance of each bacteria species was compared *via* Mann-Whitney *U* test. We found that the NW microbiome of children during healthy state or at baseline was more diverse than microbiome during AOM. At AOM, no significant difference in microbiome diversity was found between NW and MEF, although some bacteria species appear to differ in MEF than in NW. The microbiome of samples stored in PBS had significant greater diversity than samples stored in Trizol reagent.

Keywords: nasopharyngeal microbiome, middle ear microbiome, acute otitis media, 16S rRNA, Shannon Diversity, sample storage

INTRODUCTION

Acute otitis media (AOM) is one of the most common bacterial infections in children for which antibiotics are prescribed in the United States of America (Vergison et al., 2010; Monasta et al., 2012). The three major bacterial pathogens *Streptococcus pneumoniae*, *Haemophilus influenzae*, and *Moraxella catarrhalis* are among hundreds species of commensal microbiomes in the respiratory tract. Current prevention and treatment options are being continuously eroded by emergence of new otopathogen strains (Pettigrew et al., 2012). It is estimated that each year, more than 5 million AOM cases occur in the US (Monasta et al., 2012; Suaya et al., 2018). The annual total cost is about $6 billion in the US for health care of OM including $3 billion to 4 billion in direct costs

for treatment of OM, and the most frequent surgery in children (after circumcision) involving insertion of tympanostomy tubes (Nsouli 2019).

Nasopharyngeal (NP) colonization by potential bacterial respiratory pathogens is a frequent event in early childhood, and initial, necessary step in pathogenesis of respiratory bacterial infectious diseases such as AOM, conjunctivitis, sinusitis, chronic obstructive pulmonary disease, and pneumonia in children (Bogaert et al., 2004; Libson et al., 2005; Syrjanen et al., 2005; Revai et al., 2008; Littman and Pamer 2011; Chonmaitree et al., 2017). Previous studies have shown that the microbiome plays an important role in modulating immune homeostasis and disease susceptibility (Duan et al., 2003; Kuss et al., 2011; Littman and Pamer 2011). A large portion of this research has focused on the gut microbiome and susceptibility to enteric pathogens (Sekirov et al., 2008; Kuss et al., 2011). The role of the respiratory tract microbiome in pathogenesis and immune modulation of AOM remain unexplored. Middle ear (ME) microbiome has been reported in chronic otitis media (Santos-Cortez et al., 2016; Krueger et al., 2017; Boers et al., 2018; Johnston et al., 2019), and NP microbiome is associated with pathogenesis of upper respiratory traction infection and AOM (Lappan et al., 2018). None of these studies investigate changes in NP microbiota during onset of AOM. Here we sought to compare the microbiome in nasal wash (NW) of children 2 to 3 weeks prior to their onset of AOM (but otherwise healthy) versus those same children at onset of AOM, and compare their NW microbiome with ME microbiome during AOM.

MATERIALS AND METHODS

Study Cohorts and Samples

The NW and middle ear fluid (MEF) samples were previously collected under a US National Institutes of Health-funded study of AOM. The study design and sample collections have been described in previous publications (Xu et al., 2012; Pichichero 2016). Briefly, healthy infants without previous episodes of AOM were enrolled at 6 months of age and NW samples were prospectively collected at 6, 9, 12, 15, 18, 24, and 30 to 36 months of age. Whenever the children were diagnosed with AOM, tympanocentesis was performed on the same day. MEF samples were handled aseptically and kept on ice during transport to the lab, where it was processed immediately to confirm the diagnosis with microbiologic culture for otopathogens. The study was approved by the Institutional Review Board of Rochester General Hospital, and written informed consent was obtained from parents or guardians of all children. Samples were either directly stored in 1 ml phosphate-buffered saline (PBS) at −80°C, or centrifuged at 3,000 rpm for 10 min at 4°C, after which the pellets were stored in 1 ml of Trizol reagents (Sigma) at −80°C until use for microbiome analyses.

16S rRNA Gene Sequencing Analysis

Bacteria DNA Extraction: Bacterial ribonucleotides from NP and MEF were extracted by FastPrep bead beating lysis in TRI Reagent (Ambion) and purified on a Zymo-Spin™ IC column (Zymo). Integrity of the purified nucleotides was assessed on an Agilent BioAnalyzer. The V1–V3 region of bacterial 16S rRNA genes were amplified using dual-indexed coded primers (Fadrosh et al., 2014) and Phusion High-Fidelity Polymerase (Thermo Fisher). V1–V3 amplicons were purified and normalized using SequalPrep™ Normalization plates (Life Technologies), pooled, and validated on an Agilent BioAnalyzer. The final library was paired-end sequenced (2 × 300 bp) on an Illumina MiSeq. The individual amplicons were pooled for sequencing. This approach routinely yields high quality sequence data, with ~40 K reads per sample and assembly of 550 bp overlapping amplicons from the paired-end reads for each sample. This depth of sequencing coverage results in a high likelihood of identifying rare taxa.

To minimize the variations from sample processing, both DNA extraction and 16S rRNA gene sequencing analysis were simultaneously performed for all the samples.

Processing of 16S rRNA Sequence Reads: Raw data in the form of BCL files were processed into 2x300 FASTQ format paired end read files using Illumina's bcl2fastq version 1.8.4 without demultiplexing and with the EAMMS algorithm disabled. After preprocessing, the open source software package, Quantitative Insights Into Microbial Ecology (QIIME) (Caporaso et al., 2010), was used to remove low quality sequences and chimeras and to perform bacterial community quantification, description, and analyses. Specifically, assembled 16S rRNA reads were truncated at the beginning of the first 30 base window with a mean Phred quality score of less than 20 or at the first ambiguous base, whichever came first. Sequences were aligned and then processed by complete linkage clustering using a maximum cluster distance cutoff of 3% (97% identity) to define operational taxonomic units (OTUs). These OTUs were used to calculate Shannon and evenness diversity indices (Lozupone et al., 2007; Lozupone and Knight 2008).

Taxonomic Description of the Respiratory Microbiome: Taxonomic designations of our sequences was done using the RDP classifier tool, which uses a naive Bayesian method for taxonomic assignment and can be accessed through QIIME (Wang et al., 2007; Caporaso et al., 2010). The taxonomic OTU proportion was used to describe the NP and ME microbiomes within our population. Rank abundance plots were made listing the most frequent taxonomic OTU's within NP and ME samples. We note OTUs that are present in a given stratum but absent or at low levels in other strata. The differences in the abundance of individual taxa of interest between samples grouped by outcomes were analyzed by Mann-Whitney *U* test.

Statistical Analysis

Shannon diversity index was calculated in Microsoft excel based on the equation $H = -\sum_i^n pi \ln(pi)$. which p_i is the portion of species i among the total population of n species in a sample. To minimize the discrepancy in data collection, only data from samples processed in Trizol were included in the comparison between healthy and AOM patients, in which three samples with the lowest DNA reads were excluded. Paired one-tailed *t* test was performed to measure the statistical significance between Shannon indexes using the GraphPad Prism software.

The relative abundance of taxa was compared between samples by Mann-Whitney *U* test.

RESULTS

Comparison of NP Microbiome at Onset of AOM and During Health Prior to AOM

From our sample inventory, we identified six cases of children with a diagnosed AOM who happened to have a prospective healthy visit without any symptoms of URI or AOM at 1 to 3 weeks prior to AOM. This enabled us to perform a self-case-control analysis of NP microbiome during health vs. at onset of AOM. The results are summarized in the **Table 1** and **Figures 1** and **2**. We found that the NP microbiome had significantly greater diversity during health than at onset of AOM (**Figure 1**). The genus whose abundance was >1% were 6 ± 3 (mean ± SE) in the NW during health, 3 ± 1 in the NW during AOM, and 3 ± 2 in the MEF during AOM (**Figure 2A** and **Table 1**). The most abundant microbiome at genus level were *Moraxella* (36.89%), *Streptococcus* (21.65%), *Haemophilus* (14.16%), *Corynebacterium* (11.31%), *Veillonella* (2.97%), and *Alloiococcus* (2.12%) in NW of healthy children; *Haemophilus* (51.01%), *Moraxella* (20.69%), *Streptococcus* (16.75%), *Corynebacterium* (7.43%), and *Alloiococcus* (2.24%) in NW of AOM children; and *Haemophilus* (74.05%), *Streptococcus* (18.43%), *Corynebacterium* (3.02%), and *Alloiococcus* (2.91%) in MEF of AOM children (**Table 1**). Mann-Whitney test was performed to identify the OTUs that differ statistically significantly between the NWs during health and the NWs during AOM. They were found to be *Rothia mucilaginosa*, *Streptococcus* sp., *Veillonella dispar*, and *Prevotella melaninogenica* (**Figure 2B** and **Table 2**). On the other hand, more OTUs differed significantly between NWs during health and MEFs during AOM. They included *Haemophilus* sp., *R. mucilaginosa*, *Streptococcus* sp., *V. dispar*, *P. melaninogenica*, *Porphyromonas* sp., *Granulicatella* sp., and *Alloiococcus* sp. (**Figure 2B** and **Table 2**).

Comparison of NP and Middle Ear Microbiome at Onset of AOM

We also compared NP microbiome and MEF microbiome in children at onset of AOM. There was no significant differences in microbiome diversity between NP and MEF samples ($p = 0.31$) (**Figure 1**). However, there appeared to be some difference at the level of individual OTUs. Specifically, *Veillonella* was reduced in the MEFs relative to NPs whereas *Alloiococcus otitidis* was increased (**Figure 2B** and **Table 2**).

Comparison of Differences in Microbiome Diversities of the Samples Processed With Different Methods

We have six children whose MEF samples were stored in Trizol reagents before microbiome analysis and five children whose MEF samples were stored in PBS before microbiome analysis. We found that samples stored in PBS had significant greater diversities than those stored in Trizol (Shannon index, **Supplementary Figure 1**).

DISCUSSION

The pathogenesis, development, severity, and clinical outcomes of AOM are largely dependent on the resident composition of the NP microbiome and immune defense and few studies have provided an understanding of how the NP microbiome and molecular immune responses might be manipulated to favor the child host (Melendi et al., 2007; Alper et al., 2009; Wine and Alper 2012). The NP is the main ecological niche of AOM pathogens and is the site of transmission for otopathogens to others (contagion). Imbalance of the NP microbiome diversity (number and abundance) occurs during symptomatic infections (Pettigrew et al., 2012; Santee et al., 2016; Chonmaitree et al., 2017). Composition of the microbiome including the number of different species present (diversity), and the relative proportion of these species (evenness or abundance) are influenced by multiple factors (Lozupone and Knight 2008; Dominguez-Bello et al., 2010; Teo et al., 2015; Chonmaitree et al., 2017). In a study of 65 children with AOM and 74 children without AOM, Chonmaitree et al. (2017) have recently shown that viral URI frequency is positively associated with an increase in otopathogen colonization, and AOM frequency is associated with lower *Micrococcus* NP colonization. They also found during viral URI and AOM, increases in abundance in the NP of otopathogen genera when *Pseudomonas*, *Myroides*, *Yersinia*, and *Sphingomonas* are decreased. Finally, infant children with AOM in the first year were shown to have significant lower abundance

TABLE 1 | OTUs with > 1% abundance in NW or MEF microbiome during health prior to an AOM (<3 weeks) and at onset of AOM.

NW during health prior to AOM		MEF at onset of AOM		MEF at onset of AOM	
Moraxella;s_	36.89%	Haemophilus;s_influenzae	47.80%	Haemophilus;s_influenzae	67.79%
Haemophilus;s_influenzae	14.16%	Moraxella;s_	20.69%	Streptococcus;Other	18.43%
Streptococcus;s_	11.85%	Streptococcus;Other	16.75%	Haemophilus;Other	6.26%
Corynebacterium;s_	11.31%	Corynebacterium;s_	7.43%	Corynebacterium;s_	3.02%
Streptococcus;Other	9,80%	Haemophilus;Other	3.21%	Alloiococcus;s_otitis	2.91%
Moraxellaceae;g_;s_	2.88%	Alloiococcus;s_	2.24%		
Alloiococcus;s_	2.12%				
Veillonella;s_dispar	1.96%				
Granulicatella;s_	1.36%				
Veillonella;s_	1.01%				

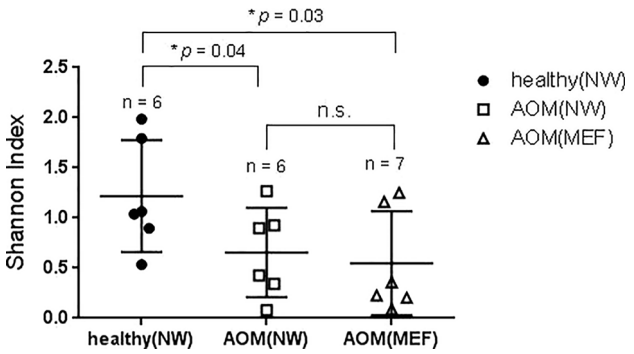

FIGURE 1 | Diversity of NP and ME microbiome during health and AOM. The nasal wash (NW) and MEF samples were collected at onset of AOM and during heath prior to the AOM with 3 weeks' time interval. The samples were analyzed by 16S rRNA gene sequencing. Shannon diversity index was calculated and compared between samples (see *MATERIALS AND METHODS*) by one-tailed *t* test.

of *Corynebacterium* and antibiotics significantly decrease *Corynebacterium* and *Dolosigranulum* (Pettigrew et al., 2012; Teo et al., 2015).

In our study, we found that NP microbiome diversity at onset of AOM significant lower compared with diversity during heath prior to AOM. The potential bacterial pathogens *Haemophilus*, *Moraxella*, and *Streptococcus* became the most abundant microbiota in the NP both during health prior to AOM and at onset of AOM. The commensal *Corynebacterium* was more abundant during health than at onset of AOM, although this difference did not reach statistical significance. Instead, *R. mucilaginosa*, *V. dispar*, *P. melaninogenica*, and certain species in the genus of *Streptococcus* appear to be less abundant in the NWs during AOM relative to health, suggesting these bacteria species may compete with the otopathogens for niche and their abundance reduces when the otopathogens prevail. Whether this is indeed the case has not been reported and may serve as new research directions in the microbiome field of AOM.

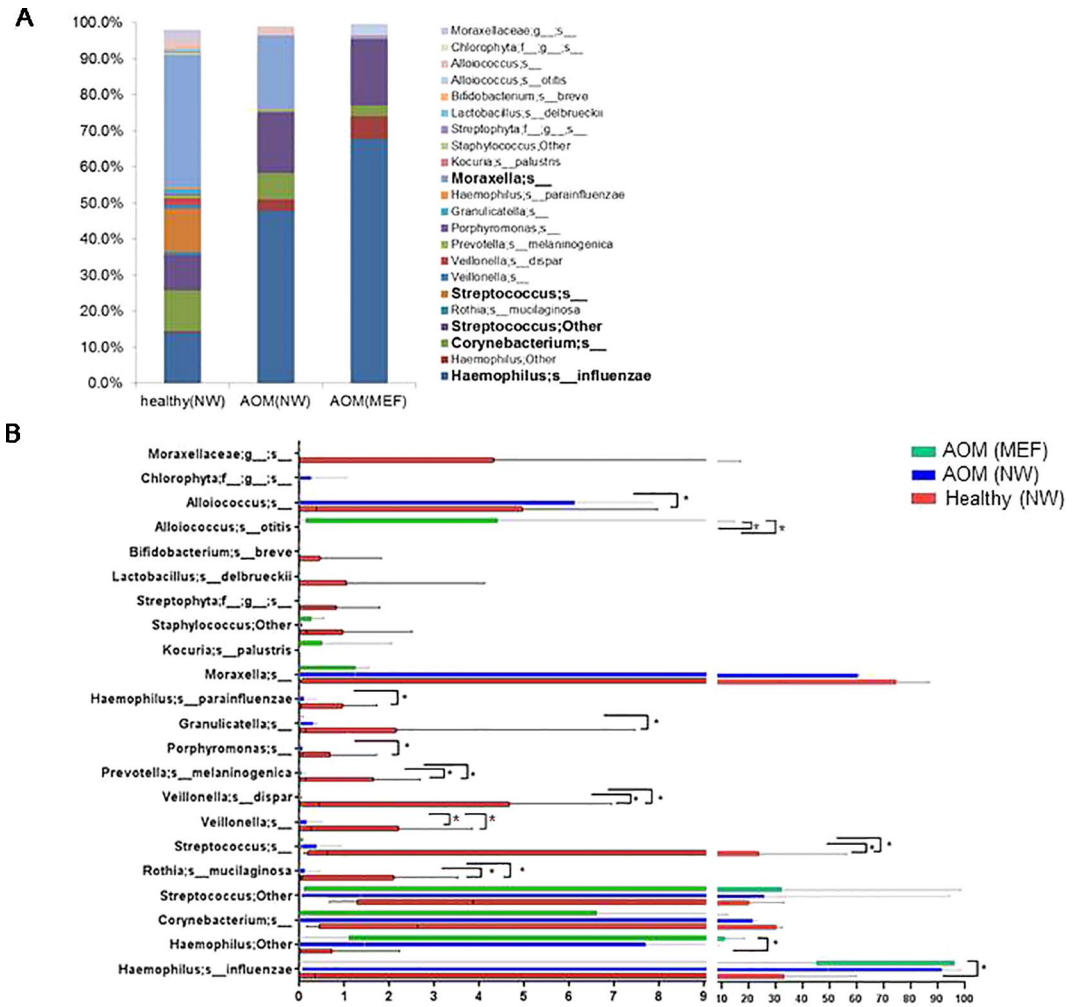

FIGURE 2 | OTUs in NWs and MEFs during heath and at onset of AOM. The NW samples were collected at onset of AOM and during heath prior to the AOM with 3 weeks' time interval. The microbiome was analyzed by 16S rRNA gene sequencing and taxonomic designations. **(A)** Average abundance of OTUs in each group was plotted. **(B)** Comparison of abundance of each individual OUT between groups by Mann-Whitney test. *$p < 0.05$.

TABLE 2 | Difference in OTUs Abundance % between Groups.

	NW		MEF	*Mann-Whitney Test*		
	health	**AOM**	**AOM**	**heath vs AOM (NW)**	**health vs AOM (MEF)**	**AOM (NW) vs AOM (MEF)**
Haemophilus;s_influenzae	14.16	47.80	67.79	not sig	$p = 0.027$	not sig
Haemophilus;Other	0.42	3.21	6.26	not sig	$p = 0.033$	not sig
Corynebacterium;s_	11.31	7.43	3.02	not sig	not sig	not sig
Streptococcus;Other	9.80	16.75	18.43	not sig	not sig	not sig
Rothia;s_mucilaginosa	0.88	0.08	0.00	$p = 0.015$	$p = 0.0026$	not sig
Streptococcus;s_	11.85	0.22	0.03	$p = 0.015$	$p = 0.015$	not sig
Veillonella;s_	1.01	0.10	0.00	not sig	$p = 0.0066$	$p = 0.025$
Veillonella;s_dispar	1.96	0.02	0.01	$p = 0.033$	$p = 0.0042$	not sig
Prevotella;s_melaninogenica	0.72	0.02	0.00	$p = 0.015$	$p = 0.0042$	not sig
Porphyromonas;s_	0.36	0.03	0.00	not sig	$p = 0.023$	not sig
Granulicatella;s_	1.36	0.11	0.02	not sig	$p = 0.01$	not sig
Haemophilus;s_parainfluenzae	0.42	0.07	0.00	not sig	$p = 0.039$	not sig
Moraxella;s_	36.89	20.69	0.53	not sig	not sig	not sig
Kocuria;s_palustris	0.00	0.00	0.34	not sig	not sig	not sig
Staphylococcus;Other	0.55	0.03	0.15	not sig	not sig	not sig
Streptophyta;f_;g_;s_	0.38	0.01	0.00	not sig	not sig	not sig
Lactobacillus;s_delbrueckii	0.69	0.00	0.00	not sig	not sig	not sig
Bifidobacterium;s_breve	0.30	0.00	0.00	not sig	not sig	not sig
Alloiococcus;s_otitis	0.00	0.00	2.91	not sig	$p = 0.01$	$p = 0.025$
Alloiococcus;s_	2.12	2.24	0.00	not sig	$p = 0.033$	not sig
Chlorophyta;f_;g_;s_	0.00	0.18	0.00	not sig	not sig	not sig
Moraxellaceae;g_;s_	2.88	0.00	0.00	not sig	not sig	not sig

Relative to the difference between NWs of healthy children and children at onset of AOM, more OTUs diverged in their abundance between the MEFs of AOM children and NWs of healthy children. This increment in disparity suggests that after establishing in the NP, the invasion of otopathogens into ME and later growth in ME is associated with reduced abundance of commensal bacteria. This may be subtle and/or vary significantly among individuals, since very few OTUs differed significantly between the NWs and MEFs in children during AOM (**Figure 2** and **Table 2**).

The ME microbiome has been investigated recently in children with otitis media with effusion (OME), chronic otitis media, or recurrent AOM (Liu et al., 2011; Jervis-Bardy et al., 2015; Chan et al., 2016; Minami et al., 2017; Lappan et al., 2018). Several reports showed that the most abundant microbiome in ME of children with OME were *A. otitidis* followed by *Haemophilus*, *Moraxella*, and *Streptococcus* (Jervis-Bardy et al., 2015; Chan et al., 2016). We also observed a significant enrichment of *A. otitidis* in MEFs of AOM children, compared with NWs in AOM children or healthy children. It is unclear if *A. otitidis* is an otopathogen, a co-pathogen that facilitates biofilm formation, or a contaminant for the external ear canal skin flora. A prior study children with recurrent AOM found *Alloiococcus*, *Staphylococcus* sp. and *Turicella* were most abundant in the ME (Lappan et al., 2018), whereas adenoids microbiome was dominated by *H. influenzae*, *M. catarrhalis*, *S. pneumoniae*, *P. aeruginosa*, and *S. aureus* (Dirain et al., 2017). On the other hand, in chronic otitis media, Krueger et al. reported that the *Haemophilus* and *Moraxella* were the most abundant microbiota in the ME of children (Krueger et al., 2017), whereas Liu et al. reported that Pseudomonadaceae dominated in the ME, Streptococcaceae in the tonsil, and Pseudomonadaceae, Streptococcaceae, Fusobacteriaceae, and Pasteurellaceae dominated in the adenoid (Liu et al., 2011). In spite of the differences, our study and others suggest a resident microbiota in the ME that differs from NP after an initial ME infection has occurred.

Sample processing approaches and preservation methods may impact microbiome analysis results (Choo et al., 2015; Penington et al., 2018; Chen et al., 2019). In this study, we found that MEF samples stored in PBS had significant greater diversity of microbiome than MEF samples stored in the Trizol reagent after going through centrifugations.

Our study has limitations. Contamination during samples collection is always a concern for microbiome analysis. Contact with the external auditory canal during MEF samples collection may influence the accuracy in microbiome abundance of skin colonizers such as *Staphylococcus*, *Pseudomonas*, and *Alloiococcus*. (Johnston et al., 2019). The MEF samples were collected by tympanocentesis. Although we tired our best to avert contamination we cannot exclude the possibility contact of the external auditory canal by the tympanocentesis needle. Our participant cohort was small and sample size is a concern to interpret microbiome analysis results (Johnston et al., 2019). The 16S reads did not allow differentiation at the species level for most organisms identified; whole genome sequencing likely would have allowed better species level results. We expected to identify *Dolosigranulum pigrum* in some NP samples (Lappan et al., 2018). A recent report suggests *D. pigrum* may be mis-identified as *Alloiococcus* species during data analyses (Lappan et al., 2018).

In summary, in this study we found that the NP microbiome during health prior to AOM had greater diversity and are enriched in certain commensal bacteria, compared with the NP microbiome during AOM. The most abundant microbiota in the NP were known potential otopathogens (*Haemophilus*, *Moraxella*, and *Streptococcus*) along with nasal commensals such as *Corynebacterium*. At onset of AOM, no significant difference was found in microbiome diversity

between NP and MEF. MEF may have a different microbiome profile than the NP suggesting a resident microbiota in the ME after a first ME infection. Sample processing and storage methods influence microbiome analysis results.

DATA AVAILABILITY STATEMENT

The raw data supporting the conclusions of this manuscript will be made available by the authors, without undue reservation, to any qualified researcher.

ETHICS STATEMENT

The studies involving human participants were reviewed and approved by IRB of Rochester General Hospital. Written informed consent to participate in this study was provided by the participants' legal guardian/next of kin.

AUTHOR CONTRIBUTIONS

QX conceived the idea for the study, coordinated data collection, performed preliminary data analyses and prepared the initial draft of the manuscript. SG provided the resource for the completion of 16S rRNA sequence analyses. LX conducted final stages of data analyses and manuscript preparation. EG provided technical assistance throughout the project. MP provided overall guidance for the study and oversaw its completion.

ACKNOWLEDGMENTS

This study was supported by Rochester General Hospital Howard J. Kidd Fund for Medical Research (to QX, LX and Pichichero). We thank Ann Gill and Alex Grier at the University of Rochester Medical Center for DNA extraction, PCR, 16S rRNA gene sequencing and data analysis. We thank Dr. Robert Zagursky for reviewing and editing the manuscript.

SUPPLEMENTARY MATERIAL

The Supplementary Material for this article can be found online at: https://www.frontiersin.org/articles/10.3389/fgene.2019.01176/full#supplementary-material

SUPPLEMENTARY FIGURE 1 | Sample processing approach affects microbiota diversity. MEF samples were either stored in PBS or in Trizol after centrifugation. Both types of samples were analyzed by 16S rRNA sequencing. Shannon diversity index was calculated and compared between the two sets of samples by one tailed t test.

REFERENCES

Alper, C. M., Winther, B., Hendley, J. O., and Doyle, W. J. (2009). Cytokine polymorphisms predict the frequency of otitis media as a complication of rhinovirus and RSV infections in children. *Eur. Arch. Oto-Rhino-Laryngology* 266 (2), 199–205. doi: 10.1007/s00405-008-0729-2

Boers, S. A., de Zeeuw, M., Jansen, R., van der Schroeff, M. P., van Rossum, A. M. C., Hays, J. P., et al. (2018). Characterization of the nasopharyngeal and middle ear microbiota in gastroesophageal reflux-prone versus gastroesophageal reflux non-prone children. *Eur. J. Clin. Microbiol. Infect. Dis.* 37 (5), 851–857. doi: 10.1007/s10096-017-3178-2

Bogaert, D., De Groot, R., and Hermans, P. W. (2004). Streptococcus pneumoniae colonisation: the key to pneumococcal disease. *Lancet Infect. Dis.* 4 (3), 144–154. doi: 10.1016/S1473-3099(04)00938-7

Caporaso, J. G., Kuczynski, J., Stombaugh, J., Bittinger, K., Bushman, F. D., Costello, E. K., et al. (2010). QIIME allows analysis of high-throughput community sequencing data. *Nat. Methods* 7 (5), 335–336. doi: 10.1038/nmeth.f.303

Chan, C. L., Wabnitz, D., Bardy, J. J., Bassiouni, A., Wormald, P. J., Vreugde, S., et al. (2016). The microbiome of otitis media with effusion. *Laryngoscope* 126 (12), 2844–2851. doi: 10.1002/lary.26128

Chen, Z., Hui, P. C., Hui, M., Yeoh, Y. K., Wong, P. Y., Chan, M. C. W., et al. (2019). Impact of preservation method and 16S rRNA hypervariable region on gut microbiota profiling. *mSystems* 4 (1) pii: e00271–18. doi: 10.1128/mSystems.00271-18

Chonmaitree, T., Jennings, K., Golovko, G., Khanipov, K., Pimenova, M., Patel, J. A., et al. (2017). Nasopharyngeal microbiota in infants and changes during viral upper respiratory tract infection and acute otitis media. *PloS One* 12 (7), e0180630. doi: 10.1371/journal.pone.0180630

Choo, J. M., Leong, L. E., and Rogers, G. B. (2015). Sample storage conditions significantly influence faecal microbiome profiles. *Sci. Rep.* 5, 16350. doi: 10.1038/srep16350

Dirain, C. O., Silva, R. C., Collins, W. O., and Antonelli, P. J. (2017). The adenoid microbiome in recurrent acute otitis media and obstructive sleep apnea. *J. Int. Adv. Otol* 13 (3), 333–339. doi: 10.5152/iao.2017.4203

Dominguez-Bello, M. G., Costello, E. K., Contreras, M., Magris, M., Hidalgo, G., Fierer, N., et al. (2010). "Delivery mode shapes the acquisition and structure of the initial microbiota across multiple body habitats in newborns. *Proc. Natl. Acad. Sci. U.S.A.* 107 (26), 11971–11975. doi: 10.1073/pnas.1002601107

Duan, K., Dammel, C., Stein, J., Rabin, H., and Surette, M. G. (2003). Modulation of Pseudomonas aeruginosa gene expression by host microflora through interspecies communication. *Mol. Microbiol.* 50 (5), 1477–1491. doi: 10.1046/j.1365-2958.2003.03803.x

Fadrosh, D. W., Ma, B., Gajer, P., Sengamalay, N., Ott, S., Brotman, R. M., et al. (2014). An improved dual-indexing approach for multiplexed 16S rRNA gene sequencing on the Illumina MiSeq platform. *Microbiome* 2 (1), 6. doi: 10.1186/2049-2618-2-6

Jervis-Bardy, J., Rogers, G. B., Morris, P. S., Smith-Vaughan, H. C., Nosworthy, E., Leong, L. E., et al. (2015). The microbiome of otitis media with effusion in Indigenous Australian children. *Int. J. Pediatr. Otorhinolaryngol* 79 (9), 1548–1555. doi: 10.1016/j.ijporl.2015.07.013

Johnston, J., Hoggard, M., Biswas, K., Astudillo-Garcia, C., Radcliff, F. J., Mahadevan, M., et al. (2019). Pathogen reservoir hypothesis investigated by analyses of the adenotonsillar and middle ear microbiota. *Int. J. Pediatr. Otorhinolaryngol* 118, 103–109. doi: 10.1016/j.ijporl.2018.12.030

Krueger, A., Val, S., Perez-Losada, M., Panchapakesan, K., Devaney, J., Duah, V., et al. (2017). Relationship of the middle ear effusion microbiome to secretory mucin production in pediatric patients with chronic otitis media. *Pediatr. Infect. Dis. J.* 36 (7), 635–640. doi: 10.1097/INF.0000000000001493

Kuss, S. K., Best, G. T., Etheredge, C. A., Pruijssers, A. J., Frierson, J. M., Hooper, L. V., et al. (2011). Intestinal microbiota promote enteric virus replication and systemic pathogenesis. *Sci.* 334 (6053), 249–252. doi: 10.1126/science.1211057

Lappan, R., Imbrogno, K., Sikazwe, C., Anderson, D., Mok, D., Coates, H., et al. (2018). A microbiome case-control study of recurrent acute otitis media identified potentially protective bacterial genera. *BMC Microbiol.* 18 (1), 13. doi: 10.1186/s12866-018-1154-3

Libson, S., Dagan, R., Greenberg, D., Porat, N., Trepler, R., Leiberman, A., et al. (2005). Nasopharyngeal carriage of Streptococcus pneumoniae at the completion of successful antibiotic treatment of acute otitis media predisposes to early clinical recurrence. *J. Infect. Dis.* 191 (11), 1869–1875. doi: 10.1086/429918

Littman, D. R., and Pamer, E. G. (2011). Role of the commensal microbiota in normal and pathogenic host immune responses. *Cell Host Microbe* 10 (4), 311–323. doi: 10.1016/j.chom.2011.10.004

Liu, C. M., Cosetti, M. K., Aziz, M., Buchhagen, J. L., Contente-Cuomo, T. L., Price, L. B., et al. (2011). The otologic microbiome: a study of the bacterial microbiota in a pediatric patient with chronic serous otitis media using 16SrRNA gene-based pyrosequencing. *Arch. Otolaryngol. Head Neck Surg.* 137 (7), 664–668. doi: 10.1001/archoto.2011.116

Lozupone, C. A., and Knight, R. (2008). Species divergence and the measurement of microbial diversity. *FEMS Microbiol. Rev.* 32 (4), 557–578. doi: 10.1111/j.1574-6976.2008.00111.x

Lozupone, C. A., Hamady, M., Kelley, S. T., and Knight, R. (2007). Quantitative and qualitative beta diversity measures lead to different insights into factors that structure microbial communities. *Appl. Environ. Microbiol.* 73 (5), 1576–1585. doi: 10.1128/AEM.01996-06

Melendi, G. A., Laham, F. R., Monsalvo, A. C., Casellas, J. M., Israele, V., Polack, N. R., et al. (2007). Cytokine profiles in the respiratory tract during primary infection with human metapneumovirus, respiratory syncytial virus, or influenza virus in infants. *Pediatr.* 120 (2), e410–e415. doi: 10.1542/peds.2006-3283

Minami, S. B., Mutai, H., Suzuki, T., Horii, A., Oishi, N., Wasano, K., et al. (2017). Microbiomes of the normal middle ear and ears with chronic otitis media. *Laryngoscope* 127 (10), E371–E377. doi: 10.1002/lary.26579

Monasta, L., Ronfani, L., Marchetti, F., Montico, M., Vecchi Brumatti, L., Bavcar, A., et al. (2012). Burden of disease caused by otitis media: systematic review and global estimates. *PloS One* 7 (4), e36226. doi: 10.1371/journal.pone.0036226

Nsouli, T. (2019). "Expert interview: Talal Nsouli: Serous Otitis Media and Acute Otitis Media (middle ear infections)Serous Otitis Media and Acute Otitis Media (middle ear infections)." Retrieved April 3rd, 2019.

Penington, J. S., Penno, M. A. S., Ngui, K. M., Ajami, N. J., Roth-Schulze, A. J., Wilcox, S. A., et al. (2018). Influence of fecal collection conditions and 16S rRNA gene sequencing at two centers on human gut microbiota analysis. *Sci. Rep.* 8 (1), 4386. doi: 10.1038/s41598-018-22491-7

Pettigrew, M. M., Laufer, A. S., Gent, J. F., Kong, Y., Fennie, K. P., and Metlay, J. P. (2012). Upper respiratory tract microbial communities, acute otitis media pathogens, and antibiotic use in healthy and sick children. *Appl. Environ. Microbiol.* 78 (17), 6262–6270. doi: 10.1128/AEM.01051-12

Pichichero, M. E. (2016). Ten-Year Study of the Stringently Defined Otitis-prone Child in Rochester, NY. *Pediatr. Infect. Dis. J.* 35 (9), 1033–1039. doi: 10.1097/INF.0000000000001217

Revai, K., Mamidi, D., and Chonmaitree, T. (2008). Association of nasopharyngeal bacterial colonization during upper respiratory tract infection and the development of acute otitis media. *Clin. Infect. Dis.* 46 (4), e34–e37. doi: 10.1086/525856

Santee, C. A., Nagalingam, N. A., Faruqi, A. A., DeMuri, G. P., Gern, J. E., Wald, E. R., et al. (2016). Nasopharyngeal microbiota composition of children is related to the frequency of upper respiratory infection and acute sinusitis. *Microbiome* 4 (1), 34. doi: 10.1186/s40168-016-0179-9

Santos-Cortez, R. L., Hutchinson, D. S., Ajami, N. J., Reyes-Quintos, M. R., Tantoco, M. L., Labra, P. J., et al. (2016). Middle ear microbiome differences in indigenous Filipinos with chronic otitis media due to a duplication in the A2ML1 gene. *Infect. Dis. Poverty* 5 (1), 97. doi: 10.1186/s40249-016-0189-7

Sekirov, I., Tam, N. M., Jogova, M., Robertson, M. L., Li, Y., Lupp, C., et al. (2008). Antibiotic-induced perturbations of the intestinal microbiota alter host susceptibility to enteric infection. *Infection Immun.* 76 (10), 4726–4736. doi: 10.1128/IAI.00319-08

Suaya, J. A., Gessner, B. D., Fung, S., Vuocolo, S., Scaife, J., Swerdlow, D. L., et al. (2018). Acute otitis media, antimicrobial prescriptions, and medical expenses among children in the United States during 2011-2016. *Vaccine* 36 (49), 7479–7486. doi: 10.1016/j.vaccine.2018.10.060

Syrjanen, R. K., Auranen, K. J., Leino, T. M., Kilpi, T. M., and Makela, P. H. (2005). Pneumococcal acute otitis media in relation to pneumococcal nasopharyngeal carriage. *Pediatr. Infect. Dis. J.* 24 (9), 801–806. doi: 10.1097/01.inf.0000178072.83531.4f

Teo, S. M., Mok, D., Pham, K., Kusel, M., Serralha, M., Troy, N., et al. (2015). The infant nasopharyngeal microbiome impacts severity of lower respiratory infection and risk of asthma development. *Cell Host Microbe* 17 (5), 704–715. doi: 10.1016/j.chom.2015.03.008

Vergison, A., Dagan, R., Arguedas, A., Bonhoeffer, J., Cohen, R., Dhooge, I., et al. (2010). Otitis media and its consequences: beyond the earache. *Lancet Infect. Dis.* 10 (3), 195–203. doi: 10.1016/S1473-3099(10)70012-8

Wang, Q., Garrity, G. M., Tiedje, J. M., and Cole, J. R. (2007). Naive Bayesian classifier for rapid assignment of rRNA sequences into the new bacterial taxonomy. *Appl. Environ. Microbiol.* 73 (16), 5261–5267. doi: 10.1128/AEM.00062-07

Wine, T. M., and Alper, C. M. (2012). Cytokine responses in the common cold and otitis media. *Curr. Allergy Asthma Rep.* 12 (6), 574–581. doi: 10.1007/s11882-012-0306-z

Xu, Q., Almudervar, A., Casey, J. R., and Pichichero, M. E. (2012). Nasopharyngeal bacterial interactions in children. *Emerg Infect. Dis.* 18 (11), 1738–1745. doi: 10.3201/eid1811.111904

Conflict of Interest: The authors declare that the research was conducted in the absence of any commercial or financial relationships that could be construed as a potential conflict of interest.

frontiers in Genetics

REVIEW
published: 26 November 2019
doi: 10.3389/fgene.2019.01230

Recent Perspectives on Gene-Microbe Interactions Determining Predisposition to Otitis Media

Rahul Mittal[1†], Sebastian V. Sanchez-Luege[1†], Shannon M. Wagner[1†], Denise Yan[1] and Xue Zhong Liu[1,2,3]*

[1] Department of Otolaryngology, University of Miami Miller School of Medicine, Miami, FL, United States, [2] Department of Pediatrics, University of Miami Miller School of Medicine, Miami, FL, United States, [3] Dr. John T. Macdonald Foundation, Department of Human Genetics and John P. Hussman Institute for Human Genomics, University of Miami Miller School of Medicine, Miami, FL, United States

A comprehensive understanding about the pathogenesis of otitis media (OM), one of the most common pediatric diseases, has the potential to alleviate a substantial disease burden across the globe. Advancements in genetic and bioinformatic detection methods, as well as a growing interest in the microbiome, has enhanced the capability of researchers to investigate the interplay between host genes, host microbiome, invading bacteria, and resulting OM susceptibility. Early studies deciphering the role of genetics in OM susceptibility assessed the heritability of the phenotype in twin and triplet studies, followed by linkage studies, candidate gene approaches, and genome-wide association studies that have helped in the identification of specific loci. With the advancements in techniques, various chromosomal regions and genes such as *FBXO11*, *TGIF1*, *FUT2*, *FNDC1*, and others have been implicated in predisposition to OM, yet questions still remain as to whether these implicated genes truly play a causative role in OM and to what extent. Meanwhile, 16S ribosomal RNA (rRNA) sequencing, microbial quantitative trait loci (mbQTL), and microbial genome-wide association studies (mGWAS) have mapped the microbiome of upper airways sites and therefore helped in enabling a more detailed study of interactions between host polymorphisms and host microbiome composition. Variants of specific genes conferring increased OM susceptibility, such as *A2ML1*, have also been shown to influence the microbial composition of the outer and middle ear in patients with OM, suggesting their role as mediators of disease. These interactions appear to impact the colonization of known otopathogens (*Streptococcus pneumoniae*, *Haemophilus influenzae*, and *Moraxella catarrhalis),* as well as *Neisseria*, *Gemella*, *Porphyromonas*, *Alloprevotella*, and *Fusobacterium* populations that have also been implicated in OM pathogenesis. Meanwhile, studies demonstrating an increased abundance of *Dolosigranulum* and *Corynebacterium* in healthy patients compared to those with OM suggest a protective role for these bacteria, thereby introducing potential avenues for future probiotic treatment. Incorporating insights from these genetic, microbiome, and host-pathogen studies will allow for a more robust, comprehensive understanding of OM pathogenesis that can ultimately facilitate in the development of exciting new treatment modalities.

Keywords: otitis media, genetics, microbiome, gene-microbe interactions, twin studies, mouse models

OPEN ACCESS

Edited by:
Regie Santos-Cortez, University of Colorado Denver, United States

Reviewed by:
Emma Kaitlynn Sliger, St. Jude Children's Research Hospital, United States
Rachael Lappan, University of Western Australia, Australia

***Correspondence:**
Xue Zhong Liu
xliu@med.miami.edu

†These authors have contributed equally to this work

Specialty section:
This article was submitted to Genetic Disorders, a section of the journal Frontiers in Genetics

Received: *24 July 2019*
Accepted: *06 November 2019*
Published: *26 November 2019*

Citation:
Mittal R, Sanchez-Luege SV, Wagner SM, Yan D and Liu XZ (2019) Recent Perspectives on Gene-Microbe Interactions Determining Predisposition to Otitis Media. Front. Genet. 10:1230. doi: 10.3389/fgene.2019.01230

INTRODUCTION

Otitis media (OM) is one of the most common childhood diseases. With prevalence reaching as high as 5,000,000 annually in the United States, OM is a leading cause for pediatrician office visits and antibiotic prescriptions each year (Kaur et al., 2017). The associated medical expenditures account for as high as $4.1 billion, contributing to a significant healthcare utilization burden for both the healthcare system and patients (Gates, 1996; Bondy et al., 2000; Coticchia et al., 2013; Ahmed et al., 2014; Kaur et al., 2017). OM primarily affects children between the ages of 6 and 24 months, with 80–90% infants likely to experience OM disease at least once before reaching school age despite the introduction of the heptavalent pneumococcal conjugate vaccine in 2000 and its tri-decavalent counterpart in 2010 (Pichichero et al., 2008; Harmes et al., 2013; Kaur et al., 2016; Kaur et al., 2017). With resistance to standard antibiotic treatment continuing to increase steadily, the need for a more comprehensive understanding of OM pathogenesis and potential treatment modalities has become an immediate priority for pediatric and otolaryngology clinicians.

The specific diagnostic classification of OM varies according to its clinical presentation, which is characterized by specific signs and symptoms, disease progression, and the effectiveness of treatment. OM can be classified as acute otitis media (AOM) or otitis media with effusion (OME) when findings include an accumulation of fluid (middle ear effusion) behind the tympanic membrane (Harmes et al., 2013; Schilder et al., 2016). According to the latest guidelines, a diagnosis of AOM requires a moderate to severe bulging of the tympanic membrane, otorrhea, and ear pain with erythema; in contrast, these symptoms are often absent in OME (Lieberthal et al., 2013; Siddiq and Grainger, 2015). When AOM/OME persists despite treatment with antibiotics and/or surgical methods, chronic otitis media (COM), chronic otitis media with effusion (COME), or chronic suppurative otitis media (CSOM) may be indicated. COM is defined as recurrent infection of the middle ear with dry tympanic membrane perforation. COME shares a similar clinical presentation but with the addition of continuous serous drainage, while CSOM features purulent drainage leaking from a perforated tympanic membrane or ventilation tube (Mittal et al., 2015; Schilder et al., 2016). Chronic OM etiologies tend to be more serious for patients, as frequent and/or persistent dysfunction of the Eustachian tube may lead to significant hearing loss, thereby negatively impacting language acquisition and behavioral development in children (Cripps and Kyd, 2003; Santos-Cortez et al., 2016; Walker et al., 2019).

In many clinical cases, the manifestations of OM may overlap and co-occur. Therefore, the diagnostic distinctions between the many OM etiologies are important as they help in determining the adequate course of treatment and expected duration of disease. Some physicians utilize watchful waiting even with diagnosed OM cases to allow for the activation and response of the patient's immune response that may help in the clearance of infection. Symptomatic therapy is indicated in the vast majority of OM cases, with antibiotic treatment regimens only appropriate when cases are persistent. Surgical methods such as tympanostomy tube or grommet insertion are implemented when case recurrence is especially severe (Pichichero et al., 2001; Kozyrskyj et al., 2010). Beyond guiding treatment, however, diagnostic classifications have also been linked to particular offending pathogenic microorganisms despite the fact that obtaining a culture-confirmed diagnosis is not routine in the clinical setting. *Streptococcus pneumoniae*, non-typeable *Haemophilus influenzae* (NTHi), and *Moraxella catarrhalis* are the three main otopathogens known to cause AOM worldwide (Casey et al., 2010; Casey et al., 2013; Kaur et al., 2017; Lappan et al., 2018). International epidemiological studies of Latin American and Caribbean populations have also confirmed *S. pneumoniae* and NTHi as the most frequent AOM bacterial pathogens (Bardach et al., 2011). In addition to these known and culturable otopathogens, a growing body of research has helped highlight how other bacterial, fungal, and/or viral species differentially contribute to the pathogenesis of various OM subtypes (Chonmaitree et al., 2008; Pettigrew et al., 2011; Chonmaitree et al., 2016). For example, clinical and animal studies both demonstrate how inflammation and microbiome disruption of an initial viral and/or bacterial infection of the upper respiratory tract often contributes to the pathogenesis of AOM (Coticchia et al., 2013; Schilder et al., 2016; Dewan et al., 2019). Progression of AOM to COM is largely believed to be due to the complex interactions between bacterial, environmental, and host factors. *Pseudomonas aeruginosa* and *Staphylococcus aureus* (Mittal et al., 2015; Mittal et al., 2019) are the most common pathogens associated with CSOM. However, our current knowledge about COM, especially CSOM, is still very limited and further studies are warranted to understand the pathogenesis of disease.

Early studies attempted to identify the microbiological causes of OM that were limited to culturable bacteria. However, the expansion of 16S ribosomal RNA (rRNA) sequencing and other culture-independent methods have allowed for the identification of microorganisms within the nasopharynx (NP) and middle ear (ME) that play an important role in both resident microbiota and intruding pathogenic populations (Broides et al., 2009; Pichichero, 2009; Kaur et al., 2010). The advancement of these bioinformatic and genomic detection methods have allowed researchers to incorporate insights from the host genome and microbiome that have both deepened and complicated our knowledge of OM pathogenesis. Decades of research have helped uncover links between host genes and OM susceptibility, but our expanding repository of microbiome literature across many fields has introduced new questions regarding the host microbiota's role in pathogenesis, progression, and persistence of many disease etiologies. For instance, recent studies exploring the interplay between individual genes and microbiome composition in the gastrointestinal system, such as the gene-microbe interaction found to drive the development of Crohn's disease-like colitis in mice, suggesting the potential of this interdisciplinary approach for future OM research (Caruso et al., 2019). The goal is that these insights will lead to the development of novel treatment modalities such as probiotic therapies, thereby addressing concerns of growing antibiotic resistance amidst continuously high OM disease burden (Lappan et al., 2018; Mittal et al., 2018). In this article, we describe the recent developments in

OM research that elucidate the interactions between host genes, microbiome composition, and OM pathogenesis, and we identify relevant gaps in understanding that should we believe should be prioritized in future research.

Genetics of Otitis Media

Twin Studies

The first studies to assess the role of genetics in acquiring recurrent OM were mainly twin studies (**Table 1**). One of these initial studies was a retrospective study comprising of 2,750 pairs of Norwegian twins born between 1967 and 1974 (Kvaerner et al., 1997). A series of eight structural equation models were constructed to estimate genetic effects, individual environmental effects, common familial environment effects in males, and dominance effects in females on the predisposition to develop OM (Kvaerner et al., 1997). After selecting a model that best fit the data, it was found that heritability of OM was estimated at 45 and 75% in males and females, respectively (Kvaerner et al., 1997). It is important to note that, despite common misinterpretation, these heritability values do not suggest that OM is 45 or 75% caused by genetics. Instead, the heritability values suggest that 45 and 75% of the variability in developing OM can be attributed to genetic differences in the populations studied. Twin studies are vital in guiding further scientific research to study the role of genetics in OM. A few other important twin studies are described below.

Another study, a prospective twin and triplet study, investigated the genetic component of recurrent ME effusion and AOM (Casselbrant et al., 1999) (**Table 1**). From 1982 to 1995, 168 same-sex twin pairs and 7 same-sex triplet sets younger than 2 months old were recruited for the study mainly from Magee-Women's Hospital in Pittsburgh, PA (Casselbrant et al., 1999). Only same-sex twin and triplet sets were included in the study due to differences in incidence of OM between males and females. From the 168 twin and triplet sets first recruited, 126 were followed for 2 years and any episodes of ME effusion or AOM were documented. From these 126 twin and triplet sets, the estimated degrees of discordance for three or more episodes of ME effusion were 0.04 and 0.37 for monozygotic and dizygotic twins, respectively. For an episode of AOM, the estimates of discordance were 0.04 in monozygotic twins and 0.49 in dizygotic twins. These discordance values imply that monozygotic twins shared similar presence of illness compared to dizygotic twins, who did not become ill in conjunction with each other as often. These results suggest genetics play some role in susceptibility of the illness since monozygotic twins showed more concordance with disease than dizygotic twins. Lastly, the heritability of recurrent ME effusion was estimated at 0.73 after 2 years, which suggests genetics plays a significant role in the individual variation of OM cases. In 1987, researchers altered the protocol to extend the follow-up period to 5 years (Casselbrant et al., 2004). Eighty-three sets of twins or triplets were followed for 5 years, and the heritability of recurrent ME effusion within 5 years of life was estimated at 0.72, further suggesting genetics may play a large role in susceptibility to OM (Casselbrant et al., 2004).

To further understand the extent of genetic predisposition for OM, the Twin Early Development Study, a longitudinal study of same-sex twins born in England and Wales in 1994, was conducted (Rovers et al., 2002). Unlike previous studies, this study set out to estimate the heritability of different manifestations and symptoms of OM compared to those of chronic airway blockage, which frequently accompanies persistent effusion (Rovers, 2002). The researchers followed 1,373 twin pairs for 2, 3, and 4 years, assessing the occurrence of OM symptoms (earache, ears leaking pus or mucus, pulling or scratching ears, and red or sore ears) and chronic airway blockage symptoms (breathing through the mouth and snoring or snorting in sleep). When the OM and the chronic airway blockage symptoms were combined, the heritability was estimated at 0.49, 0.66, and 0.71 for ages 2, 3, and 4, respectively. When tested separately, the heritability of OM symptoms averaged over all years was estimated to be 0.57, and the effect of twin shared environment was 0.18. The chronic airway blockage symptoms when tested alone showed higher heritability (0.72) and a lower effect of twin shared environment (0.10) compared to those of OM. This investigation elucidates the importance of separating the symptoms of OM from those of chronic airway blockage instead of considering the two as undifferentiated OM.

As briefly mentioned before, these twin studies, although a good starting point for investigating the role of genetics in OM, provide minimal evidence compared to other studies of genetic causation or predisposition to developing OM. The main reason for the poor level of evidence is that a twin study only provides information about the role of genetics in the variation of the disease in a population. Heritability values cannot be used at the individual level to declare that a specific disease is caused by genetic factors some percentage of the time. The

TABLE 1 | Significant heritability values from various twin and triplet studies.

Heritability	Ages affected	Case definition	Reference
Males: 0.45 Females: 0.75	0–7	Individuals with recurrent ear infections before 7 years old	Kvaerner et al., 1997
0.73	0–2	AOM: presence of effusion, at least one symptom (fever, otalgia, or irritability), and one sign of inflammation (erythema, bulging/fullness, or otorrhea) OME: presence of middle ear effusion without symptoms of AOM	Casselbrant et al., 1999
0.72	0–5	AOM: presence of effusion, at least one symptom (fever, otalgia, or irritability), and one sign of inflammation (erythema, bulging/fullness, or otorrhea) OME: presence of middle ear effusion without symptoms of AOM	Casselbrant et al., 2004
0.57	0–4	OM: earache, ears leaking pus/mucus, pulling or scratching ears, and red or sore ears	Rovers et al., 2002

other issue with twin studies is that they provide no insight as to the specific genetic loci that may be implicated in OM, only a general sense of genetic heritability. It is important to note that the heritability measures are applicable/specific only to the cohort in which they are estimated.

Linkage Studies

Besides twin investigations, there has been interest in investigating genetic determinants of chronic and recurrent OM across the entire genome using linkage studies (Daly et al., 2004) (**Table 2**). In a linkage analysis, researchers assess the statistical linkage of segments of the genome with the phenotype of interest among a series of families. One study recruited individuals who received tympanostomy tube surgery to treat chronic or recurrent OM and their families (Daly et al., 2004). From 133 families, they acquired 591 DNA samples, 238 of which were affected by chronic or recurrent OM, for genetic screening. The DNA samples were then screened for 404 fluorescent microsatellite markers and analyzed by single- and multipoint nonparametric linkage (NPL). The single-point NPL analyses suggested significant evidence of linkage on chromosome 10q26.3 at marker *D10S212* (LOD 3.78) and suggestive evidence of linkage on chromosome 19q13.43 at marker *D19S254* (LOD 2.61). The multipoint NPL analyses suggested strong evidence of linkage on chromosome 19q near marker *D19S254* (LOD 2.53). Interestingly, the multipoint NPL analyses showed decreased linkage on chromosome 10q near marker *D10S212* (LOD 1.64). Conditional analyses were then performed on samples that supported linkage on 10q and 19q in order to potentially increase other significant regions of the genome (Daly et al., 2004). The conditional analyses revealed linkage for chronic or recurrent OM on a region of chromosome 3p [conditional (10q) LOD 2.43; conditional (19q) LOD 1.84; unconditional LOD 0.60]. These analyses suggest that there exists an interaction between several regions of the genome that plays a role in the risk of chronic or recurrent OM.

Another study also attempted a linkage analysis to further identify possible genes that increase the risk of OM (Casselbrant et al., 2009). The researchers recruited families with two or more full siblings who received tympanostomy tube insertions due to a history of OM. Four hundred and three Caucasian families (1,431 individuals) and 26 African American families (75 individuals) were genotyped. The researchers carried out an NPL analysis using 8,802 single-nucleotide polymorphisms (SNPs) on the larger Caucasian data set, at first by itself and then in conjunction with the African American data set. When analyzed by itself, the Caucasian data set suggested strong linkage on chromosome 17q12 (LOD 2.83) and 6p25.1 (LOD 2.25). There were also three other suggestive linkages on 10q22.3, 7q33, and 4p15.2, but these were not as significant as the linkage on 17q12. When the data sets were combined, the peaks on chromosomes 17, 6, and 4 became less significant, but the linkage on chromosome 10q22.3 became more significant. The authors also suggest that these linkage signals are near previously implicated genes *SFTPA2, IFNG,* and *TNF* (Casselbrant et al., 2009).

To further localize significant linkage signals, another study set out to fine map chromosome 19, the chromosome previously implicated in Daly et al. (2004) (Chen et al., 2011). The researchers recruited individuals who received tympanostomy tube surgery to treat chronic or recurrent OM and their families. The participants included all subjects from the initial study and an additional six new families (a total of 607 individuals from 139 families). The researchers performed an NPL analysis of 1,091 SNPs, the majority of them were from chromosome 19. The NPL analysis suggested significant linkage on chromosome 19 at position 63.4 mb (LOD 3.75) with LOD-1 support interval between 61.6 and 63.8 mb. This region of the genome contains over 90 known genes and includes several genes implicated in inflammatory and immune processes (Chen et al., 2011).

These linkage analysis studies were large leaps forward in illustrating the potential genetics of OM because they isolated specific genomic sequences that statistically linked with cases of OM. Despite these promising findings, though, linkage analysis has its limitations. In linkage analysis, there can be a significant increase in the rate of false positives and a reduction of statistical power (Ferreira, 2004). Therefore the results of linkage studies should be evaluated with caution. In an attempt to overcome the drawbacks of linkage analysis studies, researchers focused their efforts in candidate gene approach studies to test the statistical association between specific genes and/or markers implicated in OM from previous studies and cases of OM in a population.

TABLE 2 | List of chromosomes implicated in otitis media based on various nonparametric linkage analyses.

Chromosome	LOD score	Marker	Case definition	Reference
10q26.3*	3.78	*D10S212*	At least two data sources indicated positive results for ear examination, tympanogram, self-reported history, and/ or medical record OR 1 data source indicated positive results for above findings and current middle-ear findings presumptive of COME/ROM history	Daly et al., 2004
19q13.43*	2.61	*D19S254*		
19q	2.53	Near *D19S254*		
10q	1.64	Near *D10S212*		
3p[a]	2.43	NA		
3p[b]	1.84	NA		
3p[c]	0.6	NA		
17q12	2.83	NA	Insertion of tympanostomy tube at least once for recurrent/ persistent OM	Casselbrant et al., 2009
6p25.1	2.25	NA		
19	3.75	63.4 mb	Tympanostomy tube insertion for COME/ROM, presence of OM sequelae, and/or abnormal middle ear mechanics	Chen et al., 2011

**Single-point nonparametric linkage (NPL) analyses; all other linkages found from multipoint NPL analyses. [a]Conditional analysis with 10q. [b]Conditional analysis with 19q. [c]Unconditional analysis (not significant). NA, not analyzed.*

Otitis Media in Mouse Models

The mouse model is a useful tool to study and identify the genes relevant to OM. There are genes that are essential for the maintenance of the ME epithelial cell integrity and health and mutations/deletion in these genes can determine predisposition to OM: 1) *Tgif1*—it functions as a negative regulator of the transforming growth factor beta (TGFβ) signaling pathway. *Tgif1* mutant mice have significantly raised auditory thresholds due to a conductive deafness arising from OM (Tateossian et al., 2013). 2) *Phex*—the mutation in the *Phex* gene primarily upregulates the expression level of the *Fgf23* gene in the MEs and is linked to predisposition to OM in mice (Han et al., 2012). *Fgf23* mutant mice have also been shown to have mixed hearing loss and ME malformation (Lysaght et al., 2014). 3) *Oxgr1*—the *Oxgr1* gene encodes oxoglutarate receptor 1. The ligand for OXGR1 is believed to be involved in the regulation of vascular endothelial growth factor, an important inducer of angiogenesis and vascular permeability. Kerschner et al. (2013) showed presence of inflammatory cells, changes in the mucosal epithelium, and ME fluid in *Oxgr1* deficient mice. 4) *Mcph1*—the *Mcph1*-deficient mice had mild to moderate hearing loss (around 70% penetrance). Other defects of *Mcph1*-deficient mice included small skull sizes, increased micronuclei in red blood cells, increased B cells, and ocular abnormalities (Chen et al, 2013). 5) *Lmna—Lmna* mutant mice have profound early-onset hearing deficits and abnormal positioning of the Eustachian tube accompanied by OM (Zhang et al., 2012).

There is also evidence of the involvement of signaling pathways and inflammatory factors involved in OM. *Pai-1* knockout mice showed significant pathological changes of tympanosclerosis (Shin et al., 2014); mice deficient in the *C5a* gene have been shown to have reduced levels of IL-6, mKC, and MCP-1, in association with decrease in inflammatory cell recruitment, mucosal inflammation, and bacterial clearance (Tong et al., 2014); mice lacking the *IL-17A* gene, encoding interleukin 17A (IL-17A), a neutrophil inducing factor, were associated with abnormal recruitment and apoptosis of neutrophils (Wang et al., 2014).

Mouse-To-Man Candidate Gene Study

All cohorts for OM reported thus far have low power to detect common genetic risk factors for disease and have low resolution. The specific genetic susceptibility loci for OM can be identified, however, through genome-wide or candidate gene association studies. Candidate gene studies can theoretically overcome these issues of low power and resolution by focusing directly on the association between disease and genetic variants with strong support for their involvement in the biology. Through candidate gene association studies, efforts have been made to test the association of chronic OM with specific genetic loci that have been identified as potential risk loci of OM in mouse models. In candidate gene studies, the frequencies of a genetic marker are compared between affected study subjects and control subjects. The control subjects can be unrelated healthy controls (case-control study) or healthy siblings or other family members (family study). But with the candidate gene approach, ascertaining relevant loci for testing can be difficult and thus are likely to miss many causal regions. Increasingly, genetically altered mouse models, such as those discussed earlier, have been used to study OM because of the technology available to genetically alter this species and translate the analysis of suspected genes to the human model.

Bhutta et al. (2017) performed a genetic association study on a large cohort of children with COME, and tested SNPs at candidate loci derived from four genetically altered mouse models that have identified *Fbxo11*, *Evi1*, *Tgif1*, and *Nisch* as potential risk loci for chronic OM. Of the 1,296 families analyzed, evidence of association was found at rs881835 and rs1962914 at the *TGIF1* locus, with odds ratios of 1.4–1.6. There was a weaker association with rs10490302 and rs2537742, two SNPs within *FBXO11*, with odds ratios of around 1.2. All these SNPs are located in intronic regions. However, no evidence of association with the loci *EVI1* or *NISCH* was detected. Both the *TGIF1* and *FBXO11* loci are thought to be involved in TGF-β signaling, which implies that this pathway may be critical in the transition from acute to chronic ME inflammation. However, Bhutta et al. (2017) reported that these results failed to replicate in a case-control cohort in Finland of 402 children with chronic OM with effusion and 777 control participants.

In previous studies, Rye et al. (2011), in an analysis of 434 families predominantly suffering from recurrent AOM ($p = 0.009$) from Western Australia, showed an association with the major A allele at SNP rs330787 at *FBXO11*, with replication of this finding in an independent cohort ($p = 6.9 \times 10{-}6$, OR = 1.55). Segade et al. (2006) also reported nominal evidence of *association to the* SNP rs2134056 ($p = 0.017$) at *FBXO11* in their cohort of 142 families from the US (with a mixed OM phenotype). The *TGIF1* locus, found to be associated with risk of COME, has not been evaluated in any previous genetic association study. *EVI1* and *NISCH* were not associated with OM (Sale et al., 2011).

The data therefore indicate that regulation of the TGF-β pathway may be critical for the development of persistent inflammation in the ME. TGF-β has already been reported as a key regulator of inflammatory response, through its effects on chemotaxis, activation, and survival of lymphocytes, natural killer cells, dendritic cells, macrophages, mast cells, and granulocytes (Yoshimura et al., 2010).

Other studies have attempted to isolate particular genetic loci associated with susceptibility to OM using a candidate gene association approach. What follows is a brief description of various other studies and their findings. A candidate gene study on 15 genes with single-nucleotide polymorphisms (SNPs) in 142 families with 618 subjects was conducted by Sale et al. (2011). Nominal genetic association was found for *MUC5AC* [rs2735733, $P = .002$, odds ratio (OR) = 0.646; rs7396030, $P = .049$, OR = 1.565; rs2075859, $P = .041$, OR = 0.744]. A trend toward association was also found in three other SNPs at three genes: *SCN1B* (rs810008, $P = .013$), *SFTPD* (rs1051246, $P = .039$), and *TLR4* (rs2770146, $P = .038$). Rye et al. (2013) have shown functional evidence for a role for *SLC11A1* in susceptibility to OM and have studied the candidate gene in 660 affected children from 531 families in a case/pseudo-control study. The best SNP association was detected at the rs2776631 ($P = .025$).

Furthermore, haplotype analysis revealed the 3_C_C_G haplotype (rs34448891_rs2276631_rs3731865_rs2695343) to be more common in the affected individuals ($P = .0008$). MacArthur et al. (2014), in a candidate gene study of 192 SNPs from eight genes on 100 cases and 79 controls, reported that 8 SNPs on four genes (*TLR4*, *MUC5B*, *SMAD2*, *SMAD4*) showed a potential trend toward association (P unadjusted = 0.007, rs10116253 on *TLR4*). It is important to note, though, that these eight SNPs did not show significant association after correcting for multiple statistical testing (P adjusted = 0.625, rs10116253 on TLR4). Also, an increased risk for OM proneness was found associated with the *CX3CR1* gene (Thr280Met, OR = 6.23, $P = .038$) in a study of 21 SNPs as risk factors for upper respiratory tract infections, OM, and OM proneness in 653 children (Nokso-Koivisto et al., 2014). Ilia et al. (2014) conducted studies in a Greek cohort of 96 children on eight SNPs of five cytokine genes, that have demonstrated that *IL-10* (−592, −819, and −1082) and *TGF*β (codon 10C > T) were associated with an increased number of acute OM episodes ($P < .001$, $P < .001$, $P < .001$, and $P = .002$, respectively); *IL-10* (−1082) and *TGF*β (codon 10C > T) were also associated with a later onset of AOM ($P = .007$ and $P = .0039$, respectively). Gessner et al. (2013) reported in 1,032 study subjects from Alaska that individuals homozygous for the arctic variant of *CPT1A* (c.1436C > T) demonstrated a trend to more likely have OM (OR = 3.6, 95% confidence interval: 1.4–8.9). Hafren et al. (2015)performed a candidate gene study with 53 SNPs on 624 study subjects with recurrent acute OM and/or chronic OM with effusion and 778 control subjects. The positive result for *TLR4* (rs5030717, OR = 1.33, $P = .003$) was further investigated by a tagging SNP analysis and has resulted in the identification of two additional SNPs (rs1329060 and rs1329057). There was an increased association among patients with a more severe phenotype: those with OM starting before the age of 6 months (OR = 2.42, $P = .0005$, for rs1329060) and those with repeated insertions of tympanostomy tubes (OR = 1.65, $P = .00004$ for rs1329060). The finding was replicated in a Finnish OM cohort of 205 children (s1329060, OR = 1.32, $P = .002$; rs1329057, OR = 1.30, $P = .003$; rs5030717, OR = 1.34, $P = .002$). However, in three other cohorts (two in the United States and one in the United Kingdom), the three SNPs failed to show an association with the risk for OM. Finally, a variant, Asp299Gly (rs4986790) in *TLR4,* was found to be related to the colonization of *M. catarrhalis* in the upper respiratory tract of children (43%) in comparison with the *TLR4* wild type (9%) (RR = 4.91, P = .0001) (Hafren et al., 2015).

Lastly, another large-scale candidate gene study investigated the role of *FUT2*, a gene whose protein product regulates the expression of red blood cell Lewis and ABO antigens and that had previously been associated with increased risk of recurrent urinary tract infections, in familial OM (Santos-Cortez et al., 2018). For this study, families with children affected by OM were recruited. The participants were recruited from various ethnic backgrounds, including 137 individuals of indigenous Filipino descent (Santos-Cortez et al., 2015), 257 trios of mother, father, and child from Texas, 76 individuals from Colorado, 140 families from a previous family cohort from the University of Minnesota (Sale et al., 2011), 105 families from Helsinki University Hospital (Hafren et al., 2012), and 19 families from the southern Punjab province of Pakistan (Santos-Cortez et al., 2018). This study suggests an association of the c.412C > T variant of *FUT2* with chronic or recurrent OM in European-American children and family trios in the United States. Additionally, an association between the c.461G > A variant and transmission in family trios in the United States as well as shifts in the microbiota composition in the ME were observed. Lastly, they reported an association of the c.604C > T variant with OM in the Filipino data set, though 17 individuals did not show shifts in ME microbiota composition due to this variant. The authors proposed that *FUT2* variants confer higher risk for OM by modification of the microbiome in the ME. The authors also tested the expression and localization of *Fut2* and found that there is a transient increase in expression in the ME of mice inoculated with *H. influenzae* (Santos-Cortez et al., 2018). This study's extensive array of results seems to suggest that different genetic variants and environmental factors influence susceptibility to OM (Santos-Cortez et al., 2018).

These candidate gene association studies have moved the field forward by suggesting an association between OM susceptibility and these various genetic variants, but unfortunately the statistical power of these studies remains quite low. Up to now, most existing association studies in OM have been poorly phenotyped and used small sample sizes (Bhutta, 2013), which significantly reduces the statistical power, decreasing thus the probability of replication. The latter can also be due to variation in study design, particularly if phenotypes are poorly matched. For example, there is some evidence suggesting that chronic OM should be evaluated and analyzed as distinct from acute OM. Yet, many studies on genetic risk of chronic OM have used candidate loci involved in innate or acute inflammatory pathways and included cases of both recurrent acute and chronic OM. Furthermore, epidemiological studies have demonstrated that AOM is a risk factor for ME effusion, although many children with COME have no preceding history of AOM (Bhutta, 2014). Also, mouse transcript studies have shown that genes upregulated in the initial phase of inflammation are different to those found as inflammation resolves, suggesting that there is a molecular transition from acute to chronic inflammation (Hernandez et al., 2015). Other reasons for failure of replication may be that the genetic structure might be disparate (Lao et al, 2008), or that different pathogenic mechanisms exist in different populations.

Genome-Wide Association Studies

Since very few genes that contribute to the development of OM had been identified, genome-wide association studies (GWAS) have been used to decipher the genetic etiology of the disease by assessing whether any genetic variants throughout the entire genome associate with cases of OM (**Table 3**). A study recruited 416 cases (at least 3 episodes of AOM by the age of 3) and 1,075 controls from the Western Australian Pregnancy Cohort (Raine) Study, a longitudinal cohort study in Western Australia of 2,868 children whose mothers were recruited in early pregnancy from 1989 to

TABLE 3 | List of genes implicated in otitis media from genomic association studies.

Gene	Allele or variant	Chromosome	Odds ratio, LOD score, or p-value	Case definition	Reference
FBXO11	A allele at rs10490302 G allele at rs2537742	2p16.3	OR 1.17 OR 1.16	COME: symptomatic effusion for at least 3 months and effusion at operation	Bhutta et al., 2017
TGIF1	T allele at rs881835 G allele at rs1962914	18p11.31	OR 1.39 OR 1.58		
FUT2	c.412C > T at rs1800022 c.461G > A at rs601338 c.604C > T at rs1800028	19q13.33	p = 0.01* p = 0.01* LOD 4.0	Study assessed multiple different cohorts—case definition slightly different for each cohort	Santos-Cortez et al., 2018
CAPN14 *GALNT14*	rs6755194 rs1862981	2p23.1	OR 1.90 OR 1.60	Clinical exam within 3 years of life indicated presence of inflamed/retracted/scarred tympanic membrane, middle ear effusion, or tympanostomy tube OR parents reported 3 or more episodes of AOM within first 3 years of life	Rye et al., 2012
KIF7	rs1110060	15q26.1	$p = 9.1 \times 10^{-7}$ [a] p = 0.072 [b]	Insertion of tympanostomy tube at least once for recurrent/persistent OM	Allen et al., 2013
CDCA7 and SP3[d]	rs10497394	2q31.1	$p = 2.9 \times 10^{-5}$ [a] $p = 4.7 \times 10^{-5}$ [b]		
FNDC1	rs2932989	6q25.3	$p = 4.36 \times 10^{-8}$ [a] $p = 2.15 \times 10^{-9}$ [c]	CHOP cohort: AOM defined using ICD-9 codes Generation R Study cohort: survey data on OM, otorrhea, fever with earache, and/or use of ear drops per subscription	Van Ingen et al., 2016

**Transmission disequilibrium test. [a]Initial data. [b]Replication data. [c]Combined meta-analysis of initial and replication data. [d]These genes border the corresponding marker, rs10497394.*

1991 (Rye et al., 2012). Despite a predominantly Caucasian cohort, it was reported that principle component analysis showed evidence for population stratification, or differences in allelic frequencies between subpopulations. The data set was corrected to account for this population substructure by adjusting for two principal components. Genome-wide association analysis of the corrected data set identified various SNPs showing association, the strongest of which were at *CAPN14* and *GALNT14* on chromosome 2p23.1. When the data set was tested without accounting for the population stratification, analysis did not reveal one significant genetic variant. Replication of the results was also attempted in a cohort of 793 affected individuals (55% with recurrent AOM and 45% with COM with effusion) from the Western Australian Family Study of OM. Twenty SNPs within seven candidate genes, including *CAPN14* and *GALNT14*, were genotyped, but no significant variants were identified. It was proposed that the lack of replication might be due to phenotypic and sample size differences in the populations (Rye et al., 2012). Another study attempted to replicate the results from the Western Australian Pregnancy Cohort (Raine) Study. Twenty-six autosomal SNPs from the Raine Study were analyzed for association in the sample of families with children affected by chronic OM with effusion and recurrent OM from the Daly et al. (2004), study discussed previously (Allen et al., 2014). No significant association was found with any of the 26 SNPs tested; the p-values ranged from 0.03 to 0.93, never crossing the significance threshold of p = 0.001 (Allen et al., 2014).

A second GWAS study attempted to elucidate potential genes by genotyping 229 controls and 373 children who received tympanostomy tube surgery to treat COM with effusion or recurrent OM (Allen et al., 2013). Analysis of 324,748 SNPs revealed various SNPs on a number of chromosomes that showed suggestive or strong association with OM. The strongest of these variants was rs1110060 on chromosome 15 ($p = 9.1 \times 10^{-7}$). Replication of the findings from this genome-wide association analysis was attempted in a cohort of 652 controls and 932 affected children who also received tympanostomy tube insertion for chronic or recurrent OM (Allen et al., 2013). Of the 53 tested for replication genotyping, 4 significant SNPs ($p < 0.10$) were identified. One of these 4 SNPs was rs1110060 on chromosome 15 (p = 0.072), the most significant result from the initial study, but rs10497394 on chromosome 2 was the most significant replication (initial study: $p = 2.9 \times 10^{-5}$; replication study: $p = 4.7 \times 10^{-5}$) (Allen et al., 2013). The significant SNP variants identified in this study have been added to the list of candidate genes, such as *KIF7* (in rs1110060) and *CDCA7* and *SP3* (which both border rs10497394), that require further research (Allen et al., 2013).

Another study performed a meta-analysis of two cohorts consisting of 825 cases/7,936 controls and 1,219 cases/1,067 controls from the Children's Hospital of Philadelphia (CHOP) and the Generation R Study (GenR) at Erasmus University Medical Center, the Netherlands, respectively (Van Ingen et al., 2016). The cases were defined as individuals with AOM prior to 3 years old. The GWAS suggested a significant association between the variant rs2932989 on chromosome 6q25.3 and AOM ($p = 2.15 \times 10^{-9}$). These findings were then replicated in an independent cohort of 293 cases of AOM and 1,719 controls recruited from the Children's Hospital of Philadelphia. This SNP lies in an intergenic region near the *FNDC1* locus, so expression and methylation tests were performed to determine whether this gene could be associated with these findings. FNDC1 expression was found in multiple tissue types in mice and humans, in

addition to mice ME (Van Ingen et al., 2016). The expression of *Fndc1* was also upregulated in mouse ME after treatment with lipopolysaccharide, which induces an inflammatory response and stimulates TGF-beta, TNF-alpha, and IL-1 signaling (Van Ingen et al., 2016). Lastly, the increase in *Fndc1* expression may be explained by experiments that show lower levels of methylation of human *FNDC1* in the SNP of interest (Van Ingen et al., 2016).

Although these GWAS present promising results of associations between specific genetic markers and OM, GWAS also struggles with the dichotomy of high false positive rates and lower than desired power. Commonly in GWAS, the false positive rate is maintained at 5%. As a result, though, the study loses power because the p-value threshold becomes very small in order to be considered significant (Tam et al., 2019). Since the p-value is so low, there can be a number of SNPs that have associations with the trait that do not get detected because their p-value does not cross the very strict threshold. Even though there are replicable associations between some genetic variants and OM, there still remains the issue of causality. A GWAS on its own cannot explain the role of the genetic variants on the pathophysiology of OM, so studies must be carried out to further elaborate the potential mechanistic involvement of these genes.

Genetics and the Microbiome

The composition and diversity of the microbiome, as well as the exogenous and endogenous factors that affect it, is notoriously difficult to study. However, high-throughput sequencing analysis techniques such as 16S rRNA and metagenomics (MGS) have contributed significantly to the field, allowing a more detailed study of microbiome composition, specific genetic loci, and disease progression (Turnbaugh et al., 2009; Yatsunenko et al., 2012; Kurilshikov et al., 2017; Awany et al., 2019). A more comprehensive study is valuable in light of the growing understanding of how the microbiome can either prevent or foster infectious, metabolic, inflammatory, atopic, and neurological disease through predominantly immuno-modulatory processes (Tremlett et al., 2017; Aydin et al., 2018; Imhann et al., 2018; Lee et al., 2018; Liang et al., 2018). Of note, these advancements have been facilitated by the development of microbial genome-wide association studies (mGWAS) techniques to probe the genome for loci directly influencing bacterial populations. mGWAS studies have already identified hundreds of microbial quantitative trait loci (mbQTLs) associated with alpha-diversity, beta-diversity, and abundance of particular taxonomic groups and have mapped them to polymorphisms related to mucosal immunity and metabolic processes (Goodrich et al., 2014; Bonder et al., 2016; Turpin et al., 2016; Wang et al., 2016; Hall et al., 2017; Kurilshikov et al., 2017). For example, innate immune factors such as C-type lectins, toll-like receptor (TLR) regulators including *Irak2*, and NOD-like receptors (*NOD1/NOD2*) have all been shown to affect microbial environment, while genes such as *FUT2, LCT, CARD9* have linked the host and microbiota metabolism, all of which carry implications for disease susceptibility, progression, and treatment (Blekhman et al., 2015; Lamas et al., 2016; Kurilshikov et al., 2017).

In an attempt to extricate the environmental impact from that of a host's genome, a study reviewed mGWAS studies and methodologies and reports that mGWAS's earliest use helped identify 83 microbiome-loci associations, with follow-up studies especially supporting the discovered link between the *LCT* lactase gene and *Bifidobacterium* (Blekhman et al., 2015; Weissbrod et al., 2018). Meanwhile, other studies demonstrated that 10.43% of microbiome variability (beta-diversity) between individuals can be attributed to 42 genetic loci, and that microbial diversity is particularly affected by the *VDR* (vitamin D receptor) gene (Wang et al., 2016; Hall et al., 2017). However, the majority of these existing mGWAS studies analyze gut microbiota, thereby limiting the direct application to the OM field. One of the only mGWAS studies exploring the composition of the nasal vestibule and NP microbiome was performed using 16S rRNA methods to compare a small, 144-person cohort with the alpha diversity, beta diversity, and relative abundance of bacterial taxa (Igartua et al., 2017). The study identified 37 significant associations (mbQTLs) out of 148,653 genetic variants ($q < 0.05$), the most significant of which linked *Dermacoccus* and the variant rs117042385 located upstream of terminal differentiation induced non-coding RNA, a non-coding RNA binding to the mRNA of *PGLYRP3* encoding a known antimicrobial protein important for epidermal differentiation (Igartua et al., 2017). Importantly, the study also found a significant association between shared genetics and similar microbiome composition even after controlling for a shared household environment. Igartua et al. therefore was able to establish an association between genes, microbial populations in the upper airways, and innate mucosal immunity, thereby encouraging the further use of this new technology to the study of OM and other upper respiratory tract infections.

It is important to note some limitations of these new contributions. The conflicting results from analyses of the same data sets have been reported, though this has been ascribed to differences in statistical methods and significance cutoffs. Also, much like the limitations introduced by GWAS studies, associations identified by mGWAS are often weak at best, spread out across the genome, and therefore impose a comparatively insignificant effect. Finally, the ever-changing nature of the microbiome—a bacterial population susceptible to both short- and long-term changes influenced by diet, transient infections, and a slew of other behavioral variations of the host—complicates reproducibility of data. Therefore, carefully designed studies are needed in both the OM and the gastrointestinal fields in order to clarify links between a fixed, heritable genome to a variable as dynamic as the microbiome.

Otitis Media and the Microbiome

The microbiome has been implicated in the pathogenesis of OM, primarily in its role as an immunomodulator and as a competitor against invading bacteria seeking both nutrients and space. A number of studies have determined alteration in microbiome profile in OM prone individuals (**Table 4**). As mentioned before, the microbiome may carefully modulate host inflammatory processes through intricate cross talk between immune cells and the resident microbiota (Sokolowska et al.,

TABLE 4 | A summary of studies determining microbiome of upper respiratory tract in individuals susceptible to otitis media.

Sample type	Age of subjects	Sample size	Results	References
MEF, NP swab, adenoid swab	3–10 years	11 indigenous children with OME	- *Alloiococcus, Haemophilus, Streptococcus, Moraxella*	Jervis-Bardy et al., 2015
Nasal aspirates	2–12 months	234 infants	- *Moraxella, Streptococcus, Haemophilus*	Teo et al., 2015
MEF, adenoid swab	1–12 years	23 children with COME, 10 children without COME with respiratory surgery	- *Alloiococcus* inversely related to *Haemophilus* - Abundance of *Alloiococcus otitidis* and *Staphylococcus* in MEF	Chan et al., 2016
ME and mastoid swab	6 months–87 years	46 children/adults with COM	- *Haemophilus, Staphylococcus, Alloiococcus*	Neeff et al., 2016
MEF and external auditory canal lavage	1–14 years	18 children with OME	- Predominance of *A. otitidis* and *Haemophilus* in MEF - Abundance of *A. otitidis* and *Staphylococcus* in ear canal	Chan et al., 2017
MEF	5 months–2.5 years	79 children with AOM	- Predominance of *S. pneumoniae*, *Haemophilus influenza*, and *Moraxella catarrhalis* - *A. otitidis, Turicella otitidis*, and *Staphylococcus auricularis*	Sillanpää et al., 2017
NP swab	<12 months	65 children with AOM; 74 children without AOM	- *Staphylococcus* and *Sphingobium* associated with decreased risk of AOM development - Infants having AOM showed reduction in numbers of *Corynebacterium*	Chonmaitree et al., 2017
MEF	3 months–14.6 years	55 children with COME	- *Haemophilus, Moraxella, Turicella*	Krueger et al., 2017
MEF and NP swab	<12 years	9 children with gastroesophageal reflux-associated OM; 21 children with OM only	- *Alloiococcus* and *Turicella* in MEF - *Haemophilus* and *Streptococcus* detected in MEF if also present in NP -No difference between reflux and non-reflux microbiota	Boers et al., 2018
MEF and ME aspirates, ear canal swab, nasal swab	0–60 months	93 children with rAOM and 103 healthy controls	- *Haemophilus, Turicella, Alloiococcus, Staphylococcus*	Lappan et al., 2018
MEF (otorrhea) and NP swab	<5 years	94 children with AOM+ grommets	- MEF had less microbial diversity than nasopharynx - There was an abundance of *Corynebacterium* and *Dolosigranulum*	Man et al, 2019a
NP adenoid swabs, palatine tonsillar swabs	15–65 years	14 adults with tonsil/adenoid hyperplasia; 14 adults with secretory OM	- *S. pneumoniae*, *H. influenzae*, and *M. catarrhalis* exclusively in adenoids	Fagö-Olsen et al., 2019
ME, adenoid, and tonsil swab	2–10 years	10 children with OME	- *Fusobacterium, Haemophilus, Neisseria, Porphyromonas*	Johnston et al., 2019

2018). Effective communication between host commensals and host immune cells is essential for both dampening inflammatory cascades when not required and promoting immune responses against invading pathogens threaten stability. The composition and integrity of the microbiome is therefore a key factor in OM pathogenesis, and next-generation sequencing technologies have allowed us to better study gene-environment interactions at this microscopic level. Herein we explore the association between both the NP and ME microbiota and their relationship with invasive, OM-causing pathogens.

Microbiome of the Nasopharynx

Microbiome ecosystems are highly specific to their immediate environment, and their composition can vary widely depending on their anatomic location within the host. For this reason, studies have repeatedly uncovered distinct resident microbiota compositions in the gut, upper respiratory tract, NP, and both the middle as well as the inner ear (Cho and Blaser, 2012). However, AOM research often cites the first step of pathogenesis as bacterial colonization and/or viral disturbance of the NP, from which the disease eventually progresses through the Eustachian tube to the ear. Animal studies have also demonstrated this time course, with initial inoculation of bacteria in the NP followed by eventual migration to the ME, where they may persist for days, weeks, and even months (Cripps and Kyd, 2003; Coticchia et al., 2013; Schilder et al., 2016; Dewan et al., 2019). Thus, analysis of both the ME and NP microbiota is essential for obtaining a comprehensive understanding of the host-pathogen interactions leading to OM development. However, obtaining nasopharyngeal swab samples is often easier, cheaper, and less invasive than samples from the ME. Therefore, the nasopharyngeal microbiome has been more extensively studied than the ME microbiome.

The various morphologies and presentations of OM disease [AOM, recurrent AOM (rAOM), CSOM, OME, and/or COM] is about as varied and dynamic as the bacterial, viral, and fungal microorganisms that contribute to OM pathogenesis. However, the research has well-established the link between rAOM and the major otopathogens *S. pneumoniae*, non-typeable *Haemophilus influenza* (NTHi), and *M. catarrhalis*, and these species are consistently found at higher levels of the NP in studies comparing the microbiota of rAOM and COME cases *versus* healthy controls (Lappan et al., 2018; Walker et al., 2019). Yet the presence of these same organisms, albeit at lower levels, in the controls suggest their potential role as endogenous pathobionts even in the absence of disease. NTHi was found to be the most abundant of three otopathogens in the ME with 18.5% of ME reads attributable to this species, though NTHi was still more abundant in the NP than the ME of rAOM cases. A study sequencing ME fluids/rinses, ear canal swabs, and NP using 16S rRNA observed that *Neisseria* (10.9% RA) was associated with cases of AOM specifically, while *Gemella* (3.2% RA), *Porphyromonas* (3.6% RA), *Alloprevotella* (2.4% RA), and *Fusobacterium* (2.7% RA) were also present in cases but absent (<0.3% RA) in the NP of healthy controls (Lappan et al., 2018). Taken together, the unique presence of these bacteria in rAOM

cases has demonstrated an increased level of microbiota diversity in cases compared to healthy controls.

This finding is somewhat controversial, as many other studies have instead shown increased diversity in healthy controls compared to OM cases, suggesting increased bacterial diversity as a protective factor against invading pathogenic bacteria. For example, one recent study compared the NP microbiota of 3 to 4-year-old patients undergoing tympanostomy for COME and found overall microbiota diversity to be decreased in cases compared to controls, as measured by both a lower Shannon diversity index as well as cluster analyses showing an increased number of profiles dominated by one spp. in the case compared to the control group (Walker et al., 2019). However, the group's analysis still found greater levels of standard otopathogens in cases, as well as a greater level of expected commensal species such as a-hemolytic *Streptococci* and *Lactococci* in controls (Walker et al., 2019). The discrepancy in microbial diversity results may be attributable to the differences in disease processes between acute COM (aCOM) and COME, as the pathogenesis of COME distinctly occurs when bacteria in the biofilm state trigger and maintain a mucoid or serous inflammatory effusion.

Nevertheless, diversity analyses warrant future study, as only about half of all existing studies comparing microbiome diversity between AOM cases *versus* control samples have also found diversity to be higher in healthy controls. Currently, alterations in microbiome diversity are generally attributed to antibiotic use. Studies have explored how microbiota populations are near-permanently altered following the administration and completion of antibiotic regimens, with single opportunistic pathogens initially dominating but new pathogens establishing with time (Kaur et al., 2013). Of note, all current data in the literature are acquired from cross-sectional cohort studies involving diseased and healthy populations; therefore, the temporality of the association cannot be empirically established. Other than chronic antibiotic use, alternative hypotheses to explain the link between increased microbial diversity and increased incidence of disease include the role of synergism in polymicrobial etiologies of OM. Animal-model studies utilizing bacterial and viral co-infections have been shown to significantly increase the incidence of bacterial OM. For example, recent studies demonstrate that the presence of different bacteria not only affects the rates and burden of nasopharyngeal colonization but can also enhance the incidence and severity of OM (Krishnamurthy et al., 2009). Other studies have also noted that *M. catarrhalis* is more likely to be observed within mixed bacterial observations than isolated alone, and that this polymicrobial environment can affect the incidence of *S. pneumoniae* OM (Krishnamurthy et al., 2009; Pichichero, 2009).

As OM disease more commonly affects pediatric populations, studies aiming to discern the distinct microbiome of children have helped uncover differences in the microbiota of healthy children *versus* those suffering from respiratory disease. For example, a prospective birth cohort study featuring 1,616 samples from healthy children and 1,423 samples from children with respiratory disease highlighted microbiome profile groups dominated by *Haemophilus*, *Streptococcus*, *Moraxella*, *Staphylococcus*, *Corynebacterium*, and *Alloiococcus* in 91% of samples (Lang et al., 2019). Importantly, the study noted increased abundances of *Haemophilus* (OR 3.9, p58.4x10−16), *Streptococcus* (OR 3.8, p58.9x10−18), and *Moraxella* (OR 2.1, p53.4x10−12) within the context of disease, while *Staphylococcus*, *Corynebacterium*, and *Alloiococcus* profiles were inversely correlated with disease (OR 0.22/p = 52.5x10−4, OR 0.49/p = 53.8x10−9, and OR 0.25/p = 53.7x10−17, respectively). Meanwhile, an elegant case-control study performed in the Netherlands found similar microbiome compositions within the lower respiratory tract and the NP of children, while also demonstrating that microbial profiles dominated by *H. influenzae/haemolyticus* and *S. pneumoniae* were associated with disease (Man et al., 2019b). The study also identified the importance of a combined classification model (bacterial microbiome, viral microbiome, and external factors such as antibiotic use and breastfeeding) in reliably predicting clinical disease, thereby stressing the multifactorial nature of disease (Man et al., 2019b).

Dolosigranulum and Corynebacterium: The Discovery and Role of Protective Bacteria

While the comparison of NP microbiota generally highlights the unique presence of bacterial species in AOM cases rather than controls, two species of bacteria have instead emerged in increased abundance within the NP microbiome of healthy volunteers. The increased relative abundance of *Dolosigranulum* (16.34% case RA/1.86% control RA) and *Corynebacterium* (13.34% case RA/1.63% control RA) suggests the potential protective role of these bacteria against competing pathological bacteria seeking space and nutrients within the respiratory tract ecosystem (Lappan et al., 2018). The two species were found to correlate together, thereby suggesting a symbiotic relationship potentially mediated by *Dolosigranulum*'s production of lactic acid into the environment. These findings are supported by previous reports of *Dolosigranulum* and *Corynebacterium* predominating the NP of both healthy adults and children, their association with a decreased risk of OM/AOM diagnosis or pneumococcal colonization, and a shorter duration of otorrhea (Laufer et al., 2011; Pettigrew et al., 2012; Bomar et al., 2016; Chonmaitree et al., 2017; Man et al., 2019a). Interestingly, other studies have linked increased *Dolosigranulum* and *Corynebacterium* levels with both breastfeeding and vaginal (compared to *Cesarean*) deliveries, thereby suggesting a mechanism to explain the reported link between breastfeeding and OM resistance (Biesbroek et al., 2014; Biesbroek et al., 2014b).

As described previously, however, the diminished presence of these species in rAOM case cohorts may instead be attributed to rAOM patients' heightened exposure to long-term antibiotics, and studies have indeed found *Dolosigranulum* and *Corynebacterium* relatively depleted in patients with recent history of children using antibiotics (Pettigrew et al., 2012). Antibiotic treatments not only disrupt the host microbiome by temporarily reducing certain bacterial populations, but are also capable of inducing long-term dysbiosis, leaving hosts susceptible to infection as well as atopic and inflammatory diseases (Francino, 2015). Despite this, some experiments have attempted to identify a causal link between the abundance of these two species and the health of the NP. One study uncovered a

mechanism in which *Corynebacterium* species *Corynebacterium accolens* was able to utilize triacylglycerols found on the human skin to assemble free fatty acids that inhibited growth of S. pneumoniae (Bomar et al., 2016). Another report found *Corynebacteria* to eradicate *S. aureus* in healthy nasopharynges of adults, and yet another demonstrated how the introduction of *Corynebacteria* helped mice resist both respiratory syncytial virus and secondary pneumococcal infection, presumably through host immune modulation (Uehara et al., 2000; Kanmani et al., 2017). Preliminary *in vitro* experiments show multiple strains of *Corynebacteria* inhibiting growth of *M. catarrhalis*, and though the mechanism is still unclear, it appears more a result of resource competition than particular bactericidal activity (Lappan, 2019). The potential of these two species as protection against OM-causing bacteria certainly warrants further exploration, especially in light of the potential to develop novel probiotic therapies that would reduce antibiotic use. Other species demonstrating a potential clinical benefit, such as *Haemophilus haemolyticus* and *Streptococcus salivarius*, also present the opportunity for further therapeutic development (Marchisio et al., 2015; Pickering et al., 2016). Future research should incorporate *in vivo* models to incorporate relevant host immune factors, address the impact of environmental factors that modulate host-pathogen interaction (pH, lactic acid, etc.), as well as clinical studies that control for past antibiotic exposure.

Middle Ear Microbiome

The use of nasopharyngeal washes and/or swabs as a less invasive methodical approach for the analysis of host microbiota has produced an abundance of NP microbiome analyses. Meanwhile, studies involving the extraction of ME samples are rare. One study attempting to address this discrepancy by obtaining ME saline washes and ME fluids of children undergoing grommet insertion for rAOM (Lappan et al., 2018). Using 16S rRNA sequencing methods, researchers identified *Alloiococcus otitidis*, *Turicella otitidis*, and *Staphylococcus* spp. as uniquely present in the ME of patients undergoing grommet insertion for severe rAOM diagnoses. The absence of these species in nasopharyngeal swab samples also obtained from the same patients suggests these species' role as normal auricle flora and/or as standard ME pathogens in cases of OM (Lappan et al., 2018). The standard otopathogens *S. pneumoniae*, NTHi, and *M. catarrhalis* were found to be present in the ME of rAOM cases, albeit at lower levels than in the NP, and also in lower levels than the standard ME pathogens previously described. However, their presence in the ME suggests bacterial migratory patterns originating in the oropharynx and extending through the Eustachian tube and into the ME, which is consistent with known OM pathogenesis. Finally, ME diversity was found to be lower than NP diversity in case samples, further establishing the NP's role as a robust reservoir for microorganisms in both the presence and absence of disease (Lappan et al., 2018).

Genetics, The Microbiome, and Otitis Media

As previously described, a healthy microbiome is dependent on effective communication between host commensals and host immune systems, with microbiome composition and diversity in part determined by the host genome. Therefore, genetic defects affecting key biomolecular messengers/signals within this network of crosstalk can have profound effects on the integrity of this balance and therefore the microbiome itself. Within the specific context of OM pathogenesis, researchers have discovered a candidate gene that seems to shape micro-environments favoring particular groups of OM pathobionts. A rare duplication variant of *A2ML1* (α2-macroglobulin-like 1), a gene encoding a middle-ear specific protease inhibitor, has been identified to confer an increased susceptibility to OM (Santos-Cortez et al., 2015). The study incorporated samples from a 250-member intermarried indigenous Filipino community with a 49.6% prevalence of OM, which ultimately identified the *A2ML1* duplication c.2478_2485dupGGCTAAAT (p.Ser829Trpfs*9) as co-segregating with OM with a logarithm of odds (LOD) of 7.5. The study also compared these findings with 123 otitis-prone and 118 non-otitis prone children from the University of Texas Medical Branch (UTMB). Within the Texas cohort, 3 of the 123 otitis-prone children were found to have the same A2ML1 variant, all of whom reported early-onset severe OM that ultimately required tympanostomy tube insertion surgeries.

While this initial study identified the candidate gene and therefore suggested the genetic link to OM susceptibility, follow-up studies uncovered the host microbiome composition as an essential mediator of the association. Using 16S rRNA gene sequencing for microbiome analysis of outer and ME, samples from carriers of the *A2ML1* variant were found to have higher levels of *Fusobacterium, Porphyromonas, Peptostreptococcus, Parvimonas*, and *Bacteroides* compared to wild-type COM cases, and variant carriers also demonstrated an increased alpha-diversity *via* mean Shannon diversity index (Santos-Cortez et al., 2016). Meanwhile, microbiota from wild-type cases were more likely to feature well-known otopathogens such as *Alloiococcus*, *Staphylococcus, Proteus*, and *Haemophilus*. It is important to note that study limitations were characterized by issues of statistical significance due to small sample sizes, as the study cohort included only 16 indigenous Filipino patients, 11 of whom carry the *A2ML1* variant. However, these studies are the first of their kind in that they specifically apply the genome-microbiome interaction to OM disease susceptibility, offering exciting new avenues for further exploration in our field especially.

CONCLUSION AND FUTURE DIRECTIONS

Genetic predisposition to OM has been elucidated through twin studies, linkage association studies, candidate gene approaches, and genome-wide association studies, but further research is necessary to precisely understand the genetic etiology and determine which genes are at play. Through these studies, a number of genes and SNPs have been implicated, including *FBXO11, TGIF1, FUT2, CAPN14, GALNT14, KIF7, CDCA7, SP3,* and *FNDC1,* yet replication of these results has been unsuccessful. One major issue with replication of genetic findings is that it is incredibly difficult to find cohorts with the exact same clinical phenotype for OM. Further, some cohorts

focus on healthy *versus* AOM, others focus on acute OM *vs.* recurrent OM/COME. In addition to these studies, a growing body of research incorporating bioinformatical analysis of host microbiota is beginning to identify how these particular genes influence OM susceptibility through mediation of the host microbiota, such as the *A2ML1* variant's association with *Fusobacterium* and *Bacteroides* anaerobic bacteria within the NP of chronic AOM patients. Meanwhile, studies are comparing resident host microbiota of healthy controls *versus* COM cases within both the NP and the ME/ear canal. While data from these studies reinforce conclusions regarding *S. pneumoniae,* NTHi, and *M. catarrhalis* as primary otopathogens, they also found these three species at higher levels in the NP than the ME, which was instead predominantly colonized with *Staphylococcus* spp., *A. otitidis*, and *T. otitidis.* However, these studies demonstrate the highest level of bacterial diversity in the NP of OM cases when compared to NP and ME bacterial populations within both case and control patients. These findings challenge a series of studies that have found higher bacterial diversity to be associated with healthy microbiota compared to COME microbiota, though the controversy reinforces the need to establish temporality in future studies due to antibiotic use as a potential confounding variable. These studies also have identified higher levels of *Dolosigranulum* and *Corynebacterium* in healthy control NP microbiota, thereby suggesting a potential protective effect that may be harnessed in the form of novel probiotic therapies. This hypothesis must be tested within the context of longitudinal studies, as *Dolosigranulum* and *Corynebacterium* may simply be more susceptible to long-term antibiotic use more prevalent in the aCOM case group. However, as studies highlighting the gene-microbiome interactions are especially new and offer the greatest potential in the coming years, we anticipate the expansion of new insights that may be applicable to the development of novel probiotic therapies for OM.

AUTHOR CONTRIBUTIONS

All the authors listed contributed intellectually in writing of the manuscript and approved the final version of the manuscript for publication.

FUNDING

Dr. Liu's Laboratory is supported by R01 DC005575, R01DC017264, T32 DC015995, and R01 DC012115 grants from the National Institutes of Health/National Institute on Deafness and Other Communication Disorders.

ACKNOWLEDGMENTS

We are thankful to Dr. Valerie Gramling for critical reading of the manuscript.

REFERENCES

Ahmed, S., Shapiro, N. L., and Bhattacharyya, N. (2014). Incremental health care utilization and costs for acute otitis media in children. *Laryngoscope.* 124 (1), 301–305. doi: 10.1002/lary.24190

Allen, E. K., Chen, W. M., Weeks, D. E., Chen, F., Hou, X., Mattos, J. L., et al. (2013). A genome-wide association study of chronic otitis media with effusion and recurrent otitis media identifies a novel susceptibility locus on chromosome 2. *J. Assoc. Res. Otolaryngol.* 14 (6), 791–800. doi: 10.1007/s10162-013-0411-2

Allen, E. K., Manichaikul, A., Chen, W. M., Rich, S. S., Daly, K. A., and Sale, M. M. (2014). Evaluation of replication of variants associated with genetic risk of otitis media. *PloS One* 9 (8), e104212. doi: 10.1371/journal.pone.0104212

Awany, D., Allali, I., Dalvie, S., Hemmings, S., Mwaikono, K. S., Thomford, N. E., et al. (2019). Host and microbiome genome-wide association studies: current state and challenges. *Front. Genet.* 9, 637. doi: 10.3389/fgene.2018.00637

Aydin, Ö., Nieuwdorp, M., and Gerdes, V. (2018). The gut microbiome as a target for the treatment of type 2 diabetes. *Curr. Diabetes Rep.* 18 (8), 55. doi: 10.1007/s11892-018-1020-6

Bardach, A., Ciapponi, A., Garcia-Marti, S., Glujovsky, D., Mazzoni, A., Fayad, A., et al. (2011). Epidemiology of acute otitis media in children of Latin America and the Caribbean: a systematic review and meta-analysis. *Int. J. Pediatr. Otorhinolaryngol* 75, 1062–1070. doi: 10.1016/j.ijporl.2011.05.014

Bhutta, M. F., Lambie, J., Hobson, L., Goel, A., Hafrén, L., Einarsdottir, E., et al. (2017). A mouse-to-man candidate gene study identifies association of chronic otitis media with the loci TGIF1 and FBXO11. *Sci. Rep.* 7 (1), 12496. doi: 10.1038/s41598-017-12784-8

Bhutta, M. F., Cheeseman, M. T., Herault, Y., Yu, Y. E., and Brown, S. D. (2013). Surveying the Down syndrome mouse model resource identifies critical regions responsible for chronic otitis media. *Mamm. Genome* 24, 439–45. doi: 10.1007/s00335-013-9475-x

Bhutta, M. F. (2014). Epidemiology and pathogenesis of otitis media: construction of a phenotype landscape. *Audiol. Neurotol.* 19 (3), 210–223. doi: 10.1159/000358549

Biesbroek, G., Bosch, A., Wang, X., Keijser, B., Veenhoven, R., and Sanders, E. (2014a). The impact of breastfeeding on nasopharyngeal microbial communities in infants. *Am. J. Respir. Crit. Care Med.* 190 (3), 298–308. doi: 10.1164/rccm.201401-0073OC

Biesbroek, G., Tsivtsivadze, E., Sanders, E., Montijn, R., Veenhoven, R., Keijser, B., et al. (2014b). Early respiratory microbiota composition determines bacterial succession patterns and respiratory health in Children. *Am. J. Respir. Crit. Care Med.* 190 (11), 1283–1292. doi: 10.1164/rccm.201407-1240OC

Blekhman, R., Goodrich, J. K., Huang, K., Sun, Q., Bukowski, R., Bell, J. T., et al. (2015). Host genetic variation impacts microbiome composition across human body sites. *Genome Biol.* 16 (1), 191. doi: 10.1186/s13059-015-0759-1

Boers, S. A., de Zeeuw, M., Jansen, R., van der Schroeff, M. P., van Rossum, A. M. C., Hays, J. P., et al. (2018). Characterization of the nasopharyngeal and middle ear microbiota in gastroesophageal reflux-prone versus gastroesophageal reflux non-prone children. *Eur. J. Clin. Microbiol. Infect. Dis.* 37 (5), 851–857. doi: 10.1007/s10096-017-3178-2

Bomar, L., Brugger, S., Yost, B., Davies, S., and Lemon, K. (2016). Corynebacterium accolens releases antipneumococcal free fatty acids from human nostril and skin surface triacylglycerols. *mBio.* 7 (1), e01725–e01715. doi: 10.1128/mBio.01725-15

Bonder, M. J., Kurilshikov, A., Tigchelaar, E. F., Mujagic, Z., Imhann, F., Vich, A., et al. (2016). The effect of host genetics on the gut microbiome. *Nat. Genet.* 48 (11), 1407–1412. doi: 10.1038/ng.3663

Bondy, J., Berman, S., Glazner, J., and Lezotte, D. (2000). Direct expenditures related to otitis media diagnoses: extrapolations from a pediatric Medicaid cohort. *Pediatrics.* 105 (6), E72. doi: 10.1542/peds.105.6.e72

Broides, A., Dagan, R., Greenberg, D., Givon-Lavi, N., and Leibovitz, E. (2009). Acute otitis media caused by Moraxella catarrhalis: epidemiologic and clinical characteristics. *Clin. Infect. Dis.* 49 (11), 1641–1647. doi: 10.1086/647933

Caruso, R., Mathes, T., Martens, E. C., Kamada, N., Nusrat, A., Inohara, N., et al. (2019). A specific gene-microbe interaction drives the development of Crohn's disease–like colitis in mice. *Sci. Immunol.* 4 (34), eaaw4341. doi: 10.1126/sciimmunol.aaw4341

Casey, J. R., Adlowitz, D. G., and Pichichero, M. E. (2010). New patterns in the otopathogens causing acute otitis media six to eight years after introduction of pneumococcal conjugate vaccine. *Pediatr. Infect. Dis. J.* 29 (4), 304–309. doi: 10.1097/INF.0b013e3181c1bc48

Casey, J. R., Kaur, R., Friedel, V. C., and Pichichero, M. E. (2013). Acute otitis media otopathogens during 2008 to 2010 in Rochester, New York. *Pediatr. Infect. Dis. J.* 32 (8), 805–809. doi: 10.1097/INF.0b013e31828d9acc

Casselbrant, M. L., Mandel, E. M., Fall, P. A., Rockette, H. E., Kurs-Lasky, M., Bluestone, C. D., et al. (1999). The heritability of otitis media: a twin and triplet study. *JAMA*. 282 (22), 2125–2130. doi: 10.1001/jama.282.22.2125

Casselbrant, M. L., Mandel, E. M., Rockette, H. E., Kurs-Lasky, M., Fall, P. A., Bluestone, C. D., et al. (2004). The genetic component of middle ear disease in the first 5 years of life. *Arch. Otolaryngol. Head Neck Surg.* 130 (3), 273–278. doi: 10.1001/archotol.130.3.273

Casselbrant, M. L., Mandel, E. M., Jung, J., Ferrell, R. E., Tekely, K., Szatkiewicz, J. P., et al. (2009). Otitis media: a genome-wide linkage scan with evidence of susceptibility loci within the 17q12 and 10q22.3 regions. *BMC Med. Genet.* 10, 85. doi: 10.1186/1471-2350-10-85

Chan, C. L., Wabnitz, D., Bardy, J. J., Bassiouni, A., Wormald, P. J., Vreugde, S., et al. (2016). The microbiome of otitis media with effusion. *Laryngoscope* 126 (12), 2844–2851. doi: 10.1002/lary.26128

Chan, C. L., Wabnitz, D., Bassiouni, A., Wormald, P., Vreugde, S., and Psaltis, A. J. (2017). Identification of the Bacterial Reservoirs for the Middle Ear Using Phylogenic Analysis. *JAMA Otolaryngol. Head Neck Surg.* 143 (2), 155–161. doi: 10.1001/jamaoto.2016.3105

Chen, W. M., Allen, E. K., Mychaleckyj, J. C., Chen, F., Hou, X., Rich, S. S., et al. (2011). Significant linkage at chromosome 19q for otitis media with effusion and/or recurrent otitis media (COME/ROM). *BMC Med. Genet.* 12, 124. doi: 10.1186/1471-2350-12-124

Chen, J., Ingham, N., Clare, S., Raisen, C., Vancollie, V. E., Ismail, O., et al. (2013). Mcph1-deficient mice reveal a role for MCPH1 in otitis media. *PloS One* 8 (3), e58156. doi: 10.1371/journal.pone.0058156

Cho, I., and Blaser, M. J. (2012). The human microbiome: at the interface of health and disease. *Nat. Rev. Genet.* 13 (4), 260–270. doi: 10.1038/nrg3182

Chonmaitree, T., Revai, K., Grady, J. J., Clos, A., Patel, J. A., Nair, S., et al. (2008). Viral upper respiratory tract infection and otitis media complication in young children. *Clin. Infect. Dis.* 46 (6), 815–823. doi: 10.1086/528685

Chonmaitree, T., Trujillo, R., Jennings, K., Alvarez-Fernandez, P., Patel, J. A., Loeffelholz, M. J., et al. (2016). Acute otitis media and other complications of viral respiratory infection. *Pediatrics* 137 (4), e20153555. doi: 10.1542/peds.2015-3555

Chonmaitree, T., Jennings, K., Golovko, G., Khanipov, K., Pimenova, M., Patel, J., et al. (2017). Nasopharyngeal microbiota in infants and changes during viral upper respiratory tract infection and acute otitis media. *PloS One* 12 (7), e0180630. doi: 10.1371/journal.pone.018063

Coticchia, J. M., Chen, M., Sachdeva, L., and Mutchnick, S. (2013). New paradigms in the pathogenesis of otitis media in children. *Front. Pediatr.* 1, 52. doi: 10.3389/fped.2013.00052

Cripps, A. W., and Kyd., J. M. (2003). Bacterial otitis media: Current vaccine development strategies. *Immunol. Cell Biol.* 81 (1), 46–51. doi: 10.1046/j.08018-9641.2002.01141.x

Daly, K. A., Brown, W. M., Segade, F., Bowden, D. W., Keats, B. J., Lindgren, B. R., et al. (2004). Chronic and recurrent otitis media: a genome scan for susceptibility loci. *Am. J. Hum. Genet.* 75 (6), 988–997. doi: 10.1086/426061

Dewan, K. K., Taylor-Mulneix, D. L., Campos, L. L., Skarlupka, A. L., Wagner, S. M., Ryman, V. E., et al. (2019). A model of chronic, transmissible otitis media in mice. *PloS Pathog.* 15 (4), e1007696. doi: 10.1371/journal.ppat.1007696

Fagö-Olsen, H., Dines, L. M., Sørensen, C. H., and Jensen, A. (2019). The adenoids but not the palatine tonsils serve as a reservoir for bacteria associated with secretory otitis media in small children. *mSystems* 4 (1), e00169–e00118. doi: 10.1128/mSystems.00169-18

Ferreira, M. A. (2004). Linkage analysis: principles and methods for the analysis of human quantitative traits. *Twin Res.* 7 (5), 513–530. doi: 10.1375/twin.7.5.513

Francino, M. P. (2015). Antibiotics and the human gut microbiome: dysbioses and accumulation of resistances. *Front. Microbiol.* 6, 1543. doi: 10.3389/fmicb.2015.01543

Gates, G. A. (1996). Cost-effectiveness considerations in otitis media treatment. *Otolaryngol. Head Neck Surg.* 114 (4), 525–530. doi: 10.1016/S0194-5998(96)70243-7

Gessner, B. D., Gillingham, M. B., Wood, T., and Koeller, D. M. (2013). Association of a genetic variant of carnitine palmitoyltransferase 1A with infections in Alaska Native children. *J. Pediatr.* 163 (6), 1716–1721. doi: 10.1016/j.jpeds.2013.07.010

Goodrich, J. K., Waters, J. L., Poole, A. C., Sutter, J. L., Koren, O., Blekhman, R., et al. (2014). Human genetics shape the gut microbiome. *Cell* 159 (4), 789–799. doi: 10.1016/j.cell.2014.09.053

Hafren, L., Kentala, E., Jarvinen, T. M., Leinonen, E., Onkamo, P., Kere, J., et al. (2012). Genetic background and the risk of otitis media. *Int. J. Pediatr. Otorhinolaryngol.* 76 (1), 41–44. doi: 10.1016/j.ijporl.2011.09.026

Hafren, L., Einarsdottir, E., Kentala, E., Hammaren-Malmi, S., Bhutta, M. F., MacArthur, C. J., et al. (2015). Predisposition to childhood otitis media and genetic polymorphisms within the Toll-like receptor 4 (TLR4) locus. *PloS One* 10 (7), e0132551. doi: 10.1371/journal.pone.0132551

Hall, A. B., Tolonen, A. C., and Xavier, R. J. (2017). Human genetic variation and gut microbiome disease. *Nat. Rev. Genet.* 18 (11), 690–699. doi: 10.1038/nrg.2017.63

Han, F., Yu, H., Li, P., Zhang, J., Tian, C., Li, H., et al. (2012). Mutation in Phex gene predisposes BALB/c-Phex(Hyp-Duk)/Y mice to otitis media. *PloS One* 7 (9), e43010. doi: 10.1371/journal.pone.0043010

Harmes, K. M., Blackwood, R. A., Burrows, H. L., Cooke, J. M., Harrison, R. V., and Passamani, P. P. (2013). Otitis media: Diagnosis and treatment. *Am. Fam. Physician* 88 (7), 435–440.

Hernandez, M., Leichtle, A., Pak, K., Webster, N. J., Wasserman, S. I., and Ryan, A. F. (2015). The transcriptome of a complete episode of acute otitis media. *BMC Genomics* 16 (1), 259. doi: 10.1186/s12864-015-1475-7

Igartua, C., Davenport, E. R., Gilad, Y., Nicolae, D. L., Pinto, J., and Ober, C. (2017). Host genetic variation in mucosal immunity pathways influences the upper airway microbiome. *Microbiome* 5 (1), 16. doi: 10.1186/s40168-016-0227-5

Ilia, S., Goulielmos, G. N., Samonis, G., and Galanakis, E. (2014). Polymorphisms in IL-6, IL-10, TNF-alpha, IFN-gamma and TGF-beta1 genes and susceptibility to acute otitis media in early infancy. *Pediatr. Infect. Dis. J.* 33 (5), 518–521. doi: 10.1097/INF.0000000000000229

Imhann, F., Vila, A. V., Bonder, M. J., Fu, J., Gevers, D., Visschedijk, M. C., et al. (2018). Interplay of host genetics and gut microbiota underlying the onset and clinical presentation of inflammatory bowel disease. *Gut* 67 (1), 108–119. doi: 10.1136/gutjnl-2016-312135

Jervis-Bardy, J., Leong, L. E., Marri, S., Smith, R. J., Choo, J. M., Smith-Vaughan, H. C., et al. (2015). Deriving accurate microbiota profiles from human samples with low bacterial content through post-sequencing processing of illumina miSeq data. *Microbiome* 3, 19. doi: 10.1186/s40168-015-0083-8

Johnston, J., Hoggard, M., Biswas, K., Astudillo-García, C., Radcliff, F. J., Mahadevan, M., et al. (2019). Pathogen reservoir hypothesis investigated by analyses of the adenotonsillar and middle ear microbiota. *Int. J. Pediatr. Otorhinolaryngol.* 118, 103–109. doi: 10.1016/j.ijporl.2018.12.030

Kanmani, P., Clua, P., Vizoso-Pinto, M. G., Rodriguez, C., Alvarez, S., Melnikov, V., et al. (2017). Respiratory commensal bacteria Corynebacterium pseudodiphtheriticum improves resistance of infant mice to respiratory syncytial virus and streptococcus pneumoniae superinfection. *Front. Microbiol.* 8, 1613. doi: 10.3389/fmicb.2017.01613

Kaur, R., Adlowitz, D. G., Casey, J. R., Zeng, M., and Pichichero, M. E. (2010). Simultaneous assay for four bacterial species including Alloiococcus otitidis using multiplex- PCR in children with culture negative acute otitis media. *Pediatr. Infect. Dis. J.* 29 (8), 741–745. doi: 10.1097/INF.0b013e3181d9e639

Kaur, R., Casey, J. R., and Pichichero, M. E. (2013). Relationship with original pathogen in recurrence of acute otitis media after completion of amoxicillin/clavulanate: bacterial relapse or new pathogen. *Pediatr. Infect. Dis. J.* 32 (11), 1159–1162. doi: 10.1097/INF.0b013e31829e3779

Kaur, R., Casey, J. R., and Pichichero, M. E. (2016). Emerging Streptococcus pneumoniae strains colonizing the nasopharynx in children after 13-valent Pneumococcal conjugate vaccination in comparison to the 7-valent era,

2006-2015. *Pediatr. Infect. Dis. J.* 35 (8), 901–906. doi: 10.1097/INF.0000000000001206

Kaur, R., Morris, M., and Pichichero, M. E. (2017). Epidemiology of acute otitis media in the postpneumococcal conjugate vaccine era. *Pediatrics* 140 (3), e20170181. doi: 10.1542/peds.2017-0181

Kerschner, J. E., Hong, W., Taylor, S. R., Kerschner, J. A., Khampang, P., Wrege, K. C., et al. (2013). A novel model of spontaneous otitis media with effusion (OME) in the Oxgr1 knock-out mouse. *Int. J. Pediatr. Otorhinolaryngol.* 77 (1), 79–84. doi: 10.1016/j.ijporl.2012.09.037

Kozyrskyj, A., Klassen, T. P., Moffatt, M., and Harvey, K. (2010). Short-course antibiotics for acute otitis media. *Cochrane Database Syst. Rev.* 9, CD001095. doi: 10.1002/14651858.CD001095.pub2

Krishnamurthy, A., McGrath, J., Cripps, A. W., and Kyd, J. M. (2009). The incidence of Streptococcus pneumoniae otitis media is affected by the polymicrobial environment particularly Moraxella catarrhalis in a mouse nasal colonisation model. *Microbes Infect.* 11 (5), 545–553. doi: 10.1016/j.micinf.2009.03.001

Krueger, A., Val, S., Pérez-Losada, M., Panchapakesan, K., Devaney, J., Duah, V., et al. (2017). Relationship of the middle ear effusion microbiome to secretory mucin production in pediatric patients with chronic otitis media. *Pediatr. Infect. Dis. J.* 36 (7), 635–640. doi: 10.1097/INF.0000000000001493

Kurilshikov, A., Cisca, W., Fu, J., and Zhernakova, A. (2017). Host genetics and gut microbiome: challenges and perspectives. *Trends Immunol.* 38 (9), 633–647. doi: 10.1016/j.it.2017.06.003

Kvaerner, K. J., Tambs, K., Harris, J. R., and Magnus, P. (1997). Distribution and heritability of recurrent ear infections. *Ann. Otol. Rhinol. Laryngol.* 106 (8), 624–632. doi: 10.1177/000348949710600802

Lamas, B., Richard, M. L., Leducq, V., Pham, H. P., Michel, M. L., Da Costa, G., et al. (2016). CARD9 impacts colitis by altering gut microbiota metabolism of tryptophan into aryl hydrocarbon receptor ligands. *Nat. Med.* 22 (6), 598–605. doi: 10.1038/nm.4102

Lang, A., Holt, K. E., Inouye, M., Holt, P. G., Teo, S. M., Tang, H. H., et al. (2019). Nasopharyngeal microbiome during health and illness in early life. *J. Allergy Clin. Immunol.* 141 (2), AB109. doi: 10.1016/j.jaci.2017.12.348

Lao, O., Lu, T. T., Nothnagel, M., Junge, O., Freitag-Wolf, S., Caliebe, A., et al. (2008). Correlation between genetic and geographic structure in Europe. *Curr. Biol.* 18 (16), 1241–1248. doi: 10.1016/j.cub.2008.07.049

Lappan, R., Imbrogno, K., Sikazwe, C., Anderson, D., Mok, D., Coates, H., et al. (2018). A microbiome case-control study of recurrent acute otitis media identified potentially protective bacterial genera. *BMC Microbiol.* 18 (1), 13. doi: 10.1186/s12866-018-1154-3

Lappan, R. J. (2019). Using omics technologies to understand pathogenesis and seek alternative therapies for otitis media in children. doi.org/10.26182/5cf73acaee262.

Laufer, A., Metlay, J., Gent, J., Fennie, K., Kong, Y., and Pettigrew, M. (2011). Microbial communities of the upper respiratory tract and otitis media in children. *mBio* 2 (1), e00245–e00 10. doi: 10.1128/mBio.00245-10

Lee, S., Lee, E., Park, Y., and Hong, S. (2018). Microbiome in the gut-skin axis in atopic dermatitis. *Allergy Asthma Immunol. Res.* 10 (4), 354–362. doi: 10.4168/aair.2018.10.4.354

Liang, D., Leung, R., Guan, W., and Au, W. (2018). Involvement of gut microbiome in human health and disease: brief overview, knowledge gaps, and research opportunities. *Gut Pathog.* 10, 3. doi: 10.1186/s13099-018-0230-4

Lieberthal, A. S., Carroll, A. E., Chonmaitree, T., Ganiats, T. G., Hoberman, A., Jackson, M. A., et al. (2013). The diagnosis and management of acute otitis media. *Pediatrics* 131 (3), e965–e999. doi: 10.1542/peds.2012-3488

Lysaght, A. C., Yuan, Q., Fan, Y., Kalwani, N., Caruso, P., Cunnane, M., et al. (2014). FGF23 deficiency leads to mixed hearing loss and middle ear malformation in mice. *PloS One* 9 (9), e107681. doi: 10.1371/journal.pone.0107681

MacArthur, C. J., Wilmot, B., Wang, L., Schuller, M., Lighthall, J., and Trune, D. (2014). Genetic susceptibility to chronic otitis media with effusion: candidate gene single nucleotide polymorphisms. *Laryngoscope* 124 (5), 1229–1235. doi: 10.1002/lary.24349

Man, W., van Dongen, T., Venekamp, R., Puimakers, V., Chu, M., van Houten, M., et al. (2019a). Respiratory microbiota predicts clinical disease course of acute otorrhea in children with tympanostomy tubes. *Pediatr. Infect. Dis. J.* 38 (6), e116–e125. doi: 10.1097/INF.0000000000002215

Man, W. H., van Houten, M. A., Mérelle, M. E., Vlieger, A. M., Chu, M. L., Jansen, N. J., et al. (2019b). Bacterial and viral respiratory tract microbiota and host characteristics in children with lower respiratory tract infections: a matched case-control study. *Lancet Respir. Med.* 7 (5), 417–426. doi: 10.1016/S2213-2600(18)30449-1

Marchisio, P., Santagati, M., Scillato, M., Baggi, E., Fattizzo, M., Rosazza, C., et al. (2015). Streptococcus salivarius 24SMB administered by nasal spray for the prevention of acute otitis media in otitis-prone children. *Eur. J. Clin. Microbiol. Infect. Dis.* 34 (12), 2377–2383. doi: 10.1007/s10096-015-2491-x

Mittal, R., Lisi, C. V., Gerring, R., Mittal, J., Mathee, K., Narasimhan, G., et al. (2015). Current concepts in the pathogenesis and treatment of chronic suppurative otitis media. *J. Med. Microbiol.* 64, 1103–1116. doi: 10.1099/jmm.0.000155

Mittal, R., Parrish, J. M., Soni, M., Mittal, J., and Mathee, K. (2018). Microbial otitis media: recent advancements in treatment, current challenges and opportunities. *J. Med. Microbiol.* 67 (10), 1417–1425. doi: 10.1099/jmm.0.000810

Mittal, R., Debs, L. H., Patel, A. P., Nguyen, D., Blackwelder, P., Yan, D., et al. (2019). Otopathogenic Staphylococcus aureus invades human middle ear epithelial cells primarily through cholesterol dependent pathway. *Sci Rep.* 9, 10777. doi: 10.1038/s41598-019-47079-7

Neeff, M., Biswas, K., Hoggard, M., Taylor, M. W., and Douglas, R. (2016). Molecular microbiological profile of chronic suppurative otitis media. *J. Clin. Microbiol.* 54 (10), 2538–2546. doi: 10.1128/JCM.01068-16

Nokso-Koivisto, J., Chonmaitree, T., Jennings, K., Matalon, R., Block, S., and Patel, J. A. (2014). Polymorphisms of immunity genes and susceptibility to otitis media in children. *PloS One* 9 (4), e93930. doi: 10.1371/journal.pone.0093930

Pettigrew, M. M., Gent, J. F., Pyles, R. B., Miller, A. L., Nokso-Koivisto, J., and Chonmaitree, T. (2011). Viral-bacterial interactions and risk of acute otitis media complicating upper respiratory infection. *J. Clin. Microbiol.* 49 (11), 3750–3755. doi: 10.1128/JCM.01186-11

Pettigrew, M., Laufer, A., Gent, J., Kong, Y., Fennie, K., and Metlay, J. (2012). Respiratory tract microbial communities, acute otitis media pathogens, and antibiotic use in healthy and sick children. *Appl. Environ. Microbiol.* 78 (17), 6262–6270. doi: 10.1128/AEM.01051-12

Pichichero, M. E., Marsocci, S. M., Murphy, M. L., Hoeger, W., Francis, A. B., and Green, J. L. (2001). A prospective observational study of 5-, 7-, and 10-day antibiotic treatment for acute otitis media. *Otolaryngol. Head Neck Surg.* 124 (4), 381–387. doi: 10.1067/mhn.2001.114311

Pichichero, M. E., Casey, J. R., Hoberman, A., and Schwartz, R. (2008). Pathogens causing recurrent and difficult-to-treat acute otitis media, 2003-2006. *Clin. Pediatr. (Phila)* 47 (9), 901–906. doi: 10.1177/0009922808319966

Pichichero, M. (2009). Widening differences in acute otitis media study populations. *Clin. Infect. Dis.* 49 (11), 1648–1649. doi: 10.1086/647934

Pickering, J., Prosser, A., Corscadden, K., de Gier, C., Richmond, P., Zhang, G., et al. (2016). *Haemophilus haemolyticus* Interaction with Host Cells Is Different to Nontypeable *Haemophilus influenzae* and Prevents NTHi Association with Epithelial Cells. *Front. Cell Infect. Microbiol.* 6, 50. doi: 10.3389/fcimb.2016.00050

Rovers, M., Haggard, M., Gannon, M., Koeppen-Schomerus, G., and Plomin, R. (2002). Heritability of symptom domains in otitis media: a longitudinal study of 1,373 twin pairs. *Am. J. Epidemiol.* 155 (10), 958–964. doi: 10.1093/aje/155.10.958

Rye, M. S., Wiertsema, S. P., Scaman, E. S., Oommen, J., Sun, W., Francis, R. W., et al. (2011). FBXO11, a regulator of the TGFbeta pathway, is associated with severe otitis media in Western Australian children. *Genes Immun.* 12 (5), 352–359. doi: 10.1038/gene.2011.2

Rye, M. S., Warrington, N. M., Scaman, E. S., Vijayasekaran, S., Coates, H. L., Anderson, D., et al. (2012). Genome-wide association study to identify the genetic determinants of otitis media susceptibility in childhood. *PloS One* 7 (10), e48215. doi: 10.1371/journal.pone.0048215

Rye, M. S., Wiertsema, S. P., Scaman, E. S., Thornton, R., Francis, R. W., Vijayasekaran, S., et al. (2013). Genetic and functional evidence for a role for SLC11A1 in susceptibility to otitis media in early childhood in a Western Australian population. *Infect. Genet. Evol.* 16, 411–418. doi: 10.1016/j.meegid.2013.03.023

Sale, M. M., Chen, W. M., Weeks, D. E., Mychaleckyi, J. C., Hou, X., Marion, M., et al. (2011). Evaluation of 15 functional candidate genes for association with chronic otitis media with effusion and/or recurrent otitis media (COME/ROM). *PloS One* 6 (8), e22297. doi: 10.1371/journal.pone.0022297

Santos-Cortez, R. L. P., Chiong, C. M., Reyes-Quintos, M. R. T., Tantoco, M. L. C., Wang, X., Acharya, A., et al. (2015). Rare A2ML1 variants confer susceptibility to otitis media. *Nat. Genet.* 47 (8), 917–920. doi: 10.1038/ng.33447

Santos-Cortez, R. L. P., Hutchinson, D. S., Ajami, N. J., Reyes-Quintos, M. R. T., Tantoco, M. L. C., Labra, P. J., et al. (2016). Middle ear microbiome differences in indigenous filipinos with chronic otitis media due to a duplication in the A2ML1 gene. *Infect. Dis. Poverty* 5, 97. doi: 10.1186/s40249-016-0189-7

Santos-Cortez, R. L. P., Chiong, C. M., Frank, D. N., Ryan, A. F., Giese, A. P. J., Roberts, T. B., et al. (2018). FUT2 variants confer susceptibility to familial otitis media. *Am. J. Hum. Genet.* 103 (5), 679–690. doi: 10.1016/j.ajhg.2018.09.010

Schilder, A. G., Chonmaitree, T., Cripps, A. W., Rosenfeld, R. M., Casselbrant, M. L., Haggard, M. P., et al. (2016). Otitis media. *Nat. Rev. Dis. Primers* 2, 16063. doi: 10.1038/nrdp.2016.63

Segade, F., Daly, K. A., Allred, D., Hicks, P. J., Cox, M., Brown, M., et al. (2006). Association of the FBXO11 gene with chronic otitis media with effusion and recurrent otitis media: the Minnesota COME/ROM Family Study. *Arch. Otolaryngol. Head Neck Surg.* 132 (7), 729–733.

Shin, S., Koh, S., Woo, C., and Lim, J. (2014). PAI-1 inhibits development of chronic otitis media and tympanosclerosis in a mouse model of otitis media. *Acta Otolaryngol.* 134 (12), 1231–1238. doi: 10.3109/00016489.2014.940554

Siddiq, S., and Grainger, J. (2015). The diagnosis and management of acute otitis media: American Academy of Pediatrics Guidelines 2013. *Arch. Dis. Child Educ. Pract. Ed.* 100, 193–197.

Sillanpää, S., Kramna, L., Oikarinen, S., Sipilä, M., Rautiainen, M., Aittoneiemi, J., et al. (2017). Next-generation sequencing combined with specific PCR assays to determine the bacterial 16S rRNA gene profiles of middle ear fluid collected from children with acute otitis media. *mSphere* 2 (2), e00006–e00017. doi: 10.1128/mSphere.00006-17

Sokolowska, M., Frei, R., Lunjani, N., Akdis, C. A., and O'Mahony., L. (2018). Microbiome and asthma. *Asthma Res. Pract.* 4, 1. doi: 10.1186/s40733-017-0037-y

Tam, V., Patel, N., Turcotte, M., Bosse, Y., Pare, G., and Meyre, D. (2019). Benefits and limitations of genome-wide association studies. *Nat. Rev. Genet.* 20 (8), 467–484. doi: 10.1038/s41576-019-0127-1

Tateossian, H., Morse, S., Parker, A., Mburu, P., Warr, N., Acevedo-Arozena, A., et al. (2013). Otitis media in the Tgif knockout mouse implicates TGFbeta signaling in chronic middle ear inflammatory disease. *Hum. Mol. Genet.* 22 (13), 2553–2565. doi: 10.1093/hmg/ddt103

Teo, S. M., Mok, D., Pham, K., Kusel, M., Serralha, M., Troy, N., et al. (2015). The infant nasopharyngeal microbiome impacts severity of lower respiratory infection and risk of asthma development. *Cell Host Microbe* 17 (5), 704–715. doi: 10.1016/j.chom.2015.03.008

Tong, H. H., Lambert, G., Li, Y. X., Thurman, J. M., Stahl, G. L., Douthitt, K., et al. (2014). Deletion of the complement C5a receptor alleviates the severity of acute pneumococcal otitis media following influenza A virus infection in mice. *PloS One* 9 (4), e95160. doi: 10.1371/journal.pone.0095160

Tremlett, H., Bauer, K., Appel-Cresswell, S., Finlay, B., and Waubant, E. (2017). The gut microbiome in human neurological disease: a review. *Ann. Neurol.* 81 (3), 369–382. doi: 10.1002/ana.24901

Turnbaugh, P. J., Hamady, M., Yatsunenko, T., Cantarel, B. L., Duncan, A., Ley, R. E., et al. (2009). A core gut microbiome in obese and lean twins. *Nature* 457 (7228), 480–484. doi: 10.1038/nature07540

Turpin, W., Espin-Garcia, O., Xu, W., Silverber, M. S., Kevans, D., Smith, M. I., et al. (2016). Association of host genome with intestinal microbial compositionin a large healthy cohort. *Nat. Genet.* 48 (11), 1413–1417. doi: 10.1038/ng.3693

Uehara, Y., Nakama, H., Agematsu, K., Uchida, M., Kawakami, Y., Fattah, A. S. M., et al. (2000). Bacterial interference among nasal inhabitants: eradication of *Staphylococcus aureus* from nasal cavities by artificial implantation of *Corynebacterium* sp. *J. Hosp. Infect.* 44 (2), 127–133. doi: 10.1053/jhin.1999.0680

Van Ingen, G., Li, J., Goedegebure, A., Pandey, R., Li, Y. R., March, M. E., et al. (2016). Genome-wide association study for acute otitis media in children identifies FNDC1 as disease contributing gene. *Nat. Commun.* 7, 12792. doi: 10.1038/ncomms12792

Walker, R. E., Walker, C. G., Camargo, C. A., Bartley, J., Flint, D., Thompson, J. M. D., et al. (2019). Nasal microbial composition and chronic otitis media with effusion: A case-control study. *PloS One* 14 (2), e0212473. doi: 10.1371/journal/pone/0212473

Wang, W., Zhou, A., Zhang, X., Xiang, Y., Huang, Y., Wang, L., et al. (2014). Interleukin 17A promotes pneumococcal clearance by recruiting neutrophils and inducing apoptosis through a p38 mitogen-activated protein kinase dependent mechanism in acute otitis media. *Infect. Immun.* 82 (6), 2368–2377. doi: 10.1128/IAI.00006-14

Wang, J., Thingholm, L. B., Skiecevičienė, J., Rausch, P., Kummen, M., Hov, J. R., et al. (2016). Genome-wide association analysis identifies variation in vitamin D receptor and other host factors influencing the gut microbiota. *Nat. Genet.* 48 (11), 1396–1406. doi: 10.1038/ng.3695

Weissbrod, O., Rothschild, D., Barkan, E., and Segal, E. (2018). Host genetics and microbiome associations through the lens of genome wide association studies. *Curr. Opin. Microbiol.* 44, 9–19. doi: 10.1016/j.mib.2018.05.003

Yatsunenko, T., Rey, F. E., Manary, M. J., Trehan, I., Dominguez-Bello, M. G., Contreras, M., et al. (2012). Human gut microbiome viewed across age and geography. *Nature* 486 (7402), 222–227. doi: 10.1038/nature11053

Yoshimura, A., Wakabayashi, Y., and Mori, T. (2010). Cellular and molecular basis for the regulation of inflammation by TGF-beta. *J. Biochem.* 147 (6), 781–792. doi: 10.1093/jb/mvq043

Zhang, Y., Yu, H., Xu, M., Han, F., Tian, C., Kim, S., et al. (2012). Pathological features in the LmnaDhe/+ mutant mouse provide a novel model of human otitis media and laminopathies. *Am. J. Pathol.* 181 (3), 761–774. doi: 10.1016/j.ajpath.2012.05.031

Conflict of Interest: The authors declare that the research was conducted in the absence of any commercial or financial relationships that could be construed as a potential conflict of interest.

frontiers in Genetics

ORIGINAL RESEARCH
published: 17 January 2020
doi: 10.3389/fgene.2019.01352

Identification of Novel Genes and Biological Pathways That Overlap in Infectious and Nonallergic Diseases of the Upper and Lower Airways Using Network Analyses

*Erin E. Baschal[1], Eric D. Larson[1], Tori C. Bootpetch Roberts[1], Shivani Pathak[1], Gretchen Frank[1], Elyse Handley[1,2], Jordyn Dinwiddie[1,2], Molly Moloney[1], Patricia J. Yoon[1,2], Samuel P. Gubbels[1], Melissa A. Scholes[1,2], Stephen P. Cass[1], Herman A. Jenkins[1], Daniel N. Frank[3], Ivana V. Yang[3], David A. Schwartz[3], Vijay R. Ramakrishnan[1] and Regie Lyn P. Santos-Cortez[1]**

[1] Department of Otolaryngology, School of Medicine, University of Colorado Anschutz Medical Campus, Aurora, CO, United States, [2] Department of Pediatric Otolaryngology, Children's Hospital Colorado, Aurora, CO, United States, [3] Department of Medicine, School of Medicine, University of Colorado Anschutz Medical Campus, Aurora, CO, United States

OPEN ACCESS

Edited by:
Prashant Kumar Verma,
All India Institute of Medical Sciences, Rishikesh, India

Reviewed by:
Anand Kumar Andiappan,
Singapore Immunology Network (A*STAR), Singapore
Theodora Katsila,
National Hellenic Research Foundation, Greece

***Correspondence:**
Regie Lyn P. Santos-Cortez
regie.santos-cortez@cuanschutz.edu

Specialty section:
This article was submitted to Genetic Disorders, a section of the journal Frontiers in Genetics

Received: 26 July 2019
Accepted: 10 December 2019
Published: 17 January 2020

Citation:
Baschal EE, Larson ED, Bootpetch Roberts TC, Pathak S, Frank G, Handley E, Dinwiddie J, Moloney M, Yoon PJ, Gubbels SP, Scholes MA, Cass SP, Jenkins HA, Frank DN, Yang IV, Schwartz DA, Ramakrishnan VR and Santos-Cortez RLP (2020) Identification of Novel Genes and Biological Pathways That Overlap in Infectious and Nonallergic Diseases of the Upper and Lower Airways Using Network Analyses. Front. Genet. 10:1352. doi: 10.3389/fgene.2019.01352

Previous genetic studies on susceptibility to otitis media and airway infections have focused on immune pathways acting within the local mucosal epithelium, and outside of allergic rhinitis and asthma, limited studies exist on the overlaps at the gene, pathway or network level between the upper and lower airways. In this report, we compared [1] pathways identified from network analysis using genes derived from published genome-wide family-based and association studies for otitis media, sinusitis, and lung phenotypes, to [2] pathways identified using differentially expressed genes from RNA-sequence data from lower airway, sinus, and middle ear tissues, in particular cholesteatoma tissue compared to middle ear mucosa. For otitis media, a large number of genes (n = 1,806) were identified as differentially expressed between cholesteatoma and middle ear mucosa, which in turn led to the identification of 68 pathways that are enriched in cholesteatoma. Two differentially expressed genes *CR1* and *SAA1* overlap in middle ear, sinus, and lower airway samples and are potentially novel genes for otitis media susceptibility. In addition, 56 genes were differentially expressed in both tissues from the middle ear and either sinus or lower airways. Pathways that are common in upper and lower airway diseases, whether from published DNA studies or from our RNA-sequencing analyses, include chromatin organization/remodeling, endocytosis, immune system process, protein folding, and viral process. Taken together, our findings from genetic susceptibility and differential tissue expression studies support the hypothesis that the unified airway theory wherein the upper and lower respiratory tracts act as an integrated unit also applies to infectious and nonallergic airway epithelial disease. Our results may be

used as reference for identification of genes or pathways that are relevant to upper and lower airways, whether common across sites, or unique to each disease.

Keywords: cholesteatoma, immune pathways, lower airway, mucosa, networks, otitis media, RNA-sequencing, sinusitis

INTRODUCTION

The unified airway theory proposes that the respiratory tract acts as an integrated unit, from the middle ear through the distant bronchioles (Krouse, 2008). Structurally, the mucosae of the middle ear, nose/sinuses, and lower respiratory tract are highly similar, lined by mostly ciliated epithelium, which is involved in the transport of mucosa and particulate matter. Additionally, bacterial communities in healthy lungs are highly similar to those in the upper respiratory tract (Charlson et al., 2011; Segata et al., 2012; Hanshew et al., 2017). The unified airway model has typically been applied to allergic rhinitis and asthma, with the observations that allergic rhinitis is present in at least 80% of asthma patients, and that asthma is found in up to 40% of patients with allergic rhinitis (Feng et al., 2012; Giavina-Bianchi et al., 2016). In addition, treatment of allergic rhinitis symptoms has been found to improve asthma symptoms and pulmonary function. This is believed to be due to a shared inflammation model, with local inflammatory processes producing systemic mediators that affect disease in other areas of the respiratory tract (Krouse, 2008). Specifically, it has been found that if one area of the airway mucosa is stimulated with antigen, within hours system-wide inflammatory changes are observed. Additionally, atopic patients undergoing surgery for otitis media (OM) with effusion have similar cellular and cytokine profiles in both the middle ear effusion and nasopharynx (Nguyen et al., 2004). It is hypothesized that the middle ear is capable of participating in a T_H2 inflammatory response and that the inflammation in OM with effusion is not limited to the middle ear (Nguyen et al., 2004).

Limited nonallergic observations of the unified airway have been described in the literature. At least 40% and up to 88% of chronic obstructive pulmonary disease (COPD) patients have sinonasal symptoms, which are increased during COPD exacerbations (Hens et al., 2008; Burgel, 2015). In addition, a study of sinus CT in bronchiectasis patients found that the severity of sinus disease was worse in bronchiectasis patients than in allergic rhinitis patients (Ramakrishnan et al., 2013). In our study, we wanted to further apply the unified airway theory to infectious and nonallergic airway epithelial disease in the middle ear, sinus, and lung. We predicted that the host genetic background contributes to susceptibility to upper and lower airway epithelial diseases, with the hypothesis that genes and enriched pathways identified from either DNA or RNA studies will be shared between upper and lower airway diseases.

Abbreviations: BAL, bronchoalveolar lavage; COPD, chronic obstructive pulmonary disease; CRS, chronic rhinosinusitis; DEG, differentially expressed gene; eQTL, expression quantitative trait locus; GEO, gene expression omnibus; GO, gene ontology; GTEx, Genotype-Tissue Expression Project; GWAS, genome-wide association study; NP, nasal polyp; NTM, nontuberculous mycobacterial infection; OM, otitis media; PTB, pulmonary tuberculosis; RNA-Seq, RNA-sequencing.

METHODS

The study is divided into three parts (**Supplementary Methods**; **Supplementary Figure 1**): ***Part 1*** consists of network analyses and pathway identification using published genes based on genome-wide significant variants from DNA studies and eGenes derived from expression quantitative trait loci (eQTL); ***Part 2*** includes analyses of RNA-sequence data from middle ear, sinus, and lung tissue, and identification of common genes and pathways from network analyses across different sites; and ***Part 3*** involves the comparison of network analysis results from DNA literature and RNA-sequence data in order to find common genes and pathways across the upper and lower airways.

Network Analyses for Published Genes and eGenes (Part 1)

Generation of Gene Lists From the Literature and UK Biobank

A literature search on DNA studies was performed for upper and lower airway phenotypes, including OM, chronic rhinosinusitis (CRS) and/or nasal polyps (NP), chronic bronchitis, bronchiolitis, acute bronchitis, pneumonia, pulmonary nontuberculous mycobacterial (NTM) infection, pulmonary tuberculosis (PTB), and bronchiectasis. Specific terms used for the search and the exclusion criteria are listed in the **Supplementary Methods**. Only studies with genome-wide significant results were included. Genome-wide significance criteria were as follows: [1] variant or gene identified using linkage analyses in family-based studies (LOD≥3.3); [2] variant or gene identified by population-based genome-wide association study (GWAS; $p < 5.0\text{x}10^{-8}$ if using single-variant analyses, $p < 2.5\text{x}10^{-6}$ if using gene-based tests). The variants and genes meeting these criteria are included in **Supplementary Table 1** that lists the design, sample size and ancestry of each cited study cohort from which the power of each study may be assessed. Aside from published literature, genome-wide significant variants ($p < 5.0\text{x}10^{-8}$) were extracted from publicly available GWAS results on selected phenotypes from the UK Biobank [**Supplementary Table 2**, (Neale, 2018)]. Variants classified as "low confidence" in the UK Biobank data set were removed from further analyses.

From variants identified by single-variant GWAS either in literature or the UK Biobank, only the most significant variant in each peak was selected for further analyses and annotated using the hg19 version of the UCSC Variant Annotation Integrator

(Kent et al., 2002; Hinrichs et al., 2016). Furthermore, variants were annotated as eQTLs using the GTEx v7 portal (GTEx Portal, 2017). In this study, we identified the significant eGenes for the variants identified from the literature or UK Biobank in 26 selected tissues (**Supplementary Table 3**) and annotated the results using Ensembl BioMart (Zerbino et al., 2018). Note that GTEx has eQTL data for lung but not for middle ear or sinonasal tissues, thus we were limited to identification of eQTLs based on other mucosal, respiratory or lymphoid tissues in GTEx (**Supplementary Table 3**). Multiple significant eGenes were typically identified for each variant, but intergenic variants that were not identified as eQTLs for the 26 tissues selected in GTEx were not considered further.

Gene lists were compiled for each phenotype (**Supplementary Table 4**), which includes the following: [1] Genes were significant by gene-based GWAS or linkage analyses from the literature. [2] From the literature and UK Biobank, for variants identified by single-variant GWAS, genes were only included if the variant was located in a gene (coding, intronic, or UTR), not if it was upstream or downstream. [3] For all types of variants from single-variant GWAS whether from literature or the UK Biobank, eGenes were identified from single-tissue eQTL analysis in GTEx. Duplicate genes were removed within each list. Additionally, the genes identified for the lower airway phenotypes were combined into a single list ("Lower").

Network Analysis for Lists of Published Genes and eGenes

NetworkAnalyst was used to generate networks (Xia et al., 2014; Xia et al., 2015; Zhou et al., 2019). The input used were the gene lists identified from the literature and UK Biobank for Part 1 (**Supplementary Table 4**), with separate networks created for OM, CRS, and Lower (**Supplementary Methods**). Networks were created using the Generic PPI, with the IMEx Interactome database from InnateDB (Breuer et al., 2013). The default network creation method was used for the module and PANTHER Biological Process (BP) analyses, which adds in the first neighbors (interacting genes) for the seed genes (genes on the input list). Module analysis was performed on each subnetwork, to break the larger subnetworks into smaller, more densely connected clusters or modules (Xia et al., 2014), using the Walktrap algorithm (Pons and Latapy, 2005). Nodes representing genes within a module are likely to work collectively to perform a biological function. When phenotypes were combined, a combined network was created in NetworkAnalyst and visualized using Cytoscape software, in order to delineate overlaps and differences between phenotypes (Shannon et al., 2003; Assenov et al., 2008; Doncheva et al., 2012).

PANTHER BP enrichment analysis was completed for each significant module within the larger subnetworks (Mi et al., 2019). Each node (gene) is annotated with PANTHER BP Gene Ontology (GO) Terms or pathways. PANTHER uses a subset of GO Terms to simplify and condense results. The output of the PANTHER BP enrichment analysis are the pathways that are enriched in the nodes in the module or subnetwork. Significant pathways [false-discovery rate (FDR)-adjusted $p < 0.05$] were compiled into a final list for each phenotype (**Supplementary Table 5**). The Multiple List Comparator (http://www.molbiotools.com/listcompare.html) was used to make comparisons and generate Venn diagrams for either gene or pathway lists.

Network Analyses Using RNA-Sequence Data for Upper and Lower Airway Phenotypes (Part 2)

RNA-Sequencing for Middle Ear Tissues From Individuals With OM

Prior to start of the study, recruitment of patients undergoing OM surgery was approved by the Colorado Multiple Institutional Review Board. All study participants provided written informed consent. Three cholesteatoma samples (considered "case" tissue) and four middle ear mucosa samples ("control" tissue) were collected from patients undergoing OM surgery at the University of Colorado Hospital or Children's Hospital Colorado, and these samples were submitted for RNA-sequencing (RNA-Seq). For cholesteatoma samples, the median RIN was 5.8 and median DV% was 89.2, while for mucosa samples median RIN was 1.5 and median DV% was 52.8. Tissue samples were processed as described in the **Supplementary Methods**. Libraries were constructed using the NuGEN Trio RNA-Seq kit (Tecan, Redwood City, CA, USA), which includes an rRNA depletion step. Sequencing was completed on the Illumina NovaSeq, with paired-end 2x151bp reads. An average of 11.3 million read pairs were obtained per sample (range 4.5 to 23.2 million read pairs). One sample (3086) was removed from further analyses due to an insufficient mapping rate to the human genome (5%) and not clustering with the other OM samples in the principal components analysis (**Supplementary Figure 2**).

RNA-Seq Data for CRS, NTM, and COPD

Previously, uncinate mucosa tissue from three patients with CRS and four control individuals underwent RNA-Seq (Ramakrishnan et al., 2017). For lung phenotypes, a search of the NCBI Gene Expression Omnibus (GEO) database (http://www.ncbi.nlm.nih.gov/geo/) did not identify transcriptome data on lower airway tissue biopsies. However two RNA-Seq data sets were available on bronchoalveolar lavage (BAL) fluid samples for NTM cases and controls [GSE103852, unpublished, three cases and three controls] and large airway brushings for COPD cases and controls [GSE124180, (Morrow et al., 2019), three COPD cases and four controls, all without emphysema]. Raw RNA-Seq results were not available for the COPD data set, and therefore we used the nonnormalized count data that was available. On the other hand, the CRS and NTM data sets had the raw read data available for analysis.

Processing of RNA-Seq Data and Differential Expression Analysis

Reads were trimmed with either Trimmomatic for the CRS and NTM data sets or BBDuk software for OM (Bolger et al., 2014; Bushnell et al., 2017). Transcripts were quantified using Salmon, run in mapping-based mode, which includes indexing and quantification (Patro et al., 2017). The tximport package was

used to extract counts from the salmon quantification output (Soneson et al., 2015). The DESeq2 workflow was followed for the tximport steps and DESeq2 analyses [http://bioconductor.org/packages/devel/bioc/vignettes/DESeq2/inst/doc/DESeq2.html, (Love et al., 2014)].

For OM, CRS, and NTM, the nonnormalized counts from tximport were used for the DESeq2 analyses. For COPD, the nonnormalized counts were available in the GEO database and were used as the input. Counts were filtered to have an average of more than three reads in either the cases or controls. The plotPCA function in DESeq2 was used to generate principal components (PC) plots for each data set. DESeq2 was run with default parameters, and included read count normalization followed by differential expression analysis. DESeq2 analysis was performed for each of the four phenotypes individually (OM, CRS, NTM, COPD). Multiple testing correction was performed using adjustment for FDR, with significance threshold for differentially expressed genes (DEGs) at adj-$p < 0.05$.

Network Analysis for Differentially Expressed Genes

For Part 2, network analysis using the same workflow as in section 2.1.2 was performed using NetworkAnalyst with the DEGs and fold-change as input. A "Lower" list was created that combined the DEGs for NTM and for COPD, while OM and CRS were analyzed separately. Chord and Venn diagrams were created to compare the DEGs across OM, CRS, and Lower phenotypes. Significant pathways were compiled into a final list for each phenotype group (**Supplementary Table 5**). Venn diagrams were also made to quantify pathway overlaps among phenotypes.

Literature Review for Transcriptome Studies

A literature search on RNA studies was performed for upper and lower airway phenotypes, using the same workflow as in section 2.1.1. Specific terms used for the search are included in the **Supplementary Methods**. Studies were excluded if RNA was not extracted from the disease tissue of interest. Genome-wide significance was not required for transcriptome studies. Articles meeting the criteria were summarized (**Supplementary Table 6**).

Comparisons Between Published and RNA-Seq Data (Part 3)

In order to detect concordance between genome-wide significant genes and eGenes (Part 1) and DEGs from RNA-Seq data (Part 2), the gene lists from each part were compared by phenotype (OM, CRS, Lower) and Venn diagrams were created. Likewise, comparisons were made between Parts 1 and 2 for lists of pathways by phenotype.

RESULTS

Genes and Pathways Identified in the Literature and UK Biobank GWAS (Part 1)

Upon review of the literature, 46 genome-wide significant variants and 64 genes were identified from GWAS and family-based studies (**Supplementary Table 1**). No variants overlap between phenotypes, but there is some overlap at the gene level, namely, *HLA-DRB1* in both OM and pneumonia and *MUC6* in both bronchiolitis and pneumonia. In addition, 40 significant variants and 21 genes from the Neale UK Biobank single-variant GWAS were identified (**Supplementary Table 2**). Two variants (rs338598 and rs34210653 in CRS/NP) and three genes (*ALOX15*, *CYP2S1*, and *FOXP1* in CRS/NP) were identified in both the literature and UK Biobank data. The literature source for the CRS/NP data was a paper that performed a GWAS in both deCODE and UK Biobank, so the results would be expected to overlap (Kristjansson et al., 2019). When only the most significant variant in each peak was selected from single-variant GWAS, 84 genome-wide significant variants remained and were queried in the GTEx portal for association with gene expression levels (eQTLs). In total, 122 eGenes were identified from 84 variants (**Supplementary Table 3**). Eighteen variants were excluded because the variant was not located in a gene and was not a significant eQTL in the selected GTEx tissues. **Table 1** lists the final gene counts for each phenotype, including OM and CRS. The lower airway phenotypes (bronchiolitis, chronic bronchitis, pneumonia, and acute bronchitis, and NTM and PTB) were included in a single "Lower" list for further analyses. Fifteen genes (8%) overlap between upper and lower airway phenotypes (**Table 1**; **Supplementary Table 4**). The majority of these genes are immune-related (**Supplementary Table 4**).

TABLE 1 | Counts of published genes and eGenes by phenotype (Part 1)[1].

Phenotype	Published genes[2]	eGenes[3]	Total genes	References
OM	19	49	68	(Allen et al., 2013; Santos-Cortez et al., 2015; Einarsdottir et al., 2016; van Ingen et al., 2016; Tian et al., 2017; Santos-Cortez et al., 2018)
CRS	16	25	41	(Kristjansson et al., 2019)
Bronchiolitis	17	30	47	(Salas et al., 2017)
Chronic Bronchitis	4	1	5	(Lee et al., 2014; Cho et al., 2015; Dijkstra et al., 2015)
Pneumonia and Acute Bronchitis	18	21	39	(Kenyan Bacteraemia Study Group et al., 2016; Hayden et al., 2017; Tian et al., 2017; Salas et al., 2018)
NTM and PTB	9	12	21	(Curtis et al., 2015; Sveinbjornsson et al., 2016; Chen et al., 2017; Zheng et al., 2018)
All phenotypes combined	81	99	180	–
Overlap between upper and lower airways	1	14	15 (8%)	–

[1]*Genes are listed in* ***Supplementary Table 4***.
[2]*Published genes include genes that harbor genome-wide significant variants.*
[3]*eGenes were identified in eQTL analyses using published genome-wide significant variants that control expression in 26 selected tissues in the GTEx database.*

In the network created from the combined gene list for OM, CRS, and Lower (**Supplementary Figure 3**), there is minimal overlap between the upper and lower airways at a gene level. The different phenotypes are interconnected in the network, but the phenotypic associations are not necessarily with the same genes.

In order to generate lists of significant pathways for each phenotype, we also analyzed the networks per phenotype. The network input was the gene list for each phenotype (OM, CRS, and Lower), and the network was created based on known protein-protein interactions. For OM, four subnetworks were generated, composed of 20 modules, all of which were significant. For CRS, four subnetworks were generated, composed of 10 modules, all of which were significant. For Lower, two subnetworks were generated, composed of 22 modules, 21 of which were significant. PANTHER BP enrichment analysis was completed on each module individually. Significantly enriched GO Terms/pathways were identified and compiled into a single list for each phenotype (**Supplementary Table 5**). Significant pathways were identified for OM (n = 36), CRS (n = 13), and Lower (n = 37; **Supplementary Figure 4**). Overall, based on published genes and eGenes, 22 pathways (41%) overlap between the upper and lower airways, and seven pathways were common to all three phenotypes (OM, CRS, and Lower, **Supplementary Figure 4**). These seven pathways include antigen processing and presentation, endocytosis, immune system process and response, protein folding, and viral process (**Supplementary Figure 4**).

Genes and Pathways Identified by RNA-Seq (Part 2)

Differential expression analysis was completed separately for each phenotype (OM, CRS, Lower). For OM, a large number of genes (n = 1,806) were identified as differentially expressed between cholesteatoma and middle ear mucosa (**Supplementary Table 7**). Overall, 19 genes (0.9%) overlap between upper and lower airway phenotypes (**Figure 1**). The two DEGs that are present in all three phenotypes are *CR1* and *SAA1* (**Supplementary Table 7**). Three DEGs were shared between CRS and Lower, namely, *RDH10, SAA2,* and *SLC7A11* (**Supplementary Table 7**). Of the 14 DEGs that were identified in OM and Lower data sets, half of the genes are known to perform various enzymatic functions, while four genes are involved in gene regulation (**Supplementary Table 7**).

From networks identified in OM RNA-Seq data, four subnetworks were generated, composed of 96 modules, 16 of which were significant. For CRS, six subnetworks were generated, composed of 64 modules, 56 of which were significant. For Lower, three subnetworks were generated, composed of 29 modules, 26 of which were significant. Using the same PANTHER BP enrichment analysis workflow in Part 1 and the DEGs as input, significant pathways were identified for OM (n = 68), CRS (n = 56), and Lower (n = 34; **Supplementary Figure 5**; **Supplementary Table 5**). Overall, based on DEGs, 32 pathways (38%) overlap between the upper and lower airways, and 27 pathways were common to all three phenotypes (OM, CRS, and Lower; **Supplementary Figure 5**; **Supplementary Table 5**). Notably about half of these 27 pathways that were common in OM, CRS, and Lower also overlap with DEGs identified in previous microarray and RNA-Seq studies (Liu et al., 2004; Kwon et al., 2006; Lee et al., 2006; Payne et al., 2008; Raju et al., 2008; Stankovic et al., 2008; Rostkowska-Nadolska et al., 2011; Klenke et al., 2012; Macias et al., 2013; Wang et al., 2016; Ramakrishnan et al., 2017; Wang et al., 2017; Gao et al., 2018a; Gao et al., 2018b; Kato et al., 2018; Langelier et al., 2018; Ninomiya et al., 2018; Okada et al., 2018; Jovanovic et al., 2019; Walter et al., 2019; Yao et al., 2019). The common pathways from Part 2 RNA-Seq data that were identified in the transcriptome literature are apoptosis, cell adhesion, cell cycle, cell proliferation, chromatin organization/remodeling,

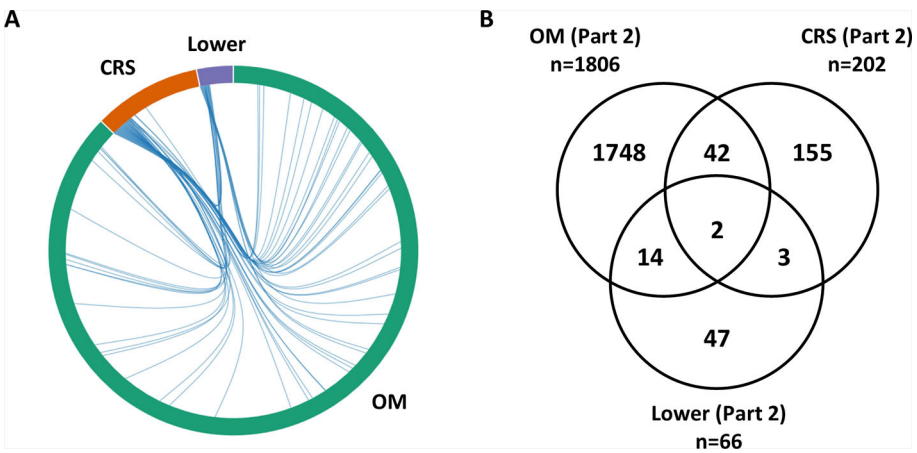

FIGURE 1 | Overlap between lists of differentially expressed genes from RNA-Seq data (Part 2). **(A)** The chord diagram presents the overlap between the differentially expressed genes (DEGs) for each phenotype (otitis media [OM], chronic rhinosinusitis [CRS], Lower including nontuberculous mycobacterial [NTM and chronic obstructive pulmonary disease [COPD]). The connecting lines within the chord diagram show the overlap, at a gene level, between phenotypes. **(B)** Venn diagram showing the overlap in the Part 2 gene lists between OM, CRS, and Lower (**Supplementary Table 6**). Nineteen genes (0.9%) overlap between upper and lower airway phenotypes.

endocytosis, glycogen metabolic process, immune system process, muscle contraction, protein phosphorylation, proteolysis, RNA metabolic process, and transcription (**Supplementary Table 6**).

Comparison of Genes and Pathways From the Literature or UK Biobank GWAS vs. RNA-Seq Data (Part 3)

For each phenotype (OM, CRS, and Lower), we compared the genes and pathways identified from review of literature on DNA studies vs. RNA-Seq results in order to determine if commonalities in genetic background in the susceptibility to upper and lower airway diseases are supported by both types of studies (**Figure 2**). For OM, five genes (*ABO, CDHR3, HLA-DQB2, IER3, SURF1*, 0.3%) were identified in both the DNA literature (Part 1) and RNA-Seq (Part 2). For CRS, only the *NGEF* gene (0.4%) was identified in both Parts 1 and 2. For the lower airway, the *HCP5* gene (0.6%) was identified in both Parts 1 and 2. Of note, there are a large number of genes that do not overlap between Parts 1 and 2 for all three phenotypes. In addition, all genes common between Parts 1 and 2 were unique to each phenotype.

The same comparisons were made at the pathway level (**Supplementary Table 5**; **Figure 2**). For OM, 21 pathways (25%) were identified in the literature (Part 1) and RNA-Seq (Part 2). For CRS, 11 pathways (19%), and for the lower airway, 21 pathways (42%) were identified in both Parts 1 and 2. We also looked at the pathways that were common between Parts 1 and 2 individually for each phenotype, then compared them across the phenotypes. The common pathways among the three phenotypes (OM, CRS, and Lower) are chromatin organization/remodeling, endocytosis, immune system process, protein folding, and viral process (**Figure 2**). The additional pathways that are common between the upper and lower airway phenotypes are apoptotic process, cell cycle, DNA repair, glycogen metabolic process, transcription, and translation. In total, 12 (35%) pathways overlap between upper and lower airway phenotypes (**Supplementary Table 5**; **Figure 2**).

DISCUSSION

Here, we report the results of an investigation of the unified airway theory in infectious and nonallergic airway epithelial conditions, both for genetic susceptibility (Part 1) and differentially expressed genes (Part 2). Five pathways namely chromatin organization/remodeling, endocytosis, immune system process, protein folding, and viral process were shown

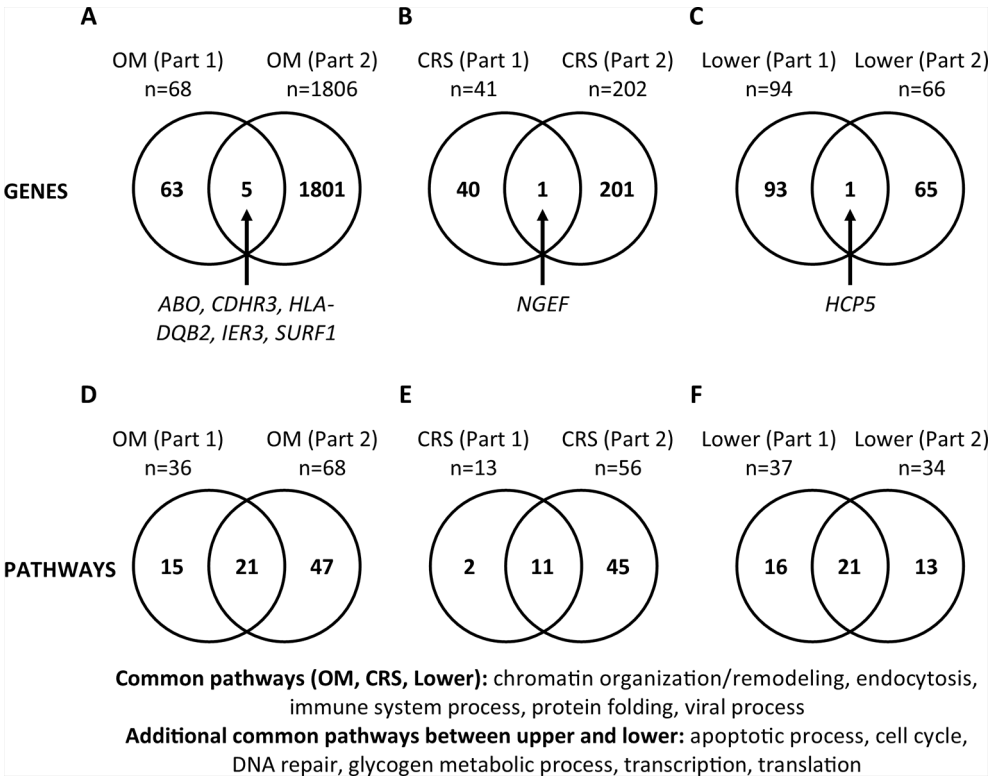

FIGURE 2 | Comparisons between gene and pathway lists (Part 3). **(A–C)** Significant genes were compared between Part 1 (published genes and eGenes) and Part 2 (RNA-Seq) for each phenotype (otitis media [OM], chronic rhinosinusitis [CRS], and Lower). Genes are listed in **Supplementary Tables 4** and **6**. **(D–F)** The lists of significant PANTHER Biological Process Gene Ontology (GO) Terms/pathways were compared between Parts 1 and 2 for each phenotype (**Supplementary Figures 3** and **5**; **Supplementary Table 5**). Twelve (35%) pathways were present in both the upper and lower airway phenotypes (**Supplementary Table 5**).

to overlap among OM, CRS, and Lower airway phenotypes in both Part 1 and Part 2 (**Figure 2**), indicating that our approach is a viable route for finding overlaps among significant pathways for diseases across the upper and lower airways. Three of these pathways (chromatin organization/remodeling, endocytosis, and immune system process) were also identified in previously published transcriptome studies (**Supplementary Table 6**). These three pathways have the strongest evidence for involvement in both the upper and lower airway infectious and nonallergic disease processes. While this study was focused on the unified airway theory and therefore the pathways that are common between OM, CRS, and the Lower airway, the pathways that are unique to each disease site are also of interest, particularly those that overlap between DNA and RNA studies (**Supplementary Table 5**). These pathways may also provide insight into disease-specific susceptibility and pathogenesis.

In each Part of this study, we identified more overlap between upper and lower airway at the pathway level than at the gene level (**Figure 1**; **Supplementary Figures 4** and **5**; **Supplementary Table 5**). This finding may indicate that the genes responsible differ between the diseases, but that those genes impact the same pathways and cause disease or disease susceptibility in a similar manner. While Part 1 measures changes that occur at the DNA level and relate to genetic susceptibility for a disease, Part 2 measures changes that occur at the RNA level. The latter may be related to the genetic susceptibility and downstream processes that are affected, or they may be related to the changes that occur as a result of the disease process itself. While we saw overlap in the results from Part 1 and Part 2, especially at the pathway level, it is reasonable to see that the results did not overlap completely. On the other hand, genes and pathways that overlap in both DNA and RNA studies for the same or similar phenotype(s) provide strong evidence for their involvement in disease.

Cholesteatoma is a middle ear lesion of keratinized epithelium surrounding squamous debris that usually occurs as part of chronic OM, and is characterized by uncontrolled growth and proliferation. This is the first report using RNA-Seq in OM patients with middle ear cholesteatoma compared to middle ear mucosal tissue as a control. Previous studies have used either skin or granulation tissue as control tissue in cholesteatoma studies (Kwon et al., 2006; Klenke et al., 2012; Macias et al., 2013; Gao et al., 2018a; Jovanovic et al., 2019). In our study, 1,806 genes were differentially expressed between cholesteatoma and mucosa samples (**Supplementary Table 7**; **Figure 1**). This large number of DEGs may be explained by the growth characteristics of the cholesteatoma tissue. In addition, 68 pathways were enriched in cholesteatoma tissue (**Supplementary Table 5**). These RNA-Seq findings may provide insight into the disease mechanism for cholesteatoma, which is still poorly understood. Both the DEGs and pathways identified here provide a resource for future studies, e.g., for prioritizing candidate genes from sequencing studies whether by DEGs or expression levels in middle ear and sinonasal tissues.

For example, of the five OM genes that overlap between Parts 1 and 2, *CDHR3*, *HLA-DQB2*, and *IER3* are annotated with viral process, apoptotic process, and DNA repair, which are some of the PANTHER BP terms that were found as overlapping pathways in Parts 1 and 2. *HLA-DQB2* (MIM 615161) is a well-known immune gene, while *IER3* (MIM 602996) regulates genes involved in apoptosis. *CDHR3* (MIM 615610) encodes a transmembrane epithelial protein and was previously identified in GWAS for childhood ear infections (Pickrell et al., 2016) and also for asthma exacerbations in children primarily due to viral respiratory infections (Bønnelykke et al., 2014; Everman et al., 2019). While the GWAS finding of *CDHR3* variant rs114947103 as a protective factor against OM has not been replicated (Pickrell et al., 2016), the downregulation of *CDHR3* in cholesteatoma compared to mucosal middle ear tissue (adj-p = 0.004) in our RNA-Seq study strongly supports a role for *CDHR3* in OM.

However because *CDHR3* was identified in a GWAS for asthma, this gene was not included in overlaps between OM and Lower airway. Of the 14 DEGs that overlap between OM and Lower, all the genes except *MUCL1* are in overlapping pathways in OM and Lower (**Supplementary Table 5**). On the other hand, there are 42 DEGs that overlap between OM and CRS in the RNA-Seq data, and are not shared with the Lower airway phenotype (**Figure 1**). This suggests that at the gene level there are more genes that overlap between OM and CRS (n = 42) compared to OM and Lower airway (n = 14) or between the upper and lower airway overall (n = 19). The shared number of DEGs between OM and CRS at the RNA-Seq level may help explain why, in addition to the physical proximity and connectedness of the middle ear to the sinonasal complex, OM and CRS are more similar to each other than either is to the Lower airway phenotypes.

By comparing the RNA-Seq results from middle ear, sinus, and lung, we identified two potentially novel genes for OM, i.e. *CR1* and *SAA1,* that are involved in susceptibility to both upper and lower airway disease. *CR1* (MIM 120620), which encodes the complement C3b/C4b receptor 1 (Knops blood group), was a significant DEG in OM, CRS, and Lower (−3.6, +1.8, and −1.5 log2 fold change, respectively). The GO BP pathway annotations for *CR1* include immune system process, viral process, and negative regulation of complement activation. CR1 is important for the host response to bacteria, and mediates immune adherence and phagocytosis (Smith et al., 2002; Li et al., 2010). In CRS, CR1 was reported to have denser localization in the mucosa of CRS patients than in normal mucosa (Miyaguchi et al., 1988), and higher levels of CR1 were found in granulocytes from the circulation and sinus pus in patients with purulent sinusitis (Berg et al., 1989). In pneumonia, CR1 had significantly higher levels on neutrophils in patients with bacterial pneumonia compared to those with viral pneumonia (Hohenthal et al., 2006). The *CR1* gene was reported to be important for host defense against pneumococcal infection in mice (Ren et al., 2004). In addition, deficiency of CR1 was reported in a patient with OM, sinusitis, and pneumonia (Sadallah et al., 1999). In our study, *CR1* was found to be downregulated in OM cholesteatoma and NTM BAL, but upregulated in CRS. This could be consistent with a

potential deficiency of CR1 resulting in susceptibility to infections in the OM and NTM patients.

SAA1 (MIM 104750), encoding serum amyloid A1, was significantly differentially expressed in OM, CRS, and Lower (−2.5, +2.9, −4.6 log2 fold change, respectively). The *SAA1* GO BP annotations include positive regulation of cytokine secretion, receptor-mediated endocytosis, and positive regulation of cell adhesion. Elevated plasma levels of SAA1 is a well-documented clinical indicator for inflammatory conditions, and is suggested to have a role in host defense against bacterial infection. *SAA1* has been reported to be upregulated in lung parenchyma and bronchi of patients with COPD compared with smoking controls (Lopez-Campos et al., 2013). During TB treatment, *SAA1* expression is reduced, and the reduction is greater for patients who culture-converted at later time points (Sigal et al., 2017; Kedia et al., 2018). In our study, this gene was found to be downregulated in OM cholesteatoma and COPD large airway brushings, but upregulated in CRS. Interestingly for both *CR1* and *SAA1* the direction of regulation of expression is opposite in OM vs. CRS but the same in OM vs. Lower. This may be primarily due to the differences in types of tissues used; alternatively it may also be due to disease-specific processes in each site.

One limitation of the OM RNA-Seq study is that we were unable to collect paired cholesteatoma and mucosa samples from the same patients due to technical reasons. This prevents us from comparing the expression levels of genes in the same patients, which could provide additional valuable information about the disease process. Other limitations are [1] the small amount of middle ear tissues available resulting in lower RIN values, and [2] the small sample size for RNA-Seq studies. On the other hand, the rRNA depletion protocol used for RNA-Seq allowed us to have analyzable data for comparison and genetic results were replicated in other data sets, indicating that our main findings are not false-positive results. Nevertheless following up these findings in a well-powered cohort particularly for OM will help validate the identified DEGs, enable identification of additional novel DEGs, and also allow for inclusion of covariates such as patient age, sex and ethnicity. Based on our OM RNA-Seq data set with ~15,000 genes for testing, ~1,800 DEGs, minimum fold change≥2, and average read counts of ~900, we will have sufficient power ≥80% with an expanded data set of 28 middle ear tissues, preferably with paired samples.

In summary, we have confirmed support for the unified airway theory for infectious and nonallergic airway epithelial disease, using both genetic susceptibility and differential tissue expression studies. We also identified two potentially novel genes for OM susceptibility, *CR1* and *SAA1,* in addition to 56 OM DEGs that are also DEGs for CRS or lower airways. Moreover we identified a total of 1,806 DEGs and 68 pathways that are enriched in cholesteatoma compared to middle ear mucosa. In the process we have created a data set that can be used as reference for finding genes or pathways that are relevant to upper and lower airways, whether common across sites, or unique to each disease.

DATA AVAILABILITY STATEMENT

The data generated for this article can be found in dbGAP, accession phs001941.v1.p1.

ETHICS STATEMENT

The studies involving human participants were reviewed and approved by Colorado Institutional Review Board. Written informed consent to participate in this study was provided by adult participants or for children, the participants' parents.

AUTHOR CONTRIBUTIONS

RS-C, VR, DS, IY, and DF conceptualized the study. GF, EH, JD, MM, PY, SG, MS, SC, and HJ collected middle ear samples. TB performed isolation of RNA from tissue samples and submitted RNA samples for sequencing. EB and EL performed RNA sequence analyses. EB and SP extracted data from literature. EB extracted data from UK Biobank and GTEx and performed network analyses. EB and RS-C wrote the manuscript. All authors read and approved the manuscript.

FUNDING

This work was funded by the National Institute on Deafness and Other Communication Disorders (NIDCD) of the National Institutes of Health grants R01 DC015004 (to RS-C), K23 DC014747 (to VR), and a training grant T32 DC012280 to the Department of Otolaryngology at the University of Colorado.

ACKNOWLEDGMENTS

We thank the patients who provided samples and A Fung and C Brands for general support. We are also very grateful to the laboratory of Dr. Benjamin Neale at Harvard Medical School and Broad Institute who made their GWAS results on the UK Biobank public. The Genotype-Tissue Expression (GTEx) Project database that was used in this study was supported by the Common Fund of the Office of the Director of the National Institutes of Health (NIH), and by NCI, NHGRI, NHLBI, NIDA, NIMH, and NINDS. The data used for the analyses described in this manuscript were obtained from the GTEx Portal on 02/21/2019. The content is solely the responsibility of the authors and does not necessarily represent the official views of the National Institutes of Health.

SUPPLEMENTARY MATERIAL

The Supplementary Material for this article can be found online at: https://www.frontiersin.org/articles/10.3389/fgene.2019.01352/full#supplementary-material

REFERENCES

Allen, E. K., Chen, W. M., Weeks, D. E., Chen, F., Hou, X., Mattos, J. L., et al. (2013). A genome-wide association study of chronic otitis media with effusion and recurrent otitis media identifies a novel susceptibility locus on chromosome 2. *J. Assoc. Res. Otolaryngol.* 14 (6), 791–800. doi: 10.1007/s10162-013-0411-2

Assenov, Y., Ramirez, F., Schelhorn, S. E., Lengauer, T., and Albrecht, M. (2008). Computing topological parameters of biological networks. *Bioinformatics* 24 (2), 282–284. doi: 10.1093/bioinformatics/btm554

Bønnelykke, K., Sleiman, P., Nielsen, K., Kreiner-Moller, E., Mercader, J. M., Belgrave, D., et al. (2014). A genome-wide association study identifies CDHR3 as a susceptibility locus for early childhood asthma with severe exacerbations. *Nat. Genet.* 46 (1), 51–55. doi: 10.1038/ng.2830

Berg, O., Carenfelt, C., Hallden, G., and Hed, J. (1989). CR1-expression and C3b-mediated phagocytosis of granulocytes in purulent maxillary secretion and peripheral blood from patients with sinusitis. *Acta Otolaryngol.* 107 (1-2), 130–135. doi: 10.3109/00016488909127489

Bolger, A. M., Lohse, M., and Usadel, B. (2014). Trimmomatic: a flexible trimmer for Illumina sequence data. *Bioinformatics* 30 (15), 2114–2120. doi: 10.1093/bioinformatics/btu170

Breuer, K., Foroushani, A. K., Laird, M. R., Chen, C., Sribnaia, A., Lo, R., et al. (2013). InnateDB: systems biology of innate immunity and beyond–recent updates and continuing curation. *Nucleic Acids Res.* 41 (Database issue), D1228–D1233. doi: 10.1093/nar/gks1147

Burgel, P. R. (2015). United airway diseases. Should we add upper airway inflammatory disorders to the list of chronic obstructive pulmonary disease comorbidities? *Ann. Am. Thorac. Soc.* 12 (7), 968–970. doi: 10.1513/AnnalsATS.201505-309ED

Bushnell, B., Rood, J., and Singer, E. (2017). BBMerge - Accurate paired shotgun read merging *via* overlap. *PloS One* 12 (10), e0185056. doi: 10.1371/journal.pone.0185056

Charlson, E. S., Bittinger, K., Haas, A. R., Fitzgerald, A. S., Frank, I., Yadav, A., et al. (2011). Topographical continuity of bacterial populations in the healthy human respiratory tract. *Am. J. Respir. Crit. Care Med.* 184 (8), 957–963. doi: 10.1164/rccm.201104-0655OC

Chen, F., Szymanski, E. P., Olivier, K. N., Liu, X., Tettelin, H., Holland, S. M., et al. (2017). Whole-Exome Sequencing Identifies the 6q12-q16 Linkage Region and a Candidate Gene, TTK, for Pulmonary Nontuberculous Mycobacterial Disease. *Am. J. Respir. Crit. Care Med.* 196 (12), 1599–1604. doi: 10.1164/rccm.201612-2479OC

Cho, M. H., Castaldi, P. J., Hersh, C. P., Hobbs, B. D., Barr, R. G., Tal-Singer, R., et al. (2015). A Genome-Wide Association Study of Emphysema and Airway Quantitative Imaging Phenotypes. *Am. J. Respir. Crit. Care Med.* 192 (5), 559–569. doi: 10.1164/rccm.201501-0148OC

Curtis, J., Luo, Y., Zenner, H. L., Cuchet-Lourenco, D., Wu, C., Lo, K., et al. (2015). Susceptibility to tuberculosis is associated with variants in the ASAP1 gene encoding a regulator of dendritic cell migration. *Nat. Genet.* 47 (5), 523–527. doi: 10.1038/ng.3248

Dijkstra, A. E., Postma, D. S., van Ginneken, B., Wielputz, M. O., Schmidt, M., Becker, N., et al. (2015). Novel genes for airway wall thickness identified with combined genome-wide association and expression analyses. *Am. J. Respir. Crit. Care Med.* 191 (5), 547–556. doi: 10.1164/rccm.201405-0840OC

Doncheva, N. T., Assenov, Y., Domingues, F. S., and Albrecht, M. (2012). Topological analysis and interactive visualization of biological networks and protein structures. *Nat. Protoc.* 7 (4), 670–685. doi: 10.1038/nprot.2012.004

Einarsdottir, E., Hafren, L., Leinonen, E., Bhutta, M. F., Kentala, E., Kere, J., et al. (2016). Genome-wide association analysis reveals variants on chromosome 19 that contribute to childhood risk of chronic otitis media with effusion. *Sci. Rep.* 6, 33240. doi: 10.1038/srep33240

Everman, J. L., Sajuthi, S., Saef, B., Rios, C., Stoner, A. M., Numata, M., et al. (2019). Functional genomics of CDHR3 confirms its role in HRV-C infection and childhood asthma exacerbations. *J. Allergy Clin. Immunol.* 144, 962–971. doi: 10.1016/j.jaci.2019.01.052

Feng, C. H., Miller, M. D., and Simon, R. A. (2012). The united allergic airway: connections between allergic rhinitis, asthma, and chronic sinusitis. *Am. J. Rhinol. Allergy* 26 (3), 187–190. doi: 10.2500/ajra.2012.26.3762

Gao, J., Tang, Q., Zhu, X., Wang, S., Zhang, Y., Liu, W., et al. (2018a). Long noncoding RNAs show differential expression profiles and display ceRNA potential in cholesteatoma pathogenesis. *Oncol. Rep.* 39 (5), 2091–2100. doi: 10.3892/or.2018.6320

Gao, M., Wang, K., Yang, M., Meng, F., Lu, R., Zhuang, H., et al. (2018b). Transcriptome analysis of bronchoalveolar lavage fluid from children with Mycoplasma pneumoniae pneumonia reveals natural killer and T cell-proliferation responses. *Front. Immunol.* 9, 1403. doi: 10.3389/fimmu.2018.01403

Giavina-Bianchi, P., Aun, M. V., Takejima, P., Kalil, J., and Agondi, R. C. (2016). United airway disease: current perspectives. *J. Asthma Allergy* 9, 93–100. doi: 10.2147/JAA.S81541

GTEx Portal (2017). Data from: *GTEx Analysis V7*. https://www.gtexportal.org/home/.

Hanshew, A. S., Jette, M. E., Rosen, S. P., and Thibeault, S. L. (2017). Integrating the microbiota of the respiratory tract with the unified airway model. *Respir. Med.* 126, 68–74. doi: 10.1016/j.rmed.2017.03.019

Hayden, L. P., Cho, M. H., McDonald, M. N., Crapo, J. D., Beaty, T. H., Silverman, E. K., et al. (2017). Susceptibility to Childhood Pneumonia: A Genome-Wide Analysis. *Am. J. Respir. Cell Mol. Biol.* 56 (1), 20–28. doi: 10.1165/rcmb.2016-0101OC

Hens, G., Vanaudenaerde, B. M., Bullens, D. M., Piessens, M., Decramer, M., Dupont, L. J., et al. (2008). Sinonasal pathology in nonallergic asthma and COPD: 'united airway disease' beyond the scope of allergy. *Allergy* 63 (3), 261–267. doi: 10.1111/j.1398-9995.2007.01545.x

Hinrichs, A. S., Raney, B. J., Speir, M. L., Rhead, B., Casper, J., Karolchik, D., et al. (2016). UCSC Data Integrator and Variant Annotation Integrator. *Bioinformatics* 32 (9), 1430–1432. doi: 10.1093/bioinformatics/btv766

Hohenthal, U., Nuutila, J., Lilius, E. M., Laitinen, I., Nikoskelainen, J., and Kotilainen, P. (2006). Measurement of complement receptor 1 on neutrophils in bacterial and viral pneumonia. *BMC Infect. Dis.* 6, 11. doi: 10.1186/1471-2334-6-11

Jovanovic, I., Zivkovic, M., Djuric, T., Stojkovic, L., Jesic, S., and Stankovic, A. (2019). Perimatrix of middle ear cholesteatoma: A granulation tissue with a specific transcriptomic signature. *Laryngoscope*. doi: 10.1002/lary.28084

Kato, Y., Takabayashi, T., Sakashita, M., Imoto, Y., Tokunaga, T., Ninomiya, T., et al. (2018). Expression and functional analysis of CST1 in intractable nasal polyps. *Am. J. Respir. Cell Mol. Biol.* 59 (4), 448–457. doi: 10.1165/rcmb.2017-0325OC

Kedia, K., Wendler, J. P., Baker, E. S., Burnum-Johnson, K. E., Jarsberg, L. G., Stratton, K. G., et al. (2018). Application of multiplexed ion mobility spectrometry towards the identification of host protein signatures of treatment effect in pulmonary tuberculosis. *Tuberculosis (Edinb)* 112, 52–61. doi: 10.1016/j.tube.2018.07.005

Kent, W. J., Sugnet, C. W., Furey, T. S., Roskin, K. M., Pringle, T. H., Zahler, A. M., et al. (2002). The human genome browser at UCSC. *Genome Res.* 12 (6), 996–1006. doi: 10.1101/gr.229102

Kenyan Bacteraemia Study Group and Wellcome Trust Case Control Consortium, Rautanen, A., Pirinen, M., Mills, T. C., Rockett, K. A., et al. (2016). Polymorphism in a lincRNA associates with a doubled risk of pneumococcal bacteremia in Kenyan children. *Am. J. Hum. Genet.* 98 (6), 1092–1100. doi: 10.1016/j.ajhg.2016.03.025

Klenke, C., Janowski, S., Borck, D., Widera, D., Ebmeyer, J., Kalinowski, J., et al. (2012). Identification of novel cholesteatoma-related gene expression signatures using full-genome microarrays. *PloS One* 7 (12), e52718. doi: 10.1371/journal.pone.0052718

Kristjansson, R. P., Benonisdottir, S., Davidsson, O. B., Oddsson, A., Tragante, V., Sigurdsson, J. K., et al. (2019). A loss-of-function variant in ALOX15 protects against nasal polyps and chronic rhinosinusitis. *Nat. Genet.* 51 (2), 267–276. doi: 10.1038/s41588-018-0314-6

Krouse, J. H. (2008). The unified airway–conceptual framework. *Otolaryngol. Clin. North Am.* 41 (2), 257–266. doi: 10.1016/j.otc.2007.11.002

Kwon, K. H., Kim, S. J., Kim, H. J., and Jung, H. H. (2006). Analysis of gene expression profiles in cholesteatoma using oligonucleotide microarray. *Acta Otolaryngol.* 126 (7), 691–697. doi: 10.1080/00016480500475633

Langelier, C., Kalantar, K. L., Moazed, F., Wilson, M. R., Crawford, E. D., Deiss, T., et al. (2018). Integrating host response and unbiased microbe detection for

lower respiratory tract infection diagnosis in critically ill adults. *Proc. Natl. Acad. Sci. U.S.A.* 115 (52), E12353–E12362. doi: 10.1073/pnas.1809700115

Lee, J. Y., Lee, S. H., Lee, H. M., Lee, S. H., Jung, H. H., Lee, S. W., et al. (2006). Analysis of gene expression profiles of normal human nasal mucosa and nasal polyp tissues by SAGE. *J. Allergy Clin. Immunol.* 118 (1), 134–142. doi: 10.1016/j.jaci.2006.02.048

Lee, J. H., Cho, M. H., Hersh, C. P., McDonald, M. L., Crapo, J. D., Bakke, P. S., et al. (2014). Genetic susceptibility for chronic bronchitis in chronic obstructive pulmonary disease. *Respir. Res.* 15, 113. doi: 10.1186/s12931-014-0113-2

Li, J., Wang, J. P., Ghiran, I., Cerny, A., Szalai, A. J., Briles, D. E., et al. (2010). Complement receptor 1 expression on mouse erythrocytes mediates clearance of Streptococcus pneumoniae by immune adherence. *Infect. Immun.* 78 (7), 3129–3135. doi: 10.1128/IAI.01263-09

Liu, Z., Kim, J., Sypek, J. P., Wang, I. M., Horton, H., Oppenheim, F. G., et al. (2004). Gene expression profiles in human nasal polyp tissues studied by means of DNA microarray. *J. Allergy Clin. Immunol.* 114 (4), 783–790. doi: 10.1016/j.jaci.2004.04.052

Lopez-Campos, J. L., Calero, C., Rojano, B., Lopez-Porras, M., Saenz-Coronilla, J., Blanco, A. I., et al. (2013). C-reactive protein and serum amyloid a overexpression in lung tissues of chronic obstructive pulmonary disease patients: a case-control study. *Int. J. Med. Sci.* 10 (8), 938–947. doi: 10.7150/ijms.6152

Love, M. I., Huber, W., and Anders, S. (2014). Moderated estimation of fold change and dispersion for RNA-seq data with DESeq2. *Genome Biol.* 15 (12), 550. doi: 10.1186/s13059-014-0550-8

Macias, J. D., Gerkin, R. D., Locke, D., and Macias, M. P. (2013). Differential gene expression in cholesteatoma by DNA chip analysis. *Laryngoscope* 123 Suppl S5, S1–21. doi: 10.1002/lary.24176

Mi, H., Muruganujan, A., Ebert, D., Huang, X., and Thomas, P. D. (2019). PANTHER version 14: more genomes, a new PANTHER GO-slim and improvements in enrichment analysis tools. *Nucleic Acids Res.* 47 (D1), D419–D426. doi: 10.1093/nar/gky1038

Miyaguchi, M., Uda, H., Sakai, S., Kubo, T., and Matsunaga, T. (1988). Immunohistochemical studies of complement receptor (CR1) in cases with normal sinus mucosa and chronic sinusitis. *Arch. Otorhinolaryngol.* 244 (6), 350–354. doi: 10.1007/bf00497463

Morrow, J. D., Chase, R. P., Parker, M. M., Glass, K., Seo, M., Divo, M., et al. (2019). RNA-sequencing across three matched tissues reveals shared and tissue-specific gene expression and pathway signatures of COPD. *Respir. Res.* 20 (1), 65. doi: 10.1186/s12931-019-1032-z

Neale, B. (2018). Data from: *UK Biobank GWAS Round 2.* http://www.nealelab.is/uk-biobank/.

Nguyen, L. H., Manoukian, J. J., Sobol, S. E., Tewfik, T. L., Mazer, B. D., Schloss, M. D., et al. (2004). Similar allergic inflammation in the middle ear and the upper airway: evidence linking otitis media with effusion to the united airways concept. *J. Allergy Clin. Immunol.* 114 (5), 1110–1115. doi: 10.1016/j.jaci.2004.07.061

Ninomiya, T., Noguchi, E., Haruna, T., Hasegawa, M., Yoshida, T., Yamashita, Y., et al. (2018). Periostin as a novel biomarker for postoperative recurrence of chronic rhinosinitis with nasal polyps. *Sci. Rep.* 8 (1), 11450. doi: 10.1038/s41598-018-29612-2

Okada, N., Nakayama, T., Asaka, D., Inoue, N., Tsurumoto, T., Takaishi, S., et al. (2018). Distinct gene expression profiles and regulation networks of nasal polyps in eosinophilic and non-eosinophilic chronic rhinosinusitis. *Int. Forum. Allergy Rhinol.* 8 (5), 592–604. doi: 10.1002/alr.22083

Patro, R., Duggal, G., Love, M. I., Irizarry, R. A., and Kingsford, C. (2017). Salmon provides fast and bias-aware quantification of transcript expression. *Nat. Methods* 14 (4), 417–419. doi: 10.1038/nmeth.4197

Payne, S. C., Han, J. K., Huyett, P., Negri, J., Kropf, E. Z., Borish, L., et al. (2008). Microarray analysis of distinct gene transcription profiles in non-eosinophilic chronic sinusitis with nasal polyps. *Am. J. Rhinol.* 22 (6), 568–581. doi: 10.2500/ajr.2008.22.3233

Pickrell, J. K., Berisa, T., Liu, J. Z., Segurel, L., Tung, J. Y., and Hinds, D. A. (2016). Detection and interpretation of shared genetic influences on 42 human traits. *Nat. Genet.* 48 (7), 709–717. doi: 10.1038/ng.3570

Pons, P., and Latapy, M. (2005). *Computing Communities in Large Networks Using Random Walks* (Berlin Heidelberg: Springer), 284–293.

Raju, B., Hoshino, Y., Belitskaya-Levy, I., Dawson, R., Ress, S., Gold, J. A., et al. (2008). Gene expression profiles of bronchoalveolar cells in pulmonary TB. *Tuberculosis (Edinb)* 88 (1), 39–51. doi: 10.1016/j.tube.2007.07.003

Ramakrishnan, V. R., Ferril, G. R., Suh, J. D., Woodson, T., Green, T. J., and Kingdom, T. T. (2013). Upper and lower airways associations in patients with chronic rhinosinusitis and bronchiectasis. *Int. Forum. Allergy Rhinol.* 3 (11), 921–927. doi: 10.1002/alr.21204

Ramakrishnan, V. R., Gonzalez, J. R., Cooper, S. E., Barham, H. P., Anderson, C. B., Larson, E. D., et al. (2017). RNA sequencing and pathway analysis identify tumor necrosis factor alpha driven small proline-rich protein dysregulation in chronic rhinosinusitis. *Am. J. Rhinol. Allergy* 31 (5), 283–288. doi: 10.2500/ajra.2017.31.4457

Ren, B., McCrory, M. A., Pass, C., Bullard, D. C., Ballantyne, C. M., Xu, Y., et al. (2004). The virulence function of Streptococcus pneumoniae surface protein A involves inhibition of complement activation and impairment of complement receptor-mediated protection. *J. Immunol.* 173 (12), 7506–7512. doi: 10.4049/jimmunol.173.12.7506

Rostkowska-Nadolska, B., Kapral, M., Fraczek, M., Kowalczyk, M., Gawron, W., and Mazurek, U. (2011). A microarray study of gene expression profiles in nasal polyps. *Auris Nasus Larynx* 38 (1), 58–64. doi: 10.1016/j.anl.2010.05.002

Sadallah, S., Gudat, F., Laissue, J. A., Spath, P. J., and Schifferli, J. A. (1999). Glomerulonephritis in a patient with complement factor I deficiency. *Am. J. Kidney Dis.* 33 (6), 1153–1157. doi: 10.1016/S0272-6386(99)70155-1

Salas, A., Pardo-Seco, J., Cebey-Lopez, M., Gomez-Carballa, A., Obando-Pacheco, P., Rivero-Calle, I., et al. (2017). Whole exome sequencing reveals new candidate genes in host genomic susceptibility to Respiratory Syncytial Virus Disease. *Sci. Rep.* 7 (1), 15888. doi: 10.1038/s41598-017-15752-4

Salas, A., Pardo-Seco, J., Barral-Arca, R., Cebey-Lopez, M., Gomez-Carballa, A., Rivero-Calle, I., et al. (2018). Whole exome sequencing identifies new host genomic susceptibility factors in empyema caused by Streptococcus pneumoniae in children: a pilot study. *Genes (Basel)* 9 (5), 240. doi: 10.3390/genes9050240

Santos-Cortez, R. L., Chiong, C. M., Reyes-Quintos, M. R., Tantoco, M. L., Wang, X., Acharya, A., et al. (2015). Rare A2ML1 variants confer susceptibility to otitis media. *Nat. Genet.* 47 (8), 917–920. doi: 10.1038/ng.3347

Santos-Cortez, R. L. P., Chiong, C. M., Frank, D. N., Ryan, A. F., Giese, A. P. J., Bootpetch Roberts, T., et al. (2018). FUT2 Variants confer susceptibility to familial otitis media. *Am. J. Hum. Genet.* 103 (5), 679–690. doi: 10.1016/j.ajhg.2018.09.010

Segata, N., Haake, S. K., Mannon, P., Lemon, K. P., Waldron, L., Gevers, D., et al. (2012). Composition of the adult digestive tract bacterial microbiome based on seven mouth surfaces, tonsils, throat and stool samples. *Genome Biol.* 13 (6), R42. doi: 10.1186/gb-2012-13-6-r42

Shannon, P., Markiel, A., Ozier, O., Baliga, N. S., Wang, J. T., Ramage, D., et al. (2003). Cytoscape: a software environment for integrated models of biomolecular interaction networks. *Genome Res.* 13 (11), 2498–2504. doi: 10.1101/gr.1239303

Sigal, G. B., Segal, M. R., Mathew, A., Jarlsberg, L., Wang, M., Barbero, S., et al. (2017). Biomarkers of tuberculosis severity and treatment effect: a directed screen of 70 host markers in a randomized clinical trial. *EbioMed.* 25, 112–121. doi: 10.1016/j.ebiom.2017.10.018

Smith, B. O., Mallin, R. L., Krych-Goldberg, M., Wang, X., Hauhart, R. E., Bromek, K., et al. (2002). Structure of the C3b binding site of CR1 (CD35), the immune adherence receptor. *Cell* 108 (6), 769–780. doi: 10.1016/s0092-8674(02)00672-4

Soneson, C., Love, M. I., and Robinson, M. D. (2015). Differential analyses for RNA-seq: transcript-level estimates improve gene-level inferences. *F1000Res* 4, 1521. doi: 10.12688/f1000research.7563.2

Stankovic, K. M., Goldsztein, H., Reh, D. D., Platt, M. P., and Metson, R. (2008). Gene expression profiling of nasal polyps associated with chronic sinusitis and aspirin-sensitive asthma. *Laryngoscope* 118 (5), 881–889. doi: 10.1097/MLG.0b013e31816b4b6f

Sveinbjornsson, G., Gudbjartsson, D. F., Halldorsson, B. V., Kristinsson, K. G., Gottfredsson, M., Barrett, J. C., et al. (2016). HLA class II sequence variants influence tuberculosis risk in populations of European ancestry. *Nat. Genet.* 48 (3), 318–322. doi: 10.1038/ng.3498

Tian, C., Hromatka, B. S., Kiefer, A. K., Eriksson, N., Noble, S. M., Tung, J. Y., et al. (2017). Genome-wide association and HLA region fine-mapping studies

identify susceptibility loci for multiple common infections. *Nat. Commun.* 8 (1), 599. doi: 10.1038/s41467-017-00257-5

van Ingen, G., Li, J., Goedegebure, A., Pandey, R., Li, Y. R., March, M. E., et al. (2016). Genome-wide association study for acute otitis media in children identifies FNDC1 as disease contributing gene. *Nat. Commun.* 7, 12792. doi: 10.1038/ncomms12792

Walter, J. M., Ren, Z., Yacoub, T., Reyfman, P. A., Shah, R. D., Abdala-Valencia, H., et al. (2019). Multidimensional assessment of the host response in mechanically ventilated patients with suspected pneumonia. *Am. J. Respir. Crit. Care Med.* 199 (10), 1225–1237. doi: 10.1164/rccm.201804-0650OC

Wang, W., Gao, Z., Wang, H., Li, T., He, W., Lv, W., et al. (2016). Transcriptome analysis reveals distinct gene expression profiles in eosinophilic and noneosinophilic chronic rhinosinusitis with nasal polyps. *Sci. Rep.* 6, 26604. doi: 10.1038/srep26604

Wang, K., Gao, M., Yang, M., Meng, F., Li, D., Lu, R., et al. (2017). Transcriptome analysis of bronchoalveolar lavage fluid from children with severe Mycoplasma pneumoniae pneumonia reveals novel gene expression and immunodeficiency. *Hum. Genomics* 11 (1), 4. doi: 10.1186/s40246-017-0101-y

Xia, J., Benner, M. J., and Hancock, R. E. (2014). NetworkAnalyst–integrative approaches for protein-protein interaction network analysis and visual exploration. *Nucleic Acids Res.* 42 (Web Server issue), W167–W174. doi: 10.1093/nar/gku443

Xia, J., Gill, E. E., and Hancock, R. E. (2015). NetworkAnalyst for statistical, visual and network-based meta-analysis of gene expression data. *Nat. Protoc.* 10 (6), 823–844. doi: 10.1038/nprot.2015.052

Yao, Y., Xie, S., and Wang, F. (2019). Identification of key genes and pathways in chronic rhinosinusitis with nasal polyps using bioinformatics analysis. *Am. J. Otolaryngol.* 40 (2), 191–196. doi: 10.1016/j.amjoto.2018.12.002

Zerbino, D. R., Achuthan, P., Akanni, W., Amode, M. R., Barrell, D., Bhai, J., et al. (2018). Ensembl 2018. *Nucleic Acids Res.* 46 (D1), D754–D761. doi: 10.1093/nar/gkx1098

Zheng, R., Li, Z., He, F., Liu, H., Chen, J., Chen, J., et al. (2018). Genome-wide association study identifies two risk loci for tuberculosis in Han Chinese. *Nat. Commun.* 9 (1), 4072. doi: 10.1038/s41467-018-06539-w

Zhou, G., Soufan, O., Ewald, J., Hancock, R. E. W., Basu, N., and Xia, J. (2019). NetworkAnalyst 3.0: a visual analytics platform for comprehensive gene expression profiling and meta-analysis. *Nucleic Acids Res.* 47, W234–W241. doi: 10.1093/nar/gkz240

Conflict of Interest: The authors declare that the research was conducted in the absence of any commercial or financial relationships that could be construed as a potential conflict of interest.

frontiers in Genetics

REVIEW
published: 07 February 2020
doi: 10.3389/fgene.2019.01395

Current Understanding of Host Genetics of Otitis Media

Ruishuang Geng[1], *Qingzhu Wang*[1,2], *Eileen Chen*[3] *and Qing Yin Zheng*[3]*

[1] College of Special Education, Binzhou Medical University, Yantai, China, [2] Department of Otolaryngology, Guangdong Second Provincial General Hospital, Guangzhou, China, [3] Department of Otolaryngology, Case Western Reserve University, Cleveland, OH, United States

The pathogenesis of otitis media (OM), an inflammatory disease of the middle ear (ME), involves interplay between many different factors, including the pathogenicity of infectious pathogens, host immunological status, environmental factors, and genetic predisposition, which is known to be a key determinant of OM susceptibility. Animal models and human genetics studies have identified many genes and gene variants associated with OM susceptibility: genes that encode components of multiple signaling pathways involved in host immunity and inflammatory responses of the ME mucosa; genes involved in cellular function, such as mucociliary transport, mucin production, and mucous cell metaplasia; and genes that are essential for Eustachian tube (ET) development, ME cavitation, and homeostasis. Since our last review, several new mouse models with mutations in genes such as *CCL3*, *IL-17A,* and *Nisch* have been reported. Moreover, genetic variants and polymorphisms in several genes, including *FNDC1, FUT2, A2ML1, TGIF1*, *CD44,* and *IL1-RA* variable number tandem repeat (VNTR) allele 2, have been identified as being significantly associated with OM. In this review, we focus on the current understanding of the role of host genetics in OM, including recent discoveries and future research prospects. Further studies on the genes identified thus far and the discovery of new genes using advanced technologies such as gene editing, next generation sequencing, and genome-wide association studies, will advance our understanding of the molecular mechanism underlying the pathogenesis of OM and provide new avenues for early screening and developing effective preventative and therapeutic strategies to treat OM.

Keywords: otitis media, genetics, susceptibility, immunity, inflammatory response, host, pathogenicity

OPEN ACCESS

Edited by:
Regie Santos-Cortez, University of Colorado, United States

Reviewed by:
Jian_Dong Li, Georgia State University, United States
Derek William Hood, Medical Research Council, United Kingdom

***Correspondence:**
Qing Yin Zheng
qyz@case.edu

Specialty section:
This article was submitted to Genetic Disorders, a section of the journal Frontiers in Genetics

Received: *31 October 2019*
Accepted: *20 December 2019*
Published: *07 February 2020*

Citation:
Geng R, Wang Q, Chen E and Zheng QY (2020) Current Understanding of Host Genetics of Otitis Media. Front. Genet. 10:1395. doi: 10.3389/fgene.2019.01395

INTRODUCTION

Otitis media (OM) is an inflammatory disease of the middle ear (ME) that is most commonly caused by bacterial pathogens, such as *Streptococcus pneumoniae* (Spn), nontypeable *Haemophilus influenzae* (NTHi), and *Moraxella catarrhalis*, and is one of the most common diseases in young children. There are several types of OM, such as acute OM (AOM), chronic OM with effusion (COME), and chronic suppurative OM (CSOM). More than 80% of children under the age of three suffer at least one episode of AOM; however, only a small subset of children experience recurrent or chronic OM (COM), and the reason for this remains unclear (Kong and Coates, 2009). Although

most cases of OM are resolved by the age of six, prolonged ME inflammation can lead to hearing loss and other complications in some cases.

The pathogenesis of OM is known to be multifactorial, involving pathogen virulence, host immune status, genetic predisposition, and environmental factors, alongside other risk factors that affect the occurrence of COM, such as allergy/atopy, prior upper respiratory tract viral infection, early or recurrent AOM, and passive smoking (Zhang et al., 2014). Genetics has also been shown to play a critical role in host susceptibility to OM; therefore, identifying genetic loci that are associated with OM could help to elucidate potential disease mechanisms and develop effective therapies. Many host genes identified and associated with OM have been reviewed before (Rye et al., 2011a; Kurabi et al., 2016; Bhutta et al., 2017b; Lin et al., 2017). In this review, we provide an update on the identification of new host genes, make progress in our understanding of previously identified genes in OM predisposition, and discuss the prospects for future research in this field.

INNATE IMMUNE AND INFLAMMATORY RESPONSES IN OM

The epithelial lining of the ME possesses several defense mechanisms; for instance, ME epithelial cells secret mucin and other defense molecules (e.g. defensins, interferons, lactoferrin, and nitric oxide) to attack and trap pathogens, particles, and dead cells, which are conveyed toward the nasopharynx *via* the Eustachian tube (ET) and cleared from the ME by the constant unidirectional beating of the cilia of ciliated epithelial cells. ME epithelial cells also express pattern recognition receptors (PRRs), such as Toll-like receptors (TLRs) and Nod-like receptors (NLRs), which recognize bacterial pathogens by binding to pathogen-associated molecular patterns (PAMPs) on their surface. The binding of PRRs and PAMPs activates downstream MAPK or NFκB signaling cascades to induce the expression and activation of pro-inflammatory transcription factors, such as NFκB and interferon-regulatory factors (IRFs). These transcription factors translocate to nucleus and induce the production and release of inflammatory cytokines and chemokines, which recruit and activate neutrophils, macrophages, and monocytes that destroy and clear invading bacterial pathogens (Leichtle et al., 2011; Kurabi et al., 2016).

Genes Involved in Inflammatory Responses in OM

During the past decade, considerable progress has been made in our understanding of the fundamental molecular mechanisms underlying the role of innate immunity and inflammatory responses in OM (Kurabi et al., 2016). The innate immune system plays important roles in the initiation of inflammation, clearance of invading pathogens, and recovery in AOM. Many genes have been identified that are involved in immunity and inflammatory responses in OM, and their functions have been studied in animal models. The most important discoveries of mouse models and gene association studies are briefly summarized and discussed below.

Pro-inflammatory molecules, such as TNF-α, IL-1β, and C-C motif chemokine ligand 3 (CCL3), play key roles in the recruitment of inflammatory cells into the ME and the activation of these cells for microbial clearance. Mice deficient in pro-inflammatory molecules, such as TNF-α and CCL3, displayed diminished but prolonged leukocyte recruitment, defective macrophage function, and failure to clear NTHi from the ME cavity (Leichtle et al., 2010; Deniffel et al., 2017). Moreover, exogenous CCL3 can restore phagocytosis and fully restore OM recovery, suggesting that CCL3 acts downstream of TNF-α (Leichtle et al., 2010). These data pinpoint the essential roles of pro-inflammatory molecules in the initiation and recovery in AOM.

Mouse mutants deficient in PRRs (TLR2, TLR4, and TLR9), NLRs [apoptosis-associated speck-like protein containing a caspase-activating and recruitment domain (ASC)], and adaptor proteins (MyD88 and TRIF) display reduced production and maturation of pro-inflammatory cytokines, such as IL-1 and TNF-α, which leads to reduced leukocyte recruitment to the ME and, more profoundly, persistent inflammation with impaired bacterial clearance, and this is consistent with their roles in mediating the production of pro-inflammatory cytokines in response to pathogens and in the recovery of AOM (Hirano et al., 2007; Hernandez et al., 2008; Han et al., 2009; Leichtle et al., 2009a; Leichtle et al., 2009b; Leichtle et al., 2012). Similarly, in children, genetic polymorphisms in TLR2, TLR4, and the TLR co-receptor CD14 have been found to be associated with an increased incidence of OM, while TLR4 also plays a role in acquired adaptive mucosal immunity in the ME (Wiertsema et al., 2006; Emonts et al., 2007; Hafren et al., 2015; Toivonen et al., 2017).

The active form of IL-1β is a cleavage product formed by the inflammasome, a multi-protein complex that consists of the NLRs ASC and pro-caspase 1. ASC-deficient mutants display a lack of IL-1β maturation in the ME, reduced leukocyte recruitment and infiltration in the ME cavity, and reduced NTHi phagocytosis (Kurabi et al., 2015). Moreover, ASC deficiency increases the degree and duration of mucosal epithelial hyperplasia in the ME and delays bacterial clearance in the infected ME cavity (Kurabi et al., 2015). In a microphage cell model infected with Spn, IL-1β and TNF-α secretion were significantly reduced by treatment with inhibitors of c-Jun N-terminal kinase (JNK) or spleen tyrosine kinase (Syk). Furthermore, it has been demonstrated that JNK is required for ASC oligomerization and caspase-1 activation, and that JNK activation *via* phosphorylation is regulated by Syk (Feng et al., 2018) with similar results having also been obtained in neutrophils upon Spn infection. In addition to JNK, neutrophil serine proteases have also been found to participate in IL-1β secretion by regulating ASC oligomerization and caspase-1 activation (Zhang et al., 2019).

It has also been shown that IL-17A levels are significantly upregulated in ME fluid during AOM. Wang et al. reported that IL-17A promotes neutrophil recruitment to the ME cavity and

neutrophil apoptosis for bacterial clearance *via* the p38 MAPK signaling pathway during Spn infection (Wang et al., 2014a). The same group found that IL-17A also induces ME injury since *IL-17A* knockout (KO) mice display less severe pathological changes in their ME and lower pro-inflammatory cytokine and myeloperoxidase (MPO) levels. Furthermore, the group showed that neutrophil MPO production is mediated by the p38 MAPK signaling pathway (Wang et al., 2017).

In summary, the innate immune system mediated by TLR, NLR, and their downstream effectors and signaling pathways play critical roles in the production of pro-inflammatory molecules in response to pathogens for the recruitment of leukocytes into ME and recovery of AOM. Other signaling pathways, such as JNK and MAPK, also participate in the initiation of inflammation and ME injury, which may be caused by prolonged existence of leukocytes and elevated level of myeloperoxidase in the ME.

Genes Involved in Anti-Inflammatory Responses in OM

While pro-inflammatory responses fight infection and damage host tissue, they are balanced by anti-inflammatory responses that are thought to protect against host tissue damage and initiate repair and healing to restore tissue homeostasis. Both pro- and anti-inflammatory cytokines and cytokine signaling genes are rapidly upregulated in response to NTHi, as shown by transcriptome assays performed during a complete episode of AOM (Hernandez et al., 2015). IL-6, which acts as both a pro- and anti-inflammatory cytokine, is significantly upregulated 3–6 h after NTHi inoculation, with its decline followed by significant increases in other pro-inflammatory cytokines (IL-1 β and TNF-α) and anti-inflammatory cytokines (IL-1 receptor antagonist (IL-1RA) and IL-10) (Hernandez et al., 2015). It has been found that IL-10 is associated with OM and plays a critical role in protecting the cochlea from inflammation-mediated tissue damage by negatively regulating *MCP-1/CCL2* expression (Ilia et al., 2014; Woo et al., 2015). Deubiquitinase cylindromatosis (CYLD) has been found to suppress NTHi-induced inflammation by inhibiting the expression of the key pro-inflammatory chemokine IL-8 *via* the MAP kinase phosphatase 1 (MKP-1)–dependent inhibition of extracellular signal-regulated kinase (ERK) (Wang et al., 2014b). In a recent study, Zivkovic et al. found that the *IL-1RA* VNTR allele 2 was associated with a chronic OM patient in Serbia and suggested that the allele is associated with higher IL-1RA levels, consistent with the increase in IL-1RA observed in mouse models of OM (Zivkovic et al., 2018).

*Several TGF*β signaling pathway genes have been associated with AOM in humans, and the TGFβ signaling pathway has been shown to be involved in anti-inflammatory function in mouse models of OM (Ilia et al., 2014; Rye et al., 2014). The immunomodulatory gene transforming growth interacting factor 1 (TGIF1) is a negative regulator of the TGFβ signaling pathway, and *Tgif1* knockout mice develop spontaneous COME, which is characterized by significant thickening of the ME mucosa lining and goblet cell population expansion (Tateossian et al., 2013). In addition, studies in *Fbxo11*- and *Evi1-deficient* mouse models have indicated that OM is *associated with defects in the regulation of* TGFβ signaling. Evi1 is known to repress TGFβ signaling in several pathological processes by interacting with different proteins and negatively regulate NTHi-induced inflammation by inhibiting NFκB activity (Kurokawa et al., 1998; Izutsu et al., 2001; Sato et al., 2008; Xu et al., 2012). Moreover, Evi1 dominant mutations lead to the spontaneous development of OM in mice under specific pathogen-free conditions (Parkinson et al., 2006; Hood et al., 2016). *Fbxo11 is also involved in* TGFβ signaling by regulating phosphoSmad2 levels in the epithelial cells of palatal shelves, while a recent report showed that $Fbxo11^{lf/+}$ mutations cause failed mesenchymal regression during bulla cavitation, which may be the underlying cause of OM (Tateossian et al., 2009; Del-Pozo et al., 2019a). FBXO11 and TGIF1 have also been associated with COM in humans (Segade et al., 2006; Rye et al., 2011b; Bhutta et al., 2017a), and the involvement of EVI1, FBXO11, and TGIF1 in the development of COM may be mediated *via* vascular endothelial growth factor (VEGF) signaling, which was found to be upregulated in the leukocytes of these mutant mice during the bulla fluid response to inflammatory hypoxia (Cheeseman et al., 2011). Furthermore, VEGF signaling has also been demonstrated in the effusions of children with COME, while NFκB has been detected in the mucosa of patients with CSOM (Sekiyama et al., 2011; Jesic et al., 2014). These data further suggest the regulation of ME inflammation involves complex interactions between several signaling pathways. Continuing study is needed to reveal the molecular mechanism underlying the pathogenesis of COM.

Other Genes Involve in Innate Immune and Inflammatory Response in OM

BPIFA1 (SPLUNC1), which is abundant in the mammalian nasal, oral, and respiratory mucosa, has broad-spectrum antimicrobial activity and can act as a chemoattractant that recruits macrophages and neutrophils to the site of infection (Sayeed et al., 2013). In mice, BPIFA1 is highly expressed in the surface epithelium, submucosal glands in the ME, and ET, while BPIFA1-deficient mice display an increased COM frequency, as characterized by the accumulation of neutrophils, proteinaceous fluid, and mucus in the ME and extensive remodeling of the ME walls (Bartlett et al., 2015). Recently, Mulay et al. found that *Bpifa1* deletion in $Evi1^{Jbo/+}$ mice significantly worsened the OM phenotype, thickening the ME mucosa and increased collagen deposition, without significantly increasing pro-inflammatory gene expression. The authors concluded that BPIFA1 is involved in maintaining homeostasis within the ME and its loss causes more severe OM *via* a mechanism other than the inflammatory response (Mulay et al., 2018). In this study, the deletion of *BPIFA1* alone does not increase the susceptibility to OM, which is different from the ENU $Bpifa1^{-/-}$ mutant. This discrepancy in the predisposition to OM may be due to the fact that the mutations are in different genetic backgrounds (Bartlett et al., 2015; Mulay et al., 2018).

Recently, Wang et al. found a multifunctional growth factor, Progranulin (PGRN), was involved in AOM in an unusual way in

the study of PGRN-deficient ($PGRN^{-/-}$) mouse model (Wang et al., 2018). After Spn inoculation, $PGRN^{-/-}$ mice exhibited increased macrophage recruitment in ME but delayed bacteria clearance. They found the production of CCL2 is increased, which could contribute to enhanced macrophage recruitment, whereas the delayed bacteria clearance is most likely due to impaired endocytosis capacity of macrophages (Wang et al., 2018).

Many studies have induced AOM in rodent models using Spn, NTHi, and influenzae A virus to conduct transcriptomic analyses and thereby identify genes and associated pathways involved in OM. These studies have found that expression of the inflammatory cytokines *Cxcl1, Cxcl2*, and *IL-6*, and genes involved in NFκB signaling, innate immune, and inflammatory responses are upregulated in OM. These data further support the roles of inflammatory cytokines and innate immune response in AOM (MacArthur et al., 2013; Hernandez et al., 2015). Genes that are important for craniofacial structure and ME cellular function in OM.

The coordinated movement of cilia toward the pharynx *via* the ET is essential for trapping pathogens and mucociliary clearance. Many OM mouse models are characterized by gene mutations that cause defects in craniofacial anatomy or ME cellular function, including mucin production, ciliated cell function, ET structure and function, ME cavitation, and mucosal hyperplasia. Many of these mouse mutants spontaneously develop COME and thus can serve as good models for studying COME (Bhutta et al., 2017b; Lin et al., 2017).

In the past few years, continuing efforts have been made to identify new genes and further characterize existing mouse models. Mutations in TNF-like ligand ectodysplasin (Eda) and its receptor, Edar, result in the impaired development or loss of submucosal glands, leading to reduced ET gating and the ascension of bacteria and foreign body particles into the ME cavity as well as reduced mucociliary clearance in mice and rats (Azar et al., 2016; Del-Pozo et al., 2019b). Mutations in the EYA transcriptional coactivator and phosphatase 4 *(Eya4) and Fbxo11, which cause delayed or failed* mesenchyme regression during ME cavitation, have also been associated with OM (Depreux et al., 2008; Del-Pozo et al., 2019a). T-box transcription factor 1 (Tbx1) deficiency disrupts the function of the muscles that control ET function (Fuchs et al., 2015; Funato and Yanagisawa, 2018), while OM model mice carrying mutations in the cell adhesion protein Cdh11 display ME cavitation defects (Kiyama et al., 2018). Further study of many of previous identified genes in mouse models is needed to elucidate the cellular and molecular mechanism of these genes in OM.

RECENTLY IDENTIFIED GENES ASSOCIATED WITH OM

In the past decade, a number of genetic loci, such as those at 10q26.3, 19q13.43, 17q12, 10q22.3, and 2q31.1, and genes including *A2ML1, BPIFA1, CAPN14, GALNT14*, *FBXO11*, *FNDC1, FUT2*, and *TGIF1,* have been reported to be associated with OM (Daly et al., 2004; Casselbrant et al., 2009; Chen et al., 2011; Rye et al., 2011b; Rye et al., 2012; Allen et al., 2013; Rye et al., 2014; Santos-Cortez et al., 2015; Einarsdottir et al., 2016; Santos-Cortez et al., 2016; van Ingen et al., 2016; Bhutta et al., 2017a; Santos-Cortez et al., 2018). In addition, several genes have been identified as associated with childhood ear infection *via* a genome-wide association study (GWAS), such as *FUT2, TBX1, ABO, MKX*, *FGF3*, *AUTS2, CDHR3, and PLG (*Tian et al., 2017*).* Among these, *FUT2 and TBX1 were associated with OM by separate studies;* however, many of these associations did not reach the genome-wide significance threshold ($p < 5 \times 10^{-8}$), therefore their *involvement in OM requires further validation. Fortunately,* during the past three years, an increasing number of genes have been identified by GWAS, exome sequencing, linkage analysis, and the use of mouse mutants.

The alpha-2-macroglobulin-like 1 (*A2ML1*) gene encodes an ME-specific protease inhibitor with 41% identity and 59% similarity with alpha-2-macroglobulin (*A2M*), an inflammatory marker of the ME and oral cavity. A number of rare *A2ML1* variants have been associated with OM susceptibility in indigenous Filipino and in European- and Hispanic-American children (Santos-Cortez et al., 2015; Santos-Cortez et al., 2016; Larson et al., 2019). An RNAseq analysis has shown that *A2ML1* upregulation *is correlated with the* differential expression of genes in the keratinocyte and epidermal cell differentiation pathways, further suggesting that these rare *A2ML1* variants play a role in ME mucosal pathology.

FUT2, which encodes alpha-(1,2)-fucosyltransferase, is a human secretion gene that controls the expression of the Lewis and ABO(H) antigens on the mucosal epithelia, *via* which bacterial pathogens bind (Goto et al., 2016). GWAS identified *FUT2 as a potential susceptibility gene for ear infections in children (*Tian et al., 2017*), while* Santos-Cortez *et al. found that common and rare FUT2* variants confer susceptibility to recurrent/chronic OM in patients from various ethnicities. FUT2 likely modulates the ME microbiome by regulating A antigen levels in epithelial cells (Santos-Cortez et al., 2018).

Van Ingen et al. identified that the fibronectin type III domain containing 1 (*FNDC1*) gene is significantly associated with AOM *via* GWAS (van Ingen et al., 2016). Previous reports have suggested that FNDC1 is involved in multiple cellular processes, including inflammation. The AOM-associated *FNDC1* variants were correlated with the methylation status of the *FNDC1* gene and their association surpassed the threshold of genome-wide significance and was replicated in an independent cohort. Moreover, Fndc1 is expressed in the ME tissue of mice and its expression upregulated upon lipopolysaccharide treatment, which is known to potently induce inflammation and stimulate TGF-β, TNF-α, and IL-1 signaling. Thus, these studies imply that *FNDC1* may be involved in the pathogenesis of OM by modulating immunity or inflammatory responses (van Ingen et al., 2016).

CD44 is a transmembrane glycoprotein receptor for hyaluronic acid that is widely expressed on the surface of leukocytes, endothelial cells, epithelial cells, fibroblasts, and keratinocytes and is involved in cell-cell interactions, cell adhesion, and migration. Mice deficient in CD44 exhibit reduced early mucosal hyperplasia and leukocyte recruitment

and delayed bacterial clearance, suggesting it plays a critical role in the cellular function of leukocytes and epithelial cells as wells as in the pathogenesis and recovery of OM (Lim et al., 2019).

Nischarin is a cytosolic protein that is involved in the regulation of cell motility, cell invasion, vesicle maturation, and tumor suppression by interacting with multiple interacting partners. Crompton et al. reported that mice with a mis-sense mutation in the *Nisch* gene spontaneously develop OM, with progression to chronic OM evidenced by histological examinations (Crompton et al., 2017). Moreover, the mutant mice exhibit serous or granulocytic effusions, become increasingly macrophage- and neutrophil-rich with age, and develop a thickened, inflamed mucoperiosteum. Significant genetic interactions have also been observed between *Nisch* and *Itga5* mutations in the penetrance and severity of chronic OM, while immunohistochemical staining and protein expression analysis have implicated PAK1, RAC1, and downstream LIM domain kinase 1 (LIMK1) and NFκB pathway signaling in the development of chronic OM (Crompton et al., 2017). Further study on the molecular pathways involve these recently identified genes could provide insight into the pathogenesis of OM.

MicroRNAs AND OM

Several reports have suggested that miRNAs are involved in the pathogenesis of OM. Song et al. identified 15 differentially expressed miRNAs from human ME epithelial cells (HMEECs) treated with lipopolysaccharides (LPS), which are a cell wall component of gram-negative bacteria. The predicted target genes of these miRNAs are involved in developmental processes, regulating cell growth, innate immune responses, acute inflammatory responses, the IκB kinase/NFκB cascade, complement activation, cell communication, and cell differentiation, among others (Song et al., 2011). Val et al. detected miRNAs from chronic OM ME effusions and identified five miRNAs (miR-378a-3p + miR-378i, miR-200a-3p, miR-378g, miR30d-5p, and miR-222-3p) that were significantly induced in exosomes from HMEECs exposed to NTHi lysates, all of which are known to target innate immunity genes (Val et al., 2018). Associations between miRNAs and OM have also been reported in humans; for instance, miR-146 expression is increased in the ME of OM patients and *in vitro* cultured ME epithelial cells stimulated with proinflammatory cytokines. Therefore, identifying miRNA target genes and their downstream pathways could provide new insights into OM (Samuels et al., 2016).

CONCLUDING REMARKS

During the past decade, mutagenesis and mutant characterization studies in mouse models have identified many genes as predisposing factors to OM which are predominantly involved in host immune and inflammatory responses, cellular function in mucin production, mucociliary transport, and the development of the ME cavity and craniofacial structure. Genetic studies in human patients have identified far fewer genes and loci that are significantly associated with OM due to small patient sample sizes, poor phenotyping, and more complex genetic polymorphisms. However, there has been some consistency between the genes identified by human and mouse genetic studies, with polymorphisms or variants of the human orthologs of mouse genes, such as *TLR2, TLR4, FBXO11, and BPIFA1*, also found to be significantly associated with OM in humans. Moreover, some OM-associated syndromic disease genes have also been identified in mice.

Studies in both human and mouse models have shown that the host innate immune system plays crucial roles in the pathogenesis and recovery of AOM. Deficiency in PRRs and downstream signaling molecules that affect pro-inflammatory factor production delay OM recovery, while mouse mutants with ME cellular function defects and craniofacial abnormalities often spontaneously develop chronic OM. Chronic OM has also been associated with genetic polymorphisms or mutations in genes involved in or mediated by innate immunity, VEGF, *and TGF*β signaling pathways, such as *Tlr4, Evi1, Nisch, Bpifa1, Tgif1*, and *Fbxo11*.

Mouse mutants have been shown to recapitulate many features of human chronic OM, including ME leukocyte infiltration, mucosal hyperplasia, and the production of mucus-rich effusions, thus serve as excellent models for studying the pathology and mechanism underlying the pathogenesis and recovery of OM. The human counterparts of these mouse genes associated with OM predisposition should be investigated as candidate genes for genetic linkage or association studies in human OM patients of different ancestries. However, the majority of studies in animal models are phenotypic or pathophysiological, and little is known about the disease-related pathways or molecular mechanisms underlying the pathogenesis of chronic OM. Thus, further studies on these animal models are necessary.

There are several limitations to the study of OM using mouse models. Firstly, they may not fully recapitulate the features of human OM; for example, there is no mouse model of CSOM. Secondly, the human counterparts of COME causal genes in mice, such as those causing syndromic disease and craniofacial abnormalities, may not account for the high prevalence of OM in humans as the correlation between ET abnormalities and chronic OM susceptibility in young children remains unclear (Sade et al., 1986; Takasaki et al., 2007). Instead, craniofacial abnormalities may be more associated with chronic OM in adult patients (Dinc et al., 2015; Nemade et al., 2018). OM susceptibility is likely to be polygenic. Thirdly, many of these mouse models have been obtained by mutagenesis in isogenic inbred lines housed in clean facilities, whereas the human population has huge genetic variation and polymorphisms, experiences diverse living conditions, and is exposed to different environments. Studying OM gene function in outbred laboratory animals may

be a better approach. Nevertheless, mice still serve as good models for studying the etiology, pathophysiology, and recovery process of human OM. Therefore, the genes that have been associated with OM in humans but failed to exceed genome-wide significance thresholds or could not be replicated in different cohorts should be further investigated in mice using reverse genetics tools, such as gene editing.

In the past three years, promising results have been obtained by using GWAS, exome sequencing, and linkage analysis to identify human genes associated with OM. Genetic variants and polymorphisms in several genes, such as *FNDC1, FUT2, A2ML1, TGIF1,* and *CD44*, have been identified as significantly associated with OM, confirming that the genome-wide significance of genetic associations can be improved by increasing the size of the study group. With continuing advancements in genetic analysis technologies and experimental design, such as increased sample size, more defined phenotyping, and less diversity in the ancestry of the study group, future studies should be able to identify more novel OM-predisposing genes to advance our understanding of the mechanism underlying the pathogenesis and recovery of OM. This information would, in turn, provide new options for efficient diagnosis and developing effective therapies that target the specific etiology of OM.

AUTHOR CONTRIBUTIONS

RG, QW, EC, and QZ collected data and wrote the manuscript. All authors have read and approved the submitted form.

FUNDING

This work was supported by the National Institute of Health (R01DC015111 and R21DC005846); the National Natural Science Foundation of China (81530030, 35281873679, 81500797, and 81700902); the Taishan Scholar Foundation (ZR2019PH06); and Binzhou Medical University start-up fund.

REFERENCES

Allen, E. K., Chen, W. M., Weeks, D. E., Chen, F., Hou, X., Mattos, J. L., et al. (2013). A genome-wide association study of chronic otitis media with effusion and recurrent otitis media identifies a novel susceptibility locus on chromosome 2. *J. Assoc. Res. Otolaryngol.* 14, 791–800. doi: 10.1007/s10162-013-0411-2

Azar, A., Piccinelli, C., Brown, H., Headon, D., and Cheeseman, M. (2016). Ectodysplasin signalling deficiency in mouse models of hypohidrotic ectodermal dysplasia leads to middle ear and nasal pathology. *Hum. Mol. Genet.* 25, 3564–3577. doi: 10.1093/hmg/ddw202

Bartlett, J. A., Meyerholz, D. K., Wohlford-Lenane, C. L., Naumann, P. W., Salzman, N. H., and Mccray, P. B.Jr. (2015). Increased susceptibility to otitis media in a Splunc1-deficient mouse model. *Dis. Model Mech.* 8, 501–508. doi: 10.1242/dmm.019646

Bhutta, M. F., Lambie, J., Hobson, L., Goel, A., Hafren, L., Einarsdottir, E., et al. (2017a). A mouse-to-man candidate gene study identifies association of chronic otitis media with the loci TGIF1 and FBXO11. *Sci. Rep.* 7, 12496. doi: 10.1038/s41598-017-12784-8

Bhutta, M. F., Thornton, R. B., Kirkham, L. S., Kerschner, J. E., and Cheeseman, M. T. (2017b). Understanding the aetiology and resolution of chronic otitis media from animal and human studies. *Dis. Model Mech.* 10, 1289–1300. doi: 10.1242/dmm.029983

Casselbrant, M. L., Mandel, E. M., Jung, J., Ferrell, R. E., Tekely, K., Szatkiewicz, J. P., et al. (2009). Otitis media: a genome-wide linkage scan with evidence of susceptibility loci within the 17q12 and 10q22.3 regions. *BMC Med. Genet.* 10, 85. doi: 10.1186/1471-2350-10-85

Cheeseman, M. T., Tyrer, H. E., Williams, D., Hough, T. A., Pathak, P., Romero, M. R., et al. (2011). HIF-VEGF pathways are critical for chronic otitis media in Junbo and Jeff mouse mutants. *PloS Genet.* 7, e1002336. doi: 10.1371/journal.pgen.1002336

Chen, W. M., Allen, E. K., Mychaleckyj, J. C., Chen, F., Hou, X., Rich, S. S., et al. (2011). Significant linkage at chromosome 19q for otitis media with effusion and/or recurrent otitis media (COME/ROM). *BMC Med. Genet.* 12, 124. doi: 10.1186/1471-2350-12-124

Crompton, M., Purnell, T., Tyrer, H. E., Parker, A., Ball, G., Hardisty-Hughes, R. E., et al. (2017). A mutation in Nischarin causes otitis media *via* LIMK1 and NF-kappaB pathways. *PloS Genet.* 13, e1006969. doi: 10.1371/journal.pgen.1006969

Daly, K. A., Brown, W. M., Segade, F., Bowden, D. W., Keats, B. J., Lindgren, B. R., et al. (2004). Chronic and recurrent otitis media: a genome scan for susceptibility loci. *Am. J. Hum. Genet.* 75, 988–997. doi: 10.1086/426061

Del-Pozo, J., Macintyre, N., Azar, A., Glover, J., Milne, E., and Cheeseman, M. (2019a). Chronic otitis media is initiated by a bulla cavitation defect in the FBXO11 mouse model. *Dis. Model Mech.* 12, 1–20. doi: 10.1242/dmm.038315

Del-Pozo, J., Macintyre, N., Azar, A., Headon, D., Schneider, P., and Cheeseman, M. (2019b). Role of ectodysplasin signalling in middle ear and nasal pathology in rat and mouse models of hypohidrotic ectodermal dysplasia. *Dis. Model Mech.* 12, 1–9. doi: 10.1242/dmm.037804

Deniffel, D., Nuyen, B., Pak, K., Suzukawa, K., Hung, J., Kurabi, A., et al. (2017). Otitis media and nasopharyngeal colonization in ccl3(-/-) mice. *Infect. Immun.* 85, 1–14. doi: 10.1128/IAI.00148-17

Depreux, F. F., Darrow, K., Conner, D. A., Eavey, R. D., Liberman, M. C., Seidman, C. E., et al. (2008). Eya4-deficient mice are a model for heritable otitis media. *J. Clin. Invest.* 118, 651–658. doi: 10.1172/JCI32899

Dinc, A. E., Damar, M., Ugur, M. B., Oz, I. I., Elicora, S. S., Biskin, S., et al. (2015). Do the angle and length of the eustachian tube influence the development of chronic otitis media? *Laryngoscope* 125, 2187–2192. doi: 10.1002/lary.25231

Einarsdottir, E., Hafren, L., Leinonen, E., Bhutta, M. F., Kentala, E., Kere, J., et al. (2016). Genome-wide association analysis reveals variants on chromosome 19 that contribute to childhood risk of chronic otitis media with effusion. *Sci. Rep.* 6, 33240. doi: 10.1038/srep33240

Emonts, M., Veenhoven, R. H., Wiertsema, S. P., Houwing-Duistermaat, J. J., Walraven, V., De Groot, R., et al. (2007). Genetic polymorphisms in immunoresponse genes TNFA, IL6, IL10, and TLR4 are associated with recurrent acute otitis media. *Pediatrics* 120, 814–823. doi: 10.1542/peds.2007-0524

Feng, S., Huang, Q., Ye, C., Wu, R., Lei, G., Jiang, J., et al. (2018). Syk and JNK signaling pathways are involved in inflammasome activation in macrophages infected with Streptococcus pneumoniae. *Biochem. Biophys. Res. Commun.* 507, 217–222. doi: 10.1016/j.bbrc.2018.11.011

Fuchs, J. C., Linden, J. F., Baldini, A., and Tucker, A. S. (2015). A defect in early myogenesis causes Otitis media in two mouse models of 22q11.2 Deletion Syndrome. *Hum. Mol. Genet.* 24, 1869–1882. doi: 10.1093/hmg/ddu604

Funato, N., and Yanagisawa, H. (2018). Deletion of the T-box transcription factor gene, Tbx1, in mice induces differential expression of genes associated with cleft palate in humans. *Arch. Biol.* 95, 149–155. doi: 10.1016/j.archoralbio.2018.08.001

Goto, Y., Uematsu, S., and Kiyono, H. (2016). Epithelial glycosylation in gut homeostasis and inflammation. *Nat. Immunol.* 17, 1244–1251. doi: 10.1038/ni.3587

Hafren, L., Einarsdottir, E., Kentala, E., Hammaren-Malmi, S., Bhutta, M. F., Macarthur, C. J., et al. (2015). Predisposition to childhood otitis media and genetic polymorphisms within the toll-Like receptor 4 (TLR4) locus. *PloS One* 10, e0132551. doi: 10.1371/journal.pone.0132551

Han, F., Yu, H., Tian, C., Li, S., Jacobs, M. R., Benedict-Alderfer, C., et al. (2009). Role for Toll-like receptor 2 in the immune response to Streptococcus pneumoniae infection in mouse otitis media. *Infect. Immun.* 77, 3100–3108. doi: 10.1128/IAI.00204-09

Hernandez, M., Leichtle, A., Pak, K., Ebmeyer, J., Euteneuer, S., Obonyo, M., et al. (2008). Myeloid differentiation primary response gene 88 is required for the resolution of otitis media. *J. Infect. Dis.* 198, 1862–1869. doi: 10.1086/593213

Hernandez, M., Leichtle, A., Pak, K., Webster, N. J., Wasserman, S. I., and Ryan, A. F. (2015). The transcriptome of a complete episode of acute otitis media. *BMC Genomics* 16, 259. doi: 10.1186/s12864-015-1475-7

Hirano, T., Kodama, S., Fujita, K., Maeda, K., and Suzuki, M. (2007). Role of Toll-like receptor 4 in innate immune responses in a mouse model of acute otitis media. *FEMS Immunol. Med. Microbiol.* 49, 75–83. doi: 10.1111/j.1574-695X.2006.00186.x

Hood, D., Moxon, R., Purnell, T., Richter, C., Williams, D., Azar, A., et al. (2016). A new model for non-typeable Haemophilus influenzae middle ear infection in the Junbo mutant mouse. *Dis. Model Mech.* 9, 69–79. doi: 10.1242/dmm.021659

Ilia, S., Goulielmos, G. N., Samonis, G., and Galanakis, E. (2014). Polymorphisms in IL-6, IL-10, TNF-alpha, IFN-gamma and TGF-beta1 genes and susceptibility to acute otitis media in early infancy. *Pediatr. Infect. Dis. J.* 33, 518–521. doi: 10.1097/INF.0000000000000229

Izutsu, K., Kurokawa, M., Imai, Y., Maki, K., Mitani, K., and Hirai, H. (2001). The corepressor CtBP interacts with Evi-1 to repress transforming growth factor beta signaling. *Blood* 97, 2815–2822. doi: 10.1182/blood.V97.9.2815

Jesic, S., Jotic, A., Tomanovic, N., and Zivkovic, M. (2014). Expression of toll-like receptors 2, 4 and nuclear factor kappa B in mucosal lesions of human otitis: pattern and relationship in a clinical immunohistochemical study. *Ann. Otol. Rhinol. Laryngol.* 123, 434–441. doi: 10.1177/0003489414527229

Kiyama, Y., Kikkawa, Y. S., Kinoshita, M., Matsumoto, Y., Kondo, K., Fujimoto, C., et al. (2018). The adhesion molecule cadherin 11 is essential for acquisition of normal hearing ability through middle ear development in the mouse. *Lab. Invest.* 98, 1364–1374. doi: 10.1038/s41374-018-0083-y

Kong, K., and Coates, H. L. (2009). Natural history, definitions, risk factors and burden of otitis media. *Med. J. Aust.* 191, S39–S43. doi: 10.5694/j.1326-5377.2009.tb02925.x

Kurabi, A., Lee, J., Wong, C., Pak, K., Hoffman, H. M., Ryan, A. F., et al. (2015). The inflammasome adaptor ASC contributes to multiple innate immune processes in the resolution of otitis media. *Innate Immun.* 21, 203–214. doi: 10.1177/1753425914526074

Kurabi, A., Pak, K., Ryan, A. F., and Wasserman, S. I. (2016). Innate Immunity: Orchestrating Inflammation and Resolution of Otitis Media. *Curr. Allergy Asthma Rep.* 16, 6. doi: 10.1007/s11882-015-0585-2

Kurokawa, M., Mitani, K., Imai, Y., Ogawa, S., Yazaki, Y., and Hirai, H. (1998). The t(3;21) fusion product, AML1/Evi-1, interacts with Smad3 and blocks transforming growth factor-beta-mediated growth inhibition of myeloid cells. *Blood* 92, 4003–4012. doi: 10.1182/blood.V92.11.4003

Larson, E. D., Magno, J. P. M., Steritz, M. J., Llanes, E., Cardwell, J., Pedro, M., et al. (2019). A2ML1 and otitis media: novel variants, differential expression and relevant pathways. *Hum. Mutat.* 40 (8), 1156–1171. doi: 10.1002/humu.23769

Leichtle, A., Hernandez, M., Pak, K., Webster, N. J., Wasserman, S. I., and Ryan, A. F. (2009a). The toll-Like receptor adaptor TRIF contributes to otitis media pathogenesis and recovery. *BMC Immunol.* 10, 45. doi: 10.1186/1471-2172-10-45

Leichtle, A., Hernandez, M., Pak, K., Yamasaki, K., Cheng, C. F., Webster, N. J., et al. (2009b). TLR4-mediated induction of TLR2 signaling is critical in the pathogenesis and resolution of otitis media. *Innate Immun.* 15, 205–215. doi: 10.1177/1753425909103170

Leichtle, A., Hernandez, M., Ebmeyer, J., Yamasaki, K., Lai, Y., Radek, K., et al. (2010). CC chemokine ligand 3 overcomes the bacteriocidal and phagocytic defect of macrophages and hastens recovery from experimental otitis media in TNF-/- mice. *J. Immunol.* 184, 3087–3097. doi: 10.4049/jimmunol.0901167

Leichtle, A., Lai, Y., Wollenberg, B., Wasserman, S. I., and Ryan, A. F. (2011). Innate signaling in otitis media: pathogenesis and recovery. *Curr. Allergy Asthma Rep.* 11, 78–84. doi: 10.1007/s11882-010-0158-3

Leichtle, A., Hernandez, M., Lee, J., Pak, K., Webster, N. J., Wollenberg, B., et al. (2012). The role of DNA sensing and innate immune receptor TLR9 in otitis media. *Innate Immun.* 18, 3–13. doi: 10.1177/1753425910393539

Lim, H. W., Pak, K., Kurabi, A., and Ryan, A. F. (2019). Lack of the hyaluronan receptor CD44 affects the course of bacterial otitis media and reduces leukocyte recruitment to the middle ear. *BMC Immunol.* 20, 20. doi: 10.1186/s12865-019-0302-3

Lin, J., Hafren, L., Kerschner, J., Li, J. D., Brown, S., Zheng, Q. Y., et al. (2017). Panel 3: Genetics and Precision Medicine of Otitis Media. *Otolaryngol. Head Neck Surg.* 156, S41–S50. doi: 10.1177/0194599816685559

Macarthur, C. J., Hausman, F., Kempton, J. B., Choi, D., and Trune, D. R. (2013). Otitis media impacts hundreds of mouse middle and inner ear genes. *PloS One* 8, e75213. doi: 10.1371/journal.pone.0075213

Mulay, A., Hood, D. W., Williams, D., Russell, C., Brown, S. D. M., Bingle, L., et al. (2018). Loss of the homeostatic protein BPIFA1, leads to exacerbation of otitis media severity in the Junbo mouse model. *Sci. Rep.* 8, 3128. doi: 10.1038/s41598-018-21166-7

Nemade, S. V., Shinde, K. J., Rangankar, V. P., and Bhole, P. (2018). Evaluation and significance of Eustachian tube angles and pretympanic diameter in HRCT temporal bone of patients with chronic otitis media. *World J. Otorhinolaryngol. Head Neck Surg.* 4, 240–245. doi: 10.1016/j.wjorl.2017.12.012

Parkinson, N., Hardisty-Hughes, R. E., Tateossian, H., Tsai, H. T., Brooker, D., Morse, S., et al. (2006). Mutation at the Evi1 locus in Junbo mice causes susceptibility to otitis media. *PloS Genet.* 2, e149. doi: 10.1371/journal.pgen.0020149

Rye, M. S., Bhutta, M. F., Cheeseman, M. T., Burgner, D., Blackwell, J. M., Brown, S. D., et al. (2011a). Unraveling the genetics of otitis media: from mouse to human and back again. *Mamm. Genome* 22, 66–82. doi: 10.1007/s00335-010-9295-1

Rye, M. S., Wiertsema, S. P., Scaman, E. S., Oommen, J., Sun, W., Francis, R. W., et al. (2011b). FBXO11, a regulator of the TGFbeta pathway, is associated with severe otitis media in Western Australian children. *Genes Immun.* 12, 352–359. doi: 10.1038/gene.2011.2

Rye, M. S., Warrington, N. M., Scaman, E. S., Vijayasekaran, S., Coates, H. L., Anderson, D., et al. (2012). Genome-wide association study to identify the genetic determinants of otitis media susceptibility in childhood. *PloS One* 7, e48215. doi: 10.1371/journal.pone.0048215

Rye, M. S., Scaman, E. S., Thornton, R. B., Vijayasekaran, S., Coates, H. L., Francis, R. W., et al. (2014). Genetic and functional evidence for a locus controlling otitis media at chromosome 10q26.3. *BMC Med. Genet.* 15, 18. doi: 10.1186/1471-2350-15-18

Sade, J., Luntz, M., Yaniv, E., Yurovitzki, E., Berger, G., and Galrenter, I. (1986). The eustachian tube lumen in chronic otitis media. *Am. J. Otol.* 7, 439–442.

Samuels, T. L., Yan, J., Khampang, P., Mackinnon, A., Hong, W., Johnston, N., et al. (2016). Association of microRNA 146 with middle ear hyperplasia in pediatric otitis media. *Int. J. Pediatr. Otorhinolaryngol.* 88, 104–108. doi: 10.1016/j.ijporl.2016.06.056

Santos-Cortez, R. L., Chiong, C. M., Reyes-Quintos, M. R., Tantoco, M. L., Wang, X., Acharya, A., et al. (2015). Rare A2ML1 variants confer susceptibility to otitis media. *Nat. Genet.* 47, 917–920. doi: 10.1038/ng.3347

Santos-Cortez, R. L., Reyes-Quintos, M. R., Tantoco, M. L., Abbe, I., Llanes, E. G., Ajami, N. J., et al. (2016). Genetic and environmental determinants of otitis media in an indigenous filipino population. *Otolaryngol. Head Neck Surg.* 155, 856–862. doi: 10.1177/0194599816661703

Santos-Cortez, R. L. P., Chiong, C. M., Frank, D. N., Ryan, A. F., Giese, A. P. J., Bootpetch Roberts, T., et al. (2018). FUT2 variants confer susceptibility to familial otitis media. *Am. J. Hum. Genet.* 103, 679–690. doi: 10.1016/j.ajhg.2018.09.010

Sato, T., Goyama, S., Nitta, E., Takeshita, M., Yoshimi, M., Nakagawa, M., et al. (2008). Evi-1 promotes para-aortic splanchnopleural hematopoiesis through up-regulation of GATA-2 and repression of TGF-b signaling. *Cancer Sci.* 99, 1407–1413. doi: 10.1111/j.1349-7006.2008.00842.x

Sayeed, S., Nistico, L., St Croix, C., and Di, Y. P. (2013). Multifunctional role of human SPLUNC1 in Pseudomonas aeruginosa infection. *Infect. Immun.* 81, 285–291. doi: 10.1128/IAI.00500-12

Segade, F., Daly, K. A., Allred, D., Hicks, P. J., Cox, M., Brown, M., et al. (2006). Association of the FBXO11 gene with chronic otitis media with effusion and recurrent otitis media: the Minnesota COME/ROM Family Study. *Arch. Otolaryngol. Head Neck Surg.* 132, 729–733. doi: 10.1001/archotol.132.7.729

Sekiyama, K., Ohori, J., Matsune, S., and Kurono, Y. (2011). The role of vascular endothelial growth factor in pediatric otitis media with effusion. *Auris Nasus Larynx* 38, 319–324. doi: 10.1016/j.anl.2010.10.008

Song, J. J., Kwon, S. K., Cho, C. G., Park, S. W., and Chae, S. W. (2011). Microarray analysis of microRNA expression in LPS induced inflammation of human middle ear epithelial cells (HMEECs). *Int. J. Pediatr. Otorhinolaryngol.* 75, 648–651. doi: 10.1016/j.ijporl.2011.02.001

Takasaki, K., Takahashi, H., Miyamoto, I., Yoshida, H., Yamamoto-Fukuda, T., Enatsu, K., et al. (2007). Measurement of angle and length of the eustachian tube on computed tomography using the multiplanar reconstruction technique. *Laryngoscope* 117, 1251–1254. doi: 10.1097/MLG.0b013e318058a09f

Tateossian, H., Hardisty-Hughes, R. E., Morse, S., Romero, M. R., Hilton, H., Dean, C., et al. (2009). Regulation of TGF-beta signalling by Fbxo11, the gene mutated in the Jeff otitis media mouse mutant. *Pathogenetics* 2, 5. doi: 10.1186/1755-8417-2-5

Tateossian, H., Morse, S., Parker, A., Mburu, P., Warr, N., Acevedo-Arozena, A., et al. (2013). Otitis media in the Tgif knockout mouse implicates TGFbeta signalling in chronic middle ear inflammatory disease. *Hum. Mol. Genet.* 22, 2553–2565. doi: 10.1093/hmg/ddt103

Tian, C., Hromatka, B. S., Kiefer, A. K., Eriksson, N., Noble, S. M., Tung, J. Y., et al. (2017). Genome-wide association and HLA region fine-mapping studies identify susceptibility loci for multiple common infections. *Nat. Commun.* 8, 599. doi: 10.1038/s41467-017-00257-5

Toivonen, L., Vuononvirta, J., Mertsola, J., Waris, M., He, Q., and Peltola, V. (2017). Polymorphisms of Mannose-binding Lectin and Toll-like Receptors 2, 3, 4, 7 and 8 and the Risk of Respiratory Infections and Acute Otitis Media in Children. *Pediatr. Infect. Dis. J.* 36, e114–e122. doi: 10.1097/INF.0000000000001479

Val, S., Krueger, A., Poley, M., Cohen, A., Brown, K., Panigrahi, A., et al. (2018). Nontypeable Haemophilus influenzae lysates increase heterogeneous nuclear ribonucleoprotein secretion and exosome release in human middle-ear epithelial cells. *FASEB J.* 32, 1855–1867. doi: 10.1096/fj.201700248RR

Van Ingen, G., Li, J., Goedegebure, A., Pandey, R., Li, Y. R., March, M. E., et al. (2016). Genome-wide association study for acute otitis media in children identifies FNDC1 as disease contributing gene. *Nat. Commun.* 7, 12792. doi: 10.1038/ncomms12792

Wang, W., Zhou, A., Zhang, X., Xiang, Y., Huang, Y., Wang, L., et al. (2014a). Interleukin 17A promotes pneumococcal clearance by recruiting neutrophils and inducing apoptosis through a p38 mitogen-activated protein kinase-dependent mechanism in acute otitis media. *Infect. Immun.* 82, 2368–2377. doi: 10.1128/IAI.00006-14

Wang, W. Y., Komatsu, K., Huang, Y., Wu, J., Zhang, W., Lee, J. Y., et al. (2014b). CYLD negatively regulates nontypeable Haemophilus influenzae-induced IL-8 expression *via* phosphatase MKP-1-dependent inhibition of ERK. *PloS One* 9, e112516. doi: 10.1371/journal.pone.0112516

Wang, W., Liu, W., Liu, J., Wang, Z., Fan, F., Ma, Y., et al. (2017). Interleukin-17A Aggravates Middle Ear Injury Induced by Streptococcus pneumoniae through the p38 Mitogen-Activated Protein Kinase Signaling Pathway. *Infect. Immun.* 85, 1–14. doi: 10.1128/IAI.00438-17

Wang, Z., He, Q., Zhang, X., Ma, Y., Fan, F., Dong, Y., et al. (2018). Innate anti-microbial and anti-chemotaxis properties of progranulin in an acute otitis media mouse model. *Front. Immunol.* 9, 2952. doi: 10.3389/fimmu.2018.02952

Wiertsema, S. P., Herpers, B. L., Veenhoven, R. H., Salimans, M. M., Ruven, H. J., Sanders, E. A., et al. (2006). Functional polymorphisms in the mannan-binding lectin 2 gene: effect on MBL levels and otitis media. *J. Allergy Clin. Immunol.* 117, 1344–1350. doi: 10.1016/j.jaci.2006.01.031

Woo, J. I., Kil, S. H., Oh, S., Lee, Y. J., Park, R., Lim, D. J., et al. (2015). IL-10/HMOX1 signaling modulates cochlear inflammation *via* negative regulation of MCP-1/CCL2 expression in cochlear fibrocytes. *J. Immunol.* 194, 3953–3961. doi: 10.4049/jimmunol.1402751

Xu, X., Woo, C. H., Steere, R. R., Lee, B. C., Huang, Y., Wu, J., et al. (2012). EVI1 acts as an inducible negative-feedback regulator of NF-kappaB by inhibiting p65 acetylation. *J. Immunol.* 188, 6371–6380. doi: 10.4049/jimmunol.103527

Zhang, Y., Xu, M., Zhang, J., Zeng, L., Wang, Y., and Zheng, Q. Y. (2014). Risk factors for chronic and recurrent otitis media-a meta-analysis. *PloS One* 9, e86397. doi: 10.1371/journal.pone.0086397

Zhang, T., Du, H., Feng, S., Wu, R., Chen, T., Jiang, J., et al. (2019). NLRP3/ASC/Caspase-1 axis and serine protease activity are involved in neutrophil IL-1beta processing during Streptococcus pneumoniae infection. *Biochem. Biophys. Res. Commun.* 513, 675–680. doi: 10.1016/j.bbrc.2019.04.004

Zivkovic, M., Kolic, I., Jesic, S., Jotic, A., and Stankovic, A. (2018). The allele 2 of the VNTR polymorphism in the gene that encodes a natural inhibitor of IL-1beta, IL-1RA is favorably associated with chronic otitis media. *Clin. Exp. Otorhinolaryngol.* 11, 118–123. doi: 10.21053/ceo.2017.01060

Conflict of Interest: The authors declare that the research was conducted in the absence of any commercial or financial relationships that could be construed as a potential conflict of interest.

frontiers in Genetics

BRIEF RESEARCH REPORT
published: 11 February 2020
doi: 10.3389/fgene.2020.00050

Mutation in *Fbxo11* Leads to Altered Immune Cell Content in *Jeff* Mouse Model of Otitis Media

Pratik P. Vikhe, Hilda Tateossian, Gurpreet Bharj, Steve D.M. Brown and Derek W. Hood*

Mammalian Genetics Unit, MRC Harwell Institute, Oxfordshire, United Kingdom

The *Jeff* mouse mutant carries a mutation in the F-box only 11 gene (*Fbxo11*) and heterozygous animals display conductive deafness due to the development of otitis media (OM). The *Fbxo11* locus is also associated with chronic otitis media with effusion (COME) and recurrent OM in humans. The *Jeff* mutation affects the ability of FBXO11 to stabilize p53 that leads to perturbation in the TGF-beta/Smad2 signaling pathway important in immunity and inflammation. In the current study, we evaluated the effect of the *Jeff* mutation on the immune cell content using multicolor flow cytometry. In blood of *Jeff* heterozygotes, we observed a significant increase in the number of NK, dendritic (CD11b+), neutrophils, and natural killer T (NKT) cells and a significant decrease in effector T-helper and B-lymphocytes compared to wild-type controls. The percentage of NK cells significantly decreased in the lungs of *Jeff* heterozygotes, with a concomitant reduction in B-lymphocytes and T-cytotoxic cells. In the spleen, *Jeff* heterozygotes displayed a significant decrease in mature B-lymphocytes, effector T-helper, and naïve T-cytotoxic cells. Neutrophils, dendritic, and NKT cells dominated bulla fluid in *Jeff* heterozygote mice. Similar analysis carried out on *Fbxo11*$^{tm2b/+}$ heterozygotes, which carry a null allele, showed no difference when compared to wild-type. Cytokine/chemokine analysis revealed a significant increase in the G-CSF, GM-CSF, sTNFRI, TPO, and IL-7 levels in *Jeff* heterozygote serum compared to wild-type. This analysis increases our understanding of the role played by *Fbxo11*, a gene associated with human OM, in the systemic and localized cellular immune response associated with increased susceptibility to OM.

Keywords: *Fbxo11*, otitis media, *Jeff* mouse, immune cells, natural killer cells

OPEN ACCESS

Edited by:
Allen Frederic Ryan, University of California, San Diego, United States

Reviewed by:
Jian Dong Li, Georgia State University, United States
Anke Leichtle, Universität zu Lübeck, Germany

****Correspondence:***
Pratik P. Vikhe
p.vikhe@har.mrc.ac.uk

Specialty section:
This article was submitted to Genetic Disorders, a section of the journal Frontiers in Genetics

Received: *24 July 2019*
Accepted: *16 January 2020*
Published: *11 February 2020*

Citation:
Vikhe PP, Tateossian H, Bharj G, Brown SDM and Hood DW (2020) Mutation in Fbxo11 Leads to Altered Immune Cell Content in Jeff Mouse Model of Otitis Media. Front. Genet. 11:50. doi: 10.3389/fgene.2020.00050

INTRODUCTION

Otitis media (OM) is a very common middle ear disease in children that is characterized by middle ear inflammation and fluid accumulation (Schilder et al., 2016). Pathology of OM can manifest in different ways and chronic and recurrent OM (ROM), often accompanied by effusion (chronic OM with effusion, COME), can lead to hearing loss and developmental delays with a significant burden on the healthcare system (Veenhoven et al., 2003). Tympanostomy to alleviate COME remains the commonest cause of surgery in children. There is a significant genetic component to COME (Sale et al., 2011), and recently the discovery of a number of mouse genetic models of COME has led to

insights into the genetic and molecular pathways involved in the pathophysiology of chronic middle ear disease (Li et al., 2013; Bhutta et al., 2017b). *Jeff* (Hardisty et al., 2003), *Junbo* (Parkinson et al., 2006), and *edison* (Crompton et al., 2017) mutants are COME mouse models each with single point mutation in the *Fbxo11, Evi1,* and *nischarin* genes respectively, identified at MRC Harwell through a deafness screen as a part of a larger scale N-ethyl-N-nitrosourea (ENU) mouse mutagenesis program (Nolan et al., 2000).

Following the identification of a number of genes involved in COME in the mouse there have been several studies to explore the association of these genes with COME in the human population. Association studies have shown that several human genes may increase susceptibility toward OM, including *FBXO11* (Sale et al., 2011). One of the largest association studies employing samples from 1,296 families (3,828 individuals) uncovered a significant link between FBXO11 and OM susceptibility (Bhutta et al., 2017a). Moreover, two similar studies carried out on western Australian children (Rye et al., 2011) and Minnesota COME/ROM families (Segade et al., 2006) showed a direct link between polymorphisms at the *FBXO11* locus and OM susceptibility.

FBXO11 is part of the SCF (SKP1-cullin-F-box) complex, a multi-protein E3 ubiquitin-ligase complex catalyzing the ubiquitination of proteins destined for proteasomal degradation. FBXO11 is involved in ubiquitination of BCL6 (Duan et al., 2012) and phosphorylated SNAIL (Zheng et al., 2014), and neddylation of p53 (Abida et al., 2007), which play critical roles in regulation of the mammalian cell cycle and function. FBXO11, through regulation of BCL6, modulates B-cell survival and plays a crucial role in B-cell lymphoma (Duan et al., 2012). Other than regulation of B-cell survival in lymphoma, the role played by FBXO11 in modulating other immune cells and the relevance of this to OM remains unclear.

In the current study, we used the well-characterized COME *Jeff* mouse model (Hardisty et al., 2003; Hardisty-Hughes et al., 2006) which carries a missense mutation in the *Fbxo11* gene. The homozygotes of this mutant mouse line do not survive beyond birth and show a severe lung phenotype (Tateossian et al., 2009), whereas the heterozygote mice survive with chronic OM (Hardisty et al., 2003). FBXO11 can function as a Nedd8-ligase for p53 promoting its neddylation and inhibiting its transcription activity. The *Fbxo11* mutation in the *Jeff* mouse results in a decreased level of p53 and increased pSmad2 levels; pSmad2 is directly involved in the regulation of the TGF-beta pathway (Tateossian et al., 2009; Tateossian et al., 2015). The TGF-beta pathway plays a critical role in maintaining homeostasis by regulating remodeling of injury in disease and modulating the immune and inflammatory response (Wan and Flavell, 2007).

The association of *FBXO11* locus polymorphisms with OM in the human population and the corresponding phenotype observed in the *Jeff* mouse with a mutation in the orthologous gene makes it a vital model to dissect important immune changes that are associated with OM. In the current study, we analyzed the cellular immune changes that occur due to the *Fbxo11* mutation in the heterozygote *Jeff* mouse using a comprehensive flow cytometry panel that classified granulocytes, monocytes, macrophages, eosinophils, dendritic, natural killer, B and T cells. The *Jeff* mutation significantly altered the immune cell content in the blood, mostly affecting the natural killer cells, and adaptive B and T immune cells, which underlines the significance of FBXO11 in the immune/genetic regulation of these cells. Further, we carried out a similar analysis with the heterozygote *Fbxo11* knockout mouse in order to better understand the role of FBXO11 in the cellular immune response. The *Fbxo11* knockout mouse did not show significant differences in the immune cells as was observed in the *Jeff* mouse, suggesting that the *Fbxo11* mutation in the *Jeff* mouse has gain of function effects that lead to altered immune cell content. Also, using a mouse model, this study is the first to report systemic immune cell differences due to a genetic aberration leading to localized middle ear inflammation and OM.

MATERIALS AND METHODS

Mice

The humane care and use of mice in this study was carried out under the appropriate UK Home Office license and the local ethics review committee reviewed the experimental procedures.

Heterozygote $Fbxo11^{Jf/+}$ (also referred to as *Jeff* Het) mice and their *Jeff* wild-type littermates (also referred to as *Jeff* Wt) were generated by inter-crossing F1 $Fbxo11^{Jf/+}$ C57BL/6J C3H/HeH males with F1 $Fbxo11^{+/+}$ C57BL/6J C3H/HeH wild-type females. Heterozygote $Fbxo11^{tm2b/+}$ (also referred to as *Fbxo11* knockout) and their $Fbxo11^{+/+}$ wild-type littermates were generated by inter-crossing F1 $Fbxo11^{tm2b/+}$-PL-TM2B-C57BL/6NJ with C57BL/6NJ females. The mice were specific pathogen free and used at 8 weeks of age.

Sample Preparation

Blood was collected by retro-orbital bleeding under terminal anesthesia induced by an intraperitoneal overdose of sodium pentobarbital in lithium heparin tubes. For flow cytometry analysis, 50 µl of blood was resuspended in 1 ml of red blood cell (RBC) lysis buffer (Biolegend™) for 10 min on ice followed by centrifugation and two washes with 1 ml phosphate buffer saline (PBS). The final pellet was resuspended in FACS buffer (5 mM EDTA, 0.5% fetal calf serum in PBS). Middle ear fluid for flow cytometry and cytokine/chemokine analyses was collected as described previously (Vikhe et al., 2019). Briefly, middle ear fluid was collected from unskinned heads obtained from mice under terminal anesthesia. After removal of any material on the external surface of the tympanic membrane, a hole was made in the membrane while removing the malleus from the middle ear using a sterile pair of forceps and fluid was collected with a pipette and microtip in 10 µl cold PBS. Other tissues (spleens and lungs) were collected in gentleMACS™ C tubes with 3 ml RPMI supplemented with 10 µg/ml collagenase II (Serlabo™) and 166 µg/ml DNAse I (Sigma™). The tissue was homogenized in a gentleMACS™ Dissociator and the single cell suspension was

separated from tissue debris by passing through a 70 µm Cell Strainer. The cell pellet obtained after centrifugation at 800 x g for 2 min was resuspended in RBC lysis buffer. Finally, after RBC lysis, the cells were pelleted by centrifugation then resuspended in FACS buffer for flow cytometry analysis.

Flow Cytometry Analysis

Middle ear fluid, blood, lung, and spleen samples were diluted with FACS buffer, and a cell count was obtained. The samples were transferred to a 96 well plate at the concentration of 2 X 10^5 cells/well. Cells were centrifuged and washed twice with FACS buffer. For the analysis of different types of immune cells, the resuspended cells were incubated for 15 min with CD16/CD32 antibody (BD Pharmagen™) at a dilution of 1:100. After centrifugation at 800 x g for 1 min, cell pellets were resuspended in 100 µl of either of panel 1 or panel 2 (**Table S1**) antibody cocktail and incubated for 20 min in the dark. Cells were centrifuged and washed twice with FACS buffer and finally resuspended in 100 µl of Sytox DNA stain (1:10,000). After making up the final volume to 250 µl with FACS buffer, flow cytometry was performed using a BD FACSCanto™ II system. FlowJo software (Tree Star™) was used to analyze the data obtained (**Figures S1**, **S2** and **Table S2**).

Cytokine/Chemokine Analysis

Cytokine and chemokine levels were measured using a mouse cytokine antibody array (Mouse Cytokine Array C1, RayBiotech Inc.™) as described previously (Vikhe et al., 2019). Changes in IL-7 and IL-15 were analyzed by Mouse IL-7 and IL-15 DuoSet ELISA (R&D systems™) according to the manufacturer's instructions. The color change was measured at 450 nm on an Epoch BioTek™ plate reader and the IL-7 and IL-15 concentrations were calculated by using the standard curve obtained.

Data Analysis

We used the unpaired t test assuming equal variance for comparing the cytokine/chemokine changes between *Fbxo11*$^{Jf/+}$ serum to the *Jeff* wild-type whereas non-parametric Mann-Whitney U test was used to compare the flow cytometry data. A *P* value of less than 0.05 was considered significant.

RESULTS

Innate Immune Cell Population in *Fbxo11*$^{Jf/+}$ Mouse

Innate immune cells play a critical role in the initiation of the inflammatory response and the onset and maintenance of OM (Mittal et al., 2014). The *Fbxo11*$^{Jf/+}$ mouse is characterized by middle ear inflammation that mimics the human OM and also exhibits a defective lung phenotype (Tateossian et al., 2009). To understand the effect of the *Jeff* mutation in the *Fbxo11* gene on the innate immune cell population we analyzed the neutrophils, eosinophils, macrophages, monocytes, dendritic cells (DC) (CD11b+ve and –ve), progenitor DC, and natural killer (NK) cells present in blood, spleen, lungs, and middle ear fluids obtained from the *Fbxo11*$^{Jf/+}$ mouse (**Table 1**). Significant differences were observed in the proportion of blood neutrophils, macrophages, DCs, and NK cells in *Fbxo11*$^{Jf/+}$

TABLE 1 | Immune cell percentage in *Jeff* wild-type (*Jeff* Wt) and *Fbxo11*$^{Jf/+}$ (*Jeff* Het) mouse obtained by flow cytometry.

Immune cells	Blood		Lungs		Spleen		MEF
	Jeff Wt	*Jeff* Het	*Jeff* Wt	*Jeff* Het	*Jeff* Wt	*Jeff* Het	*Jeff* Het
Granulocytes	**16.60 (± 1.76)**	**19.30 (± 0.85)**	6.21 (± 0.79)	5.34 (± 0.43)	3.53 (± 0.43)	2.77 (± 0.31)	10.34 (± 4.11)
Eosinophils	0.18 (± 0.07)	0.29 (± 0.05)	0.035 (± 0.01)	0.028 (± 0.01)	0.05 (± 0.03)	0.021 (± 0.01)	0.14 (± 0.05)
Macrophages	**0.20 (± 0.06)**	**0.57 (± 0.16)**	0.21 (± 0.04)	0.22 (± 0.03)	0.34 (± 0.04)	0.23 (± 0.02)	0.22 (± 0.06)
Monocytes	5.54 (± 0.88)	8.41 (± 1.55)	**1.58 (± 0.21)**	**0.81 (± 0.22)**	0.89 (± 0.03)	0.84 (± 0.12)	0.34 (± 0.16)
DC CD8 type	27.5 (± 2.78)	20.44 (± 2.19)	13.52 (± 1.53)	13.17 (± 1.43)	43.60 (± 0.70)	42.30 (± 1.58)	3.69 (± 0.72)
DC CD11b type	**1.29 (± 0.28)**	**3.31 (± 0.53)**	1.06 (± 0.15)	1.35 (± 0.13)	1.81 (± 0.17)	1.92 (± 0.11)	4.54 (± 0.99)
Progenitor DC (pDC)	7.54 (± 1.96)	7.99 (± 1.06)	10.65 (± 0.89)	11.13 (± 1.36)	5.43 (± 0.75)	4.50 (± 0.43)	6.69 (± 1.46)
NK cells	**5.87 (± 0.72)**	**10.84 (± 1.71)**	2.80 (± 0.17)	0.91 (± 0.23)	4.09 (± 0.63)	3.12 (± 0.20)	0.79 (± 0.35)
T helper (Th) effector	**2.63 (± 0.72)**	**0.69 (± 0.03)**	0.37 (± 0.13)	0.17475 (± 0.12)	**1.28 (± 0.06)**	**0.72 (± 0.01)**	0.22 (± 0.07)
T helper (Th) resting	4.49 (± 0.59)	4.54 (± 0.68)	2.45 (± 0.50)	1.22 (± 0.32)	7.73 (± 0.71)	8.93 (± 0.61)	0.16 (± 0.07)
T regulator (T reg) effector	0.86 (± 0.08)	0.66 (± 0.06)	0.68 (± 0.12)	0.52 (± 0.12)	0.53 (± 0.05)	0.46 (± 0.03)	0.28 (± 0.08)
T regulator (T reg) resting	**0.14 (± 0.02)**	**0.43 (± 0.06)**	0.35 (± 0.06)	0.22 (± 0.07)	**0.82 (± 0.01)**	**1.34 (± 0.09)**	0.029 (± 0.01)
T cytotoxic effector	0.47 (± 0.09)	0.31 (± 0.01)	0.31 (± 0.10)	0.11 (± 0.03)	0.53 (± 0.08)	0.34 (± 0.03)	0.68 (± 0.27)
T cytotoxic naive	3.62 (± 0.67)	2.53 (± 0.38)	**1.25 (± 0.12)**	**0.58 (± 0.12)**	5.56 (± 0.73)	6.92 (± 0.72)	0.07 (± 0.04)
T cytotoxic resting	**1.56 (± 0.35)**	**0.67 (± 0.12)**	**0.44 (± 0.07)**	**0.10 (± 0.03)**	**2.44 (± 0.25)**	**1.64 (± 0.17)**	0.04 (± 0.02)
B2 total	**24.82 (± 2.80)**	**11.16 (± 1.22)**	11.53 (± 1.09)	9.22 (± 0.91)	34.90 (± 1.07)	28.87 (± 0.95)	1.37 (± 0.34)
B2 mature	**2.31 (± 0.25)**	**1.55 (± 0.09)**	2.69 (± 0.48)	3.75 (± 0.27)	3.38 (± 0.28)	2.97 (± 0.09)	0.26 (± 0.11)
B2 immature	**21.98 (± 2.79)**	**9.26 (± 1.13)**	**8.52 (± 0.85)**	**5.14 (± 0.70)**	30.67 (± 0.91)	25.20 (± 0.83)	1.03 (± 0.23)
B1 total	**0.73 (± 0.09)**	**0.58 (± 0.03)**	**3.14 (± 0.48)**	**5.81 (± 0.76)**	3.43 (± 0.38)	4.90 (± 0.44)	1.74 (± 0.32)
NKT effector	**0.77 (± 0.14)**	**2.04 (± 0.27)**	12.92 (± 0.88)	16.22 (± 2.22)	1.29 (± 0.18)	0.95 (± 0.07)	3.15 (± 0.99)
Invariant NKT (iNKTs)	**0.57 (± 0.07)**	**2.23 (± 0.33)**	6.21 (± 1.09)	8.98 (± 1.40)	1.13 (± 0.24)	1.47 (± 0.15)	1.99 (± 0.67)
NKT resting	**0.46 (± 0.05)**	**1.43 (± 0.16)**	**0.96 (± 0.11)**	**1.43 (± 0.35)**	**0.78 (± 0.11)**	**1.63 (± 0.20)**	0.68 (± 0.17)

Values are the percentage of total live cells. Values in blue are significantly increased whereas those in red are significantly decreased in Jeff Het (Fbxo11$^{Jf/+}$*) compared to Jeff Wt (Jeff wild-type) mice. MEF, middle ear fluid; DC, dendritic cell; NK, natural killer cell.*

when compared to the *Jeff* wild-type litter mates. The greatest difference was observed in blood NK cell levels, which were 10.84% of live cells in the *Fbxo11*$^{Jf/+}$ mouse compared to 5.87% in the *Jeff* wild-type counterpart (**Figure 1A–C**). The *Fbxo11*$^{Jf/+}$ mouse had 3.31% of CD11b+ve DCs compared to 1.29% present in *Jeff* wild-type blood. Similarly, slight but significantly higher levels of macrophages (0.57%) were observed in *Fbxo11*$^{Jf/+}$ compared to 0.20% in *Jeff* wild-type blood. Blood granulocyte levels were significantly higher in the *Fbxo11*$^{Jf/+}$ (19.30%) compared to *Jeff* wild-type (16.60%) mouse. In contrast to blood, a significantly lower proportion of NK cells was observed in lungs of *Fbxo11*$^{Jf/+}$ (0.91%) compared to *Jeff* wild-type (2.80%) mice. Further, *Fbxo11*$^{Jf/+}$ lungs had 0.81% of monocytes compared to 1.58% in the *Jeff* wild-type mouse. No significant difference was observed in *Fbxo11*$^{Jf/+}$ spleen innate immune cells when compared to the *Jeff* wild-type mouse. The middle ear fluid from *Fbxo11*$^{Jf/+}$ had a high percentage of granulocytes and DCs. The middle ear fluid comprised 10.34% neutrophils and 6.69% progenitor dendritic cells (pDCs). Compared to pDC's, the percentage of CD11b-ve DCs and CD11b+ DCs in the *Fbxo11*$^{Jf/+}$ middle ear fluid was less: 3.69 and 4.54% respectively (**Table 1**).

A similar analysis carried out on the *Fbxo11*$^{tm2b/+}$ heterozygote *Fbxo11* knockout mouse (**Table S3**), did not show the major differences in innate immune cell content as observed in the *Fbxo11*$^{Jf/+}$mouse in comparison to their respective wild-type countertypes. The only significant difference observed for the *Fbxo11*$^{tm2b/+}$ compared to *Fbxo11*$^{+/+}$ mouse was for blood and lung macrophages and blood CD11b+ DC's. *Fbxo11*$^{tm2b/+}$ had a slight but significantly higher percentage of blood macrophages (1.72%) compared to the *Fbxo11*$^{+/+}$ mouse (0.95%). Also, CD11b+ DC's were 3.61% in *Fbxo11*$^{tm2b/+}$ mouse compared to 2.65% in the *Fbxo11*$^{+/+}$ mouse blood. In lungs of the *Fbxo11*$^{tm2b/+}$ mouse, macrophage numbers were significantly elevated (0.86%) compared to its wild-type counterpart, *Fbxo11*$^{+/+}$ (0.39%). We observed minor

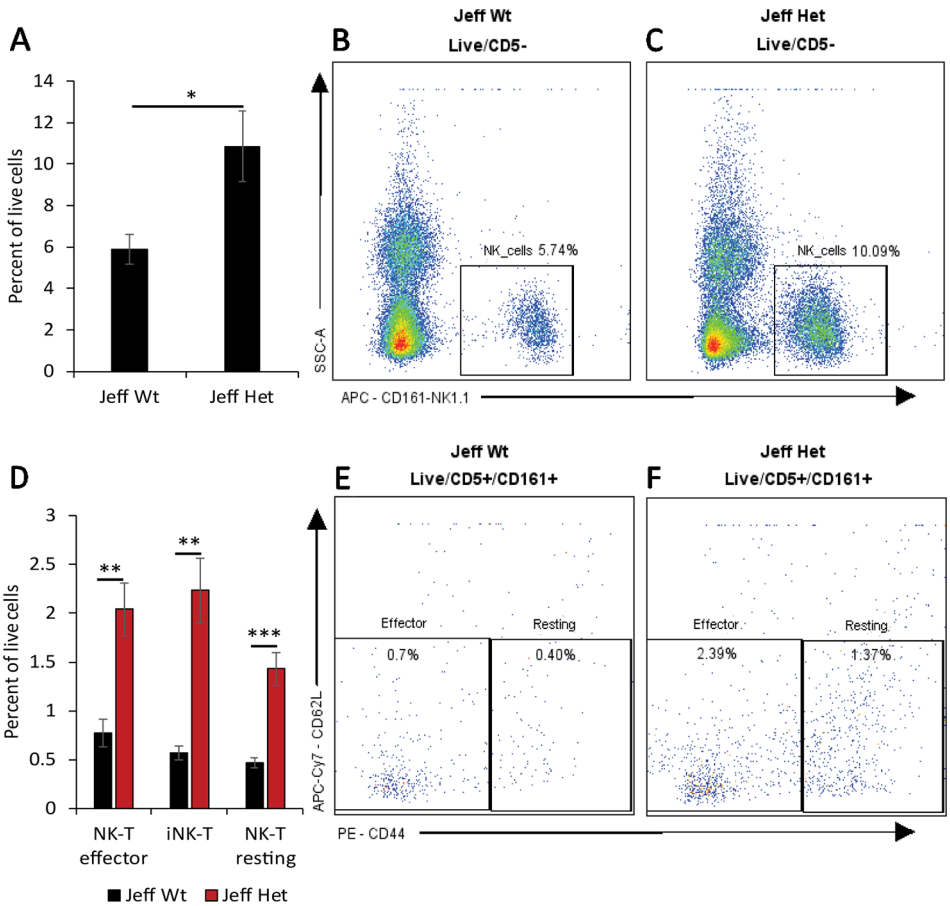

FIGURE 1 | Natural killer (NK) cell percentage in *Jeff* mice (*Fbxo11*$^{Jf/+}$ and *Jeff* Wt). **(A)** Average difference in the percentage of blood NK cells in *Jeff* Het (*Fbxo11*$^{Jf/+}$) and *Jeff* wild type (*Jeff* Wt) mice. The error bars show standard error of mean where n = 4 and *P < 0.05. Representative flow cytometry plot for NK cell analysis of bloods from *Jeff* Wt **(B)** and *Jeff* Het (*Fbxo11*$^{Jf/+}$) **(C)** mice. **(D)** Average difference in the percentage of blood effector NKT, resting NKT, and invariant NKT (iNKT) cells in *Jeff* Het (*Fbxo11*$^{Jf/+}$) and *Jeff* Wt mice. The error bars show standard error of mean where n = 4 and *P < 0.05, **P < 0.01, ***P < 0.001. Representative flow cytometry plot for NKT cell analysis of bloods from *Jeff* Wt **(E)** and *Jeff* Het (*Fbxo11*$^{Jf/+}$) **(F)** mice.

immune cell differences between the *Jeff* wild-type and $Fbxo11^{+/+}$ wild-type mice. It is known that mouse background affects immunity and the mouse immune response to infection. The *Jeff* wild-type and $Fbxo11^{+/+}$ mouse vary in their background: *Jeff* wild-type is on mixed C57BL/6J C3H/HeH background whereas the $Fbxo11^{+/+}$ mouse is on a C57BL/6NJ background, we predict that this difference in background could be influencing the difference in immune cell content observed between these wild-types.

Our observed differences in innate immune cells between the $Fbxo11^{Jf/+}$ and the $Fbxo11^{tm2b/+}$ mouse indicates the significant role played by the *Fbxo11* gene in immunogenetic control of these cells and OM.

Adaptive Immune Cell Population in *Jeff* Mouse

We characterized the content of adaptive immune cells (**Table 1**): T cells (helper and cytotoxic), B cells, and natural killer T (NKT) cells in $Fbxo11^{Jf/+}$ mouse blood, lung, spleen, and middle ear fluid. The percentage of T helper (Th) effector cells in the blood was significantly less in $Fbxo11^{Jf/+}$ (0.69%) compared to the *Jeff* wild-type counterpart. The percentage of blood resting T cytotoxic cells was also significantly less in the $Fbxo11^{Jf/+}$ (0.67%) compared to *Jeff* wild-type (1.56%) mouse. In contrast, the percentage of blood T regulatory (T reg) resting cells was significantly higher in the $Fbxo11^{Jf/+}$ compared to *Jeff* wild-type mouse. The greatest difference was observed in the proportion of blood immature B cells; $Fbxo11^{Jf/+}$ had significantly less (9.26%) immature B cells compared to the *Jeff* wild-type (21.98%) mouse (**Figure 2A–C**). In contrast, NKT cell levels in the blood were significantly higher in the $Fbxo11^{Jf/+}$ compared to *Jeff* wild-type mouse. $Fbxo11^{Jf/+}$ mouse blood had a significantly higher level of effector NKT cells, 2.04% compared to 0.77% in *Jeff* wild-type. A similar trend was observed in the levels of resting NKT cells and invariant NKT (iNKT) cells (**Figure 1D–F**, **Table 1**).

Analysis of cells derived from the lung did not show a significant difference in T-helper cells, but a significant reduction in the levels of naïve and resting T-cytotoxic cells was observed in the $Fbxo11^{Jf/+}$ compared to the *Jeff* wild-type mouse. The $Fbxo11^{Jf/+}$ lung had 0.58 and 0.1% of naïve and resting T cytotoxic cells respectively compared to 1.25 and 0.44% (naïve and resting respectively) in *Jeff* wild-type. Other than T-cytotoxic cells, the only significant reduction observed was in B2-immature cells; the $Fbxo11^{Jf/+}$ lung had 5.14% of B2-immature cells compared to 8.52% in the *Jeff* wild-type mouse. The percent of effector Th cells was significantly lower (0.72%) in $Fbxo11^{Jf/+}$ compared to 1.28% observed in the *Jeff* wild-type mouse whereas the resting T reg percentage was significantly higher in $Fbxo11^{Jf/+}$ spleen (1.34%) compared to that found in *Jeff* wild-type (0.82%). Also, a higher percentage of resting NKT cells was observed in $Fbxo11^{Jf/+}$ spleen (1.63%) compared to its wild-type counterpart (0.78%). In the middle ear fluid, the highest percentage of adaptive immune cells observed was NKT cells at 5.83%; among these NKT cells nearly 55% were effector cells. After NKT cells, B cells were the second highest adaptive immune cells observed in the $Fbxo11^{Jf/+}$ mouse middle ear fluid. The percentages of B1 and B2 cells in the $Fbxo11^{Jf/+}$ middle ear fluid were 1.74 and 1.37%, respectively and nearly 75% of the B2 cells were mature (**Table 1**).

Similar analysis carried out on the $Fbxo11^{tm2b/+}$ knockout mouse did not show major differences in adaptive immune cells as had been observed for the $Fbxo11^{Jf/+}$ mouse compared to the respective wild type (**Table S3**). Other than splenic immature B2 cells, no other significant differences were observed in the $Fbxo11^{tm2b/+}$ knockout compared to its wild-type counterpart $Fbxo11^{+/+}$mouse. The $Fbxo11^{tm2b/+}$ mouse spleen had a significantly higher proportion of immature B2 cells (16.23%) compared to its wild-type counterpart $Fbxo11^{+/+}$ (8.60%). Our analysis indicates that the mutation in the $Fbxo11^{Jf/+}$ mouse affects not only the innate immune cell content but also adaptive

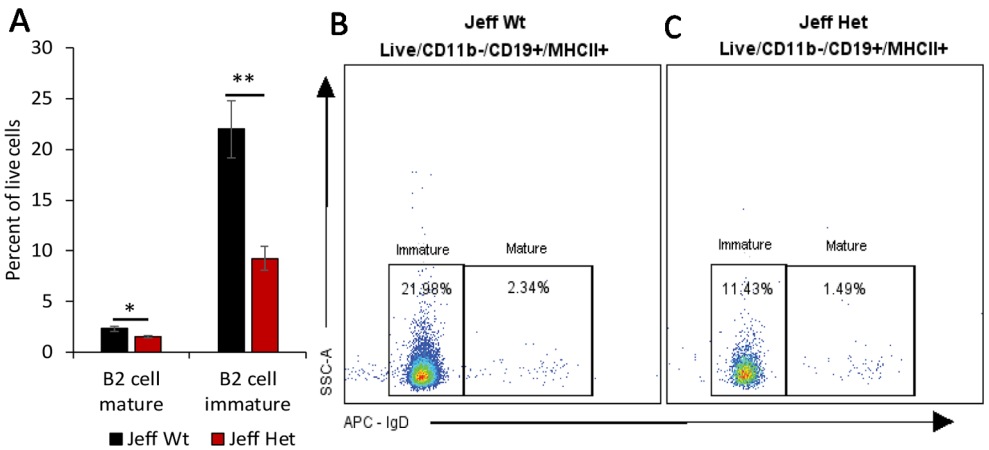

FIGURE 2 | B cell percentage in *Jeff* mice ($Fbxo11^{Jf/+}$ and *Jeff* Wt). **(A)** Average difference in the percentage of mature and immature blood B2 cells in *Jeff* Het ($Fbxo11^{Jf/+}$) and *Jeff* Wt mice. The error bars show standard error of mean where n = 4 and *P < 0.05, **P < 0.01. Representative flow cytometry plot for B cell analysis of bloods from *Jeff* Wt **(B)** and *Jeff* Het ($Fbxo11^{Jf/+}$) **(C)** mice.

immune cells. The absence of cellular immune changes in the *Fbxo11*$^{tm2b/+}$ mouse that were observed in the *Fbxo11*$^{Jf/+}$ mouse suggests that the ENU mutation in the *Fbxo11* gene could be gain of function which alters the regulation of immune cells, leading to lung and middle ear phenotypes observed in the *Fbxo11*$^{Jf/+}$ mice.

Cytokine/Chemokine Levels in *Jeff* Mouse

Mutation in the *Fbxo11* gene leads to systemic and local differences in the *Fbxo11*$^{Jf/+}$ mouse immune cells. To understand the influence of the autocrine and paracrine signals on the differences observed, levels of the specific cytokines/chemokines that modulate the functional response in the immune cells were analyzed (**Figure 3A**). A significant increase in G-CSF, GM-CSF, sTNFRI (soluble TNFRI), and TPO levels was observed in the *Fbxo11*$^{Jf/+}$ serum compared to the *Jeff* wild-type. The significant increase in the NK cells observed in the *Fbxo11*$^{Jf/+}$ mouse could correlate with the major cytokines known to modulate NK cell number and function, IL-7 and IL-15 (**Figure 3B**). Of these two cytokines, only IL-7 was significantly higher in *Fbxo11*$^{Jf/+}$ serum compared to its wild-type counterpart mouse. A majority of the cytokine/chemokines in the *Fbxo11*$^{Jf/+}$ mouse middle ear fluid were relatively high: IL-12p40/p70, IL-12p70, CCL2, sTNFRI, and TPO. High levels of IL-7 were also observed in the *Fbxo11*$^{Jf/+}$ middle ear fluid.

DISCUSSION

One of the best characterized animal models for chronic OM is the *Jeff* mouse mutant, which carries a mutation in the *Fbxo11* gene that is known to be associated with human OM (Hardisty et al., 2003; Segade et al., 2006; Bhutta et al., 2017a). To understand the effect of this mutation on the systemic and localized immune cell content, we analyzed the immune cell population in the *Jeff* mutant mouse.

The most significant difference observed between *Jeff* heterozygotes (*Fbxo11*$^{Jf/+}$) and wild-type mice was in the increased percentage of NK cells in blood, which are

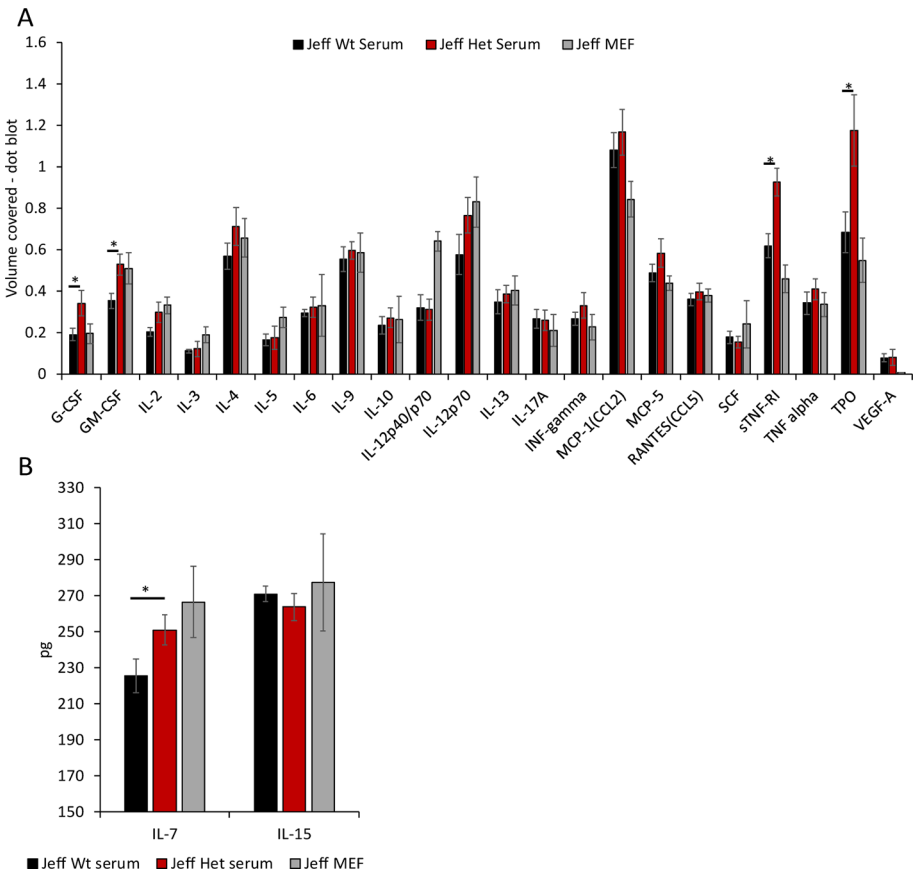

FIGURE 3 | Cytokine and chemokine levels in *Jeff* mouse (*Fbxo11*$^{Jf/+}$ and *Jeff* Wt) serum and middle ear fluid (MEF). **(A)** The volume coverage represents the cytokine/chemokine levels obtained after analyses of 10 µl serum from *Jeff* Het (*Fbxo11*$^{Jf/+}$) and *Jeff* Wt and 1 µl MEF from *Jeff* Het (*Fbxo11*$^{Jf/+}$). Volume cover was calculated using Image Lab (BioRadTM) analysis on the RayBioRc C-Series mouse cytokine antibody array C1. **(B)** Interleukin (IL)-7 and IL-15 levels in the serum from *Jeff* Het (*Fbxo11*$^{Jf/+}$) and *Jeff* Wt and MEF from *Jeff* Het (*Fbxo11*$^{Jf/+}$), using mouse IL-7 or IL-15 DuoSet ELISA (R&D systems™). The concentrations in pg/ml were obtained from the standard graph of concentration against absorbance at 450 nm. The error bars show standard error of mean where n = 4 and *P < 0.05.

significantly raised in the mutant. Similarly, the percentage of NKT cells (effector, resting, and iNKT) was high in the *Fbxo11*$^{Jf/+}$ compared to the wild-type mouse. Analysis carried out on otitis-prone children has shown similar findings; children prone to OM have a higher proportion of NK cells in blood compared to a healthy control group. The authors of the study postulate that the increase in NK cell numbers is due to prolonged exposure to upper respiratory tract infection (Seppanen et al., 2018). However, our current study provides the possibility of a genetic link being responsible for the increase in the circulating NK cells. The *Fbxo11*$^{Jf/+}$ mice utilized in the present study are bred in specific pathogen-free conditions (Hood et al., 2016). The development of OM in *Fbxo11*$^{Jf/+}$ mice is spontaneous at a young age (Hardisty et al., 2003). A similar analysis carried out in the *Fbxo11*$^{tm2b/+}$ knockout mouse did not show any difference in the NK cell population when compared to its wild-type counterpart. This indicates that the increase in the NK cells in the circulation can be purely attributed to the specific mutation in the *Fbxo11* gene in the *Fbxo11*$^{Jf/+}$ mouse.

One of the major cytokines that plays a critical role in NK cell development, homeostasis, and activation is IL-15 (Marçais et al., 2013). Mice deficient in IL-15 do not produce NK cells, supporting its significance in NK cell development (Ranson et al., 2003). Analysis of IL-15 levels in the *Fbxo11*$^{Jf/+}$ mouse serum did not show a significant difference compared to its wild-type counterpart indicating that the *Fbxo11* mutation does not affect the paracrine signaling for NK cell modulation through IL-15. IL-15 maintains the peripheral NK cell numbers by increasing the anti-apoptotic BCL6 family proteins (Ranson et al., 2003). BCL6 is targeted for ubiquitination and proteasomal degradation by an SKP1–CUL1–F- box protein (SCF) ubiquitin ligase complex that contains the FBXO11 protein (Duan et al., 2012). The increased blood NK cell percentage in the *Fbxo11*$^{Jf/+}$ mouse indicates the possible alteration of the SCF mediated BCL6 degradation, specifically in the NK cells. Another important cytokine that regulates NK cell function is TGF-beta, levels of which were not significantly different in the *Fbxo11*$^{Jf/+}$ mouse compared to its wild-type counterpart. Earlier studies carried out on the *Fbxo11*$^{Jf/+}$ mouse have highlighted the significance of the *Jeff* mutation on the Smad2 mediated TGF-beta induced intracellular signaling in the developmental pathways (Tateossian et al., 2009). Even though we did not observe any significant difference in the levels of TGF-beta in the *Fbxo11*$^{Jf/+}$ mouse, the intracellular signaling induced by TGF-beta in the NK cells could play a vital role in their increased levels and function.

Along with NK cells, we also observed a significant increase in the circulating T cell population in the *Fbxo11*$^{Jf/+}$mouse. One of the cytokines that can stimulate the release of lymphocytes from bone marrow and thymus is IL-7 (von Freeden-Jeffry et al., 1995); levels of this cytokine were significantly higher in the *Fbxo11*$^{Jf/+}$ serum compared to its wild-type counterpart. Along with increasing lymphocyte numbers, this elevated level of IL-7 can also result in increased thymic NK cell numbers (Marçais et al., 2013). IL-7 also increases the release of B cells from bone marrow and thymus (von Freeden-Jeffry et al., 1995) but in *Fbxo11*$^{Jf/+}$ the percentage of B cells was significantly lower than in the wild-type mouse. FBXO11 is known to play a critical role in maintenance of B cell levels *via* the BCL6 pathway and FBXO11 loss of function is frequently observed in B cell lymphoma cell lines and increased B-cell levels (Duan et al., 2012), as we observed in the *Fbxo11*$^{tmb2/+}$ knockout mouse. Restoration of BCL6 function in the B cell lymphoma cell lines has been shown to inhibit B-cell lymphogensis (Duan et al., 2012), indicating a potential critical role played by FBXO11 in the modulation of B cell survival. Our observation of reduced levels of B cells in the *Fbxo11*$^{Jf/+}$ mouse indicates that the *Jeff* mutation in the B-cells could be inducing the apoptotic pathways, possibly through BCL6. This novel role of *Fbxo11* in the modulation of B cell survival warrants further studies but suggest that the *Jeff* mutation may be manifesting gain of function phenotypes in the regulation of B cell numbers.

The other cytokines that were significantly increased in the *Fbxo11*$^{Jf/+}$ serum compared to wild-type were G-CSF and GM-CSF. Both these cytokines play a critical role in the regulation of neutrophil development (Roberts, 2005), which could correspond with the significantly higher blood granulocyte levels observed in the *Fbxo11*$^{Jf/+}$ mouse. G-CSF also inhibits NK cell activity (Schlahsa et al., 2011). IL-2 is one of the major cytokines released after activation of NK cells. In the *Fbxo11*$^{Jf/+}$ mouse, even with the high percentage of NK cells in the circulation, no difference in IL-2 levels was observed compared to wild type. Neutrophil numbers also play a critical role in perturbation of inflammation in the middle ear. In other animal models, the extracellular neutrophil DNA in the middle ear fluid contributes to NTHi biofilm formation (Jurcisek and Bakaletz, 2007; Juneau et al., 2011). In the case of *Fbxo11*$^{Jf/+}$ mice, the neutrophil percentage in the middle ear fluid was high and most of these were living. This might be a contributing factor toward the significantly lower NTHi titers and infection rate observed in *Fbxo11*$^{Jf/+}$ compared to *Junbo* mice (Hood et al., 2016); the latter has high levels of necrotic cells in the middle ear fluid (Vikhe et al., 2019).

The level of soluble TNFRI (sTNFR1) in the *Fbxo11*$^{Jf/+}$ serum was significantly higher than that found in wild-type, whereas TNF–alpha levels were not different. sTNFRI has a high affinity for TNF-alpha (Wang et al., 2004), modulating its slow release and thus suppressing inflammation. It is well established that inhibiting TNF-alpha decreases middle ear inflammation in OM (Jeun et al., 2001). Trans-tympanic membrane treatment of mice with sTNFRI and anti-TNF-alpha inhibits LPS induced middle ear inflammation and OM (Jeun et al., 2001). The molecular level regulation for the release of sTNFRI is still unclear. The increase in sTNFRI in the *Fbxo11*$^{Jf/+}$ mouse serum indicates a role for FBXO11 in its regulation; this mouse model could play an essential role in understanding the regulation of this critical cytokine at the genetic level.

Another cytokine/growth factor that was significantly higher in *Fbxo11*$^{Jf/+}$ mouse serum was thrombopoietin (TPO). TPO is a growth factor that initiates the process of megakaryocyte production and generation of platelets (Lupia et al., 2012).

Increased levels of TPO are found in patients with inflammatory bowel disease (Kapsoritakis et al., 2000) and *Streptococcus pneumoniae* induced bacterial meningitis in mice (Hoffmann et al., 2011). The relevance of TPO in cardiovascular damage and inflammatory diseases is known (Lupia et al., 2012), but its role in OM has yet to be evaluated. We were not able to classify platelet population in the *Fbxo11*$^{Jf/+}$ mouse in our current study but increased levels of TPO are indicative of abnormal platelet function and its relevance in OM can be investigated using this mutant mouse model.

In conclusion, our studies of the *Jeff* (*Fbxo11*$^{Jf/+}$) mouse model identify immune cell changes which can play a critical role in inflammation. A significant increase in blood neutrophil, NK cells, NKT cells and dendritic cells were observed in the *Fbxo11*$^{Jf/+}$ mutant mouse compared to wild-type. The heterozygote *Fbxo11* knockout mouse did not show these differences, consistent with a gain of function for the *Jeff* mutation that leads to these immune cell changes. Interestingly, as we report elsewhere (Kubinyecz *et al.* manuscript submitted), the *Fbxo11*$^{tm2b/+}$ heterozygous knockout mouse does not develop a spontaneous OM phenotype as observed in *Fbxo11*$^{Jf/+}$, which is also indicative of gain of function effects. In conclusion, this study paves the way for further studies using the *Jeff* model to dissect the genetic interrelationships between the control of immune cells and OM.

DATA AVAILABILITY STATEMENT

All datasets generated for this study are included in the article/ **Supplementary Material**.

ETHICS STATEMENT

The animal study was reviewed and approved by MRC Harwell Institute ethics review committee and this study was carried out under the appropriate UK Home Office license.

AUTHOR CONTRIBUTIONS

PV designed and conceptualized the experiments. PV, HT, and GB performed the experiments. PV, and GB analyzed the data. PV and HT participated in collecting animals testes. PV drafted the manuscript. PV, HT, DH, and SB edited and wrote the final manuscript. All authors approved the manuscript for submission.

FUNDING

This work was funded by the Medical Research Council (MRC funding award no. MC_U142684175).

ACKNOWLEDGMENTS

We thank the staff in the Mary Lyon Centre for the husbandry and humane care of these mice, clinical chemistry, pathology and histology teams, and the genotyping core, at MRC Harwell Institute.

SUPPLEMENTARY MATERIAL

The Supplementary Material for this article can be found online at: https://www.frontiersin.org/articles/10.3389/fgene.2020.00050/full#supplementary-material

FIGURE S1 | Flow cytometry panel 1 gating strategy.

FIGURE S2 | Flow cytometry panel 2 gating strategy.

TABLE S1 | Flow cytometry antibody and panels.

TABLE S2 | Flow cytometry gating strategy.

TABLE S3 | Immune cell percentage in *Fbxo11*$^{tmb2/+}$ (*Fbxo11* knockout) and *Fbxo11*$^{+/+}$ mouse obtained by flow cytometry.

REFERENCES

Abida, W. M., Nikolaev, A., Zhao, W., Zhang, W., and Gu, W. (2007). FBXO11 promotes the Neddylation of p53 and inhibits its transcriptional activity. *J. Biol. Chem.* 282, 1797–1804. doi: 10.1074/jbc.M609001200

Bhutta, M. F., Lambie, J., Hobson, L., Goel, A., Hafrén, L., Einarsdottir, E., et al. (2017a). A mouse-to-man candidate gene study identifies association of chronic otitis media with the loci TGIF1 and FBXO11. *Sci. Rep.* 7, 18–24. doi: 10.1038/s41598-017-12784-8

Bhutta, M. F., Thornton, R. B., Kirkham, L.-A. S., Kerschner, J. E., and Cheeseman, M. T. (2017b). Understanding the aetiology and resolution of chronic otitis media from animal and human studies. *Dis. Model. Mech.* 10, 1289–1300. doi: 10.1242/dmm.029983

Crompton, M., Purnell, T., Tyrer, H. E., Parker, A., Ball, G., Hardisty-Hughes, R. E., et al. (2017). A mutation in Nischarin causes otitis media via LIMK1 and NF-κB pathways. *PloS Genet.* 13 (8), e1006969. doi: 10.1371/journal.pgen.1006969

Duan, S., Cermak, L., Pagan, J. K., Rossi, M., Martinengo, C., Celle, F., et al. (2012). FBXO11 targets BCL6 for degradation andis inactivated in diffuse large B-cell lymphomas. *Nature.* 481, 90–94. doi: 10.1038/nature10688

Hardisty, R. E., Erven, A., Logan, K., Morse, S., Guionaud, S., Sancho-Oliver, S., et al. (2003). The deaf mouse mutant Jeff (Jf) is a single gene model of otitis media. *J. Assoc. Res. Otolaryngol.* 4, 130–138. doi: 10.1007/S10162-002-3015-9

Hardisty-Hughes, R. E., Tateossian, H., Morse, S. A., Romero, M. R., Middleton, A., Tymowska-Lalanne, Z., et al. (2006). A mutation in the F-box gene, Fbxo11, causes otitis media in the Jeff mouse. *Hum. Mol. Genet.* 15, 3273–3279. doi: 10.1093/hmg/ddl403

Hoffmann, O., Rung, O., Im, A.-R., Freyer, D., Zhang, J., Held, J., et al. (2011). Thrombopoietin contributes to neuronal damage in experimental bacterial meningitis. *Infect. Immun.* 79, 928–936. doi: 10.1128/IAI.00782-10

Hood, D., Moxon, R., Purnell, T., Richter, C., Williams, D., Azar, A., et al. (2016). A new model for non-typeable Haemophilus influenzae middle ear infection in the Junbo mutant mouse. *Dis. Model. Mech.* 9, 69–79. doi: 10.1242/dmm.021659

Jeun, E.-J., Park, Y.-S., Yeo, S. W., Choi, Y.-C., and Jung, T. T. K. (2001). Effect of inhibitor of tumor necrosis factor-alpha on experimental otitis media with effusion. *Ann. Otol. Rhinol. Laryngol.* 110, 917–921. doi: 10.1177/000348940111001005

Juneau, R. A., Pang, B., Weimer, K. E. D., Armbruster, C. E., and Swords, W. E. (2011). Nontypeable Haemophilus influenzae initiates formation of neutrophil extracellular traps. *Infect. Immun.* 79, 431–438. doi: 10.1128/IAI.00660-10

Jurcisek, J. A., and Bakaletz, L. O. (2007). Biofilms formed by nontypeable Haemophilus influenzae in vivo contain both double-stranded DNA and type IV pilin protein. *J. Bacteriol.* 189, 3868–3875. doi: 10.1128/JB.01935-06

Kapsoritakis, A. N., Potamianos, S. P., Sfiridaki, A. I., Koukourakis, M. I., Koutroubakis, I. E., Roussomoustakaki, M. I., et al. (2000). Elevated thrombopoietin serum levels in patients with inflammatory bowel disease. *Am. J. Gastroenterol.* 95, 3478–3481. doi: 10.1111/j.1572-0241.2000.03364.x

Li, J.-D., Hermansson, A., Ryan, A. F., Bakaletz, L. O., Brown, S. D., Cheeseman, M. T., et al. (2013). Panel 4: recent advances in otitis media in molecular biology, biochemistry, genetics, and animal models. *Otolaryngol. Head. Neck Surg.* 148, E52–E63. doi: 10.1177/0194599813479772

Lupia, E., Goffi, A., Bosco, O., and Montrucchio, G. (2012). Thrombopoietin as biomarker and mediator of cardiovascular damage in critical diseases. *Mediators Inflamm.* 2012, 1–12. doi: 10.1155/2012/390892

Marçais, A., Viel, S., Grau, M., Henry, T., Marvel, J., and Walzer, T. (2013). Regulation of mouse NK cell development and function by cytokines. *Front. Immunol.* 4, 450. doi: 10.3389/fimmu.2013.00450

Mittal, R., Kodiyan, J., Gerring, R., Mathee, K., Li, J.-D., Grati, M., et al. (2014). Role of innate immunity in the pathogenesis of otitis media. *Int. J. Infect. Dis.* 29, 259–267. doi: 10.1016/j.ijid.2014.10.015

Nolan, P. M., Peters, J., Strivens, M., Rogers, D., Hagan, J., Spurr, N., et al. (2000). A systematic, genome-wide, phenotype-driven mutagenesis programme for gene function studies in the mouse. *Nat. Genet.* 25, 440–443. doi: 10.1038/78140

Parkinson, N., Hardisty-Hughes, R. E., Tateossian, H., Tsai, H. T., Brooker, D., Morse, S., et al. (2006). Mutation at the Evi1 locus in Junbo mice causes susceptibility to otitis media. *PloS Genet.* 2, 1556–1564. doi: 10.1371/journal.pgen.0020149

Ranson, T., Vosshenrich, C. A. J., Corcuff, E., Richard, O., Müller, W., and Di Santo, J. P. (2003). IL-15 is an essential mediator of peripheral NK-cell homeostasis. *Blood* 101, 4887–4893. doi: 10.1182/blood-2002-11-3392

Roberts, A. W. (2005). G-CSF: a key regulator of neutrophil production, but that's not all! *Growth Factors* 23, 33–41. doi: 10.1080/08977190500055836

Rye, M. S., Wiertsema, S. P., Scaman, E. S. H., Oommen, J., Sun, W., Francis, R. W., et al. (2011). FBXO11, a regulator of the TGFβ pathway, is associated with severe otitis media in Western Australian children. *Genes Immun.* 12, 352–359. doi: 10.1038/gene.2011.2

Sale, M. M., Chen, W.-M., Weeks, D. E., Mychaleckyj, J. C., Hou, X., Marion, M., et al. (2011). Evaluation of 15 functional candidate genes for association with chronic otitis media with effusion and/or recurrent otitis media (COME/ROM). *PloS One* 6, e22297. doi: 10.1371/journal.pone.0022297

Schilder, A. G. M., Chonmaitree, T., Cripps, A. W., Rosenfeld, R. M., Casselbrant, M. L., Haggard, M. P., et al. (2016). Otitis media. *Nat. Rev. Dis. Prim.* 2, 16063. doi: 10.1038/nrdp.2016.63

Schlahsa, L., Jaimes, Y., Blasczyk, R., and Figueiredo, C. (2011). Granulocyte-colony-stimulatory factor: a strong inhibitor of natural killer cell function. *Transfusion* 51, 293–305. doi: 10.1111/j.1537-2995.2010.02820.x

Segade, F., Daly, K. A., Allred, D., Hicks, P. J., Cox, M., Brown, M., et al. (2006). Association of the FBXO11 gene with chronic otitis media with effusion and recurrent otitis media: the Minnesota COME/ROM Family Study. *Arch. Otolaryngol. Head. Neck Surg.* 132, 729–733. doi: 10.1001/archotol.132.7.729

Seppanen, E., Tan, D., Corscadden, K. J., Currie, A. J., Richmond, P. C., Thornton, R. B., et al. (2018). Evidence of functional cell-mediated immune responses to nontypeable Haemophilus influenzae in otitis-prone children. *PloS One* 13, e0193962. doi: 10.1371/journal.pone.0193962

Tateossian, H., Hardisty-Hughes, R. E., Morse, S., Romero, M. R., Hilton, H., Dean, C., et al. (2009). Regulation of TGF-β signalling by Fbxo11, the gene mutated in the Jeff otitis media mouse mutant. *Pathogenetics* 2, 5. doi: 10.1186/1755-8417-2-5

Tateossian, H., Morse, S., Simon, M. M., Dean, C. H., and Brown, S. D. M. (2015). Interactions between the otitis media gene, Fbxo11, and p53 in the mouse embryonic lung. *Dis. Model. Mech.* 8, 1531–1542. doi: 10.1242/dmm.022426

Veenhoven, R., Bogaert, D., Uiterwaal, C., Brouwer, C., Kiezebrink, H., Bruin, J., et al. (2003). Effect of conjugate pneumococcal vaccine followed by polysaccharide pneumococcal vaccine on recurrent acute otitis media: a randomised study. *Lancet* 361, 2189–2195. doi: 10.1016/S0140-6736(03)13772-5

Vikhe, P. P., Purnell, T., Brown, S. D. M., and Hood, D. W. (2019). Cellular content plays a crucial role in Non-typeable Haemophilus influenzae infection of preinflamed Junbo mouse middle ear. *Cell. Microbiol.* 21, 1–11. doi: 10.1111/cmi.12960

von Freeden-Jeffry, U., Vieira, P., Lucian, L. A., McNeil, T., Burdach, S. E., and Murray, R. (1995). Lymphopenia in interleukin (IL)-7 gene-deleted mice identifies IL-7 as a nonredundant cytokine. *J. Exp. Med.* 181, 1519–1526. doi: 10.1084/jem.181.4.1519

Wan, Y. Y., and Flavell, R. A. (2007). Yin-Yang functions of transforming growth factor-beta and T regulatory cells in immune regulation. *Immunol. Rev.* 220, 199–213. doi: 10.1111/j.1600-065X.2007.00565.x

Wang, M., Meng, X., Tsai, B., Wang, J.-F., Turrentine, M., Brown, J. W., et al. (2004). Preconditioning up-regulates the soluble TNF receptor I response to endotoxin. *J. Surg. Res.* 121, 20–24. doi: 10.1016/j.jss.2004.02.017

Zheng, H., Shen, M., Zha, Y.-L., Li, W., Wei, Y., Blanco, M. A., et al. (2014). PKD1 phosphorylation-dependent degradation of SNAIL by SCF-FBXO11 regulates epithelial-mesenchymal transition and metastasis. *Cancer Cell* 26, 358–373. doi: 10.1016/J.CCR.2014.07.022

Conflict of Interest: The authors declare that the research was conducted in the absence of any commercial or financial relationships that could be construed as a potential conflict of interest.

frontiers in Cellular and Infection Microbiology

REVIEW
published: 14 February 2020
doi: 10.3389/fcimb.2020.00051

Reviewing the Pathogenic Potential of the Otitis-Associated Bacteria *Alloiococcus otitidis* and *Turicella otitidis*

Rachael Lappan[1,2], *Sarra E. Jamieson*[3] *and Christopher S. Peacock*[1,3]*

[1] *The Marshall Centre for Infectious Diseases Research and Training, School of Biomedical Sciences, The University of Western Australia, Perth, WA, Australia,* [2] *Wesfarmers Centre of Vaccines and Infectious Diseases, Telethon Kids Institute, The University of Western Australia, Perth, WA, Australia,* [3] *Telethon Kids Institute, The University of Western Australia, Perth, WA, Australia*

Alloiococcus otitidis and *Turicella otitidis* are common bacteria of the human ear. They have frequently been isolated from the middle ear of children with otitis media (OM), though their potential role in this disease remains unclear and confounded due to their presence as commensal inhabitants of the external auditory canal. In this review, we summarize the current literature on these organisms with an emphasis on their role in OM. Much of the literature focuses on the presence and abundance of these organisms, and little work has been done to explore their activity in the middle ear. We find there is currently insufficient evidence available to determine whether these organisms are pathogens, commensals or contribute indirectly to the pathogenesis of OM. However, building on the knowledge currently available, we suggest future approaches aimed at providing stronger evidence to determine whether *A. otitidis* and *T. otitidis* are involved in the pathogenesis of OM. Such evidence will increase our understanding of the microbial risk factors contributing to OM and may lead to novel treatment approaches for severe and recurrent disease.

Keywords: *Alloiococcus*, *Turicella*, otitis media, middle ear, otopathogen

OPEN ACCESS

Edited by:
Regie Santos-Cortez,
University of Colorado, United States

Reviewed by:
Kevin Mason,
The Ohio State University, United States
Joshua Chang Mell,
Drexel University, United States

***Correspondence:**
Christopher S. Peacock
christopher.peacock@uwa.edu.au

Specialty section:
This article was submitted to Microbiome in Health and Disease, a section of the journal Frontiers in Cellular and Infection Microbiology

Received: *29 August 2019*
Accepted: *27 January 2020*
Published: *14 February 2020*

Citation:
Lappan R, Jamieson SE and Peacock CS (2020) Reviewing the Pathogenic Potential of the Otitis-Associated Bacteria Alloiococcus otitidis and Turicella otitidis. Front. Cell. Infect. Microbiol. 10:51. doi: 10.3389/fcimb.2020.00051

INTRODUCTION

Otitis media (OM) is a polymicrobial disease most common in young children, characterized by inflammation of the middle ear and the presence of fluid behind the tympanic membrane. OM is a significant health care burden, affecting over 80% of children by the age of 3 (Teele et al., 1989) at an estimated annual cost of AUD$100 to 400 million in Australia (Taylor et al., 2009). The signs and symptoms of OM have been described as a phenotypic landscape of disease (Bhutta, 2014), but are commonly divided into two broad categories; acute OM (AOM) and OM with effusion (OME). In AOM, signs of an acute infection are present with a bulging tympanic membrane and often purulent fluid in the middle ear. Episodes of AOM may recur, becoming recurrent AOM (rAOM) if 3 or more episodes are experienced within 6 months, or $\geq$ 4 in 12 months (Kong and Coates, 2009). In OME, there are no signs of acute infection with the fluid more commonly serous or mucoid. If the fluid persists for $\geq$3 months, this is diagnosed as chronic OME (COME) (Bluestone et al., 2002). The onset of AOM will often occur subsequent to a viral upper respiratory infection, and may develop into OME (Bhutta, 2014). Chronic suppurative OM (CSOM) may follow untreated rAOM

or COME, where the tympanic membrane perforates and there is persistent discharge (otorrhea) from the middle ear (Kong and Coates, 2009), allowing infection from external sources. Untreated OM can result in conductive hearing loss and consequent speech and language delays (Kong and Coates, 2009).

Three major bacterial pathogens are known to be involved in OM (known as otopathogens); *Streptococcus pneumoniae,* non-typeable *Haemophilus influenzae* (NTHi), and *Moraxella catarrhalis*. These otopathogens are frequently detected in middle ear fluid (MEF) from both children with OME and with AOM (Bluestone et al., 1992). As colonizers of the nasopharynx, these otopathogens are thought to ascend the Eustachian tube to the middle ear, often following an episode of an upper respiratory tract viral infection (Chonmaitree et al., 2008). Respiratory viruses are capable of increasing the adherence of otopathogens to host cells, compromising Eustachian tube function, stimulating the immune system and inducing mucus production which may contribute to the otopathogens' ability to colonize the middle ear (Bakaletz, 2002). These otopathogens are capable of intracellular invasion and the formation of biofilm in the middle ear (Thornton et al., 2011); a matrix of extracellular DNA, polysaccharides and proteins. With these mechanisms, otopathogens are protected from antibiotic molecules and the host immune system and are able to later recolonise the middle ear, likely contributing to the recurrent or persistent nature of severe OM (Hall-Stoodley et al., 2006). Colonization with multiple otopathogens in the nasopharynx is more common in children with rAOM than in healthy children (Wiertsema et al., 2011). However, in some studies utilizing PCR, substantial proportions (18–31%) of children with AOM do not appear to have any evidence of the three major otopathogens in the middle ear fluid (Leskinen et al., 2004; Harimaya et al., 2006a; Kaur et al., 2010; Holder et al., 2012); suggesting other microbes are also involved in the pathogenesis of OM.

There are other bacterial species often isolated from the middle ear fluid of children with OM that are not currently considered major otopathogens. The two organisms most frequently reported are *Alloiococcus otitidis* and *Turicella otitidis.* These bacteria have primarily been observed in the middle ear fluid of children with OME (Ashhurst-Smith et al., 2007; Jervis-Bardy et al., 2015; Chan et al., 2016), including Indigenous Australian children; however, these organisms have also been identified as normal flora of the external auditory canal (Stroman et al., 2001). It has been speculated for over 25 years that these species are involved in the development of OM (Faden and Dryja, 1989; Funke et al., 1994), but there remains no substantial evidence describing their role, if any, in the disease.

In this review, we aim to summarize the current knowledge on these two species and their association with OM. We extensively review reports of their prevalence and abundance in the MEF from children with OM by culture, species-specific PCR and next generation sequencing methods, which have limitations in accurately estimating the abundance of these organisms. We explore the major issues with interpreting these organisms as otopathogens, including their natural colonization of the external ear canal and their relative absence in the nasopharynx; features not characteristic of major otopathogen species. We also evaluate the minimal evidence available from studies that have aimed to demonstrate a pathogenic role. As these organisms' involvement in OM currently remains equivocal we propose directions for future research that could firmly establish how these "controversial" organisms relate to the health of children with OM.

Alloiococcus otitidis

A. otitidis is a Gram positive coccus first reported as an unknown organism isolated from the MEF of children with OME in 1989 (Faden and Dryja, 1989). It was characterized as slow-growing, aerobic, catalase positive, and oxidase negative and was distinguishable from the phenotypically similar *Aerococcus*, *Gemella, Enterococcus,* and *Micrococcus* (Faden and Dryja, 1989). In 1992, the 16S rRNA sequence of the novel organism was analyzed and it was named *Alloiococcus* ("different coccus") *otitis* (Aguirre and Collins, 1992). This nomenclature was later revised (von Graevenitz, 1993) to *A. otitidis*. Placed within the *Carnobacteriaceae* family, it is the only species in its genus and is most closely related to *Dolosigranulum* by 16S rRNA sequence homology (Vos et al., 2009). *Dolosigranulum* is a nasopharyngeal commensal of relevance to OM, and their similarity leads to misclassification in 16S rRNA gene surveys using older taxonomic databases (Lappan et al., 2018). *A. otitidis* strains have been characterized as resistant to trimethoprim-sulfamethoxazole and macrolides, and susceptible or intermediately resistant to penicillin and ampicillin (Bosley et al., 1995; Ashhurst-Smith et al., 2007; Marsh et al., 2012), though they are β-lactamase negative (Bosley et al., 1995).

Turicella otitidis

The first description of *T. otitidis* was in 1993, when it was independently determined that unidentified coryneforms from MEF specimens (primarily from children with AOM), whilst phenotypically similar to *Corynebacterium afermentans,* were biochemically distinct from this species (Funke et al., 1993; Simonet et al., 1993). The 16S rRNA sequences of these strains showed they were also phylogenetically distinct and the new genus and species *T. otitidis* was proposed (Funke et al., 1994). *T. otitidis* is a Gram positive bacillus; catalase positive, oxidase negative and aerobic (Funke et al., 1994). Like *A. otitidis, T. otitidis* is the only member of its genus and was placed in the *Corynebacteriaceae* family with its closest relative, *Corynebacterium* (Goodfellow et al., 2012); though it has recently been proposed that *T. otitidis* is a true member of the *Corynebacterium* genus (Baek et al., 2018). Like *A. otitidis, T. otitidis*' closest relative is also a nasopharyngeal commensal, and *Corynebacterium* and *Dolosigranulum* commonly co-occur in healthy children (Biesbroek et al., 2014; Lappan et al., 2018). *T. otitidis* is similarly misclassified as *Corynebacterium* in at least one ribosomal taxonomic database (Lappan et al., 2018). *T. otitidis*is sensitive to tetracyclines and amoxicillin, but is resistant to sulfamethoxazole and co-trimoxazole (Troxler et al., 2001) and some strains have developed mutations conferring

macrolide resistance (Gómez-Garcés et al., 2004; Boumghar-Bourtchai et al., 2009).

WHY HAVE THESE ORGANISMS BEEN IMPLICATED IN OTITIS MEDIA?

Both *Alloiococcus* and *Turicella* were first isolated by culture from the MEF of children with OM, prompting suggestions of their association with the disease (Faden and Dryja, 1989; Funke et al., 1993; Simonet et al., 1993). This is the primary niche from which these organisms have since been consistently detected, though they have not been studied as extensively as the three major otopathogen species. *A. otitidis* has appeared more frequently than *T. otitidis* in the scientific literature, with 97 results for "*Alloiococcus*" and 44 for "*Turicella*" in the Scopus database as at 2019-02-07; this literature has been used for this review. This disparity is likely because *A. otitidis* can be detected by both culture and PCR methods, whereas there are currently no published primer pairs specific to *T. otitidis*. Additionally, cultured *T. otitidis* isolates are not often distinguished from commensal skin coryneforms (von Graevenitz and Funke, 2014). **Table 1** summarizes the studies that have evaluated the prevalence of *A. otitidis* in MEF by either microbiological culture or targeted PCR, including the OM phenotype and extent of ear canal avoidance for each. Few studies describe the prevalence of *T. otitidis* (see section *T. otitidis* Has Been Detected in MEF by Culture, But Is Seldom Reported).

A. otitidis Can Be Difficult to Detect by Culture

A. otitidis was originally detected by microbiological culture from MEF and was thus implicated as a cause of OME. However, it has remained a challenging organism to grow, requiring extended incubation times and producing small colonies (Ashhurst-Smith et al., 2007) so it may have been overlooked as an otopathogen in early studies. At its discovery, it was successfully cultured at 37°C with 5% CO_2 on blood agar for 2–5 days (Faden and Dryja, 1989). Subsequent studies apparently failed to culture the organism, with rates of 0% reported until 2007 when Ashhurst-Smith et al. (2007) successfully cultured the organism in 40% of MEF samples using a slightly lower temperature (35°C) and higher CO_2 (7.5%). Only six studies since the 1989 paper have reported the prevalence of *A. otitidis* in MEF by culture; five cultured it from 1 to 40% of samples from children with OME or COME (Ashhurst-Smith et al., 2007; de Miguel Martínez and Ramos Macías, 2008; Khoramrooz et al., 2012; Garibpour et al., 2013; Sheikh et al., 2015) and one cultured it from 46% of qPCR-positive otorrhoea swabs from children with AOM and perforation (Marsh et al., 2012). Due to the varying culture conditions used to isolate the organism (see **Table 1**) and the potential for overgrowth of other organisms to mask the presence of small *A. otitidis* colonies, it is not clear whether the prevalence of *A. otitidis* by culture is comparable to that of the three major otopathogens. A clearer picture can be obtained from those studies that have detected these organisms via species-specific PCR.

A. otitidis Is Commonly Detected in MEF by PCR

In 1997, *A. otitidis* was incorporated as part of a multiplex PCR method with the three major otopathogens, NTHi, *S. pneumonia*, and *M. catarrhalis* (Hendolin et al., 1997). The use of PCR has substantially improved the detection rate of these four organisms in MEF specimens compared to microbiological culture, as demonstrated by studies where both methods were used (Hendolin et al., 1997, 1999; Leskinen et al., 2002; Pereira et al., 2004; Harimaya et al., 2006a; Kaur et al., 2010; Aydin et al., 2012; Khoramrooz et al., 2012; Sheikh et al., 2015; Sillanpää et al., 2016; Slinger et al., 2016). In children with OME or COME, *A. otitidis* has been reported by PCR in 18.5–60.5% of MEF specimens (13 studies), and in children with AOM or rAOM, 7–50% (5 studies). Two studies compared the prevalence of *A. otitidis* in purulent and non-purulent MEF; *A. otitidis* was detected in 18.4 and 22.6% of purulent fluids, and in 25.4 and 25.7% of non-purulent fluids (Holder et al., 2012, 2015). However, there were 4–8 times as many non-purulent fluids tested in these studies as purulent fluids. One study has measured the bacterial load of *A. otitidis* in children with AOM with perforation and demonstrated that it was present at a comparable load to *H. influenzae*, the most dominant otopathogen (Marsh et al., 2012); but this is the only study to have done so.

The information currently available on the prevalence of *A. otitidis* suggests it is more commonly associated with persistence (OME) than acute infection (AOM). The within study-comparisons of purulent and non-purulent fluid support this (Holder et al., 2012, 2015), though no other studies have made a direct comparison between phenotypes and the difference in proportions is not large. It therefore may be hypothesized that the role of *A. otitidis* in OM is in the perpetuation of inflammation rather than as a direct pathogenic cause of acute infection. Further studies are needed to test this hypothesis, however some caution is required as the apparent association may be due to publication bias with few reported studies having sought to detect *A. otitidis* in children with AOM. Importantly, the prevalence and abundance of *A. otitidis* in MEF is possibly overestimated due to its habitation of the external ear canal. Several of the studies in **Table 1** either did not describe measures that were taken to avoid contamination with the ear canal, disinfected it only with 70% alcohol (which does not destroy DNA) or included children whose tympanic membranes had previously been breached.

Of the 16 studies summarized in **Table 1** that have reported the prevalence *A. otitidis, S. pneumoniae,* NTHi, and *M. catarrhalis* by species-specific PCR, *A. otitidis* was detected more frequently than each of the major otopathogens in 9 of them (for two of these studies, in non-purulent fluid only). **Table 2** describes those studies that have reported whether *A. otitidis* occurs alone or is detected together with the major otopathogens. Both scenarios are reported, with *A. otitidis*, present in the fluid-filled middle ear with and without the presence of the major otopathogen species. Therefore, if *A. otitidis* is involved in the pathogenesis of OM, it may directly cause disease or it may contribute by supporting the main otopathogens in some way.

TABLE 1 | Detection of *A. otitidis* in MEF specimens by culture and PCR methods.

References	Phenotype	Method of detection	*A. otitidis* prevalence	Major otopathogen prevalence[a]			Contact with the ear canal	Participants	Culture details for *A. otitidis*
				Hi	Spn	Mcat			
Faden and Dryja (1989)	OME	Culture	16 isolates of *A. otitidis* from 10 children	23%	14%	11%	Not described	320 samples from 200 children aged 0–2 years	37°C with 5% CO_2 for 2–5 days on blood agar
Hendolin et al. (1997)	OME (effusion ≥ 1 month)	Culture PCR	Not cultured 5/25 (20%)	2/25 (8%) 13/25 (52%)	2/25 (8%) 2/25 (8%)	4/25 (16%) 4/25 (16%)	Ear canal mechanically cleaned	25 samples from 16 children aged 1–7 years (median age 3 years)	NA
Beswick et al. (1999)	COME (effusion ≥ 6 months)	Culture PCR[b]	0/12 (0%) 6/12 (50%)	0/12 (0%) 1/12 (8.3%)	0/12 (0%) 0/12 (0%)	0/12 (0%) 1/12 (8.3%)	Care taken to avoid canal via sealed sampling system	12 samples from 10 children aged 5–10 years and 2 adults (28 and 59 y)	37°C with 5% CO_2 for a maximum of 5 days on blood agar
Hendolin et al. (1999)	OME	Culture PCR	0/67 (0%) 31/67 (46.3%)	6/67 (9%) 12/67 (17.9%)	2/67 (3%) 14/67 (20.9%)	6/67 (9%) 25/67 (37.3%)	Ear canal mechanically cleaned, all children had intact tympanic membrane	67 samples from 48 children aged 13 months−9 years and 2 months (median age 3 years 8 months)	Conditions not specified, on blood agar
Hendolin et al. (2000)	OME	PCR	14/73 (19.2%)	24/73 (32.9%)	26/73 (35.6%)	39/73 (53.4%)	Ear canal mechanically cleaned	73 samples from children	NA
Kalcioglu et al. (2002)[c]	COME	PCR	10/54 (18.5%)	7/54 (13%)	2/54 (3.7%)	4/54 (7.4%)	Not available	54 samples from 32 children	NA
Leskinen et al. (2002)	OME (effusion ≥ 1 month)	Culture PCR	0/123 (0%) 25/123 (20.3%)	18/123 (14.6%) 40/123 (32.5%)	14/123 (11.4%) 43/123 (35%)	8/123 (6.5%) 78/123 (63.4%)	Cleaned of cerumen, all children had intact tympanic membranes	123 samples from 123 children aged 7 months−12 years (median age 2 years 5 months)	Not described
Leskinen et al. (2004)	AOM	Culture PCR	NA 30/118 (25.4%)	22/118 (18.6%) 13/118 (11%)	26/118 (22%) 24/118 (20.3%)	12/118 (10.2%) 32/118 (27.1%)	Excluded children with spontaneous perforations or current tubes. 10% had previously had tympanostomy.	118 samples from 118 children aged 3 months−7 years 5 months (median age 2 years 6 months)	NA
Pereira et al. (2004)[d]	rAOM and COME (effusion ≥ 3 months)	Culture PCR	0/128 (0%) 67/128 (52.3%)	13/128 (10.2%) 50/128 (39.1%)	8/128 (6.3%) 16/128 (12.5%)	5/128 (3.9%) 13/128 (10.2%)	Cerumen removed and canal disinfected with 70% alcohol	128 samples from 75 children aged 11 months−10 years	37°C for a maximum of 5 days on blood and chocolate agar
Harimaya et al. (2006a)	AOM and COME (effusion ≥ 3 months)	Culture	0/40 (0%) in AOM 0/76 (0%) in OME	2/40 (5%) in AOM 4/76 (5.3%) in OME	5/40 (12.5%) in AOM 1/76 (1.3%) in OME	0/40 (0%) in AOM 1/76 (1.3%) in OME	Disinfected with povidone-iodine	116 samples from 88 children aged 9 months to 8 years (median age 3.5 years) for AOM; 6 months to 12 years (median age 4 years) for OME.	Conditions not specified, for up to 14 days on blood and chocolate agar

(Continued)

TABLE 1 | Continued

References	Phenotype	Method of detection	*A. otitidis* prevalence	Major otopathogen prevalence[a]			Contact with the ear canal	Participants	Culture details for *A. otitidis*
				Hi	Spn	Mcat			
		PCR	20/40 (50%) in AOM 46/76 (60.5%) in OME	3/40 (7.5%) in AOM 9/76 (11/8%) in OME	5/40 (12.5%) in AOM 6/76 (7.9%) in OME	8/40 (20%) in AOM 5/76 (6.6%) in OME			
Harimaya et al. (2006b)	recurrent OM ("otitis-prone") and non-recurrent OM ("non-otitis-prone")	Culture PCR	0/83 (0%) 16/25 (64%) in recurrent OM 8/58 (13.8%) in non-recurrent OM	NA	NA	NA	Disinfected with povidone-iodine	83 samples from 56 children aged 8 months to 10 years (median age 4 years)	Conditions not specified, for up to 14 days on blood and chocolate agar
Ashhurst-Smith et al. (2007)	COME	Culture	20/50 (40%)	2/50 (4%)	1/50 (2%)	0/50 (0%)	Cerumen removed and canal disinfected with povidone-iodine	50 samples from 50 children aged 1–10 years	35°C in 7.5% CO_2 for 7 days on blood, chocolate, MacConkey and colistin-nalidixic acid blood agar
de Miguel Martínez and Ramos Macías (2008)	AOM and OME	Culture	0/40 (0%) in AOM 14/40 (35%) in OME	10/40 (25%) in AOM 5/40 (12.5%) in OME	16/40 (40%) in AOM 1/40 (2.5%) in OME	0/80 (0%)	External ear canal was avoided, and children with previous tubes or perforations excluded	80 samples from 80 children with OME (mean age 4.1 years) and AOM (mean age 3.2 years)	37°C for 3 days on blood agar
Güvenç et al. (2010)	OME	PCR[b]	12/46 (26.1%)	7/46 (15.2%)	1/46 (2.2%)	1/46 (2.2%)	Disinfected with 70% alcohol and care taken to avoid contact during sampling	46 samples from 28 children aged 2–12 years (mean age 7 years)	NA
Kaur et al. (2010)	AOM	Culture PCR (culture-negative samples)	0/170 (0%) 16/49 (32.7%)	54/170 (31.8%) 17/49 (34.7%)	35/170 (20.6%) 25/49 (51%)	13/170 (7.6%) 7/49 (14.3%)	Not described	170 samples from 97 children aged 6 months−3 years	37°C with 5% CO_2, time not specified, on blood and chocolate agar[e]
Aydin et al. (2012)	COME (effusion $\geq$ 3 months)	Culture PCR	0/34 (0%) 12/34 (35.3%)	0/34 (0%) 1/34 (2.9%)	0/34 (0%) 3/34 (8.8%)	0/34 (0%) 3/34 (8.8%)	Disinfected with povidone-iodine	34 samples from 34 children aged 3 16 years (mean age 8 years)	35°C with 5% CO_2 for 7 days on blood and chocolate agar
Holder et al. (2012)	rAOM and COME	PCR	7/38 (18.4%) in purulent MEF 43/169 (25.4%) in non-purulent MEF	25/38 (65.8%) in purulent MEF 40/169 (23.7%) in non-purulent MEF	2/38 (5.3%) in purulent MEF 8/169 (4.7%) in non-purulent MEF	7/38 (18.4%) in purulent MEF 29/169 (17.2%) in non-purulent MEF	Not described. Children with previous ear tubes included.	207 samples from 207 children aged < 18 years (50% aged 1–3 years)	NA

(Continued)

TABLE 1 | Continued

References	Phenotype	Method of detection	*A. otitidis* prevalence	Major otopathogen prevalence[a]			Contact with the ear canal	Participants	Culture details for *A. otitidis*
				Hi	Spn	Mcat			
Khoramrooz et al. (2012)	COME (effusion ≥ 3 months)	Culture PCR	15/63 (23.8%) 25/63 (39.7%)	3/63 (4.8%) 7/63 (11.1%)	6/63 (9.5%) 7/63 (11.1%)	6/63 (9.5%) 6/63 (9.5%)	Disinfected with povidone-iodine and children with perforations or previous tubes excluded	63 samples from 48 children aged 1.7–12 years (mean age 7 years)	35°C in 5% CO_2 for 14 days on blood agar
Marsh et al. (2012)	AOM with perforation	Culture qPCR	5/11 (45.5%) of qPCR-positive swabs 11/31 (35.4%)	4/11 Ao-positive swabs 10/11 Ao-positive swabs	2/11 Ao-positive swabs 3/11 Ao-positive swabs	1/11 Ao-positive swabs 4/11 Ao-positive swabs	Samples were ear discharge swabs from perforations	31 samples from 27 Indigenous Australian children aged 6 months−4 years (median age 1.2 years)	37°C for 2–21 days on blood agar
Garibpour et al. (2013)[d]	OME	Culture PCR	15/65 (23%) 26/65 (40%)	NA	NA	NA	Not available	65 samples from 50 children	Not available
Holder et al. (2015)	AOM and OME (purulent and non-purulent MEF)	PCR	7/31 (22.6%) purulent MEF 63/245 (25.7%) non purulent MEF	16/31 (51.6%) in purulent MEF 45/245 (18.4%) in non-purulent MEF	6/31 (19.4%) in purulent MEF 9/245 (3.7%) in non-purulent MEF	8/31 (25.8%) purulent MEF 30/245 (12.2%) nonpurulent MEF	Not described. Children with previous tubes included.	276 samples from 276 children aged 0–18 years (mean age 2.7 years)	NA
Sheikh et al. (2015)	OME	Culture PCR	1/70 (1.4%) 18/70 (25.7%)	0/70 (0%) 14/70 (20%)	2/70 (2.8%) 14/70 (20%)	3/70 (4.2%) 9/70 (12.9%)	Disinfected with 70% alcohol, MEF collected by swab	70 samples from 45 children aged 1–15 years (mean 4.5 years)	35°C with 5% CO_2 for 2 weeks on blood agar
Slinger et al. (2016)	OME	Culture qPCR	0/48 (0%) 15/48 (31.3%)	3/48 (6.3%) 5/48 (10.4%)	2/48 (4.2%) 15/48 (31.3%)	5/48 (10.4%) 14/48 (29.2%)	Disinfected with 70% alcohol	48 samples from 30 children aged 11 months−10 years (median age 2.8 years)	37°C for 5 days on blood, chocolate and MacConkey agar
Sillanpää et al. (2016)	AOM (some with perforation)	Culture qPCR	0/90 (0%) 6/90 (6.7%)	17/90 (18.9%) 30/90 (33.3%)	15/90 (16.7%) 27/90 (30%)	8/90 (8.9%) 42/90 (46.7%)	Some children had drainage from tube or perforation	90 samples from 79 children aged 5 months−3.3 years (median age 1.6 years)	35°C with 5% CO_2 for 24 hours on blood and chocolate agar

PCR detection utilized species-specific primers unless otherwise indicated.

[a] *Hi, Haemophilus influenzae; Spn, Streptococcus pneumoniae; Mcat, Moraxella catarrhalis; Ao, Alloiococcus otitidis.*

[b] *PCR targeting 16S rRNA, amplicons identified by sequencing.*

[c] *Only abstract available.*

[d] *Only abstract and tables available in English.*

[e] *Casey et al. (2010).*

TABLE 2 | Distribution of *A. otitidis* detected with at least one otopathogen species or as the sole detected organism.

References	Detection with at least one otopathogen (%)	Detection as sole organism (%)	Phenotype
Hendolin et al. (1999)	58	42	OME
Leskinen et al. (2002)	96	4	OME
Pereira et al. (2004)	45	55	rAOM and COME
Aydin et al. (2012)	42	58	COME
Holder et al. (2012)	71	29	Purulent fluid
	49	51	Non-purulent fluid
Holder et al. (2015)	71	29	Purulent fluid
	27	73	Non-purulent fluid

Studies that have reported the number of A. otitidis-positive samples that also contained one or more otopathogenic species are included. All detection is by PCR. Percentages represent the proportion of total A. otitidis-positive samples.

T. otitidis Has Been Detected in MEF by Culture, but Is Seldom Reported

Detection of *T. otitidis* has been described infrequently in the literature. This is likely due to the difficulty in phenotypically distinguishing it from other coryneforms, which are often considered contaminants and do not appear to be routinely identified to species level (von Graevenitz and Funke, 2014). Additionally, no PCR primers have been described in the literature for the detection of *T. otitidis,* so it has only been detected by standard culture methods and next generation sequencing. Like *A. otitidis*, it has primarily been observed and reported in the MEF of children with OM, so both organisms may have been overlooked as otopathogens.

Since original detection of the organism in MEF in two independent studies (Funke et al., 1993; Simonet et al., 1993), very few studies have reported detection of *T. otitidis* by culture. Renaud et al. (1996) reported that otorrheal fluid from a child with a perforated tympanic membrane produced several colonies of *T. otitidis* (Renaud et al., 1996). Its prevalence appears to be low, with 7/112 (6.3%) of MEF samples in a 2004 study producing *T. otitidis* colonies (Gómez-Garcés et al., 2004). In 5 of these 7 samples the children had perforations and the MEF was collected from the external ear canal. One study has assessed the prevalence of *T. otitidis* where perforations were not present, reporting it in 10% of MEF samples from children with COME, compared to the major otopathogens at 3.3–8.3% (Holzmann et al., 2002). In this study, where *T. otitidis* was detected in the MEF, it was also detected in the external auditory canal; though the canal was disinfected between sampling each site. As we describe later in this review, the contribution of canal flora is challenging to tease out from the detection of both *A. otitidis* and *T. otitidis* in the MEF.

Detection of *A. otitidis* and *T. otitidis* in MEF Has Increased With Next Generation Sequencing

In recent years, several studies have utilized next generation DNA sequencing to study the whole bacterial community present in MEF specimens (**Table 3**). By amplifying and sequencing a segment of the 16S rRNA gene, the microbial profile (or microbiome) can be characterized, including bacteria that are challenging to isolate in culture or are not targeted by commonly-used species-specific PCRs. The advantage of this method is that these potentially overlooked organisms can not only be detected, but their relative abundance in a sample can be estimated and compared between samples. However, the major disadvantage is that only part of the gene is sequenced, providing little to no taxonomic resolution beyond the genus level (or broader, depending on the taxa and the region sequenced).

In the microbiota of MEF, *Alloiococcus* appears to be one of the dominant genera (Jervis-Bardy et al., 2015; Chan et al., 2016, 2017b; Boers et al., 2018; Lappan et al., 2018; Val et al., 2018; Johnston et al., 2019). *Turicella* is less often reported, but has been identified as a member of the MEF microbiota in 8 of the 12 MEF microbiota studies reported in **Table 3** (Jervis-Bardy et al., 2015; Krueger et al., 2017; Minami et al., 2017; Sillanpää et al., 2017; Boers et al., 2018; Lappan et al., 2018; Val et al., 2018; Johnston et al., 2019). However, due to the compositional nature of microbiome data it remains difficult to interpret which organisms are more abundant than others. Microbiome composition may also vary with the efficacy of the chosen DNA extraction method and amplicon primers on different organisms, and the variation in numbers of copies of the 16S rRNA gene amongst different bacterial genera; qPCR is still a more reliable indicator of whether there are greater numbers of *Alloiococcus* than other organisms within the same sample.

What Does Their Presence in MEF Tell us?

A. otitidis, and to a lesser extent *T. otitidis,* are prevalent in MEF specimens from children with OM. *A. otitidis* in particular is often detected at a similar or higher frequency to the three major otopathogen species. These two organisms may have been overlooked as potential otopathogens as they can be challenging to detect, though studies of the microbiome of MEF have revealed that they are not insignificant members of the microbiota of the otitis-prone middle ear. However, the observations from the studies summarized thus far only describe their prevalence and abundance, and do not assess their potential role in the pathogenesis of OM.

WHY IS THE ROLE OF THESE ORGANISMS IN OTITIS MEDIA STILL UNDER DEBATE?

Despite their prevalence in the MEF of children with OM, the role of *A. otitidis* and *T. otitidis* as potential otopathogens remains under debate. This is mostly due to two complicating factors: their presence in the external auditory canal (EAC), where the major otopathogens are rarely observed; and their infrequency in the nasopharynx, the site where major otopathogens initially colonize before ascension via the Eustachian tube to the middle ear.

TABLE 3 | Genus-level relative abundance of *A. otitidis* and *T. otitidis* in MEF specimens by 16S rRNA gene sequencing.

References	Phenotype	*A. otitidis* relative abundance	*T. otitidis* relative abundance	Main otopathogen relative abundance			Contact with the ear canal	Participants
				Haemophilus	*Streptococcus*	*Moraxella*		
Jervis-Bardy et al. (2015)	COME (effusion ≥ 6 months)	>50% in 6/11 samples	Detected in 3/11 samples	>50% in 3/11 samples	>50% in 1/11 samples	Detected in 2/11 samples	Minimized contact	11 samples from Indigenous Australian children aged 3–9 years (mean age 5.3 years)
Chan et al. (2016)	COME (effusion > 3 months)	23% (cumulative)	Not reported	22% (cumulative)	5% (cumulative)	5% (cumulative)	Care taken to avoid contact	35 samples from 23 children aged 1–8 years (mean age 3.3 years)
Neeff et al. (2016)[a]	CSOM (with and without cholesteatoma) and healthy ME controls	Absent from healthy controls and non-cholesteatoma CSOM. ∼10% in CSOM patients with cholesteatoma.	Not reported	Very low abundance in healthy controls. Absent from non-cholesteatoma CSOM. ∼25% in CSOM patients with cholesteatoma.	Reported in both MEF and healthy ME, abundance not described.	Absent from healthy controls and cholesteatoma CSOM. <1% in non-cholesteatoma CSOM.	All CSOM patients had perforations	22 samples from healthy controls aged 6 months−85 years, and 24 samples from CSOM patients aged 1–75 years (16 with and 8 without cholesteatoma).
Santos-Cortez et al. (2016)	CSOM	0% (median)	Not reported	0.17% (median)	Not reported	Not reported	All patients perforated. Canal also sampled.	16 Indigenous Filipino individuals aged 4–24 years (median age 9.5 years)
Chan et al. (2017b)	OME	37.5% (mean)	Not reported[b]	14.4% (mean)	3.8% (mean)	10.0% (mean)	Care taken to avoid direct contact. Canal also sampled. 18% had previous tubes.	18 samples from children aged 1–14 years (mean age 4 years)
Krueger et al. (2017)	COME	5.1%	7.8%	22.5%	4.2%	11.1%	Not described	55 samples from children aged 3 months−14.7 years (mean age 3.4 years)
Minami et al. (2017)[c]	COME and healthy ME controls	Not described	2% across all samples	Not described	Reported in one COME sample	Not described	Some patients with perforation. Care taken to avoid contact	88 individuals with COME (44 with active inflammation and MEF aged 9–84 years, mean age 57 years; 44 without active inflammation or MEF aged 6–83 years, mean age 59 years) and 67 healthy ME controls aged 1–72 years (mean age 22 years)
Sillanpää et al. (2017)[d]	AOM	0.7% (mean)	1.9% (mean)	14.0% (mean)	13.8% (mean)	6.1% (mean)	Some patients with perforation or previous tubes	90 samples from 79 children aged 5 months−3.5 years (median age 1.6 years)
Boers et al. (2018)[d]	rAOM and OME	24.9% (mean)	23.3% (mean)	9.1% (mean)	6.9% (mean)	0.26% (mean)	Some patients with previous tubes	19 samples from children aged 0.8–12.8 years

(Continued)

TABLE 3 | Continued

References	Phenotype	*A. otitidis* relative abundance	*T. otitidis* relative abundance	Main otopathogen relative abundance			Contact with the ear canal	Participants
				Haemophilus	*Streptococcus*	*Moraxella*		
Lappan et al. (2018)	rAOM	49.8% (cumulative)	6.7% (cumulative)	18.5% (cumulative)	3.5% (cumulative)	2.2% (cumulative)	Canal also sampled	127 samples from children with median age 1.9 years (IQR 1.3–2.8y)
Val et al. (2018)[e]	COME (effusion > 3 months)	~15% (mean)	~6% (mean)	~20% (mean)	~6% (mean)	~12% (mean)	Not described	5 samples; mean age for this subset of cohort not reported.
Johnston et al. (2019)[f]	COME (effusion ≥ 6 months)	~12%	~7%	~11%	~6%	0%	Not described. MEF collected by swab.	10 samples from children aged 2–10 years (mean age 5 years)

Where the information was available, relative abundance is reported as either the total relative abundance across all sequence reads (cumulative) or mean/median relative abundance across all samples (mean/median). ME, middle ear.

[a] *Values interpreted from Figure 3 (relative abundance of dominant genera).*

[b] *Possibly reported as Corynebacterium (3.1% mean relative abundance), as GreenGenes database was used for classification. The GreenGenes v13_8 database contains Turicella sequence labeled as its close relative Corynebacterium.*

[c] *This study primarily reported results at phylum level or for small groups of samples.*

[d] *Values calculated from Figure 1 (heatmap of relative abundance per sample with values).*

[e] *Values interpreted from Figure 5 (relative abundance of genera above 5%, per sample). If genus not shown, value taken as 0%.*

[f] *Values estimated from Figure 1 (stacked barplot of genera across all MEF samples).*

A. otitidis and *T. otitidis* Are Found in the External Auditory Canal

When first discovered, *A. otitidis* was reported not to be found in the EAC (Faden and Dryja, 1989), but both *A. otitidis* and *T. otitidis* have since been proposed as members of the normal EAC flora. Both organisms have been observed in the EACs of healthy adults and children (Stroman et al., 2001; Frank et al., 2003; Tano et al., 2008; De Baere et al., 2010), indicating that they are capable of growth in the EAC without causing disease. Given this finding, it becomes important to establish whether the detection of *A. otitidis* and *T. otitidis* in MEF is a result of contamination during sampling, or if they inhabit both sites. Currently, this is difficult to determine as only three studies, to our knowledge, have been in a position to address this question by looking for these organisms in EAC and MEF samples from the same ear in children with OM and intact tympanic membranes.

A 2002 study cultured *T. otitidis* from the EAC and MEF of children with OME, and found that the frequency of *T. otitidis* was higher in the EAC of children with OME (23%) than in healthy control children (11%) (Holzmann et al., 2002). Additionally, they noted that it was never isolated from the MEF alone; every MEF in which it was present had a positive result for the corresponding EAC sample. Because of this finding, they suggested that it resides only in the EAC, noting that many studies observing *T. otitidis* in MEF did not look for it in the EAC and that this was the likely source.

A recent study by Chan et al. (2017b) using 16S rRNA amplicon sequencing on samples from the EAC and MEF of children with OME did not observe *T. otitidis,* but reported *A. otitidis* as the most abundant species in both sites. They noted its high abundance in children who had previously had grommets, and suggested that the EAC may serve as a reservoir of infection for the middle ear via a tympanic membrane perforation. This study detailed their care in sampling the MEF without touching the EAC and concluded it unlikely that the abundance of *A. otitidis* in the MEF was the result of contamination from the EAC during sampling.

We recently took a similar approach, undertaking 16S rRNA amplicon sequencing on EAC and MEF samples from children with rAOM (Lappan et al., 2018). We observed *A. otitidis* and *T. otitidis* as dominant organisms in both sites in a cohort where the majority of children had no known current tympanic membrane perforations or previous grommets. While it is unlikely that these children had suffered tympanic membrane perforations, a perforation history was not obtained. The relative abundance of both *A. otitidis* and *T. otitidis* was significantly higher in the EAC than in the MEF. As with the Chan et al. study, care was taken to ensure the MEF was sampled without touching the EAC, however as we did not identify any bacteria unique to the EAC we could not rule out contamination of the MEF during sampling.

Based on the studies above, it is plausible that these organisms are present in both sites, but the evidence currently suggests that their primary habitat is the EAC. In support of this possibility, other studies have detected *A. otitidis* and *T. otitidis* in the EAC by culture and PCR, commonly observing a higher frequency in the EAC of children with OM than in healthy children

(Gómez-Hernando et al., 1999; Durmaz et al., 2002; Holzmann et al., 2002). Tano et al. found *A. otitidis* more frequently in the EAC of healthy individuals (29%) than patients with OM (6%), but sampled from adults and children and did not report these results separately (Tano et al., 2008). In the EAC of healthy children and adults, Stroman et al. (2001) cultured *A. otitidis* as the most common streptococci/enterococci-like organism, and *T. otitidis* as the dominant coryneform. While most of the *A. otitidis* isolates were from children, it was also detected in adults and *T. otitidis* isolates were found across both age groups. Frank et al. (2003) undertook a similar assessment of EAC samples from adults and children using 16S rRNA cloning and sequencing. They observed *A. otitidis* and *T. otitidis* (referred to as *Corynebacterium otitidis*) as the most prevalent sequence types, representing 57 and 20% of all clones, respectively, and with *A. otitidis* common in children. A more recent study also suggested that the organisms are not specific to children, detecting *A. otitidis* by PCR in 83% of EAC samples from healthy young adults, where *T. otitidis* was also cultured from 5 of 10 randomly selected samples (De Baere et al., 2010).

It therefore seems likely that *A. otitidis* and *T. otitidis* found in MEF originate from the EAC; but if these organisms do colonize the middle ear, their mechanism of entry remains unknown. It has been hypothesized that these organisms could enter the middle ear through a perforation in the tympanic membrane (De Baere et al., 2010; Marsh et al., 2012; Chan et al., 2017b). However, there are some studies that have reported the detection of *A. otitidis* in children with intact tympanic membranes when care is taken to avoid contact with the EAC (Leskinen et al., 2002, 2004; de Miguel Martínez and Ramos Macías, 2008; Khoramrooz et al., 2012). It is possible that small perforations sufficient for bacterial entry may not be detected by parents or physicians; and perhaps inflammation of the middle ear increases permeability of the tympanic membrane. However, understanding their entry into the middle ear does not indicate whether they are responsible for causing disease once inside. The sparsity of the major otopathogens in the EAC compared to *A. otitidis* and *T. otitidis* (Stroman et al., 2001; Frank et al., 2003; De Baere et al., 2010; Chan et al., 2017b; Lappan et al., 2018) indicates that *A. otitidis* and *T. otitidis* either have a different pathway for involvement in OM compared to the major otopathogens, or they are not otopathogenic organisms.

They Are Infrequently Found in the Nasopharynx

A. otitidis and *T. otitidis* show dissimilarity to the major otopathogens not only because they are found in the EAC, but also because they are rarely found in the nasopharynx. It is commonly accepted that the major otopathogens colonize the nasopharynx before ascension to the middle ear and subsequent infection (Chonmaitree et al., 2008). The low detection rates of *A. otitidis* and *T. otitidis* in the nasopharynx are another indicator that these organisms behave differently compared to the major otopathogens.

A. otitidis has infrequently been reported in the nasopharynx, and then only by PCR. The first study to do so was Durmaz et al. (2002), where it was detected in 15% of 27 nasopharyngeal samples from children with chronic OM (Durmaz et al., 2002). It has been observed more frequently in the nasopharynx of children with a history of otitis media episodes (>3 in 6 months, >4 in 12 months, or > 4 by 2 years of age; 29.4%) than those with fewer episodes (2.6%) (Harimaya et al., 2006b). It was also observed in 9% of nasopharyngeal samples from children with AOM (Kaur et al., 2010) and in 7% of children with an upper respiratory tract infection (Tano et al., 2008). It is very rare in the nasopharynx of healthy children, seen in 0.5% in one study (Janapatla et al., 2011) whilst in others was not detected (Durmaz et al., 2002; Aydin et al., 2012). It was also found to be absent from the nasopharynx of healthy young adults (De Baere et al., 2010). Where these studies also observed *A. otitidis* in the MEF or ear canal, it was found more commonly in these sites than in the nasopharynx (Harimaya et al., 2006b; Tano et al., 2008; De Baere et al., 2010; Kaur et al., 2010; Aydin et al., 2012), with one exception (Durmaz et al., 2002). *A. otitidis* also appears to be absent, or has been detected at very low abundance, on the tonsils (Aydin et al., 2012) and adenoids (Khoramrooz et al., 2012; Jervis-Bardy et al., 2015; Chan et al., 2016) of children with OME, suggesting that these lymphatic tissues are not a source of the organism in the middle ear. To our knowledge, *T. otitidis* has not been reported in the nasopharynx by culture or by PCR.

Both *A. otitidis* and *T. otitidis* have occasionally been detected in the nasopharynx by 16S rRNA amplicon sequencing. However, both organisms are likely to be misclassified depending on the reference database used. *A. otitidis* was reported in the nasopharynx of healthy infants (Teo et al., 2015) and in sinonasal swabs from adults with chronic rhinosinusitis (Lal et al., 2017), however both studies used the GreenGenes 13_8 taxonomic database for classification. This database does not contain *Dolosigranulum,* a nasopharyngeal commensal, and will misclassify it as *Alloiococcus.* These studies may similarly have not been able to detect *Turicella* in the nasopharynx as the GreenGenes database will report it as *Corynebacterium.* Similarly, nasopharyngeal microbiome studies that aggregate taxa at broader levels will have missed these genera. In 16S rRNA studies that did not use GreenGenes, *Alloiococcus,* and *Turicella* were not reported in the nasopharynx of children with OM (Laufer et al., 2011; Pettigrew et al., 2012; Jervis-Bardy et al., 2015). *Alloiococcus* was present at very low relative abundance in nasopharyngeal samples from children with rAOM (0.19% across all samples) and in healthy controls (0.17%) in our own study—significantly lower abundance than in the MEF (49.8%) (Lappan et al., 2018). *Turicella* was similarly present at 0.03% in the nasopharynx of both groups of children, again significantly lower than in the MEF (6.7%) (Lappan et al., 2018). In the nasopharynx, both genera were present at a similar level to known contaminants in negative control samples, indicating that caution should be taken to interpret the organisms as present in the nasopharynx.

These studies indicate that if *A. otitidis* and *T. otitidis* are present in the nasopharynx of children with OM then it is only at low abundance; they appear to be even more scarce in the nasopharynx of healthy individuals. The nasopharynx is therefore unlikely to represent a reservoir for these organisms, or

their presence there is transient and potentially originates from the middle ear. If they do not originate from the nasopharynx, then it is also unlikely that they follow the same pathway as the major otopathogens to the middle ear. This may be because these organisms are indeed not otopathogens, or it may be because the EAC, rather than the nasopharynx, is their predominant niche. The studies summarized so far do not provide any causal or mechanistic link between the presence of these organisms and the development of OM.

ARE THESE ORGANISMS CAPABLE OF CAUSING DISEASE?

In addition to understanding their mechanism for colonizing the middle ear (and indeed confirmation that they are not simply contaminants from the EAC introduced during sampling), the other aspect of *A. otitidis* and *T. otitidis*' ecology that we lack is an understanding of whether they are capable of causing disease. Very few studies have attempted to investigate the behavior and potential pathogenic activity of these two species, with all published articles that have investigated this issue focusing on *A. otitidis*. Evaluating their pathogenic potential is an integral part of understanding whether these organisms are causative of OM, if they contribute indirectly to pathogenesis, or whether they are aural commensals that are not involved in the pathogenesis of OM.

A. otitidis Provokes an Immune Response

There are a handful of studies that have assessed the ability of *A. otitidis* to elicit an immune response, as a proxy measure to indicate pathogenic potential. Initial studies assessed the production of interleukins (IL) from THP-1 cells (IL-8 and IL-12) and Hep-2, HeLa and U937 cells (IL-8) in response to *A. otitidis*. These studies demonstrated that viable *A. otitidis* was capable of stimulating IL-8 and IL-12 at similar levels to the three major otopathogens (Himi et al., 2000; Kita et al., 2000). The effect was reduced when cells were stimulated with whole killed *A. otitidis* and when viable cells were prevented from direct contact, but soluble proteins from *A. otitidis* elicited a response for both cytokines (Himi et al., 2000; Kita et al., 2000). Whole killed *A. otitidis* can also induce expression of CD69 (indicating activation of lymphocytes) in blood and adenoidal lymphocytes at comparable levels to the major otopathogens (Harimaya et al., 2005), but the response is lower than that induced by *Staphylococcus aureus* (Tarkkanen et al., 2000). Whole killed *A. otitidis* has also been shown to activate signaling pathways for the production of IL-8, similarly to *S. pneumoniae* (Harimaya et al., 2007a). Formalin-killed cells from clinical isolates of *A. otitidis* have induced IL-1β, IL-6, IL-8, and TNF-α on a cell line *in vitro* at or above levels induced by *S. pneumoniae* (Ashhurst-Smith et al., 2014a). An experiment with cell-free filtrates from these isolates indicated that extracellular proteins rather than peptodiglycan may be responsible for the induction (Ashhurst-Smith et al., 2014b).

The production of pro-inflammatory cytokines provides preliminary evidence that the human immune system responds to *A. otitidis*. However, these studies lack replication in a middle ear epithelial environment, have not involved comparisons with non-pathogenic bacteria, and are potentially strain-dependent. For example, some strains of the nasopharyngeal commensal *Haemophilus haemolyticus* have been shown to elicit an inflammatory response *in vitro* (Pickering et al., 2016). It remains unclear from these studies whether these inflammatory responses are characteristic of the response in the middle ear of children with OM, and whether they are evidence for pathogenicity.

Two further studies by Harimaya et al. have explored the immune response to *A. otitidis* within the middle ear. In 2007, they determined that MEF from children with *A. otitidis*-positive OM (in the absence of other detectable otopathogens) contained IgG, secretory IgA, IgG2, and IgM specific to *A. otitidis* (Harimaya et al., 2007b). In 2009, they also discovered that *A. otitidis*-positive MEF contained similar levels of pro-inflammatory cytokines and chemokines as *S. pneumoniae*-positive MEF (both in the absence of other otopathogens detectable by culture or PCR) (Harimaya et al., 2009). While these preliminary studies require replication, it is important to note that *A. otitidis* does appear to elicit an innate and adaptive immune response in the middle ear of children with OM.

Observations of Bacterial Activity

There is also some limited evidence for *Alloiococcus* having pathogenic potential based on how the organism behaves. Upon its initial discovery, *Alloiococcus* was reported to be found intracellularly, which the authors suggested was an indication of pathogenic capability (Faden and Dryja, 1989); though this may have been an observation of engulfment by neutrophils. Two reports of intracellular bacteria found in the middle ear mucosa described Gram positive cocci (Coates et al., 2008) and other, unidentified bacteria (Thornton et al., 2011), though no studies since have indicated the presence of intracellular *Alloiococcus*. In children with AOM and perforation, the *Alloiococcus* bacterial load in MEF was comparable to *H. influenzae* (Marsh et al., 2012). *A. otitidis* has been observed more frequently than the major otopathogens in non-purulent MEF (Holder et al., 2012, 2015) and more commonly in persistent (≥3 month duration) effusions than those of shorter duration (Leskinen et al., 2002), suggesting involvement in chronicity. It is similarly prevalent in purulent effusions (Holder et al., 2012, 2015), though its presence in the MEF of children with AOM appears to be unrelated to disease severity (Leskinen et al., 2004). *A. otitidis* is strictly aerobic, as its viability decreases greatly when grown anaerobically (Matsuo et al., 2011). Its presence in middle ear fluids is therefore somewhat unexpected, as the fluid-filled middle ear in OM is thought to be hypoxic (Cheeseman et al., 2011). Interestingly, the organism has recently been shown to form biofilms in broth culture, both with *H. influenzae* and independently as a single-species biofilm (Chan et al., 2017a). Furthermore, *A. otitidis* improved the growth of *H. influenzae* when in media without its required X and V factors and at suboptimal temperatures, suggesting its enhancement of biofilm production by otopathogens may allow *A. otitidis* to indirectly contribute to the pathogenesis of OM. This multispecies biofilm was also less susceptible to antimicrobial killing, and it is possible

that *A. otitidis*' ability to also form biofilm alone may contribute to the perpetuation of inflammation and chronic OM (Chan et al., 2017a). Understanding whether *A. otitidis* DNA detected in MEF originates from live or dead cells, and whether residence in biofilm improves its tolerance to low oxygen conditions would be highly informative regarding its persistence in the middle ear.

For *Turicella*, very little has been investigated with respect to pathogenicity other than its resistance to antimicrobials. *Turicella* strains have shown resistance to macrolides and clindamycin (Gómez-Garcés et al., 2007; Boumghar-Bourtchai et al., 2009), though are susceptible to amoxicillin-clavulanic acid (Funke et al., 1996; Troxler et al., 2001) which is more commonly used to treat AOM (Antibiotic Expert Group, 2014). The draft genome sequence of a strain isolated from MEF of a child with OM apparently did not contain any candidate virulence factors, but no detail was given as to how these were sought (Brinkrolf et al., 2012). We therefore currently have minimal evidence for the pathogenicity of *T. otitidis*.

Assessment in Animal Models

To our knowledge, there has only been one published study investigating *Alloiococcus* in an animal model to evaluate pathogenicity, and none investigating *Turicella*. In 2008, Tano et al. inoculated $>10^8$ CFU/ml of *Alloiococcus* into the middle ear of 7 rats (a 10-fold higher concentration than required of the major otopathogens) (Tano et al., 2008). Reactions were mild; after 3 days, all rats had an amber-colored (but not purulent) effusion in the middle ear but by day 14 all ears were normal. In conjunction with their observations that *Alloiococcus* was found in the EAC of healthy adults and rarely in the nasopharynx of children, Tano et al. concluded that *Alloiococcus* is not an otopathogen. This study requires replication, though it suggests that *A. otitidis* is not overtly pathogenic on its own; an observation consistent with the association of *A. otitidis* with OME and persistent inflammation rather than AOM. However, effective animal models of AOM often make use of a viral infection to predispose the animal to AOM, as occurs in humans (Davidoss et al., 2018); so it remains possible that *A. otitidis* would produce or exacerbate disease in the presence of a co-infecting virus or organism. This would be congruent with the observations of coinfection summarized in **Table 2**, and with *A. otitidis*' ability to enhance the survival of NTHi in biofilm (Chan et al., 2017a).

Pathogenicity in Diseases Other Than Otitis Media

There have been isolated reports of *A. otitidis* and *T. otitidis* as causative agents of diseases seemingly unrelated to otitis media. *A. otitidis* has been described as the causative agent in two case reports, where it was isolated from vitreous fluid of a patient with acute-onset endopthalmitis (Marchino et al., 2013) and from blood cultures in a young adult with endocarditis (Guler et al., 2015). Both infections are usually caused by the Gram positive cocci *Streptococcus* and *Staphylococcus* (Marchino et al., 2013; Guler et al., 2015); it is possible that the cause was misidentified as these reports do not provide any detail on how the isolates were identified as *A. otitidis*. In the endocarditis case, the patient had chronic OME with perforation which had apparently been a problem since childhood, so it is possible that in long-term severe disease *A. otitidis* can opportunistically infect the bloodstream. *T. otitidis* has similarly had few instances of unrelated opportunistic infection. Two case reports isolated *T. otitidis* from the blood of an immunocompromised child (Loïez et al., 2002) and an elderly hospitalized patient (Bîrlutiu et al., 2017) with bacteraemia. In the case of the child, otitis externa was apparently present at the time and *T. otitidis* was also isolated from an external ear swab (Loïez et al., 2002). It has also been isolated in pure culture from a posterior auricular abscess (Reynolds et al., 2001) and a case of mastoiditis (Dana et al., 2001), both in young children. The *T. otitidis* strain TD1, whose genome was recently sequenced (Greninger et al., 2015), was isolated from a venous catheter. It is therefore plausible that the genomic contents of this strain are not representative of strains involved in OM.

Thus, there is weak evidence for both *A. otitidis* and *T. otitidis* to have opportunistic pathogenicity outside of the ear; these reports are infrequent and not replicated. Samples taken from in or around the ear have the potential to have been contaminated with the organisms from the EAC; outside of these few case reports these species have only been reported in the middle or external ear. It is unknown how these organisms would migrate to the blood, and it is likely that the connection between these patients' ear disease and bacteraemia is a result of sample contamination or transient bacteraemia rather than invasive infection by these organisms.

These sparse reports of pathogenic activity are in contrast to the major otopathogens, each of which can reside asymptomatically but are also responsible for a wide range of infections (Verduin et al., 2002; Bogaert et al., 2004; Van Eldere et al., 2014). Overall, there is currently minimal evidence for the pathogenicity of *A. otitidis* and *T. otitidis* as the immunological and animal studies lack a comparison to commensal organisms known *not* to cause OM, and the work is lacking replication.

SUMMARY AND FUTURE DIRECTIONS

What we Currently Know

Our summary of the literature available at the time of writing suggests that *A. otitidis* and *T. otitidis* are primarily organisms of the human ear. They are found abundantly in both the MEF and EAC of children with OM, but are also present in the EAC of healthy children and adults. Current evidence suggests that *A. otitidis* and *T. otitidis* in MEF may originate from the EAC as they are uncommonly found in the nasopharynx. This pattern of detection is opposite to what is commonly observed of the major otopathogens, which typically colonize the nasopharynx to ascend to the middle ear and are rarely found in the EAC. Curiously, the closest relatives of *Alloiococcus* and *Turicella* are *Dolosigranulum,* and *Corynebacterium,* respectively; both organisms being usual nasopharyngeal commensals. These organisms may have diverged to inhabit the middle ear and the nasopharynx, where they have potentially developed specialized but very different interactions with the other dominant organisms in these niches (the otopathogen genera).

The majority of available studies on *A. otitidis* and *T. otitidis* only *hypothesize* their role in the pathogenesis of OM by describing their prevalence and abundance, but relatively few studies set out to *test* these hypotheses to better define their role in disease. Thus, we have minimal information on whether or how these organisms contribute to the development of OM.

The few studies that have aimed to directly investigate pathogenic potential have tested only *A. otitidis*. There is evidence that it is capable of forming biofilm and supporting the survival of NTHi, stimulating release of pro-inflammatory cytokines *in vitro*, and stimulating the production of specific antibodies. However, these studies have compared *A. otitidis* only with the major otopathogens and not with known commensal species; it is possible that a commensal organism would still elicit these responses. There is still much that is unknown about the role of *A. otitidis* and *T. otitidis* in the pathogenesis of OM, and a targeted research effort is required to further characterize their function.

Designing Future Studies to Clarify Their Role in Otitis Media

Even after more than 25 years since their discovery, there is much about the behavior of *A. otitidis* and *T. otitidis* in the middle ear and EAC that remains unknown. Firstly, while there are many studies describing their prevalence in the MEF of children with OM, and some in the EAC, these studies are often confounded with the possibility of EAC flora contaminating MEF samples during collection. However, several studies have reported the presence of *A. otitidis* or *T. otitidis* in specimens from children in which tympanic membrane perforations (including previous grommets) had not occurred (Hendolin et al., 1999; Leskinen et al., 2002, 2004; de Miguel Martínez and Ramos Macías, 2008; Khoramrooz et al., 2012). This suggests three possibilities: 1) *A. otitidis* and *T. otitidis* inhabit the normal middle ear, prior to the onset of OM; 2) they enter the middle ear through undetectable, minor tympanic membrane perforations; 3) they are detectable in MEF specimens as a result of contamination from the EAC during sampling.

The first possibility is challenging to address, as the healthy middle ear is a very low biomass environment, where samples are highly prone to environmental contamination and the area is inaccessible without surgery. Some attempts have been made to survey the microbiota of the healthy middle ear, and these studies have not consistently reported the presence of *A. otitidis* and *T. otitidis* (Antonelli and Ojano-Dirain, 2013; Neeff et al., 2016; Minami et al., 2017) and some have not found evidence for the presence of bacteria in the normal middle ear at all (de Miguel Martínez and Ramos Macías, 2008; Westerberg et al., 2009; Thornton et al., 2011; Papp et al., 2016). The second possibility is also challenging, but may be explored with animal or tissue models of an inflamed tympanic membrane to test its permeability to bacteria. These will also be important studies if it is found that viable *A. otitidis* and *T. otitidis* in the MEF originate from the EAC, even in children with intact tympanic membranes. The final possibility of MEF contamination is the most straightforward to test, and these experiments are also useful for addressing the second possibility. A well-designed study aiming to isolate viable *A. otitidis* and *T. otitidis* from the two sites independently is required. This may be achieved by sampling the EAC, sterilizing it thoroughly, sampling it again, and then opening the tympanic membrane to sample the MEF with all care taken not to contact the EAC. This should be carried out in children who have never had a known tympanic membrane perforation as well as those who have, or have had tympanostomy tubes in the past. Such a study would also be well-positioned to answer the subsequent question, addressing the minor perforation hypothesis: if these organisms reside in the MEF, how do they get there? The isolates from the EAC and MEF of the same ear may be phenotypically or genetically compared to determine if the EAC is the likely origin of the isolates from the MEF. Higher similarity between EAC and MEF strains of the same patient than between strains from different patients may indicate the transferral of strains between the EAC and MEF in the absence of sampling contamination. Metagenomics is also a useful tool for answering this question if isolation of live bacteria is a challenge (which could be informative in itself). Metagenomic analysis would also allow for the characterization of other EAC community members to aid in the assessment of contamination and strain relatedness between the EAC and MEF communities. Bacterial load estimation via species-specific qPCR would also be useful to determine whether there is a larger population of *A. otitidis* and *T. otitidis* in the EAC or in the MEF, keeping in mind that there may be differences in the live and dead populations of *A. otitidis* and *T. otitidis*. Longitudinal sampling of the EAC may also indicate whether the presence or abundance of these organisms in the EAC is associated with episodes of OM. These experiments should provide a solid body of evidence to a) show whether *A. otitidis* and *T. otitidis* do inhabit the MEF and are not present due to contamination; and b) whether they enter the middle ear from the EAC, and how they do so.

The second major gap in current knowledge is that the functions these organisms perform in the EAC and MEF is entirely unknown. To begin to understand the behavior of these organisms in the middle ear, metagenomics and other new "'omics" techniques may be able to answer many of these questions. The genomes of *A. otitidis* and *T. otitidis* isolates are currently in draft stage; complete, annotated genomes will allow us to understand whether they contain genes that may allow them to cause disease. The assembly of many additional genomes will aid an understanding of their metabolic functions and strain heterogeneity Transcriptomics and proteomics analysis of MEF could directly indicate their activity in the inflamed middle ear; this could be compared to their activity in the EAC. *In vitro* analyses making use of middle ear epithelial cell lines could confirm the pro-inflammatory stimulation by *A. otitidis,* and *T. otitidis* could be studied in this manner as well. These experiments would also be useful to determine whether the species are capable of residing intracellularly in the middle ear mucosa, as a mechanism for immune or antibiotic evasion. Further work with animal models would also fill gaps in our knowledge of the behavior of *A. otitidis* and *T. otitidis* in the middle ear, perhaps allowing us to determine if the presence of these organisms in OM caused by the major otopathogens results in a more severe phenotype. With these models, we may

determine whether these organisms can produce OM on their own, or whether the presence of otopathogens or viruses is required. It can be assessed whether the phenotype is more severe in the presence of *A. otitidis* or *T. otitidis*. Understanding what functions these organisms perform in the MEF is essential to understand whether they play a pathogenic role, by themselves or in synergism with the otopathgoens.

CONCLUSION

Research focusing on the development of new therapies to treat severe OM has focused on the major otopathogens; with advances in the areas of vaccinations, tackling biofilm and restoring the commensal flora of the nasopharynx. Despite these advances in prevention and treatment, OM remains a very common childhood disease that can be difficult to treat. The complex polymicrobial nature of the disease and the role dominant organisms like *A. otitidis* and *T. otitidis* may play has remained equivocal for decades. The current understanding of these organisms is limited, and there are many ways in which they can be further characterized. It is important to understand their role, if any, in the pathogenesis of OM, as it is plausible that they are supporting otopathogen growth or contributing to the persistence and recurrence of chronic OM; potentially entering the middle ear through minor tympanic membrane perforations. These organisms may be useful targets for treatment, which are perpetually overlooked as their commensal residence in the external ear canal continues to confound efforts to understand their pathogenicity. Establishing their role in the otitis-prone middle ear will allow the advancement of new therapies, or will ensure that resources are not overspent investigating commensals that are uninvolved in the disease.

AUTHOR CONTRIBUTIONS

RL undertook the literature review and drafted the manuscript. SJ and CP provided critical feedback on the manuscript. All authors have read and approved the final manuscript.

FUNDING

RL was supported by an Australian Government Research Training Program Scholarship and a top-up scholarship from the Wesfarmers Centre of Vaccines and Infectious Diseases, Telethon Kids Institute.

ACKNOWLEDGMENTS

The authors would like to acknowledge Professor Alexander von Graevenitz, who kindly airmailed a copy of his article for inclusion in this review: (Funke et al., 1993).

REFERENCES

Aguirre, M., and Collins, M. D. (1992). Phylogenetic analysis of *Alloiococcus otitis* gen. nov., sp. nov., an organism from human middle ear fluid. *Int. J. Syst. Evol. Microbiol.* 42, 79–83. doi: 10.1099/00207713-42-1-79

Antibiotic Expert Group (2014). *Therapeutic Guidelines: Antibiotic. Version 15.* Melbourne, VIC: Therapeutic Guidelines Limited.

Antonelli, P. J., and Ojano-Dirain, C. P. (2013). Microbial flora of cochlear implants by gene pyrosequencing: *Otol. Neurotol.* 34, e65–e71. doi: 10.1097/MAO.0b013e3182941101

Ashhurst-Smith, C., Hall, S. T., Burns, C. J., Stuart, J., and Blackwell, C. C. (2014a). *In vitro* inflammatory responses elicited by isolates of *Alloiococcus otitidis* obtained from children with otitis media with effusion. *Innate Immun.* 20, 320–326. doi: 10.1177/1753425913492181

Ashhurst-Smith, C., Hall, S. T., Burns, C. J., Stuart, J., and Blackwell, C. C. (2014b). Induction of inflammatory responses from THP-1 cells by cell-free filtrates from clinical isolates of *Alloiococcus otitidis*. *Innate Immun.* 20, 283–289. doi: 10.1177/1753425913490535

Ashhurst-Smith, C., Hall, S. T., Walker, P., Stuart, J., Hansbro, P. M., and Blackwell, C. C. (2007). Isolation of *Alloiococcus otitidis* from Indigenous and non-Indigenous Australian children with chronic otitis media with effusion. *FEMS Immunol. Med. Microbiol.* 51, 163–170. doi: 10.1111/j.1574-695X.2007.00297.x

Aydin, E., Taştan, E., Yücel, M., Aydogan, F., Karakoç E., Arslan, N., et al. (2012). Concurrent assay for four bacterial species including *Alloiococcus otitidis* in middle ear, nasopharynx and tonsils of children with otitis media with effusion: a preliminary report. *Clin. Exp. Otorhinolaryngol.* 5, 81–85. doi: 10.3342/ceo.2012.5.2.81

Bîrlutiu, V., Mihaila, R. G., Bîrlutiu, R. M., and Cipaian, C. R. (2017). Bacteremia with *Turicella otitidis* in an institutionalized elderly patient with multiple hospital admissions: a case report. *Biomed. Res.* 28, 2196–2198. Available online at: https://www.alliedacademies.org/abstract/bacteremia-with-turicella-otitidis-in-an-institutionalized-elderly-patient-with-multiple-hospital-admissions-a-case-report-6715.html

Baek, I., Kim, M., Lee, I., Na, S. I., Goodfellow, M., and Chun, J. (2018). Phylogeny trumps chemotaxonomy: a case study involving *Turicella otitidis*. *Front. Microbiol.* 9. doi: 10.3389/fmicb.2018.00834

Bakaletz, L. O. (2002). "Otitis Media," in *Polymicrobial Diseases*, eds K. Brogden and J. Guthmiller (Washington, DC: ASM Press). Available online at: https://www.ncbi.nlm.nih.gov/books/NBK2482/ (accessed August 11, 2017).

Beswick, A. J., Lawley, B., Fraise, A. P., Pahor, A. L., and Brown, N. L. (1999). Detection of *Alloiococcus otitis* in mixed bacterial populations from middle-ear effusions of patients with otitis media. *Lancet* 354, 386–389. doi: 10.1016/S0140-6736(98)09295-2

Bhutta, M. F. (2014). Epidemiology and pathogenesis of otitis media: construction of a phenotype landscape. *Audiol. Neurotol.* 19, 210–223. doi: 10.1159/000358549

Biesbroek, G., Tsivtsivadze, E., Sanders, E. A. M., Montijn, R., Veenhoven, R. H., Keijser, B. J. F., et al. (2014). Early respiratory microbiota composition determines bacterial succession patterns and respiratory health in children. *Am. J. Respir. Crit. Care Med.* 190, 1283–1292. doi: 10.1164/rccm.201407-1240OC

Bluestone, C. D., Gates, G. A., Klein, J. O., Lim, D. J., Mogi, G., Ogra, P. L., et al. (2002). Definitions, terminology, and classification of otitis media. *Ann. Otol. Rhinol. Laryngol.* 111:8. doi: 10.1177/00034894021110S304

Bluestone, C. D., Stephenson, J. S., and Martin, L. M. (1992). Ten-year review of otitis media pathogens. *Pediatr. Infect. Dis. J.* 11, S7–11. doi: 10.1097/00006454-199208001-00002

Boers, S. A., de Zeeuw, M., Jansen, R., van der Schroeff, M. P., van Rossum, A. M. C., Hays, J. P., et al. (2018). Characterization of the nasopharyngeal and middle ear microbiota in gastroesophageal reflux-prone versus gastroesophageal reflux non-prone children. *Eu. J. Clin. Microbiol. Infect. Dis.* 37, 851–857. doi: 10.1007/s10096-017-3178-2

Bogaert, D., de Groot, R., and Hermans, P. (2004). *Streptococcus pneumoniae* colonisation: the key to pneumococcal disease. *Lancet Infect. Dis.* 4, 144–154. doi: 10.1016/S1473-3099(04)00938-7

Bosley, G. S., Whitney, A. M., Pruckler, J. M., Moss, C. W., Daneshvar, M., Sih, T., et al. (1995). Characterization of ear fluid isolates of *Alloiococcus*

otitidis from patients with recurrent otitis media. *J. Clin. Microbiol.* 33:2876. doi: 10.1128/JCM.33.11.2876-2880.1995

Boumghar-Bourtchai, L., Chardon, H., Malbruny, B., Mezghani, S., Leclercq, R., and Dhalluin, A. (2009). Resistance to macrolides by ribosomal mutation in clinical isolates of *Turicella otitidis*. *Int. J. Antimicrob. Agents* 34, 274–277. doi: 10.1016/j.ijantimicag.2009.03.023

Brinkrolf, K., Schneider, J., Knecht, M., Rückert, C., and Tauch, A. (2012). Draft genome sequence of *Turicella otitidis* ATCC 51513, isolated from middle ear fluid from a child with otitis media. *J. Bacteriol.* 194, 5968–5969. doi: 10.1128/JB.01412-12

Casey, J. R., Adlowitz, D. G., and Pichichero, M. E. (2010). New patterns in the otopathogens causing acute otitis media six to eight years after introduction of pneumococcal conjugate vaccine. *Pediatr. Infect. Dis. J.* 29, 304–309. doi: 10.1097/INF.0b013e3181c1bc48

Chan, C. L., Richter, K., Wormald, P.-J., Psaltis, A. J., and Vreugde, S. (2017a). *Alloiococcus otitidis* forms multispecies biofilm with *Haemophilus influenzae*: effects on antibiotic susceptibility and growth in adverse conditions. *Front. Cell Infect. Microbiol.* 7:344. doi: 10.3389/fcimb.2017.00344

Chan, C. L., Wabnitz, D., Bardy, J. J., Bassiouni, A., Wormald, P.-J., Vreugde, S., et al. (2016). The microbiome of otitis media with effusion. *Laryngoscope* 126, 2844–2851. doi: 10.1002/lary.26128

Chan, C. L., Wabnitz, D., Bassiouni, A., Wormald, P.-J., Vreugde, S., and Psaltis, A. J. (2017b). Identification of the bacterial reservoirs for the middle ear using phylogenic analysis. *JAMA Otolaryngol. Head Neck Surg.* 143:155. doi: 10.1001/jamaoto.2016.3105

Cheeseman, M. T., Tyrer, H. E., Williams, D., Hough, T. A., Pathak, P., Romero, M. R., et al. (2011). HIF–VEGF pathways are critical for chronic otitis media in junbo and jeff mouse mutants. *PLoS Genet.* 7:e1002336. doi: 10.1371/journal.pgen.1002336

Chonmaitree, T., Revai, K., Grady, J. J., Clos, A., Patel, J. A., Nair, S., et al. (2008). Viral upper respiratory tract infection and otitis media complication in young children. *Clin. Infect. Dis.* 46, 815–823. doi: 10.1086/528685

Coates, H., Thornton, R., Langlands, J., Filion, P., Anthony, D. K., Vijayasekaran, S., et al. (2008). The role of chronic infection in children with otitis media with effusion: evidence for intracellular persistence of bacteria. *Otolaryngol. Head Neck Surg.* 138, 778–781. doi: 10.1016/j.otohns.2007.02.009

Dana, A., Fader, R., and Sterken, D. (2001). *Turicella otitidis* mastoiditis in a healthy child. *Pediatr. Infect. Dis. J.* 20, 84–85. doi: 10.1097/00006454-200101000-00020

Davidoss, N. H., Varsak, Y. K., and Santa Maria, P. L. (2018). Animal Models of Acute Otitis Media – A Review with Practical Implications for Laboratory Research. *Eur. Ann. Otorhinolaryngol. Head Neck Dis.* 135, 183–190. doi: 10.1016/j.anorl.2017.06.013

De Baere, T., Vaneechoutte, M., Deschaght, P., Huyghe, J., and Dhooge, I. (2010). The prevalence of middle ear pathogens in the outer ear canal and the nasopharyngeal cavity of healthy young adults. *Clin. Microbiol. Infect.* 16, 1031–1035. doi: 10.1111/j.1469-0691.2009.02928.x

de Miguel Martínez, I., and Ramos Macías, Á. (2008). Serous otitis media in children: implication of *Alloiococcus otitidis*. *Otol. Neurotol.* 29, 526–530. doi: 10.1097/MAO.0b013e318170b5f8

Durmaz, R., Ozerol, I. H., Kalcioglu, M. T., Oncel, S., Otlu, B., Direkel, S., et al. (2002). Detection of *Alloiococcus otitidis* in the nasopharynx and in the outer ear canal. *New Microbiol.* 25, 265–268. Available online at: www.researchgate.net/publication/11351598_Detection_of_Alloiococcus_otitidis_in_the_nasopharynx_and_in_the_outer_ear_canal

Faden, H., and Dryja, D. (1989). Recovery of a unique bacterial organism in human middle ear fluid and its possible role in chronic otitis media. *J. Clin. Microbiol.* 27, 2488–2491. doi: 10.1128/JCM.27.11.2488-2491.1989

Frank, D. N., Spiegelman, G. B., Davis, W., Wagner, E., Lyons, E., and Pace, N. R. (2003). Culture-independent molecular analysis of microbial constituents of the healthy human outer ear. *J. Clin. Microbiol.* 41, 295–303. doi: 10.1128/JCM.41.1.295-303.2003

Funke, G., Pfyffer, G. E., and von Graevenitz, A. (1993). A hitherto undescribed coryneform bacterium isolated from patients with otitis media. *Med. Microbiol. Lett.* 2, 183–190.

Funke, G., Pünter, V., and von Graevenitz, A. (1996). Antimicrobial susceptibility patterns of some recently established coryneform bacteria. *Antimicrob. Agents Chemother.* 40, 2874–2878. doi: 10.1128/AAC.40.12.2874

Funke, G., Stubbs, S., Altwegg, M., Carlotti, A., and Collins, M. D. (1994). *Turicella otitidis* gen. nov., sp. nov., a coryneform bacterium isolated from patients with otitis media. *Int. J. Syst. Bacteriol.* 44, 270–273. doi: 10.1099/00207713-44-2-270

Garibpour, F., Khoramrooz, S. S., Mirsalehian, A., Emaneini, M., Jabalameli, F., Darban-Sarokhalil, D., et al. (2013). Isolation and detection of *Alloiococcus otitidis* in children with otitis media with effusion using culture and PCR methods. *J Mazandaran Univ Med Sci.* 23, 52–60. Available online at: http://jmums.mazums.ac.ir/browse.php?a_id=2175&sid=1&slc_lang=en

Gómez-Garcés, J. L., Alhambra, A., Alos, J. I., Barrera, B., and García, G. (2004). Acute and chronic otitis media and *Turicella otitidis*: a controversial association. *Clin. Microbiol. Infect.* 10, 854–857. doi: 10.1111/j.1198-743X.2004.00965.x

Gómez-Garcés, J. L., Alos, J. I., and Tamayo, J. (2007). In vitro activity of linezolid and 12 other antimicrobials against coryneform bacteria. *Int. J. Antimicrob. Agents* 29, 688–692. doi: 10.1016/j.ijantimicag.2006.11.032

Gómez-Hernando, C., Toro, C., Gutiérrez, M., Enríquez, A., and Baquero, M. (1999). Isolation of *Alloiococcus otitidis* from the external ear in children. *EJCMID* 18, 69–70. doi: 10.1007/s100960050230

Goodfellow, M., Kämpfer, P., Busse, H. J., Trujillo, M. E., Suzuki, K., Ludwig, W., et al. (eds.). (2012). *Bergey's Manual of Systematic Bacteriology: Volume 5: The Actinobacteria*. New York, NY: Springer New York. doi: 10.1007/978-0-387-68233-4

Greninger, A. L., Kozyreva, V., Truong, C.-L., Graves, M., and Chaturvedi, V. (2015). Draft genome sequence of *Turicella otitidis* TD1, isolated from a patient with bacteremia. *Genome Announc.* 3:e01060-15. doi: 10.1128/genomeA.01060-15

Guler, A., Sahin, M. A., Yesil, F. G., Yildizoglu, U., Demirkol, S., and Arslan, M. (2015). Chronic otitis media resulting in aortic valve replacement: a case report. *J. Tehran Univ Heart Center* 10:98.

Güvenç, M. G., Midilli, K., Inci, E., Kuşkucu, M., and Tahamiler, R., Özergil, E., et al. (2010). Lack of Chlamydophila pneumoniae and predominance of *Alloiococcus otitidis* in middle ear fluids of children with otitis media with effusion. *Auris Nasus Larynx* 37, 269–273. doi: 10.1016/j.anl.2009.09.002

Hall-Stoodley, L., Hu, F. Z., Gieseke, A., Nistico, L., Nguyen, D., Hayes, J., et al. (2006). Direct detection of bacterial biofilms on the middle-ear mucosa of children with chronic otitis media. *JAMA* 296, 202–211. doi: 10.1001/jama.296.2.202

Harimaya, A., Fujii, N., and Himi, T. (2009). Preliminary study of proinflammatory cytokines and chemokines in the middle ear of acute otitis media due to *Alloiococcus otitidis*. *Int. J. Pediatr. Otorhinolaryngol.* 73, 677–680. doi: 10.1016/j.ijporl.2008.12.033

Harimaya, A., Himi, T., Fujii, N., Tarkkanen, J., Carlson, P., Ylikoski, J., et al. (2005). Induction of CD69 expression and Th1 cytokines release from human peripheral blood lymphocytes after in vitro stimulation with *Alloiococcus otitidis* and three middle ear pathogens. *FEMS Immunol. Med. Microbiol.* 43, 385–392. doi: 10.1016/j.femsim.2004.10.014

Harimaya, A., Koizumi, J.-I., Fujii, N., and Himi, T. (2007a). Interleukin-8 induction via NF-κB, p38 mitogen-activated protein kinase and extracellular signal-regulated kinase1/2 pathways in human peripheral blood mononuclear cells by *Alloiococcus otitidis*. *Int. J. Pediatric Otorhinolaryngol.* 71, 1465–1470. doi: 10.1016/j.ijporl.2007.06.003

Harimaya, A., Takada, R., Hendolin, P. H., Fujii, N., Ylikoski, J., and Himi, T. (2006a). High incidence of *Alloiococcus otitidis* in children with otitis media, despite treatment with antibiotics. *J. Clin. Microbiol.* 44, 946–949. doi: 10.1128/JCM.44.3.946-949.2006

Harimaya, A., Takada, R., Himi, T., Yokota, S., and Fujii, N. (2007b). Evidence of local antibody response against *Alloiococcus otitidis* in the middle ear cavity of children with otitis media. *FEMS Immunol. Med. Microbiol.* 49, 41–45. doi: 10.1111/j.1574-695X.2006.00166.x

Harimaya, A., Takada, R., Somekawa, Y., Fujii, N., and Himi, T. (2006b). High frequency of *Alloiococcus otitidis* in the nasopharynx and in the middle ear cavity of otitis-prone children. *Int. J. Pediatric Otorhinolaryngol.* 70, 1009–1014. doi: 10.1016/j.ijporl.2005.10.012

Hendolin, P. H., Kärkkäinen, U., Himi, T., Markkanen, A., and Ylikoski, J. (1999). High incidence of *Alloiococcus otitis* in otitis media with effusion. *Pediatr. Infect. Dis. J.* 18, 860–865. doi: 10.1097/00006454-199910000-00005

Hendolin, P. H., Markkanen, A., Ylikoski, J., and Wahlfors, J. J. (1997). Use of multiplex PCR for simultaneous detection of four bacterial species in middle ear effusions. *J. Clin. Microbiol.* 35, 2854–2858. doi: 10.1128/JCM.35.11.2854-2858.1997

Hendolin, P. H., Paulin, L., and Ylikoski, J. (2000). Clinically applicable multiplex PCR for four middle ear pathogens. *J. Clin. Microbiol.* 38, 125–132. Available online at: https://jcm.asm.org/content/38/1/125

Himi, T., Kita, H., Mitsuzawa, H., Harimaya, A., Tarkkanen, J., Hendolin, P., et al. (2000). Effect of *Alloiococcus otitidis* and three pathogens of otitis media in production of interleukin-12 by human monocyte cell line. *FEMS Immunol. Med. Microbiol.* 29, 101–106. doi: 10.1111/j.1574-695X.2000.tb01511.x

Holder, R. C., Kirse, D. J., Evans, A. K., Peters, T. R., Poehling, K. A., Swords, W. E., et al. (2012). One third of middle ear effusions from children undergoing tympanostomy tube placement had multiple bacterial pathogens. *BMC Pediatr.* 12:87. doi: 10.1186/1471-2431-12-87

Holder, R. C., Kirse, D. J., Evans, A. K., Whigham, A. S., Peters, T. R., Poehling, K. A., et al. (2015). Otopathogens detected in middle ear fluid obtained during tympanostomy tube insertion: contrasting purulent and non-purulent effusions. *PLoS ONE* 10:e0128606. doi: 10.1371/journal.pone.0128606

Holzmann, D., Funke, G., Linder, T., and Nadal, D. (2002). *Turicella otitidis* and *Corynebacterium auris* do not cause otitis media with effusion in children. *Pediatr. Infect. Dis J* 21, 1124–1126. doi: 10.1097/00006454-200212000-00007

Janapatla, R. P., Chang, H. J., Hsu, M. H., Hsieh, Y. C., Lin, T. Y., and Chiu, C. H. (2011). Nasopharyngeal carriage of Streptococcus pneumoniae, *Haemophilus influenzae*, *Moraxella catarrhalis*, and *Alloiococcus otitidis* in young children in the era of pneumococcal immunization, Taiwan. *Scand. J. Infect. Dis.* 43, 937–942. doi: 10.3109/00365548.2011.601754

Jervis-Bardy, J., Rogers, G. B., Morris, P. S., Smith-Vaughan, H. C., Nosworthy, E., Leong, L. E. X., et al. (2015). The microbiome of otitis media with effusion in Indigenous Australian children. *Int. J. Pediatr. Otorhinolaryngol.* 79, 1548–1555. doi: 10.1016/j.ijporl.2015.07.013

Johnston, J., Hoggard, M., Biswas, K., Astudillo-García, C., Radcliff, F. J., Mahadevan, M., et al. (2019). Pathogen reservoir hypothesis investigated by analyses of the adenotonsillar and middle ear microbiota. *Int. J. Pediatr. Otorhinolaryngol.* 118, 103–109. doi: 10.1016/j.ijporl.2018.12.030

Kalcioglu, M. T., Oncel, S., Durmaz, R., Otlu, B., Miman, M. C., and Ozturan, O. (2002). Bacterial etiology of otitis media with effusion; focusing on the high positivity of *Alloiococcus otitidis*. *New Microbiol.* 25, 31–35.

Kaur, R., Adlowitz, D. G., Casey, J. R., Zeng, M., and Pichichero, M. E. (2010). Simultaneous assay for four bacterial species including *Alloiococcus otitidis* using multiplex-PCR in children with culture negative acute otitis media. *Pediatr. Infect. Dis. J.* 29, 741–745. doi: 10.1097/INF.0b013e3181d9e639

Khoramrooz, S. S., Mirsalehian, A., Emaneini, M., Jabalameli, F., Aligholi, M., Saedi, B., et al. (2012). Frequency of *Alloicoccus otitidis*, *Streptococcus pneumoniae*, *Moraxella catarrhalis* and *Haemophilus influenzae* in children with otitis media with effusion (OME) in Iranian patients. *Auris Nasus Larynx* 39, 369–373. doi: 10.1016/j.anl.2011.07.002

Kita, H., Himi, T., Fujii, N., and Ylikoski, J. (2000). Interleukin-8 secretion of human epithelial and monocytic cell lines induced by middle ear pathogens. *Microbiol. Immunol.* 44, 511–517. doi: 10.1111/j.1348-0421.2000.tb02526.x

Kong, K., and Coates, H. L. C. (2009). Natural history, definitions, risk factors and burden of otitis media. *Med. J. Aust.* 191, S39–S43. doi: 10.5694/j.1326-5377.2009.tb02925.x

Krueger, A., Val, S., Pérez-losada, M., Panchapakesan, K., Devaney, J., Duah, V., et al. (2017). Relationship of the middle ear effusion microbiome to secretory mucin production in pediatric patients with chronic otitis media. *Pediatr. Infect. Dis. J.* 36, 635–640. doi: 10.1097/INF.0000000000001493

Lal, D., Keim, P., Delisle, J., Barker, B., Rank, M. A., Chia, N., et al. (2017). Mapping and comparing bacterial microbiota in the sinonasal cavity of healthy, allergic rhinitis, and chronic rhinosinusitis subjects. *Int. Forum Allergy Rhinol.* 7, 561–569. doi: 10.1002/alr.21934

Lappan, R., Imbrogno, K., Sikazwe, C., Anderson, D., Mok, D., Coates, H., et al. (2018). A microbiome case-control study of recurrent acute otitis media identified potentially protective bacterial genera. *BMC Microbiol.* 18:13. doi: 10.1186/s12866-018-1154-3

Laufer, A. S., Metlay, J. P., Gent, J. F., Fennie, K. P., Kong, Y., and Pettigrew, M. M. (2011). Microbial communities of the upper respiratory tract and otitis media in children. *mBio* 2, e00245–e00210. doi: 10.1128/mBio.00245-10

Leskinen, K., Hendolin, P., Virolainen-Julkunen, A., Ylikoski, J., and Jero, J. (2002). The clinical role of *Alloiococcus otitidis* in otitis media with effusion. *Int. J. Pediatr. Otorhinolaryngol.* 66, 41–48. doi: 10.1016/S0165-5876(02)00186-6

Leskinen, K., Hendolin, P., Virolainen-Julkunen, A., Ylikoski, J., and Jero, J. (2004). *Alloiococcus otitidis* in acute otitis media. *Int. J. Pediatr. Otorhinolaryngol.* 68, 51–56. doi: 10.1016/j.ijporl.2003.09.005

Loïez, C., Wallet, F., Fruchart, A., Husson, M.-O., and Courcol, R. J. (2002). *Turicella otitidis* in a bacteremic child with acute lymphoblastic leukemia. *Clin. Microbiol. Infect.* 8, 758–759. doi: 10.1046/j.1469-0691.2002.00474.x

Marchino, T., Vela, J. I., Bassaganyas, F., Sánchez, S., and Buil, J. A. (2013). Acute-onset endophthalmitis caused by *Alloiococcus otitidis* following a dexamethasone intravitreal implant. *COP* 4, 37–41. doi: 10.1159/000348809

Marsh, R. L., Binks, M. J., Beissbarth, J., Christensen, P., Morris, P. S., Leach, A. J., et al. (2012). Quantitative PCR of ear discharge from Indigenous Australian children with acute otitis media with perforation supports a role for *Alloiococcus otitidis* as a secondary pathogen. *BMC Ear Nose Throat Disord.* 12:11. doi: 10.1186/1472-6815-12-11

Matsuo, J., Yamaguchi, H., Harimaya, A., Fukumoto, T., Nakamura, S., Yoshida, M., et al. (2011). Impact of anaerobic and oligotrophic conditions on survival of *Alloiococcus otitidis*, implicated as a cause of otitis media. *J. Infect. Chemother.* 17, 478–482. doi: 10.1007/s10156-010-0199-5

Minami, S. B., Mutai, H., Suzuki, T., Horii, A., Oishi, N., Wasano, K., et al. (2017). Microbiomes of the normal middle ear and ears with chronic otitis media. *Laryngoscope* 127, E371–E377. doi: 10.1002/lary.26579

Neeff, M., Biswas, K., Hoggard, M., Taylor, M. W., and Douglas, R. (2016). Molecular microbiological profile of chronic suppurative otitis media. *J. Clin. Microbiol.* 54, 2538–2546. doi: 10.1128/JCM.01068-16

Papp, Z., Elgabsi, H., and Tóth, L. (2016). MALDI-TOF mass spectrometry reveals a highly complex bacterial profile of otitis media with effusion. *Int. J. Pediatr. Otorhinolaryngol.* 86, 189–192. doi: 10.1016/j.ijporl.2016.05.004

Pereira, M. B. R., Cantarelli, V., Pereira, D. R. R., and da Costa, S. S. (2004). High incidence of *Alloiococcus otitidis* in otitis media with effusion measured by multiplex PCR. *Braz. J. Otorhinolaryngol.* 70, 217–224. doi: 10.1590/S0034-72992004000200012

Pettigrew, M. M., Laufer, A. S., Gent, J. F., Kong, Y., Fennie, K. P., and Metlay, J. P. (2012). Upper respiratory tract microbial communities, acute otitis media pathogens, and antibiotic use in healthy and sick children. *Appl. Environ. Microbiol.* 78, 6262–6270. doi: 10.1128/AEM.01051-12

Pickering, J. L., Prosser, A., Corscadden, K. J., de Gier, C., Richmond, P. C., Zhang, G., et al. (2016). *Haemophilus haemolyticus* interaction with host cells is different to nontypeable *Haemophilus influenzae* and prevents NTHi association with epithelial cells. *Front. Cell Infect. Microbiol.* 6:50. doi: 10.3389/fcimb.2016.00050

Renaud, F. N., Grégory, A., Barreau, C., Aubel, D., and Freney, J. (1996). Identification of *Turicella otitidis* isolated from a patient with otorrhea associated with surgery: differentiation from *Corynebacterium afermentans* and *Corynebacterium auris*. *J. Clin. Microbiol.* 34, 2625–2627. doi: 10.1128/JCM.34.10.2625-2627.1996

Reynolds, S. J., Behr, M., and McDonald, J. (2001). *Turicella otitidis* as an unusual agent causing a posterior auricular abscess. *J. Clin. Microbiol.* 39, 1672–1673. doi: 10.1128/JCM.39.4.1672-1673.2001

Santos-Cortez, R. L. P., Hutchinson, D. S., Ajami, N. J., Reyes-Quintos, M. R. T., Tantoco, M. L. C., Labra, P. J., et al. (2016). Middle ear microbiome differences in indigenous Filipinos with chronic otitis media due to a duplication in the A2ML1 gene. *Infect. Dis. Poverty* 5:97. doi: 10.1186/s40249-016-0189-7

Sheikh, A. F., Saki, N., Roointan, M., Ranjbar, R., Yadyad, M. J., Kaydani, A., et al. (2015). Identification of *Alloiococcus otitidis*, *Streptococcus pneumoniae*, *Moraxella catarrhalis* and *Haemophilus influenzae* in children with otitis media with effusion. *Jundishapur J. Microbiol.* 8:e17985. doi: 10.5812/jjm.17985

Sillanpää, S., Kramna, L., Oikarinen, S., Sipilä, M., Rautiainen, M., Aittoniemi, J., et al. (2017). Next-generation sequencing combined with specific PCR assays to determine the bacterial 16S rRNA gene profiles of middle ear fluid collected from children with acute otitis media. *mSphere* 2:e00006–17. doi: 10.1128/mSphere.00006-17

Sillanpää, S., Oikarinen, S., Sipilä, M., Kramna, L., Rautiainen, M., Huhtala, H., et al. (2016). *Moraxella catarrhalis* might be more common than expected in acute otitis media in young finnish children. *J. Clin. Microbiol.* 54, 2373–2379. doi: 10.1128/JCM.01146-16

Simonet, M., De Briel, D., Boucot, I., Minck, R., and Veron, M. (1993). Coryneform bacteria isolated from middle ear fluid. *J. Clin. Microbiol.* 31, 1667–1668. doi: 10.1128/JCM.31.6.1667-1668.1993

Slinger, R., Duval, M., Langill, J., Bromwich, M., MacCormick, J., Chan, F., et al. (2016). Direct molecular detection of a broad range of bacterial and viral organisms and *Streptococcus pneumoniae* vaccine serotypes in children with otitis media with effusion. *BMC Res. Notes* 9:247. doi: 10.1186/s13104-016-2040-4

Stroman, D. W., Roland, P. S., Dohar, J., and Burt, W. (2001). Microbiology of normal external auditory canal. *Laryngoscope* 111, 2054–2059. doi: 10.1097/00005537-200111000-00035

Tano, K., Von Essen, R., Eriksson, P. O., and Sjöstedt, A. (2008). *Alloiococcus otitidis* - otitis media pathogen or normal bacterial flora? *APMIS* 116, 785–790. doi: 10.1111/j.1600-0463.2008.01003.x

Tarkkanen, J., Carlson, P., Himi, T., Ylikoski, J., Atshushi, H., and Mattila, P. S. (2000). Stimulation of adenoidal lymphocytes by *Alloiococcus otitidis*. *Ann. Otol. Rhinol. Laryngol.* 109, 958–964. doi: 10.1177/000348940010901010

Taylor, P. S., Faeth, I., Marks, M. K., Del Mar, C. B., Skull, S. A., Pezzullo, M. L., et al. (2009). Cost of treating otitis media in Australia. *Expert Rev. Pharmacoecon. Outcomes Res.* 9, 133–141. doi: 10.1586/erp.09.6

Teele, D. W., Klein, J. O., Rosner, B., and Greater Boston Otitis Media Study Group (1989). Epidemiology of otitis media during the first seven years of life in children in greater boston: a prospective, cohort study. *J. Infect. Dis.* 160, 83–94. doi: 10.1093/infdis/160.1.83

Teo, S. M., Mok, D., Pham, K., Kusel, M., Serralha, M., Troy, N., et al. (2015). The infant airway microbiome in health and disease impacts later asthma development. *Cell Host Microbe* 17, 704–715. doi: 10.1016/j.chom.2015.03.008

Thornton, R. B., Rigby, P. J., Wiertsema, S. P., Filion, P., Langlands, J., Coates, H. L., et al. (2011). Multi-species bacterial biofilm and intracellular infection in otitis media. *BMC Pediatr.* 11:94. doi: 10.1186/1471-2431-11-94

Troxler, R., Funke, G., Von Graevenitz, A., and Stock, I. (2001). Natural antibiotic susceptibility of recently established coryneform bacteria. *Eur. J. Clin. Microbiol. Infect. Dis.* 20, 315–323. doi: 10.1007/s100960100503

Val, S., Poley, M., Anna, K., Nino, G., Brown, K., Pérez-Losada, M., et al. (2018). Characterization of mucoid and serous middle ear effusions from patients with chronic otitis media: implication of different biological mechanisms? *Pediatr. Res.* 84, 296–305. doi: 10.1038/s41390-018-0060-6

Van Eldere, J., Slack, M. P. E., Ladhani, S., and Cripps, A. W. (2014). Non-typeable *Haemophilus influenzae*, an under-recognised pathogen. *Lancet Infect. Dis.* 14, 1281–1292. doi: 10.1016/S1473-3099(14)70734-0

Verduin, C. M., Hol, C., Fleer, A., Dijk, H., van, and Belkum, A., van (2002). *Moraxella catarrhalis*: from emerging to established pathogen. *Clin. Microbiol. Rev.* 15, 125–144. doi: 10.1128/CMR.15.1.125-144.2002

von Graevenitz, A. (1993). Revised nomenclature of *Alloiococcus otitis*. *J. Clin. Microbiol.* 31:472. doi: 10.1128/JCM.31.2.472-472.1993

von Graevenitz, A., and Funke, G. (2014). *Turicella otitidis* and *Corynebacterium auris*: 20 years on. *Infection* 42, 1–4. doi: 10.1007/s15010-013-0488-x

Vos, P., Garrity, G., Jones, D., Krieg, N. R., Ludwig, W., Rainey, F. A., et al. (2009). *Bergey's Manual of Systematic Bacteriology: Volume 3: The Firmicutes, 2nd Edn*. New York, NY: Springer Science & Business Media.

Westerberg, B. D., Kozak, F. K., Thomas, E. E., Blondel-Hill, E., Brunstein, J. D., and Patrick, D. M. (2009). Is the healthy middle ear a normally sterile site? *Otol. Neurotol.* 30, 174–177. doi: 10.1097/MAO.0b013e31819225a0

Wiertsema, S. P., Kirkham, L.-A. S., Corscadden, K. J., Mowe, E. N., Bowman, J. M., Jacoby, P., et al. (2011). Predominance of nontypeable *Haemophilus influenzae* in children with otitis media following introduction of a 3 + 0 pneumococcal conjugate vaccine schedule. *Vaccine* 29, 5163–5170. doi: 10.1016/j.vaccine.2011.05.035

Conflict of Interest: The authors declare that the research was conducted in the absence of any commercial or financial relationships that could be construed as a potential conflict of interest.

frontiers in Genetics

ORIGINAL RESEARCH
published: 21 February 2020
doi: 10.3389/fgene.2019.01327

Transcript Analysis Reveals a Hypoxic Inflammatory Environment in Human Chronic Otitis Media With Effusion

Mahmood F. Bhutta[1], Jane Lambie[2], Lindsey Hobson[3], Debbie Williams[4], Hayley E. Tyrer[5], George Nicholson[6], Steve D.M. Brown[4], Helen Brown[7], Chiara Piccinelli[8], Guillaume Devailly[9], James Ramsden[3] and Michael T. Cheeseman[8]*

[1] Department of ENT, Brighton & Sussex University Hospitals NHS Trust, Brighton, United Kingdom, [2] Nuffield Department of Surgical Sciences, University of Oxford, John Radcliffe Hospital, Oxford, United Kingdom, [3] Department of ENT, Oxford University Hospitals NHS Trust, John Radcliffe Hospital, Oxford, United Kingdom, [4] Mammalian Genetics Unit, MRC Harwell Institute, Harwell, United Kingdom, [5] Faculty of Health and Wellbeing, University of Lancashire, Preston, United Kingdom, [6] Department of Statistics, University of Oxford, Oxford, United Kingdom, [7] The Roslin Institute, University of Edinburgh, Midlothian, United Kingdom, [8] The Royal (Dick) School of Veterinary Studies, University of Edinburgh, Midlothian, United Kingdom, [9] GenPhySE, Université de Toulouse, INRA, ENVT, Castanet Tolosan, France

OPEN ACCESS

Edited by:
Allen Frederic Ryan, University of California, San Diego, United States

Reviewed by:
Diego Preciado, Children's National Health System, United States
Theodora Katsila, National Hellenic Research Foundation, Greece

***Correspondence:**
Mahmood F. Bhutta
m.bhutta@nhs.net

Specialty section:
This article was submitted to Genetic Disorders, a section of the journal Frontiers in Genetics

Received: *21 July 2019*
Accepted: *05 December 2020*
Published: *21 February 2020*

Citation:
Bhutta MF, Lambie J, Hobson L, Williams D, Tyrer HE, Nicholson G, Brown SDM, Brown H, Piccinelli C, Devailly G, Ramsden J and Cheeseman MT (2020) Transcript Analysis Reveals a Hypoxic Inflammatory Environment in Human Chronic Otitis Media With Effusion. Front. Genet. 10:1327. doi: 10.3389/fgene.2019.01327

Chronic otitis media with effusion (COME) is the most common cause of childhood hearing loss in the developed world. Underlying pathophysiology is not well understood, and in particular the factors that lead to the transition from acute to chronic inflammation. Here we present the first genome-wide transcript analysis of white blood cells in the effusion of children with COME. Analysis of microarray data for enriched pathways reveals upregulation of hypoxia pathways, which is confirmed using real-time PCR and determining VEGF protein titres. Other pathways upregulated in both mucoid and serous effusions include Toll-like receptor signaling, complement, and RANK-RANKL. Cytology reveals neutrophils and macrophages predominated in both serous and mucoid effusions, however, serous samples had higher lymphocyte and eosinophil differential counts, while mucoid samples had higher neutrophil differential counts. Transcript analysis indicates serous fluids have CD4+ and CD8+ T-lymphocyte, and NK cell signatures. Overall, our findings suggest that inflammation and hypoxia pathways are important in the pathology of COME, and targets for potential therapeutic intervention, and that mucoid and serous COME may represent different immunological responses.

Keywords: otitis media, effusion, transcript, inflammation, hypoxia

INTRODUCTION

Otitis media with effusion (OME) or "glue ear" is the most common cause of hearing loss in children in a developed world environment. The disease is characterized by an inflammatory effusion that prevents transmission of sound through the middle ear space, and if chronic (chronic OME, COME) is associated with potential effects on language acquisition and learning.

The pathophysiology underlying OME is not fully understood. It often follows an episode of acute otitis media (AOM), where ascent of bacteria from the nasopharynx leads to a purulent effusion in the middle ear. As this purulent effusion resolves, the serous or mucoid effusion of OME replaces it. The effusion of OME is usually short-lived, but in a minority of cases the effusion persists as COME (defined as OME of duration >3 months). COME affects 5–6% of all children in their second year of life (Bhutta, 2014), and if associated with hearing disability may be treated with the surgical insertion of grommets (ventilation tubes) which eliminate the effusion.

Data from mouse models demonstrate differing expression of cytokines in the middle ear, and differing involvement of leucocytes and epithelial cells, through the onset, development, and resolution of an episode of AOM (Hernandez et al., 2015). Expression of inflammation-associated genes has also been found in peripheral blood mononuclear cells in children with AOM (Liu et al., 2012; Liu et al., 2013). However, the molecular events that may be pivotal in the transition from acute to chronic inflammation in the middle ear are not known (Bhutta et al., 2017). The high heritability of time with middle ear effusion (Casselbrant et al., 1999) suggests that host response is relevant.

This question is important. Unlike some chronic inflammatory disorders, chronic otitis media can and usually does improve in later life (Caye-Thomasen et al., 2008). In addition COME is sometimes a risk factor for more serious ear disorders such as cholesteatoma (Jennings et al., 2017). An understanding of what causes chronic inflammation in the middle ear could therefore allow us not only to understand what causes disease but could also highlight potential molecular targets to affect earlier and more reliable resolution. To date molecular analysis of the effusion in COME has been fragmentary.

Proteomic analysis of effusions from children undergoing grommet surgery shows abundance of innate immunity products of neutrophil leukocytes, neutrophil extracellular traps (NETs), epithelial/glandular anti-microbial proteins (such as BPIFB1, also known as LPLUNC and BPIFA1, also known as SPLUNC) and mucins such as MUC5B (Val et al., 2016). Cytokine analysis reveals a wide spectrum of pro-inflammatory cytokines, among which is IL-8 the neutrophil leukocyte chemotaxic protein (Matkovic et al., 2007; Val et al., 2016). Hypoxia signaling pathway members such as vascular endothelial growth factor (VEGF) protein and mRNA are also present in the effusion and middle ear mucosa (Jung et al., 1999; Sekiyama et al., 2011; Val et al., 2016; Val et al., 2018).

The effusion in younger patients with COME is predominantly mucoid rather than serous (Duah et al., 2016). There are microbiome difference between mucoid and serous effusions (Krueger et al., 2017), and proteomic analysis reveals a higher content of MUC5B in mucoid effusions, as well as DNA (Val et al., 2018). Mucoid effusions also have a global tendency to increased pro-inflammatory mediators, but serous effusions have greater acute phase proteins IL-1b and IL-10, suggestive of a differing immunological response (Val et al., 2018).

In this study we perform the first whole genome transcript analysis of white blood cell (wbc) gene expression from effusions in children with COME. We compare samples with peripheral venous blood as a baseline, and then make comparisons of serous versus mucoid effusions. We also examine the cytology of such effusions.

We report that microarray analysis of effusions showed upregulation of hypoxia signaling, response to hypoxia, Toll-Like Receptor signaling, the complement and the RANK-RANKL pathways. RTqPCR showed upregulation of hypoxia signaling genes and VEGF protein titres were elevated. Mucoid and serous effusions had different cytological profiles that parallel differences in T-lymphocyte, NK cell and myeloid cell signatures in the microarray analysis.

MATERIALS AND METHODS

Ethics Statement

This study was approved by Oxfordshire Research Committee C (reference 11/SC/0057). Informed consent was obtained from the child's guardian for the collection, retention and analysis of samples. All patient records and associated metadata (age, racial ethnicity, duration of disease, vaccination history, antibiotic use, previous grommet surgery, and occurrence of atopy) were anonymized.

Chronic OME Phenotypes

Children with COME were diagnosed using standard clinical and audiological tests that met the UK National Institute for Health and Care Excellence guidelines for surgical management of glue ear (http://publications.nice.org.uk/ifp60). Clinical samples were collected under general anesthesia from children undergoing grommet (ventilation tube) insertion. Syndromic children were excluded. No children had been given glucocorticoid steroids or antibiotics in the three months prior to surgery.

Sample Collection

A 3.5 ml venous blood sample was collected from the hand vein using a BD vacutainer and 1ml transferred to a lithium heparin tube (Kabe LaborTechnik GmbH) for plasma sample preparation and 2.5 ml Intracellular RNA from blood was isolated with PAXgene Blood RNA kit (PreAnalytiX, Qiagen) following manufacturer's instructions.

Individual COME fluid samples from each middle ear were collected through a myringotomy using a Juhn Tym-Tap® aspirator/collector device (Medtronic). The surgeon evaluated the gross appearance and viscosity of the effusion at time of surgery and characterized the aspirate as serous, mucoid or intermediate, and noted whether or not the sample was blood-stained.

A cytology preparation was made (see below) and the remainder was snap frozen on dry ice and stored at −70°C.

Glue Ear Cytology

Forty-eight cytology smears were made from 30 children (one ear sample per child), and 9 children (samples from both ears). Material adherent to the aspirator tube was used to make a cytology smear on a glass slide. These were methanol fixed and Giemsa stained and graded for mucus; red blood cells, and overall cellularity, white blood cell differential performed on 200 cells; leukocyte morphology; presence of bacteria and epithelial cells. The criteria

used for grading the samples are given in **Table S1**. The patient ID and effusion phenotype was blinded for evaluation.

Mixed models were used to compare the leukocyte proportions between the mucoid categories (serous, intermediate and mucoid treated as ordinal). Patients were fitted as random effects and mucoid category as a fixed effect. These models take into account any correlation occurring between measurements taken from the ears of the same children. Each type of leucocyte (i.e. lymphocytes, neutrophils, etc.) was analyzed using a separate mixed model. Mixed models with the same structure were used to compare leukocyte measurements between other categories (e.g. bloody ear, first grommet, and demographic characteristics).

Cell cytological characteristics (macrophage vacuolation, macrophage erythrophagocytosis) were analyzed using mixed ordinal regression models. Again patient effects were fitted as random to allow for any correlation between the results from ears of the same children. Generalized linear mixed models (GLMMs) were used to examine associations between binary outcomes (e.g. bloody ear) and other characteristics. In situations where data were very sparse and the model did not converge, then a Fisher's exact test was used. However, this takes no account of the potential correlation between data from the ears from same children.

RNA Isolation

Intracellular RNA from blood was isolated with PAXgene Blood RNA kit (PreAnalytiX, Qiagen) following manufacturer's instructions and its quality was assessed using a bioanalyzer (Agilent Tecnologies).

RNA from middle ear effusions was extracted using the NucleoSpin® kit (Macherey-Nagel) following manufacturer's instructions. Due to the large volume of some effusions the initial volume of lysis buffer and β-mercaptoethanol was increased to 1 ml and the sample run through the tube through several rounds of centrifugation. Due to the larger sample volumes at this initial stage, flow-through was collected in 15 ml tubes.

cDNA Synthesis

cDNA was generated following manufacturer's instructions using a high capacity cDNA reverse transcriptase kit containing MultiScribe™ Reverse Transcriptase (Applied Biosystems). Samples were either used immediately in RT-qPCR reactions or stored long term at −80°C.

Transcriptional Profiling

Transcriptome analysis was performed on 6 serous COME effusions from six children and 6 mucoid effusions from five children (samples from both ears in one child), and their matching 11 blood samples. Transcriptional profiling was performed on an Affymetrix GeneChip® Human Gene 2.0 ST Array platform. The selection of samples was based on the quantity and quality of the RNA sample judged by RNA integrity number (RIN). In the first experiment 6 mucoid samples (RIN 6.1-7.2) and corresponding patient blood samples were analyzed. In the second 6 serous samples (RIN 6.4-7.7) and corresponding blood sample. Two of the serous ear samples came from the right and left ear of the same child. Corresponding blood samples from these patients RIN scores ranged from 8.1–9.1

Microarray Analysis

CEL files were processed and normalized using AromaAffymetrix (https://statistics.berkeley.edu/tech-reports/745) and a chip definition file provided by Brainarray (Dai et al., 2005). Differentially expressed genes were found using limma (Ritchie et al., 2015) with an adjusted *P*-value cut-off of 0.01 and a minimal difference of a factor 2 (ie absolute value of the log2 of the fold change equal or greater than 1). Unique HUGO identifier of differentially expressed genes were passed to the Enrichr web application (Kuleshov et al., 2016) for functional enrichment analysis. The data discussed in this publication (including raw and processed files, expression values for each gene in each sample, and fold change and adjusted *P*-value for each gene in the three comparisons: mucoid vs blood, serous vs blood, mucoid vs serous) have been deposited in NCBI's Gene Expression Omnibus [46] and are accessible through GEO Series accession number GSE125532 (https://www.ncbi.nlm.nih.gov/geo/query/acc.cgi?acc=GSE125532).

R code used to perform the analysis and produce the plot is available through a GitHub repository: https://github.com/gdevailly/oitis_array_analysis.

RT-qPCR

Thirty-two RNA extracts were made from wbcs in COME effusion (one ear sample per child) and matching blood samples were analyzed RNA from both blood and middle ear effusion were run on custom designed 96-well TaqMan Fast array plates (Applied Biosystems) following manufacturer's instructions. There were 32 patient samples (2/32 serous, 2/32 intermediate, 2 non-classified and 26/32 mucoid) with RNA RIN scores ranging from 2.3 to 7.7; corresponding blood samples from these patients had RIN scores ranging from 7.9 to 9.0. RT-qPCR data was analyzed by ΔΔCt method. The efficiency of the assays was ensured by the use of inventory TaqMan assays.

Selection of Appropriate Control Genes

Our set of endogenous control genes was selected from: *ACTB, B2M, HPRT1, HRAS, NRAS, PPIA*, and *TBP*. Two criteria were applied: (A) there should be no evidence of differential expression between blood and exudate at any of the control genes used; and (B) the variance of the normalization factor (calculated from the set of selected control genes) should be small. To address criterion (A), a paired t-test (paired within participants) was applied at each gene to test for non-zero mean difference in Ct value between blood and exudate; all genes apart from *HPRT1, HRAS,* and *NRAS* were significantly differentially expressed between blood and exudate at the 5% level, and so all genes except these three were excluded from further consideration. Then, to fulfill criterion (B), the variance of the normalization factor was estimated for each subset of these three genes using the methodology described by Chervoneva et al., (2010).

Figures analogous to theirs led us to select an optimal subset comprising all three genes—*HPRT1, HRAS*, and *NRAS*. This subset provided a normalization factor with relatively low variance in each of our sub-experiments (plates and individual assays).

Statistical Analysis of RT-qPCR Data

Fold changes for each patient were calculated using DataAssist software v3.0 by comparing gene expression levels of middle ear fluid using a patient's own blood as a control. Statistical significance was established using a two tailed paired student t-test with *P*-values adjusted using the Benjamin-Hochberg false discovery rate.

VEGF Protein Assay

Thirty-seven COME effusion samples (one ear sample per child) and matching plasma samples were analyzed for VEGF. Tubes containing samples were weighed and blanked against an empty tube to estimate fluid volume. Depending on sample weight and viscosity the samples were diluted with 0.5, 1.0, 1.5, or 2.0 ml of PBS dispersed by vortexing for 1 min then pelleted at 3000 rpm for 10 min at 4°C. Supernatant COME effusion samples and corresponding patient serum samples were assayed for VEGF protein using MSD® MULTI-ARRAY® Human VEGF assay (Meso Scale Discovery). The COME effusions data was normalized to plasma volume by multiplying the COME assay value by its dilution (weight of glue and volume of PBS diluent). The assay read out is calibrated against standard curve and VEGF titres are in units of pg/ml.

VEGF titres in effusion and plasma titres were not normally distributed ($P \geq 0.01$; D'Agostino & Pearson omnibus normality tests) and were therefore analyzed with a Wilcoxon matched-pairs signed rank test. We performed a Spearman correlation analysis between patient age and COME VEGF titre. Data were graphed using Prism Graph Pad.

RESULTS

Patients and Patient Samples

The patient cohort consisted of children undergoing grommet surgery for COME. There were 12 girls age range 1.4–8.0 years of age (4.93 ± 0.57 mean ± SEM) and 40 boys age range 3.1–9.4 (5.36 ± 0.25). The average age of the girls and boys was not significantly different ($P = 0.50$; 2 tailed t-test with unequal variance).

Effusion samples were characterized as serous, mucoid or intermediate in consistency and whether or not blood-staining was present (see *Methods and Materials* for details). The frequency of unilateral glue ear was not significantly different in boys (8/40) and girls (2/12) ($P = 1.0$, Fisher exact). The frequencies of each sample category were not significantly different in boys (17/69 serous, 10/69 intermediate, 42/69 mucoid; 3 samples were too small to assess) and girls (3/22 serous, 1/22 intermediate, 18/22 mucoid; $P = 0.30$, Fisher Exact).

The volume and quality of COME samples varied and not all were suitable for analysis. We found it impractical to split COME effusion samples at the time of collection or subsequently in the lab, so contralateral ear samples from each child were used for either RNA or for protein analysis. Whole blood was collected into two tubes, one for RNA, a second for plasma.

The breakdown of samples used in each assay can be summarized as follows. Thirty-two matched pairs of COME effusion (one sample per child from either the right or left ear) and blood samples were analyzed by RTqPCR; 37 matched pairs of COME effusions samples (one ear sample per child) and plasma were analyzed for VEGF protein. Transcriptome analysis was performed on 6 serous COME effusions from six children and 6 mucoid effusions from five children (samples from both ears in one child), and their matching 11 blood samples. Forty-eight cytology smears were made from 30 children (one ear sample per child), and 9 children (samples from both ears).

Glue Ear Cytology

Forty-eight samples with mucoid n = 31, intermediate n = 8, and serous n = 9 gross appearance yielded good quality slide preparations for full cytological examination. Cytological categorization of mucus was graded as heavy, intermediate or low/absent which we hereafter refer to as mucoid, intermediate and serous. See **Table S1** for cytology grading classification.

COME samples showed varying degrees of cellularity and cellular composition, but leukocytes largely predominated in all samples and only occasional suspected epithelial cells were noted. Cellularity appeared slightly higher in mucoid samples (**Table S2**), however a more precise quantification (e.g. cell counts on the fluid) rather than the estimated grading from the smears would be needed to better investigate this finding. Neutrophils and macrophages predominated in all sample classes. However, serous samples had significantly higher lymphocyte and eosinophil differential counts, while mucoid samples had significantly higher neutrophil differential counts. Macrophage differentials did not differ significantly between serous, intermediate and mucoid samples (**Figure 1**). Occasional macrophages showing erythrophagocytosis were observed in low numbers of samples (12.5%); this may suggest that in those cases the presence of RBCs may not only be due to iatrogenic contamination during the sampling procedure, but minimal true hemorrhage may have occurred. Occasional columnar epithelial cells were observed in 14.6% of samples.

We explored associations for cytology features with patient metadata (age, racial ethnicity, duration of disease, vaccination history, antibiotic use, previous grommet surgery, occurrence of atopy). Blood stained effusions were associated with higher levels of lymphocytes, mucus and red blood cell count, and macrophage erythrophagocytosis was higher in serous than mucoid effusions. Male children had significantly more serous effusions as well as higher lymphocytes (**Table S2**). Additional analyses were performed with adjustment for blood-stained effusions and for gender, which confirmed the differences in leucocytes between mucoid and serous effusions were not confounded by these factors.

Other borderline significant associations which may warrant further investigation are listed in **Table S2**.

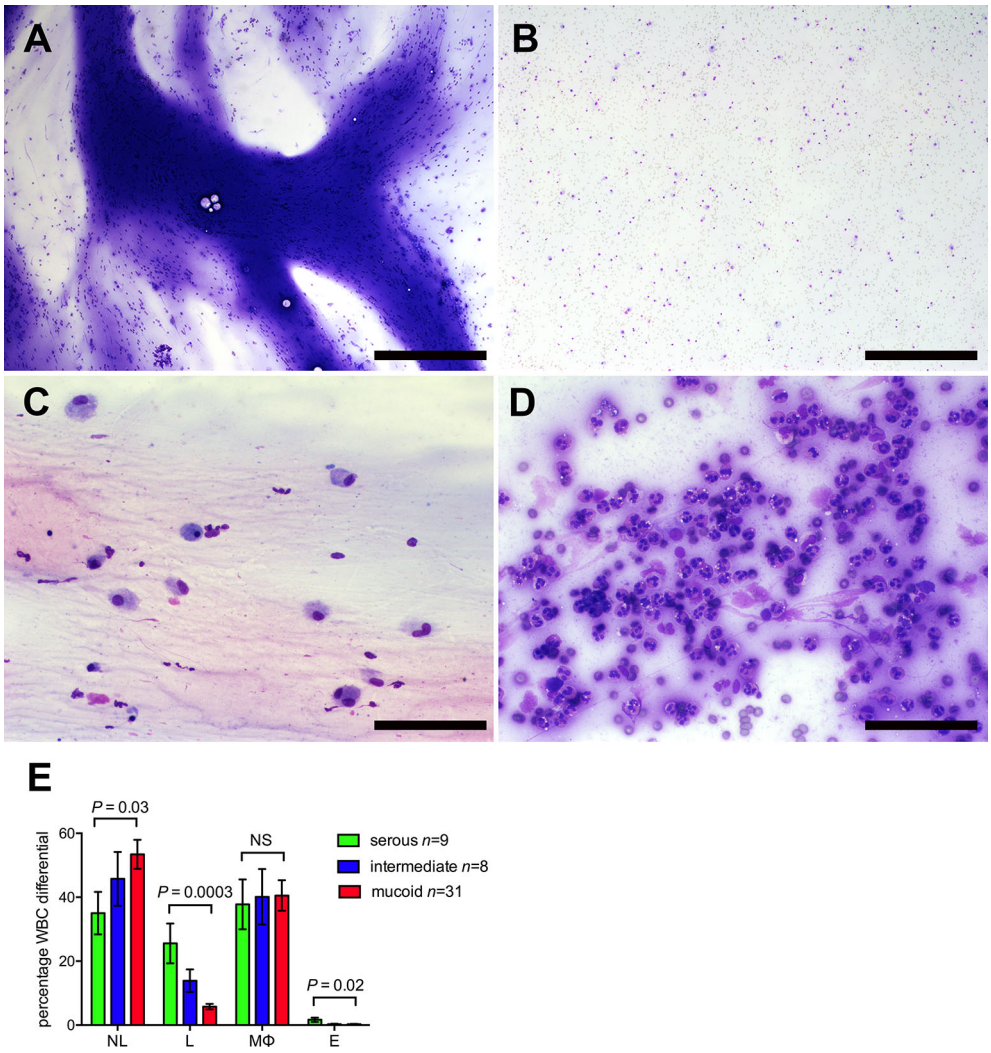

FIGURE 1 | Glue ear cytology. Examples of different cytological appearance of the glue ear samples graded on an ordinal scale 1–3 (See **Table S1** for cytology grading criteria). **(A)** Sample with high mucus score and moderate cellularity. **(B)** Sample with low mucus score and moderate cellularity. **(C)** Sample with low cellularity and high proportion of macrophages (75%) **(D)** Sample with high cellularity and high proportion of neutrophils (94%). May-Grünwald Giemsa stained direct smear preparations. Scale bars **(A, B)** 500 µm, **(C, D)** = 100 µm. **(E)** Cytology differentials for serous, intermediate and mucoid samples. Mixed statistical models were used to compare serous and mucoid samples (see Methods and Materials). NL, neutrophil leukocytes; L, lymphocytes; MØ, macrophages; NS, probability not significant P > 0.05.

Microarray Analysis

To gain a better understanding of gene expression profiles of mucoid and serous effusions we performed microarray analysis of wbc RNA extract from effusions with a high RNA yield: Transcriptome analysis was performed on 6 serous COME effusions from six children and 6 mucoid effusions from five children (samples from both ears in one child), and their matching 11 blood samples. We used the Affymetrix Human Gene 2.0 ST microarray, using annotations provided by BrainArray (Molecular and Behavioral Neuroscience Institute, University of Michigan) (Xuan et al., 2010). After data normalisation using AromaAffymetrix (http://aroma-project.org/), we performed a multidimensional scaling of the data (**Figure S1**).

Dimension 1 clearly discriminates blood from ear effusions, while dimension 2 discriminates the different ear effusions, notably but incompletely splitting mucoid from serous effusion. No association from pairs of effusion—wbc samples was detectable neither on dimension 1 nor on dimension 2. Thus we performed a differential gene expression analysis by comparing all mucoid effusion samples against all blood samples, all serous effusion samples against all blood samples, and all mucoid effusion samples against all serous effusion samples (**Figure 2**). As expected from the multidimensional scaling, more genes were differentially expressed between mucoid effusion and blood, and between serous effusion and blood, than between mucoid and serous effusions. Due to our experiment design, differences in

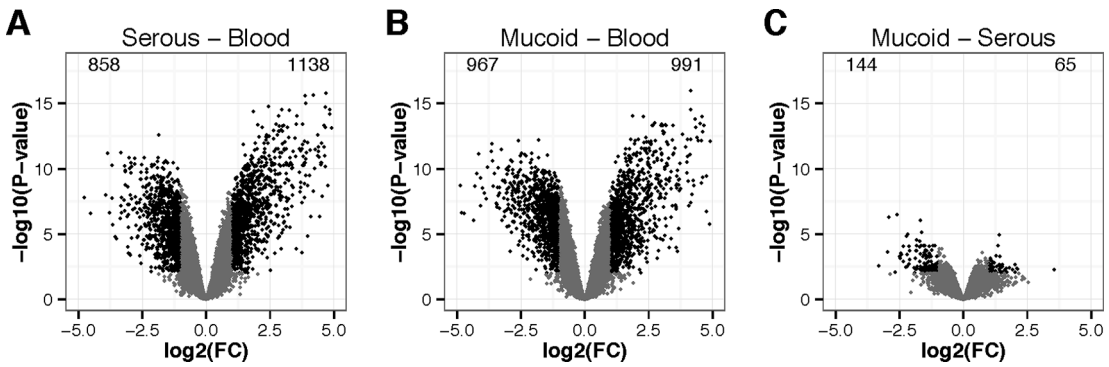

FIGURE 2 | Volcano plots of differentially expressed genes in wbcs. **(A)** middle ear serous effusion versus blood, **(B)** middle ear mucoid effusion versus blood, and **(C)** mucoid versus serous effusions. X-axis represent the log2 of the fold change (FC). Y-axis represents –log10 of the *P*-value of the difference. Black points represent genes with a fold change greater than 2 or lower than 0.5 and a *P*-value lower than 0.01.

gene expression may be the results of difference in wbc populations as well as difference in gene expression in one or several cell types.

Figure S2 represents a heatmap view of all differentially expressed genes identified from the microarrays, using as a threshold a minimum absolute log2 fold change (FC) of 1, and a maximal adjusted *P*-value of 0.01 (FDR correction for multiple testing). It shows that most of the differences observed in gene expression were shared in serous and mucoid effusion as compared to blood. **Table S4** presents limma gene expression data for mucoid COME effusion and blood; serous COME effusion and blood; and mucoid COME effusion and serous COME effusion. We note that there is differential expression of epithelial genes such as MUC5B that is significantly higher (adjusted value $P = 0.0354$) in mucoid versus serous COME samples, which we attribute as originating from the small numbers of columnar epithelial cells that are found in COME effusions.

Functional enrichment of the differentially expressed genes using Enrichr (Chen et al., 2013; Kuleshov et al., 2016) reveals characteristics of the effusion of COME patients (**Table 1**). It shows that the effusion is an inflammatory and hypoxic environment, enriched in CD33+ myeloid cells (granulocyte and macrophage lineages) and CD14+ monocyte cells. Its transcriptional signature overlaps those of RELA, SOX2, and MITF (amongst other) transcription factors.

Differences in gene expression were observed when comparing mucoid against serous effusion RNA extracts (**Table S3**). For example, IL1RN, SERPINE1 were more expressed in mucoid fluid, while CXCL9, CXCL10, CXCL11, CXCL12, CD3D, CD96, IL32, and APOBEC3G were significantly more expressed in serous fluids (**Table S4**). Functional enrichment of the differentially expressed genes using Enrichr reveals that serous fluid had a transcriptomic signature enriched in CD8+, CD4+, and CD56+_NK cells and had a stronger T cell signature whereas mucoid samples had borderline enrichment in myeloid cells and monocytes (**Table S3**).

RTqPCR Analysis Shows Upregulation of Hypoxia Signaling Pathways in COME Effusions

Thirty-two RNA wbc extracts were made from COME effusion (one ear sample per child) and matching blood samples were analyzed for 52 selected genes by RTqPCR. This confirmed significant upregulation of hypoxia signaling pathway genes including VEGF ligands (*VEGFA, VEGFB*) receptors (*KDR, FLT1*) adapter proteins (*NRP1, NRP2*), and HIF transcription factor (*HIF1A*) in COME relative to blood (**Figure S3**).

Overall there was reasonably good concordance between RTqPCR and microarray data as 22 over 27 (81%) of the differentially expressed genes according to the array were also differentially expressed according to RTqPCR experiment (*P*-value < 0.01, **Figure S3**). RTqPCR identified 14 additional genes differentially expressed in wbcs from COME effusion and blood that were not differentially expressed in our microarray analysis, suggesting that in our experimental design RTqPCR was more sensitive than microarrays, albeit with more variability.

VEGF Protein Is Elevated in COME Effusions

Thirty-seven COME effusion samples (one ear sample per child) and matching plasma samples were analyzed for VEGF.VEGF protein titer is elevated in COME fluid samples (mixed categories) (median 6,427 pg/ml, 95% CI 3,541–12,923) compared with plasma (median 69 pg/ml 95% CI 61–92; $P < 0.00010$ 2-tailed Wilcoxon matched pairs signed rank test, n=37 pairs). It confirms at the protein level the increase of VEGF expression as observed in both micro-array and RTqPCR data. There was a small and borderline statistically significant negative correlation between COME VEGF titre and increasing child age (Spearman r −0.3241, 95% CL −0.5930 to 0.009839, n = 37 XY pairs; $P = 0.050$).

DISCUSSION

The Effusion in COME Reveals Upregulation of Hypoxia Signaling Pathways

We report that hypoxia signaling pathways are upregulated in wbcs from both mucoid and serous COME fluids compared to wbcs in venous blood. Significant upregulation was shown by

TABLE 1 | List of enriched categories in genes upregulated in middle ear effusions as compared to blood, as identified with the Enrichr web tools.

	Enrichr database	Dataset	Mucoid vs blood *P*-value	Serous vs blood *P*-value
Ontologies and pathways	WikiPathways 2015	Toll-like receptor signaling pathway (Homo sapiens)	0.001995	0.005231
		RANKL/RANK signaling Pathway (Homo sapiens)	0.0006495	0.005231
	BioCarta 2015	hypoxia-inducible factor in the cardiovascular system	0.001801	0.006227
		classical complement pathway	0.005481	0.004845
	GO Biological Process	inflammatory response (GO:0006954)	7.78E-08	0.000002643
		response to hypoxia (GO:0001666)	6.61E-07	0.00009897
		regulation of leukocyte activation (GO:0002694)	0.00002025	8.04E-08
Enriched cell types	Human Gene Atlas	CD33+_Myeloid	0.000008913	0.028
		CD14+_Monocytes	0.01814	0.07511
	Mouse Gene Atlas	macrophage_peri_LPS_thio_0hrs	3.42E-13	1.15E-11
Regulation	ChEA	RELA-24523406-FIBROSARCOMA-HUMAN	6.51E-88	2.94E-49
		SOX2-20726797-SW620-HUMAN	2.03E-79	3.70E-73
		MITF-21258399-MELANOMA-HUMAN	1.11E-141	5.50E-154
		ZNF217-24962896-MCF7-HUMAN	4.39E-67	7.37E-67
		NR1H3-23393188-ATHEROSCLEROTIC-FOAM-HUMAN	2.11E-50	2.13E-49
		TP63-23658742-EP156T-HUMAN	3.01E-83	2.38E-75
	TRANSFAC and JASPAR PWMs	FOXC1 (human)	5.74E-16	4.60E-17
		TCF4 (human)	1.14E-18	1.27E-18
		JUN (human)	9.37E-16	1.20E-18
		ETS1 (human)	3.32E-14	5.51E-16
		GATA2 (human)	1.81E-13	3.77E-14
	ENCODE TF ChIP-seq 2015	IKZF1_GM12878_hg19	4.28E-28	3.94E-25
		SMARCC1_HeLa-S3_hg19	3.14E-18	2.57E-20
	NCI-Nature	HIF-1-alpha transcription factor network	4.78E-07	0.000002112
		HIF-2-alpha transcription factor network	0.004811	0.07746
	Single Gene Perturbations from GEO up	RARA Activation - AM580 (RARA Agonist) human GSE5679 sample 2385	2.55E-67	4.65E-55

microarray data analysis using Enrichr annotation strategies, including ontology and pathway analysis (using the WikiPathways database and the GO Biological Processes database), and HIF-1A regulatory pathway analysis (using the NCI-Nature database, **Table 1**). Findings were confirmed by RTqPCR for selected pathway genes (VEGF ligands, VEGF receptors and adapters, and HIF transcription factor).

We also found significantly elevated VEGF protein in COME fluids when compared to plasma. Other studies have reported the presence of VEGF protein in the effusion and the middle ear mucosa of patients with COME (Jung et al., 1999; Val et al., 2016; Val et al., 2018). The present study finding of hypoxia on transcriptional profiling was the result of an unbiased approach to whole transcript analysis and provides further evidence of wbc hypoxia in human COME. We found a small and borderline statistically significant negative correlation between COME effusion VEGF protein titre with increasing child age. This small effect requires further study, but may be interpreted as a trend towards resolution of inflammation and hypoxia and improved oxygenation of the bulla.

Upregulated hypoxia signaling in the bulla has been demonstrated in several animal models of otitis media: genetic mouse models of COME [*Fbxo11*$^{lf/+}$, *Mecom*$^{lbo/+}$ (Cheeseman et al., 2011), *Tgif*$^{-/-}$ (Tateossian et al., 2013), *Nischarin* $^{edsn/edsn}$ (Crompton et al., 2017) and *Eda*^{Ta} (Azar et al., 2016)], after cauterization of the Eustachian tube in the rat (Huang et al., 2012), and that induced by intrabullar injection of Non-typeable *Haemophilus influenzae* in the mouse (Husseman et al., 2012) or gastric-content in the rabbit (Basoglu et al., 2012). This underlines the common association between hypoxia with inflammation (see below) regardless of the initiating cause of OM, duration of inflammation, effusion phenotype or species differences.

Hypoxia signaling is a common finding in inflamed microenvironments, and it is unclear whether such signaling is the cause or the result of inflammation. Surgical ventilation of the middle ear in the *Mecom*$^{lbo/+}$ mouse model reduces tissue hypoxia and inflammation (Bhutta et al., 2014), suggesting that alleviation of tissue hypoxia may be a contributory therapeutic mechanism underlying grommet insertion for treatment of COME. In addition, administration of VEGF receptor inhibitors to young *Mecom*$^{lbo/+}$ mice at the time of initiation of OM moderates the progression of hearing loss (Cheeseman et al., 2011). The efficacy of such treatment in chronic OM has not yet been established. It seems worthwhile to further explore the potential for targeting hypoxia pathways in chronic OM.

Upregulation of Other Inflammatory Networks in COME

Hypoxia in mucoid and serous bulla effusions is accompanied by myeloid cell signature and upregulation of inflammatory networks (**Table 1**). Enrichr analysis revealed upregulation invoked in the Toll-like receptor (TLR) pathway, the complement pathway, and the RANK/RANKL pathway.

TLRs are components of the innate immune system, and typically respond to "pathogen associated molecular patterns" (PAMPs) on microbial cell walls or pathogen membranes. However, TLRs can also be activated by "damage-associated molecular patterns" (DAMPs): endogenous intra or extracellular proteins released as a result of cell

necrosis from host tissue injury. Why TLRs respond to endogenous signals is not known, but in such circumstances TLR activation may perpetuate inflammation, risking further tissue damage. TLR activation is thought to contribute to chronic inflammation in diseases such as rheumatoid arthritis and atherosclerosis (Drexler and Foxwell, 2010), and our transcriptome data suggest TLRs are also active in chronic otitis media. A previous genetic association study found that polymorphism in the *TLR4* receptor is a risk factor for childhood COME (although this finding was not replicated) (Hafren et al., 2015), and a *Tlr* deficient mouse exhibits altered immune response to bacterial challenge of the middle ear (Tyrer et al., 2013).

Microbiome analysis of human COME samples (Liu et al., 2011; Jervis-Bardy et al., 2015; Chan et al., 2016; Krueger et al., 2017) shows the presence of diverse bacterial communities that are a potential stimulus for TLR activation along with ongoing host tissue damage. Targeting induction of TLR pathways, for example through administration of anti-microbials, specific antibodies or proteases (Piccinini and Midwood, 2010), are logical strategies to counteract this effect.

Complement consists of a cascade of innate immune proteins that respond to pattern recognition molecules displayed on the surface of potential pathogens or damaged cells, including apoptotic or necrotic host cells (Ricklin and Lambris, 2013a). In mouse models mutation at complement loci alters the duration of induced otitis media (Tyrer et al., 2013). In COME it may be that complement activation is a consequence of persistent pathogen presence, presence of necrotic or apoptotic hosts cells (as often found in a hypoxic inflammatory environment), a result of cross-talk with activated TLR pathways (Song, 2012), or via other mechanisms. Like TLR pathways, experimental data suggest that complement pathways could be antagonized with small molecules or antibodies (Ricklin and Lambris, 2013b).

The RANK–RANKL pathway affects bone remodeling and repair as well as immune regulation. This pathway mediates interactions between osteoblasts and osteoclasts as well as between T cells and dendritic cells, which in turn can affect function of fibroblasts (Walsh and Choi, 2014). The role of RANKL in inflammation is still not well understood, but is thought to be an immunoregulatory role, largely through activation of the transcription factor NFkB. Some mouse models carrying mutations at loci in the NFkB pathway develop chronic OM (Tyrer et al., 2013). Again there are compounds to target the RANK-RANKL pathway, which have previously been used to treat osteoporosis (Walsh and Choi, 2014).

Hence, our transcript analysis reveals upregulation of hypoxia, TLR, complement and RANK-RANKL pathways. It suggests that targeting one of these pathways, or perhaps targeting several of them with a cocktail of molecular inhibitors, could be a mechanism to antagonize and moderate inflammation in COME.

Differences in Immune Cell Profiles in Mucoid and Serous COME

Cytology differentials showed neutrophils and macrophages are predominant inflammatory cell types in COME samples with heavy, intermediate, and low mucus, however mucoid samples have a significantly higher percentage of neutrophils, while serous effusions have a significantly higher percentage of lymphocytes and eosinophils. Eosinophils represent <2% of overall wbc population in our study of childhood COME. These eosinophil percentages are similar (2.6%) to older patients ~50 years-of age with COME, and contrast with much higher eosinophil differentials (13.4%) in patients with eosinophilic OM (Uchimizu et al., 2015).

While our cytological analysis did not characterize lymphocyte sub-populations, the transcript analysis indicates serous fluids have CD4+ and CD8+ T-lymphocyte, and NK cell signatures, whereas mucoid effusions have an enriched myeloid cell signature (**Table S3**). In flow cytometry analysis of COME effusions (not subdivided into mucoid and serous effusions), CD4+ and CD8+ T-lymphocytes, but not NK cells, were elevated with respect to blood populations (Skotnicka et al., 2005).

Earlier studies employing immunological techniques [e.g. cell rosetting assays (Bernstein et al., 1978)] and/or cytochemistry to characterize lymphoid cell subsets (Palva et al., 1978; Palva et al., 1980; Palva et al., 1980) emphasize the importance of lymphocytes in COME fluids. T cell differentials in serous and mucoid samples are equivalent (Palva et al., 1980), and the presence of T lymphocytes in mucoid COME is suggestive of delayed-type hypersensitivity, or mucosal injury by immune complexes (Palva et al., 1980). In another study comparing serous, seromucinous and mucoid samples recognize macrophages and lymphocytes in all samples, with serous samples containing predominantly macrophages and T cells; seromucinous samples, macrophages, T and B cells; and mucoid samples mainly B cells (Bernstein et al., 1978).

The high prevalence of neutrophils in mucoid, serous and intermediate COME effusions in this study is consistent with the proteomic findings of neutrophils and NETs described by Val et al. (2016). A subsequent proteomic analysis by these authors focusing on the differences between mucoid and serous COME samples indicated that higher neutrophil signature NET's in mucoid COME associated with greater MUC5B, and that serous COME samples have higher early innate immunity markers, complement and immunoglobulins (Val et al., 2018).

Taken together these data shows there are significant differences in the inflammatory cell profiles suggestive of an underlying difference in immunological basis for serous versus mucoid COME. There may be several contributory factors. Lim et al. (Lim et al., 1979) found that neutrophils predominated in COME effusions that had culturable pathogenic bacteria whereas lymphocytes were prominent in culture negative effusions and furthermore, variation in effusion microbiome had an impact on mucin content (Krueger et al., 2017). We did not collect sample microbiome data that would allow us to evaluate this possibility.

Strengths and Limitations of This Study

To our knowledge this is the first reported whole genome transcript analysis of the effusion in human COME. The strengths of our study are that we had a well phenotyped patient population and, by grouping COME samples into grossly mucoid and serous we were able to perform cross-comparisons and whole genome transcript analysis revealing differences in immune cell population and gene expression. Parallel differences were observed in mucoid and serous sample cytology. Results from the microarray were validated for the hypoxia-signaling pathway with RTqPCR.

Here we analyzed transcripts from the effusion in COME without extracting or differentiating the cells within that effusion, although cytological analysis would suggest that this is largely the signature from leucocytes. Future studies may aim to analyse the transcript in middle ear mucosa. We used peripheral blood wbc as control for gene expression in bulla effusion wbc, which will constitutively be different, but absence of immune cells and fluids in the healthy non-inflamed bulla means that a better control tissue is not available. For the same reason, we used plasma as the baseline control for VEGF protein in COME fluids. There is however a rationale for comparing bulla fluids with blood as the wbcs in COME effusions will have been recruited from the blood and effusion proteins will contain a transudate of plasma. We also acknowledge the general problems with the analysis of mRNA transcriptome, in that this may not directly correlate to protein expression. The microbiota was not assayed in COME effusions and this may be a determinant of glue ear MUC5B content (Krueger et al., 2017).

CONCLUSION

The cytological and transcriptome data from this study confirm that COME is an inflammatory disorder, with infiltration by a leucocyte population largely composed of neutrophils and macrophages, albeit with differences in cell populations in serous versus mucoid effusions. Transcriptome pathway analysis indicates upregulation of hypoxia signaling, the TLR pathway, complement, and the RANK-RANKL pathway. The prospects for utilizing transcriptome data to identify new targets for medical interventions depend on validation of candidate target proteins and a precise understanding of their role in effusion and mucosal inflammation. Pre-clinical animal models such as mouse models of chronic otitis media may assist future drug trials, ideally utilizing compounds that would be administered locally to the chronically inflamed middle ear.

DATA AVAILABILITY STATEMENT

The datasets generated for this study can be found in the GEO Series accession number GSE125532.

ETHICS STATEMENT

The studies involving human participants were reviewed and approved by Oxfordshire Research Ethics Committee. Written informed consent to participate in this study was provided by the participants' legal guardian/next of kin.

AUTHOR CONTRIBUTIONS

MB: Clinical lead for project, initial draft of paper. JL: Consent, and initial processing of samples. LH: Study coordinator, and initial processing of samples. DW: Transcript analysis. HT: Laboratory assistance. GN: Statistical analysis. SB: Study design. HB: Statistical analysis, CP: Cytological analysis, GD: Bioinformatic analysis and initial draft of paper. JR: Lead for ethical approval of study. MC: Scientific lead for project, initial draft of paper.

FUNDING

This work was funded through a Medical Research Council Technology Development Gap Fund grant A853-0092 and a BBSRC Institute Strategic Programme Grant BB/J004316/1 to the Roslin Institute. The microarray data were generated in the OXION facility at Oxford University and this was supported by Wellcome Trust grant 084655. MRC Harwell provided the open access publication costs.

ACKNOWLEDGMENTS

Thanks to Anagha Joshi for assistance with the study and Tertius Hough (MRC Harwell) for generating the VEGF data.

SUPPLEMENTARY MATERIAL

The Supplementary Material for this article can be found online at: https://www.frontiersin.org/articles/10.3389/fgene.2019.01327/full#supplementary-material

REFERENCES

Azar, A., Piccinelli,C., Brown, H., Headon, D., and Cheeseman, M. (2016). Ectodysplasin signalling deficiency in mouse models of hypohidrotic ectodermal dysplasia leads to middle ear and nasal pathology. *Hum. Mol. Genet.* 25 (16), 3564–3577. doi: 10.1093/hmg/ddw202

Basoglu, M. S., Eren, E., Aslan, H., Kolatan, H. E., Ozbay, C., Inan, S., et al. (2012). Increased expression of VEGF, iNOS, IL-1beta, and IL-17 in a rabbit model of gastric content-induced middle ear inflammation. *Int. J. Pediatr. Otorhinolaryngol.* 76 (1), 64–69. doi: 10.1016/j.ijporl.2011.10.001

Bernstein, J. M., Szymanski, C., Albini, B., Sun, M., and Ogra, P. L. (1978). Lymphocyte subpopulations in otitis media with effusion. *Pediatr. Res.* 12 (7), 786–788. doi: 10.1203/00006450-197807000-00009

Bhutta, M. F., Cheeseman, M. T., and Brown, S. D. (2014). Myringotomy in the Junbo mouse model of chronic otitis media alleviates inflammation and cellular hypoxia. *Laryngoscope* 124, E377–EE83. doi: 10.1002/lary.24698

Bhutta, M. F., Thornton, R.B., Kirkham, L. S., Kerschner, J. E., and Cheeseman, M. T. (2017). Understanding the aetiology and resolution of chronic otitis media from animal and human studies. *Dis. Models Mech.* 10 (11), 1289–1300. doi: 10.1242/dmm.029983

Bhutta, M. F. (2014). Epidemiology and pathogenesis of otitis media: construction of a phenotype landscape. *Audiol. Neuro-Otol.* 19 (3), 210–223. doi: 10.1159/000358549

Casselbrant, M. L., Mandel, E. M., Fall, P. A., Rockette, H. E., Kurs-Lasky, M., Bluestone, C. D., et al. (1999). The heritability of otitis media: a twin and triplet study. *JAMA* 282 (22), 2125–2130. doi: 10.1001/jama.282.22.2125

Caye-Thomasen, P., Stangerup, S. E., Jorgensen, G., Drozdziewic, D., Bonding, P., and Tos, M. (2008). Myringotomy versus ventilation tubes in secretory otitis media:

eardrum pathology, hearing, and eustachian tube function 25 years after treatment. *Otol. Neurotol.* 29 (5), 649–657. doi: 10.1097/MAO.0b013e318173035b

Chan, C.L., Wabnitz, D., Bardy, J. J., Bassiouni, A., Wormald, P. J., Vreugde, S., et al. (2016). The microbiome of otitis media with effusion. *Laryngoscope* 126 (12), 2844–2851. doi: 10.1002/lary.26128

Cheeseman, M. T., Tyrer, H. E., Williams, D., Hough, T. A., Pathak, P., Romero, M. R., et al. (2011). HIF-VEGF pathways are critical for chronic otitis media in Junbo and Jeff mouse mutants. *PloS Genet.* 7 (10), e1002336. doi: 10.1371/journal.pgen.1002336

Chen, E. Y., Tan, C. M., Kou, Y., Duan, Q., Wang, Z., Meirelles, G. V., et al. (2013). Enrichr: interactive and collaborative HTML5 gene list enrichment analysis tool. *BMC Bioinf.* 14, 128. doi: 10.1186/1471-2105-14-128

Chervoneva, I., Li, Y., Schulz, S., Croker, S., Wilson, C., Waldman, S. A., et al. (2010). Selection of optimal reference genes for normalization in quantitative RT-PCR. *BMC Bioinf.* 11, 253. doi: 10.1186/1471-2105-11-253

Crompton, M., Purnell, T., Tyrer, H. E., Parker, A., Ball, G., Hardisty-Hughes, R. E., et al. (2017). A mutation in Nischarin causes otitis media via LIMK1 and NF-kappaB pathways. *PloS Genet.* 13 (8), e1006969. doi: 10.1371/journal.pgen.1006969

Dai, M., Wang, P., Boyd, A. D., Kostov, G., Athey, B., Jones, E. G., et al. (2005). Evolving gene/transcript definitions significantly alter the interpretation of GeneChip data. *Nucleic Acids Res.* 33 (20), e175. doi: 10.1093/nar/gni179

Drexler, S. K., and Foxwell, B. M. (2010). The role of toll-likereceptors in chronic inflammation. *Int. J. Biochem. Cell Biol.* 42 (4), 506–518. doi: 10.1016/j.biocel.2009.10.009

Duah, V., Huang, Z., Val, S., DeMason, C., Poley, M., and Preciado, D. (2016). Younger patients with COME are more likely to have mucoid middle ear fluid containing mucin MUC5B. *Int. J. Pediatr. Otorhinolaryngol.* 90, 133–137. doi: 10.1016/j.ijporl.2016.09.009

Hafren, L., Einarsdottir, E., Kentala, E., Hammaren-Malmi, S., Bhutta, M. F., MacArthur, C. J., et al. (2015). Predisposition to childhood otitis media and genetic polymorphisms within the Toll-Like Receptor 4 (TLR4) Locus. *PloS One* 10 (7), e0132551. doi: 10.1371/journal.pone.0132551

Hernandez, M., Leichtle,A., Pak, K., Webster, N. J., Wasserman, S. I., and Ryan, A. F. (2015). The transcriptome of a complete episode of acute otitis media. *BMC Genomics* 16, 259. doi: 10.1186/s12864-015-1475-7

Huang,Q., Zhang,Z., Zheng,Y., Zheng,Q., Chen, S., Xu, Y., et al. (2012). Hypoxia-inducible factor and vascular endothelial growth factor pathway for the study of hypoxia in a new model of otitis media with effusion. *Audiol. Neuro-Otol.* 17 (6), 349–356. doi: 10.1159/000341163

Husseman,J., Palacios, S. D., Rivkin, A. Z., Oehl,H., and Ryan, A. F. (2012). The role of vascular endothelial growth factors and fibroblast growth factors in angiogenesis during otitis media. *Audiol. Neuro-Otol.* 17 (3), 148–154. doi: 10.1159/000333805

Jennings, B. A., Prinsley, P., Philpott, C., Willis, G., and Bhutta, M. F. (2017). The genetics of cholesteatoma. A systematic review using narrative synthesis. *Clin. Otolaryngol.* 43 (1), 55–67. doi: 10.1111/coa.12900

Jervis-Bardy,J., Rogers, G. B., Morris, P.S., Smith-Vaughan, H. C., Nosworthy, E., Leong, L. E., et al. (2015). The microbiome of otitis media with effusion in Indigenous Australian children. *Int. J. Pediatr. Otorhinolaryngol.* 79 (9), 1548–1555. doi: 10.1016/j.ijporl.2015.07.013

Jung, H. H., Kim, M. W., Lee, J. H., Kim, Y. T., Kim, N. H., Chang, B. A., et al. (1999). Expression of vascular endothelial growth factor in otitis media. *Acta Oto-Laryngol.* 119 (7), 801–808. doi: 10.1080/00016489950180450

Krueger, A., Val, S., Perez-Losada, M., Panchapakesan, K., Devaney, J., Duah, V., et al. (2017). Relationship of the middle ear effusion microbiome to secretory mucin production in pediatric patients with chronic otitis media. *Pediatr. Infect. Dis. J.* 36 (7), 635–640. doi: 10.1097/INF.0000000000001493

Kuleshov, M. V., Jones, M. R., Rouillard, A. D., Fernandez, N. F., Duan, Q., Wang, Z., et al. (2016). Enrichr: a comprehensive gene set enrichment analysis web server 2016 update. *Nucleic Acids Res.* 44 (W1), W90–W97. doi: 10.1093/nar/gkw377

Lim, D. J., Lewis, D. M., Schram, J. L., and Birck, H. G. (1979). Otitis media with effusion. Cytological and microbiological correlates. *Arch. Otolaryngol.* 105 (7), 404–412. doi: 10.1001/archotol.1979.00790190030006

Liu, C. M., Cosetti, M. K., Aziz, M., Buchhagen, J. L., Contente-Cuomo, T. L., Price, L. B., et al. (2011). The otologic microbiome: a study of the bacterial microbiota in a pediatric patient with chronic serous otitis media using 16SrRNA gene-based pyrosequencing. *Arch. Otolaryngol.–Head Neck Surg.* 137 (7), 664–668. doi: 10.1001/archoto.2011.116

Liu, K., Chen, L., Kaur, R., and Pichichero, M. (2012). Transcriptome signature in young children with acute otitis media due to Streptococcus pneumoniae. *Microbes Infect.* 14 (7–8), 600–609. doi: 10.1016/j.micinf.2012.01.006

Liu, K., Chen, L., Kaur, R., and Pichichero, M. E. (2013). Transcriptome signature in young children with acute otitis media due to non-typeable Haemophilus influenzae. *Int. Immunol.* 25 (6), 353–361. doi: 10.1093/intimm/dxs154

Matkovic, S., Vojvodic, D., and Baljosevic, I. (2007). Cytokine levels in groups of patients with different duration of chronic secretory otitis. *Eur. Arch. Otorhinolaryngol.* 264 (11), 1283–1287. doi: 10.1007/s00405-007-0373-2

Palva, T., Hayry, P., and Ylikoski, J. (1978). Lymphocyte morphology in mucoid middle ear effusions. *Ann. Otol. Rhinol. Laryngol.* 87 (3 Pt 1), 421–425. doi: 10.1177/000348947808700325

Palva, T., Hayry, P., and Ylikoski, J. (1980). Lymphocyte morphology in middle ear effusions. *Ann. Otol. Rhinol. Laryngol. Suppl.* 89 (3 Pt 2), 143–146. doi: 10.1177/00034894800890s336

Palva, T., Hayry, P., Raunio, V., and Ylikoski, J. (1980). Immunologic aspects of otitis media. *Acta Oto-Laryngol.* 89 (3–4), 177–181. doi: 10.3109/00016488009127125

Piccinini, A. M., and Midwood, K. S. (2010). DAMPening inflammation by modulating TLR signalling. *Mediators Inflammation* 2010, 672395. doi: 10.1155/2010/672395

Ricklin, D., and Lambris, J. D. (2013a). Complement in immune and inflammatory disorders: pathophysiological mechanisms. *J. Immunol.* 190 (8), 3831–3838. doi: 10.4049/jimmunol.1203487

Ricklin, D., and Lambris, J. D. (2013b). Complement in immune and inflammatory disorders: therapeutic interventions. *J. Immunol.*190 (8), 3839–3847. doi: 10.4049/jimmunol.1203200

Ritchie, M. E., Phipson, B., Wu, D., Hu, Y., Law, C. W., Shi, W., et al. (2015). limma powers differential expression analyses for RNA-sequencing and microarray studies. *Nucleic Acids Res.* 43 (7), e47. doi: 10.1093/nar/gkv007

Sekiyama, K., Ohori, J., Matsune, S., and Kurono, Y. (2011). The role of vascular endothelial growth factor in pediatric otitis media with effusion. *Auris Nasus Larynx* 38 (3), 319–324. doi: 10.1016/j.anl.2010.10.008

Skotnicka, B., Stasiak-Barmuta, A., Hassmann-Poznanska, E., and Kasprzycka, E. (2005). Lymphocyte subpopulations in middle ear effusions: flow cytometry analysis. *Otol. Neurotol.* 26 (4), 567–571. doi: 10.1097/01.mao.0000169050.61630.da

Song, W. C. (2012). Crosstalk between complement and toll-like receptors. *Toxicol. Pathol.* 40 (2), 174–182. doi: 10.1177/0192623311428478

Tateossian, H., Morse, S., Parker, A., Mburu, P., Warr, N., Acevedo-Arozena, A., et al. (2013). Otitis media in the Tgif knockout mouse implicates TGFβ signalling in chronic middle ear inflammatory disease. *Hum. Mol. Genet.* 22 (13), 2553–65. doi: 10.1093/hmg/ddt103

Tyrer, H. E., Crompton, M., and Bhutta, M. F. (2013). What have we learned frommurine models of otitis media? *Curr. Allergy Asthma Rep.* 13 (5), 501–511. doi: 10.1007/s11882-013-0360-1

Uchimizu, H., Matsuwaki, Y., Kato, M., Otori, N., and Kojima, H. (2015). Eosinophil-derived neurotoxin, elastase, and cytokine profile in effusion from eosinophilic otitis media. *Allerg. Int.* 64 (Suppl), S18–S23. doi: 10.1016/j.alit.2015.03.007

Val, S., Poley, M., Brown, K., Choi, R., Jeong, S., Colberg-Poley, A., et al. (2016). Proteomic characterization of middle ear fluid confirms neutrophil extracellulartraps as a predominant innate immune response in chronic otitis media. *PloS One* 11 (4), e0152865. doi: 10.1371/journal.pone.0152865

Val, S., Poley, M., Anna, K., Nino, G., Brown, K., Perez-Losada, M., et al. (2018). Characterization of mucoid and serous middle ear effusions from patients with chronic otitis media: implication of different biological mechanisms? *Pediatr. Res.* doi: 10.1371/journal.pone.0152865. eCollection 2016.

Walsh, M. C., and Choi, Y. (2014). Biology of the RANKL-RANK-OPG System in Immunity, Bone, and Beyond. *Front. Immunol.* 5, 511. doi: 10.3389/fimmu.2014.00511

Xuan, W., Dai,M., Buckner,J., Mirel,B., Song, J., Athey, B., et al. (2010). Cross-domain neurobiology data integration and exploration. *BMC Genomics* 11 (Suppl 3), S6. doi: 10.1186/1471-2164-11-S3-S6

Conflict of Interest: The authors declare that the research was conducted in the absence of any commercial or financial relationships that could be construed as a potential conflict of interest.

frontiers in Genetics

ORIGINAL RESEARCH
published: 15 April 2020
doi: 10.3389/fgene.2020.00358

Single-Cell Transcriptomes Reveal a Complex Cellular Landscape in the Middle Ear and Differential Capacities for Acute Response to Infection

Allen F. Ryan[1], Chanond A. Nasamran[2], Kwang Pak[1], Clara Draf[1], Kathleen M. Fisch[2], Nicholas Webster[3] and Arwa Kurabi[1]*

[1] Departments of Surgery/Otolaryngology, UC San Diego School of Medicine, VA Medical Center, La Jolla, CA, United States, [2] Medicine/Center for Computational Biology & Bioinformatics, UC San Diego School of Medicine, VA Medical Center, La Jolla, CA, United States, [3] Medicine/Endocrinology, UC San Diego School of Medicine, VA Medical Center, La Jolla, CA, United States

OPEN ACCESS

Edited by:
Amélie Bonnefond, Institut National de la Santé et de la Recherche Médicale (INSERM), France

Reviewed by:
Fabien Delahaye, Institut Pasteur de Lille, France
Nelson L. S. Tang, The Chinese University of Hong Kong, China

***Correspondence:**
Allen F. Ryan
afryan@ucsd.edu

Specialty section:
This article was submitted to Genetic Disorders, a section of the journal Frontiers in Genetics

Received: *09 August 2019*
Accepted: *24 March 2020*
Published: *15 April 2020*

Citation:
Ryan AF, Nasamran CA, Pak K, Draf C, Fisch KM, Webster N and Kurabi A (2020) Single-Cell Transcriptomes Reveal a Complex Cellular Landscape in the Middle Ear and Differential Capacities for Acute Response to Infection. Front. Genet. 11:358. doi: 10.3389/fgene.2020.00358

Single-cell transcriptomics was used to profile cells of the normal murine middle ear. Clustering analysis of 6770 transcriptomes identified 17 cell clusters corresponding to distinct cell types: five epithelial, three stromal, three lymphocyte, two monocyte, two endothelial, one pericyte and one melanocyte cluster. Within some clusters, cell subtypes were identified. While many corresponded to those cell types known from prior studies, several novel types or subtypes were noted. The results indicate unexpected cellular diversity within the resting middle ear mucosa. The resolution of uncomplicated, acute, otitis media is too rapid for cognate immunity to play a major role. Thus innate immunity is likely responsible for normal recovery from middle ear infection. The need for rapid response to pathogens suggests that innate immune genes may be constitutively expressed by middle ear cells. We therefore assessed expression of innate immune genes across all cell types, to evaluate potential for rapid responses to middle ear infection. Resident monocytes/macrophages expressed the most such genes, including pathogen receptors, cytokines, chemokines and chemokine receptors. Other cell types displayed distinct innate immune gene profiles. Epithelial cells preferentially expressed pathogen receptors, bactericidal peptides and mucins. Stromal and endothelial cells expressed pathogen receptors. Pericytes expressed pro-inflammatory cytokines. Lymphocytes expressed chemokine receptors and antimicrobials. The results suggest that tissue monocytes, including macrophages, are the master regulators of the immediate middle ear response to infection, but that virtually all cell types act in concert to mount a defense against pathogens.

Keywords: single-cell, middle ear, otitis media, cluster-profiling, homeostasis

INTRODUCTION

The middle ear (ME) is a bone-encased, air-filled cavity that links the external ear to the inner ear. Bounded externally by the tympanic membrane, it houses the three ossicles that transmit acoustic vibrations from the eardrum to the cochlea. It is connected to the nasopharynx by the

Eustachian tube, which provides intermittent ventilation and pressure release, as well as clearance via ciliary activity.

The ME is a frequent site of infection, especially in children. More than 90% of children experience otitis media (OM), which is chronic-recurrent in 15−20% (Rosenfeld and Bluestone, 2003). It is the most common cause of physician visits and surgery at ages less than 5 years (Cullen et al., 2009). OM leads to hearing loss during a critical period of language acquisition and learning, and has been associated with deficits in both language and learning (Friel-Patti et al., 1982; Wendler-Shaw et al., 1993). OM can be well-controlled by therapy, but the annual cost in the United States is estimated at >$5 billion (Ahmed et al., 2014). In contrast, OM is a very serious disease in developing countries due to limited access to medical care. Under-treated suppurative OM is estimated by the World Health Organization to be responsible for 28,000 annual deaths due to intracranial infection and to cause half of the world's burden of severe hearing loss, approximately 240 million cases (Arguedas et al., 2010). The resolution of uncomplicated, acute OM occurs in less than one week, even without antibiotic treatment. This is too rapid for the *de novo* elaboration of cognate immunity, suggesting that OM is normally resolved by innate immunity. Indeed, deficiencies in innate immune genes have been linked to OM susceptibility in both mice and humans (Leichtle et al., 2011; Rye et al., 2011).

The ME is an atypical mucosal site, characterized by a largely rudimentary cellular structure, yet with the capability to rapidly transform into a respiratory-type epithelium. The majority of the resting ME cavity is lined by a monolayer of simple squamous epithelial cell overlying a sparse stroma and vasculature. However, upon infection and inflammation, hyperplasia can produce a 20-fold increase in thickness, into a pseudostratified, columnar epithelium populated with ciliated, goblet and secretory cells, within a few days. Upon the resolution of infection, the mucosa returns to its baseline structure (Lim, 1979).

The cells that make up the normal ME mucosa have been studied primarily morphologically. Early studies were limited to the observation of a simple squamous lining epithelium with ciliated cells in some areas, especially near the orifice of the Eustachian tube (e.g., Kolmer and Mellendorff, 1927; Wolff, 1943). Later investigations noted morphological details that confirmed a simple squamous epithelial structure with minimal stroma throughout much of the ME, but with some areas of cuboidal, columnar and pseudostratified epithelium, primarily near the Eustachian tube but also in recesses and corners of the ME (e.g., Hentzer, 1970). Blood vessels, lymphatics, and small numbers of immunocytes including macrophages, lymphocytes and plasma cells were also noted in the stroma, as were melanocytes (Lin and Zak, 1982). In addition, histochemistry was used to demonstrate the presence of mucopolysaccharides within both ciliated and non-ciliated epithelial cells (e.g., Sade, 1966).

The introduction of electron microscopy to ME studies added significant details regarding ME cell types. Based on their ultrastructure, Lim and Hussl (1969) classified ME epithelial cells as non-ciliated without secretory granules, mucus-secreting goblet cells with abundant secretory granules, intermediary secretory cells with fewer secretory granules, ciliated cells, and subsurface basal cells. Hentzer (1976) added a sixth class that he termed intermediate cells, which he proposed could differentiate into any of the other surface cell types, with intermediary secretory cells a transitional stage into goblet cells. Ultrastructural studies also noted pericytes in association with the endothelial cells of vessels.

Additional information has been added by immunohistochemistry. Takahashi et al. (1989) identified macrophages, T-cells and B-cells in the subepithelial stroma of the normal ME. However, these cells were sparse, with on average less than one B cell in a histological section through the entire ME, and 1−5 macrophages and T-cells per section. They thus comprised a very small fraction of the cells present in the normal ME, as observed morphologically by Lim (1979). Immunohistochemistry was also used to document the presence of melanocytes (Lin and Zak, 1982), pericytes (Zhang et al., 2015), natural killer cells (Jecker et al., 1996), and mast cells (Stenfors et al., 1985).

More recently, a lineage study found that the ME mucosal epithelium in mice has two distinct embryonic origins. Epithelial cells in approximately half of the ME cavity closest to the Eustachian tube orifice originate from the endoderm of the branchial arches, while the remainder originates from the neural crest. In the normal ME, ciliated and goblet cells were observed only in cells of endodermal origin, although many non-ciliated, non-secretory cells were also present (Thompson and Tucker, 2013). More recently, ciliated cells have been documented in the region of neural crest origin (Luo et al., 2017). However, the dual origin of cells adds yet another layer of complexity to ME cell types.

Recent studies have also evaluated the transcriptome of the normal ME mucosa (MacArthur et al., 2013; Hernandez et al., 2015). These studies, which utilized bulk RNA, identified genes expressed in the normal ME. However, they could not address the genes expressed individually by the different ME cell types. Cell-specific patterns of genes expression would help to define the functions of various cell types and their ability to respond to ME infection.

The purpose of the present study was to document the expression of genes in individual ME cells. We sought to identify the cell types present in the ME cavity at a single-cell resolution, to illuminate their functional characteristics, and to evaluate the cellular distribution of genes known to be important for the pathogenesis and resolution of OM.

MATERIALS AND METHODS

Animals

Young adult (60−90 day old) wildtype C57Bl/6J mice (Charles River, Wilmington, MA, United States) were used. All procedures were performed to National Institutes of Health guidelines and approved by the Institutional Animal Care and Use Committee of the VA San Diego Medical Center.

Preparation of Cell Suspensions

Groups of six mice were deeply anesthetized (ketamine 50 mg/kg, xylazine 1 mg/kg, acepromazine 5 mg/kg in 50 μl, i.p.) and sacrificed by decapitation, avoiding significant pressure on the neck to prevent the rupture of blood vessels in the ME. Six animals were required to generate a sufficient number of cells for a 10X Genomics run, because a ME tissue sample from a single animal are small. The ME bullae were isolated and opened along the suture that divides the lateral from the medial ME. ME mucosal tissue was gently harvested from the bullar bone. Care was taken not to include any tissue from the ME muscles. The pooled tissue was incubated with 0.5 mg/ml thermolysin (Sigma-Aldrich, #T7902) in Leibovitz's buffer for 25–30 min in a 37°C/5% CO_2 humidified tissue culture incubator to dissociate the extracellular matrix. The thermolysin was then aspirated, the tissue rinsed, and the sample incubated in FACSMax cell dissociation solution (Genlantis, #T200100). The cell mixture was triturated with a pipette and further dissociated into single cells mechanically by passing through a 23 G blunt-ended needle. Dissociated cells were passed through a 40 μm cell strainer (BD Biosciences) to eliminate clumps before sorting and collected into a FACS tube on ice containing PBS buffer with 0.04% BSA. Cell viability was assessed by Trypan blue exclusion staining and cells counted with a hemocytometer (Countess II, Thermo Fisher Scientific). Cell viability was greater than 95%. Following counting, the samples were diluted to 700 cells/μL. Three replicates were performed since the typical yield of a 10X genomics run is about 2,000 cells, and we wanted to evaluate a higher number, plus we wanted independent biological samples to assess replicability of the data.

Single-Cell Library Preparation and Sequencing

Libraries were prepared using the Chromium Controller (10X Genomics, Pleasanton, CA, United States) in conjunction with the Single Cell 3' Reagent Kit v2 kit user guide. Briefly, the cell suspensions were diluted with nuclease-free water according to manufacturer instructions to achieve an estimated cell count of 1,950 to 2,858 per sample. cDNA synthesis, barcoding, and library preparation were then carried out in the Chromium controller according to the manufacturers' instructions. The libraries were sequenced on an Illumina HiSeq 2500 (Illumina, San Diego, United States) with a read length of 26 bp for read 1 [cell barcode and unique molecule identifier (UMI)], 8 bp i7 index read (sample barcode), and 98 bp for read 2 (actual RNA read). Reads were first sequenced in the rapid run mode, allowing for fine-tuning of sample ratios in the following high-output run. Combining the data from both flow cells yielded approximately 200 million reads per sample.

Single-Cell Data Analysis

Reads were demultiplexed using Cellranger 2.0.2 (10X Genomics) and mkfastq in conjunction with bcl2fastq 2.17.1.14 (Illumina). The reads were subsequently aligned to the murine reference genome (mm10 with annotations from Ensembl release 84), filtered, and quantified using the Cellranger count command. Cellranger aggr (10X Genomics) was further used to generate an initial secondary analysis (t-distributed stochastic neighbor embedding; t-SNE), principal component analysis (PCA) clustering. Graph-based, as well as K-means (K = 2–10) analysis of gene expression was used to identify the 50 most differentially regulated genes that distinguished each PCA cell cluster. Cellranger aggr was used to merge the count matrices from 3 independent samples.

Additional clustering analysis was conducted using R package Seurat (Satija et al., 2015) to merge the data from the three independent samples and generate overall cell clusters. Cells were filtered based on quality control measurements recommended by the Seurat developers. Genes that were expressed in less than 0.1% of cells and cells that expressed less than 750 unique genes were excluded from the analysis. Cells that expressed greater than 7.5% mitochondrial genes were also excluded, as they represent dead or injured cells. After filtering, 6,370 of 6,770 cells remained.

After quality filtering, counts were log normalized. The FindVariableGenes function in Seurat was used to identify 2,207 highly variable genes that were used for downstream analysis. Finally, the data were scaled and subject to PCA to reduce the dimensionality of the dataset.

We used overrepresentation enrichment analysis (ORA) from R package WebGestaltR. Searched geneontology biological process database. Looked for enrichment in significantly differentially expressed genes (adjusted p-value < 0.05) for each cluster versus all highly variable genes (n = 2,207).

Identification of Cell Types

Cells were identified by assessing gene expression in the clusters of the three independent samples. Two methods were used to evaluate each of the samples. In the first, the expression of well-recognized cell marker genes was mapped to the graph-based clusters. For a second means of identification, the top 50 differentially expressed genes in each cluster were evaluated for their known expression by different cell types using the GeneCards database and the literature. From both methods, exclusively expressed genes (defined as being expressed by >50% of the cells in a cluster at high levels versus <2.5% of the cells of all other clusters at low levels) that were associated with an individual cell type were then assessed for their known cellular expression in the literature and in the GeneCards database.

Immunohistochemistry

Expression of select genes used for cell identification was verified by immunohistochemistry. Paraffin sections of MEs were deparaffinized, and antigen retrieval performed with citrate buffer, pH 6.0. The sections were exposed to primary antibodies to: EPCAM (Sino Biological), DYNLRB2 (Thermo Fisher Scientific), COL1A2 (LSBio), LRG (Proteintech), CSFR1 (LSBio) and PTPRCAP (Antibodies.online), DEFB1 (BiossUSA), AREG (LSBio), ECRG4 (Biorbyt), followed by secondary antibodies labeled with Alexa 488 (Abcam).

Expression of Innate Immune Genes

Acute OM in most children resolves in less than a week even in the absence of antibiotic treatment (Little et al., 2001), a

TABLE 1 | Single cell metrics.

Sample	Reads	Total cells	Genes/cell	Reads/cell	Total genes	UMIs/cell
1	54.0 M	2,858	1,637	18,886	17,719	3,933
2	45.0 M	1,962	1,490	20,920	17,110	3,744
3	41.9 M	1,950	1,600	21,468	17,138	4,005

Metrics for the three independent samples of ME mucosa, each representing six mouse MEs.

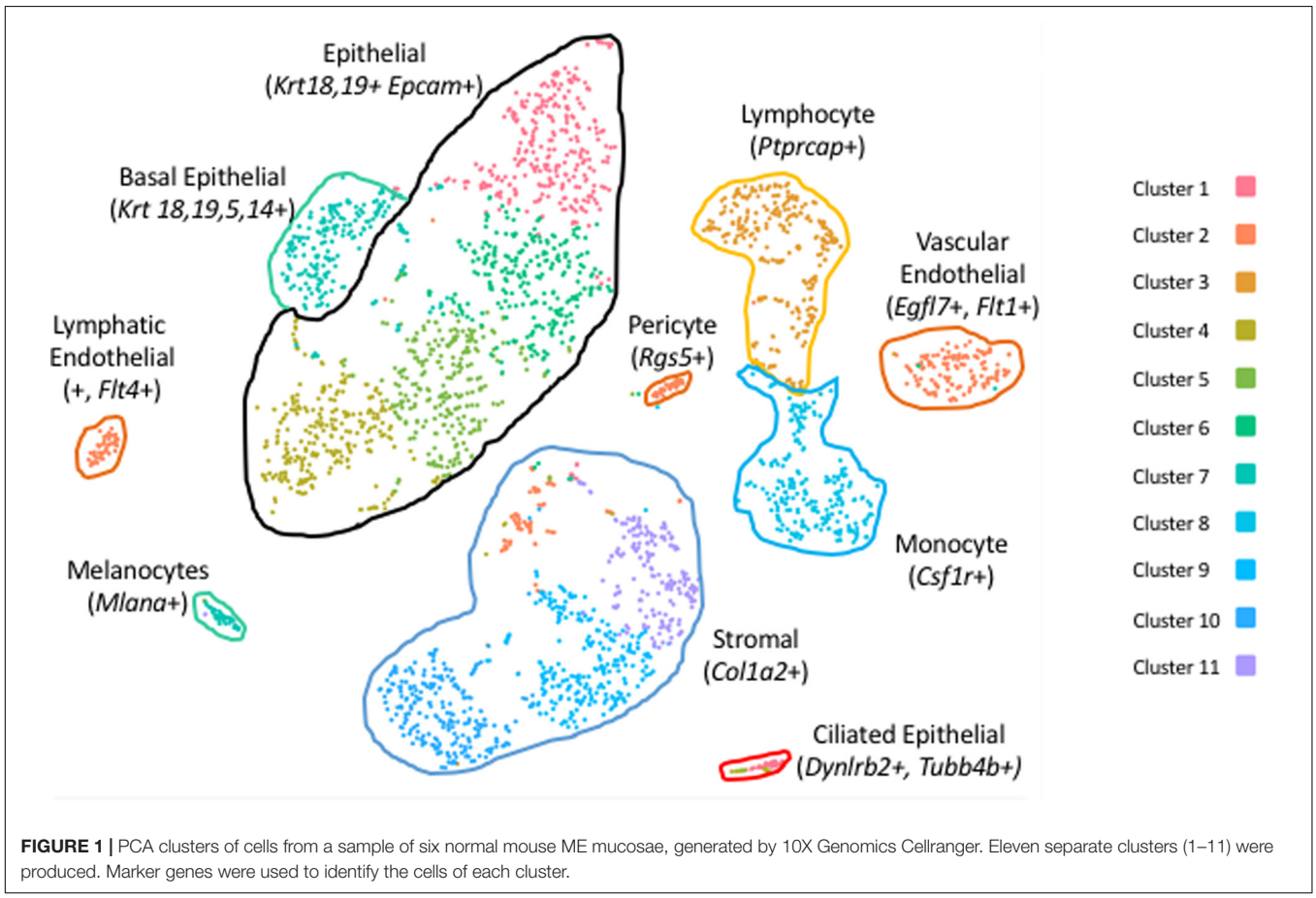

FIGURE 1 | PCA clusters of cells from a sample of six normal mouse ME mucosae, generated by 10X Genomics Cellranger. Eleven separate clusters (1–11) were produced. Marker genes were used to identify the cells of each cluster.

period too short for the full engagement of cognate immunity. This implicates innate immunity in the normal resolution of ME infection. In order to assess the capacity of resting ME cells to rapidly engage innate immunity, we assessed the expression levels of innate immune genes in our single-cell transcriptomes. For this analysis we used the Mouse Genome Informatics gene ontology (GO) list of 1599 innate immune transcripts representing 809 individual genes: GO:0045087.

RESULTS

Single-Cell Metrics

The mean number of transcriptomes per sample was 2,257, typical for a single-cell sample on the 10X genomics device, for a total of 6,770 cells. As noted above, quality control eliminating cells with a high proportion of mitochondrial genes likely to be dead or dying cells as well as outliers, left a total of 6,370 cells. A mean of 45.6 million reads/sample resulted in the detection of 17,322 genes for each tissue sample, with an average 20,425 reads/cell, 3,894 UMIs/cell and 1,576 genes/cell. The quality control metrics for each sample are presented in **Table 1**.

Generation of Cell Clusters

Clustering of ME cell transcriptomes using the 10X Cellranger pipeline resulted in a similar pattern of cell groupings for each of the samples, identifying 11 (**Figure 1**), 8 and 7 clusters in the three separate samples. Some of these clusters were subdivisions of spatially contiguous cell groups, and generally it was variation in the number of these subgroups that produced differences in cluster number between samples. However, later analysis confirmed that marker genes present in the sample with the most clusters (11) also distinguished cell groups in the two samples with fewer clusters, even though they had not been separated

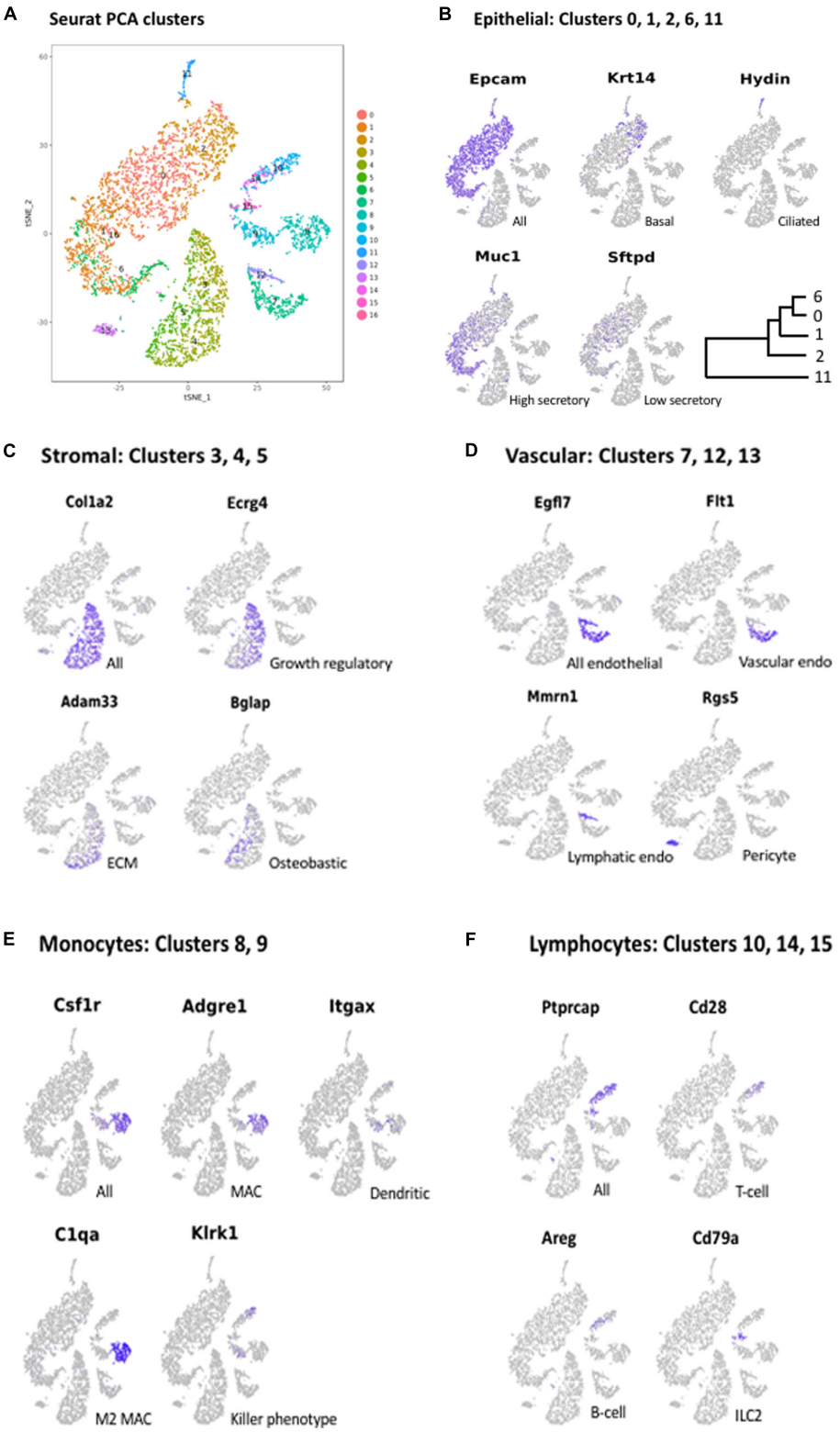

FIGURE 2 | (A) PCA clusters generated from the cells of all three mucosal samples, generated with Seurat. Seventeen clusters (0–16) were identified. Marker genes were again used to determine the cells types present in each cluster. Some cell types that were grouped in contiguous clusters by Cellranger were separated in the Seurat analysis. Marker gene expression in: **(B)** Epithelial cell clusters (0, 1, 2, 6, 11); **(C)** Stromal cell clusters (3, 4, 5); **(D)** Vascular cell clusters (7, 12, 13); **(E)** Monocyte clusters (8, 9); and **(F)** Lymphocyte clusters (10, 14, 15).

by PCA. To increase the depth of analysis, cell sequences from the three samples were merged and analyzed using Seurat. Seurat t-SNE clustering of the merged samples yielded 17 cell clusters, which are illustrated in **Figure 2A**. Several clusters consisted of discrete groups of cells. Others were parts of multi-cluster cell groupings, as observed in the Cellranger analysis.

Identification of ME Cell Types

As noted above, the expression of cell type marker genes that are well recognized in the literature was used to identify ME cell types (**Figure 2**). Evaluation of cluster-specific genes (expressed by the majority of cells in a single cluster and very few cells from other clusters) was also used to confirm ME cell type identity, when the literature or the GeneCards database indicated that expression was limited to a single cell type. Genes used to identify ME cell types are presented in **Table 2**.

TABLE 2 | Genes used to identify ME cell types.

Epithelial cells (all)	*Epcam, Krt18, Krt19*
Basal	*Krt5, Krt14*
Ciliated	*Spag6l, Hydin*
Secretory	*Muc1, Lyz*
Stromal cells (all)	*Col1a2*
Endothelial cells	*Egfl7*
Vascular	*Flt4*
Lymphatic	*Flt1*
Pericytes	*Rgs5*
Melanocytes	*Mlana*
Monocytes (all)	*Csf1r*
Macrophages	*Adgre1* (F4/80)
M2	*C1qa*
Dendritic cells	*Itgax*
Cytotoxic phenotype	*Klrk1*
Lymphocytes (all)	*Ptprcap*
T-cell	*Cd3d*
B-cell	*Cd79a*
Type 2 Lymphoid cell	*Areg*

These genes were reliable indicators of cell types in the normal ME.

Epithelial Cells

The largest number of cells (51.5% of all cells in the merged samples) showed expression of genes typical of epithelia (Hackett et al., 2011), including the epithelial cell adhesion gene *Epcam* (**Figure 2B**), the cytokeratin genes *Krt18* and *Krt19*, several claudin genes, and *Muc16*. This included the cells of Seurat Clusters 0, 1, 2, 6, and 11. Two of these clusters were readily identified as epithelial subtypes: Cluster 2 exclusively expressed *Krt5*, *Krt14* (**Figure 2B**), and *Krt17*, recognized markers of basal epithelial cells. Cluster 11, physically separate from the other epithelial clusters in the Seurat PCA analysis (**Figure 2A**), exclusively expressed many genes characteristic of ciliated cells (Hoh et al., 2012), including those encoding dynein axosomal heavy (e.g., *Dnah5*) *Intermediate* and light chains, the dynein regulator *Dynlrb2* (dynein light chain roadblock 2) as well as *Hydin* (axonemal central pair apparatus protein) (**Figure 2B**).

Melanocytes

Embedded within the larger epithelial cell grouping that included Clusters 0, 1, 2 and 6 was a small number of cells (Cluster 16, consisting of only 1.8% of all cells) that did not express epithelial markers. The cells of this cluster uniquely expressed markers for melanocytes (Yang et al., 2014), including many involved in melanin synthesis: *Pmel* (premelanosome protein), *Mlana* (melan-A) which is required for PMEL function, *Dct* (dopamine tautomerase, involved in PMEL synthesis), *Slc45a2* (Solute carrier family 45 member 2) involved in melanin synthesis and *Tyrp1* (tyrosine-related protein 1) which regulates melanin synthesis).

Stromal Cells

After epithelial cells, the next largest group of cells (22.6% of all cells) expressed genes typical of stromal cells. This included Clusters 3, 4, and 5 (**Figure 2A**), the cells of which expressed numerous extracellular matrix (ECM)/connective tissue proteins, such as *Col1a1* (collagen type 1 alpha 1), *Col1a2* (**Figure 2C**), *Fbln1* (fibulin 1, a fibrillar ECM), *Wisp2* (Wnt1 inducible signaling pathway protein, a connective tissue growth factor); *Adamts5* (ADAM metallopeptidase with thrombospondin type 1), a connective tissue organization factor, *Fmod* (fibromodulin) collagen fibrillogenesis factor involved in ECM assembly, and *Cdh11* (cadherin 11), an ECM synthesis regulator.

Endothelial Cells and Pericytes

Cells associated with the vasculature comprised 9.2% of all cells on our samples. Clusters 7 and 12 exclusively expressed the endothelial cell marker *Egfl7* (encoding a secreted endothelial protein involved in angiogenesis) (**Figure 2D**). They were also the only cells expressing several other genes related to angiogenesis including Lrg*1* (A TGF-beta binding protein), *Mmrn2* (A TGF-beta antagonist), *Rasip1*, *Vegfr2*, and *Sox18*. In addition, they expressed *Selp* (P selectin) and *Icam2*, both involved in endothelial recruitment of leukocytes. The cells of Cluster 13 expressed marker genes for pericytes, including *Rgs5* (**Figure 2D**), a hypoxia-inducible G-protein regulatory subunit involved in angiogenesis and regulation of leukocyte extravasation.

Monocytes

Monocyte lineage cells comprised 8.52% of our samples. The cells of Clusters 8 and 9 uniquely expressed many monocyte marker genes, including *Csf1r* (colony stimulating factor 1 receptor) (**Figure 2E**), *Aif1* (monocyte activation) *c300d* (receptor involved in innate immunity), *Lst1* (lymphocyte proliferation inhibitor), *Clec12a* (negative regulator of monocyte and granulocyte function) and *Ccl2* (macrophage chemoattractant). Cluster 8 cells also exclusively expressed macrophage-specific markers, such as *Adgre1* (F4/80 antigen) (**Figure 2E**), *Ccl3* (MIP1alpha) and *Mrc1* (macrophage mannose receptor). Many but not all cells in Cluster 9 preferentially expressed *Itgax* (mature dendritic cell marker) (**Figure 2E**) and *Cd209a* (dendritic cell adhesion molecule), consistent with dendritic cell identity. The non-macrophage, non-dendritic cell monocytes were a mixed population of

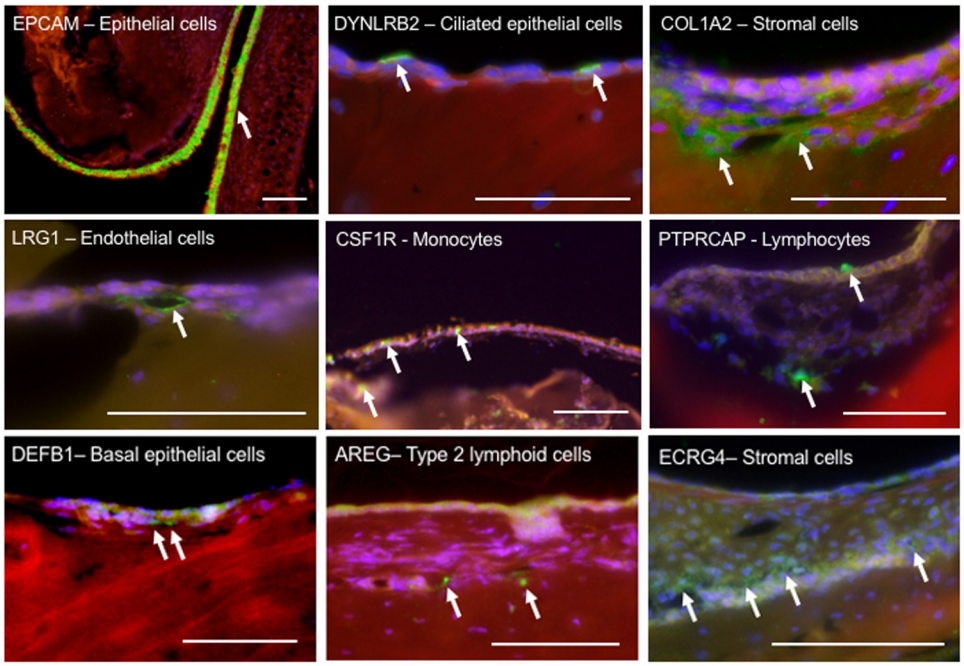

FIGURE 3 | Immunohistochemical localization of select proteins encoded by marker genes, used to identify cell types in the ME mucosa. Paraffin sections were labeled with phalloidin (red), DAPI (blue) and Alexa 488-conjugated secondary antibodies (green). The upper six panels represent marker genes used to identify cell types known to be present in the ME. The three lower panels represent less expected findings: DEFB1 expression in basal epithelial cells; AREG indicating type II lymphoid cells; and ECRG4, often expressed in epithelia, in stromal cells. Scale bars represents 100 μm.

inflammatory (*Ccr2*$^{+}$, *Ly6C2*$^{+}$) and resident, homeostatic (*Cx3cr1*$^{+}$, *Ly6C2*$^{-}$) phenotypes (Gordon and Taylor, 2005).

Lymphocytes

The lymphocytes of Clusters 10, 14, and 15 (comprised 6.2% of our samples. All exclusively expressed a murine lymphocyte-specific gene *Ptprcap* (encoding a key regulator of lymphocyte activation) (**Figure 2F**). Cluster 10 cells also expressed *Cd2* and *Cd28* (**Figure 2F**), markers of both T- and NK-cells. The cells of Cluster 14 did not express specific T-cell or B-cell markers. However, they exclusively expressed *Areg* (**Figures 2F**, **3**), an immunoregulatory member of the EGF family which is produced by type 2 innate lymphoid cells (ILC2s) (Zaiss et al., 2015). Consistent with an ILC2 phenotype, they also expressed *Il7r* and *Thy1*, *Il13*, and *Gata3* (Gasteiger et al., 2017). Cluster 15 cells expressed B-cell markers including *Cd19*, *Cd79a* (**Figure 2F**) and *Cd79b* (involved in B-cell antigen recognition), *H2-dmb2* (a B-cell class II molecule), *Mzb1* (which regulates Ca^{2+} stores to diversify B-cell function).

The expression of selected genes used to identify ME cell types is further illustrated by immunohistochemical labeling in **Figure 3**.

Differential Expression of Genes by ME Cell Clusters

The above analysis employed marker genes to identify cell types in our ME samples. However, the majority of the genes that were significantly differentially expressed between clusters, and which defined them in PCA analysis, were not markers for a given cell type. A total of 2,207 genes were differentially expressed between Seurat t-SNE clusters. For purposes of illustration, **Figure 4** shows a heat map of the top 5 genes that were differentially regulated between each of the various clusters, and that contributed to cluster generation. It can be seen from the figure that most clusters expressed gene sets that clearly differentiated them from other cell groups. Genes that were highly expressed by different ME cell types, either exclusive to that type (as defined previously) or strongly preferentially, are described below.

Epithelial Cells

Many of the genes exclusively expressed by cells in all five ME epithelial populations are involved in fluid or solute regulation, including *Aqp5*, *Cldns 3, 4, and 7*, *Fxyd3*, *Kcnj16*; *Atp1b1*, *Fxyd3* and *Slc6a1*.

The cells of Clusters 0, 1, and 6 appeared to be closely related and expressed relatively few genes exclusively. Rather, this group of clusters expressed genes in common, often exhibiting relative differences in expression. A number of genes were expressed in these clusters in a gradient, with the descending order 1, 6 and 0. This included *Muc1* (**Figure 2B**), *Muc5b*, *Muc16*, *Tff2* (Trefoil factor 2, mucin stabilization gene), *Reg3g* (secreted lectin), as well as *Lyz2* (lysozyme) and *Ltf* (lactotransferrin), both antimicrobials. Also expressed with this gradient were *Agr2* (anterior gradient 2) involved in mucin assembly and *Mgst1* (microsomal glutathione S-transferase 1) involved in leukotriene and prostaglandin synthesis. These gene gradients

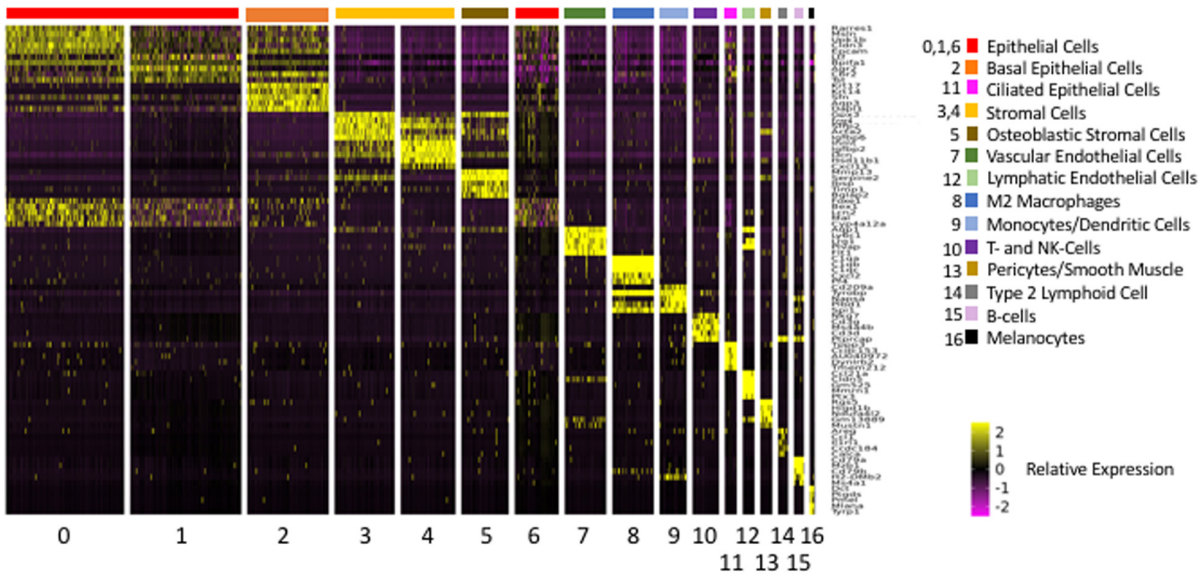

FIGURE 4 | Heatmap illustrating the 5 most differentially regulated genes for each of the 17 Seurat cell clusters. Most clusters were clearly delineated by the differential gene expression. However, three epithelial clusters (0, 1, and 6) showed somewhat overlapping patterns of expression.

are consistent with Cluster 1 cells exhibiting the highest level of secretory activity. Cluster 1 cells also expressed high levels of *Upk1b*, involved in the stabilization and strengthening of apical cell membranes, suggesting presence at the luminal surface of the mucosa.

Genes expressed with an opposite gradient, highest in Cluster 0 and lowest in Cluster 1, included *Bcam* and *Igfbp5*, involved in ECM binding, and *Sftpd* (**Figure 2B**) encoding surfactant protein D. Genes that defined Cluster 6 included *Cyp4a12a* (iron binding oxyreductase), *Mal* (vesicle trafficking from Golgi), *Lcn2* (iron sequestration), *Bex1* (growth factor signaling) and *Foxe1* (transcription factor involved in TGF and WNT regulation). However, these genes were also expressed in Clusters 0, at higher levels than in Cluster 6, and to a lesser extent in Clusters 1 and 2 (see **Figure 4**).

The basal epithelial cells of Cluster 2 cells strongly expressed *Sfn* (a regulator of cell signaling and cell cycle), *Aqp3*, *Dapl1* (G coupled receptor activity), and *Anax8*. Aquaporin 3 is found in the basolateral membranes of kidney collecting duct cells, where it provides a pathway for water to exit these cells. This may play a similar role in the exit of water from the ME mucosal epithelium at its basal surface. Annexin 8 is a calcium binding protein found in mature and functional epithelial cells, where it participates in exocytosis. Interestingly, basal epithelial cells were also the only ME cells to strongly express *Defb1*, encoding the antimicrobial, beta defensin 1 (**Figure 3**).

In addition to many genes related to cilia, the ciliated epithelial cells of Cluster 11 exclusively expressed *Muc4*, encoding a membrane mucin that can activate ERBB2 and stimulate epithelial proliferation. They also preferentially expressed an unusually high number of genes for which no function has been well described, including among others *Tmem212*, *Ccdc153*, *C9orf116*, *Fam183b*, *Sec14l3*, and antisense IncRNA *AU40972*.

Stromal Cells

Cluster 3 was distinguished from other clusters by significantly higher levels of expression of growth regulators, including *Ecrg4* (epithelial cell growth regulator) (**Figures 2C**, **3**) which in other tissues is often expressed in epithelial cells (Kurabi et al., 2013), *Sfrp2* (Wnt signaling modulator), *Serpinf1* (angiogenesis and cell differentiation inhibitor) and *Aspn* (TGFß and BMP inhibitor).

Cluster 4 exclusively expressed *Adam33* (cell−ECM interactions) (**Figure 2C**), *Dpt* (ECM assembly) and *Col28a1* (collagen chain trimerization). The cluster preferentially expressed other genes related to ECM generation: including *Gpc6* (growth factor and ECM receptor), *Dcn* (ECM assembly), *Mfap4* and *Mfap5* (ECM proteins); as well as genes involved in defense against infection: *Cxcl13* (anti-microbial, B-cell chemoattractant) and *Adm* (antimicrobial and fluid regulation).

The cells of Cluster 5 strongly expressed *Mmp13* (ECM breakdown), *Serpine2* (regulator of cell signaling) and *Timp1* (MMP inhibitor). They also exclusively expressed several genes consistent with osteoblast function, including *Bglap* (an abundant Ca-binding bone protein) (**Figure 2C**), *Bglap2* (a hormone secreted by osteoblasts), *Ibsp* (a major structural protein in bone) and *Sfrp4* (involved in bone morphogenesis), as well as *Tnc* (ECM protein tenascin C), *Podnl1* (collagen binding), and *Ackr4* (a decoy receptor that inactivates cytokines).

Endothelial Cells

Of the two groups of endothelial cells, Cluster 7 strongly expressed *Aqp1*, *Ly6c1* (an immunocyte antigen also expressed by endothelial cells), *Lrg1* (TGFß receptor binding) and *Plvap* (microvascular permeability). They exclusively expressed *Flt1* (VEGFR1) (**Figure 2D**), *Aplnr* and *Vwf (Von Willebrand factor)*, consistent with vascular endothelium, as well as the scavenger cytokine receptor *Ackr1*. Cluster 12 cells exclusively

expressed *Prox1 (a homeobox protein)*, *Flt4 (VEGF receptor 3)* and *Reln (Reelin),* all markers for lymphatic endothelial cells, as well as *Ccl21a* (T-cell chemotaxis), *Cldn5* (tight junction protein), *Gm525* (unknown function), *Ptx3* (angiogenesis and inflammation), *Mmrn1* (a factor V/Va receptor) (**Figure 2D**) and the cytokine scavenger receptor gene *Ackr2*.

Pericytes

The pericytes of Cluster 13 exclusively expressed three hypoxia-inducible mitochondrial genes involved in regulating the shift between glucose and glycogen metabolism: *Higd1b*; *Ndufa4l2* and *Cox4i2*. They were the only ME cells to express genes involved in regulating vascular tone, including *Des*, *Olf558*, *Myh11*, *Myocd* and *Kcne4* (Jepps et al., 2015). They also expressed *Cspg4*, encoding a proteoglycan that stimulates endothelial cell motility during microvascular morphogenesis and *Ephx3*, encoding a protein involved in water permeability barriers. They strongly expressed *GM13889* (unknown function) and *Mustn1* (muscle development).

Macrophages

The macrophages of Cluster 8 preferentially expressed genes observed in M2 (alternatively activated) macrophages, such as those encoding the complement components *C1qa* (**Figure 2E**), *C1qb* and *Ciqc* and the fractalkine receptor *Cx3cr1* (Italiani and Boraschi, 2014). They also strongly expressed *Cxcl2* (macrophage inflammatory protein 2), *Pf4* (neutrophil and monocyte chemotaxis) *Tyrobp* (neutrophil activation), *Plbd1* (hydrolase activity) and *Spi1* (macrophage differentiation). Interestingly, none of the cells in this clusters expressed the mature macrophage marker *Itgam* (MAC-1), but many expressed *Cd33*, characteristic of immature macrophages.

Dendritic Cells/Monocytes

Most of the cells in Cluster 9 preferentially expressed *Itgax* (mature dendritic cell marker) and *Cd209a* (dendritic cell adhesion molecule), consistent with dendritic cell identity. However, these cells also expressed the NK gene *Klrk1* (**Figure 2E**). This indicates that they are primarily NK dendritic cells, which possess cytotoxic capability. These cells are usually present as a small subset of dendritic cells in blood and tissue (Chan et al., 2006), but appear to represent about 40% of dendritic cells ($Itgax^{+}$) in the ME. In common with Cluster 8, the dendritic cells and monocytes of Cluster 9 strongly expressed *Tyrobp*, *Plbd1* and *Spi*. They also exclusively expressed *Cd209a* (pathogen receptor). As noted above, less differentiated monocytes expressed genes consistent with either the classical (pro-inflammatory) or resident (homeostatic) phenotypes.

Lymphocytes

Many of the lymphocytes of Clusters 10 expressed the T-cell receptor genes *Cd3d* and *Cd3g*, as well as *CD3e* and *Cd3z*, indicating that they are gamma/delta T-cells. Consistent with this identity, very few expressed *Cd4*. Gamma/delta T-cells are common in mucosal and other barrier tissues where they serve as part of the front-line defense against infection. Many also expressed *Nkg7* (a natural killer cell granule protein) suggesting a cytotoxic phenotype. A small subpopulation expressed *Cd8a* and *Cd8b1*. *Cd8ab*-positive gamma-delta T-cells have been identified as a unique cytotoxic population that is negatively correlated with disease states (Kadivar et al., 2016). The larger population of $Cd8^{-}/Cd4^{-}$ cells are known as double-negative T-cells. In other tissues, the majority of double-negative T-cells bear the alpha/beta receptors consistent with cognate immunity (Antonelli et al., 2006). However, in the ME mucosa the majority appear to bear the gamma/delta receptor more consistent with innate immune function. Gamma/delta T-cells are also involved in M2 macrophage polarization (Mathews et al., 2015). Cluster 10 cells also strongly expressed *Ms4a4b*, a negative regulator of T-cell proliferation.

The ILC2 cells of Cluster 14 type exclusively expressed *Il5* and *Il13*, Th2 cytokines associated with this cell type, as well as *Il1rl1* and *Icos*, which have been associated with helper cell function, and *Cxcr6*, associated with memory, naïve ($Cd28^{+}$) and regulatory ($Il7r^{+}$) T-cells. They also strongly expressed, *Il1rl1* (possibly helper T-cell function), *Ccdc184* (unknown function), and Calca (calcium regulation, antimicrobial).

The B-cells of Cluster 15 expressed many genes related to B-cell function, including *Cd22* (essential for B-cell—B-cell interactions); *Dank1* (mobilization of intracellular B-cell stores); *Spi6* (B-cell development); *Pou2af1* (essential for B-cell response to antigens), *Ms4a1* (B-cell development) and various Fc receptor genes involved in B-cell activation. They also expressed *Pax5*, involved in early but not late B-cell development, suggesting that ME B-cells are not fully mature. A small number of cluster cells expressed *Jchain*, involved in the production of secretory factor.

In addition to evaluating differentially expressed genes, we applied an analysis of the GO: biological processes the genes for which were most highly expressed by different cell clusters. Not surprisingly the results summarized in **Table 3**, are largely consistent with functions that can be inferred from the differentially regulated genes presented above.

Expression of Innate Immune Genes by ME Cell Types

The genes reviewed above were identified based purely on differential expression across cell clusters. In order to evaluate the expression of genes specifically related to OM, we first assessed genes related to innate immunity across ME cell clusters and types. Acute OM in the average child resolves in less than one week (Little et al., 2001). This is not sufficient time to mount a robust cognate immune response, which implies that normal resolution of acute OM is mediated by innate immunity. Indeed, studies in mice with deletions of individual genes for innate immune receptors or effectors have found that, while lack of some genes leads to more severe deficits in recovery from bacterial OM, virtually all show a deficit (Kurabi et al., 2016). This finding indicates that the innate immune system participates in normal OM recovery, and that the genetic machinery with which to initiate innate immunity resides in the cells of the normal ME. We therefore evaluated the expression of genes in Mouse Genome Informatics GO category 0045087 "Innate Immunity." Out of 809 genes in the category, expression of 805 was detected in cells of the normal ME.

TABLE 3 | Single-cell cluster enrichment of GO: biological process.

GO category	*P*-value
Cluster 0 (Epithelial cells)	
Negative regulation of cell motility	2.0631e−7
Negative regulation of cell migration	9.0561e−7
Extracellular matrix organization	8.8733e−8
Negative regulation of cellular component movement	3.3807e−7
Negative regulation of locomotion	6.5930e−7
Cluster 1 (Epithelial cells)	
Extracellular matrix assembly	0.0000088218
Collagen metabolic process	0.0000034043
Extracellular matrix organization	4.0817e−9
Extracellular structure organization	2.7391e−8
Cell growth	0.0000029102
Cluster 6 (Epithelial cells)	
Protein trimerization	0.00018877
Cellular response to amino acid stimulus	0.000026320
Cellular response to acid chemical	0.000072229
Lung development	0.00018877
Respiratory tube development	0.00022526
Cluster 2 (Basal epithelial cells)	
Collagen biosynthetic process	0.000040927
Collagen metabolic process	0.00018409
Protein localization to plasma membrane	0.000059560
Bone mineralization	0.000055506
Transforming growth factor beta receptor signaling pathway	0.000045449
Cluster 11 (Ciliated epithelial cells)	
Axoneme assembly	0
Cilium movement	0
Cilium or flagellum-dependent cell motility	1.9154e−10
Cilium-dependent cell motility	1.9154e−10
Axonemal dynein complex assembly	1.9154e−10
Cluster 3 (Stromal cells)	
Collagen fibril organization	0.0000091862
Collagen metabolic process	0.0000037847
Protein processing	0.000068852
Extracellular matrix organization	4.5168e−9
Extracellular structure organization	7.6653e−8
Cluster 4 (Stromal cells)	
Collagen fibril organization	0.0000043023
Embryonic skeletal system development	0.000014268
Negative regulation of cellular response to growth factor stimulus	0.0000039117
Collagen metabolic process	0.0000068214
Extracellular matrix organization	3.7315e−11
Cluster 5 (Stromal cells)	
Collagen fibril organization	1.5268e−9
Regulation of bone mineralization	5.1255e−8
Regulation of biomineral tissue development 6.3049e−9	
Bone mineralization	7.6798e−10
Biomineral tissue development	1.7298e−11
Cluster 7 (Vascular endothelial cells)	
Negative regulation of cellular component movement	2.5616e−8
Regulation of plasma membrane bounded cell projection	4.2233e−8
Regulation of cell projection organization	5.2664e−8
Angiogenesis	6.4595e−11
Blood vessel morphogenesis	9.2663e−11
Cluster 12 (Lymphatic endothelial cells)	
Endothelial cell differentiation	0.0000057055
Endothelium development	0.0000080317
Sprouting angiogenesis	0.000010961
Negative regulation of angiogenesis	0.0000091829
Negative regulation of blood vessel morphogenesis	0.000013967
Cluster 13 (Pericytes)	
Membrane repolarization	0.000084352
Actin-mediated cell contraction	0.0000096969
Actin filament-based movement	0.000018559
Notch signaling pathway	0.0000090719
Regulation of heart contraction	0.00017208
Cluster 8 (Macrophages)	
Tumor necrosis factor production	5.0342e−8
Regulation of tumor necrosis factor production	3.3417e−8
Cellular response to molecule of bacterial origin	4.9622e−8
Response to molecule of bacterial origin	2.1447e−8
Response to organonitrogen compound	3.3417e−8
Cluster 9 (Monocytes, Dendritic cells)	
Cellular response to radiation	0.000033926
Activation of innate immune response	0.000071442
Tumor necrosis factor production	0.000017344
Regulation of tumor necrosis factor superfamily cytokine production	0.000043714
Tumor necrosis factor superfamily cytokine production	0.000043714
Cluster 10 (T-cells, NK cells)	
T-cell receptor signaling pathway	5.3595e−7
Positive regulation of leukocyte cell-adhesion	3.9513e−7
Positive regulation of lymphocyte activation	2.3319e−7
T-cell differentiation	9.7306e−8
T-cell activation	4.4670e−12
Cluster 14 (ILC2s)	
Positive regulation of leukocyte differentiation	0.0000018086
Regulation of lymphocyte differentiation	0.0000011529
Positive regulation of hemopoiesis	0.0000013987
Positive regulation of lymphocyte activation	0.000002159
Regulation of hemopoiesis	1.1023e−7
Cluster 15 (B-cells)	
B cell receptor signaling pathway	2.9347e−11
Regulation of B cell proliferation	7.1741e−8
B cell proliferation	3.0189e−8
B cell activation	6.8834e−15
Antigen receptor-mediated signaling pathway	2.8936e−9
Cluster 16 (Melanocytes)	
Sister chromatid segregation	8.2230e−10
DNA packaging	2.8980e−9
DNA conformation change	5.2742e−10
Chromosome segregation	9.2013e−11
Nuclear chromosome segregation	1.4193e−9

(Continued)

The five GO categories with the highest enrichment ratios are listed for each single-cell cluster.

For a few genes, there was broad expression across all ME cell types. These included *Bipfa1* (contributes to airway surface liquid homeostasis and proper clearance of mucus) as well as three ribosomal proteins with innate immune subfunctions: *Rpl13a* (suppression of inflammatory genes); Rpl39 (viral gene transcription) and Rps19 (suppression of interferon production).

For a total of 520 innate immune genes, there were significant expression differences between cell types. A heat map illustrating the expression of the 520 genes across all ME cells is presented in **Supplementary Figure S1**, while **Figure 5** shows the expression of a more readily visualized set of 109 innate immune genes, those with the most robust expression, ordered by cell type. **Table 4** lists the most differentially expressed innate immune genes for each cell cluster. All clusters expressed distinct sets of innate immune genes.

The epithelial cells of Cluster 0 expressed *Lbp* (component of the endotoxin receptor), *Lcl2* (antibacterial protein) *Sftpd* (surfactant protein D), *Xrcc5* (antiviral response) *Cd55* (negative complement regulator) and *Hmgb2* (innate immune DNA/RNA receptor). They also expressed genes related to leukocyte recruitment and activation, including *Csf1* (macrophage differentiation) and *Cxcl16* (T-cell recruitment). Cluster 1 epithelial cells expressed the genes for the anti-microbials lactoferrin and REG3γ, and the interferon-stimulated antivirals CD25 and ISG20. The basal epithelial cells of Cluster 2 expressed several complement genes, as well as *Axl* (TLR inhibition), *Rab20* (antibacterial response), and the anti-viral gene *Ifit1*. Cluster 6 epithelial cells expressed *Sftpd*. The ciliated epithelial cells of Cluster 11 expressed a small set of diverse innate immune genes including *Hist1b2bc* (antibacterial responses), *Il1rn1* (receptor-blocking inhibitor of IL1ß), *Ifit1,* and *Aqp4*.

Innate immune genes expressed by all stromal cells of Clusters 3, 4 and 5 included *Colec12*, (antimicrobial response), *Mmp2* (positive regulator of inflammatory NFκB signaling), *Rarres2* (chemotactic and anti-inflammatory factor), and *Serpinb1* (negative complement regulation). Clusters 3 and 4 uniquely expressed several complement factors and *Lgals9* (soluble, negative regulator of T- and NK-cells). Cluster 4 expressed the complement factor gene *C2*. Clusters 3 and 5 expressed *Cfn* (negative complement regulator), while Cluster 5 expressed *Tgfb1* (multifunctional, including inhibition of T-cell Th1, Th2 and cytotoxic phenotypes) and *Tspan6* (negative regulator of innate immunity).

The vascular endothelial cells of Clusters 7 expressed *Adam15* (epithelial−T-cell interactions) *Cav1* (T-cell activation, negative regulation of TGFß1), *Cebpg* (IL4 gene activation), *Dab2ip* (participates in TNF, IFN and LPS signaling pathways), *Iigp1* (IFN-inducible antimicrobial), *Irf1* (IFN production), *Irgm1* (IFN-induced negative regulator of mucosal immune responses), *Vim* (viral and bacterial attachment) and *Samhd1* (response to virus, mediation of TNF response).

The lymphatic endothelial cells of Cluster 12 strongly expressed *Tspan6*, *Mrc1*, *Ccl21a* (all described above) as well as *Bst2* (antiviral), *Arrb2* (involved in multiple signaling pathways including that of CCL19), *Ptx3* (positive regulation of innate response to pathogens) and *Serinc3* (resistance to viral infection).

The pericytes of Cluster 13 expressed the complement gene *C1s1*, *Cav1* (negative regulator of inflammation) and *Ifitm1*.

Some of the innate immune genes expressed by Cluster 8 macrophages are marker genes for this cell types, as noted above. Also expressed preferentially by this cell type were nine genes related to pathogen receptor signaling, a total of ten chemotactic chemokine genes, four genes related to complement response, six immune modulators including four negative regulators and the antibacterial gene *Scl11a1*.

Cluster 9 monocytes and dendritic cells preferentially expressed a subset of the genes expressed by Cluster 8 macrophages, but also expressed two genes encoding NK cell lectins related to cytotoxicity, *Klrd1* and *Klrk1*; *Lgals3* (PMN and mast cell activation, macrophage chemotaxis); *Rnase6* (antibacterial); *Samhd1* (antiviral responses); *Sirpa* (negative regulation of dendritic cells and phagocytosis); Slamf7 (killer cell activation); and *Unc93b1* (intracellular TLR transport).

The T-cells and NK cells of cluster 10 strongly expressed *Coro1a (required for lytic granule secretion from cytotoxic cells)*, *Klrd1*, *Klrk1*, *Ccl5* (leukocyte chemoattractant or chemotaxis inhibitor, depending on splicing), *Hmgb2* (innate immune DNA/RNA receptor), *Rpl14a* (ribosomal protein upregulated by endotoxin, Ceppi et al., 2009) and *Txk* (involved in Th1 cytokine production). The ILC2s of Cluster 14 expressed *Cor1a*, *Samhd1*, *Ccl1* (monocyte chemotaxis), *Arg1* (promotes acute type 2 inflammation), and *C1qbp* (involved in multiple infection and inflammatory responses). The B cells of Cluster 15 expressed *Cd74* (MIF receptor), *Coro1a*, *Irf8* (regulates IFN responses), *Ly86* (involved in endotoxin response with TLR4), *Ptpn6* (hematopoietic cell signaling), *Slamf7* (NK cell activation) and *Unc93b1*.

The melanocytes of Cluster 16 strongly expressed *Vim*, *Gapdh* (in innate immunity, IFNg-induced transcript-selective translation inhibition) and *Mif* (regulation of macrophage function).

DISCUSSION

The results of this study provide, for the first time, a molecular landscape of the cells that make up the normal mucosal lining of the ME prior to OM. They also identify the resting ME cells that express major determinants of innate immunity. As noted above, innate immunity is responsible for the normal resolution of OM (e.g., Underwood and Bakaletz, 2011; Kurabi et al., 2016). The immediate response provided by the cell of the normal ME is critical to initiating this first line of defense against infection. We found that the cells of the ME have distinctly different potential capacities to contribute immediately to innate immunity. Our results also provide a baseline against which to measure the responses of ME cells to infection in future studies.

Cell Types of the Normal ME

Seurat PCA analysis of 6,370 ME cells identified 17 cell clusters, each of which displayed a distinct set of genes. The expression of key genes by most of these clusters correspond to cell types that

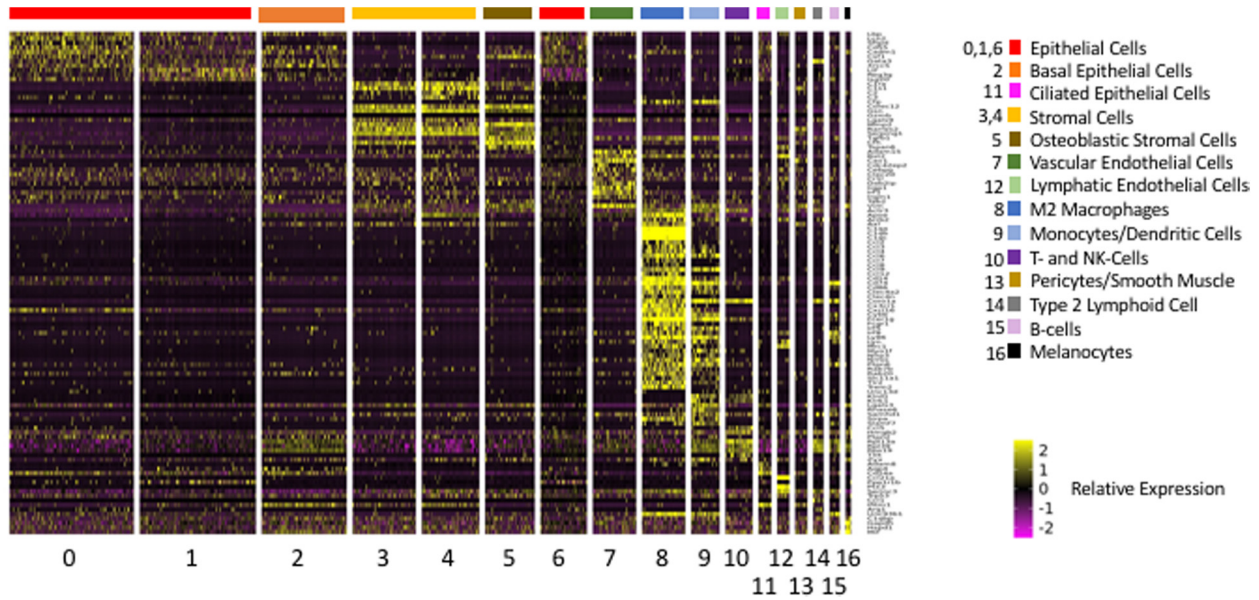

FIGURE 5 | Heatmap illustrating the expression of the 109 most differentially regulated innate immune genes, arranged by cell cluster in which they are differentially expressed. Cluster 8 cells (macrophages) expressed the greatest number.

have been observed previously in the ME, while others identify cells not previously known to be present.

Epithelial Cells

As noted above, previous authors have proposed five (Lim and Hussl, 1969; Lim, 1979) or six (Hentzer, 1976) morphological categories of ME epithelial cells: basal, intermediate, non-secretory, intermediary secretory, secretory and ciliated epithelial cells. Our transcriptome data are more consistent with five subtypes. Of the five clusters of cells expressing epithelial markers, basal (Cluster 2) and (Cluster 11) ciliated epithelial cell clusters were clearly identified. The three remaining clusters, 0, 1, and 6, were less differentiated by gene expression and presumably less specialized. However, Cluster 1 showed the highest expression of genes encoding secreted factors, including mucins, indicating that this cluster likely consists of fully developed secretory epithelial cells. Secretory genes were expressed at progressively lower levels in Clusters 6 and 0. However, Cluster 0 exclusively expressed surfactant D, also suggestive of an epithelial surface location, and the most innate immune genes of any epithelial type, indicating a prominent role in initial defense of the ME. This cluster may thus represent the morphologically defined "non-secretory" surface epithelial cells. Cluster 6 gene expression was intermediate between that of Clusters 0 and 1, consistent with an intermediate epithelial cell capable of transitioning into either of these two phenotypes.

Regarding the two disparate origins of ME epithelial cells noted by Thompson and Tucker (2013), neural crest versus branchial arch endoderm, there are no recognized adult gene markers for cells of neural crest origin. The small number of melanocytes observed in Cluster 16, which were scattered through epithelial clusters in the Seurat analysis and are assumed to be of neural crest origin (Lin and Zak, 1982), did not express epithelial markers. In addition, we saw no categories of ME epithelial cells that might reasonably be supposed to correspond to this division. It seems likely that dissection of the ME mucosa from the corresponding regions prior to single-cell analysis would be required to determine whether different embryologic origins correspond to any transcriptome and/or functional variations.

Stromal Cells

Based on their morphology, ME stromal cells have generally been classified as fibrocytes, with little further distinction. Clusters 3, 4, and 5 were identified as stromal by the expression of many ECM genes. Cluster 5, expressing bone formation genes, appears to correspond to osteoblastic cells. The ME has a strong propensity to generate new bone beneath the stromal layer during OM (Cayé-Thomasen et al., 1999). Cluster 3 was characterized by preferential expression of genes targeting tissue growth, including that of epithelial cells, while cluster 4 expressed genes encoding antimicrobials. These clusters indicate the presence of two additional classes of stromal cells in the ME, cell types not previously recognized on morphological or histochemical grounds.

Vascular Cells

Blood vessels, although sparse in the ME, have long been recognized (Lim, 1979). Therefore the vascular endothelial cells of Cluster 8 were to be expected. Morphological studies have also noted the presence of lymphatics in the ME based (Lim and Hussl, 1975), and drainage from the ME to lymph nodes of the neck has been demonstrated (Galich, 1973; Lim and Hussl, 1975),

TABLE 4 | Single-cell Cluster Expression of Innate Immune Genes.

Gene	Protein	Innate immune function
Cluster 0 (Epithelial cells)		
Lbp	LPS Binding Protein	Endotoxin receptor component
Hmgb2	High mobility group box 2	Innate immune DNA/RNA receptor
Csf1	Colony stimulating factor 1	Macrophage differentiation
Cxcl16	Chemokine CXCL16	T-cell recruitment
Ptpn2	PTP2	T-cell activitation, tissue growth
Cadm1	CADM1	NK and T-cell regulation by other cell types
Cd24a	CD24A	B-cell differentiation, tissue growth
Lcn2	Lipocalin2	Antibacterial
Sftpd	surfactant D	Antibacterial, surfactant
Xrcc5	DNA repair XRCC5	Antiviral
Cd55	DAF	Negative complement regulator
Cluster 1 (Epithelial cells)		
Cd25	IL2 receptor α	Control of regulatory T-cell, tissue growth
Ppp1r1b	PPP1R1B	Regulatory T-cell activation, cell survival
Ltf	Lactoferrin	Antimicrobial
Reg3γ	REG3γ	Antimicrobial
Isg20	ISG20	IFN-stimulated antiviral
Cluster 6 (Epithelial cells)		
Sftpd	surfactant D	antibacterial, surfactant
Cluster 2 (Basal epithelial cells)		
Lbp	LPS Binding	endotoxin receptor component
Hmgb2	High mobility group box 2	innate immune DNA/RNA receptor
Cadm1	CADM1	NK and T-cell regulation by other cell types
Gata3	GATA3	Immune cell differentiation, tissue growth
Rab20	RAB20	endocytosis, antibacterial responses
Xrcc5	DNA repair XRCC5	antiviral response
Ifitm1	IFITM1	Inhibition of viral entry
Rpl39	Ribosomal protein L39	Viral gene transcription
Rpl13a	Ribosomal	Suppression of inflammation
Rps19	Ribosomal	Suppression of interferon
Axl	AXL receptor tyrosine kinase	TLR inhibition
Cd55	DAF	negative complement regulator
Cluster 11 (Ciliated epithelial cells)		
Adam8	ADAM8	leukocyte migration
Cd24a	CD24A	B-cell differentiation, tissue growth
Ifitm1	IFITM1	inhibition of viral entry
Aqp4	Aquaporin4	water permeability,response to inflammation
Clusters 3, 4, 5 (All stromal cells)		
Gsn	Gelsolin	TLR endocytosis
Rarres2	Chemerin	Chemotactic, anti-inflammatory
C1ra	Complement C1 component	Complement response
Colec12	Collectin-12	Antimicrobial responses
Serping1	Serpin G1	Negative complement regulator
Axl	AXL receptor tyrosine kinase	TLR inhibition
Cluster 3 (Stromal cells)		
C1s1	Complement C1 component	Complement response
Cr1l	C1 receptor like	Complement activation
Samhd1	SAMHD1	Mediates TNF inflammatory responses
Lgals9	Galactin9	Negative regulation of T- and NK-cells
Ifitm1	IFITM1	Inhibition of viral entry
Clec2d	CLEC2D	Protection against NK cell lysis
Cluster 4 (Stromal cells)		
C1s1	Complement C1 component	Complement response
C2	Complement C2	Complement response
C3	Complement C3	Complement response
Apoe	Apolipoprotein E	Leukocyte regulation, lipid metabolism
Zyx	Zyxin	Viral pathogen receptor signaling
Bst2	Tetherin	Antiviral
Serinc3	Serine incorporator 3	Antiviral
Trp53	P53	Antiviral
Ifitm1	IFITM1	Inhibition of viral entry
Lgals9	Galectin 9	Negative regulator of T- and NK-cells
Cluster 5 (Stromal cells)		
Lgals3	Galectin 3	Acute inflammation activator
Csf1	Colony stimulating factor 1	Macrophage differentiation
Trp53	P53	Antiviral
Tgfb1	TGFβ1	Multifunctional, immunocyte inhibition
Tspan6	Tetraspanin 6	Negative innate immune regulator
Cluster 7 (Vascular endothelial cells)		
Vim	Vimentin	Viral and bacterial attachment
Samhd1	SAMHD1	Mediates TNF inflammatory responses
Dab2ip	DAB2 interacting protein	TNF, IFN and LPS signaling pathways
Irf1	IFN response factor	IFN production
Adam15	ADAM15	Epithelial−T-cell interaction
Cav1	Caveolin 1	T-cell activation, TGFß1 inhibition
Iigp1	IFN-inducible G Protein 1	IFN-inducible antimicrobial
Cebpg	CEBPG	IL4 gene activation

(Continued)

TABLE 4 | Continued

Gene	Protein	Innate immune function
Irgm1	IRGM1	Mucosal immune response inhibition
Cluster 12 (Lymphatic endothelial cells)		
Mrc1	Mannose receptor C1	Pathogen neutralization
Ptx3	Pentraxin 3	Positive regulation of innate immunity
Ccl21	Chemokine CCL21	T-cell chemotaxis
Arrb2	Arrestin β2	Cytokine/chemokine signaling pathways
Bst2	Tetherin	Anti-viral
Serinc3	Serine incorporator 3	Antiviral
Tspan6	Tetraspanin 6	Negative innate immune regulator
Cluster 13 (Pericytes)		
C1s1	Complement C1 component	Complement response
Cav1	Caveolin 1	T-cell activation, TGFß1 inhibition
Ifitm1	IFITM1	Inhibition of viral entry
Cluster 8 (Macrophages)		
Tlr2	Toll-like receptor 2	Pathogen receptor
Cd14	CD14	LPS receptor component
Ly86	MD-1	LPS receptor component
Nlrp3	NALP3	Pathogen receptor, inflammasome
MyD88	MYD88	TLR signaling adaptor
Mrc1	Mannose receptor C1	Pathogen neutralization
Unc93b1	UNC93B1	Required for TLR DNA recognition
Cfp	Complement factor P	Alternative complement response
C1qa,b,c	Three C1q A-chains	Complement response
Irf5, Irf8	IFN response factors	IFN production
Cd86	CD86	T-cell activation, IL2 production
Actr3	ACTR3	Phagocytosis
Trem2	TREM2	Immune activation in phagocytes
Cd74	CD74	MHC class II antigen processing
Clec4a2	Lectin-like immunoreceptor	Antigen presentation
Apoe	Apolipoprotein E	Macrophage, T- and NK-cell regulation
Arrb2	Arrestin β2	Cytokine/chemokine signaling pathways
Ccl2	Chemokine CCL2	Macrophage chemotaxis
Ccl3	Chemokine CCL3, MIP1α	Monocyte, PMN chemotaxis
Ccl4	Chemokine CCL4, MIP1β	NK cell, monocyte chemotaxis
Ccl5	Chemokine CCL5, RANTES	T-cell chemotaxis
Ccl9	Chemokine CCL9, MRP2	Dendritic cell chemotaxis
Cxcl16	Chemokine CXCL16	T-cell, NK-cell chemotaxis
Coro1a	Coronin 1A	Lytic granule secretion
Cx3cr1	Fractalkine receptor	T-cell, monocyte chemotaxis
Fcer1g	FCER1γ	IgE receptor component
Lyn	LYN	Diverse immune signaling pathways
Nrros	Negative regulator of ROS	TGFβ1 activation in macrophages
Ptpn6	PTPN6	Hematopoietic cell signaling
Rab20	RAB20	Endocytosis, antibacterial responses
Slc11a1	SLC11A1	Iron transporter, antibacterial
Bst2	Tetherin	Anti-viral
Sirpa	SIRPA	Dendritic cell activation inhibitor
Tgfb1	TGFβ1	Multifunctional, immunocyte inhibition
Axl	AXL receptor tyrosine kinase	TLR inhibition
Rab7b	RAB7B	Negative regulation of TLRs
Cluster 9 (Monocytes, Dendritic cells)		
Cluster 9 cells expressed a subset of genes expressed by the macrophages of Cluster 8: *Cfp, Tgfb1, Vim, Actr3, Ccl6, Ccl9, Cd74, Coro1a, Cybb, Fcer1g, Ly86, Nrros, Ptpn6* and *Unc93b1*. However, they also expressed:		
Myo1f	Myosin 1F	Immune cell motility
Klrd1	KLRD1	MHC recognition by cytotoxic cells
Klrk1	KIRK1	Cytotoxicity of virus-infected cells
Slamf7	SLAMF7	NK cell activation
Lgals3	Galectin 3	Monocyte, macrophage chemotaxis
Rnase6	RNASE6	Antibacterial
Rpl39	Ribosomal protein L39	Viral gene translation
Rps19	Ribosomal protein S19	Viral gene translation
Cluster 10 (T-cells, NK cells)		
Hmgb2	HMGB2	Innate immune DNA/RNA receptor
Txk	TXK tyrosine kinase	Th1 cytokine production
Coro1a	Coronin 1A	Lytic granule secretion
Klrd1	KLRD1	MHC recognition by cytotoxic cells
Klrk1	KIRK1	Cytotoxicity of virus-infected cells
Ccl5	Chemokine CCL5, RANTES	T-cell chemotaxis
Rpl14a	Ribosomal protein 14a	Viral replication and gene translation
Cluster 14 (ILC2s)		
Coro1a	Coronin 1A	Lytic granule secretion
Samhd1	SAMHD1	Mediates TNF inflammatory responses
Arg1	Arginase 1	Promotes acute type 2 inflammation
C1qbp	C1q binding protein	Multiple immune/inflammatory responses
Ccl1	Chemokine CCL1	Monocyte chemotaxis

(Continued)

TABLE 4 | Continued

Gene	Protein	Innate immune function
Cluster 15 (B-cells)		
Ly86	MD-1	LPS receptor component
Unc93b1	UNC93B1	Required for TLR DNA recognition
Cd74	CD74	MHC class II antigen processing
Ptpn6	PTPN6	
Coro1a	Coronin 1A	Lytic granule secretion
Slamf7	SLAMF7	NK cell activation
Irf8	IFN response factor 8	Regulates IFN responses
Cluster 16 (Melanocytes)		
Vim	Vimentin	Viral and bacterial attachment
Mif	MMIF	Pro-inflammatory mediator
Gapdh	GAPDH	Inhibits IFN-induced gene expression

validating lymphatic endothelial cells of Cluster 9 cells. The documentation of capillaries and post-capillary venules in the ME (e.g., Goldie and Hellström, 1990) makes the observation of pericytes in Cluster 13 unremarkable. Gene expression related to hypoxia, contractility and water permeability are consistent with pericyte regulation of vascular tone, based on oxygen tension, and fluid entry into the ME.

Leukocytes

Clusters 8 and 9 expressed monocyte markers, while most Cluster 8 cells also expressed macrophage genes consistent with an M2 (alternatively activated) phenotype. Macrophages have been documented in the normal ME (Takahashi et al., 1989; Jecker et al., 1996), but the M2 phenotype has not previously been appreciated. The dendritic cells and less defined monocytes of Cluster 9 have also been noted before in the ME (Jecker et al., 1996). The expression of genes associated with cytotoxicity by dendritic cells indicates a killer phenotype, not recognized previously at this site. Less differentiated monocytes of the classical and resident phenotypes have also not previously been differentiated in the resting ME.

Cells in Clusters 10, 14, and 15 expressed a lymphocyte marker gene *Ptprcap*. Cluster 10 also expressed T-cell and NK-cell genes, while Cluster 15 expressed genes found in B-cells. All three of these lymphocyte types have been reported from the ME (Takahashi et al., 1989). However, the ILC2s of Cluster 14 were not previously reported to be present in the ME.

The number of leukocytes in the normal ME mucosa has often been reported to be relatively low (e.g., Takahashi et al., 1989), and lymphocytes to be especially uncommon (Jecker et al., 1996). However, we observed a substantial number of leukocytes (14.7%) in our normal ME cell samples. This disparity could be caused by differential survival of cells through the tissue digestion and cellular dispersion processes employed. However, it seems unlikely that leukocytes would be dramatically more resistant to these procedures than other cells. Another potential explanation is the diversity of subtypes and the difficulty of definitively identifying leukocytes. For example, many investigators have used the MAC1 antibody, which labels the *Itgam* gene product present in mature macrophages, to identify these cells. However, we found that few macrophages in the normal ME expressed this gene, since the macrophages were likely M2 cells of incomplete maturity.

It should be noted that not all leukocytes known to be present in the ME were found in this study. Several groups (e.g., Watanabe et al., 1991), including our own (Ebmeyer et al., 2005), have documented the presence of mast cells in the normal ME mucosa. Despite this, we were unable to identify any consistent mast cell gene signatures in our cell samples. For example, the entire family of seven mast cell protease (Mcpt) genes showed no expression in any of our ME cells. Other mast cell markers were either absent or were expressed in various cells that had been identified as other cell types with no consistent pattern. The reasons for this are not clear. The number of mast cells in the ME mucosa is not high, so this could represent a sampling issue. Alternatively, the C57BL/6 mouse used in this study may lack ME mast cells, as compared to the guinea pig or WB/B6F1 hybrid mice used in the above studies. However, it seems most likely that mast cells did not survive the cell dissociation method used in this study. The fragility of mast cells isolated from tissues has been noted by others (Kulka and Metcalfe, 2010).

With the exception of mast cells, we were thus able to identify all of the cell types that have been identified previously in the ME using alternative methodologies. In addition, we added new types not previously identified in the normal tympanic cavity. Finally, we obtained a sufficient number of cells for each type to evaluate their individual transcriptomes. This allowed us to achieve our goal of documenting the differences in cell function, as well as the expression of innate immune genes across ME cell types.

Differential Functions of ME Cell Types

Expression differences identified by clustering analysis and screening of innate immune gene beyond those that specified cell identity, provided clues as to the functional role of cells in the normal ME.

Epithelial Cells

The movement of fluids across the mucosal epithelium into and out of the ME is clearly an important aspect of ME homeostasis, OM pathogenesis and fluid clearance during recovery from infection. As indicated by *claudin* gene expression, the cells of the epithelium are joined by tight junctions. Therefore the expression of genes involved in fluid/solute transport across cell membranes by all epithelial clusters is not unexpected, as is expression of the surface liquid layer homeostasis gene *Bipfa1*. Cluster 1 epithelial cells also expressed many genes consistent with presence at the epithelial surface and with secretory activity, including cell-surface and secreted mucins as well as antimicrobials. Cluster 0 similarly expressed antimicrobials, along with surfactant D and ECM-binding genes, suggesting a possible role in basement membrane interactions and that secretory activity is distributed across more than one epithelial cell type. As noted above, Cluster 6 gene expression overlapped with that of Cluster 0 and 1, suggesting an intermediate

phenotype. The expression of genes related to tissue proliferation by the basal epithelial cells of Cluster 2 are consistent with them being a source of epithelial cells. However, they also expressed beta defensin 1, further evidence that secretory activity is distributed. Assuming that basal cells are located below the epithelial surface, this antimicrobial may defend against bacteria that invade the mucosa. Cluster 11 ciliated cells expressed *Aqp4* and *Muc4*. Altogether, epithelial cells of the ME mucosa appear specialized for fluid transport and secretory activity.

Stromal Cells

The expression of genes by stromal cell clusters was dominated by those related to ECM generation and remodeling. Cluster 3 cells appear also to be specialized for the regulation of epithelial and stromal cell growth, while Cluster 5 cells are likely involved in bone maintenance and remodeling.

Vascular Cells

The vascular endothelial cells of Cluster 7 expressed many genes involved in vascular permeability and fluid transport. They therefore work in combination with epithelial cells as the principle regulators of fluid balance in the ME. Not surprisingly, they also expressed genes involved in the recruitment of leukocytes and angiogenesis. Interestingly, vascular and lymphatic endothelial cells each preferentially expressed a different decoy cytokine receptor, which could serve to limit inflammation. Expression of genes involved in hypoxia responses and in regulating vascular tone is typical of pericytes.

Leukocytes

Not surprisingly, most of the genes preferentially expressed by leukocytes were involved in immune and inflammatory responses. However, the M2 phenotype and expression of negative immune regulators by the macrophages of Cluster 8 are consistent with a homeostatic and anti-inflammatory role, rather than the pro-inflammatory phenotype of classically activated macrophages. Gene expression by dendritic cells and other monocytes of Cluster 9 was similar, although somewhat fewer genes were preferentially expressed. The lymphocyte types of Clusters 10, 14 and 15 preferentially expressed genes consistent with their expected functions.

Innate Immune Genes and the Defense of the ME

Infection of the ME activates an innate immune response extremely rapidly (MacArthur et al., 2013; Hernandez et al., 2015). This initial response is likely based largely on the repertoire of innate immune receptor and effector genes that are expressed by the cells of the normal ME. Disruption of many individual innate immune genes in mice has been shown to reduce the effectiveness of this innate response to infection, and to prolong OM. Moreover, several studies have identified polymorphisms in human innate immune genes that are linked to otitis media proneness in patients (see Kurabi et al., 2016 for a recent review). These studies underscore the importance of innate immunity in the immediate and long-term defense of the ME, which was our rationale for focusing on these genes in ME cell transcriptomes.

As can be seen from **Figure 5**, expression of innate immune genes is distributed across the various cell types of the ME. Epithelial cells appear specialized for the detection and response to pathogens, including the secretion of antibacterial peptides. However, they also expressed genes related to leukocyte recruitment and activation.

Stromal cells expressed several complement factors and pro-inflammatory genes, suggesting potential involvement in active inflammation. They also expressed many negative immune regulators, not only of complement but also of innate immunity in general as well as T- and NK-cells. They thus appear to serve as inhibitory modulators of inflammation to a greater extent than epithelial cells.

Endothelial cells and pericytes expressed several genes involved in the activation of inflammatory pathways and T-cells, but also several negative immune regulators.

The M2 macrophages in the ME expressed by far the most innate immune genes, with an emphasis on pathogen detection, leukocyte chemotaxis, complement activation, and both positive and negative inflammatory regulation. Their phenotype is consistent with immune homeostasis, but also readiness to act in case of infection. Monocytes/dendritic cell gene expression was similar to that seen in macrophages, but cytotoxic genes were additionally expressed.

The lymphocytes of cluster 10 were primarily gamma-delta T-cells that typically have an innate immune function, and consequently expressed several pathogen receptors and innate immune effectors. Cytotoxic T-cells and NK-cells were also present in this cluster. The ILC2s of cluster 14 expressed several genes involved in T-cell regulation and induction of inflammation. The B-cells of cluster 15, as expected, expressed genes related to antibody production.

In addition to individual genes, the GO: biological process gene categories that were most regulated in macrophages and monocytes are all subcategories of the GO category for innate immunity. For the remaining ME cell types, innate immunity was not among the GO categories with the highest degree of regulation. This is not surprising, since unlike macrophages and monocytes, the primary functions of these cells are not innate immunity. However, the fact that they also express many innate immune genes underscores the importance of innate immunity in virtually all ME cell types.

A striking feature of innate immune gene expression in normal ME cells was the large number of negative regulators of immunity and inflammation observed in the transcriptomes of many different cell types, in parallel with to pro-inflammatory genes. This pattern of expression suggests that, while the cells of the ME are primed to respond to infection by generating inflammation and other antimicrobial responses, these processes are actively held in check by immune inhibitory genes to ensure ME mucosal homeostasis. This not only must pro-inflammatory gene products be activated by pathogens at the initiation of

OM, anti-inflammatory genes may need to be downregulated to allow maximally effective innate immunity to defend the ME. Other investigators have noted the importance of endogenous negative regulators in ameliorating OM Pathogenesis (e.g., Li et al., CYLD). Our results add a large number of additional negative regulators which were distributed across diverse ME cell types.

Limitations of the Study

Our analysis of single-cell transcriptomes is subject to a number of methodological limitations. As noted above, the numbers of different cell types recovered is dependent upon the survival of cells through the enzymatic digestion and dispersion techniques. While we were able to document an effect of this for mast cells, the extent to which selection bias may have influenced our other cell populations is not clear. Fortunately, we obtained sufficient numbers of cells in all cell populations to adequately survey gene transcription. However, the proportions of each cell type in our samples should not be taken to represent their relative abundance *in vivo*.

Another limiting effect is related to the limited number of genes that can be recovered from an individual cell. This means that abundant mRNAs are more likely to be represented than scarce transcripts. It has been argued that the detection of scarce mRNAs is stochastic, and that combining the results of 20 or more cells approaches the results of bulk RNASeq (Marinov et al., 2014). However, the possibility that scarcer transcripts were missed in a given cell population must be considered.

Other limitations reflect the nature of gene responses to infection. It is of course certain that the expression of innate immune and other genes by ME cells would change dramatically upon infection, and that some of these changes would be very rapid (MacArthur et al., 2013; Hernandez et al., 2015). Therefore, the roles of ME cells in the initial stage of OM, and beyond, would correspondingly change. Our data reflect only pre-existing mRNAs that may be expressed in readiness for a pathogen challenge. We plan to assess the results of infection on the transcriptomes of ME cell types. This work is in progress, and will be the basis of a future report. We felt that including results from infected ME cells would have made this paper unacceptably long.

CONCLUSION

The results of this study establish, for the first time, the differences that exist between the transcriptomes of cells in the normal ME. They identify not only previously known cell types, but also show the presence of novel cell types and subtypes. The genes that differentiate these cell types provide information on their roles in ME homeostasis, and their ability to respond immediately to infection. The results also provide a baseline from which to assess the molecular responses of ME cells to infection.

DATA AVAILABILITY STATEMENT

The single cell transcriptome data is available in GEO (GSE146244, https://www.ncbi.nlm.nih.gov/geo/query/acc.cgi?acc=GSE146244).

ETHICS STATEMENT

The animal study was reviewed and approved by the Institutional Animal Care and Use Committee of the VA San Diego Medical Center.

AUTHOR CONTRIBUTIONS

AR and AK wrote the main manuscript. KP, CD, and AK preformed the wet laboratory experiments. CN, KF, and NW performed the bioinformatics analyses. AR and CN generated the figures and table. All authors reviewed the final version of the manuscript.

FUNDING

This study was supported by grants from the NIH/NIDCD (DC006279, DC000129, and DC012595) and the Research Service of the VA (1I1BX001205) to AR, CA196853, CA155435, CA023100, and HD012303 and VA Merit Review I01BX000130 and Senior Research Career Scientist Award BX002709 to NW, and NIH grant UL1TR001442 to the UCSD Clinical and Translational Research Institute.

SUPPLEMENTARY MATERIAL

The Supplementary Material for this article can be found online at: https://www.frontiersin.org/articles/10.3389/fgene.2020.00358/full#supplementary-material

FIGURE S1 | A heat map illustrating the expression of the 520 differentially expressed genes, arranged alphabetically, across ME cell clusters.

REFERENCES

Ahmed, S., Shapiro, N. L., and Bhattacharyya, N. (2014). Incremental health care utilization and costs for acute otitis media in children. *Laryngoscope* 124, 301–305. doi: 10.1002/lary.24190

Antonelli, L. R., Dutra, W. O., Oliveira, R. R., Torres, K. C., Guimarães, L. H., Bacellar, O., et al. (2006). Disparate immunoregulatory potentials for double-negative (CD4− CD8−) αβ and γδ T cells from human patients with cutaneous leishmaniasis. *Infect. Immun.* 74, 6317–6323. doi: 10.1128/iai.00890-06

Arguedas, A., Kvaerner, K., Liese, J., Schilder, A. G., and Pelton, S. I. (2010). Otitis media across nine countries: disease burden and management. *Int. J. Pediatr. Otorhinolaryngol.* 74, 1419–1424. doi: 10.1016/j.ijporl.2010.09.022

Cayé-Thomasen, P., Hermansson, A., Tos, M., and Prellner, K. (1999). Bone modeling dynamics in acute otitis media. *Laryngoscope* 109, 723–729. doi: 10.1097/00005537-199905000-00009

Ceppi, M., Clavarino, G., Gatti, E., Schmidt, E. K., de Gassart, A., Blankenship, D., et al. (2009). Ribosomal protein mRNAs are translationally-regulated during human dendritic cells activation by LPS. *Immunome Res.* 5:5. doi: 10.1186/1745-7580-5-5

Chan, C. W., Crafton, E., Fan, H. N., Flook, J., Yoshimura, K., Skarica, M., et al. (2006). Interferon-producing killer dendritic cells provide a link between innate and adaptive immunity. *Nat. Med.* 12, 207–213. doi: 10.1038/nm1352

Cullen, K. A., Hall, M. J., and Golosinskiy, A. (2009). Ambulatory surgery in the United States. *Natl. Health Stat. Rpt.* 11, 1–25.

Ebmeyer, J., Furukawa, M., Pak, K., Ebmeyer, U., Sudhoff, H., Broide, D., et al. (2005). Role of mast cells in otitis media. *J. Allergy Clin. Immunol.* 116, 1129–1135.

Friel-Patti, S., Finitzo-Hieber, T., Conti, G., and Brown, K. C. (1982). Language delay in infants associated with middle ear disease and mild, fluctuating hearing impairment. *Pediatr. Infect Dis.* 1, 104–109. doi: 10.1097/00006454-198203000-00008

Galich, R. (1973). Lymphatics in middle ear effusion. *Laryngoscope* 83, 1713–1716. doi: 10.1288/00005537-197310000-00011

Gasteiger, G., D'Osualdo, A., Schubert, D. A., Weber, A., Bruscia, E. M., and Hartl, D. (2017). Cellular innate immunity: an old game with new players. *J. Innate Immun.* 9, 111–125. doi: 10.1159/000453397

Goldie, P., and Hellström, S. (1990). Identification and characterization of middle ear vascular leakage sites in experimental otitis media. *Ann. Otol. Rhinol. Laryngol.* 99, 810–816. doi: 10.1177/000348949009901011

Gordon, S., and Taylor, P. R. (2005). Monocyte and macrophage heterogeneity. *Nat. Rev. Immunol.* 5, 953–964. doi: 10.1038/nri1733

Hackett, N. R., Shaykhiev, R., Walters, M. S., Wang, R., Zwick, R. K., Ferris, B., et al. (2011). The human airway epithelial basal cell transcriptome. *PLoS One* 6:e18378. doi: 10.1371/journal.pone.0018378

Hentzer, E. (1970). Histologic studies of the normal mucosa in the middle ear, mastoid cavities and Eustachian tube. *Ann. Otol. Rhinol. Laryngol.* 79, 825–833. doi: 10.1177/000348947007900414

Hentzer, E. (1976). Ultrastructure of the middle ear mucosa. *Ann. Otol. Rhinol. Laryngol.* 85, 30–35. doi: 10.1177/00034894760850s208

Hernandez, M., Leichtle, A., Pak, K., Webster, N. J., Wasserman, S. I., and Ryan, A. F. (2015). The transcriptome of a complete episode of acute otitis media. *BMC Genomics* 16:259. doi: 10.1186/s12864-015-1475-7

Hoh, R., Stowe, T., Turk, E., and Stearns, T. (2012). Transcriptional program of ciliated epithelial cells reveals new cilium and centrosome components and links to human disease. *PLoS One* 7:e52166. doi: 10.1371/journal.pone.0052166

Italiani, P., and Boraschi, D. (2014). From monocytes to M1/M2 macrophages: phenotypical vs. functional differentiation. *Front. Immunol.* 5:514. doi: 10.3389/fimmu.2014.00514

Jecker, P., Pabst, R., and Westermann, J. (1996). The mucosa of the middle ear and Eustachian tube in the young rat: number of granulocytes, macrophages, dendritic cells, NK cells and T and B lymphocytes in healthy animals and during otitis media. *Acta Otolaryn.* 116, 443–450. doi: 10.3109/00016489609137871

Jepps, T., Carr, G., Lundegaard, P., Olesen, S., and Greenwood, I. (2015). Fundamental role for the KCNE4 ancillary subunit in Kv7.4 regulation of arterial tone. *J. Physiol.* 593, 5325–5340. doi: 10.1113/jp271286

Kadivar, M., Petersson, J., Svensson, L., and Marsal, J. (2016). CD8$\alpha\beta^+$ $\gamma\delta$ T cells: a novel T cell subset with a potential role in inflammatory bowel disease. *J. Immunol.* 197, 4584–4592. doi: 10.4049/jimmunol.1601146

Kolmer, W., and Mellendorff, M. (1927). Handbuch der mikroskopische anatomie des menchen. *JAMA* 89, 2215–2216.

Kulka, M., and Metcalfe, D. D. (2010). Isolation of tissue mast cells. *Curr. Protoc. Immunol.* 7, 7–25.

Kurabi, A., Pak, K., Dang, X., Coimbra, R., Eliceiri, B. P., Ryan, A. F., et al. (2013). Ecrg4 attenuates the inflammatory proliferative response of mucosal epithelial cells to infection. *PLoS One* 8:e61394. doi: 10.1371/journal.pone.0061394

Kurabi, A., Pak, K., Ryan, A. F., and Wasserman, S. I. (2016). Innate immunity: orchestrating inflammation and resolution of otitis media. *Curr. Allergy Asthma Rep.* 16:6.

Leichtle, A., Lai, Y., Wollenberg, B., Wasserman, S. I., and Ryan, A. F. (2011). Innate signaling in otitis media: pathogenesis and recovery. *Curr. Allergy Asthma Rep.* 11, 78–84. doi: 10.1007/s11882-010-0158-3

Lim, D. J. (1979). Normal and pathological mucosa of the middle ear and eustachian tube. *Clin. Otolaryngol. Allied Sci.* 4, 213–232. doi: 10.1111/j.1365-2273.1979.tb01888.x

Lim, D. J., and Hussl, B. (1969). Human middle ear epithelium. An ultrastructural and cytochemical study. *Arch. Otolaryngol.* 89, 835–849. doi: 10.1001/archotol.1969.00770020837009

Lim, D. J., and Hussl, B. (1975). Macromolecular transport by the middle ear and its lymphatic system. *Acta Otolaryngol.* 80, 19–31. doi: 10.3109/00016487509121296

Lin, C. S., and Zak, F. G. (1982). Studies on melanocytes. VI. Melanocytes in the middle ear. *Arch. Otolaryngol.* 108, 489–490. doi: 10.1001/archotol.1982.00790560027007

Little, P., Gould, C., Williamson, I., Moore, M., Warner, G., and Dunleavey, J. (2001). Pragmatic randomised controlled trial of two prescribing strategies for childhood acute otitis media. *BMJ* 322, 336–342. doi: 10.1136/bmj.322.7282.336

Luo, W., Yi, H., Taylor, J., Li, J. D., Chi, F., Todd, N. W., et al. (2017). Cilia distribution and polarity in the epithelial lining of the mouse middle ear cavity. *Sci. Rep.* 7:45870.

MacArthur, C. J., Hausman, F., Kempton, J. B., Choi, D., and Trune, D. R. (2013). Otitis media impacts hundreds of mouse middle and inner ear genes. *PLoS One* 8:e75213. doi: 10.1371/journal.pone.0075213

Marinov, G., Williams, B., Gertz, J., Myers, R., and Wold, B. (2014). From single-cell to cell-pool transcriptomes: stochasticity in gene expression and RNA splicing. *Genome Res.* 24, 496–510. doi: 10.1101/gr.161034.113

Mathews, J. A., Kasahara, D. I., Ribeiro, L., Wurmbrand, A. P., Ninin, F. M., and Shore, S. A. (2015). $\gamma\delta$ T cells are required for m2 macrophage polarization and resolution of ozone-induced pulmonary inflammation in mice. *PLoS One* 10:e0131236. doi: 10.1371/journal.pone.0131236

Rosenfeld, R., and Bluestone, C. (2003). *Evidence Based Otitis Media*, 2nd Edn. Philadelphia, PA: Decker.

Rye, M. S., Bhutta, M. F., Cheeseman, M. T., Burgner, D., Blackwell, J. M., Brown, S. D., et al. (2011). Unraveling the genetics of otitis media: from mouse to human and back again. *Mamm. Genome* 22, 66–82. doi: 10.1007/s00335-010-9295-1

Sade, J. (1966). Middle ear mucosa. *Arch. Otolaryngol.* 84, 137–143.

Satija, R., Farrell, J. A., Gennert, D., Schier, A. F., and Regev, A. (2015). Spatial reconstruction of single-cell gene expression data. *Nat. Biotechnol.* 33, 495–502. doi: 10.1038/nbt.3192

Stenfors, L. E., Albiin, N., Bloom, G. D., Hellström, S., and Widemar, L. (1985). Mast cells and middle ear effusion. *Am. J. Otolaryngol.* 6, 217–219. doi: 10.1016/s0196-0709(85)80088-0

Takahashi, M., Peppard, J., and Harris, J. P. (1989). Immunohistochemical study of murine middle ear and Eustachian tube. *Acta Otolaryngol.* 107, 97–103. doi: 10.3109/00016488909127485

Thompson, H., and Tucker, A. (2013). Dual origin of the epithelium of the mammalian middle ear. *Science* 339, 1453–1456. doi: 10.1126/science.1232862

Underwood, M., and Bakaletz, L. (2011). Innate immunity and the role of defensins in otitis media. *Curr. Allergy Asthma Rep.* 11, 499–507. doi: 10.1007/s11882-011-0223-6

Watanabe, T., Kawauchi, H., Fujiyoshi, T., and Mogi, G. (1991). Distribution of mast cells in the tubotympanum of guinea pigs. *Ann. Otol. Rhinol. Laryngol.* 100, 407–412. doi: 10.1177/000348949110000511

Wendler-Shaw, P., Menyuk, P., and Teele, D. (1993). "Effects of otitis media in first year of life on language production in the second year of life," in *Recent Advances in Otitis Media*, ed. D. Lim (Philadephia, PA: Decker).

Wolff, D. (1943). The auditory eustachian tube. *Laryngoscope* 51, 3–11.

Yang, R., Zheng, Y., Li, L., Liu, S., Burrows, M., Wei, Z., et al. (2014). Direct conversion of mouse and human fibroblasts to functional melanocytes by defined factors. *Nat. Commun.* 5:5807.

Zaiss, D. M. W., Gause, W. C., Osborne, L. C., and Artis, D. (2015). Emerging functions of amphiregulin in orchestrating immunity, inflammation, and tissue repair. *Immunity* 42, 216–226. doi: 10.1016/j.immuni.2015.01.020

Zhang, J., Chen, S., Hou, Z., Cai, J., Dong, M., and Shi, X. (2015). Lipopolysaccharide-induced middle ear inflammation disrupts the cochlear intra-strial fluid-blood barrier through down-regulation of tight junction proteins. *PLoS One* 10:e0122572. doi: 10.1371/journal.pone.0122572 doi: 10.1371/journal.pone.0122572

Conflict of Interest: AR is a co-founder of Otonomy Inc., serves as a member of the Scientific Advisory Board, and holds an equity position in the company. The UCSD Committee on Conflict of Interest has approved this relationship. Otonomy, Inc., played no part in the research reported here.

The remaining authors declare that the research was conducted in the absence of any commercial or financial relationships that could be construed as a potential conflict of interest.

frontiers in Genetics

MINI REVIEW
published: 23 April 2020
doi: 10.3389/fgene.2020.00313

Genomics of Otitis Media (OM): Molecular Genetics Approaches to Characterize Disease Pathophysiology

Arnaud P. J. Giese[1]†, Saadat Ali[2]†, Amal Isaiah[1], Ishrat Aziz[3], Saima Riazuddin[1] and Zubair M. Ahmed[1]**

[1] Department of Otorhinolaryngology—Head and Neck Surgery, University of Maryland School of Medicine, Baltimore, MD, United States, [2] The Institute of Biochemistry and Biotechnology, University of Veterinary and Animal Sciences, Lahore, Pakistan, [3] Department of Biotechnology, Virtual University of Pakistan, Lahore, Pakistan

OPEN ACCESS

Edited by:
Regie Santos-Cortez,
University of Colorado, United States

Reviewed by:
Lena Hafren,
University of Helsinki, Finland
Gijs Van Ingen,
Erasmus Medical Center, Netherlands

***Correspondence:**
Arnaud P. J. Giese
agiese@som.umaryland.edu
Zubair M. Ahmed
zmahmed@som.umaryland.edu

† These authors have contributed equally to this work

Specialty section:
This article was submitted to Genetic Disorders, a section of the journal Frontiers in Genetics

Received: 05 September 2019
Accepted: 16 March 2020
Published: 23 April 2020

Citation:
Giese APJ, Ali S, Isaiah A, Aziz I, Riazuddin S and Ahmed ZM (2020) Genomics of Otitis Media (OM): Molecular Genetics Approaches to Characterize Disease Pathophysiology. Front. Genet. 11:313. doi: 10.3389/fgene.2020.00313

Otitis media (OM) is an infective and inflammatory disorder known to be a major cause of hearing impairment across all age groups. Both acute and chronic OM result in substantial healthcare utilization related to antibiotic prescription and surgical procedures necessary for its management. Although several studies provided evidence of genetics playing a significant role in the susceptibility to OM, we had limited knowledge about the genes associated with OM until recently. Here we have summarized the known genetic factors that confer susceptibility to various forms of OM in mice and in humans and their genetic load, along with associated cellular signaling pathways. Spotlighted in this review are fucosyltransferase (FUT) enzymes, which have been implicated in the pathogenesis of OM. A comprehensive understanding of the functions of OM-associated genes may provide potential opportunities for its diagnosis and treatment.

Keywords: otitis media (OM), omic, genetic, FUT, fucosyltransferase, A2ML1

INTRODUCTION

Otitis media (OM) is defined as an infective and inflammatory disorder of the middle ear. While OM is associated with significant heterogeneity in clinical presentation, the broad types include acute otitis media (AOM), chronic suppurative otitis media (CSOM), and chronic otitis media with effusion (OME). Previous studies have shown that the pooled incidence of AOM is about 11% worldwide, with 51% of cases occurring in children under the age of five (Monasta et al., 2012). The recurrence of AOM may lead to OME, which has a worldwide incidence rate of up to 5% (Monasta et al., 2012). Both AOM and OM continue to be associated with healthcare utilization in the form of antibiotic therapy, physician and emergency room visits, and common surgical procedures such as tympanostomy tubes, although the advent of effective antimicrobial therapy has led to a substantial reduction in the burden of CSOM (Thomas et al., 2004). A smaller number of studies have also described an association between middle ear infections and speech and language deficits, emphasizing the role of OM in childhood development (Roberts et al., 2004).

The most common bacteria isolated from the middle ear of patients with AOM include *Streptococcus pneumoniae* and *Haemophilus influenzae*, although *Moraxella catarrhalis*,

Streptococcus pyogenes, and *Staphylococcus aureus* are less frequently observed. In contrast, *Pseudomonas aeruginosa* and *S. aureus* are the most frequently observed pathogens in CSOM (Giebink and Canafax, 1991).

OM is a multifactorial disorder that may be attributed to a combination of etiologic factors including immunologic, genetic, environmental, and anatomic characteristics. Seasonal microbial susceptibility and Eustachian tube dysfunction are the commonly observed causes (Swanson and Hoecker, 1996; Fireman, 1997). It is well-known that viruses from the respiratory airways also play a crucial role in the pathogenesis of AOM (Nokso-Koivisto et al., 2015). Further, exposure to tobacco smoke, the use of a pacifier, and daycare attendance are among the risk factors for OM, while breastfeeding and pneumococcal vaccines have protective effects (Swanson and Hoecker, 1996; Lubianca Neto et al., 2006; Abrahams and Labbok, 2011; Norhayati et al., 2017).

Beyond environmental factors, genetic background also confers susceptibility to OM, although the disease mechanism is not fully understood. Several OM-associated genes, identified through studies in humans and in animal models, are known to play fundamental roles in diverse biological processes including (1) the development of the middle ear cleft and the Eustachian tube, (2) immune response, (3) bacterial adhesion and viral infection rate, (4) regulation of extracellular matrix, and (5) clearance of pathogens (see **Tables 1**, **2** for specific studies). In this review, we summarized the genomic variants and factors that have been reported in patients with various forms of OM. Early genetic association studies, mouse, mouse-to-man, human candidate, and genome-wide association studies that correlate OM and genetic variations are also briefly discussed. However, we particularly focused on the recent findings of the associations of A2ML1 and FUT enzymes with OM and offered our perspective on the potential disease mechanism that intuitively can lead to OM in individuals harboring variants of *FUT2*.

Early Studies

The genetic contribution to OM susceptibility became evident in the 1980s after several studies showed that the prevalence of OM was disproportionately high in some ethnicities (native Americans and Australian aborigines) and relatively low in individuals of African ancestry (Clements, 1968; Bhutta, 2015). A surveillance study on ear and nasopharyngeal carriage was conducted among remote Australian aboriginal communities in 2013 and found that 50% of young children (mean age 13 months) had OME, 37% had AOM, and 12% had CSOM (Leach et al., 2016). Today, CSOM continues to be strongly implicated in the prevalence of hearing and learning disorders in Australian aboriginal communities (Morris, 1998).

One of the earliest genetic studies on OM, conducted in 1983, analyzed the blood groups (ABO) in a cohort of 610 children with chronic otitis media with effusion (COME) and concluded that blood group "A" was a genetic risk factor for OM based on their observation of its higher prevalence in children with COME as compared to non-affected children (Mortensen et al., 1983). Later studies have shown that human leukocyte antigen (HLA) 2 and HLA3 are strongly associated with AOM, while patients with COME have a lower frequency of HLA2 (Kalm et al., 1991, 1994). The heritability and genetic components of time with and the number of episodes with OME and AOM during the first 2 years of life were also investigated in a twin and a triplet study in 1999 and found a strong association between the duration or the number of episodes of OM and genetic makeup (Casselbrant et al., 1999).

The contribution of genetics to OM susceptibility is supported by studies reporting a higher incidence of OM in children with chromosomal abnormalities. For example, the prevalence of OME in children with Down syndrome approaches 38% (Austeng et al., 2013). Genes present on chromosome 21 in combination with craniofacial defects such as midfacial hypoplasia, short palate, and Eustachian tube dysfunction (Shibahara and Sando, 1989) and defects of the immune system (Ram and Chinen, 2011) observed in children with Down syndrome may contribute to their increased risk of OM. *Ets1* gene, encoding a proto-oncogene, has been recently associated with craniofacial abnormalities and OM in a mouse study (see section Mouse and Mouse-to-Man Studies) (Carpinelli et al., 2015). In humans, the *ETS2* gene that also belongs to the proto-oncogene gene family is present on chromosome 21 and may contribute to OM susceptibility in Down syndrome.

Several studies conducted on cohorts with Turner syndrome, a genetic disorder of partial or complete loss of chromosome X in females, described a highly variable (ranging from 9.1 to 91%) incidence of AOM (Sculerati et al., 1990; Bois et al., 2018). While the karyotype analysis did not reveal any significantly high-risk subgroup, females with Turner syndrome also have greater prevalence and longer duration of middle ear pathologies (Gawron et al., 2008; Bois et al., 2018). These findings implicate some of the X chromosome genes in middle ear development, function, or health.

Mouse and Mouse-to-Man Studies

The development and the phenotyping of transgenic and knockout mouse models in the last 30 years have significantly helped to identify several genes and genetic variations that confer susceptibility to OM in mice. Most of these mouse models spontaneously develop OM; studying their ear morphology and function provided insights into the disease pathophysiology at a molecular level. For instance, Eriksson et al. (2006) showed that plasminogen (*Plg*)-deficient mice spontaneously develop chronic OM by 18 weeks of age. Plasmin, the active serine proteinase enzyme form of PLG, is mainly involved in the dissociation of fibrin clots and promotes the degradation of the extracellular matrix (Ayon-Nunez et al., 2018). Plasmin plays a critical role in several cellular processes, including wound healing, immunity, tissue remodeling, inflammation, and cell migration (Tefs et al., 2006). Recent studies have shown that certain bacteria possess plasminogen-binding adhesions on their cell surface to exploit the fibrinolytic system, facilitating bacterial uptake and invasion (Raymond and Djordjevic, 2015; Ayon-Nunez et al., 2018).

The role of transcription factors in OM pathology became apparent through the studies of mutant mice lacking *Eya4*, *Evi1*, *Tgif*, *Ets1*, and *Fli1* genes (Hardisty-Hughes et al., 2006; Parkinson et al., 2006; Depreux et al., 2008; Tateossian et al., 2013; Carpinelli et al., 2015). Mice lacking *Eya4* have Eustachian

TABLE 1 | Most common loci associated with otitis media in mouse studies.

Locus	Protein	Protein function/phenotype in mouse mutant	OMIM	References
C3H/Hej	*TLR4* mice strain	*TLR4* mice are prone to bacterial infection	603030	Mitchell et al., 1997
Ccl3	C-C motif chemokine 3	Downstream of TNF-mediated inflammation pathways	182283	Leichtle et al., 2010
Cfb	Complement factor B	*Streptococcus pneumoniae* induced increased gene expression of factor B of the alternative complement pathway and C3 in mouse middle ear epithelium	138470	Li et al., 2011
Chd7	Chromodomain-helicase-DNA-binding protein 7	OM with effusion	608892	Tian et al., 2012
Eda	Ectodysplasin-A	Otitis media, rhinitis, and nasopharyngitis	300451	Azar et al., 2016
Edar	Tumor necrosis factor receptor superfamily member EDAR	Otitis media, rhinitis, and nasopharyngitis	604095	Azar et al., 2016
Enpp1	Ectonucleotide pyrophosphatase/phosphodiesterase family member 1	OM with effusion in *Enpp1*^{asj} mutant mice	173335	Tian et al., 2016
Ets1	E26 transformation-specific 1	Craniofacial abnormalities, small middle ear cavity, short nasal bone, hearing impairment, otitis media, fusion of ossicles to the middle ear wall, and deformed stapes	164720	Carpinelli et al., 2015
Evi1	Ectotropic viral integration 1	Chronic suppurative OM with otorrhea	165215	Parkinson et al., 2006
Eya4	Eyes absent homolog 4	Abnormal middle ear cavity and Eustachian tube	603550	Depreux et al., 2008
Fbxo11	F-box only protein 11	Compound heterozygotes carrying both Jeff and Mutt alleles demonstrated a shortened face, reduced hearing, and OM	607871	Hardisty-Hughes et al., 2006
Fli1	Friend leukemia integration 1 transcription factor	Craniofacial abnormalities, small middle ear cavity, short nasal bone, hearing impairment, otitis media, fusion of ossicles to the middle ear wall, and deformed stapes	193067	Carpinelli et al., 2015
Hbegf	Heparin binding EGF- like growth factor	Mucosal epithelial hyperplasia	126150	Suzukawa et al., 2014
Hif	Hypoxia inducible factor	Hypoxia and signal abruptions	603348	Cheeseman et al., 2011
Jnk1	JNK1	C57BL/6 mice deficient in JNK1 exhibit enhanced mucosal thickening	601158	Yao et al., 2014
Jnk2	JNK2	JNK2-/- mice exhibit delayed mucosal hyperplasia, delayed recruitment of neutrophils, and failure of bacterial clearance	602896	Yao et al., 2014
Lysozyme M	Lysozyme M	*Lysozyme M* deficiency leads to an increased susceptibility to *Streptococcus pneumoniae*-induced OM	153450	Shimada et al., 2008
Lmna	Prelamin-A/C	Malformation and abnormal positioning of the Eustachian tube, accompanied by OM, were observed in all of the Lmna(Dhe/+) mutant mice	150330	Zhang et al., 2012
MyD88	Myeloid differentiation primary response protein MyD88	Delayed recruitment of neutrophils and macrophages	602170	Hernandez et al., 2008
Mcp1/Ccl2	C-C motif chemokine 2	MCP-1/CCL2 contributes to inner ear inflammation secondary to NTHi -induced OM	158105	Woo et al., 2010
Math1	Protein atonal homolog 1	Important for mucous cell differentiation	601461	Nakamura et al., 2013
Mph1	Sex comb of midleg	OM with effusion in the hearing-impaired Mcph1(tm1a) (/tm1a) mutant mice	300227	Chen et al., 2013

(Continued)

TABLE 1 | Continued

Locus	Protein	Protein function/phenotype in mouse mutant	OMIM	References
Oxgr1	2-Oxoglutarate receptor 1	COME	606922	Kerschner et al., 2013
Pai1	Plasminogen activator inhibitor 1	Bullae of PAI-1 mutant mice showed low levels of inflammation against NTHi at the early stage of OM	173360	Shin et al., 2014
Pax9	Paired box protein Pax-9	Expression reduced in Slc25a21(tm1a(KOMP)Wtsi) mutant mice; leads to inflammation of the middle ear	167416	Maguire et al., 2014
Phex	Phosphate-regulating neutral endopeptidase PHEX	Mutation in *Phex* gene predisposes the BALB/c-Phex(Hyp-Duk)/Y mice to OM	300550	Han et al., 2012
Plg	Plasminogen	Infiltration of neutrophils and macrophages as well as the presence of T and B cells in the middle ear mucosa	173350	Eriksson et al., 2006
Spag6	Sperm-associated antigen 6	*Spag6* mutant mice are prone to develop OM due to accumulation of fluid and mucus secondary to the ciliary dysfunction.	605730	Li et al., 2014
Sh3pxd2b	SH3 and PX domain-containing protein 2B	Sh3pxd2b(nee) mutant mice develop craniofacial dysmorphologies and OM changes in cilia and goblet cells of the middle ear mucosa in Sh3pxd2b(nee) mutant mice were observed	613293	Yang et al., 2011
Slc25a21	Solute carrier Family 25 member 21	Homozygosity for Slc25a21(tm1a(KOMP)Wtsi) results in mice exhibiting orofacial abnormalities, alterations in carpal and rugae structures, hearing impairment, and inflammation in the middle ear	607571	Maguire et al., 2014

tube dysfunction, leading to an increased incidence of OME and hearing impairment (Depreux et al., 2008). Variants in *Evi1* in *Junbo* mice have been shown to cause susceptibility to CSOM. *Junbo* mice accumulate middle ear effusions and develop hypoxia, inflammation, and thickening of the mucoperiosteum (Parkinson et al., 2006; Bhutta et al., 2014). Later studies have shown that the loss of BPIFA1, one of the most abundant secretory proteins in the upper respiratory tract (Musa et al., 2012), exacerbates the severity of OM in *Junbo* mice. While *Bpifa1* mutant mice did not show any OM susceptibility, the deletion of *Bpifa1* in mice carrying *Evi1 Junbo* variant leads to the thickening of the middle ear mucosa and an increase of collagen deposition (Mulay et al., 2018). Loss of *Tgif1,* which encodes for TGIF1, results in OME accompanied by the thickening of the middle ear epithelial lining, an increase of goblet cell population, elevated levels of TNF-α and IL-1β in ear fluids, and conductive hearing loss in mice (Tateossian et al., 2013). Similarly, haploinsufficiency for *Ets1* and *Fli1* in mice results in craniofacial abnormalities, including a smaller middle ear cavity and fusion of ossicles to the walls of the middle ear (Carpinelli et al., 2015). Furthermore, $Fli1^{\pm}$ and $Ets1^{\pm}$ double-mutant mice have hearing impairment and their middle ear mucosa is infiltrated by proinflammatory cells, leading to OM (Carpinelli et al., 2015).

Hardisty et al. (2003) showed that *Jeff* mutant mice carrying a *Fbxo11* variant have craniofacial abnormalities, elevated hearing thresholds, and middle ear effusion. Defects in the bulla cavitation were observed in *Fbxo11* mutant mice, which ultimately result in middle ear adhesions and soft tissue mineralization of the bony anatomy (Del-Pozo et al., 2019). Using N-ethyl-N-nitrosourea mutagenesis, Crompton et al. (2017) showed that the pathogenic variant, p.Leu972Pro, also known as *edison* variant, in the *Nischarin* (*Nisch*) gene leads to mild craniofacial defects, spontaneous OM by 20 weeks, and progressive hearing loss. Recent studies have reported the association of *TGIF1* and *NISCH* loci as potential risk areas for OM in humans (Bhutta et al., 2017), thus supporting the relevance of knowledge obtained from mouse models to the pathophysiology of OM in humans.

Finally, *Eda* and *Edar* transcription factors mutant mice (Eda^{Ta} and $Edar^{dlJ/dlJ}$) also developed chronic rhinitis and OM (Azar et al., 2016). In these mutants, the nasopharyngeal glandular epithelium fails to develop, which leads to the loss of lysozyme secretion, the reduction of mucociliary clearance, and the overgrowth of commensal bacteria. The spread of nasal *S. aureus* in Eda^{Ta} mice and of *Escherichia coli* in $Edar^{dlJ/dlJ}$ mice into the middle ear bulla potentially triggers inflammation and OM (Azar et al., 2016). A non-exhaustive list of the most common loci associated with OM in mouse is presented in **Table 1**.

Human Candidate Gene-Based and Genome-Wide Association Studies

While early candidate gene-based OM studies have been done mostly on Caucasian patients with recurrent AOM and chronic OME (see section Early Studies), more recent genetic studies have been focusing on ethnic groups or communities for which marriages within the families are

TABLE 2 | Most common loci associated with otitis media in human studies.

Gene	Chr:	Protein	Function/ pathway	Marker	Country	Sample size	Significance	Clinical outcome	References
A2ML1	12	Alpha-2-macroglobulin-like protein 1 (A2ML1)	Peptidase inhibitor activity	c.2478_2485dupGGCTAAAT (p.Ser829Trpfs*9), p.Glu972*	Philippines	Familial (affected = 38, unaffected = 13)	LOD = 7.5	OM	Santos-Cortez et al., 2015
ABO	9	Histo-blood group ABO system transferase	Blood type	Type O: c.260insG(p.Val87_Thr88fs*) Type A	Finland	214 probands	Type A: (OR = 2.14; 95% CI: 1.04–4.50; $p = 0.03$) type O: (OR = 0.33; 95% CI: 0.11–1.04; $p = 0.04$)	RAOM/COME A increases risk for COME c.260insG (p.Val87_Thr88fs*) variant and type O are protective against RAOM	Wiesen et al., 2019
CD14	5	Cluster of differentiation 14 (CD14)	Immune response, co-receptor of TRL4	rs2569190	Netherlands	ca = 74, co = 35	$p = 0.004$	AOM	Wiertsema et al., 2006a
CPT1A	11	Carnitine palmitoyl transferase type 1A (CPT1A)	Fatty acid oxidation	rs80356779	Alaska	ca = 291, co = 136	$p < 0.001$	OM	Gessner et al., 2013
CX3CR1	3	CX3C chemokine receptor 1	Binds to chemokine	rs3732378	USA	ca = 653	$p = 0.038$		Nokso-Koivisto et al., 2014
FBXO11	2	F-box only protein 1 (FBXO11)	Protein ubiquitination	rs10182633 rs12620679 rs12712997 rs13430439 rs2710163 rs33787 rs6713506 rs6728843 rs12712997	Australia	ca = 253, co = 866	$p = 0.0009$ $p = 0.001$ $p = 0.0002$ $p = 0.0061$ $p = 0.0003$ $p = 6.9 \times 10^{-6}$ $p = 0.0074$ $p = 0.0061$	AOM	Rye et al., 2011
				rs330787		ca = 434 families, co = 561	$p = 0.009$ $p = 0.053$	RAOM/COME	
FCGR2A	1	Fc gamma receptor 11a (FCGR2A)	Fc gamma receptor, immune response	rs1801274	Netherlands	ca = 383	$p = 0.03$	OM after PV	Wiertsema et al., 2006b

(Continued)

TABLE 2 | Continued

Gene	Chr:	Protein	Function/ pathway	Marker	Country	Sample size	Significance	Clinical outcome	References
FNDC1	6	Fibronectin type III domain-containing protein 1 (FNDC1)	May be an activator of G protein signaling	rs2932989	European	825 cases and 7,936 control	$p_{meta} = 2.15 \times 10^{-09}$	AOM	van Ingen et al., 2016
FUT2	19	Galactoside 2-alpha-L-fucosyltransferase 2 (FUT2)	Creates H antigen, essential for the formation of ABO blood group antigens	rs1800022, rs601338, rs149356814, rs602662	Philippines, Pakistan, USA	1 Filipino consanguineous pedigree 609 multi-ethnic families and simplex case subjects with OM	LOD = 4.0	COME, AOM, OM	Santos-Cortez et al., 2018
IFNG	12	IFN γ	Cytokines, immune response	rs2430561	USA	ca = 20, co = 57	$p = 0.04$	OM with RSV infection	Gentile et al., 2003
IL10	1	Interleukin 10 (IL-10)	Cytokines, immune response	rs1554286, rs1800872, rs1800890, rs1800893, rs1800896, rs3024509	USA	142 families	p(ht) = 0.012, p(ht) = 0.039, p(ht) = 0.017, p(ht) = 0.017, p(ht) = 0.017, $p = 0.040$	RAOM/COME	Sale et al., 2011
				rs1800896	Netherlands	ca = 348, co = 463	$p = 0.01$	Protective for AOM after PV	Emonts et al., 2007
				rs1800871	Greece	ca = 96, c = nil	$p < 0.0001$	AOM	Ilia et al., 2014
				rs1800896, rs1800871, rs1800872	USA	ca = 102, co = 98	$p = 0.005$ $p = 0.05$ $p = 0.05$	OM followed RSV/RV	
IL1A	2	Interleukin I- (IL-1 alpha)	Cytokines, immune response	rs1800587	Finland	ca = 63, co = 400	$p = 0.03$	RAOM	Joki-Erkkila et al., 2002
IL1B	2	Interleukin 1-β (IL-1β)	Cytokines, immune response	rs16944	USA	ca = 653, co = nil	OR = 1.35	OM (prone)	Nokso-Koivisto et al., 2014
				rs1143634		ca = 104, co = 24	$p = 0.02$	AOM (inflammation)	

(Continued)

TABLE 2 | Continued

Gene	Chr:	Protein	Function/ pathway	Marker	Country	Sample size	Significance	Clinical outcome	References
IL6	7	Interleukin 6 (IL–6)	Cytokines, immune response	rs1800795	Netherlands	ca = 347, co = 460	OR > 1.45; $p = 0.02$	AOM	Emonts et al., 2007
				rs1800795	USA	ca = 68, co = 145	$p < 0.01$	RAOM	Revai et al., 2009
				rs1800795	USA	ca = 192, co = 192	$p = 0.03$	AOM	Patel et al., 2006
				rs1800795	USA	ca = 77, co = 80	$p < 0.01$	AOM	Nokso-Koivisto et al., 2014
MBL2	10	Mannose-binding lectins (MBL)	Immune response	rs11003125, rs1800450, rs1800451, rs5030737, rs7095891, rs7096206	Belgium	ca = 17, co = 172	OR(ht) = 2.9	AOM	Nuytinck et al., 2006
mDNA	mt	n/a	Mitochondrial DNA	p.Thr195Cys	Czech Republic	ca = 355	$p = 0.032$	AOM	Sale et al., 2011
MUC2	11	Mucin-2	Gel-forming mucin, lubrication, viscoelasticity	rs7396030	USA	142 families	$p = 0.049$	RAOM/COME	Sale et al., 2011
				rs7396030	USA	441 families	$p = 0.022$	RAOM/COME	
MUC5AC	11	Mucin-5AC	Gel-forming mucin, lubrication, viscoelasticity	MUC5AC (intronic)	USA	ca = 40, co = 40	$p = 0.025$	RAOM/COME	Ubell et al., 2010
MUC5B	11	Mucin-5B	Gel-forming mucin, lubrication, viscoelasticity	rs4963049	USA	ca = 102, co = 83	$p = 0.033$	COME	MacArthur et al., 2014
				rs2075859	USA	142 families	$p = 0.041$	RAOM/COME	Sale et al., 2011
				rs2735733	USA	142 families	$p = 0.02$	RAOM/COME	Sale et al., 2011
PAI1	7	Plasminogen activator inhibitor-1 (PAI1)	Inflammation	rs1799889	Netherlands	ca = 226, co = 122	$p = 0.02$	RAOM	Emonts et al., 2007

(Continued)

TABLE 2 | Continued

Gene	Chr:	Protein	Function/ pathway	Marker	Country	Sample size	Significance	Clinical outcome	References
SCN1B	19	Sodium channel sub-unit β1 ($SCN_1β$)	Ion channel binding, voltage-gated ion channel activity	rs8100085	USA	ca = 142 families	$p = 0.013$	RAOM/COME	Sale et al., 2011
SFTPA1	10	SFTPA1	Phospho-lipoproteins, surfactant	sa4-1a haplotype	Finland	ca = 147,co = 278	p(ht) = 0.03	RAOM	Ramet et al., 2001
SFTPD	10	SFTPD	Phospho-lipoproteins, surfactant	RS1051246	USA	142 families	$p = 0.039$	RAOM/COM	Sale et al., 2011
SLC11A1	2	Solute carrier family 11 member (SLC11A1)	Transporter, pathogen clearance	rs2276631, rs02695343, rs34448891, rs3731865	Australia	ca = 531 families, co = 660	p(ht) = 0.008	OM Proneness	Rye et al., 2013
SMAD2	18	SMAD2	Transcriptional modulator activated by TGF-beta	rs1792658	Australia	ca = 434 families, co = 561	$p = 0.038$	RAOM/COME	Rye et al., 2011
SMAD4	18	SMAD4	Transcriptional modulator activated by BMP	rs10502913	Australia	ca = 434 families, co = 561	$p = 0.048$	RAOM/COME	Rye et al., 2011
TGFB1	19	Transforming growth factor beta 1 (TGF-β1)	Antigen binding, immune response	rs1982073	Greece	ca = 96	$p = 0.002$	AOM	Ilia et al., 2014
TLR2	4	Toll-like receptor 2 (TLR2)	Inflammation, initiators of innate immunity system	rs5743708	Serbia	ca = 85, co-100	Significantly high	COME	Lee H.Y. et al., 2008
TLR4	9	Toll-like receptor 4 (TLR4)	Inflammation, initiators of innate immunity system	rs1800896, rs1800871, rs1800872	USA	ca = 172, co = 83	$p = 0.005$ $p = 0.05$ $p = 0.05$	AOM	Ilia et al., 2014

(Continued)

TABLE 2 | Continued

Gene	Chr:	Protein	Function/ pathway	Marker	Country	Sample size	Significance	Clinical outcome	References
				rs11788318, rs4837494, rs10116253, rs1927914, rs1554973	USA	ca = 102, co = 83	p = 0.008, p = 0.031, p = 0.007, p = 0.023, p = 0.021	COME	MacArthur et al., 2014
				rs10116253, rs12377632, rs22770146, rs5030717	USA	142 families	p (ht) = 0.025, p(ht) = 0.014, p = 0.026, p(ht) = 0.017	COME/RAOM	Sale et al., 2011
				rs5030717, rs1329060, rs1329057	Finland	ca = 624, co = 778 1,269 trios 403 families ca = 100, co = 104	OR 1.33, p = 0.003 OR 1.33, p = 0.002 OR 1.29, p = 0.003	COME/RAOM	Hafren et al., 2015
TNFA	6	Tumor necrosis factor α (TNF α)	Cytokines, immune response	rs1800629	USA	ca = 192, co = 192	p = 0.05	AOM	Emonts et al., 2007
				rs1800750	Netherlands	ca = 222, co = 120	p = 0.07	AOM	Revai et al., 2009
				rs1800750	USA	ca = 68, co = 145	OR = 1.42	RAOM	Revai et al., 2009

Ca, cases; Co, controls; OR, odds ratio; p, p-value; LOD, logarithm of the odds.

relatively common (e.g., indigenous Filipino community or Pakistani families) (Santos-Cortez et al., 2015, 2018). These studies have unveiled several novel genes and variants that confer susceptibility to familial OM (see section OM Susceptibility, Inbreeding, and Whole-Exome Sequencing): *A2ML1* and *FUT2* (Santos-Cortez et al., 2015, 2018).

Candidate Gene-Based Studies

Many variants in the genome have been associated with infectious diseases (Klebanov, 2018). In some instances, the clinical features and the biological mechanisms – such as immune response, inflammation, bacterial adhesion, viral infection, and mucociliary clearance – involved in those infectious diseases are compatible with the mechanisms involved during an episode of OM, thus marking the genes known for these disorders as prime candidates for OM susceptibility and recurrence. Candidate gene-based studies on OM have mainly involved genes associated with innate immunity and inflammation (Sale et al., 2011). Those studies have been performed on cohorts from all over the world including US, Finland, Australia, Netherlands, Greece, and Belgium and have identified over 100 alleles that confer susceptibility to various forms of OM (see **Table 2** for the partial list of these alleles, genes, and associated clinical features). As evident from this non-exhaustive list, the identified genes belong to several different signaling cascades and developmental processes, including (a) immune response and inflammation (*MBL2*, *TLR2*, *TLR4*, *CD14*, *FCGR2A*, *TGFB1*, and *PAI1*) (Nuytinck et al., 2006; Wiertsema et al., 2006a,b; Emonts et al., 2007; Lee Y.C. et al., 2008; Ilia et al., 2014; Hafren et al., 2015), (b) cytokines (*IL6*, *IL10*, *IL1A*, *IL1B*, *TNFA*, and *IFNG*) (Patel et al., 2006; Alper et al., 2009; Revai et al., 2009; Ilia et al., 2014), (c) tissue clearance (*SFPTA*, *SFTPA1*, *SFTPD*, *SLC11A1*, *MUC2*, *MUC5AC*, and *MUC5B*) (Ramet et al., 2001; Sale et al., 2011; Rye et al., 2013; MacArthur et al., 2014), (d) transcriptional modulation (*SMAD2* and *SMAD4*) (Rye et al., 2011), (e) chemosensitivity (*CX3CR1*) (Nokso-Koivisto et al., 2014), (f) protein modification (*CPT1A* and *FBXO11*) (Rye et al., 2011, 2012), and (g) channel activity (*SCN1B*) (Sale et al., 2011). Some of these genes, such as *FBXO11*, have been replicated in several independent studies, which further strengthen their role in susceptibility to OM (Segade et al., 2006; Rye et al., 2011).

Genome-Wide Association Studies

Several genome-wide association studies (GWAS) have been performed to identify new common (frequency of 75% or greater) low-risk markers (OR < 1.5) associated with OM subtypes. The findings of five salient GWAS are summarized here. In the Western Australian Pregnancy Cohort (Raine) study, a cohort of 416 patients prone to OM and 1,075 normal subjects was analyzed for 2,524,817 SNPs. Although the initial analysis revealed some association, no SNP reached GWAS significance ($P < 10^{-8}$) nor could be replicated both in the Australian or US cohorts (Rye et al., 2012; Allen et al., 2014). Intriguingly, the GWAS of the Minnesota and Pittsburg cohorts identified a SNP (rs10497394 on chromosome 2) that showed a significant association (GWAS discovery $P = 1.30 \times 10^{-5}$, independent otitis media population $P_{meta} = 1.52 \times 10^{-8}$) with susceptibility to either chronic OME or recurrent AOM (Allen et al., 2013). Finally, in a Finnish cohort (829 affected children and 2,118 randomly selected controls), the variants rs16974263 (GWAS discovery $P = 1.77 \times 10^{-7}$, sub-phenotype analysis $P_{meta} = 2.92 \times 10^{-8}$), rs268662 ($P = 1.564 \times 10^{-6}$), and rs4150992 ($P = 3.37 \times 10^{-6}$) were the most significant variants associated with COME (Einarsdottir et al., 2016). In van Ingen et al. (2016) performed GWAS on a cohort of AOM children of European descent and reported a statistically significant association at 6q25.3 locus (rs2932989, $P_{meta} = 2.15 \times 10^{-9}$). This study further demonstrated that the associated variants are correlated with the methylation status (cg05678571, $p = 1.43 \times 10^{-6}$) and expression levels ($p = 9.3 \times 10^{-5}$) of the *FNDC1* gene. Also, an independent GWAS study on more than 200,000 individuals of European ancestry reported 14 genomic regions, including *FUT2* (*p*-value: 3.51×10^{-30}), *TBX1* (1.17×10^{-19}), *HLA-DRB1* (rs4329147, 9.55×10^{-12}), *ABO* (3.67×10^{-11}), *EFEMP1* (1.47×10^{-10}), *AUTS2* (3.75×10^{-9}), *CDHR3* (5.40×10^{-9}), *BSN* (1.56×10^{-8}), and *PLG* (3.78×10^{-8}), that were significantly associated with childhood ear infection (Tian et al., 2017), further highlighting the contribution of genetic factors responsible for OM in humans.

OM Susceptibility, Inbreeding, and Whole-Exome Sequencing

A2ML1

In a large consanguineous indigenous Filipino pedigree with a high frequency of OM, Santos-Cortez et al. (2015) showed, by whole-exome and Sanger sequencing, that an 8 bp duplication in the *A2ML1* gene (LOD score of 7.5) was associated with susceptibility to OM. The same duplication was found in a heterozygous or a homozygous fashion in three individuals (European American and Hispanic) of another cohort of 123 children prone to OM and absent in non-otitis-prone children and more than 62,000 next-generation sequences. The authors identified seven additional heterozygous *A2ML1* variants in patients of European American and Hispanic American origin with OM. *A2ML1* encodes alpha-2-macroglobulin-like protein 1 (A2ML1), a protein that traps proteinases and cleaves them. A follow-up study identified 16 additional A2ML1 variants in OM subjects in indigenous Filipino and Pakistani families and US probands (Larson et al., 2019). Based on the expression in the murine mucosal epithelium of the middle ear, it has been speculated that A2ML1 may have a protective function by regulating the proteases present in the middle ear cavity and may also regulate the desquamation of epidermis (Galliano et al., 2006). Recently, by 16S rRNA sequencing of the microbiota of the middle ear of an indigenous Filipino community prone to OM and segregating *A2ML1* variants, although not having a statistically significant difference between the cases and the controls, a taxonomic analysis revealed the relative abundance of the phyla *Fusobacteria* and *Bacteroidetes* and the genus *Fusobacterium* in *A2ML1* carriers compared to non-carriers (Santos-Cortez et al., 2016).

FUT2

In the same large consanguineous indigenous Filipino pedigree with high frequency of OM, partly due to variants in *A2ML1*,

a subset of individuals were wild type for *A2ML1* but were prone to OM (Santos-Cortez et al., 2015). Further genetic analysis determined that the *FUT2* variant (p.Arg202*, LOD score of 4.0) confer susceptibility to OM in those individuals (Santos-Cortez et al., 2018). Screening of DNA samples from 609 additional multi-ethnic families and simplex case subjects with OM by direct Sanger sequencing, linkage analysis, Fisher exact, and transmission disequilibrium tests revealed several other *FUT2* variants (p.Arg138Cys, p.Trp154*, and p.Ala104Val) that confer susceptibility to OM (Santos-Cortez et al., 2018).

FUT enzymes are involved in the protein glycosylation pathway. FUTs transfer an L-fucose sugar derived from GDP-fucose (donor substrate) to a protein (acceptor substrate). The FUT family contains 13 members (FUT1–FUT13), and many of the FUTs are essential for the synthesis of blood group antigens. FUTs are single-pass type II membrane proteins, resident to the trans-Golgi, while the catalytic domain of FUT proteins resides in the lumen of the Golgi. In humans, *FUT1* and *FUT2* encode galactoside 2-L-fucosyltransferase, while *FUT3* encodes galactoside 3(4)-L-fucosyltransferase. FUT1 and FUT2 transfer L-fucose onto a β-D-galactosyl-(1→4)-N-acetyl-β-D-glucosaminyl derivative and create the oligosaccharide FuC-alpha [(1,2)Gal-beta-], also known as H antigen, which is a soluble precursor essential for the final step in the soluble A and B antigen synthesis pathway. FUT3 transfers L-fucose onto a β-D-galactosyl-(1→4)-N-acetyl-β-D-glucosaminyl derivative, or onto H antigen, in order to create blood group Lewis antigens.

FUT1 and *FUT2* are differentially expressed in various cell types. For instance, *FUT1* expression is restricted to cells of mesodermal origin (for example, erythrocytes), and *FUT2* expression is being restricted to cells of endodermal origin (such as the middle ear mucosal cells). Therefore, A and B antigens will be expressed at the surface of red blood cells under the control of FUT1, while A and B antigens will be expressed at the surface of mucosal cells under the control of FUT2. Genetic variations in *FUT1* and *FUT2* naturally exist. Some *FUT1* and *FUT2* variants lead to non-functional enzymes, while certain variations in *FUT2* can also lead to a reduction of its expression (Santos-Cortez et al., 2018). For instance, the FUT1 p.Tyr154Cys variant ablates the functional activity of the catalytic domain, resulting in the absence of A, B, or H antigens at the surface of erythrocytes (also known as the Bombay phenotype). Similarly, the FUT2 p.Trp154* variant causes absence of A, B, or H antigens at the surface of mucosal cells (a.k.a. non-secretor status) (Domino et al., 2001a,b). The p.Trp154* variant of FUT2 is also

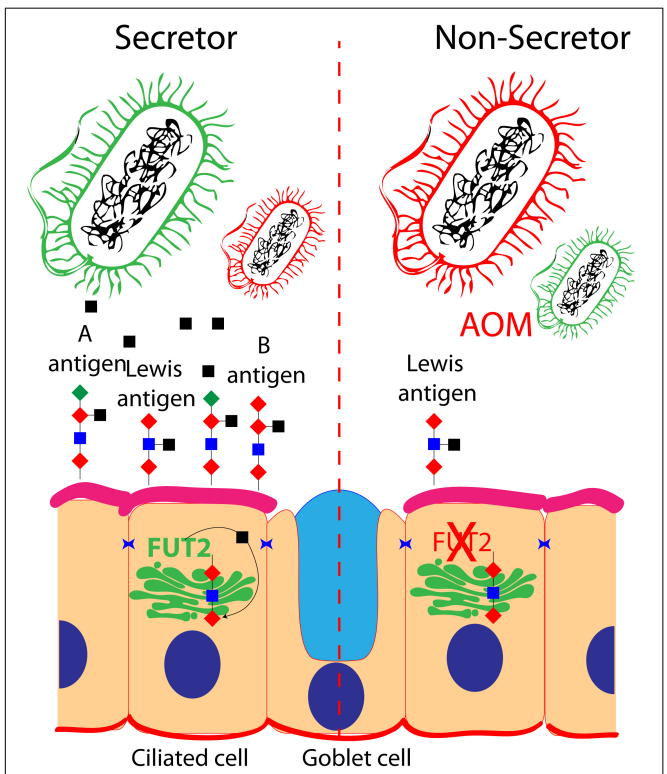

FIGURE 1 | Role of *FUT2* in the regulation of blood group and Lewis antigens at the surface of ciliated cells of the middle ear mucosa: secretor and non-secretor status are illustrated. The imbalance of optimal bacteria (green) and pathogenic bacteria (red) is shown in a non-secretor individual that is prone to acute otitis media.

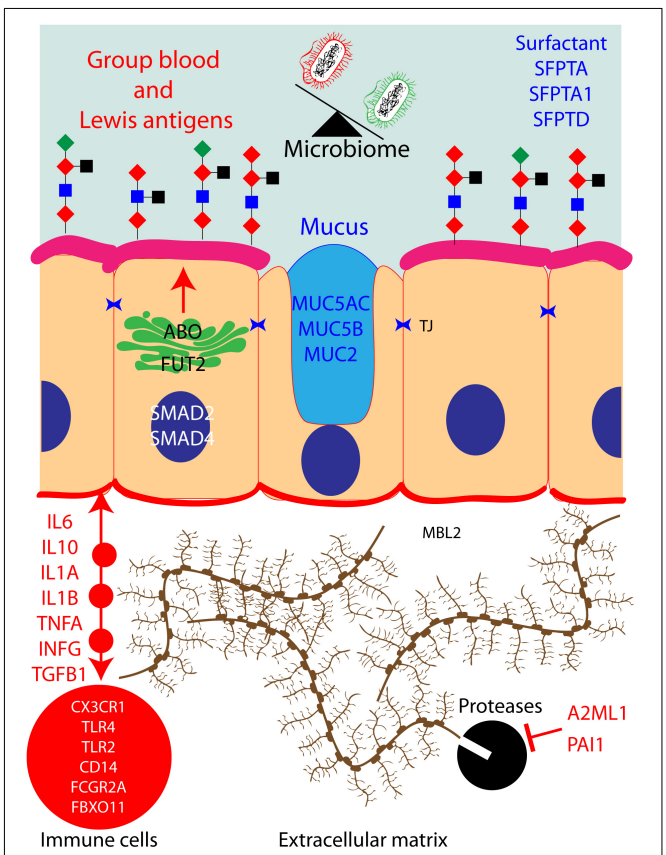

FIGURE 2 | Protein pathways contributing to otitis media (OM) in human: hypothetical network of human proteins in the middle ear mucosa that have been associated with OM. When these proteins are dysfunctional due to OM-associated genetic variants, they could potentially have an impact on the microbiota of the middle ear cavity.

responsible for the non-secretor phenotype in European and African populations (47 and 42%, respectively).

A, B, and H and Lewis antigens are known to serve as an energy source while also regulating the adhesion of bacteria to the cell surface (Ewald and Sumner, 2018; **Figure 1**). Intuitively, the different blood group antigens and their quantity at the surface of the cells of the mucosal epithelium of the middle ear would have an impact on the microbiota present in the middle ear cavity, and various blood types have been associated with OM (Wiesen et al., 2019). For instance, studies in a Finnish cohort reported a protective effect of blood type O against recurrent AOM, whereas blood type A was associated with increased risk for chronic OME (Wiesen et al., 2019). When tested *in vitro*, the four *FUT2* variants associated with OM (p.Ala104Val, p.Arg138Cys, p.Trp154*, and p.Arg202*) reduced the A antigen levels, while the two nonsense variants also reduced the FUT2 protein levels. Moreover, *Fut2* is transiently upregulated in the murine middle ear after inoculation with the non-typeable *H. influenza* (Santos-Cortez et al., 2018). It is speculated that the OM-associated *FUT2* variants are modifying the middle ear microbiome through the regulation of A antigen levels in the middle ear mucosa, thus conferring susceptibility to OM (Santos-Cortez et al., 2018).

While the microbial richness, structure, and composition differences were not statistically significant between the control individuals and the individuals prone to OM in the indigenous Filipino community segregating *FUT2* p.Arg202* variant, the individuals from a Colorado cohort prone to OM and carrier for the *FUT2* p.Trp154* variant had a relatively high abundance of *Lactobacillales* and *Gamma-proteobacteria* in their middle ears (Santos-Cortez et al., 2018). Further studies in animal models are necessary to fully understand the FUT2-associated OM mechanism.

CONCLUSION

The current genetic and molecular data revealed the association of OM with deficits in each of the following mechanisms: (1) development of the middle ear cavity and Eustachian tube, (2) immune response, (3) bacterial adhesion and viral infection, (4) regulation of the extracellular matrix, and (5) clearance of the middle ear.

In **Figure 2**, we have attempted to build a network that encompasses most of the known human proteins that have been associated with OM and our hypothesis about the potential impact on the microbiome of the middle ear cavity when these proteins are dysfunctional due to OM-associated genetic variants. Briefly, ABO and FUT2 are localized in the Golgi apparatus of the cells of the middle ear mucosa; these two proteins together create blood group Lewis antigens, potential sources of energy for microbiome. These antigens also provide an adhesion platform for the microbiota. Similarly, goblet cells secrete MUC5AC, MUC5B, MUC2 SFPTA, SFPTA1, and SFPTD to form mucus and surfactants in the middle ear cavity. Bacteria are present in these secretions and are cleared from the middle ear cavity by ciliated cells in order to maintain a healthy microbiome. Cells from the middle ear also secrete interleukins, chemokines, interferons, and necrosis and growth factors in order to recruit immune cells in the extracellular matrix. These cells fight infection and eliminate dead cells. During the inflammatory stage, the extracellular matrix is remodeled by proteases to allow immune cell infiltration. Those proteases are regulated and inhibited by A2ML1 and PAI1. A pathogenic genetic variation in any of those genes would eventually lead to middle ear infection and OM.

Future studies of the enrichment of certain microbiota in individuals with specific genetic variants may eventually help in identifying patients before chronic OM sets in or in devising a patient-specific treatment paradigm in the future.

AUTHOR CONTRIBUTIONS

AG, SA, AI, IA, SR, and ZA wrote the draft and finalized it.

FUNDING

Research in the Ahmed Laboratory was supported by the National Institutes of Health/NIDCD R01DC012564 and R01DC016295.

ACKNOWLEDGMENTS

We thank Ms. Bernadine Monari, Dimitria Gomes, and Dr. Elodie Richard for their critiques of the manuscript.

REFERENCES

Abrahams, S. W., and Labbok, M. H. (2011). Breastfeeding and otitis media: a review of recent evidence. *Curr. Allergy Asthma Rep.* 11, 508–512. doi: 10.1007/s11882-011-0218-3

Allen, E. K., Chen, W. M., Weeks, D. E., Chen, F., Hou, X., Mattos, J. L., et al. (2013). A genome-wide association study of chronic otitis media with effusion and recurrent otitis media identifies a novel susceptibility locus on chromosome 2. *J. Assoc. Res. Otolaryngol.* 14, 791–800. doi: 10.1007/s10162-013-0411-2

Allen, E. K., Manichaikul, A., Chen, W. M., Rich, S. S., Daly, K. A., Sale, M. M., et al. (2014). Evaluation of replication of variants associated with genetic risk of otitis media. *PLoS One* 9:e104212. doi: 10.1371/journal.pone.0104212

Alper, C. M., Winther, B., Hendley, J. O., and Doyle, W. J. (2009). Cytokine polymorphisms predict the frequency of otitis media as a complication of rhinovirus and RSV infections in children. *Eur. Arch. Otorhinolaryngol.* 266, 199–205. doi: 10.1007/s00405-008-0729-2

Austeng, M. E., Akre, H., Øverland, B., Abdelnoor, M., Falkenberg, E. S., and Kværner, K. J. (2013). Otitis media with effusion in children with in Down syndrome. *Int. J. Pediatr. Otorhinolaryngol.* 77, 1329–1332. doi: 10.1016/j.ijporl.2013.05.027

Ayon-Nunez, D. A., Fragoso, G., Bobes, R. J., and Laclette, J. (2018). Plasminogen-binding proteins as an evasion mechanism of the host's innate immunity in infectious diseases*. *Biosci. Rep.* 38,

Azar, A., Piccinelli, C., Brown, H., Headon, D., and Cheeseman, M. (2016). Ectodysplasin signalling deficiency in mouse models of hypohidrotic

ectodermal dysplasia leads to middle ear and nasal pathology. *Hum. Mol. Genet.* 25, 3564–3577. doi: 10.1093/hmg/ddw202

Bhutta, M. F. (2015). Evolution and otitis media: a review, and a model to explain high prevalence in indigenous populations. *Hum. Biol.* 87, 92–108. doi: 10.13110/humanbiology.87.2.0092

Bhutta, M. F., Cheeseman, M. T., and Brown, S. D. (2014). Myringotomy in the Junbo mouse model of chronic otitis media alleviates inflammation and cellular hypoxia. *Laryngoscope* 124, E377–E383. doi: 10.1002/lary.24698

Bhutta, M. F., Lambie, J., Hobson, L., Goel, A., Hafrén, L., Einarsdottir, E., et al. (2017). A mouse-to-man candidate gene study identifies association of chronic otitis media with the loci TGIF1 and FBXO11. *Sci. Rep.* 7:12496. doi: 10.1038/s41598-017-12784-8

Bois, E., Nassar, M., Zenaty, D., Léger, J., Van Den Abbeele, T., and Teissier, N. (2018). Otologic disorders in Turner syndrome. *Eur. Ann. Otorhinolaryngol. Head Neck Dis.* 135, 21–24. doi: 10.1016/j.anorl.2017.08.006

Carpinelli, M. R., Kruse, E. A., Arhatari, B. D., Debrincat, M. A., Ogier, J. M., Bories, J. C., et al. (2015). Mice haploinsufficient for Ets1 and Fli1 display middle ear abnormalities and model aspects of jacobsen syndrome. *Am. J. Pathol.* 185, 1867–1876. doi: 10.1016/j.ajpath.2015.03.026

Casselbrant, M. L., Mandel, E. M., Fall, P. A., Rockette, H. E., Kurs-Lasky, M., Bluestone, C. D., et al. (1999). The heritability of otitis media: a twin and triplet study. *JAMA* 282, 2125–2130.

Cheeseman, M. T., Tyrer, H. E., Williams, D., Hough, T. A., Pathak, P., Romero, M. R., et al. (2011). HIF-VEGF pathways are critical for chronic otitis media in Junbo and Jeff mouse mutants. *PLoS Genet.* 7:e1002336. doi: 10.1371/journal.pgen.1002336

Chen, J., Ingham, N., Clare, S., Raisen, C., Vancollie, V. E., Ismail, O., et al. (2013). Mcph1-deficient mice reveal a role for MCPH1 in otitis media. *PLoS One* 8:e58156. doi: 10.1371/journal.pone.0058156

Clements, D. A. (1968). Otitis media and hearing loss in a small aboriginal community. *Med. J. Aust.* 1, 665–667. doi: 10.5694/j.1326-5377.1968.tb28789.x

Crompton, M., Purnell, T., Tyrer, H. E., Parker, A., Ball, G., Hardisty-Hughes, R. E., et al. (2017). A mutation in Nischarin causes otitis media via LIMK1 and NF-kappaB pathways. *PLoS Genet.* 13:e1006969. doi: 10.1371/journal.pgen.1006969

Del-Pozo, J., MacIntyre, N., Azar, A., Glover, J., Milne, E., and Cheeseman, M. (2019). Chronic otitis media is initiated by a bulla cavitation defect in the FBXO11 mouse model*. *Dis. Model Mech.* 12, doi: 10.1242/dmm.038315

Depreux, F. F., Darrow, K., Conner, D. A., Eavey, R. D., Liberman, M. C., Seidman, C. E., et al. (2008). Eya4-deficient mice are a model for heritable otitis media. *J. Clin. Invest.* 118, 651–658. doi: 10.1172/JCI32899

Domino, S. E., Zhang, L., and Lowe, J. B. (2001b). Molecular cloning, genomic mapping, and expression of two secretor blood group alpha (1,2)fucosyltransferase genes differentially regulated in mouse uterine epithelium and gastrointestinal tract. *J. Biol. Chem.* 276, 23748–23756. doi: 10.1074/jbc.m100735200

Domino, S. E., Zhang, L., Gillespie, P. J., Saunders, T. L., and Lowe, J. B. (2001a). Deficiency of reproductive tract alpha(1,2)fucosylated glycans and normal fertility in mice with targeted deletions of the FUT1 or FUT2 alpha(1,2)fucosyltransferase locus. *Mol. Cell Biol.* 21, 8336–8345. doi: 10.1128/mcb.21.24.8336-8345.2001

Einarsdottir, E., Hafrén, L., Leinonen, E., Bhutta, M. F., Kentala, E., Kere, J., et al. (2016). Genome-wide association analysis reveals variants on chromosome 19 that contribute to childhood risk of chronic otitis media with effusion. *Sci. Rep.* 6:33240. doi: 10.1038/srep33240

Emonts, M., Veenhoven, R. H., Wiertsema, S. P., Houwing-Duistermaat, J. J., Walraven, V., de Groot, R., et al. (2007). Genetic polymorphisms in immunoresponse genes TNFA, IL6, IL10, and TLR4 are associated with recurrent acute otitis media. *Pediatrics* 120, 814–823. doi: 10.1542/peds.2007-0524

Eriksson, P. O., Li, J., Ny, T., and Hellström, S. (2006). Spontaneous development of otitis media in plasminogen-deficient mice. *Int. J. Med. Microbiol.* 296, 501–509. doi: 10.1016/j.ijmm.2006.04.002

Ewald, D. R., and Sumner, S. C. J. (2018). Human microbiota, blood group antigens, and disease. *Wiley Interdiscip. Rev. Syst. Biol. Med.* 10:e1413. doi: 10.1002/wsbm.1413

Fireman, P. (1997). Otitis media and eustachian tube dysfunction: connection to allergic rhinitis. *J. Allergy Clin. Immunol.* 99, S787–S797.

Galliano, M. F., Toulza, E., Gallinaro, H., Jonca, N., Ishida-Yamamoto, A., Serre, G., et al. (2006). A novel protease inhibitor of the alpha2-macroglobulin family expressed in the human epidermis. *J. Biol. Chem.* 281, 5780–5789. doi: 10.1074/jbc.m508017200

Gawron, W., Wikiera, B., Rostkowska-Nadolska, B., Orendorz-Frączkowska, K., and Noczyńska, A. (2008). Evaluation of hearing organ in patients with Turner syndrome. *Int. J. Pediatr. Otorhinolaryngol.* 72, 575–579. doi: 10.1016/j.ijporl.2008.01.021

Gentile, D. A., Doyle, W. J., Zeevi, A., Howe-Adams, J., Kapadia, S., Trecki, J., et al. (2003). Cytokine gene polymorphisms moderate illness severity in infants with respiratory syncytial virus infection. *Hum. Immunol.* 64, 338–344. doi: 10.1016/s0198-8859(02)00827-3

Gessner, B. D., Gillingham, M. B., Wood, T., and Koeller, D. M. (2013). Association of a genetic variant of carnitine palmitoyltransferase 1A with infections in Alaska Native children. *J. Pediatr.* 163, 1716–1721. doi: 10.1016/j.jpeds.2013.07.010

Giebink, G. S., and Canafax, D. M. (1991). Antimicrobial treatment of otitis media. *Semin. Respir. Infect.* 6, 85–93.

Hafren, L., Einarsdottir, E., Kentala, E., Hammarén-Malmi, S., Bhutta, M. F., MacArthur, C. J., et al. (2015). Predisposition to childhood otitis media and genetic polymorphisms within the toll-like receptor 4 (TLR4) locus. *PLoS One* 10:e0132551. doi: 10.1371/journal.pone.0132551

Han, F., Yu, H., Li, P., Zhang, J., Tian, C., Li, H., et al. (2012). Mutation in Phex gene predisposes BALB/c-Phex(Hyp-Duk)/Y mice to otitis media. *PLoS One* 7:e43010. doi: 10.1371/journal.pone.0043010

Hardisty, R. E., Erven, A., Logan, K., Morse, S., Guionaud, S., Sancho-Oliver, S., et al. (2003). The deaf mouse mutant Jeff (Jf) is a single gene model of otitis media. *J. Assoc. Res. Otolaryngol.* 4, 130–138. doi: 10.1007/s10162-002-3015-9

Hardisty-Hughes, R. E., Tateossian, H., Morse, S. A., Romero, M. R., Middleton, A., Tymowska-Lalanne, Z., et al. (2006). A mutation in the F-box gene, Fbxo11, causes otitis media in the Jeff mouse. *Hum. Mol. Genet.* 15, 3273–3279. doi: 10.1093/hmg/ddl403

Hernandez, M., Leichtle, A., Pak, K., Ebmeyer, J., Euteneuer, S., Obonyo, M., et al. (2008). Myeloid differentiation primary response gene 88 is required for the resolution of otitis media. *J. Infect. Dis.* 198, 1862–1869. doi: 10.1086/593213

Ilia, S., Goulielmos, G. N., Samonis, G., and Galanakis, E. (2014). Polymorphisms in IL-6, IL-10, TNF-alpha, IFN-gamma and TGF-beta1 genes and susceptibility to acute otitis media in early infancy. *Pediatr. Infect. Dis. J.* 33, 518–521. doi: 10.1097/INF.0000000000000229

Joki-Erkkila, V. P., Puhakka, H., and Hurme, M. (2002). Cytokine gene polymorphism in recurrent acute otitis media. *Arch. Otolaryngol. Head Neck Surg.* 128, 17–20.

Kalm, O., Johnson, U., and Prellner, K. (1994). HLA frequency in patients with chronic secretory otitis media. *Int. J. Pediatr. Otorhinolaryngol.* 30, 151–157. doi: 10.1016/0165-5876(94)90198-8

Kalm, O., Johnson, U., Prellner, K., and Ninn, K. (1991). HLA frequency in patients with recurrent acute otitis media. *Arch. Otolaryngol. Head Neck Surg.* 117, 1296–1299. doi: 10.1001/archotol.1991.01870230112019

Kerschner, J. E., Hong, W., Taylor, S. R., Kerschner, J. A., Khampang, P., Wrege, K. C., et al. (2013). A novel model of spontaneous otitis media with effusion (OME) in the Oxgr1 knock-out mouse. *Int. J. Pediatr. Otorhinolaryngol.* 77, 79–84. doi: 10.1016/j.ijporl.2012.09.037

Klebanov, N. (2018). Genetic predisposition to infectious disease. *Cureus* 10:e3210. doi: 10.7759/cureus.3210

Larson, E. D., Magno, J. P. M., Steritz, M. J., Llanes, E. G. D. V., Cardwell, J., Pedro, M., et al. (2019). A2ML1 and otitis media: novel variants, differential expression, and relevant pathways. *Hum. Mutat.* 40, 1156–1171. doi: 10.1002/humu.23769

Leach, A. J., Wigger, C., Beissbarth, J., Woltring, D., Andrews, R., Chatfield, M. D., et al. (2016). General health, otitis media, nasopharyngeal carriage and middle ear microbiology in Northern Territory Aboriginal children vaccinated during consecutive periods of 10-valent or 13-valent pneumococcal conjugate vaccines. *Int. J. Pediatr. Otorhinolaryngol.* 86, 224–232. doi: 10.1016/j.ijporl.2016.05.011

Lee, H. Y., Takeshita, T., Shimada, J., Akopyan, A., Woo, J. I., Pan, H., et al. (2008). Induction of beta defensin 2 by NTHi requires TLR2 mediated MyD88 and IRAK-TRAF6-p38MAPK signaling pathway in human middle ear epithelial cells. *BMC Infect. Dis.* 8:87. doi: 10.1186/1471-2334-8-87

Lee, Y. C., Kim, C., Shim, J. S., Byun, J. Y., Park, M. S., Cha, C. I., et al. (2008). Toll-like receptors 2 and 4 and their mutations in patients with otitis media and

middle ear effusion. *Clin. Exp. Otorhinolaryngol.* 1, 189–195. doi: 10.3342/ceo.2008.1.4.189

Leichtle, A., Hernandez, M., Ebmeyer, J., Yamasaki, K., Lai, Y., Radek, K., et al. (2010). CC chemokine ligand 3 overcomes the bacteriocidal and phagocytic defect of macrophages and hastens recovery from experimental otitis media in TNF-/- mice. *J. Immunol.* 184, 3087–3097. doi: 10.4049/jimmunol.0901167

Li, Q., Li, Y. X., Stahl, G. L., Thurman, J. M., He, Y., and Tong, H. H. (2011). Essential role of factor B of the alternative complement pathway in complement activation and opsonophagocytosis during acute pneumococcal otitis media in mice. *Infect. Immun.* 79, 2578–2585. doi: 10.1128/IAI.00168-11

Li, X., Xu, L., Li, J., Li, B., Bai, X., Strauss, J. F. I. I. I., et al. (2014). Otitis media in sperm-associated antigen 6 (Spag6)-deficient mice. *PLoS One* 9:e112879. doi: 10.1371/journal.pone.0112879

Lubianca Neto, J. F., Hemb, L., and Silva, D. B. (2006). Systematic literature review of modifiable risk factors for recurrent acute otitis media in childhood. *J. Pediatr.* 82, 87–96. doi: 10.2223/jped.1453

MacArthur, C. J., Wilmot, B., Wang, L., Schuller, M., Lighthall, J., and Trune, D. (2014). Genetic susceptibility to chronic otitis media with effusion: candidate gene single nucleotide polymorphisms. *Laryngoscope* 124, 1229–1235. doi: 10.1002/lary.24349

Maguire, S., Estabel, J., Ingham, N., Pearson, S., Ryder, E., Carragher, D. M., et al. (2014). Targeting of Slc25a21 is associated with orofacial defects and otitis media due to disrupted expression of a neighbouring gene. *PLoS One* 9:e91807. doi: 10.1371/journal.pone.0091807

Mitchell, C. R., Kempton, J. B., Scott-Tyler, B., and Trune, D. R. (1997). Otitis media incidence and impact on the auditory brain stem response in lipopolysaccharide-nonresponsive C3H/HeJ mice. *Otolaryngol. Head Neck Surg.* 117, 459–464. doi: 10.1016/s0194-5998(97)70014-7

Monasta, L., Ronfani, L., Marchetti, F., Montico, M., Vecchi Brumatti, L., Bavcar, A., et al. (2012). Burden of disease caused by otitis media: systematic review and global estimates. *PLoS One* 7:e36226.

Morris, P. S. (1998). A systematic review of clinical research addressing the prevalence, aetiology, diagnosis, prognosis and therapy of otitis media in Australian Aboriginal children. *J. Paediatr. Child Health* 34, 487–497. doi: 10.1046/j.1440-1754.1998.00299.x

Mortensen, E. H., Lildholdt, T., Gammelgård, N. P., and Christensen, P. H. (1983). Distribution of ABO blood groups in secretory otitis media and cholesteatoma. *Clin. Otolaryngol. Allied Sci.* 8, 263–265. doi: 10.1111/j.1365-2273.1983.tb01439.x

Mulay, A., Hood, D. W., Williams, D., Russell, C., Brown, S. D. M., Bingle, L., et al. (2018). Loss of the homeostatic protein BPIFA1, leads to exacerbation of otitis media severity in the Junbo mouse model. *Sci. Rep.* 8:3128. doi: 10.1038/s41598-018-21166-7

Musa, M., Wilson, K., Sun, L., Mulay, A., Bingle, L., Marriott, H. M., et al. (2012). Differential localisation of BPIFA1 (SPLUNC1) and BPIFB1 (LPLUNC1) in the nasal and oral cavities of mice. *Cell Tissue Res.* 350, 455–464. doi: 10.1007/s00441-012-1490-9

Nakamura, Y., Komori, M., Yamakawa, K., Hamajima, Y., Suzuki, M., Kim, Y., et al. (2013). Math1, retinoic acid, and TNF-alpha synergistically promote the differentiation of mucous cells in mouse middle ear epithelial cells in vitro. *Pediatr. Res.* 74, 259–265. doi: 10.1038/pr.2013.103

Nokso-Koivisto, J., Chonmaitree, T., Jennings, K., Matalon, R., Block, S., and Patel, J. A. (2014). Polymorphisms of immunity genes and susceptibility to otitis media in children. *PLoS One* 9:e93930. doi: 10.1371/journal.pone.0093930

Nokso-Koivisto, J., Marom, T., and Chonmaitree, T. (2015). Importance of viruses in acute otitis media. *Curr. Opin. Pediatr.* 27, 110–115. doi: 10.1097/MOP.0000000000000184

Norhayati, M. N., Ho, J. J., and Azman, M. Y. (2017). Influenza vaccines for preventing acute otitis media in infants and children. *Cochrane Database Syst. Rev.* 10:CD010089. doi: 10.1002/14651858.CD010089.pub3

Nuytinck, L., De Meester, E., and Van Thielen, M. (2006). Govaerts Role of mannose-binding lectin (MBL2) genotyping in predicting the risk of recurrent otitis media (rOM). *Adv. Exp. Med. Biol.* 586, 281–290. doi: 10.1007/0-387-34134-x_19

Parkinson, N., Hardisty-Hughes, R. E., Tateossian, H., Tsai, H. T., Brooker, D., Morse, S., et al. (2006). Mutation at the Evi1 locus in Junbo mice causes susceptibility to otitis media. *PLoS Genet.* 2:e149. doi: 10.1371/journal.pgen.0020149

Patel, J. A., Nair, S., Revai, K., Grady, J., Saeed, K., Matalon, R., et al. (2006). Association of proinflammatory cytokine gene polymorphisms with susceptibility to otitis media. *Pediatrics* 118, 2273–2279. doi: 10.1542/peds.2006-0764

Ram, G., and Chinen, J. (2011). Infections and immunodeficiency in Down syndrome. *Clin. Exp. Immunol.* 164, 9–16. doi: 10.1111/j.1365-2249.2011.04335.x

Ramet, M., Löfgren, J., Alho, O. P., and Hallman, M. (2001). Surfactant protein-A gene locus associated with recurrent otitis media. *J. Pediatr.* 138, 266–268. doi: 10.1067/mpd.2001.110133

Raymond, B. B., and Djordjevic, S. (2015). Exploitation of plasmin(ogen) by bacterial pathogens of veterinary significance. *Vet. Microbiol.* 178, 1–13. doi: 10.1016/j.vetmic.2015.04.008

Revai, K., Patel, J. A., Grady, J. J., Nair, S., Matalon, R., and Chonmaitree, T. (2009). Association between cytokine gene polymorphisms and risk for upper respiratory tract infection and acute otitis media. *Clin. Infect. Dis.* 49, 257–261. doi: 10.1086/599833

Roberts, J. E., Rosenfeld, R. M., and Zeisel, S. A. (2004). Otitis media and speech and language: a meta-analysis of prospective studies. *Pediatrics* 113(3 Pt 1), e238–e248. doi: 10.1542/peds.113.3.e238

Rye, M. S., Warrington, N. M., Scaman, E. S., Vijayasekaran, S., Coates, H. L., Anderson, D., et al. (2012). Genome-wide association study to identify the genetic determinants of otitis media susceptibility in childhood. *PLoS One* 7:e48215. doi: 10.1371/journal.pone.0048215

Rye, M. S., Wiertsema, S. P., Scaman, E. S., Oommen, J., Sun, W., Francis, R. W., et al. (2011). FBXO11, a regulator of the TGFbeta pathway, is associated with severe otitis media in Western Australian children. *Genes Immun.* 12, 352–359. doi: 10.1038/gene.2011.2

Rye, M. S., Wiertsema, S. P., Scaman, E. S., Thornton, R., Francis, R. W., Vijayasekaran, S., et al. (2013). Genetic and functional evidence for a role for SLC11A1 in susceptibility to otitis media in early childhood in a Western Australian population. *Infect. Genet. Evol.* 16, 411–418. doi: 10.1016/j.meegid.2013.03.023

Sale, M. M., Chen, W. M., Weeks, D. E., Mychaleckyj, J. C., Hou, X., Marion, M., et al. (2011). Evaluation of 15 functional candidate genes for association with chronic otitis media with effusion and/or recurrent otitis media (COME/ROM). *PLoS One* 6:e22297. doi: 10.1371/journal.pone.0022297

Santos-Cortez, R. L. P., Chiong, C. M., Frank, D. N., Ryan, A. F., Giese, A. P. J., Bootpetch Roberts, T., et al. (2018). FUT2 variants confer susceptibility to familial otitis media. *Am. J. Hum. Genet.* 103, 679–690. doi: 10.1016/j.ajhg.2018.09.010

Santos-Cortez, R. L., Chiong, C. M., Reyes-Quintos, M. R., Tantoco, M. L., Wang, X., Acharya, A., et al. (2015). Rare A2ML1 variants confer susceptibility to otitis media. *Nat. Genet.* 47, 917–920. doi: 10.1038/ng.3347

Santos-Cortez, R. L., Hutchinson, D. S., Ajami, N. J., Reyes-Quintos, M. R., Tantoco, M. L., Labra, P. J., et al. (2016). Middle ear microbiome differences in indigenous Filipinos with chronic otitis media due to a duplication in the A2ML1 gene. *Infect. Dis. Poverty* 5, 97.

Sculerati, N., Ledesma-Medina, J., Finegold, D. N., and Stool, S. E. (1990). Otitis media and hearing loss in Turner syndrome. *Arch. Otolaryngol. Head Neck Surg.* 116, 704–707.

Segade, F., Daly, K. A., Allred, D., Hicks, P. J., Cox, M., Brown, M., et al. (2006). Association of the FBXO11 gene with chronic otitis media with effusion and recurrent otitis media: the Minnesota COME/ROM family study. *Arch. Otolaryngol. Head Neck Surg.* 132, 729–733.

Shibahara, Y., and Sando, I. (1989). Congenital anomalies of the eustachian tube in Down syndrome. Histopathologic case report. *Ann. Otol. Rhinol. Laryngol.* 98(7 Pt 1), 543–547. doi: 10.1177/000348948909800709

Shimada, J., Moon, S. K., Lee, H. Y., Takeshita, T., Pan, H., Woo, J. I., et al. (2008). Lysozyme M deficiency leads to an increased susceptibility to Streptococcus pneumoniae-induced otitis media. *BMC Infect. Dis.* 8:134. doi: 10.1186/1471-2334-8-134

Shin, S. G., Koh, S. H., Woo, C. H., and Lim, J. H. (2014). PAI-1 inhibits development of chronic otitis media and tympanosclerosis in a mouse model of otitis media. *Acta Otolaryngol.* 134, 1231–1238. doi: 10.3109/00016489.2014.940554

Suzukawa, K., Tomlin, J., Pak, K., Chavez, E., Kurabi, A., Baird, A., et al. (2014). A mouse model of otitis media identifies HB-EGF as a mediator of inflammation-induced mucosal proliferation. *PLoS One* 9:e102739. doi: 10.1371/journal.pone.0102739

Swanson, J. A., and Hoecker, J. L. (1996). Concise review for primary-care physicians. *Mayo .Clin Proc.* 71, 179–183.

Tateossian, H., Morse, S., Parker, A., Mburu, P., Warr, N., Acevedo-Arozena, A., et al. (2013). Otitis media in the Tgif knockout mouse implicates TGFbeta signalling in chronic middle ear inflammatory disease. *Hum. Mol. Genet.* 22, 2553–2565. doi: 10.1093/hmg/ddt103

Tefs, K., Gueorguieva, M., Klammt, J., Allen, C. M., Aktas, D., Anlar, F. Y., et al. (2006). Molecular and clinical spectrum of type I plasminogen deficiency: a series of 50 patients. *Blood* 108, 3021–3026. doi: 10.1182/blood-2006-04-017350

Thomas, S. H., Meyers, A. D., Allen, G. C., and Thrasher, R. D. (2004). Otitis media with effusion. *Pediatrics* 113, 1412–1429.

Tian, C., Harris, B. S., and Johnson, K. R. (2016). Ectopic mineralization and conductive hearing loss in enpp1asj mutant mice, a new model for otitis media and tympanosclerosis. *PLoS One* 11:e0168159. doi: 10.1371/journal.pone.0168159

Tian, C., Hromatka, B. S., Kiefer, A. K., Eriksson, N., Noble, S. M., Tung, J. Y., et al. (2017). Genome-wide association and HLA region fine-mapping studies identify susceptibility loci for multiple common infections. *Nat. Commun.* 8:599. doi: 10.1038/s41467-017-00257-5

Tian, C., Yu, H., Yang, B., Han, F., Zheng, Y., Bartels, C. F., et al. (2012). Otitis media in a new mouse model for CHARGE syndrome with a deletion in the Chd7 gene. *PLoS One* 7:e34944. doi: 10.1371/journal.pone.0034944

Ubell, M. L., Khampang, A., and Kerschner, J. E. (2010). Mucin gene polymorphisms in otitis media patients. *Laryngoscope* 120, 132–138. doi: 10.1002/lary.20688

van Ingen, G., Li, J., Goedegebure, A., Pandey, R., Li, Y. R., March, M. E., et al. (2016). Genome-wide association study for acute otitis media in children identifies FNDC1 as disease contributing gene. *Nat. Commun.* 7:12792. doi: 10.1038/ncomms12792

Wiertsema, S. P., Hogenkamp, A., Wiertsema, S. P., Harthoorn, L. F., Loonstra, R., Hartog, A., et al. (2006a). Association of CD14 promoter polymorphism with otitis media and pneumococcal vaccine responses. *Clin. Vaccine Immunol.* 13, 892–897. doi: 10.1128/cvi.00100-06

Wiertsema, S. P., Veenhoven, R. H., Walraven, V., Uiterwaal, C. S., Schilder, A. G., Rijkers, G. T., et al. (2006b). Pneumococcal vaccine efficacy for mucosal pneumococcal infections depends on Fcgamma receptor IIa polymorphism. *Vaccine* 24, 792–797. doi: 10.1016/j.vaccine.2005.08.029

Wiesen, B. M., Hafrén, L., Einarsdottir, E., Kere, J., Mattila, P. S., Santos-Cortez, R. L., et al. (2019). ABO genotype and blood type are associated with otitis media. *Genet. Test Mol. Biomarkers* 23, 823–827. doi: 10.1089/gtmb.2019.0135

Woo, J. I., Pan, H., Oh, S., Lim, D. J., and Moon, S. K. (2010). Spiral ligament fibrocyte-derived MCP-1/CCL2 contributes to inner ear inflammation secondary to nontypeable H. influenzae-induced otitis media. *BMC Infect. Dis.* 10:314. doi: 10.1186/1471-2334-10-314

Yang, B., Tian, C., Zhang, Z. G., Han, F. C., Azem, R., Yu, H., et al. (2011). Sh3pxd2b mice are a model for craniofacial dysmorphology and otitis media. *PLoS One* 6:e22622. doi: 10.1371/journal.pone.0022622

Yao, W., Frie, M., Pan, J., Pak, K., Webster, N., Wasserman, S. I., et al. (2014). C-Jun N-terminal kinase (JNK) isoforms play differing roles in otitis media. *BMC Immunol.* 15:46. doi: 10.1186/s12865-014-0046-z

Zhang, Y., Yu, H., Xu, M., Han, F., Tian, C., Kim, S., et al. (2012). Pathological features in the LmnaDhe/+ mutant mouse provide a novel model of human otitis media and laminopathies. *Am. J. Pathol.* 181, 761–774. doi: 10.1016/j.ajpath.2012.05.031

Conflict of Interest: The authors declare that the research was conducted in the absence of any commercial or financial relationships that could be construed as a potential conflict of interest.

frontiers in Genetics

ORIGINAL RESEARCH
published: 24 April 2020
doi: 10.3389/fgene.2020.00323

Asian Sand Dust Particles Increased Pneumococcal Biofilm Formation *in vitro* and Colonization in Human Middle Ear Epithelial Cells and Rat Middle Ear Mucosa

Mukesh Kumar Yadav[1,2], Yoon Young Go[3], Sung-Won Chae[3], Moo Kyun Park[4] and Jae-Jun Song[3]**

[1] Institute for Medical Device Clinical Trials, Korea University College of Medicine, Seoul, South Korea, [2] Department of Biotechnology, Pachhunga University College, Mizoram Central University, Aizawl, India, [3] Department of Otorhinolaryngology-Head and Neck Surgery, Korea University College of Medicine, Seoul, South Korea, [4] Department of Otorhinolaryngology-Head and Neck Surgery, Seoul National University College of Medicine, Seoul, South Korea

OPEN ACCESS

Edited by:
Allen Frederic Ryan,
University of California, San Diego,
United States

Reviewed by:
Jorge Eugenio Vidal,
University of Mississippi Medical Center, United States
Sung K. Moon,
University of California, Los Angeles,
United States

***Correspondence:**
Moo Kyun Park
aseptic@snu.ac.kr
Jae-Jun Song
jjsong23@gmail.com

Specialty section:
This article was submitted to Genetic Disorders, a section of the journal Frontiers in Genetics

Received: 29 August 2019
Accepted: 18 March 2020
Published: 24 April 2020

Citation:
Yadav MK, Go YY, Chae S-W, Park MK and Song J-J (2020) Asian Sand Dust Particles Increased Pneumococcal Biofilm Formation in vitro and Colonization in Human Middle Ear Epithelial Cells and Rat Middle Ear Mucosa. Front. Genet. 11:323. doi: 10.3389/fgene.2020.00323

Introduction: Air pollutants such as Asian sand dust (ASD) and *Streptococcus pneumoniae* are risk factors for otitis media (OM). In this study, we evaluate the role of ASD in pneumococcal *in vitro* biofilm growth and colonization on human middle ear epithelium cells (HMEECs) and rat middle ear using the rat OM model.

Methods: *S. pneumoniae* D39 *in vitro* biofilm growth in the presence of ASD (50–300 μg/ml) was evaluated in metal ion-free BHI medium using CV-microplate assay, colony-forming unit (cfu) counts, resazurin staining, scanning electron microscopy (SEM), and confocal microscopy (CF). Biofilm gene expression analysis was performed using real-time RT-PCR. The effects of ASD or *S. pneumoniae* individually or on co-treatment on HMEECs were evaluated by detecting HMEEC viability, apoptosis, and reactive oxygen species (ROS) production. *In vivo* colonization of *S. pneumoniae* in the presence of ASD was evaluated using the rat OM model, and RNA-Seq was used to evaluate the alterations in gene expression in rat middle ear mucosa.

Results: *S. pneumoniae* biofilm growth was significantly ($P < 0.05$) elevated in the presence of ASD. SEM and CF analysis revealed thick and organized pneumococcal biofilms in the presence of ASD (300 μg/ml). However, in the absence of ASD, bacteria were unable to form organized biofilms, the cell size was smaller than normal, and long chain-like structures were formed. Biofilms grown in the presence of ASD showed elevated expression levels of genes involved in biofilm formation (*luxS)*, competence (*comA*, *comB*, *ciaR),* and toxin production (*lytA* and *ply)*. Prior exposure of HMEECs to ASD, followed by treatment for pneumococci, significantly ($P < 0.05$) decreased cell viability and increased apoptosis, and ROS production. *In vivo* experiment results showed significantly ($P < 0.05$) more than 65% increased bacteria colonization in rat middle ear mucosa in the presence of ASD. The apoptosis, cell death, DNA repair,

inflammation and immune response were differentially regulated in three treatments; however, number of genes expressed in co-treatments was higher than single treatment. In co-treatment, antimicrobial protein/peptide-related genes (S100A family, Np4, DEFB family, and RATNP-3B) and OM-related genes (CYLD, SMAD, FBXO11, and CD14) were down regulated, and inflammatory cytokines and interleukins, such as IL1β, and TNF-related gene expression were elevated.

Conclusion: ASD presence increased the generation of pneumococcal biofilms and colonization.

Keywords: Asian sand dust, *Streptococcus pneumoniae*, biofilms, colonization, otitis media, RNA-sequencing

INTRODUCTION

Otitis media (OM) is inflammation of the middle ear that affects children and elders (Monasta et al., 2012; Qureishi et al., 2014; Byeon, 2019). The recurrent OM adversely affects speech, hearing ability, and language development in children, finally leading to hearing loss (Bellussi et al., 2005; Roditi et al., 2016). Worldwide, OM-related complications result in approximately 21,000 deaths annually, and 65–300 million individuals are affected by chronic OM (COM) (Acuin, 2004). The incidence and prevalence of OM are particularly high in the Asian population (8.12–14.52%), which affect the quality of life and pose a significant social and economic burden (Monasta et al., 2012; Coleman et al., 2018; Byeon, 2019). OM is generally considered a multi-factorial abnormality of the middle ear, with many associated risk factors, including microbial exposure, environment, immunological deficiency, gender, and age (Jensen et al., 2013; Coleman et al., 2018). Among microbial agents, *Streptococcus pneumoniae* (*S. pneumoniae*) is an important commensal bacterium that colonizes asymptotically and causes infection under immune-compromised conditions (Coleman et al., 2018). Despite the introduction of a 13-valent vaccine in various countries to control pneumococcal infection, pneumococci remain the leading pathogen (Milucky et al., 2019). Moreover, *S. pneumoniae* forms biofilms, and its direct detection from biopsy samples of the middle ear mucosa of children with COM (Hall-Stoodley et al., 2006) suggests that pneumococcal biofilms are important virulence factors of OM (Blanchette et al., 2016; Vermee et al., 2019). In the nasopharyngeal cavity, pneumococci initially colonize and form biofilms that serve as a reservoir, and then, the biofilm bacteria can transit to other sterile sites causing OM, meningitis, pneumonia, bacteremia, and sepsis in immune-compromised individuals (children and elderly) (Chao et al., 2015; Weiser et al., 2018).

Recent studies have reported that particulate matter (PM) involved in air pollution is an important risk factor for OM (Park et al., 2018). Air pollution due to sand and dust storms originating in arid and semi-arid regions affects 151 countries worldwide (Middleton and Kang, 2017). A seasonal episode of Asian sand dust (ASD), which originates from arid areas of Mongolia and the Gobi desert, and affects the Korean peninsula, Japan, and China, is a major source of pollution in the East and Northeast Asia (Jung, 2016). In recent years, a growing number of reports have suggested that ASD exposure negatively affects human health, leading to respiratory diseases (Jung et al., 2012; Yu et al., 2012; Watanabe et al., 2016; Nakao et al., 2018) and significant mortality annually (Chen et al., 2004; Lee et al., 2014; Al et al., 2018). In addition, ASD contains PM of diameters < 10 μm (PM_{10}) along with inhalable hazardous chemical components such as sulfate (SO_4^{2-}) and nitrate (NO_3^-) and microbes such as bacteria, viruses, and fungi (Chen et al., 2010). One study has reported a positive association between early exposure to PM pollution and OM (Kennedy et al., 2018). Recently, a study reported the implication of air pollution containing PM_{10}, nitrogen dioxide (NO_2), ozone (O_3), sulfur dioxide, and carbon monoxide in OM (Park et al., 2018). Similarly, Girguis et al. (2018) suggested that preterm infants are most susceptible to infant bronchiolitis and OM associated with acute $PM_{2.5}$ exposure (Girguis et al., 2018). Several studies have reported that air pollution and nasopharyngeal bacteria are two known risk factors for OM (Chao et al., 2015; Park et al., 2018; Weiser et al., 2018). However, the interaction between these two factors remains unknown. Most research to date has focused on the implication of either *S. pneumoniae* or air pollutants in causing OM. Indeed, severe pneumonia and OM were reported in cigarette smokers exposed to PM and bacteria such as *S. pneumoniae* and *Haemophilus influenzae* (Nuorti et al., 2000; Givon-Lavi et al., 2006). In the nasopharynx, pneumococci and PM interact, and PM exposure increases the risk of infections and alters the function of native immune cells, impairs mucociliary clearance, and decreases phagocytosis by macrophages (Becker and Soukup, 1999; Zelikoff et al., 2002; Watanabe et al., 2016). PM including environmental tobacco smoke increases the risk of OM in children and changed the middle ear histology and eustachian tube mucosa (Kong et al., 2009; Jones et al., 2012; Bowatte et al., 2018; Nakao et al., 2018; Park et al., 2018). Previously, our group identified a potential biomarker and a signaling pathway related to OM induced by diesel exhaust particles (Kim et al., 2016). We also demonstrated that ASD exposure decreases the cell viability in a model human middle ear epithelium cell (HMEEC); affects apoptosis, cell proliferation, and oxidative stress-related gene expressions; and induces inflammatory responses in the rat middle ear epithelium (Go et al., 2015; Chang et al., 2016). However, the interaction, colonization, and virulence of *S. pneumoniae* in the presence of ASD are not known. Previous reports suggested that PM alters host immune defense (Becker and Soukup, 1999; Zelikoff et al., 2002; Watanabe et al., 2016) and induces OM (Bowatte et al., 2018; Nakao et al., 2018;

Park et al., 2018); therefore, we hypothesized that the presence of a small quantity of ASD may increase pneumococcal *in vitro* biofilms, colonization to epithelial cells and middle ear mucosa, and the risk factor for pneumococcus-mediated OM. In this study, we evaluated the effect of ASD on *S. pneumoniae in vitro* biofilm growth, colonization on HMEECs, and rat middle ear using the rat OM model.

MATERIALS AND METHODS

Ethics Statement

The animal study was approved by the Institute Review Board (IRB) of Korea University, Seoul, South Korea, with IRB approval number KOREA-2019-0029. The animal protocols were approved by Institutional Animal Care and Use Committees (IACUCs), Korea University, Seoul.

Bacteria Strain and Culture Medium

In this study, *S. pneumoniae* D39, Avery's virulence serotype 2 strain (NCTC; Salisbury, United Kingdom) was used (Avery et al., 1944). This strain is fully sequenced and well characterized and has remained highly virulent in the animal model after many years of its isolation. *Pseudomonas aeruginosa* (PA01) and *E. coli* (ATCC 24213) were purchased from ATCC, United States, and MRSA (CCARM 3903) was purchased from the culture collection of antimicrobial resistant strain (CCARM), Seoul, South Korea. Bacteria were grown in BHI broth, and glycerol stocks were maintained at −80°C. Pneumococci colonies were grown on a blood agar plate (BAP) supplemented with 5% sheep blood (Yang Chemical, Seoul, South Korea). The ASD particles used in this study were collected and composition was detected in our previous study (Chang et al., 2016). Briefly, ASD was collected using a high volume air sampler (HV500F, Sibata, Tokyo, Japan) at a flow rate of 500 L/minute, pre-filtered into filter packs (Prefilter AP, 124 mm; EMD Millipore, Bedford, MA, United States), and sieved through a filter with a 10-μm pore size (Chang et al., 2016). The stock solution of ASD was prepared in PBS and sonicated and sterilized using an autoclave.

Planktonic Growth and *in vitro* Biofilm Growth

To study the effects of ASD on bacterial growth, *S. pneumoniae* planktonic growth was evaluated with different concentrations of ASD (50, 150, and 300 μg/ml). The pneumococcal growth was detected by measuring optical density at 600 nm (OD_{600}) at different time points. *S. pneumoniae* planktonic growth was also evaluated by detecting metabolically active bacteria by resazurin staining after 48 h. Bacteria were grown in metal ion-free BHI medium based on a previous report (BHI medium treated with chelex-100) (Brown et al., 2017). *In vitro* biofilm formation ability of the bacteria, in the presence of ASD, was evaluated using a static microtiter plate assay (Christensen et al., 1982; Yadav et al., 2018). Viable bacteria in the biofilms were detected by colony-forming unit (cfu) counting, and metabolically active bacteria were detected by resazurin staining. Briefly, *S. pneumoniae* colonies grown on BAP were further grown in BHI broth up to log phase. The cells were pelleted by centrifugation and dissolved in metal ion-free medium. The diluted bacteria (1:100) in metal ion-free medium were inoculated in 96-well (200 μl) or 24-well (1 ml) plates and incubated for 48 h. After incubation, the medium was removed, and biofilms were washed twice and stained with 0.1% crystal violet for 15 min. The biofilms were washed with PBS twice and dissolved in 200 μl (96-well plate) or 1 ml (24-well plate) ethanol, and the absorbance was measured at 570 nm. Alternately, after washing with PBS, the biofilms were dissolved in sterile water followed by brief sonication (10 s). The biofilm suspension was serially diluted and spread on BAP, followed by colony counting after 24 h incubation at 37°C.

The *in vitro* biofilms of *Pseudomonas aeruginosa*, MRSA, and *E. coli* were grown as described above and quantified using resazurin staining (Yadav et al., 2017). Resazurin stain is a blue colored, non-fluorescent dye that is reduced and then emits pink fluorescence (resorufin) in the presence of actively growing bacteria. The biofilms grown in 24-well plates were dissolved and transferred to 96-well plates, followed by addition of 10% resazurin. The plates were incubated in the dark for 1 h at 37°C. Fluorescence was measured at 530/590 (excitation/emission) nm using a multimode microplate reader (Thermo Scientific, Waltham, MA, United States).

In vitro Biofilm Analysis by Scanning Electron Microscopy (SEM)

In vitro biofilms of *S. pneumoniae* D39, grown in the absence or presence of ASD (300 μg/ml), were visualized using SEM. The biofilms were grown in 24-well plates, in the metal ion-free medium for 48 h using the procedure described above. After washing with PBS, the biofilms were pre-fixed in glutaraldehyde (2%) and paraformaldehyde (2.5%) and post-fixed with osmic acid (1%) for 2 h, followed by dehydration in increasing concentrations of ethanol (60–95%). The biofilms were preserved in t-butanol and freeze-dried and platinum-coated. SEM images were captured using a field emission scanning electron microscope (Hitachi, Tokyo, Japan).

In vitro Biofilm Analysis by Confocal Microscopy

Streptococcus pneumoniae D39 *in vitro* biofilms, grown in the presence (300 μg/ml) and absence of ASD, were analyzed using confocal microscopy and peptide nucleic acid (PNA) fluorescence *in situ* hybridization (FISH) by a previously reported procedure (Malic et al., 2009). The PNA probe used for biofilm detection is a universal bacterial probe EUB338 (5′-TGCCTCCCGTAGGA-3′) (Rocha et al., 2018). It was commercially synthesized by Panagene (Dageon, South Korea) and labeled at the N-terminus with AlexaFluor488 via a double 8-amino-3,6-dioxaoctanoic acid (AEEA) linker. The biofilms were grown on μ-slides (ibidi, Germany) for 48 h in metal ion-free medium, as described above. The biofilms were washed with PBS and prefixed for 3 h in 4% paraformaldehyde. Hybridization with the probe was performed at 46°C for 3 h in hybridization buffer (5 M NaCl, 1 M Tris-HCl, 2% SDS, and 10% formamide),

followed by washing at 48°C in washing buffer (5 M NaCl, 1 M Tris–HCl, and 2% SDS). The PNA probe-labeled biofilm bacteria were analyzed using a Nikon A1 confocal microscope (Nikon Instruments, Inc., NY, United States) with FITC (green) channel.

In vitro S. pneumoniae Biofilm Gene Expression

Real-time RT-PCR was used to evaluate the expression of genes involved in competence (*comA*, *comB*, *ciaR*), biofilm formation (*luxS*), and toxin production (*ply, lytA*) in a pneumococcal biofilm. Pneumococcal biofilms were grown in metal ion-free medium, and total RNA was extracted using an RNeasy Total RNA Isolation System Kit (Qiagen, Valencia, CA, United States) as per the manufacturer's procedure. DNA contamination was removed by on-column RNase-free DNase (Qiagen) treatment for 10 min at 20–25°C. The RNA was quantified using Nanodrop, and cDNA synthesis was performed using a Bioneer cDNA synthesis kit (Seoul, South Korea). Gene list and primer sequences used in this study are presented in **Table 1**. Real-time RT-PCR was performed in a 20-μl reaction volume with 10 μl of SYBR Green, 2-pmol primers, and 2 μl of cDNA. The PCR was performed for 40 cycles with initial denaturation at 56°C for 2 min, followed by 40 cycles of denaturation at 95°C for 30 s and annealing and extension at 60°C for 1 min. Relative quantification of gene expression was performed using the $2^{-\Delta\Delta CT}$ method; a biofilm without ASD was used as the standard and 16S RNA genes as reference.

HMEEC Viability

The toxicity of *S. pneumoniae* in the presence or absence of ASD was detected by evaluating HMEEC viability upon treatment with *S. pneumoniae* or ASD, or co-treatment with both. HMEECs were kindly provided by Dr. Lim (House Ear Institutes, Los Angeles, CA, United States) (Chun et al., 2002). HMEECs were cultured (1×10^4) in a 96-well plate in airway epithelial cell growth medium (PromoCell GmbH, Sickingenstr Heidelberg Germany) supplemented with bovine pituitary extract (0.004 ml/ml), epidermal growth factor (10 ng/ml), insulin (5 μg/ml), hydrocortisone (0.5 μg/ml), epinephrine (0.5 μg/ml), triiodo-L-thyronine (6.7 ng/ml), transferrin (10 μg/ml), retinoic acid (0.1 ng/ml), and 1% fetal bovine serum for 24 h at 37°C in 5% CO_2. Then, cells were exposed to ASD (300 μg/ml) in serum-free medium for 8 h, followed by *S. pneumoniae* treatment (MOI 10) for 15 h. The viability of HMEECs was determined by using EZ-cytox cell viability kit (Dogenbio, South Korea) as per the manufacturer's instruction, and absorbance was measured at 450 nm.

TABLE 1 | List of primers used in real-time RT-PCR gene expression study.

Serial no.	Gene name	Primer sequence	Amplicon
1	*16s*	5′-AACCAAGTAACTTTGAAAGAAGAC-3′	126 bp
		5′-AAATTTAGAATCGTGGAATTTTT-3′	
2	*luxS*	5′-ACATCATCTCCAATTATGATATTC-3′	257 bp
		5′-GACATCTTCCCAAGTAGTAGTTTC-3′	
3	*comA*	GAGACGCGAGCCATTAAGG	156 bp
		GGGATCTGGATCGGCAATATGA	
4	*comB*	5′-GAACCCAGTCGTATCCTTGC-3′	95 bp
		5′-TCCCCCTTCTTAACCAGCTT-3′	
5	*ciaR*	GATGTTATGCAGGTATTTGATG	157 bp
		TAATCAGAACTGGTGTCGTAAT	
6	*ply*	TGAGACTAAGGTTACAGCTTACAG	225 bp
		CTAATTTTGACAGAGAGATTACGA	
7	*lytA*	CGTCCCAGGCACCATTATCA	95 bp
		CTGGCGGAAAGACCCAGAAT	

Detection of Apoptosis in HMEECs

Apoptosis of HMEECs treated with ASD or *S. pneumoniae* or co-treatment was detected by double staining with annexin V-fluorescein isothiocyanate and propidium iodide (BD, San Diego, CA, United States) and cytometric analysis as per manufacturer's protocol. Briefly, HMEECs (5×10^5/well) were seeded in a 6-well plate in airway epithelium cell culture medium supplemented with fetal bovine serum (1%) in 5% CO_2 atmosphere at 37°C for 24 h. Then, the HMEECs were exposed to ASD (300 μg/ml) in serum-free medium for 8 h, followed by *S. pneumoniae* treatment (MOI 10) for 15 h. The HMEECs were detached with Tris–EDTA treatment, pelleted by centrifugation, and washed twice with cold PBS. The cells were re-suspended in 1 × binding buffer [10 mM HEPES/NaOH (pH 7.4), 140 mM NaCl, and 2.5 mM $CaCl_2$] and stained with Annexin-V for 15 min at 15°C. The cells were stained with PI and evaluated using a flow cytometer (Beckman Coulter; Fullerton, CA, United States). The rates of early apoptosis and late apoptosis (necrosis) were calculated using the Beckman Coulter software.

Detection of Reactive Oxygen Species (ROS) in HMEEC

The effect of ASD and *S. pneumoniae* on ROS production by HMEECs was evaluated using OciSelect ROS assay kit (Cell Biolabs; San Diego, CA, United States). 5×10^4 HMEECs were seeded in 96-well plate (black wall clear-bottom plate) in airway epithelial growth medium and grown at 37°C in 5% CO_2 for 24 h. After washing, the cells were treated with 100 μl 2′,7′-dichlorofluorescein-diacetate (DCFH-DA) in the culture medium at 37°C for 50 min. After washing twice with PBS, HMEECs were exposed to ASD (300 μg/ml) for 2 h, followed by *S. pneumoniae* treatment for 4 h. The ROS production was detected by measuring fluorescence at 480 nm (excitation) and 530 nm (emission) using microplate (Thermo max 190, US). Hydrogen peroxide was used as a positive control.

In vivo Colonization of *S. pneumoniae* in Rat Middle Ear in the Presence of ASD Using the Rat OM Model

The *in vivo* colonization of *S. pneumoniae* in rat middle ear in the presence of ASD was evaluated using the rat OM model (Yadav et al., 2012, 2018). Thirty-two pathogen-free Sprague-Dawley rats, weighing 150–200 g, were purchased from Koatech (Pyeongtaek, South Korea). The animals were checked for any abnormality and kept for acclimatization for 2 weeks. Rats were

divided into four groups according to the treatment. Group 1 rats were inoculated with PBS (vehicle control, $n = 6$); Group 2 rats were inoculated with ASD only ($n = 8$); Group 3 rats were inoculated with *S. pneumoniae* only ($n = 9$); Group 4 rats were inoculated with ASD + *S. pneumoniae* ($n = 9$). The ASD was dissolved in PBS, and 50 μl (6 mg/ml) solution was injected (300 μg/rat) as per our previous study (Chang et al., 2016). *S. pneumoniae* cell suspensions were prepared in PBS, and 5×10^6/rat were injected in the middle ear cavity through the tympanic membrane of the right ear using a tuberculin syringe and a 27-gauge spine needle. After 5 days, the animals were scarified by CO_2 euthanasia. The rat bullae were aseptically acquired and cleaned by removing unwanted tissue surrounding the bony structure. The tympanic membranes were removed, and the middle ear was exposed and photographed. For gene expression study, bullae were harvested in RNA-later solution (Qiagen, United States). For bacterial load detection, bullae were aseptically lysed with pestle and mortar and serially diluted and plated on BAP. Bacterial cfu were counted after overnight incubation at 37°C.

For SEM analysis of rat middle mucosa, the bullae from each group were preserved in SEM solution (glutaraldehyde and paraformaldehyde). The rest of the protocol (pre-fixing, post-fixing, and dehydration) was the same as that described previously for *in vitro* biofilms SEM analysis.

Elucidation of Rat Middle Ear Mucosa Global Gene Expression Using RNA Sequencing

The mucosal membranes from bullae were recovered by scraping and three rat mucosa were pooled as one sample. Total RNA was isolated using a Qiagen RNeasy kit (Qiagen, Hilden, Germany) in accordance with the manufacturer's instructions. The RNA was quantified using a Nanodrop, and the RNA quality was assessed by analyzing the rRNA band integrity using the Agilent RNA 6000 Nano kit (Agilent Technologies, Palo Alto, CA, United States). The gene expressions of rat middle ear mucosa inoculated with ASD or bacteria or co-treatment were analyzed by QuantSeq 3′mRNA sequencing. RNA samples were processed and library was constructed using QuantSeq 3′mRNA–Seq library prep kit (Lexogen, Inc., Austria) as per the manufacturer's instructions. Total RNA (500 ng) from each sample was used with an oligo-dt primer containing an illumine-compatible sequence at its 5′ end and hybridized with the RNA followed by reverse transcription reaction. The RNA templates were digested and the synthesis of the second strand was initiated by a random primer containing an illumine-compatible linker sequence at its 5′ end. The library of double-stranded RNA was purified from reaction components using magnetic beads. The prepared library was amplified and added with the complete adapter sequences required for cluster generation. The finally finished library was purified from PCR components of reaction. The high-throughput sequencing was performed as single-end 75 sequencing using Next Seq 500 (Illumina, Inc., United States).

Bowtie2 program was used to align the QuantSeq 3′ mRNA-Seq reads (Langmead and Salzberg, 2012). Bowtie2 indices were either generated from genome assembly sequence or the representative transcript sequences for aligning to the genome assembly sequence or the representative transcript sequences for aligning to the genome and transcriptiome. Those aligned files were utilized for transcript assembling, abundance estimation, and differential gene expression detection. The differentially expressed genes were determined on the basis of unique and multiple alignments using coverage in Bedtools (Quinlan and Hall, 2010). Read count data were processed on the basis of quantile normalization method using EdgeR within R using Bioconductor (Gentleman et al., 2004). DAVID[1] and Medline databases[2] were used for gene classifications. The differentially expressed genes of rat middle ear mucosa inoculated with ASD or bacteria or co-treatment compared to untreated samples were analyzed, and fold change of ±2 was considered significant.

Statistical Analyses

The *in vitro* biofilm experiments were performed in replicates and repeated to calculate the statistical significance. Data are represented as mean ± standard deviation. Two groups were compared, and the statistical significance was detected by Student's *t* test. Three groups were compared by one-way ANOVA. The *P*-value < 0.05 was considered significant.

RESULTS

Planktonic Growth and *in vitro* Biofilm Growth

In metal ion-free medium *S. pneumoniae* growth was restricted. However, bacterial growth was significantly elevated in the presence of ASD compared to the control (**Figure 1A**). The growth of bacteria was slow initially, both in the presence and in the absence (control) of ASD. However, at 24, 36, and 48 h, bacterial growth was significantly ($P < 0.05$) high in the presence of ASD (50, 150, and 300 μg/ml) compared to the control. The metabolically active bacteria were also significantly ($P < 0.05$) increased in samples supplemented with ASD (**Figure 1B**).

The *S. pneumoniae* D39 *in vitro* biofilm growth in the presence of ASD was enhanced compared to the control. Quantification of biofilm biomass using CV-microtiter plate assay showed significant ($P < 0.05$) increase in biofilm biomass in the presence of 150 and 300 μg/ml ASD (**Figure 1C**), with a significantly ($P < 0.05$) increased number of viable bacteria (**Figure 1D**). The metabolically active bacteria within biofilms were also significantly ($P < 0.05$) higher in the presence of 150 and 300 μg/ml ASD (**Figure 1E**). *Pseudomonas aeruginosa*, MRSA, and *E. coli in vitro* biofilms were also significantly ($P > 0.05$) elevated in the presence of ASD (150 μg/ml) (**Figure 1F**).

In vitro Biofilm Analysis Using SEM

SEM analysis revealed markedly different morphology of pneumococci *in vitro* biofilms grown with ASD (300 μg/ml) with

[1]http://david.abcc.ncifcrf.gov/

[2]http://www.ncbi.nlm.nih.gov/

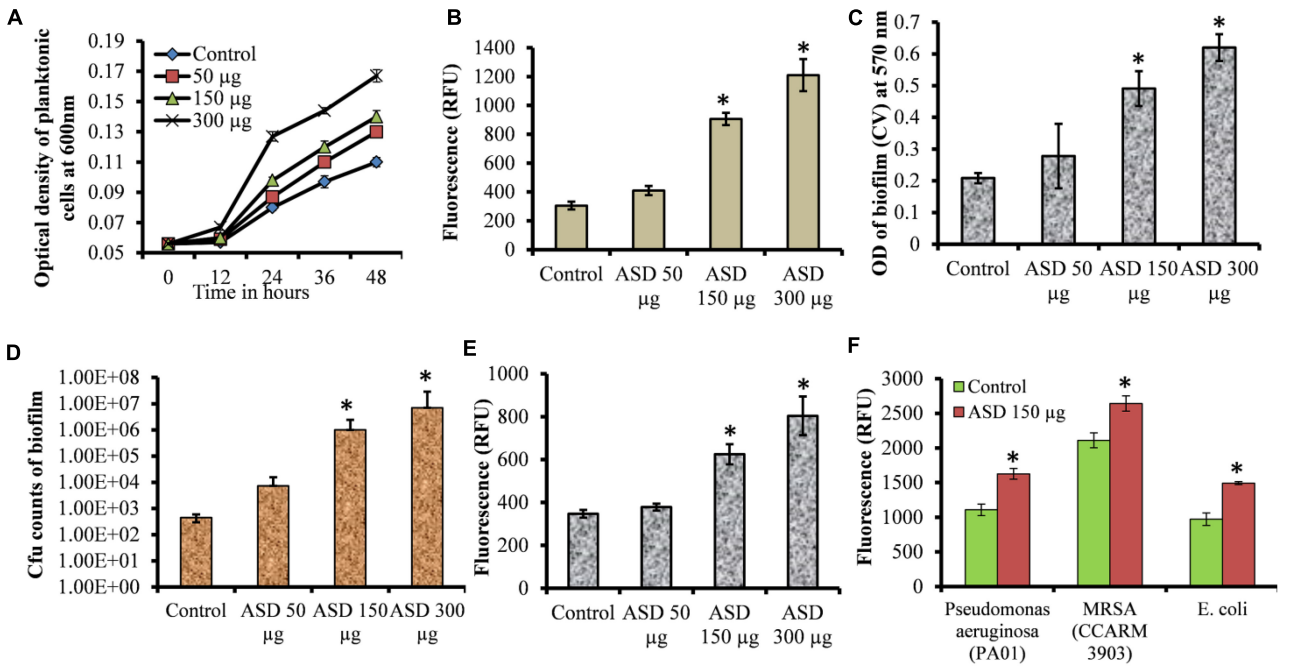

FIGURE 1 | *Streptococcus pneumoniae* D39 planktonic and biofilm growth in metal ion-free BHI medium. **(A)** Time-dependent planktonic growth from 0 to 48 h with different concentrations of ASD. Growth was detected by measuring optical density at 600 nm. **(B)** Planktonic growth detected by resazurin staining after 48 h incubation. **(C)** Quantification of *in vitro* biofilm biomass grown for 48 h using a CV-microplate assay. **(D)** Colony-forming unit (cfu) counts of *in vitro* biofilms grown for 48 h. **(E)** Quantification of *in vitro* biofilm growth using resazurin staining grown for 48 h. **(F)** Quantification of *in vitro* biofilm growth of *Pseudomonas aeruginosa,* MRSA, and *E. coli* grown for 48 h using resazurin staining. Error bars are the standard deviation from the mean. Statistical significance was calculated using the Student's *t*-test, and *P*-value < 0.05 was considered significant (*$P < 0.05$).

respect to control. The biofilms grown without ASD (control) were thin, bacteria-formed long chain-like structures, and the size of bacteria appeared smaller than the normal (**Figures 2A–C**). In contrast, in the presence of ASD, compact and thick biofilms were formed, and the bacteria were connected to each other and to the adjacent bacteria, imbedded in particulate matters (**Figures 2D–F**). The size of the bacteria appeared normal in the presence of ASD.

In vitro Biofilm Analysis Using Confocal Microscopy

The structures of biofilms, grown in the absence and presence of ASD (300 µg/ml), were analyzed by confocal microscope. The bacteria labeled with fluorescent green PNA probe were visualized. In control samples, bacteria were attached to the bottom of the plate and were unable to form organized biofilms (**Figures 3A–C**). In samples supplemented with ASD (300 µg/ml), cells were connected to each other and to the bottom of the plate and formed biofilms of significant depth (**Figures 3D,E**), and the bacteria formed three-dimensional organized biofilms (**Figure 3F**).

S. pneumoniae Biofilm Gene Expressions Altered by ASD Presence

Our study showed that pneumococcal *in vitro* biofilm growth was enhanced in the presence of ASD; therefore, to evaluate the underlying molecular mechanism, we analyzed the expressions of genes involved in competence (*ciaR)*, competence release *(comA, comB*), and biofilm formation (*luxS*) and toxin-related (*lytA*, *ply*) genes using real-time RT-PCR. The gene expression study revealed up-regulation of genes, such as *ciaR*, *comA, comB, luxS*, *lytA*, and *ply* in biofilms grown in the presence of 300 µg/ml ASD (**Figure 4**). The three genes, *ciaR*, *comA,* and *comB*, involved in *S. pneumoniae* competence production and trans-membrane release of competence stimulating peptides (CSP-1) were up-regulated by 1.8, 5.6, and 5.2-fold, respectively. The *luxS* gene, involved in autoinducer-2 production, a quorum-sensing molecular system, was up-regulated in the presence of ASD by 3.4-fold. Similarly, the pneumococcal toxin-related genes, *ply* (3.5-fold) and *lytA* (2.3-fold), were up-regulated in the presence of ASD.

ASD Exposure Decreased HMEECs Viability and Increased Apoptosis

Percent decrease in cell viability is shown in **Figure 5**. Viability of the untreated cells (control) was considered 100%, whereas that of treated cells was calculated. HMEECs viability was approximately 63% upon ASD treatment or 51% on *S. pneumoniae* treatment; however, on co-treatment (ASD + *S. pneumoniae*), the cell viability was 39% (**Figure 5A**). In co-treatment, the HMEECs viability was significantly ($P < 0.05$) decreased by 60% (**Figure 5A**).

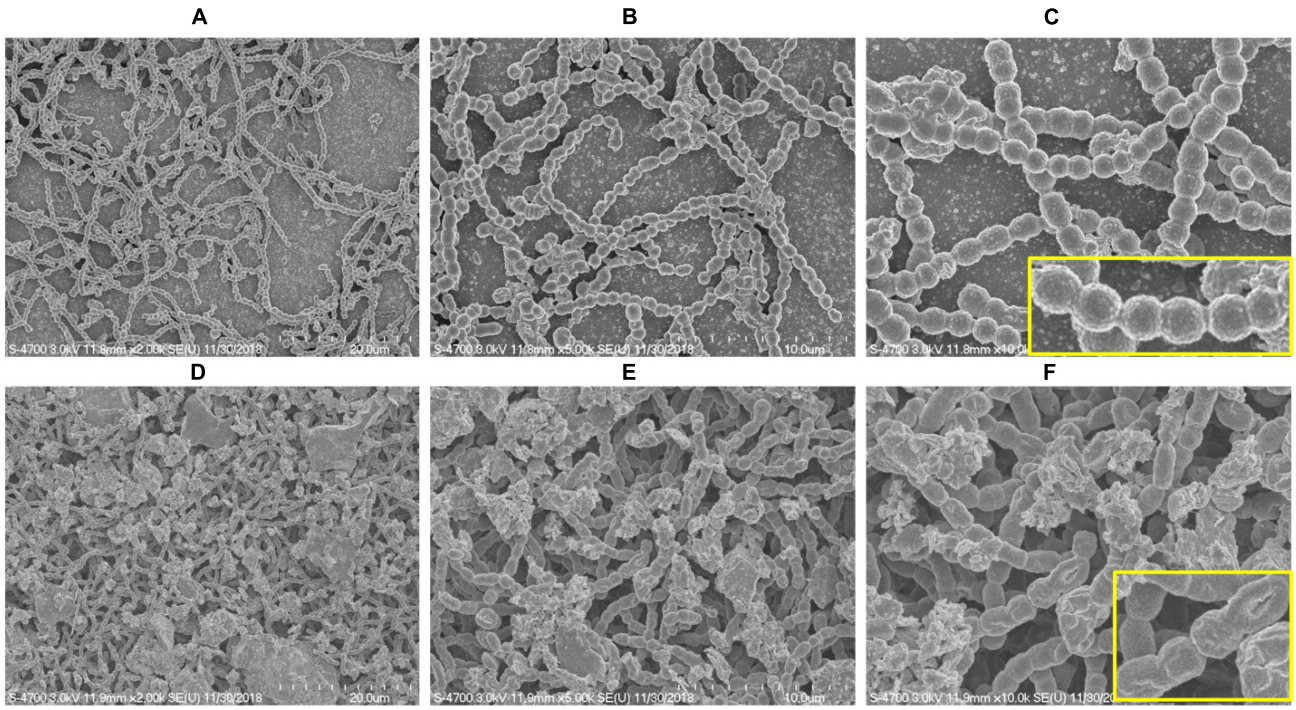

FIGURE 2 | Scanning electron microscope (SEM) images of *S. pneumoniae* D39 *in vitro* biofilms grown in metal ion-free medium for 48 h. **(A–C)** Representative SEM images of the *S. pneumoniae* biofilms grown without ASD (control). The control biofilms were thin and unorganized, bacteria formed long chains, and cell size was smaller than normal. **(D–F)** SEM images of the *S. pneumoniae* biofilms grown in the presence of ASD particles (300 μg/ml). The bacteria formed compact biofilms and were attached to each other, and the cell size appeared normal. Images from left to right are 20, 10, and 5 μm, respectively.

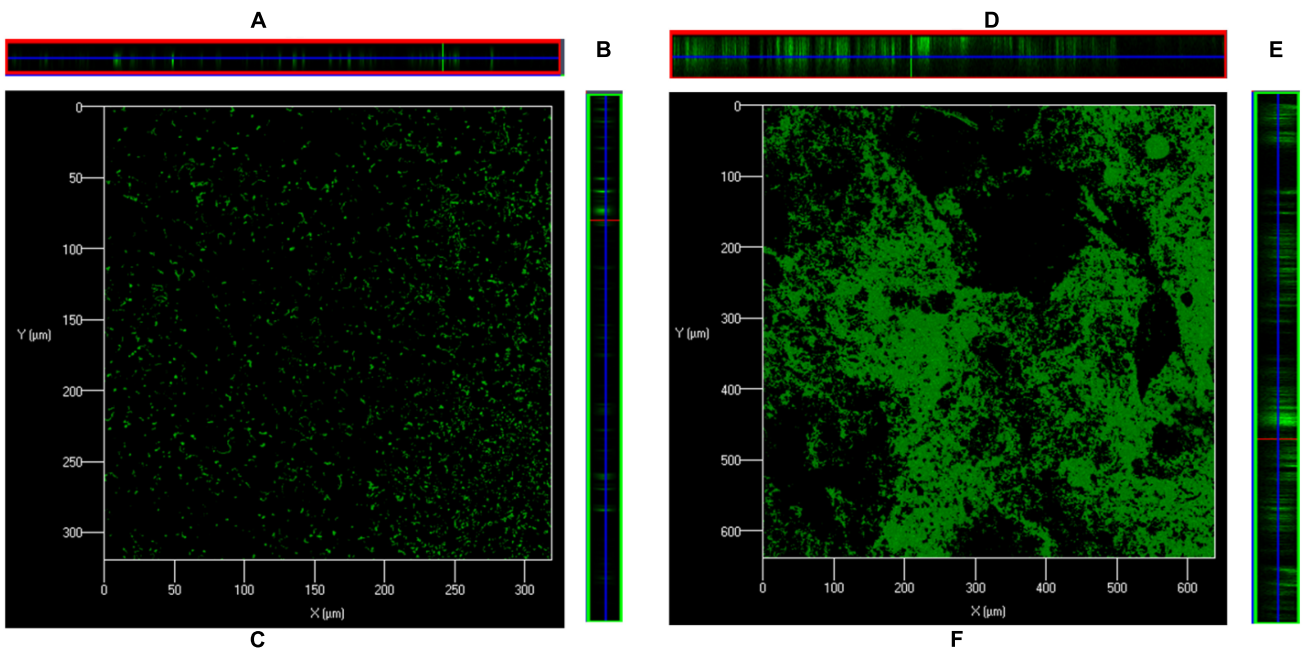

FIGURE 3 | Confocal microscopy images of *S. pneumoniae* D39 *in vitro* biofilms grown in metal ion-free medium for 48 h. **(A)** Is *XZ* and **(B)** is *YZ* plane, and **(C)** is 3-D confocal microscopy image of the *S. pneumoniae* biofilm grown without ASD (control). **(D)** Is *XZ* and **(E)** is *YZ* plane, and **(F)** is 3-D confocal microscopy image of the *S. pneumoniae* biofilm grown with ASD (300 μg/ml).

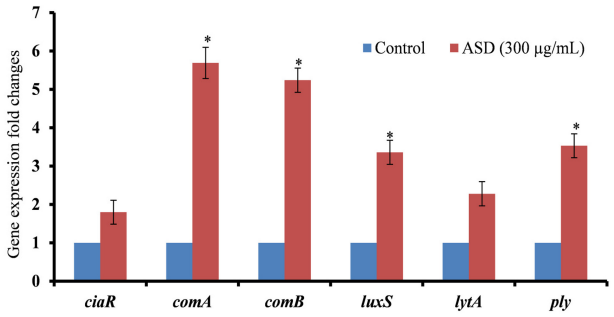

FIGURE 4 | Fold changes in the gene expression of *S. pneumoniae* D39 biofilm grown in metal ion-free medium supplied with 300 µg/ml ASD for 48 h. The differential gene expression was detected by real-time RT-PCR. The error bars representing standard deviation from mean, and statistical significance were calculated by Student's *t*-test and **P*-value less than 0.05 was considered significant.

The apoptosis of HMEECs was detected by annexin-V/PI double staining and cytometry analysis. The cytometric analysis showed that upon single treatment of HMEECs with ASD (**Figure 5C**) or *S. pneumoniae* (**Figure 5D**), a lower number of cells undergo apoptosis. However, large cells undergo apoptosis on co-treatment (**Figure 5F**). The percentage of cells undergoing apoptosis with co-treatment was markedly increased compared to that with ASD or *S. pneumoniae* single treatment (**Figure 5F**).

ASD Exposure Caused Elevated ROS Production

Treatment of HMEECs with ASD or *S. pneumoniae* causes toxicity; one of the mechanisms of toxicity is ROS production. Here, we measured ROS production in HMEECs exposed to either ASD or *S. pneumoniae* or co-treatment. ROS production was increased in HMEECs upon single treatment with ASD or *S. pneumoniae*. However, the ROS production was significantly ($P < 0.05$) elevated on co-treatment (**Figure 6**). Thus, ROS production on co-treatment can be attributed to both ASD and *S. pneumoniae*.

ASD and *S. pneumoniae* Co-treatment Increased Bacterial Colonization in Rat Middle Ear Mucosa

In vivo study showed no visible middle ear mucosal swelling in the control rat bulla (**Figure 7A**), although swelling of middle ear mucosa was visible in ASD (**Figure 7B**) or *S. pneumoniae* (**Figure 7C**) or co-treatment (**Figure 7D**). In co-treatment, severe swelling of the mucosa, with glue-like deposition, was visible. *In vivo* colonization of *S. pneumoniae* in the presence of ASD was increased. The cfu counts of the rat middle ear injected with ASD + *S. pneumoniae* showed increased bacteria colonization. In co-treatment, significantly ($P < 0.05$) > 65% more cfu counts were detected compared to the bacteria-only treatment (**Figure 7E**).

To evaluate the alteration in rat middle ear mucosa morphology upon ASD or *S. pneumoniae* colonization, SEM

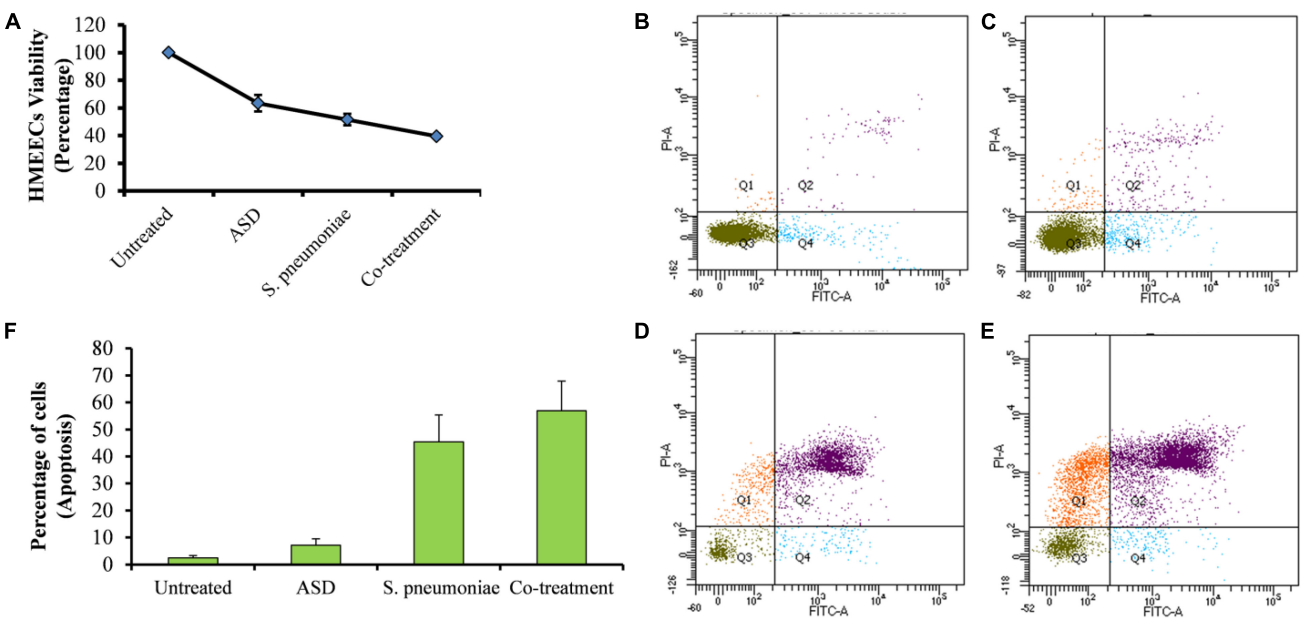

FIGURE 5 | The viability of HMEECs and apoptosis upon ASD or *S. pneumoniae* treatment or co-treatment. **(A)** Cell viability results are represented as the percentage of viable cells compared to the untreated cells (100%). The error bars represent the standard deviation. **(B)** Apoptosis of HMEECs in control, **(C)** apoptosis of HMEECs upon ASD treatment, **(D)** apoptosis upon *S. pneumoniae* treatment, and **(E)** apoptosis of HMEECs upon co-treatment, detected by annexin-V/PI double staining and cytometry analysis. **(F)** Percentage of HMEECs undergoing early and late apoptosis.

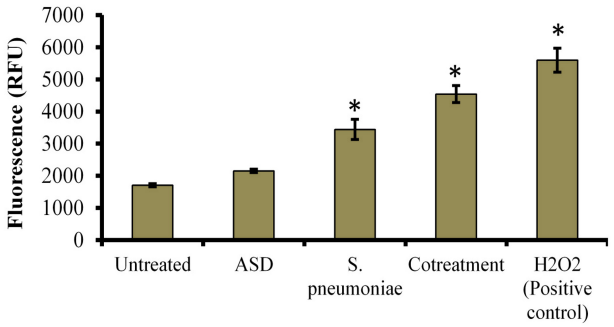

FIGURE 6 | Reactive oxygen species (ROS) production in HMEECs treated with *S. pneumoniae* or ASD or co-treatment. The error bars represent the standard deviation from the mean, and statistical significance was calculated by one-way ANOVA. *P-value less than 0.05 was considered significant.

analysis was conducted. The rat middle ear mucosa is composed of ciliated epithelium in the hypo-tympanic area and eustachian tube orifice area, and the remaining middle ear is covered with non-ciliated squamous epithelium. The SEM analysis showed a clean middle ear of the control rat (**Figures 8A,B**) with visible cilia (**Figure 8C**). The rat middle ear injected with ASD only was clean in the non-ciliated area (**Figures 8D,E**); however, the cilia of the ciliated epithelium were conglomerated (**Figure 8F**). The rat middle ear infected with *S. pneumoniae* showed some biofilm-like debris deposition on the non-ciliated epithelium (**Figures 8G,H**), and the cilia of the ciliated epithelium were conglomerated (**Figure 8I**). Interestingly, the SEM analysis of the rat middle ear injected with ASD+ *S. pneumoniae* revealed that the non-ciliated squamous epithelium was completely filled with biofilm-like debris that covered the whole middle ear (**Figures 8J,K**). The cilia of the ciliated epithelium were conglomerated, and debris was deposited on the tips of cilia (**Figure 8L**).

Elucidation of Rat Middle Ear Mucosa Global Gene Expression Using RNA Sequencing

The differential gene expressions of rat middle ear mucosa inoculated with ASD or *S. pneumoniae* or co-treatment were analyzed by Quant 3′mRNA sequencing. The differentially gene expression analysis revealed a total of 7109 genes that were differentially regulated in ASD-only treatment with respect to untreated. In bacteria-only treatment, 6583 genes were differentially regulated, while the total number of genes differentially expressed in co-treatment were 10,387 (**Figures 9A–D**).

The gene ontology (GO) analysis revealed that the genes involved in immune response, inflammatory response, DNA repair, cell cycle, cell death, apoptosis process, etc. were differentially expressed in all three treatments (**Figure 10A**). However, the number of genes differentially expressed in the above categories were higher in co-treatment compared to single treatments. For example, immune response-related genes differentially expressed in co-treatment were 338, while those in ASD or *S. pneumoniae* treatment were 283 and 277, respectively. Similarly, in co-treatment, 1472 genes related to cell differentiation were differentially regulated, while in ASD or *S. pneumoniae*, 1040 and 945 genes, respectively. The cell death-related genes differentially expressed in co-treatment or ASD or *S. pneumoniae* were 363, 249, and 216, respectively. Apoptosis-related genes differentially regulated in co-treatment

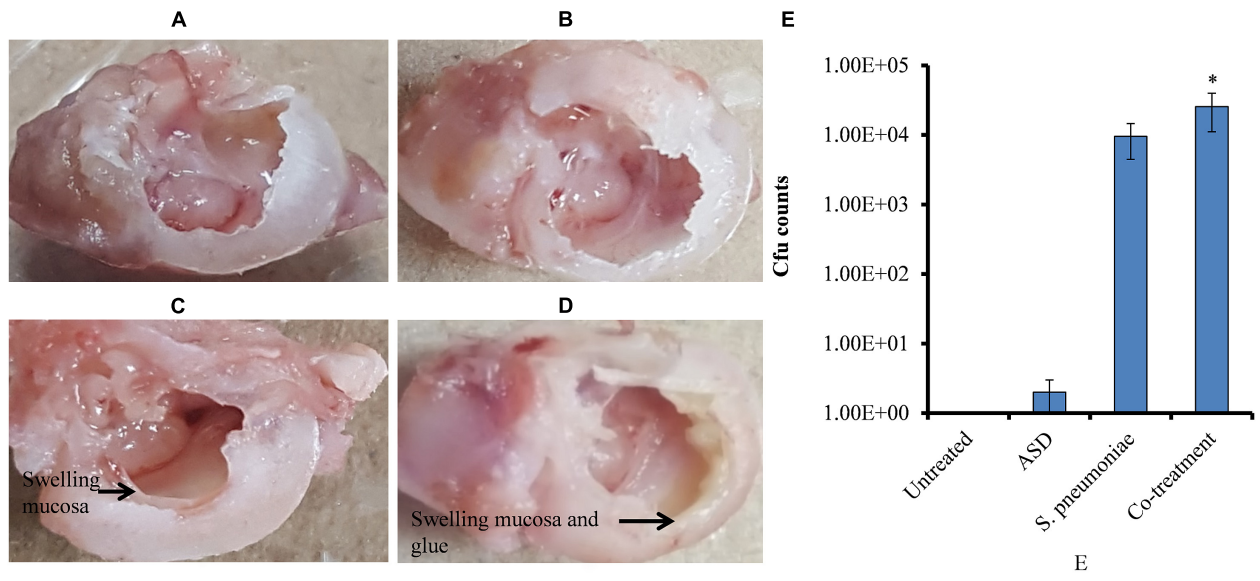

FIGURE 7 | (A–D) Digital photograph of rat middle ear injected with ASD or *S. pneumoniae* of co-treatment. **(E)** Cfu counts of rat middle ear inoculated with ASD or *S. pneumoniae* or co-treatment. The error bars representing standard deviation from mean, and statistical significance were calculated by one-way ANOVA and *P value less than 0.05 was considered significant.

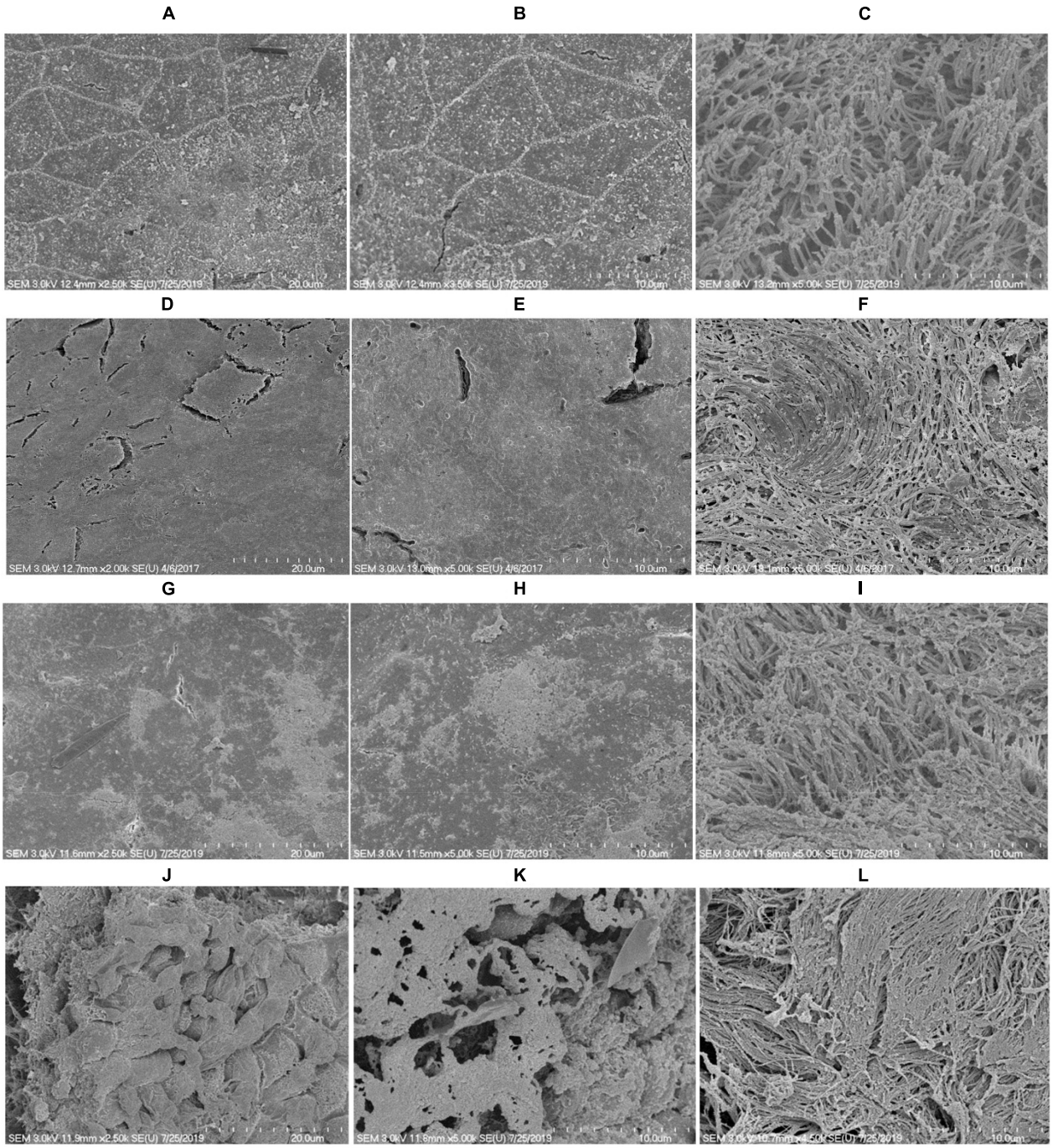

FIGURE 8 | SEM images of rat middle ear colonized with *S. pneumoniae* D39 in the presence or absence of ASD. **(A–C)** Are SEM images of rat middle ear of vehicle control. **(D–F)** Are SEM images of rat middle ear injected with ASD (300 μg/ml). **(G–I)** Are SEM images of rat middle ear infected with *S. pneumoniae* only. **(J–L)** Are SEM images of rat middle ear injected with ASD + *S. pneumoniae*.

or ASD or *S. pneumoniae* treatment were 327, 222, and 198 respectively. These results indicate that the co-treatment induces a large number of gene expressions and affects a large number of cellular processes.

The percentages of significantly differentially regulated genes and the functional category are shown in **Figure 10**. In ASD treatment, the percentage of differentially expressed genes involved in immune response, inflammatory response, DNA repair, cell cycle, cell death, and apoptosis process was 44.50, 52.54, 42.13, 43.98, and 44.31%, respectively (**Figure 10A**). In *S. pneumoniae* treatment, the percentage of differentially expressed genes involved in immune response, inflammatory

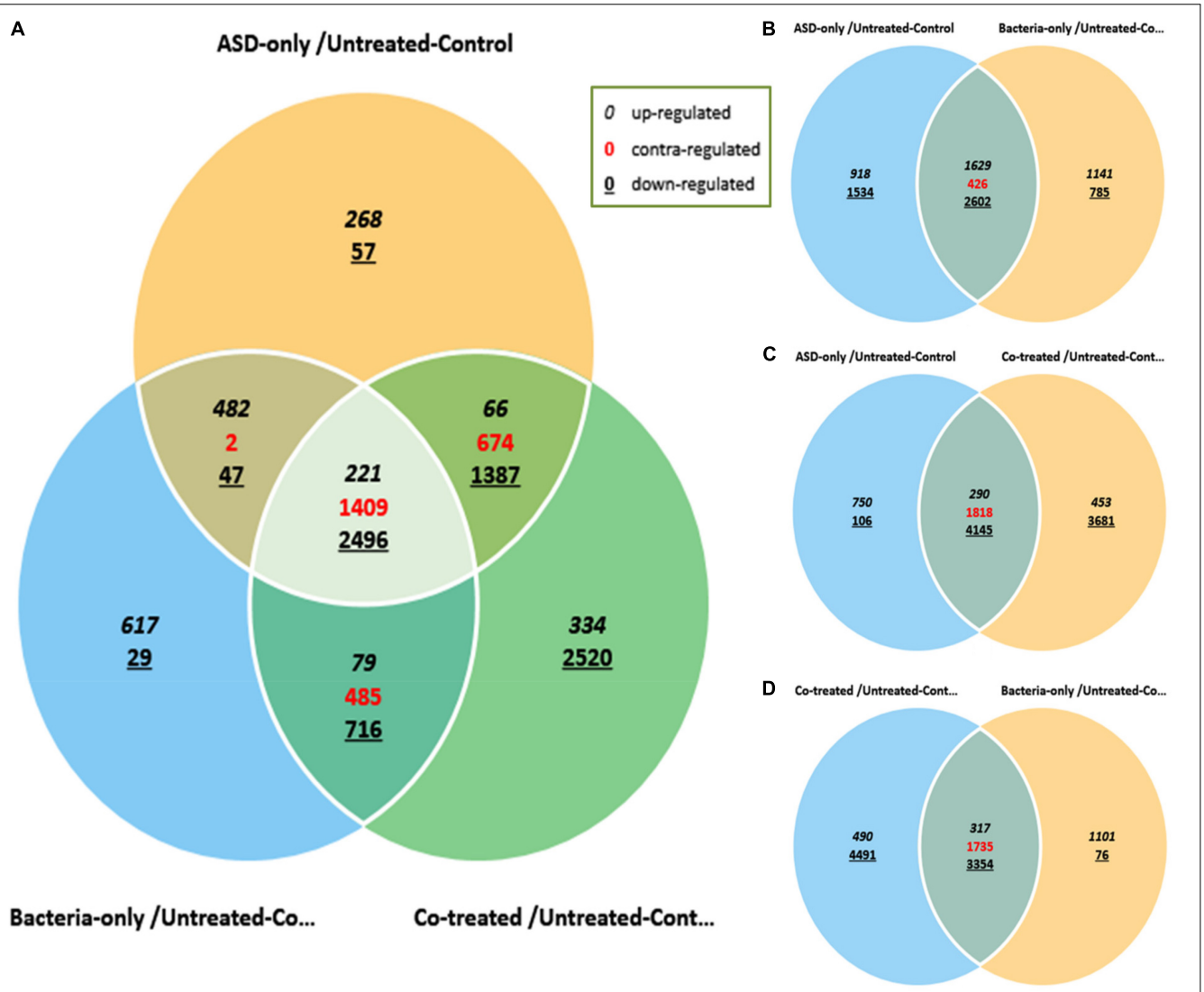

FIGURE 9 | Venn diagram showing differentially expressed genes of rat middle ear mucosa inoculated with ASD only or *S. pneumoniae* (bacteria) or co-treatment with respect to untreated. The global gene expressions were evaluated by Quant 3′m-RNA Sequencing. **(A)** Differentially expressed genes by ±2-folds in all three treatments with respect to control. **(B)** Venn diagram showing differential gene expressions in ASD or *S. pneumoniae* treatment. **(C)** Venn diagram showing differential gene expressions in ASD or co-treatment. **(D)** Venn diagram showing differential gene expressions in *S. pneumoniae* or co-treatment.

response, DNA repair, cell cycle, cell death, and apoptosis process was 43.55, 47.80, 38.72, 34.67, 38.26, and 39.21%, respectively (**Figure 10B**). However, in co-treatment, the percentage of genes that were differentially regulated in each of the above categories was significantly higher. In co-treatment, the percentage of differentially expressed genes involved in immune response, inflammatory response, DNA repair, cell cycle, cell death, and apoptosis process genes were 53.14, 51.53, 64.68, 69.66, 64.59, and 64.75%, respectively (**Figure 10C**). The significantly expressed genes involved in apoptosis, cell death, immune response, and inflammatory response and fold change in three treatments are given in the **Supplementary Table**.

OM-related genes differentially regulated in three treatments include lysine 63 deubiquitinase encoding gene (CYLD), the heme oxygenase 1 encoding gene (HMOX1), the surfactant protein D encoding gene (SFTPD), the SMAD family member 4 encoding gene (SMAD4), the F-Box protein 11 encoding (FBXO11), CD14 molecule encoding gene (CD14), tumor necrosis factor (TNF), Interleukin 1 beta encoding gene (IL1B), and Interleukin 1 alfa encoding (IL1a). In addition, the antibacterial peptide/protein encoding gene such as NP4 (encodes defensin NP-4 precursor), seven genes encoding defensin (DEFB1, DEFA5, DEFA7, DEFA8, DEFA10, DEFA11, and RATNP-3B), CTSG (encode cathepsin G), and six genes of S100 family (encoding S100 calcium binding protein) were down-regulated in co-treatment. Those genes were non-significantly (<2-fold) down-regulated or down-regulated by less folds compared to co-treatment (**Table 2**).

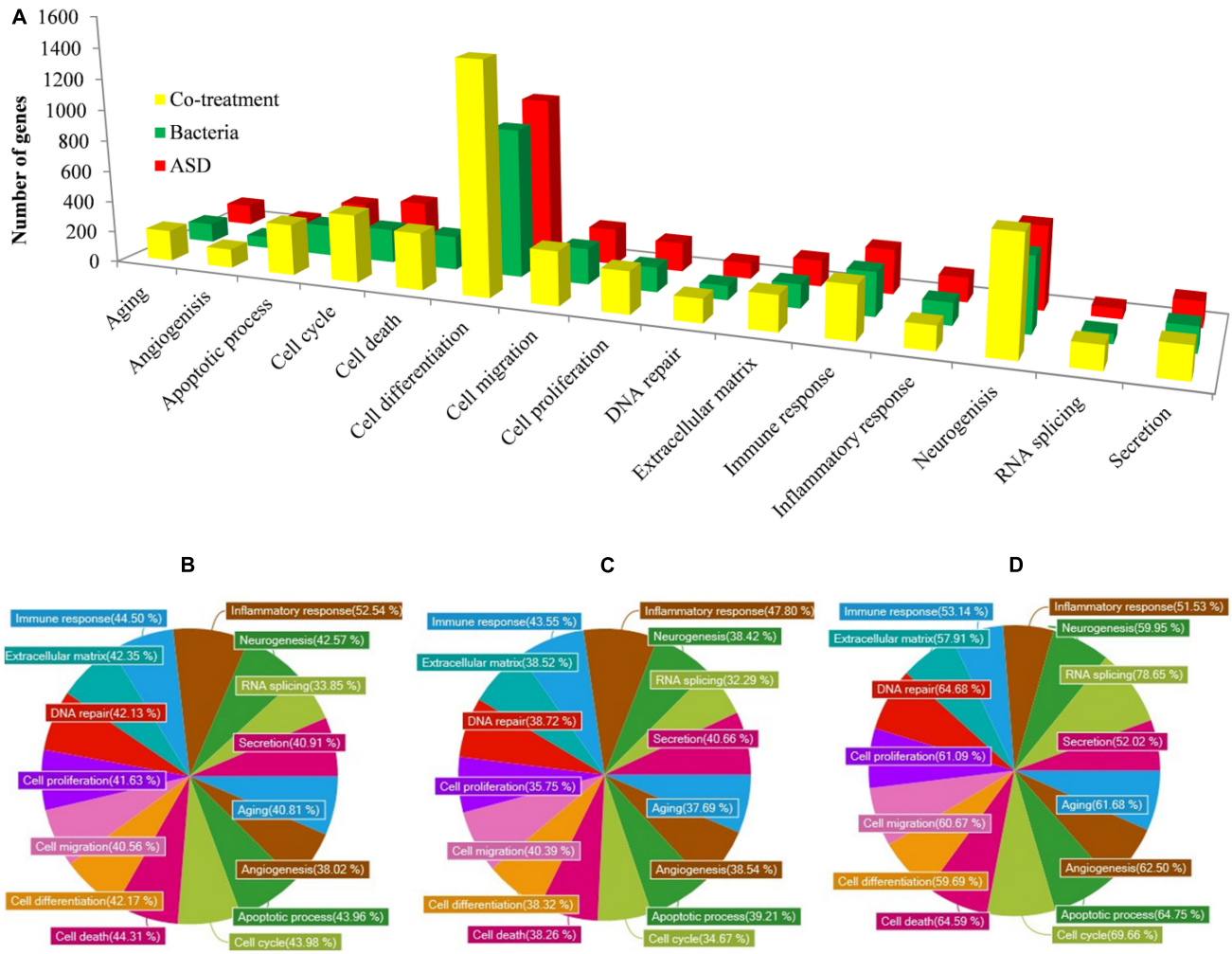

FIGURE 10 | GO (Biological term) of genes differentially expressed in rat middle ear mucosa treated with ASD or *Streptococcus pneumoniae* or co-treatment with respect to control (untreated). **(A)** Number of gene and functional categories. **(B)** Percentage of significantly differentially expressed genes involved in different functional categories and up-regulated or down-regulated upon ASD treatment, (B) *S. pneumoniae* treatment, or **(C)** co-treatment.

DISCUSSION

Streptococcus pneumoniae and ASD particulate matter are among the major risk factors causing OM worldwide; however, these two factors have been studied separately until now (Hall-Stoodley et al., 2006; Park et al., 2018). Attempts have not been made to evaluate the synergistic or additive effects of these risk factors on the outcome of OM. Furthermore, the initial interaction of ASD and pneumococci occurs in the nasopharyngeal cavity, and *S. pneumoniae* is a commensal bacterium that colonizes the nasopharyngeal cavity asymptomatically. It is not known whether the pneumococci revert to the pathogenic form on exposure to particulate matter such as ASD and cause OM. In this study, we evaluated the effect of ASD on pneumococcal biofilm growth and colonization on HMEECs and on middle ear mucosa using the rat OM model.

In this study, our results showed low bacterial growth in metal ion-free medium; however, in the presence of ASD, pneumococcal growth was significantly increased, indicating that ASD composition plays a crucial role in pneumococcal growth in the metal-devoid medium. For normal bacterial growth, metals such as Fe, Na, Mg, and Mn are essential; however, those were absent in metal ion-free medium (Weiss and Carver, 2018). Previously, Hussey et al. (2017) using Todd–Hewitt broth + 0.5% (w/v) yeast extract (THY), which contains all the required essential elements detected increased bacterial growth in the presence of black carbon. However, no reasons for elevated bacterial growth were suggested (Hussey et al., 2017). We previously reported that ASD contains various metals such as Fe, Na, Mg, and Mn (Chang et al., 2016). Since Fe, Mg, and Mn are important for *S. pneumoniae* growth and virulence, bacterial growth and virulence were disrupted in the absence of those metals (Romero-Espejel et al., 2013; Weiser et al., 2018). Pneumococci possess a specific efflux pump for the utilization of Fe and other metals (Honsa et al., 2013). Therefore,

TABLE 2 | Otitis media-related differentially expressed genes in rat mucosa treated with ASD or *Streptococcus pneumoniae* or co-treatment.

Gene function	Gene name	Fold change in ASD	Fold change in *Streptococcus pneumoniae*	Fold change co-treatment
Host defense against microbial infection	CTSG gene encodes cathepsin G transcript variant X1	0.05	0.07	0.03
	S100a13 gene encodes S100 calcium binding protein A13	0.45	0.48	0.003
	S100a16 gene encodes S100 calcium binding protein A16	1.5	1.5	0.002
	S100a3 gene encodes S100 calcium binding protein A3, transcript variant X2	0.21	0.51	0.21
	S100a8 gene encodes S100 calcium binding protein A8, transcript variant X1	0.42	0.37	0.042
	S100a9 gene encodes S100 calcium binding protein A9, transcript variant X1	0.51	0.26	0.04
	NP-4 gene encodes defensin NP-4 precursor	0.062	0.08	0.03
	DEFB1 gene encodes defensin beta 1	1.7	8.0	0.25
	DEFA5 gene encodes defensin alpha 5, transcript variant X1	0.042	0.01	0.003
	DEFA7 gene encodes defensin alpha 7	0.080	0.090	0.04
	DEFA10 gene encodes defensin alpha 10	0.41	0.38	0.31
	DEFA11 gene encodes defensin alpha 11, transcript variant X1	0.05	0.09	0.07
	RATNP-3B gene encodes defensin RatNP-3 precursor	0.12	0.2	0.07
Inflammatory response	SMAD4 gene encodes SMAD family member 4	1.471	1.439	0.02
	HMOX1 gene encodes the heme oxygenase 1 encoding gene	9.578	22.228	14.609
	CYLD gene encodes deubiquitinase cylindromatosis	Cyld	1.686	1.204
	FBXO11 gene encodes the F-Box protein 11 encoding	2.304	1.198	0.006
	CD14 gene encodes molecule encoding gene	11.958	6.473	12.230
Cytokines and interleukins	TNF gene encodes tumor necrosis factor	117.15	60.40	0.95
	IL1B gene encodes Interleukin 1 beta encoding gene	4257.707	1057.356	788.250
	IL1A gene encodes Interleukin 1 alfa encoding	397.876	98.273	0.953
Apoptosis	Ddit3 encodes DNA-damage inducible transcript 3, transcript variant X2	2.066	3.676	3.846
	Bak1 gene encodes BCL2-antagonist/killer 1, transcript variant X1	2.592	2.314	2.503

it appears that the metal contents of ASD favor pneumococcal planktonic growth.

We detected increased *in vitro* biofilm growth in the presence of ASD. The primary reason for elevated biofilm growth of pneumococci may be the increase in planktonic bacterial growth. In addition, the metal contents of ASD, including Fe (2.035%) stimulated biofilm growth. An increase in biofilm growth and virulence of pneumococci in the presence of Fe has been reported previously (Trappetti et al., 2011b). The biofilms were grown in metal-free medium, and SEM analysis revealed a significant morphological difference in the control and ASD-treated biofilms. In the absence of metal ion, pneumococci cell size appeared abnormal and formed long chain-like structures. Iron is an essential metal for bacterial growth, and its importance in pneumococcal growth is well-known (Romero-Espejel et al., 2013). In contrast, the biofilms supplemented with ASD were thick and compact and formed 3-D structures, and the bacteria size appeared normal (Moscoso et al., 2006), suggesting that metal deficiency was compensated for by the metal constituents of ASD, and the pneumococci resumed normal biofilm growth. Similarly, in the presence of Fe, up-regulation of biofilm formation has been reported for *Pseudomonas* and *E. coli* (Banin et al., 2008; Wu and Outten, 2009). Probably, the ASD particles provide a favorable surface for bacterial attachment and biofilm growth. Similar results were observed previously in the presence of black carbon (Hussey et al., 2017).

In *S. pneumoniae*, the production of biofilms was found to be regulated by competence (Com) quorum-sensing (QS) mediated by the competence-stimulating peptide (CSP) and LuxS/Autoinducer-2 (AI-2) QS (Trappetti et al., 2011a; Vidal et al., 2013; Weyder et al., 2018). In this study, up-regulation of *ciaR*, *comA*, and *comB* and *luxS* gene indicated that competence and QS were increased in the presence of ASD. Trappetti et al. (2011b) reported that *luxS* gene is the central regulator of competence, fratricide, and biofilm formation, and its expression is up-regulated in the presence of Fe in pneumococci (Trappetti et al., 2011b). In addition, the *luxS* gene is important for the synthesis of the AI-2 QS molecule that regulates pneumococcal biofilms; less biofilm formation has been reported in the *S. pneumoniae luxS* mutant (Vidal et al., 2013; Yadav et al., 2018). The *ply* genes encoding pneumolysin and *lytA* encode protein that facilitates the release of toxin that was up-regulated in biofilms (Allegrucci et al., 2006; Moscoso et al., 2006). Altogether, these results indicated that ASD induced the expression of biofilm and competence-related genes and enhanced biofilm formation.

Exposure to ASD is toxic to epithelial cells; our previous study showed a concentration-dependent decrease in HMEEC viability in the presence of ASD (Chang et al., 2016). Exposure to pneumococci also decreases the epithelial cell viability. Here, the HMEEC viability was significantly reduced in co-treatment with ASD+ *S. pneumoniae*. The significantly low viability of HMEECs in co-treatment could be due to the

pre-exposure to ASD-induced inflammation, which might result in HMMEC injury, and therefore, cells become more susceptible to pneumococci infection and cell death (Willemse et al., 2005). These results suggest that the low viability in co-treatment could be the result of additive toxicity of ASD and *S. pneumoniae*.

Here, we detected a large number of HMEECs that underwent apoptosis and produced elevated ROS in co-treatment compared to the single treatments. *S. pneumoniae* is known to produce a number of toxins, including pneumolysin that induces DNA damage and cell cycle arrest (Rai et al., 2016). In addition, it was suggested that *S. pneumoniae* produces hydrogen peroxide that damages the DNA and induces apoptosis in lung epithelial cells (Rai et al., 2015). Similarly, the toxicity of ASD is attributed to oxidative stress and apoptosis (Go et al., 2015; Chang et al., 2016; Pfeffer et al., 2018). Therefore, it appears that the additive effects of ASD and *S. pneumoniae* enhance apoptosis. It is known that ASD containing PM and *S. pneumoniae* treatment individually are toxic to epithelium cells, and one of the mechanisms of toxicity is mediated by ROS production (Li et al., 2015; Rai et al., 2015). It is reported that ASD stimulates the ROS production, and in lung infection, *S. pneumoniae*-mediated hydrogen peroxide production depended on the pneumococcal autolysin LytA (Hocke et al., 2014). In addition, *S. pneumoniae* induces autophagy in A549 cells through ROS hypergeneration (Li et al., 2015). Therefore, it appears that the ASD-only or *S. pneumoniae*-only treatment was unable to induce much toxicity, apoptosis, and ROS production in HMEECs, which was amplified in co-treatment due to combined effects.

In vivo study results showed elevated pneumococci in rat middle ear and mucosa swelling in the presence of ASD. The concentration of ASD (300 μg/ear) or the number of bacteria injected (5×10^6) was decided on the basis of our previous study, and the concentrations were reduced to exert minimum effects of single treatments (Yadav et al., 2012; Go et al., 2015; Chang et al., 2016). The cfu counts and SEM analysis indicated that a single treatment with ASD (300 μg) or *S. pneumoniae* (5×10^6) induced low toxicity; however, the presence of ASD+ *S. pneumoniae* amplified the toxicity and elevated colonization on middle ear mucosa. Previously, Hussey et al. (2017) also reported increased *in vivo* colonization of bacteria in the presence of black carbon PM (Hussey et al., 2017).

The gene expression results indicate that the co-treatment induces a large number of gene expressions and affects a large number of cellular processes, which could be due to elevated toxicity in co-treatment. The gene expression study revealed a large number of genes that were significantly differentially expressed in co-treatment are involved in apoptosis, cell death, DNA repair, immune response, and inflammatory response. Inflammatory cytokines such as IL1α, IL1β, and tumor necrosis factor produced by macrophages and monocytes in response to microbial toxin play a vital role in middle ear inflammation and OM (Yellon et al., 1991; Willett et al., 1998). Here, our results showed increased expressions of cytokine- and interleukin-related genes in all three treatments; however, the fold change varied in each treatment. The SMAD gene, CYLD gene (encodes deubiquitinase cylindromatosis), and FBXO11 (F-Box Protein 11) gene were down-regulated by >2-fold in co-treatment and non-significantly in ASD or *S. pneumoniae* treatment. The SMAD genes are mediators of the TGF-β pathway and regulate cell proliferation, apoptosis, and cell differentiation and mutation in SMAD-increased OM susceptibility (MacArthur et al., 2014). The FBXO11 is another important OM-related gene in mouse model mutation in FBXO11 that caused OM (Hardisty-Hughes et al., 2006). The deubiquitinase cylindromatosis (CYLD) gene expression involved in the suppression of the *H. influenzae* induced expression of pro-inflammatory chemokines (Wang et al., 2014). It has been suggested that PM weakens the host innate defense and obstructs the antibacterial peptides and proteins such as secretory leukocyte protease inhibitor and defensins (Chen et al., 2010, 2018). Here, our results showed down-regulation of NP4 (encodes defensin NP-4 precursor), CTSG (encode cathepsin G), six genes of the S100A family (S100A13, S100A16, S100A3, S100A6, S100A8, and S100A9) and seven genes encoding defensin (DEFB1, DEFA5, DEFA7, DEFA8, DEFA10, DEFA11, and RATNP-3B) in co-treatment. These genes encode peptides or proteins that are involved in host defense against bacterial infection, and the down-regulation in co-treatment indicates that the host defense was decreased. Defensins are broad-spectrum antimicrobial peptides that have been implicated in prevention of AOM (Underwood and Bakaletz, 2011). It was reported that deficiency of S100A8/A9 in mice could promote the progression of pneumonia caused by bacterial infection (Achouiti et al., 2015). The gene expression results indicates that co-treatment up-regulated pro-inflammatory cytokines and interleukins and down-regulated inflammation suppressor genes. Altogether, these results suggest that ASD exposure decreases host cell immune defense causing cells susceptible to establish pneumococcal infections and aggregate on the mucosa.

CONCLUSION

The results of this study showed that in the presence of ASD, pneumococcal *in vitro* biofilm growth and *in vivo* colonization to rat middle ear mucosa were elevated. The pre-exposure to ASD increased pneumococcal colonization to HMEECs, elevated ROS production and apoptosis, and increased bacteria susceptibility results in reduced HMEEC viability. The co-treatment affects a large number of genes involved in apoptosis, cell death, immune response, inflammatory response, and down-regulated defense-related genes. Altogether, these results indicate that ASD presence decreases host immune defense and increases cell susceptibility to pneumococcal infection.

DATA AVAILABILITY STATEMENT

The raw data supporting the conclusions of this manuscript will be made available by the authors, without undue reservation, to any qualified researcher.

ETHICS STATEMENT

The animal study was reviewed and approved by Institutional Animal Care and Use Committees (IACUCs), Korea University. Written informed consent was obtained from the owners for the participation of their animals in this study.

AUTHOR CONTRIBUTIONS

MY, S-WC, and J-JS: conceptualization. MY and YG: methodology. MP and J-JS: supervision. MY and J-JS: writing. MP and S-WC: review and editing.

FUNDING

This research was supported by the Basic Science Research Program of the National Research Foundation (NRF) of Korea funded by Ministry of Education grant (2017R1D1A1B03035306 to MY).

SUPPLEMENTARY MATERIAL

The Supplementary Material for this article can be found online at: https://www.frontiersin.org/articles/10.3389/fgene.2020.00323/full#supplementary-material

REFERENCES

Achouiti, A., Vogl, T., Van der Meer, A. J., Stroo, I., Florquin, S., de Boer, O. J., et al. (2015). Myeloid-related protein-14 deficiency promotes inflammation in staphylococcal pneumonia. *Eur. Respirat. J.* 46, 464–473. doi: 10.1183/09031936.00183814

Acuin, J. (2004). *Chronic Suppurative Otitis Media - Burden of Illness and Management Options*. Geneva: World Health Organization.

Al, B., Bogan, M., Zengin, S., Sabak, M., Kul, S., Oktay, M. M., et al. (2018). Effects of dust storms and climatological factors on mortality and morbidity of cardiovascular diseases admitted to ED. *Emerg. Med. Int,* 2018:7. doi: 10.1155/2018/3758506

Allegrucci, M., Hu, F. Z., Shen, K., Hayes, J., Ehrlich, G. D., Post, J. C., et al. (2006). Phenotypic characterization of *Streptococcus pneumoniae* biofilm development. *J. Bacteriol.* 188, 2325–2335. doi: 10.1128/jb.188.7.2325-2335.2006

Avery, O. T., Macleod, C. M., and McCarty, M. (1944). Studies on the chemical nature of the substance inducing transformation of pneumococcal types : induction of transformation by a desoxyribonucleic acid fraction isolated from pneumococcus type III. *J. Exp. Med.* 79, 137–158. doi: 10.1084/jem.79.2.137

Banin, E., Lozinski, A., Brady, K. M., Berenshtein, E., Butterfield, P. W., Moshe, M., et al. (2008). The potential of desferrioxamine-gallium as an anti-*Pseudomonas therapeutic* agent. *Proc. Natl. Acad. Sci. U.S.A.* 105, 16761–16766. doi: 10.1073/pnas.0808608105

Becker, S., and Soukup, J. M. (1999). Exposure to urban air particulates alters the macrophage-mediated inflammatory response to respiratory viral infection. *J. Toxicol. Environ. Health A* 57, 445–457. doi: 10.1080/009841099157539

Bellussi, L., Mandalà, M., Passàli, F. M., Passàli, G. C., Lauriello, M., and Passali, D. (2005). Quality of life and psycho-social development in children with otitis media with effusion. *Acta Otorhinolaryngol. Ital.* 25, 359–364.

Blanchette, K. A., Shenoy, A. T., Milner, J. II, Gilley, R. P., McClure, E., Hinojosa, C. A., et al. (2016). Neuraminidase A-exposed galactose promotes *Streptococcus pneumoniae* biofilm formation during colonization. *Infect. Immun.* 84, 2922–2932. doi: 10.1128/IAI.00277-16

Bowatte, G., Tham, R., Perret, J. L., Bloom, M. S., Dong, G., Waidyatillake, N., et al. (2018). Air pollution and otitis media in children: a systematic review of literature. *Int. J. Environ. Res. Public Health* 15:257. doi: 10.3390/ijerph15020257

Brown, L. R., Caulkins, R. C., Schartel, T. E., Rosch, J. W., Honsa, E. S., Schultz-Cherry, S., et al. (2017). Increased zinc availability enhances initial aggregation and biofilm formation of *Streptococcus pneumoniae*. *Front. Cell. Infect. MIcrobiol.* 7:233. doi: 10.3389/fcimb.2017.00233

Byeon, H. (2019). The association between allergic rhinitis and otitis media: a national representative sample of in South Korean children. *Sci. Rep.* 9, 1610–1610. doi: 10.1038/s41598-018-38369-7

Chang, J., Go, Y. Y., Park, M. K., Chae, S.-W., Lee, S.-H., and Song, J.-J. (2016). Asian sand dust enhances the inflammatory response and mucin gene expression in the middle ear. *Clin. Exp. Otorhinolaryngol.* 9, 198–205. doi: 10.21053/ceo.2015.01060

Chao, Y., Marks, L. R., Pettigrew, M. M., and Hakansson, A. P. (2015). *Streptococcus pneumoniae* biofilm formation and dispersion during colonization and disease. *Front. Cell. Infect. Microbiol.* 4:194. doi: 10.3389/fcimb.2014.00194

Chen, P.-S., Tsai, F. T., Lin, C. K., Yang, C.-Y., Chan, C.-C., Young, C.-Y., et al. (2010). Ambient influenza and avian influenza virus during dust storm days and background days. *Environ. Health Perspect.* 118, 1211–1216. doi: 10.1289/ehp.0901782

Chen, X., Liu, J., Zhou, J., Wang, J., Chen, C., Song, Y., et al. (2018). Urban particulate matter (PM) suppresses airway antibacterial defence. *Respir. Res.* 19, 5. doi: 10.1186/s12931-017-0700-0

Chen, Y.-S., Sheen, P.-C., Chen, E.-R., Liu, Y.-K., Wu, T.-N., and Yang, C.-Y. (2004). Effects of Asian dust storm events on daily mortality in Taipei. Taiwan. *Environ. Res.* 95, 151–155. doi: 10.1016/j.envres.2003.08.008

Christensen, G. D., Bisno, A. L., Parisi, J. T., McLaughlin, B., Hester, M. G., and Luther, R. W. (1982). Nosocomial septicemia due to multiply antibiotic-resistant staphylococcus epidermidis. *Ann. Int. Med.* 96, 1–10.

Chun, Y. M., Moon, S. K., Lee, H. Y., Webster, P., Brackmann, D. E., Rhim, J. S., et al. (2002). Immortalization of normal adult human middle ear epithelial cells using a retrovirus containing the E6/E7 genes of human papillomavirus type 16. *Ann. Otol. Rhinol. Laryngol.* 111, 507–517. doi: 10.1177/000348940211100606

Coleman, A., Wood, A., Bialasiewicz, S., Ware, R. S., Marsh, R. L., and Cervin, A. (2018). The unsolved problem of otitis media in indigenous populations: a systematic review of upper respiratory and middle ear microbiology in indigenous children with otitis media. *Microbiome* 6, 199–199. doi: 10.1186/s40168-018-0577-2

Gentleman, R. C., Carey, V. J., Bates, D. M., Bolstad, B., Dettling, M., Dudoit, S., et al. (2004). Bioconductor: open software development for computational biology and bioinformatics. *Genome Biol.* 5, R80–R80.

Girguis, M. S., Strickland, M. J., Hu, X., Liu, Y., Chang, H. H., Kloog, I., et al. (2018). Exposure to acute air pollution and risk of bronchiolitis and otitis media for preterm and term infants. *J. Exposure Sci. Environ. Epidemiol.* 28, 348–357. doi: 10.1038/s41370-017-0006-9

Givon-Lavi, N., Dagan, R., Greenberg, D., Peled, N., Broides, A., and Blancovich, I. (2006). The contribution of smoking and exposure to tobacco smoke to *Streptococcus pneumoniae* and *haemophilus influenzae* carriage in children and their mothers. *Clin. Infect. Dis.* 42, 897–903. doi: 10.1086/500935

Go, Y. Y., Park, M. K., Kwon, J. Y., Seo, Y. R., Chae, S.-W., and Song, J.-J. (2015). Microarray analysis of gene expression alteration in human middle ear epithelial cells induced by asian sand dust. *Clin. Exp. Otorhinolaryngol.* 8, 345–353. doi: 10.3342/ceo.2015.8.4.345

Hall-Stoodley, L., Hu, F. Z., Gieseke, A., Nistico, L., Nguyen, D., Hayes, J., et al. (2006). Direct detection of bacterial biofilms on the middle-ear mucosa of children with chronic otitis media. *JAMA* 296, 202–211.

Hardisty-Hughes, R. E., Tateossian, H., Morse, S. A., Romero, M. R., Middleton, A., Tymowska-Lalanne, Z., et al. (2006). A mutation in the F-box gene, Fbxo11, causes otitis media in the Jeff mouse. *Hum. Mol. Genet.* 15, 3273–3279. doi: 10.1093/hmg/ddl403

Hocke, A. C., Doehn, J.-M., Suttorp, N., Hübner, R.-H., Hippenstiel, S., Kim, Y.-J., et al. (2014). *Streptococcus pneumoniae*–induced oxidative stress in lung epithelial cells depends on pneumococcal autolysis and is reversible by resveratrol. *J. Infect. Dis.* 211, 1822–1830. doi: 10.1093/infdis/jiu806

Honsa, E. S., Johnson, M. D. L., and Rosch, J. W. (2013). The roles of transition metals in the physiology and pathogenesis of *Streptococcus pneumoniae*. *Front. Cell. Infect. Microbiol.* 3:92. doi: 10.3389/fcimb.2013.00092

Hussey, S. J. K., Purves, J., Allcock, N., Fernandes, V. E., Monks, P. S., Ketley, J. M., et al. (2017). Air pollution alters *Staphylococcus aureus* and *Streptococcus pneumoniae* biofilms, antibiotic tolerance and colonisation. *Environ. Microbiol.* 19, 1868–1880. doi: 10.1111/1462-2920.13686

Jensen, R. G., Koch, A., and Homøe, P. (2013). The risk of hearing loss in a population with a high prevalence of chronic suppurative otitis media. *Int. J. Pediatr. Otorhinolaryngol.* 77, 1530–1535. doi: 10.1016/j.ijporl.2013.06.025

Jones, L. L., Hassanien, A., Cook, D. G., Britton, J., and Leonardi-Bee, J. (2012). Parental smoking and the risk of middle ear disease in children: a systematic review and meta-analysis. *JAMA Pediatr.* 166, 18–27. doi: 10.1001/archpediatrics.2011.158

Jung, J. H., Kang, I. G., Cha, H. E., Choe, S. H., and Kim, S. T. (2012). Effect of asian sand dust on mucin production in nci-h292 cells and allergic murine model. *Otolaryngol.Head Neck Surg.* 146, 887–894. doi: 10.1177/0194599812439011

Jung, W. (2016). *Environmental Challenges and Cooperation in Northeast Asia*. Stockholm: Institute for Security and Development.

Kennedy, C. M., Pennington, A. F., Darrow, L. A., Klein, M., Zhai, X., Bates, J. T., et al. (2018). Associations of mobile source air pollution during the first year of life with childhood pneumonia, bronchiolitis, and otitis media. *Environ. Epidemiol.* 2:e007. doi: 10.1097/EE9.0000000000000007

Kim, H. J., Kim, S. Y., Kwon, J. Y., Hun, Kang S, Jang, W. H., Lee, J. H., et al. (2016). Identification of potential novel biomarkers and signaling pathways related to otitis media induced by diesel exhaust particles using transcriptomic analysis in an in vivo system. *PloS One* 11:e0166044. doi: 10.1371/journal.pone.0166044

Kong, S.-K., Chon, K.-M., Goh, E.-K., Lee, I.-W., Lee, J.-W., and Wang, S.-G. (2009). Histologic changes in the auditory tube mucosa of rats after long-term exposure to cigarette smoke. *Am. J. Otolaryngol.* 30, 376–382. doi: 10.1016/j.amjoto.2008.07.009

Langmead, B., and Salzberg, S. L. (2012). Fast gapped-read alignment with Bowtie 2. *Nat. Methods* 9, 357–259. doi: 10.1038/nmeth.1923

Lee, H., Honda, Y., Lim, Y.-H., Guo, Y. L., Hashizume, M., and Kim, H. (2014). Effect of Asian dust storms on mortality in three Asian cities. *Atmos. Environ.* 89, 309–317. doi: 10.1016/j.atmosenv.2014.02.048

Li, P., Shi, J., He, Q., Hu, Q., Wang, Y. Y., Zhang, L. J., et al. (2015). *Streptococcus pneumoniae* induces autophagy through the inhibition of the PI3K-I/Akt/mTOR Pathway and ROS hypergeneration in A549 Cells. *PLoS One* 10:e0122753. doi: 10.1371/journal.pone.0122753

MacArthur, C. J., Wilmot, B., Wang, L., Schuller, M., Lighthall, J., and Trune, D. (2014). Genetic susceptibility to chronic otitis media with effusion: candidate gene single nucleotide polymorphisms. *Laryngosc.* 124, 1229–1235. doi: 10.1002/lary.24349

Malic, S., Hill, K. E., Hayes, A., Percival, S. L., Thomas, D. W., and Williams, D. W. (2009). Detection and identification of specific bacteria in wound biofilms using peptide nucleic acid fluorescent in situ hybridization (PNA FISH). *Microbiology* 155, 2603–2611. doi: 10.1099/mic.0.028712-0

Middleton, N., and Kang, U. (2017). Sand and dust storms: impact mitigation. *Sustainability* 9:1053. doi: 10.1016/j.chemosphere.2016.04.052

Milucky, J., Morais, T. M. L., Pontes, H. A. R., de Almeida, O. P., de Carvalho, M. G. F., Soares, C. D., et al. (2019). *Streptococcus pneumoniae* colonization after introduction of 13-valent pneumococcal conjugate vaccine for US adults 65 years of age and older, 2015–2016. *Vaccine* 37, 1094–1100. doi: 10.1016/j.vaccine.2018.12.075

Monasta, L., Ronfani, L., Marchetti, F., Montico, M., Vecchi Brumatti, L., Bavcar, A., et al. (2012). Burden of disease caused by otitis media: systematic review and global estimates. *PloS One* 7:e36226. doi: 10.1371/journal.pone.0036226

Moscoso, M., García, E., and López, R. (2006). Biofilm formation by *Streptococcus pneumoniae*: role of choline, extracellular DNA, and capsular polysaccharide in microbial accretion. *J. Bacteriol.* 188, 7785–7795. doi: 10.1128/jb.00673-06

Nakao, M., Ishihara, Y., Kim, C.-H., and Hyun, I.-G. (2018). The impact of air pollution, including asian sand dust, on respiratory symptoms and health-related quality of life in outpatients with chronic respiratory disease in korea: a panel study. *J. Prevent. Med. Public Health* 51, 130–139. doi: 10.3961/jpmph.18.021

Nuorti, J. P., Butler, J. C., Farley, M. M., Harrison, L. H., McGeer, A., Kolczak, M. S., et al. (2000). Cigarette smoking and invasive pneumococcal disease. *N. Engl. J. Med.* 342, 681–689.

Park, M., Han, J., Jang, M.-J., Suh, M.-W., Lee, J. H., Oh, S. H., et al. (2018). Air pollution influences the incidence of otitis media in children: a national population-based study. *PloS One* 13:e0199296. doi: 10.1371/journal.pone.0199296

Pfeffer, P. E., Lu, H., Mann, E. H., Chen, Y.-H., Ho, T.-R., Cousins, D. J., et al. (2018). Effects of vitamin D on inflammatory and oxidative stress responses of human bronchial epithelial cells exposed to particulate matter. *PloS One* 13:e0200040. doi: 10.1371/journal.pone.0200040

Quinlan, A. R., and Hall, I. M. (2010). BEDTools: a flexible suite of utilities for comparing genomic features. *Bioinformatics* 26, 841–842. doi: 10.1093/bioinformatics/btq033

Qureishi, A., Lee, Y., Belfield, K., Birchall, J. P., and Daniel, M. (2014). Update on otitis media - prevention and treatment. *Infect. Drug Resist.* 7, 15–24. doi: 10.2147/IDR.S39637

Rai, P., He, F., Kwang, J., Engelward, B. P., and Chow, V. T. K. (2016). Pneumococcal pneumolysin induces DNA damage and cell cycle arrest. *Sci. Rep.* 6:22972. doi: 10.1038/srep22972

Rai, P., Parrish, M., Tay, I. J. J., Li, N., Ackerman, S., He, F., et al. (2015). *Streptococcus pneumoniae* secretes hydrogen peroxide leading to DNA damage and apoptosis in lung cells. *Proc. NatL. Acad. Sci. U.S.A.* 112, E3421–E3430. doi: 10.1073/pnas.1424144112

Rocha, R., Almeida, C., and Azevedo, N. F. (2018). Influence of the fixation/permeabilization step on peptide nucleic acid fluorescence in situ hybridization (PNA-FISH) for the detection of bacteria. *PLoS One* 13:e0196522. doi: 10.1371/journal.pone.0196522

Roditi, R. E., Veling, M., and Shin, J. J. (2016). Age: an effect modifier of the association between allergic rhinitis and Otitis media with effusion. *Laryngosc.* 126, 1687–1692. doi: 10.1002/lary.25682

Romero-Espejel, M. E., González-López, M. A., and de Jesús Olivares-Trejo, J. (2013). *Streptococcus pneumoniae* requires iron for its viability and expresses two membrane proteins that bind haemoglobin and haem. *Metallomics* 5, 384–389. doi: 10.1039/c3mt20244e

Trappetti, C., Gualdi, L., Di Meola, L., Jain, P., Korir, C. C., Edmonds, P., et al. (2011a). The impact of the competence quorum sensing system on *Streptococcus pneumoniae* biofilms varies depending on the experimental model. *BMC Microbiol.* 11:75. doi: 10.1186/1471-2180-11-75

Trappetti, C., Potter, A. J., Paton, A. W., Oggioni, M. R., and Paton, J. C. (2011b). LuxS mediates iron-dependent biofilm formation, competence, and fratricide in eptococcus pneumoniae. *Infect. Immun.* 79, 4550–4558. doi: 10.1128/IAI.05644-11

Underwood, M., and Bakaletz, L. (2011). Innate immunity and the role of defensins in otitis media. *Curr. Allergy Asthma Rep.* 11, 499–507. doi: 10.1007/s11882-011-0223-6

Vermee, Q., Cohen, R., Hays, C., Varon, E., Bonacorsi, S., Bechet, S., et al. (2019). Biofilm production by *Haemophilus influenzae* and *Streptococcus pneumoniae* isolated from the nasopharynx of children with acute otitis media. *BMC Infect. Dis.* 19:44. doi: 10.1186/s12879-018-3657-9

Vidal, J. E., Howery, K. E., Ludewick, H. P., Nava, P., and Klugman, K. P. (2013). Quorum-sensing systems LuxS/autoinducer 2 and Com regulate *Streptococcus pneumoniae* biofilms in a bioreactor with living cultures of human respiratory cells. *Infect. Immun.* 81, 1341–1353. doi: 10.1128/IAI.01096-12

Wang, W. Y., Komatsu, K., Huang, Y., Wu, J., Zhang, W., Lee, J.-Y., et al. (2014). CYLD negatively regulates nontypeable *Haemophilus influenzae*-Induced IL-8 Expression via Phosphatase MKP-1-dependent Inhibition of ERK. *PLoS One* 9:e112516. doi: 10.1371/journal.pone.0112516

Watanabe, M., Noma, H., Kurai, J., Sano, H., Mikami, M., Yamamoto, H., et al. (2016). Effect of Asian dust on pulmonary function in adult asthma patients in western Japan: a panel study. *Allergol. Int.* 65, 147–152. doi: 10.1016/j.alit.2015.10.002

Weiser, J. N., Ferreira, D. M., and Paton, J. C. (2018). *Streptococcus pneumoniae*: transmission, colonization and invasion. *Nat. Rev. Microbiol.* 16, 355–367. doi: 10.1038/s41579-018-0001-8

Weiss, G., and Carver, P. L. (2018). Role of divalent metals in infectious disease susceptibility and outcome. *Clin. Microbiol. Infect.* 24, 16–23. doi: 10.1016/j.cmi.2017.01.018

Weyder, M., Prudhomme, M., Bergé, M., Polard, P., and Fichant, G. (2018). Dynamic modeling of *Streptococcus pneumoniae* competence provides

regulatory mechanistic insights into its tight temporal regulation. *Front. Microbiol.* 9:1637. doi: 10.3389/fmicb.2018.01637

Willemse, B. W. M., ten Hacken, N. H. T., Rutgers, B., Postma, D. S., and Timens, W. (2005). Association of current smoking with airway inflammation in chronic obstructive pulmonary disease and asymptomatic smokers. *Respir. Res.* 6, 38–38.

Willett, D. N., Rezaee, R. P., Billy, J. M., Tighe, M. B., and DeMaria, T. F. (1998). Relationship of endotoxin to tumor necrosis factor–α and interleukin-1β in children with otitis media with effusion. *Ann. Otol. Rhinol. Laryngol.* 107, 28–33. doi: 10.1177/000348949810700106

Wu, Y., and Outten, F. W. (2009). IscR controls iron-dependent biofilm formation in *Escherichia col* by regulating type I fimbria expression. *J. Bacteriol.* 191, 1248–1257. doi: 10.1128/jb.01086-08

Yadav, M. K., Chae, S.-W., Go, Y. Y., Im, G. J., and Song, J.-J. (2017). *In vitro* multi-species biofilms of methicillin-resistant *Staphylococcus aureus* and *Pseudomonas aeruginosa* and their host interaction during *in vivo* colonization of an otitis media rat model. *Front. Cell. Infect. Microbiol.* 7:125. doi: 10.3389/fcimb.2017.00125

Yadav, M. K., Chae, S.-W., and Song, J.-J. (2012). In Vitro *Streptococcus pneumoniae* biofilm formation and in vivo middle ear mucosal biofilm in a rat model of acute otitis induced by *S. pneumoniae*. *Clin. Exp. Otorhinolaryngol.* 5, 139–144. doi: 10.3342/ceo.2012.5.3.139

Yadav, M. K., Vidal, J. E., Go, Y. Y., Kim, S. H., Chae, S.-W., and Song, J.-J. (2018). The LuxS/AI-2 quorum-sensing system of *Streptococcus pneumoniae* is required to cause disease, and to regulate virulence- and metabolism-related genes in a rat model of middle ear infection. *Front. Cellu. Infect. Microbiol.* 8:138. doi: 10.3389/fcimb.2018.00138

Yellon, R. F., Leonard, G., Marucha, P. T., Craven, R., Carpenter, R. J., Lehmann, W. B., et al. (1991). Characterization of cytokines present in middle ear effusions. *Laryngosc.* 101, 165–169.

Yu, H.-L., Chien, L.-C., and Yang, C.-H. (2012). Asian dust storm elevates children's respiratory health risks: a spatiotemporal analysis of children's clinic visits across Taipei (Taiwan). *PloS One* 7:e41317. doi: 10.1371/journal.pone.0041317

Zelikoff, J. T., Chen, L. C., Cohen, M. D., and Schlesinger, R. B. (2002). The toxicology of inhaled woodsmoke. *J. Toxicol. Environ. Health B Crit. Rev.* 5, 269–282. doi: 10.1080/10937400290070062

Conflict of Interest: The authors declare that the research was conducted in the absence of any commercial or financial relationships that could be construed as a potential conflict of interest.

frontiers in Genetics

BRIEF RESEARCH REPORT
published: 19 May 2020
doi: 10.3389/fgene.2020.00498

The *Jeff* Mouse Mutant Model for Chronic Otitis Media Manifests Gain-of-Function as Well as Loss-of-Function Effects

*Oana Kubinyecz, Pratik P. Vikhe, Thomas Purnell, Steve D. M. Brown and Hilda Tateossian**

Mammalian Genetics Unit, MRC Harwell Institute, Harwell, United Kingdom

Chronic otitis media (OM) is the most common cause of hearing loss worldwide, yet the underlying genetics and molecular pathology are poorly understood. The mouse mutant *Jeff* is a single gene mouse model for OM identified from a deafness screen as part of an ENU mutagenesis program at MRC Harwell. *Jeff* carries a missense mutation in the *Fbxo11* gene. *Jeff* heterozygotes (*Fbxo11*$^{Jf/+}$) develop chronic OM at weaning and have reduced hearing. Homozygotes (*Fbxo11*$^{Jf/Jf}$) display perinatal lethality due to developmental epithelial abnormalities. In order to investigate the role of FBXO11 and the type of mutation responsible for the phenotype of the *Jeff* mice, a knock-out mouse model was created and compared to *Jeff*. Surprisingly, the heterozygote knock-outs (*Fbxo11*$^{tm2b/+}$) show a much milder phenotype: they do not display any auditory deficit and only some of them have thickened middle ear epithelial lining with no fluid in the ear. In addition, the knock-out homozygote embryos (*Fbxo11*$^{tm2b/tm2b}$), as well as the compound heterozygotes (*Fbxo11*$^{tm2b/Jf}$) show only mild abnormalities compared to *Jeff* homozygotes (*Fbxo11*$^{Jf/Jf}$). Interestingly, 3 days after intranasal inoculation of the *Fbxo11*$^{tm2b/+}$ mice with non-typeable *Haemophilus influenzae* (NTHi) a proportion of them have inflamed middle ear mucosa and fluid accumulation in the ear suggesting that the *Fbxo11* knock-out mice are predisposed to NTHi induced middle ear inflammation. In conclusion, the finding that the phenotype of the *Jeff* mutant is much more severe than the knock-out indicates that the mutation in *Jeff* manifests gain-of-function as well as loss-of-function effects at both embryonic and adult stages.

Keywords: otitis media, chronic otitis media, FBXO11, mouse model, mutation

OPEN ACCESS

Edited by:
Allen Frederic Ryan, University of California, San Diego, United States

Reviewed by:
Qingyin Zheng, Case Western Reserve University, United States
Arwa Kurabi, University of California, San Diego, United States

****Correspondence:***
Hilda Tateossian
h.tateossian@har.mrc.ac.uk

Specialty section:
This article was submitted to Genetic Disorders, a section of the journal Frontiers in Genetics

Received: *24 July 2019*
Accepted: *22 April 2020*
Published: *19 May 2020*

Citation:
Kubinyecz O, Vikhe PP, Purnell T, Brown SDM and Tateossian H (2020) The Jeff Mouse Mutant Model for Chronic Otitis Media Manifests Gain-of-Function as Well as Loss-of-Function Effects. Front. Genet. 11:498. doi: 10.3389/fgene.2020.00498

INTRODUCTION

Otitis media (OM) is an inflammatory disease of the middle ear. Otitis media with effusion (OME) is a type of OM that is caused by a build-up of fluid within the middle ear and results in conductive hearing impairment. It is most common in young children. When the inflammation persists for longer it is considered as chronic otitis media with effusion (COME). COME is a

multifactorial disease with a significant impact on language development and behavior. It is also an indication for a common surgical treatment (tympanostomy) at an early age in developed countries (Kubba et al., 2000). Until recently, not much was known about the underlying cellular mechanisms leading to OM. However, a deafness screen as part of a larger scale ENU mouse mutagenesis program (Nolan et al., 2000) identified three mouse models that display conductive deafness due to the development of COME: *Jeff* (Hardisty et al., 2003), *Junbo* (Parkinson et al., 2006), and *edison* mice (Crompton et al., 2017) and throw light on the genes and pathways involved in susceptibility to OM.

Jeff is a semi-dominant mutant that in heterozygotes displays conductive hearing loss caused by the development of chronic suppurative OM at weaning age (Hardisty et al., 2003). The *Jeff* mice are smaller than their wild-type littermates and have mild craniofacial abnormalities. The homozygotes exhibit perinatal lethality due to respiratory problems, cleft palate and eyelids open at birth (Hardisty-Hughes et al., 2006). The lungs of homozygote embryos are severely affected, with a smaller average airway width and significantly lower number of airways (Tateossian et al., 2009).

The gene mutated in *Jeff* mice is *Fbxo11*, a member of the F-box family (Hardisty-Hughes et al., 2006). It is located on chromosome 17 and has two protein-coding isoforms. The mutation consists of a single base transversion, from A to T in exon 13 of the *Fbxo11* gene, causing a glutamine to leucine change in a highly conserved region of the protein (Hardisty-Hughes et al., 2006). Another point mutation in exon 7 of the *Fbxo11* gene, named *Mutt*, was identified from the same screen. It leads to a serine to leucine change, within another conserved region of the protein. A proportion of *Mutt* heterozygotes showed mild craniofacial abnormality (57%) and reduced startle response (13%) with no OM at the age of 2 months, suggesting that *Mutt* is a weaker hypomorphic allele of *Fbxo11* in comparison to the *Jeff* mutation. In addition, a large proportion (83%) of the *Mutt* homozygotes survive in comparison to the 100% lethality found in *Jeff* homozygotes, which also underlines the hypomorphic nature of the *Mutt* allele. The surviving *Mutt* homozygote mice, demonstrate short face (84%) and reduced startle response (42%) in the absence of OM (Hardisty-Hughes et al., 2006).

In order to determine if the point mutation in *Jeff* mice is a loss-of-function or a gain-of-function mutation, a knock-out strain of *Fbxo11* was created. We studied the phenotype of the heterozygote ($Fbxo11^{tm2b/+}$) and homozygote ($Fbxo11^{tm2b/tm2b}$) knock-out mice and also the compound heterozygotes ($Fbxo11^{tm2b/Jf}$) in order to compare them with the phenotype of the *Jeff* mice (both $Fbxo11^{Jf/+}$ and $Fbxo11^{Jf/Jf}$). Here we report that the phenotype of the *Jeff* mutant is much more severe than the phenotype of the *Fbxo11* knock-out mouse. The heterozygote knock-outs ($Fbxo11^{tm2b/+}$) do not display OM but some of the homozygotes ($Fbxo11^{tm2b/tm2b}$) as well as some of the compound mutants ($Fbxo11^{tm2b/Jf}$) show cleft palate abnormalities, a much milder phenotype compared to *Jeff* mice. The result supports the conclusion that the mutation in *Jeff* manifests gain-of-function as well as loss of function effects at both embryonic and adult stages.

MATERIALS AND METHODS

Mice Husbandry

Fbxo11 knock-out mice [$Fbxo11^{tm2b(EUCOMM)Wtsi}$] were produced by the European Conditional Mouse Mutagenesis Program at Harwell (Friedel et al., 2011; Skarnes et al., 2011; Bradley et al., 2012). The heterozygotes ($Fbxo11^{tm2b/+}$) were generated on and maintained on a pure C57BL/6NTac background. The *Jeff* colony was maintained on a mixed C3H/HeH-C57BL/6J background because they do not survive on a congenic C57BL/6J background. The compound mutant embryos ($Fbxo11^{tm2b/Jf}$) were generated on a mixed C57BL/6NTac and C3H/HeH-C57BL/6J background. All animal experimentation was approved by the Animal Welfare and Ethical Review Body at MRC, Harwell. The humane care and use of mice in this study was under the authority of the appropriate United Kingdom Home Office Project License.

Genotyping

The *Jeff* mice were genotyped as previously described (Hardisty-Hughes et al., 2006).

For the genotyping of the *Fbxo11* knock-out mice a qPCR based genotyping strategy was used. The following primers and probes were used:

> Primers for the wild-type allele Fbxo11-CR-LOA: forward, 5′-TTGCTGGAACAAGACCTTTGTAG-3′ and reverse, 5′-GGCAACAGGAGCTATCACTCA-3′. FAM labeled probe: 5′-AGCTGCTTGCGTGTGTAAACGC-3′. Primers for the LacZ assay: LacZ forward, 5′-CTCGCCACTTCAACATCAAC-3′ and reverse, 5′-TTATCAGCCGGAAAACCTACC-3′. FAM labeled probe: 5′- TCGCCATTTGACCACTACCATCAATCC-3′.

DNA was extracted from ear clips using Applied Biosystems™ TaqMan Sample-to-SNP Kit (4403313, Applied Biosystems™). Reaction mixtures (10 μL) contained 5 μL TaqMan GTXpress™ master mix (4401892, Applied Biosystems™), 0.225 μL 20 μM from each primer, 0.3 μL 15 μM probe, 2.5 μL 10 times diluted DNA extract and water. The samples were amplified (95°C for 20 s, followed by 40 cycles of 95°C for 3 s and 60°C for 3 s) and the results were analyzed using CopyCaller Software v2.0 from Applied Biosystems.

Histology

Adult and embryonic heads, lungs or whole bodies (embryonic stages E15.5; E18.5), were collected and fixed in 10% buffered formaldehyde, decalcified and embedded in paraffin following routine procedures. 5 μM-thick sections were obtained and stained with hematoxylin and eosin for morphological observations. Goblet cells were identified by a combined Alcian blue/Periodic acid-Schiff staining method (AB-PAS) staining method.

Auditory Brainstem Response (ABR)

One and two-months–old mice were anesthetized (ketamine hydrochloride, 100 mg/kg; xylasine, 10 mg/kg) and placed on

a heated mat in a sound attenuating chamber. Acoustic stimuli were delivered to the right ear, from a distance of 1.5 cm, via a free field transducer controlled by TDT SinGen/BioSig software. ABR responses were collected, amplified and averaged using the BioSig software. Broadband click stimuli were presented at 90 dB SPL and gradually decreased in steps of 5 dB until a threshold was visually determined by the lack of replicable response peaks. The test was analyzed as previously described (Hardisty-Hughes et al., 2010).

Tissue Collection and Preparation for Western Blot

Embryos were collected and transferred in cold PBS containing protease inhibitor cocktail (04 693 124 001, Roche). Lungs were dissected out, homogenized in extraction buffer (1% NP_40, 1M Tris, 1M NaCl; pH 8, protease and phosphatase inhibitor cocktails) in Precellys homogenizers for 20 s, and after centrifugation (10 min, 10,000 rpm, 4°C) the protein concentration of the supernatant was determined using DC™ Protein Assay kit (500–0116, Bio-Rad).

Western Blot Analysis

Lysates were resolved in NuPAGE™ 7% Tris-Acetate Gel (EA03555, Invitrogen), blotted onto a nitrocellulose membrane and incubated with two anti-FBXO11 antibodies: A301-177A and A301-178A, Bethyl Laboratories) in 1:1000 dilutions. ECL Plus system was used (32132, Thermo Scientific, Pierce™) for blot detection using X-ray film. Anti-rabbit IgG-HRP conjugated antibody was used as a secondary antibody (170-6515, Bio-Rad) and actin (A2066, Sigma) was used as a loading control.

Immunohistochemistry

Paraffin sections were de-waxed in xylene substitute and rehydrated via graded ethanol solutions. Endogenous peroxidase was blocked with 3% hydrogen peroxide in isopropanol for 30 min. Heat-induced epitope retrieval was performed using a microwave. Sections were incubated overnight with primary antibodies against: Cleaved Caspase-3 (Asp175) (5A1E); 1:1000 (9664, Cell Signaling Technology); F4/80, 1:200 (MF48005, Invitrogen); myeloperoxidase, 1:200 (ab9535, Abcam) and NTHi162sr, 1:10000, custom made (Vikhe et al., 2019). The Vectastain Elite ABC HRP kit (PK-6101, Vector Laboratories) kit was used according to the manufacturer's instructions for all of the antibodies except for F4/80 for which a goat anti rat HRP, 1:200, was used (7077S, Cell Signaling Technology). For development of the signal, the DAB + chromogen system was used (K3468, DAKO). Counterstaining was carried out with hematoxylin.

Intranasal Inoculation

Two-months-old wild-type littermates, C57BL/6NTac (n = 11), and heterozygote knock-out mice (n = 12), male and female, were inoculated as described previously (Hood et al., 2016). Briefly, mice were inoculated intranasally under gas anesthesia with 5 μL per nares of NTHi 162sr (streptomycin resistant) cell suspension at a concentration of 10^8 CFU/mL in PBS–1% gelatin. After 3 days of the challenge the mice were euthanized, half of the animals were used to collect the ears for histological analyses and from the other half, the middle ear fluid was harvested for culture. For the culturing the fluid was collected into PBS buffer (for wild-type mice the ears were just washed with PBS buffer), plated on streptomycin BHI (Brain Heart Infusion) plates with streptomycin and the bacterial colony count was obtained after overnight incubation at 37°C.

Data Analysis

We used the Chi-squared test to compare the difference between the observed and the expected number of the mutant mice from crosses. Two-tailed t-test was used for comparing mean ABR thresholds and mucoperiosteal thickness. A value of $p < 0.05$ was considered significant.

RESULTS

Generation of the *Fbxo11* Knock-Out Mice

The promoterless EUCOMM (European Conditional Mouse Mutagenesis Program) tm2a vector (PGS00030_B_D03) was used to generate a targeted knock-out first JM8A1.N3 embryonic stem (ES) cell clones (Friedel et al., 2011; Skarnes et al., 2011; Bradley et al., 2012). ES cell to mouse conversion (ES cell clone EPD248_1_H03) was carried out at MRC Harwell to generate chimeras, from which germline transmission of the *Fbxo11*$^{1tm2a(EUCOMM)Wtsi}$ allele was achieved. The floxed critical region containing *Fbxo11* exon 4 (ENSMUSE00000539085) is excised by cre recombinase to yield the lacZ-tagged null *Fbxo11*$^{tm2b(EUCOMM)Wtsi}$ allele (**Figure 1A**).

To confirm that the gene was successfully knocked-out we used western blots to measure the protein levels in mouse embryonic lungs. The FBXO11 mouse protein has two main protein-coding isoforms, 104 and 94 kDa. We used two antibodies; A301-178A which can recognize both isoforms and A301-177A which is specific for the full length "canonical" sequence. We detected reduced levels of FBXO11 in the heterozygote lung and no protein present in the homozygote embryonic lung (**Figures 1B,C** and **Supplementary Figure S1**). We also detected a small band (18 kDa) in the mutant tissues corresponding to the truncated protein, which was only present in the heterozygote and homozygote. In addition a band was detected between the two main FBXO11 isoforms with both antibodies in all three samples, wild-type, heterozygote and homozygote. This cross-reactive product was previously observed by us using the same antibodies (Tateossian et al., 2015) and has been noted by others (Abbas et al., 2013).

Phenotype of the *Fbxo11*$^{tm2b/+}$ Mice

To investigate the phenotype of the heterozygote knock-out mice (*Fbxo11*$^{tm2b/+}$) we out-crossed them to C57BL/6NTac wild-type mice. We had only 37% *Fbxo11*$^{tm2b/+}$ mice at weaning age

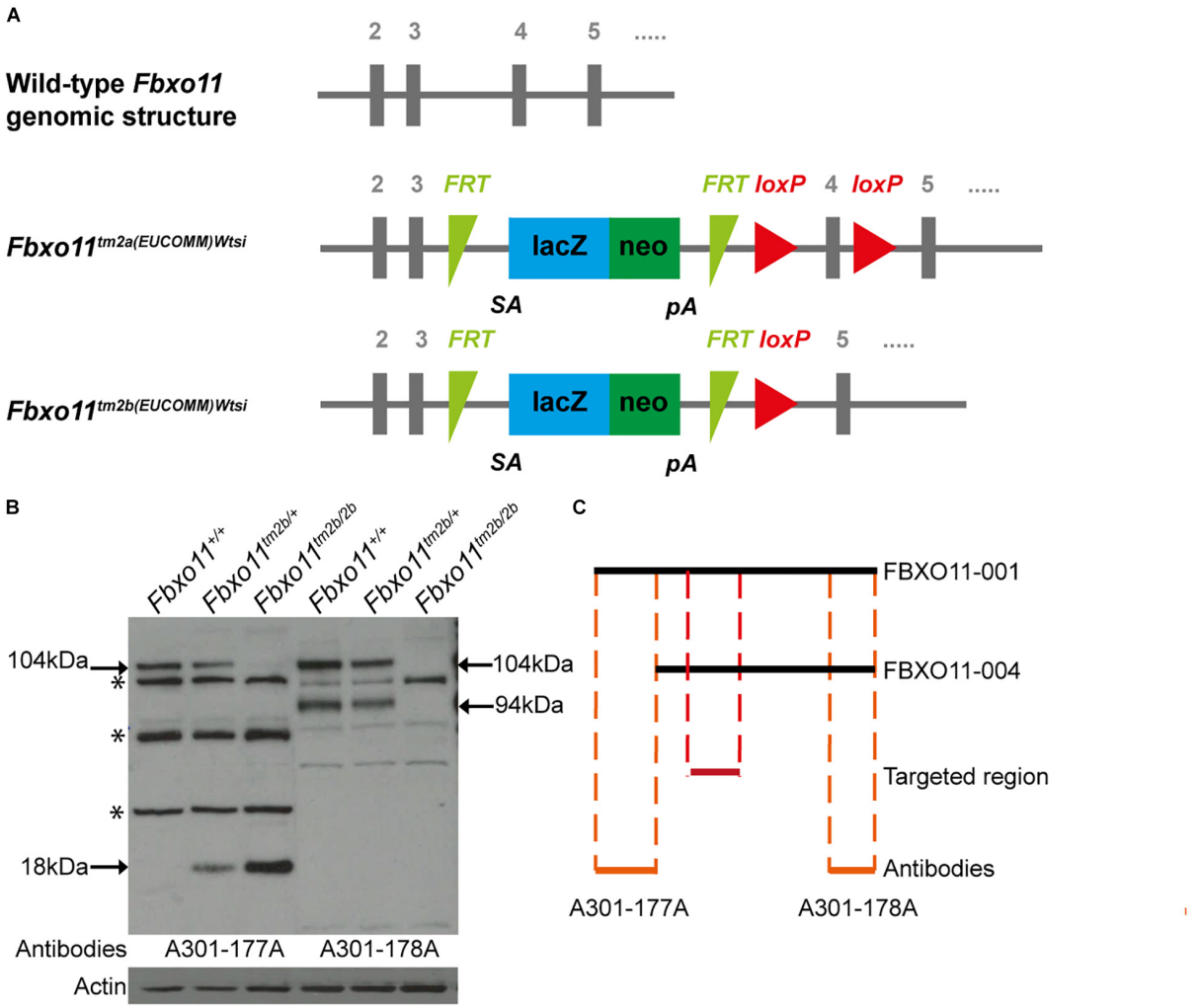

FIGURE 1 | Generation of the *Fbxo11* knock-out mice. **(A)** Schematic representation of the knock-out strategy used by EUCOMM to produce the mice (not to scale), illustrating the wild type structure of the *Fbxo11* gene from exons 2–5 and the structure of the mutant tm2a allele generated (see results). The tm2b allele is derived by cre excision of the tm2a allele, deleting exon 4. **(B)** Protein levels of FBXO11 in E18.5 embryonic lungs. Neither the 177A antibody which detects the large isoform of mouse FBXO11 (FBXO11-001, 930 aa, 104 kDa) nor the 178A, which detects both the large and small isoforms (FBXO11-001, 930 aa, 104 kDa and FBXO11-004, 855 aa, 94 kDa) detected the protein in the homozygote embryonic lung tissue. Actin was used as loading control. Truncated protein, 18 kDa, was detected in the mutant tissues. Cross- reactive bands are indicated by an asterisk. **(C)** Alignment of the two FBXO11 isoforms (FBXO11-001 and FBXO11-004), the fragments of FBXO11 protein used to produce the A301-177A and A301-178A antibodies for FBXO11 and the targeted region in the knock-out (not to scale).

(68/184) which was less than the expected 50% (p = 0.0004). We found that some pups were lost shortly after birth and prior to weaning. The surviving mice demonstrated a milder phenotype compared to *Jeff* mice (*Fbxo11*$^{Jf/+}$). Similar to *Jeff* mice, both males and females were significantly smaller than their wild-type littermates at the age of 2 months (p = 0.022 for males, p = 0.011 for females; **Figure 2B**). However, unlike *Jeff* mice (*Fbxo11*$^{Jf/+}$) they do not spontaneously develop OM. The Broadband click stimuli ABR test revealed that the *Fbxo11*$^{tm2b/+}$ mice do not have significantly reduced hearing. The ABR thresholds of the *Fbxo11*$^{tm2b/+}$ mice were comparable with the wild-type thresholds (**Figure 2D**). In addition the histological analysis of the middle ear of 3-weeks, 2- and 5-months-old *Fbxo11*$^{tm2b/+}$mutants showed no fluid in the ears (**Figure 2A**). We also measured the mucoperiosteal thickness of the middle ears of 3 weeks and 2-months-old *Fbxo11*$^{tm2b/+}$ mice. We did not find any difference in the thickness of the middle ear epithelial lining between the two genotypes at the age of 3 weeks (p = 0.930 for males, p = 0.463 for females). The result was the same between 2-months-old female *Fbxo11*$^{tm2b/+}$ mice and wild-types (p = 0.909). There was some difference in the mucosa thickness in male 2 months old *Fbxo11*$^{tm2b/+}$ mice compared to wild-type littermates, however it was not significant (p = 0.0554; **Figure 2C**). Neither female, nor male *Fbxo11*$^{tm2b/+}$ mice, displayed either a significant thickened middle ear epithelial lining or a reduced hearing phenotype.

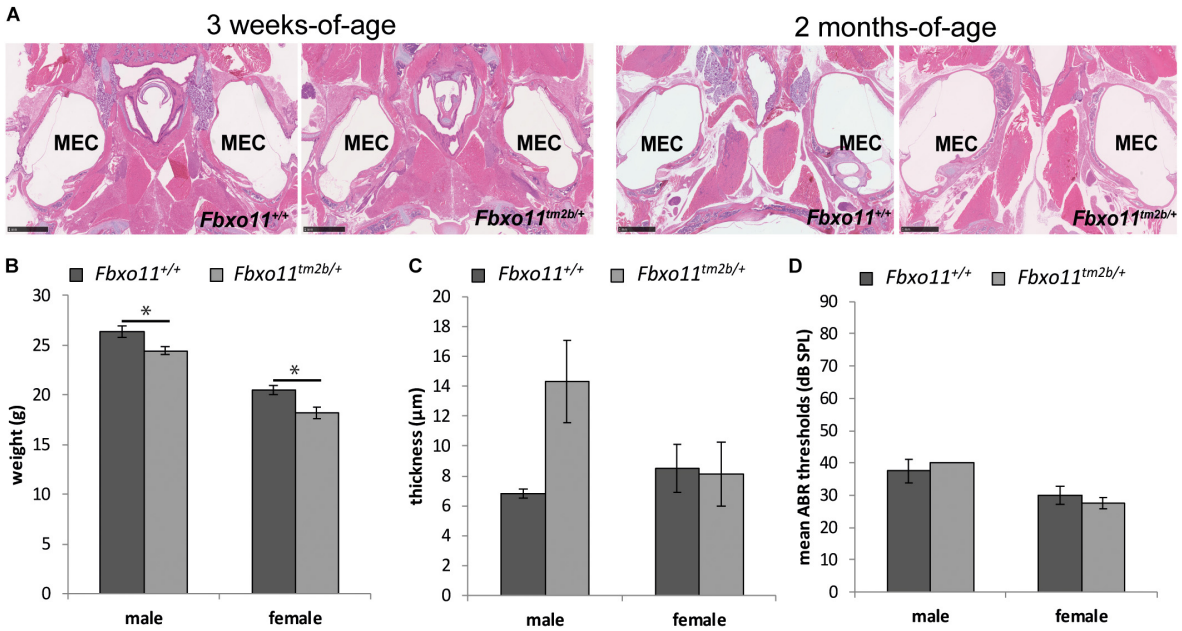

FIGURE 2 | Phenotype of the *Fbxo11*$^{tm2b/+}$ mice. **(A)** Hematoxylin-eosin stained transverse sections through the middle ear of 3-weeks and 2-months-old mice showing air-filled middle ear cavity for both heterozygote *Fbxo11*$^{tm2b/+}$ and wild-type *Fbxo11*$^{+/+}$ mice. Scale bars: 1 mM. MEC: middle ear cavity. **(B)** Comparison of the weight of the mice at the age of 2-months. The weights were taken from six mice from each sex and genotype except for the female heterozygote mice for which we had seven mice. **(C)** Comparison of the thickness of the epithelial lining of the middle ear of 2-months-old mice. The measurements were taken from three mice (six ears) from each genotype. **(D)** Broadband click stimuli ABR thresholds in the right ears of 2-months-old wild-type *Fbxo11*$^{+/+}$ and heterozygote *Fbxo11*$^{tm2b/+}$ mice. Two wild-type males, three wild-type females, two heterozygote males and three heterozygote females were used for the test. As the data was exactly the same (40dB) for both heterozygote males used for this study, the error bars are not well visible in the graph. Bars: standard error of mean. *P*-values were determined using two-tailed *t*-test, $^{*}p \leq 0.05$.

Thus, overall the phenotype of the *Fbxo11*$^{tm2b/+}$ mice resembles more closely the phenotype of *Mutt* (*Fbxo11*$^{Mutt/+}$) than *Jeff* mice (*Fbxo11*$^{Jf/+}$).

OM Phenotype of the *Fbxo11*$^{tm2b/+}$ Mice After Inoculation With NTHi

Two-month-old *Jeff* mice have been previously inoculated with NTHi162kr and it was discovered that 7 days post-inoculation they have middle ear titers of 2×10^2 colony-forming units (CFU)/µL and infection rates of 15% (Hood et al., 2016). In this study we inoculated 2-months-old *Fbxo11*$^{tm2b/+}$ mice and wild-type littermates with NTHi162sr, the middle ear fluid was collected at 3 days post-challenge, cultured and the NTHi titers were calculated. A shorter 3 days inoculation challenge was chosen because *Fbxo11*$^{tm2b/+}$ mice do not have middle ear fluid and our earlier infection studies (Hood et al., 2016; Vikhe et al., 2019) have shown that NTHi does not infect wild-type middle ears without any fluid after intranasal challenge. Samples from two out of six *Fbxo11*$^{tm2b/+}$ mice, 33% (two out of 12 ears, middle ear infection rate 16.7%) were positive for the bacteria with average 3.6×10^2 CFU/µL. There was no bacterial growth on the plates from wild-type ears. Half of the inoculated mice were used for histological examination and immunohistochemistry with different antibodies. Hematoxylin- and eosin-stained sections of middle ear bulla showed thickened epithelial lining and fluid in two out of six mice (one male with unilateral OM and one female mouse with bilateral OM), 33%. The average mucoperiosteal thickness of the middle ears was 21.5 µM compared to 8.8 µM in wild-type mice (p = 1.061 E-06; **Figures 3A,B**). In addition we detected apoptotic cells using a cleaved caspase 3 antibody; foamy macrophages with an F4/80 antibody and neutrophils using myeloperoxidase as a marker. To localize NTHi bacteria in the middle ear we used an antibody against NTHi162sr. We detected bacteria in the epithelial lining and in the fluid of the challenged mice (**Figures 3C,D**). The AB-PAS staining detected a high density of goblet cells (mucus-producing cells) in the epithelial lining of the *Fbxo11Fbxo11*$^{tm2b/+}$ mice middle ear cavity (**Figure 3E**).

Similar to *Fbxo11*$^{Jf/+}$, *Fbxo11*$^{tm2b/+}$ mice had low but significant NTHi titers. However, *Jeff* mutants have already inflamed middle ears pre-inoculation whereas in *Fbxo11*$^{tm2b/+}$ NTHi induces inflammation and fluid accumulation in the middle ear. This finding suggests that the *Fbxo11* knock-out mice are predisposed to NTHi induced middle ear inflammation.

Phenotype of the Homozygote *Fbxo11*$^{tm2b/tm2b}$

Due to the fact that the *Jeff* homozygote mice (*Fbxo11*$^{Jf/Jf}$) show perinatal lethality, only the embryonic phenotype of the *Fbxo11*$^{tm2b/tm2b}$ mice was investigated. We collected embryos

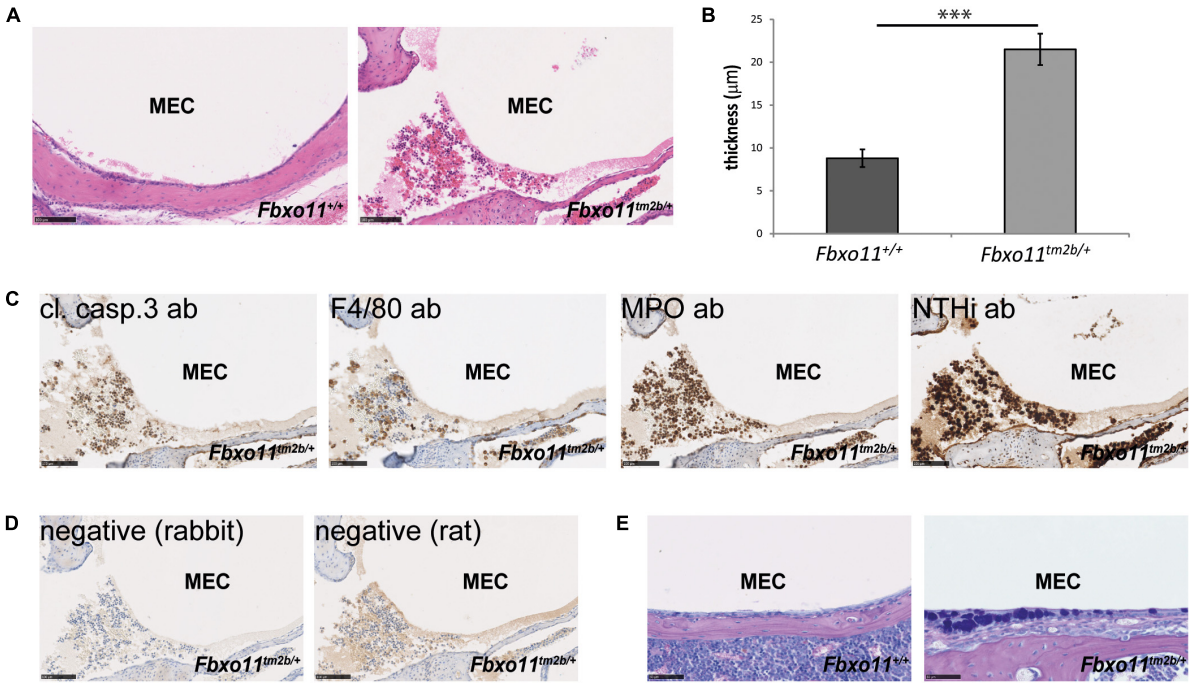

FIGURE 3 | OM phenotype of the *Fbxo11*$^{tm2b/+}$ mice after inoculation with NTHi. **(A)** Hematoxylin-eosin stained transverse sections through the middle ear of 2-months-old wild-type *Fbxo11*$^{+/+}$ and heterozygote *Fbxo11*$^{tm2b/+}$ mice after the challenge. Scale bars: 100 μM. **(B)** Comparison of the thickness of the epithelial lining of the middle ear for each genotype after the challenge. The measurements were taken from two mice (one male and one female, three ears) from each genotype. Bars: standard error of mean. *P*-values were determined using two-tailed *t*-test. ***$p \leq 0.001$. **(C)** Immunohistochemistry to detect different cell types in the middle ear fluid: cleaved caspase 3 antibody (cl. casp. 3) detecting apoptotic cells; F4/80 detecting foamy macrophages; myeloperoxidase antibody (MPO) detecting neutrophils and antibody against NTHi162sr (NTHi) detecting NTHi bacteria in the middle ear fluid. Scale bars: 100 μM. **(D)** Negative controls for the staining for antibodies raised in rat (for F4/80) or rabbit (all the other). Scale bars: 100 μM. **(E)** The AB-PAS staining detected goblet cells in the epithelial lining of the *Fbxo11*$^{tm2b/+}$ mice middle ear cavity. Scale bars: 50 μM.

at stage E15.5 and E18.5. The homozygotes composed 20% of the embryos from heterozygote intercrosses at each stage, not significantly different from the expected 25 percent (5/25, $p = 0.564$ at E15.5 and 10/50, $p = 0.414$ at E18.5). At the developmental stage E15.5, when the palatal shelves are supposed to be already fused, 80% of the *Fbxo11*$^{tm2b/tm2b}$ embryos (4/5) displayed a cleft, a phenotype similar with *Fbxo11*$^{Jf/Jf}$ embryos. At stage E18.5 however, only 10% (1/10) had a cleft, and some presented abnormalities in the fusion (**Figure 4A**) indicating a delay in the palate fusion in the knock-out mice compared to wild-type mice. None of the E18.5 embryos had an eyelid open phenotype (**Figure 4B**). We previously reported that *Jeff* new born homozygote mice (*Fbxo11*$^{Jf/Jf}$) have underdeveloped lungs (Tateossian et al., 2009) and thus investigated lung pathology in *Fbxo11*$^{tm2b/tm2b}$ mice. However, unlike *Jeff* there was no significant difference in the number ($p = 0.193$) or the width ($p = 0.431$) of airways of the lungs of the *Fbxo11*$^{tm2b/tm2b}$ embryos, compared to their wild-type littermates at either E15.5 or E18.5 (**Figures 4C–E**).

Similar to our findings with the knock-out heterozygote mice (*Fbxo11*$^{tm2b/+}$), the phenotype of the knock-out homozygote mice (*Fbxo11*$^{tm2b/tm2b}$) was found to be much milder compared to *Fbxo11*$^{Jf/Jf}$ mice.

Phenotype of the Compound Heterozygote *Fbxo11*$^{tm2b/Jf}$

We crossed mice heterozygous for *Jeff* (*Fbxo11*$^{Jf/+}$) to *Fbxo11*$^{tm2b/+}$ heterozygotes to produce compound mutants (*Fbxo11*$^{tm2b/Jf}$). Corresponding with the expected ratio, 23.5% of the total embryos at E15.5 were genotyped as compound heterozygotes (*Fbxo11*$^{tm2b/Jf}$), not significantly different from the expected 25% (4/17, $p = 0.889$). The percentage of the *Fbxo11*$^{tm2b/Jf}$ compound mutants at E18.5 was less, 11.5%, but it was also not significantly less than the expected numbers ($p = 0.075$). At E15.5, 50% of the embryos presented cleft palate, and at E18.5 25% had cleft compared to the wild-type littermates (**Figure 4A**). The result suggested that in compound mutants there is a delay in the development of the palatal shelves. We did not detect any eyelid open phenotype or underdeveloped lungs in the compound mutants (**Figures 4B–E**).

DISCUSSION

Jeff mice are one of the first mouse models of OM (Hardisty et al., 2003). They carry a missense mutation in the *Fbxo11* gene (Hardisty-Hughes et al., 2006). In order to investigate the nature

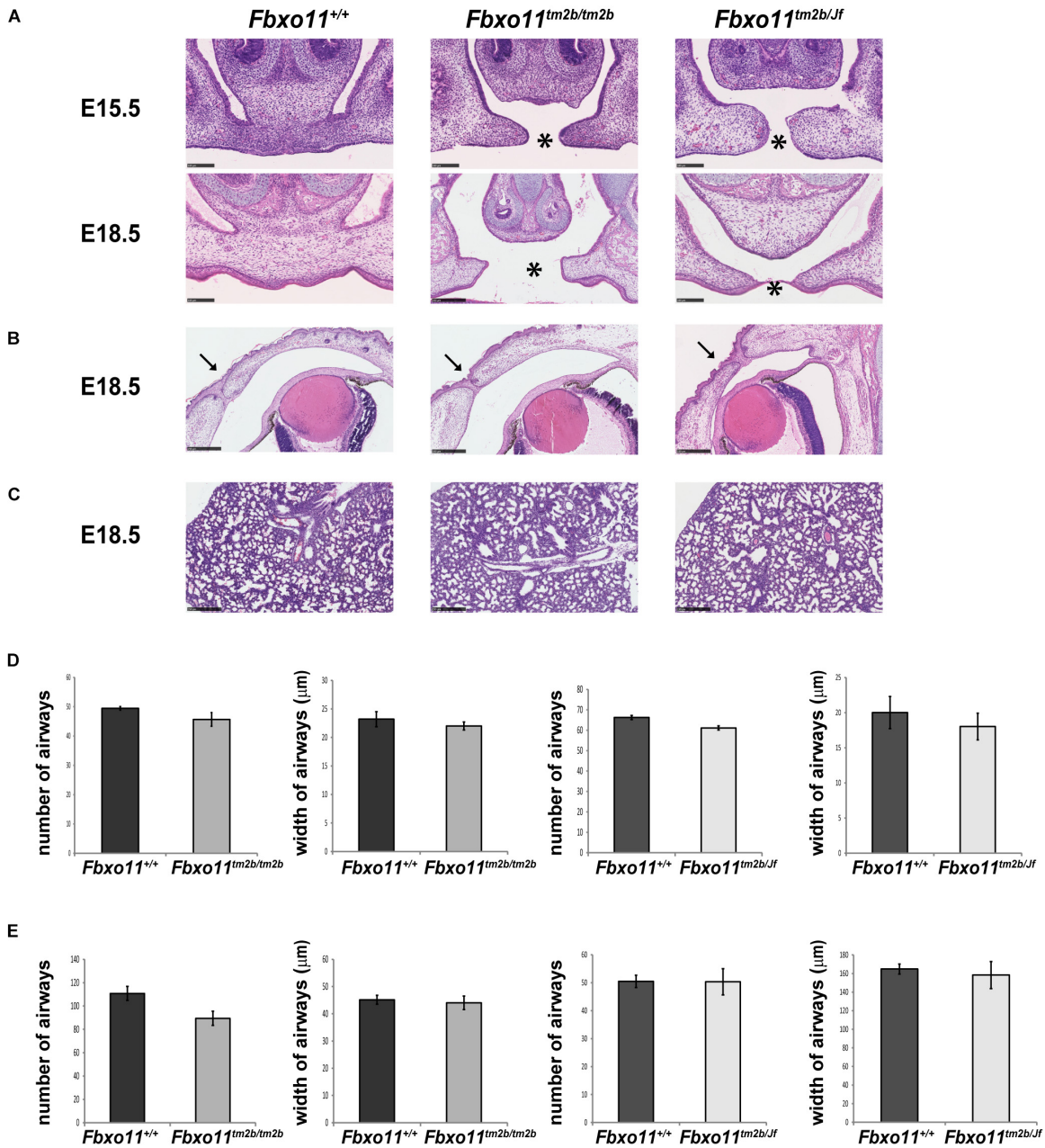

FIGURE 4 | Phenotype of homozygote knock-out *Fbxo11*$^{tm2b/tm2b}$ and compound heterozygote *Fbxo11*$^{tm2b/Jf}$ embryos. **(A)** Hematoxylin-eosin stained coronal sections through the palate of E15.5 and E18.5 embryonic heads. Scale bars: 100 μM. The cleft palate is indicated by asterisk. **(B)** Hematoxylin-eosin stained coronal sections through the eyelids of E18.5 embryonic heads. Scale bars: 250 μM. Arrows indicate the fused eyelids. **(C)** Hematoxylin-eosin stained sections through the lungs of E18.5 embryos. Scale bars: 250 μM. **(D)** Comparison of the number of airways for three regions taken at random for three E15.5 individuals from each genotype and comparison of the width of 30 airways from three sections of embryonic lungs for three E15.5 individuals from each genotype. **(E)** Comparison of the number of airways for three regions taken at random for three E18.5 individuals from each genotype and comparison of the width of 30 airways from three sections of embryonic lungs for three E15.5 individuals from each genotype. Bars: standard error of mean.

of the mutation in these mice we studied the phenotype of *Fbxo11* knock-out mice. We found that in comparison to *Jeff*, the *Fbxo11* knock-out mice appear less affected, with almost no significant differences between the wild-types and the mutants.

We have previously reported that *Jeff* heterozygotes develop OM at weaning age and the deafness phenotype is fully penetrant. They have inflamed middle ear mucosa, fluid in the middle ear and reduced hearing (Hardisty et al., 2003). We have also previously shown that the homozygotes have developmental abnormalities, cleft palate, eyelid open phenotype and perinatal lethality as a result of underdeveloped lungs (Hardisty-Hughes et al., 2006; Tateossian et al., 2009).

Surprisingly, *Fbxo11* knock-out heterozygotes ($Fbxo11^{tm2b/+}$) demonstrate a much milder phenotype. They do not develop OM at any time point, and do not display any auditory deficit. However, we found that only 37% of the pups from heterozygote matings to wild type are heterozygotes (not 50%). Some of the pups were absent from the litters shortly after birth and they might account for the missing heterozygotes, thus suggesting that the knock-out influences the survival, through a yet unknown reason. The weight of the surviving mutants was recorded to be reduced at the age of 2-months which may contribute to the reduced survival rates of the mutants.

On a BL/6 background the otitis media phenotype and viability of the *Jeff* heterozygote mice ($Fbxo11^{Jf/+}$) and the embryonic phenotype of the *Jeff* homozygote mice ($Fbxo11^{Jf/Jf}$) are very severe and it was impossible to maintain the colony on this background. For this reason, the *Jeff* colony is maintained on a mixed C3H/HeH-C57BL/6J background. The heterozygote knock-out mice ($Fbxo11^{tm2b/+}$) were generated on and maintained on an isogenic C57BL/6NTac background. Thus we analyzed the knock-out line on a severe BL/6 background. However, we cannot rule out potential differences in OM severity between a BL/6N vs. BL/6J background. What is notable is that on the BL/6N background the knock-out does not show any phenotypic indicators of OM.

Jeff mice ($Fbxo11^{Jf/+}$) have been previously inoculated with NTHi and it was discovered that 7 days post-inoculation they have middle ear titers of 2×10^2 CFU/μL and infection rates of 15% (Hood et al., 2016). To test if the knock-out heterozygote mice ($Fbxo11^{tm2b/+}$) are susceptible to middle ear inflammation we performed intranasal inoculation with bacterial pathogen NTHi162sr. Three days post-challenge a third of the mice had inflamed middle ear lining and fluid in the ears, middle ear infection rate of 16.7%. Similar to *Jeff* mice ($Fbxo11^{Jf/+}$) they also had low NTHi titers, 3.6×10^2 CFU/μL. The fact that some of the $Fbxo11^{tm2b/+}$ mice develop middle ear infection after the inoculation, irrespective of the absence of OM before the inoculation was very interesting. This finding indicates that the mutations in *Fbxo11* in both, *Jeff* and knock-out mice makes them predisposed to NTHi induced middle ear inflammation.

The embryonic development of the knock-out homozygotes ($Fbxo11^{tm2b/tm2b}$) and compound mutants ($Fbxo11^{tm2b/Jf}$) seems to be less affected than in the *Jeff* homozygotes ($Fbxo11^{Jf/Jf}$). The only similarity is in the palatal shelf development. Mouse palatogenesis takes place between E11.5 and E15.5 (Ferguson, 1988). It is a process involving palatal shelf growth and elevation above the tongue followed by fusion of the shelves at about 15.5 embryonic days. The fact that at the embryonic stage E15.5, 80% of the null embryos ($Fbxo11^{tm2b/tm2b}$) and 50% of the compound mutants ($Fbxo11^{tm2b/Jf}$) have cleft, but at E18.5 most of the palatal shelves seem to be fused, indicates that there is a delay in development at E15.5 in both mutants, but this is corrected before E18.5. In addition, all the other developmental defects seen in *Jeff* are absent in $Fbxo11^{tm2b/tm2b}$ and $Fbxo11^{tm2b/Jf}$ embryos.

The mutation in *Mutt*, a weaker hypomorphic allele of *Fbxo11*, results mainly in a mild craniofacial defect in the mice (Hardisty-Hughes et al., 2006). Fifty-seven percent of *Mutt* heterozygotes showed mild craniofacial abnormality, a shortened face. A small proportion of *Mutt* homozygotes (17%) showed perinatal lethality, mild clefting of the palate and facial clefting. The phenotype of the *Fbxo11* knock-out mice looks very similar to the phenotype of *Mutt*.

In summary, the loss-of-function effects found in the $Fbxo11^{tm2b/+}$ and $Fbxo11^{tm2b/tm2b}$ mice appear very mild compared to *Jeff* heterozygotes ($Fbxo11^{+/Jf}$) and homozygotes ($Fbxo11^{Jf/Jf}$) respectively. This is also the case for the $Fbxo11^{tm2b/Jf}$ compound heterozygote, which show a similar embryonic phenotype to $Fbxo11^{tm2b/tm2b}$ mice. We conclude from this data that the *Jeff* mutant shows gain-of-function as well as loss-of-function effects, with the gain-of-function manifesting as the severe chronic otitis media displayed in the heterozygote and the cleft palate, eyelids open and lung phenotypes along with embryonic lethality displayed in the homozygotes. We were only able to investigate the $Fbxo11^{tm2b/tm2b}$ and $Fbxo11^{tm2b/Jf}$ embryonically and were not able to study the phenotype of adult mice. But we surmise that these mice would be potentially viable and that the $Fbxo11^{tm2b/Jf}$ mice would demonstrate chronic otitis media. While these studies are focused on the *Fbxo11* knock-out and *Jeff* mutations and the nature of their pleiotropic effects across a range of tissues, including the middle ear, in order to better understand the pathways and mechanisms predisposing to middle ear inflammatory disease it will be important to develop and analyse the impact of these mutations exclusively in the middle ear using middle ear epithelial conditional mutants.

FBXO11 has a number of interacting partners and impacts on a number of pathways (Abida et al., 2007; Tateossian et al., 2009; Duan et al., 2012; Abbas et al., 2013; Rossi et al., 2013; Jin et al., 2015; Tateossian et al., 2015). FBXO11 is an E3 ubiquitin ligase, a substrate binding component of a SKP1-Cul1-Fbox protein complex involved in the post-translational modification of different target proteins. p53 has been shown to be neddylated by FBXO11 *in vitro* (Abida et al., 2007) and in the mouse developing lung (Tateossian et al., 2015). FBXO11 was reported to target BCL6 for ubiquitination and proteasomal degradation (Duan et al., 2012). Two studies demonstrated a role of FBXO11 in the ubiquitination and degradation of CDT2 (Abbas et al., 2013; Rossi et al., 2013). In addition SNAIL1/2 proteins were found to be recognized and ubiquitinated by FBXO11 (Jin et al., 2015). In our previous work we concluded that in the developing mouse FBXO11 regulates the TGFβ pathway (Tateossian et al., 2009) which is known to be critically involved with middle ear inflammation (Tateossian et al., 2013). This cross-talk may occur by interaction of FBXO11 with p53 (Tateossian et al., 2015). It is not inconceivable that mutations in FBXO11 might lead to gain-of-function effects, for example, leading to new interactions or strengthening existing interactions that would lead to dominant effects of the kind that we see in the *Jeff* mutant but not in a loss-of-function mutant. Both *in vivo* and *in vitro* characterization of the nature of interactions involving the mutant protein in *Jeff* mice may help to unravel precisely the nature of the gain-of-function effects that lead to the many changes we have already documented in relevant pathways that lead to impacts on TGFβ

and p53 signaling in the *Jeff* mouse (Tateossian et al., 2009; Tateossian et al., 2015). Moreover, further work will be required to elucidate mechanisms associated with loss of function effects.

In conclusion, by comparing the phenotype of mice carrying a null mutation in the *Fbxo11* gene with the well-characterized chronic otitis media model, *Jeff*, we have demonstrated that the *Jeff* mutation is both a loss-of-function mutation and a gain-of-function mutation. This has important lessons for our further study of the molecular mechanisms by which FBXO11 elicits COME in both mice and the human population.

DATA AVAILABILITY STATEMENT

All datasets generated for this study are included in article/**Supplementary Material**.

ETHICS STATEMENT

All animal experimentation was approved by the Animal Welfare and Ethical Review Body at MRC, Harwell.

AUTHOR CONTRIBUTIONS

OK carried out the phenotyping tests and analysis, contributed to the design of the study and the interpretation of the results, and participated in drafting the manuscript. PV and TP performed the inoculations and contributed to the interpretation of the results from these studies. HT and SB contributed to the design of the study, interpretation of results, and participated in drafting the manuscript. All authors read and approved the final manuscript.

FUNDING

This work was supported by an award from the Medical Research Council, United Kingdom to SB (MC_U142684175).

ACKNOWLEDGMENTS

We would like to thank the staff of the Mary Lyon Centre for animal husbandry, in particular Lucie Vizor and Sara Wells; Caroline Barker and Adele Austin for histology services; the staff of the Genotyping core for genotyping. We are also grateful to the Molecular and cellular biology group, in particular Lydia Teboul and Gemma Codner for generating the *Fbxo11* knock-out mice.

SUPPLEMENTARY MATERIAL

The Supplementary Material for this article can be found online at: https://www.frontiersin.org/articles/10.3389/fgene.2020.00498/full#supplementary-material

FIGURE S1 | Original image files for the western blots included in **Figure 1**.

REFERENCES

Abbas, T., Mueller, A. C., Shibata, E., Keaton, M., Rossi, M., and Dutta, A. (2013). CRL1-FBXO11 promotes Cdt2 ubiquitylation and degradation and regulates Pr-Set7/Set8-mediated cellular migration. *Mol. Cell.* 49, 1147–1158. doi: 10.1016/j.molcel.2013.02.003

Abida, W. M., Nikolaev, A., Zhao, W., Zhang, W., and Gu, W. (2007). FBXO11 promotes the Neddylation of p53 and inhibits its transcriptional activity. *J. Biol. Chem.* 282, 1797–1804. doi: 10.1074/jbc.m609001200

Bradley, A., Anastassiadis, K., Ayadi, A., Battey, J. F., Bell, C., Birling, M. C., et al. (2012). The mammalian gene function resource: the international knockout mouse consortium. *Mamm. Genome* 23, 580–586.

Crompton, M., Purnell, T., Tyrer, H. E., Parker, A., Ball, G., Hardisty-Hughes, R. E., et al. (2017). A mutation in Nischarin causes otitis media via LIMK1 and NF-kappaB pathways. *PLoS Genet.* 13:e1006969. doi: 10.1371/journal.pgen.1006969

Duan, S., Cermak, L., Pagan, J. K., Rossi, M., Martinengo, C., di Celle, P. F., et al. (2012). FBXO11 targets BCL6 for degradation and is inactivated in diffuse large B-cell lymphomas. *Nature* 481, 90–93. doi: 10.1038/nature10688

Ferguson, M. W. (1988). Palate development. *Development* 103(Suppl.), 41–60.

Friedel, R. H., Wurst, W., Wefers, B., and Kuhn, R. (2011). Generating conditional knockout mice. *Methods Mol. Biol.* 693, 205–231. doi: 10.1007/978-1-60761-974-1_12

Hardisty, R. E., Erven, A., Logan, K., Morse, S., Guionaud, S., Sancho-Oliver, S., et al. (2003). The deaf mouse mutant Jeff (Jf) is a single gene model of otitis media. *J. Assoc. Res. Otolaryngol.* 4, 130–138. doi: 10.1007/s10162-002-3015-9

Hardisty-Hughes, R. E., Parker, A., and Brown, S. D. (2010). A hearing and vestibular phenotyping pipeline to identify mouse mutants with hearing impairment. *Nat. Protoc.* 5, 177–190. doi: 10.1038/nprot.2009.204

Hardisty-Hughes, R. E., Tateossian, H., Morse, S. A., Romero, M. R., Middleton, A., Tymowska-Lalanne, Z., et al. (2006). A mutation in the F-box gene, Fbxo11, causes otitis media in the Jeff mouse. *Hum. Mol. Genet.* 15, 3273–3279. doi: 10.1093/hmg/ddl403

Hood, D., Moxon, R., Purnell, T., Richter, C., Williams, D., Azar, A., et al. (2016). A new model for non-typeable *Haemophilus influenzae* middle ear infection in the Junbo mutant mouse. *Dis. Model. Mech.* 9, 69–79.

Jin, Y., Shenoy, A. K., Doernberg, S., Chen, H., Luo, H., Shen, H., et al. (2015). FBXO11 promotes ubiquitination of the Snail family of transcription factors in cancer progression and epidermal development. *Cancer Lett.* 362, 70–82. doi: 10.1016/j.canlet.2015.03.037

Kubba, H., Pearson, J. P., and Birchall, J. P. (2000). The aetiology of otitis media with effusion: a review. *Clin. Otolaryngol. Allied Sci.* 25, 181–194. doi: 10.1046/j.1365-2273.2000.00350.x

Nolan, P. M., Peters, J., Strivens, M., Rogers, D., Hagan, J., Spurr, N., et al. (2000). A systematic, genome-wide, phenotype-driven mutagenesis programme for gene function studies in the mouse. *Nat. Genet.* 25, 440–443.

Parkinson, N., Hardisty-Hughes, R. E., Tateossian, H., Tsai, H. T., Brooker, D., Morse, S., et al. (2006). Mutation at the evi1 locus in junbo mice causes susceptibility to otitis media. *PLoS Genet.* 2:e149. doi: 10.1371/journal.pgen.100149

Rossi, M., Duan, S., Jeong, Y. T., Horn, M., Saraf, A., Florens, L., et al. (2013). Regulation of the CRL4(Cdt2) ubiquitin ligase and cell-cycle exit by the SCF(Fbxo11) ubiquitin ligase. *Mol. Cell.* 49, 1159–1166.

Skarnes, W. C., Rosen, B., West, A. P., Koutsourakis, M., Bushell, W., Iyer, V., et al. (2011). A conditional knockout resource for the genome-wide study of mouse gene function. *Nature* 474, 337–342.

Tateossian, H., Hardisty-Hughes, R. E., Morse, S., Romero, M. R., Hilton, H., Dean, C., et al. (2009). Regulation of TGF-beta signalling by Fbxo11, the gene mutated in the Jeff otitis media mouse mutant. *Pathogenetics* 2:5.

Tateossian, H., Morse, S., Parker, A., Mburu, P., Warr, N., Acevedo-Arozena, A., et al. (2013). Otitis media in the Tgif knockout mouse implicates TGFbeta signalling in chronic middle ear inflammatory disease. *Hum. Mol. Genet.* 22, 2553–2565.

Tateossian, H., Morse, S., Simon, M. M., Dean, C. H., and Brown, S. D. (2015). Interactions between the otitis media gene, Fbxo11, and p53 in the mouse embryonic lung. *Dis. Model. Mech.* 8, 1531–1542.

Vikhe, P. P., Purnell, T., Brown, S. D. M., and Hood, D. W. (2019). Cellular content plays a crucial role in Non-typeable *Haemophilus influenzae* infection of preinflamed Junbo mouse middle ear. *Cell Microbiol.* 21:e12960.

Conflict of Interest: The authors declare that the research was conducted in the absence of any commercial or financial relationships that could be construed as a potential conflict of interest.

frontiers in Genetics

ORIGINAL RESEARCH
published: 27 May 2020
doi: 10.3389/fgene.2020.00495

Role of Endoplasmic Reticulum Stress in Otitis Media

Hongchun Zhao[1,2], Yanfei Wang[2], Bo Li[3], Tihua Zheng[3], Xiuzhen Liu[4], Bo Hua Hu[5], Juan Che[2], Tong Zhao[3], Jun Chen[2], Maria Hatzoglou[6], Xiaolin Zhang[2], Zhaomin Fan[1]* and Qingyin Zheng[7]*

[1] Department of Otolaryngology-Head and Neck Surgery, Shandong Provincial ENT Hospital, Cheeloo College of Medicine, Shandong University, Jinan, China, [2] Department of Otolaryngology/Head and Neck Surgery, Institute of Otolaryngology, Affiliated Hospital of Binzhou Medical University, Binzhou, China, [3] Hearing and Speech Rehabilitation Institute, College of Special Education, Binzhou Medical University, Yantai, China, [4] Clinical Laboratory, Affiliated Hospital of Binzhou Medical University, Binzhou, China, [5] Center for Hearing and Deafness, University at Buffalo, Buffalo, NY, United States, [6] Department of Genetics, Case Western Reserve University, Cleveland, OH, United States, [7] Department of Otolaryngology-Head & Neck Surgery, Case Western Reserve University, Cleveland, OH, United States

Endoplasmic reticulum (ER) stress occurs in many inflammatory responses. Here, we investigated the role of ER stress and its associated apoptosis in otitis media (OM) to elucidate the mechanisms of OM and the signaling crosstalk between ER stress and other cell damage pathways, including inflammatory cytokines and apoptosis. We examined the expression of inflammatory cytokine- and ER stress-related genes by qRT-PCR, Western blotting, and immunohistochemistry (IHC) in the middle ear of C57BL/6J mice after challenge with peptidoglycan polysaccharide (PGPS), an agent inducing OM. We also evaluated the effect of the suppression of ER stress with tauroursodeoxycholic acid (TUDCA), an ER stress inhibitor. The study revealed the upregulation of ER stress- and apoptosis-related gene expression after the PGPS treatment, specifically ATF6, CHOP, BIP, caspase-12, and caspase-3. TUDCA treatment of PGPS-treated mice decreased OM; reduced the expression of CHOP, BIP, and caspase 3; and significantly decreased the proinflammatory gene expression of tumor necrosis factor-α (TNF-α) and interleukin-6 (IL-6). These results suggest that PGPS triggers ER stress and downstream proinflammatory gene expression in OM and that inhibition of ER stress alleviates OM. We propose that ER stress plays a critical role in inflammation and cell death, leading to the development of OM and points to ER stress inhibition as a potential therapeutic approach for the prevention of OM.

Keywords: endoplasmic reticulum (ER) stress, streptococcal peptidoglycan polysaccharide, otitis media, tauroursodeoxycholic acid, apoptosis, therapy

OPEN ACCESS

Edited by:
Regie Santos-Cortez, University of Colorado, United States

Reviewed by:
Federico Kalinec, University of California, Los Angeles, United States
Jernej Kovac, University Medical Centre Ljubljana, Slovenia

***Correspondence:**
Xiaolin Zhang
zhangxiaolinmdc@163.com
Zhaomin Fan
fanent@126.com

Specialty section:
This article was submitted to Genetic Disorders, a section of the journal Frontiers in Genetics

Received: *31 August 2019*
Accepted: *20 April 2020*
Published: *27 May 2020*

Citation:
Zhao H, Wang Y, Li B, Zheng T, Liu X, Hu BH, Che J, Zhao T, Chen J, Hatzoglou M, Zhang X, Fan Z and Zheng Q (2020) Role of Endoplasmic Reticulum Stress in Otitis Media. Front. Genet. 11:495. doi: 10.3389/fgene.2020.00495

INTRODUCTION

Otitis media (OM) is an inflammatory disorder of the middle ear associated with infection. OM is the second most common childhood disease (Hang and Brietzke, 2012). The pathogenesis of OM is related to the anatomy and immune function of patients (Gould and Matz, 2010). Both bacteria and viruses can cause an infection. Antibiotics are often recommended for infants and children with severe symptoms, such as moderate to severe ear pain and high fever, but the treatment may cause side effects such as diarrhea, vomiting, and skin rash (Han et al., 2009; Kawai and Akira, 2010;

Komori et al., 2011). Antibiotic resistance remains a major public health challenge (Venekamp et al., 2013). Therefore, there is an urgent need to understand the mechanisms of OM, which reveal novel therapeutic targets for the early intervention and prevention of OM.

The host immune response has been shown to play an important role in OM pathogenesis, but the molecular details of the response are not clear. The endoplasmic reticulum (ER) is an intracellular organelle that is essential for protein folding. Errors in protein folding can lead to protein accumulation in the ER and induce the expression of ER stress-related genes, a reaction known as the unfolded protein response (UPR) (Wang and Kaufman, 2016). The signaling pathway activated by ER stress has been studied extensively, and emerging evidence has shown the contribution of ER stress to the pathogenesis of many human diseases. Recently, signaling crosstalk between ER stress and inflammatory reactions has been reported in various inflammatory disorders (Zhang et al., 2006; Zhang and Kaufman, 2008; Hasnain et al., 2012; Qiu et al., 2013; Wang and Kaufman, 2014), especially in inflammatory bowel disease (Cao et al., 2013). Previous studies suggest that inflammatory stimuli can activate the UPR, trigger ER stress, and thus damage ER homeostasis, which leads to inflammatory diseases (Zhang et al., 2006; Menu et al., 2012). However, it is also well known that inflammatory responses can induce ER stress due to overproduction of proteins in the ER (Hasnain et al., 2012). In addition to the complexity of the interplay between ER stress and inflammation, the cellular response to ER stress has cell-type-specific components that determine either adaptation to stress conditions or maladaptation and death (Guan et al., 2017). The inflammatory gene expression programs are activated during the maladaptive response to ER stress. In fact, we have shown that such a maladaptive hyperactivation of a proinflammatory response occurs during increased intensity of an environmental stress via the actions of a novel axis of the eIF2a kinase PKR interacting with the protein PACT (Farabaugh et al., 2020). Similarly, a PACT-PKR activation mechanism during ER stress has been reported to be proapoptotic (Singh et al., 2009). Therefore, data from the recent literature suggest that ER stress can lead to proinflammatory conditions or proinflammatory conditions can cause ER stress. The role of ER stress in the pathogenesis of OM is not known. We therefore tested in an experimental mouse model of OM the presence of ER stress and inflammatory gene expression and how inhibition of ER stress can affect the proinflammatory response and the pathogenesis of OM.

As demonstrated in our previous study, inoculation with the bacterial cell wall component peptidoglycan polysaccharide (PGPS) induces inflammation in the middle ear cavity, which creates an OM model without the need for live bacteria or viruses (Zhang et al., 2015). PGPS is a pathogen-associated microbial pattern (PAMP) that can activate Toll-like receptor 2 (TLR2), leading to the activation of the immune response (Han et al., 2009; Kawai and Akira, 2010; Komori et al., 2011). We previously used C57BL/6J (B6) mice with PGPS-induced middle ear inflammation as a model to investigate the pathogenesis of OM (Zhang et al., 2015). In this study, we aimed to evaluate the role of the ER stress-related inflammatory response and cell death in the development of PGPS-induced OM. We found that PGPS-induced OM is accompanied by the increased expression of inflammation-related cytokines and the expression of ER stress-related genes. We used an ER stress inhibitor, tauroursodeoxycholic acid (TUDCA), a synthetic compound that has been widely used in the treatment of OM. Interestingly, TUDCA treatment significantly alleviated middle ear inflammation and suppressed middle ear cell death. Additionally, TUDCA treatment inhibited the expression of ER stress-associated gene expression. These findings suggest that ER stress plays a key role in OM.

MATERIALS AND METHODS

Mice and Treatments

The mice were originally obtained from the Jackson Laboratory (Bar Harbor, ME, United States). The experimental protocol was approved by the Animal Use and Care Committee of the Binzhou Medical University Hospital. A total of 168 C57BL/6JB6 mice, 8 weeks old, were used in this study. The mice were randomly assigned into three groups matched by sex and age: a PGPS-treated, a TUDCA-treated, and a PBS-treated (control) group. The PGPS-treated group was treated with PGPS (100P, BD Bioscience, San Jose, CA, United States) that was freshly prepared in 10 μl of PBS (5.5 mg/ml). This dose was selected because it balances the safety and effectiveness of the treatment, as demonstrated in our preliminary experiments (Zhang et al., 2015). The drug was injected through the tympanic membrane into the right middle ear cavity using a Hamilton syringe. The TUDCA group was treated with TUDCA (EMD Chemicals Inc., catalog no. 580549) that was freshly prepared (200 μg in 10 μl PGPS) and injected into the middle ear. The control group was treated with 0.1 M PBS. Individual mice were anesthetized intraperitoneally with 4% chloral hydrate (0.01 ml/g). Their tympanic membranes were examined at 1 h after the injection using a MedRx VetScope System® otoscopic digital imaging system (MedRx, Largo, FL, United States). The mice were examined every 12 h for 3 days post-injection.

The effects of the drug treatment were evaluated by auditory-evoked brainstem response (ABR), tympanometry, histology, and expression levels of inflammation- and apoptosis-related genes.

ABR and Tympanometry

A computer-aided evoked potential system (Intelligent Hearing Systems, Smart-EP software) and an automatic MAICO Race Car Tympanometer (MAICO Diagnostics Inc., Eden Prairie, MN, United States) were used to determine ABR thresholds and the middle ear function, respectively. The ABR and tympanometry were performed before and at 3 days post-injection with PGPS, PBS, or PGPS + TUDCA, as described previously (Zheng et al., 2007). Before entering the group, all mice had normal hearing, and electric otoscope showed normal structure without effusion and inflammation. There were no

differences found between the animals in the three groups (PBS, PGPS, and PGPS + TUDCA) before injection. Briefly, mice were anesthetized with intraperitoneal injection of 4% chloral hydrate (0.01 ml/g), and their body temperatures were maintained at 37–38°C. The testing was performed in a room with environmental noise < 50 dB SPL. The stimuli included clicks and tone bursts at 8, 16, and 32 kHz. ABRs were recorded using a computer-aided evoked potential system (Intelligent Hearing Systems, Miami, FL, United States). The threshold was defined as the lowest intensity (±5 dB) at which a visible ABR wave was seen because the minimum stimulus intensity produced an ABR wave pattern similar to that of the higher-intensity stimulus (110 dB). As previously reported, young, untreated control mice showing ABR thresholds greater than 55-dB SPL (for the click stimulus), 40-dB SPL (for 8 kHz), 35-dB SPL (for 16 kHz), or 60-dB SPL (for 32 kHz) were considered hearing impaired (Han et al., 2013). Tympanogram curves were classified as type A (normal), type B (flat, clearly abnormal), and type C (indicating a negative pressure in the middle ear, possibly indicative of pathology). The results of these tests help to determine whether the eardrum is punctured, whether the fluid is present in the ear, and whether the middle ear system is working properly.

Histological Analysis of the Middle Ear

Histological analyses were performed using the methods described previously (Han et al., 2009). On day 3 post-PGPS injection, the experimental C57BL/6J mice were euthanized with CO_2, and their bullae (including both the middle and inner ear) were collected. Then, the bulla tissues were fixed with 10% paraformaldehyde for 24 h, decalcified with 10% EDTA solution for 5 days, and embedded in paraffin. The tissue sections (5 μm) were stained with hematoxylin–eosin (H&E) and examined under a light microscope (Leica DMI4000 B).

Immunohistochemistry (IHC) Protocol

The tissue sections (5 μm) were deparaffinized as follows: two 10-min incubations in xylene followed by incubation in a graded series of ethanol (100, 95, 80, 70, and 50%) and then with ddH_2O, twice, for 5 min each. The endogenous peroxidase activity was blocked at room temperature by a 20-min incubation in 3% H_2O_2 in PBS (pH 7.4). The sections were rinsed with PBS for 5 min and blocked in normal goat serum for 20 min at room temperature. After incubation, the residual fluid was removed (without washing). Subsequently, the sections were incubated in primary antibodies against TNF-α (Proteintech, 60291-1-Ig) and CHOP (Proteintech, 15204-1-AP) for 60 min at room temperature or 4°C overnight then rinsed twice for 5 min each. An array slide was incubated with a biotin-conjugated secondary antibody at 20–37°C for 20 min. The sections were rinsed twice for 5 min each and developed using a DAB kit (control, the degree of staining with regular microscopy) to develop. The sections were subsequently washed in distilled water, stained, and differentiated in hematoxylin. Finally, slides were dehydrated and mounted.

Terminal Deoxynucleotidyl Transferase dUTP Nick-End Labeling (TUNEL) Staining

Apoptotic middle ear epithelial cells were identified by a TUNEL assay according to the manufacturer's protocol. Briefly, tissue sections (5 μm) were deparaffinized and then fixed in 4% paraformaldehyde diluted in 1 × PBS (pH 7.4) for 1 h. The surface preparations were permeabilized in 0.1% Triton X-100. The specimens were stained using a TUNEL kit (*In Situ* Cell Death Detection kit, Fluorescein, Roche) at 37°C for 1 h in a humid chamber and then counterstained with DAPI for 5 min at room temperature. The tissues were then observed under a fluorescence microscope (Leica TCS SP2).

Real-Time Quantitative PCR

The mice were sacrificed, and their right bullae (including the middle ear and inner ear) were quickly isolated. Total RNA was isolated from individual right bullae using TRIzol® reagent (Invitrogen, Carlsbad, United States) according to the manufacturer's protocol. The concentrations of RNA were measured using a Biophotometer (Eppendorf, Hamburg, Germany). The total RNA in each sample (1 μg) was reverse transcribed into cDNA using random primers following the First-Strand Synthesis protocol (Takara Bio). Quantitative real-time PCR was performed using a FastStart Universal SYBR Green Master kit (Roche, Mannheim, Germany) in a Bio-Rad iCycler iQ5 Peltier thermal cycler. The PCR thermal cycling conditions were as follows: 95°C for 10 min, 40 cycles of 95°C for 15 s, and 60°C for 1 min. Finally, a dissociation curve of 95°C for 15 s, 60°C for 1 min, 95°C for 15 s, and 60°C for 15 s was added. Primer sequences for a total of 10 genes were synthesized using Sangon Biotech Co., Ltd. (Shanghai) (see **Table 1** for the gene list and primer sequences). The levels of mRNA transcripts of target genes relative to the control of GAPDH were calculated using the $2^{-\Delta\Delta Ct}$ method (Livak and Schmittgen, 2001).

Western Blot

To further investigate the expression of inflammation- and ER stress-associated genes in OM, we examined protein expression using Western blot. The right bullae (including

TABLE 1 | Primers used for Real-time quantitative PCR.

Gene	Forward primer	Reserve primer
IL-1β	gaaatgccacctttgacagtg	tggatgctctcatcaggacag
TLR2	ctcttcagcaaacgctgttct	ggcgtctccctctattgtattg
Cas3	cggagcagtcctacatggaga	tccgtgatgtgtcgttcagat
IL-6	ggtgccctgccagtattctc	ggctcccaacacaggatga
TNF-α	gcggccacagaaaacactc	ctcccaatggtcaaggcatc
BiP	acttggggaccacctattcct	atcgccaatcagacgctcc
CHOP	ctggaagcctggtatgaggat	cagggtcaagagtagtgaaggt
Cas12	agacagagttaatgcagtttgct	ttcaccccacagattccttcc
ATF-6	tcgccttttagtccggttctt	ggctccataggtctgactcc
GAPDH	aggtcggtgtgaacggatttg	tgtagaccatgtagttgaggtca

the middle ear and inner ear) were harvested immediately after euthanasia. The bullae were lysed using ice-cold RIPA buffer with protease inhibitors (cOmplete, EDTA-free cocktail tablet, Roche) and phosphatase inhibitors (PhosSTOP tablet, Roche). Lysates were incubated for 20 min on ice and then centrifuged for 30 min at 14,000 rpm at 4°C. Then, equal amounts of proteins were subjected to SDS-PAGE and transferred to a polyvinylidene difluoride (PVDF) membrane. The PVDF membrane was blocked for 3 h in 5% skimmed milk and incubated overnight at 4°C with 1:1000 diluted primary antibodies: anti-TNF-α (Proteintech, 60291-1-Ig), anti-IL-6 (Proteintech, 66146-1-Ig), anti-IL-1β (Proteintech, 60291-1-Ig), anti-GRP78/BIP (Proteintech, 11587-1-AP), anti-caspase-3 (Proteintech, 19677-1-AP), anti-caspase-12 (Proteintech, 55238-1-Ig), anti-CHOP (Proteintech, 15204-1-AP), anti-activating transcription factor 6 (ATF6; Proteintech, 24169-1-AP), and anti-GAPDH (Hangzhou Goodhere Biotechnology Co., Ltd.). All antibodies were validated for their specificity. After washing with TBST, the membrane was incubated in 1:5000 diluted secondary antibodies (Abcam, 6721, 6789). The protein bands were visualized using ECL chemiluminescence. Band intensities were quantified using ImageJ software.

Oxidative Stress Detection

At the day 3 post-PGPS inoculation and TUDCA treatment, the mice were sacrificed, and their right bullae were dissected and placed in 10% FBS RPMI 1640 medium in a plastic culture dish. After all non-middle ear-associated tissues were removed, the mucosa in the middle ear cavity was gently removed with fine forceps and transferred to the center of a 35-mm glass-bottom culture dish and washed three times with 1 × PBS. The samples were fixed in 4% paraformaldehyde in PBS for 15 min at room temperature. Samples were washed twice in PBS to remove residual paraformaldehyde, permeabilized with 0.5% Triton X-100 in PBS for 15 min, and then washed three times in 1 × PBS. The specimens were incubated with a CellROX® Green Reagent kit (Invitrogen, 10444) at 37°C for 30 min, washed three times in 1 × PBS, and then counterstained with DAPI for 5 min at room temperature. The stained tissues were observed under an immunofluorescence microscope (Leica DFC500, Germany).

Statistical Analysis

Data are presented as the mean ± 95% confidence intervals. Statistical analyses were performed using SPSS 13.0 software. Group differences were analyzed using unpaired Student's *t* test or one-way ANOVA (for further multiple comparison between each column, Benjamini test was applied). *P* values less than 0.05 were considered significant.

RESULTS

Inflammation Presents in the Middle Ear After Inoculation With PGPS

Our previous study demonstrated that PGPS could cause inflammation of the middle ear (Zhang et al., 2015). Here, we treated the middle ear with PGPS (55 μg/10 μl) to induce OM. The PBS-treated control group had no difference in ABR thresholds and tympanometric results compared to naïve B6 mice at 8 weeks of age. Therefore, we used the PBS group as the normal control group. Mice injected with PGPS displayed greater inflammatory infiltrates in the tympanic cavity and tissue damage than the mice injected with PBS, as assessed by H&E staining (**Figure 1A**). Moreover, compared with PBS-injected mice, the PGPS-injected mice exhibited threshold shifts, as revealed by the ABR test (**Figure 1B**).

Tympanometry was used to determine the middle ear function. Most PGPS-treated mice showed a type B tympanogram, suggesting the presence of middle ear fluid and/or eardrum perforation (**Figures 1C,D**). However, the average DPOAE amplitude (in dB SPL) was not significantly decreased in the distortion product otoacoustic emission (DPOAE) test (**Figures 1E,F**). Thus, PGPS did not cause inner ear damage. These findings suggest that PGPS injection induces an inflammatory response in the middle ear cavity. We, therefore, used this model to study the effects of OM in subsequent analyses.

PGPS-Induced Inflammatory Response and Apoptosis

To investigate the response of inflammatory molecules to PGPS-induced OM, we measured the expression of a group of inflammatory cytokines using real-time PCR and Western blot. Considering that the activation of TLR2 plays a critical role in the development of OM (Komori et al., 2011; Huang et al., 2016), we measured the transcriptional and protein levels of TLR2 and other inflammation-related genes (TNF-α, IL-6, and IL-1β). We also examined the expression of caspase-3, an important apoptotic protease. All the examined molecules were significantly upregulated in the PGPS group compared to the PBS group (**Figures 2A,B**). The expression of TNF-α was also assessed with IHC analysis (**Figure 2C**). Consistent with the Western blot results, there were only a few positive cells in the middle ear epithelium in the PBS group. In contrast, the PGPS group displayed a significant increase in the number of TNF-α-expressing middle ear epithelium cells. To further evaluate the PGPS-induced apoptosis of middle ear epidermal cells, we removed the epithelial cells from the otic bulla and performed TUNEL. This analysis revealed a significant increase in the number of TUNEL-positive middle ear epidermal cells after PGPS inoculation (**Figure 2D**).

PGPS-Induced OM May Involve ER Stress

Interaction among inflammatory responses, ER stress, and apoptosis has been reported. To determine the involvement of ER stress in PGPS-induced middle ear epidermal cell apoptosis in OM, we examined the expression of ER stress-associated cell death signaling molecules using qRT-PCR and Western blot. ATF-6, GRP-78/BIP, CHOP, and cleaved caspase-12 levels were significantly increased in the PGPS group compared to the PBS group (**Figures 3A,B**). The expression of CHOP was also assessed

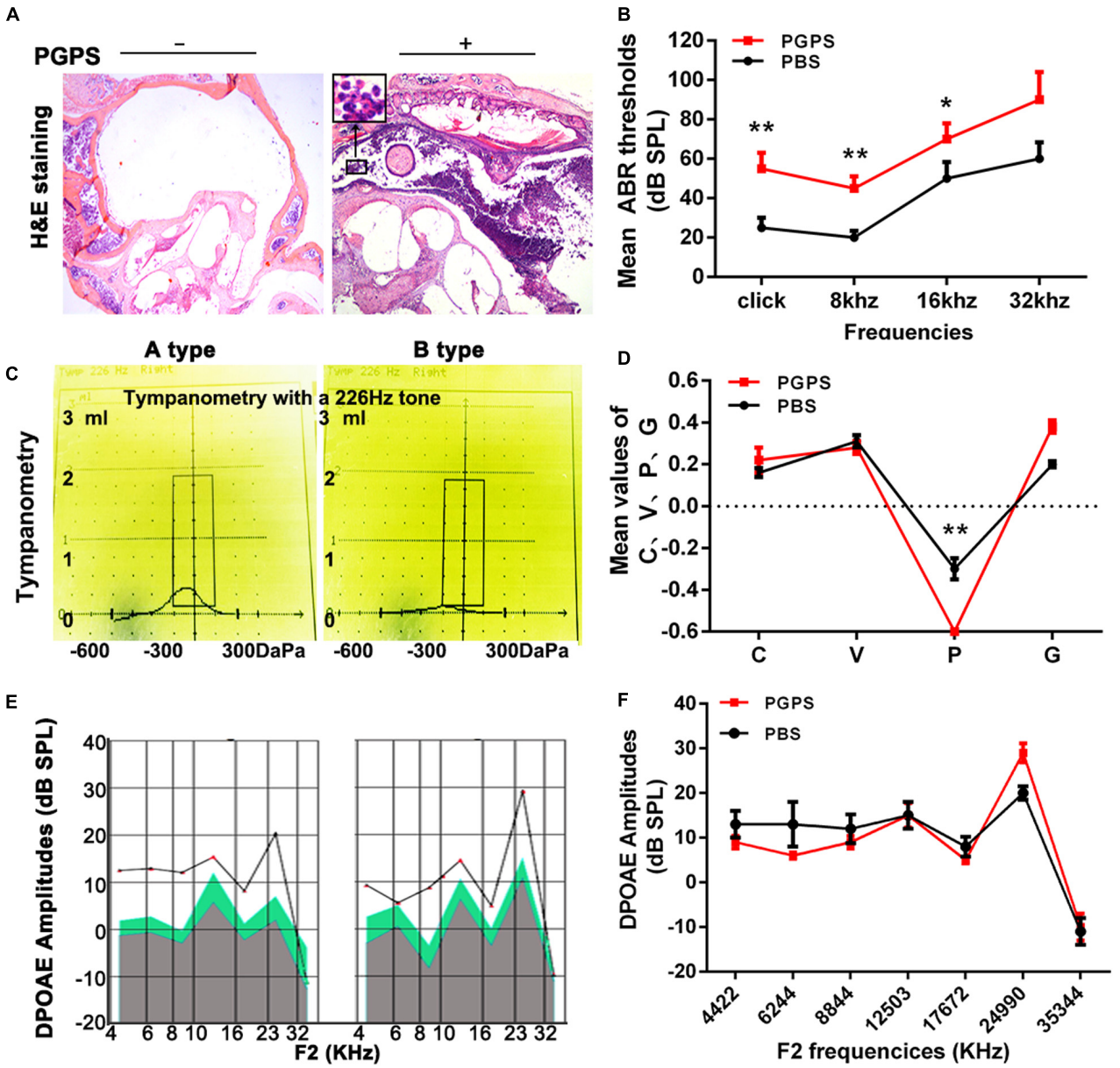

FIGURE 1 | Inoculation with PGPS induces inflammatory cell infiltration in the middle ear cavity. **(A)** Histopathological analysis (H&E staining). After PGPS inoculation, inflammation became increasingly obvious as compared to the control mice (left panel, control; right panel, PGPS). The inset in the image of the PGPS-treated tissue shows the accumulation of neutrophils. **(B)** Average ABR thresholds. The mean ABR thresholds for low-frequency stimuli (clicks and 8-kHz tone bursts) and high-frequency stimuli (16-kHz tone bursts) were significantly higher in the PGPS group than in the PBS group (data = mean ± 95% CI, n = 10 per group per time point). **(C,D)** Quantitative analysis of average tympanometry values. Tympanogram, A type – normal; B type – flat, PGPS group. V: the mean volume value; C: compliance in tympanometry parameters; G: the gradient; P: the pressure. The negative pressure of the middle ear in the PGPS group was significantly higher than that in the PBS group (data = mean ± 95% CI, n = 10 per group per time point). **(E,F)** The average DP amplitudes (in dB SPL) (data = mean ± 95% CI, n = 10 per group per time point). Individual groups of mice from separate experiments (*$P < 0.05$, **$P < 0.01$; two-tailed Student's t test).

by the IHC analysis (**Figure 3C**). The number of CHOP-positive cells in the PGPS-induced group was significantly higher than that in the control group.

Many studies have shown that oxidative stress is involved in the pathogenic process of OM. Reactive oxygen species (ROS) can trigger ER stress, and the ROS level has been used as indirect evidence for the occurrence of ER stress. To investigate the generation of ROS, middle ear epidermis was incubated with CellROX Green reagent. The green signal intensity increased in the cytoplasm and nucleus of middle ear epidermal cells in the PGPS group. The fluorescence intensity in the nuclei was significantly higher in the PGPS group than in the PBS group (**Figure 3D**), indicating that PGPS enhances the production of ROS. These findings indicate that PGPS-induced OM-activated

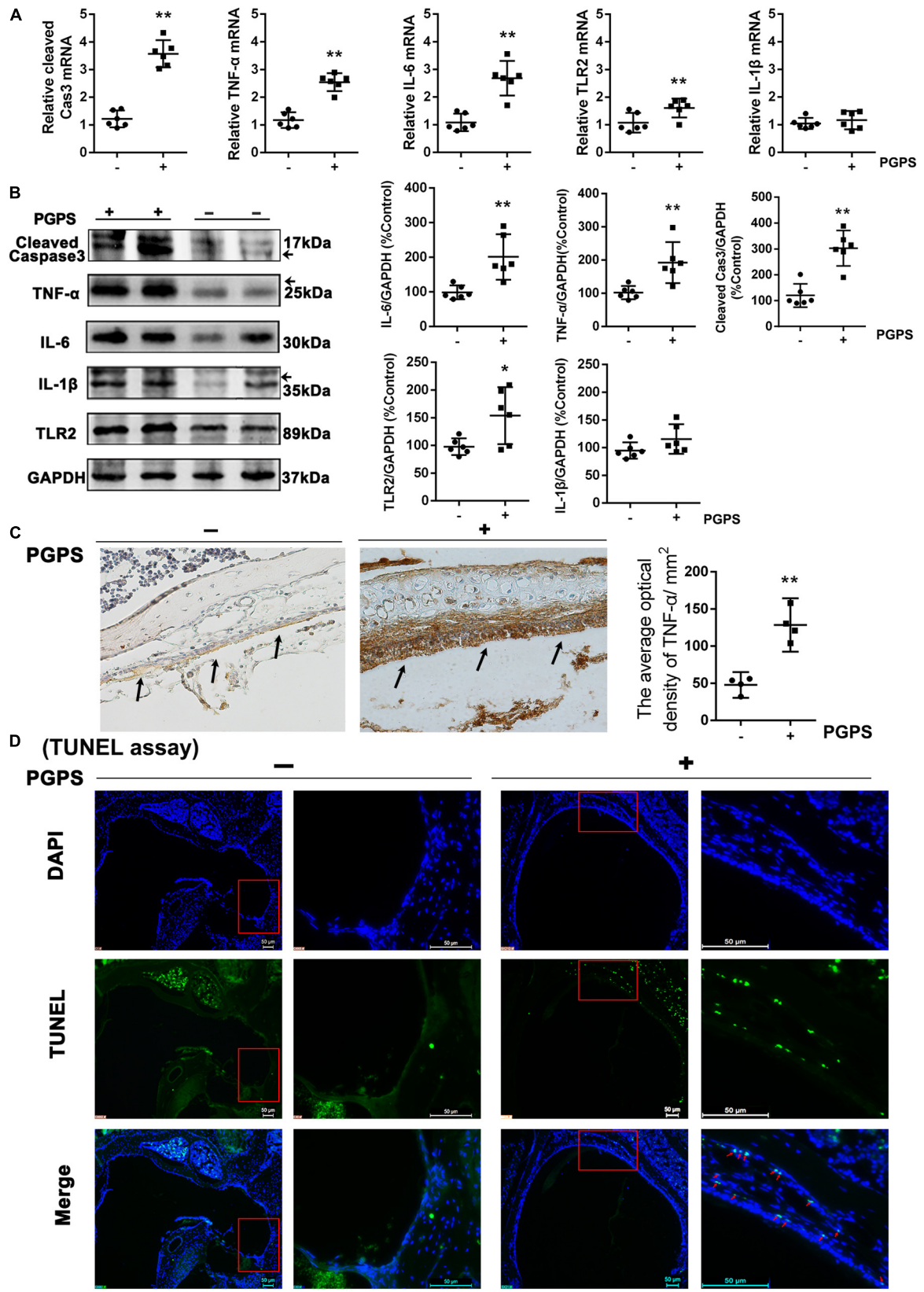

FIGURE 2 | Continued

FIGURE 2 | The inflammatory response and apoptosis are induced in PGPS-injected mice. **(A)** RT-PCR analysis for the transcriptional expression of caspase-3, TNF-α, IL-6, IL-1β, and TLR2 (data = mean ± 95% CI, $n = 6$ per group). **(B)** Western blot analysis for protein expression of caspase-3, TNF-α, IL-6, IL-1β, and TLR2 in the middle ear (data = mean ± 95% CI, $n = 6$ per group). **(C)** Immunohistochemistry analysis for TNF-α in the middle ear epidermal cell region of the PBS and PGPS groups. Quantitative analysis of the relative amount of TNF-α in the middle ear region (data = mean ± 95% CI, $n = 6$ per group). **(D)** A TUNEL assay was performed to assess apoptosis induction in the middle ear epidermal cell region after PGPS injection. Apoptotic cells are illustrated by the green signal in nuclei (TUNEL-positive) in the middle ear epidermal cell region. The left panels show the low-magnification view (50× magnification) and the right panels show the high-magnification view (400× magnification) for each group. The red arrows indicate TUNEL-positive cells in the PGPS group. $^{*}P < 0.05$, $^{**}P < 0.01$. These results confirm that the PGPS of the gram-positive bacterial cell wall is recognized by TLR2, which activates the inflammatory response and induces middle ear epidermal cell death.

TLR2 signaling increases the expression of related inflammatory cytokines, thus perturbing ER homeostasis and amplifying the inflammatory response.

PGPS-Induced ER Stress Plays a Key Role in the Inflammatory Response and Apoptosis in OM

To evaluate the role of ER stress in PGPS-induced inflammation, we treated PGPS-injected mice with TUDCA, a specific ER stress inhibitor. H&E staining showed that TUDCA treatment reduced the level of middle ear inflammation (**Figure 4A**). The areas with inflammatory cells were significantly larger, and the epithelial layer was significantly thicker in the PGPS group than those in the TUDCA group (**Figure 4B**). Moreover, the increase in ABR thresholds observed in the PGPS group was prevented by TUDCA treatment at low frequencies (8 and 16 kHz), but not at 32 kHz (**Figure 4C**). Consistent with these functional and morphological measurements, the expression analysis revealed a reduced production of inflammatory cytokines and ER stress-related proteins (**Figure 4D**). These results show that TUDCA treatment can ameliorate OM. The correction of ER stress could be a potential mechanism for reduced OM.

DISCUSSION

Otitis media is often associated with bacterial or viral infections and, therefore, is commonly treated with antibiotics. The contributing factors of OM include genetic and environmental factors. The underlying mechanisms for the pathogenesis of OM is complicated, involving a network of signal pathways. Previous studies have revealed that the levels of TLR2 and NF-κB are upregulated in OM (Yoshimura et al., 1999; Dziarski et al., 2001; Kielian et al., 2005) and promote the recruitment of neutrophils to combat pathogens in OM (Krysko et al., 2011; Arroyo et al., 2013). These findings suggest that the TLR2 signaling pathway plays an essential role in host defense against middle ear infections. Further research is urgently needed to elucidate the inflammatory response and mechanisms of related factor interactions that could serve as intervention targets to improve the treatment of OM or to prevent the disease.

Peptidoglycan polysaccharide, a component of the gram-positive bacterial cell wall, can cause acute and chronic inflammation (Komori et al., 2011; Wu et al., 2014). Our previous study showed that PGPS could induce severe OM in TLR2-deficient ($Tlr2^{-/-}$) mice (Zhang et al., 2015). In this study, we chose an optimal PGPS dose (PGPS 55 μg/10 μl) to induce OM in B6 mice to further explore the molecular mechanisms of OM. We found inflammatory infiltrates and tissue damage in the middle ear (**Figure 1**), thus suggesting that the OM model was successfully established. The levels of inflammation-related molecules (TNF-α, IL-6, IL-1β, caspase-3, and TLR2) were significantly upregulated (**Figure 2**). TLR2 enables host discrimination between self and non-self and activates the immune response to attack pathogens (Han et al., 2009). Here, PGPS was recognized by TLR2, which, in turn, activated the TLR2 signaling pathway and promoted the production of inflammatory cytokines. If the process is not controlled, inflammation occurs in the middle ear. The downstream signaling molecules, such as TNF-α, IL-6, and IL-1β, have been associated with the recurrence and persistence of OM (Mittal et al., 2014; Nokso-Koivisto et al., 2014). TNF-α is a cell-signaling protein (cytokine) involved in systemic inflammation that can be activated in the acute phase reaction. In this study, TNF-α levels were significantly increased at day 3 after PGPS injection (**Figure 2**), implying that acute inflammation occurred in the middle ear. IL-6, as an important mediator of the acute phase response or as an anti-inflammatory cytokine, is secreted by macrophages to stimulate the immune response during infection. IL-6 induces intracellular signaling cascades that give rise to inflammatory cytokine production in inflammatory cells, such as neutrophils (van der Poll et al., 1997; Gao et al., 2018; Farsakoglu et al., 2019). In our study, PGPS induced neutrophil infiltration (**Figure 1**). IL-1β, a leukocytic pyrogen, can cause a number of different autoinflammatory reactions during infection (Masters et al., 2009; Lukens et al., 2014). Our results suggest that the TNF-α, IL-6, and IL-1β play crucial roles in PGPS-induced OM. A previous study showed that TLR2 activation could cause ER stress, inflammation, and insulin resistance (Botteri et al., 2017). We hypothesized that PGPS binding to TLR2 induces ER stress to amplify inflammation in the middle ear. The expression analysis of the ER stress-related factors ATF6, BIP, CHOP, and caspase-12, supports this hypothesis (**Figure 3**).

ER stress is a cellular stress response related to the UPR, which involves three signaling pathways: PRKR-like ER kinase (PERK)–eukaryotic translation initiation factor 2α (eIF2α), inositol-requiring protein 1α (IRE1α)-X-box-binding protein 1 (XBP1), and ATF6. ATF6 is a basic leucine zipper transcription factor. Under stress, the pro-protein (approximately 90 kDa) translocates to the Golgi, where it is cleaved by proteases to form an active transcription factor (approximately 50 kDa) in the UPR. In this study, the ATF6 level was increased in PGPS-induced OM (**Figure 3**), indicating ER stress activation by ATF6 signaling pathways. Growing evidence suggests that ATF6

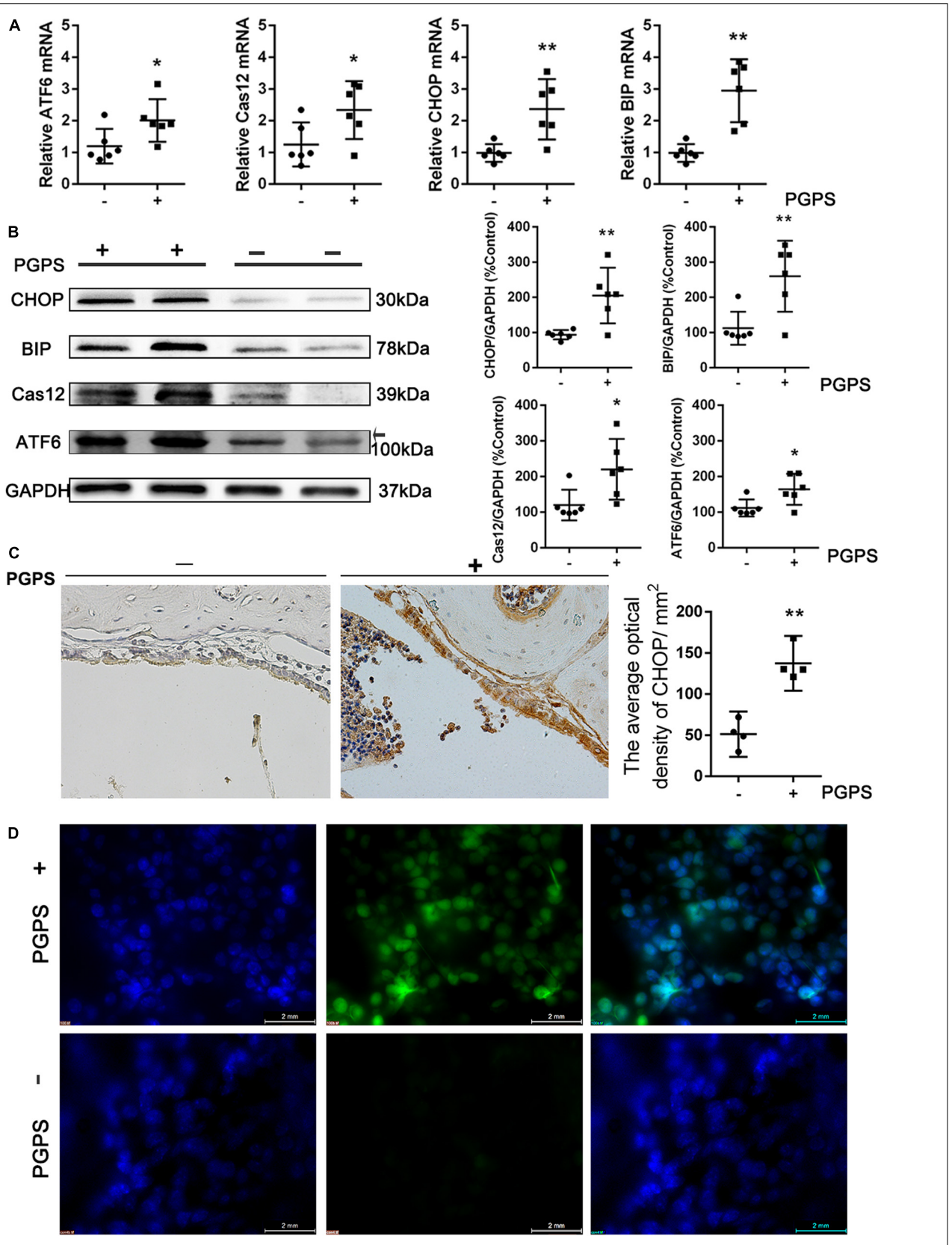

FIGURE 3 | Continued

FIGURE 3 | Endoplasmic reticulum stress is induced in PGPS-treated mice. **(A,B)** RT-PCR and Western blot analyses of ER stress-related molecules. ATF-6, GRP-78/BIP, CHOP, and cleaved caspase-12 levels were increased in PGPS-treated mice (data = mean ± 95% CI, $n = 6$ per group). **(C)** Immunohistochemistry analysis for CHOP. The number of cells showing CHOP immunoreactivity is significantly higher in the PGPS-treated ears than in the control ears (data = mean ± 95% CI, $n = 6$ per group). **(D)** ROS were detected by CellROX Green reagent. The green signal intensity increased in the cytoplasm and nucleus of the middle ear epidermal cells in the PGPS group. $^{*}P < 0.05$, $^{**}P < 0.01$.

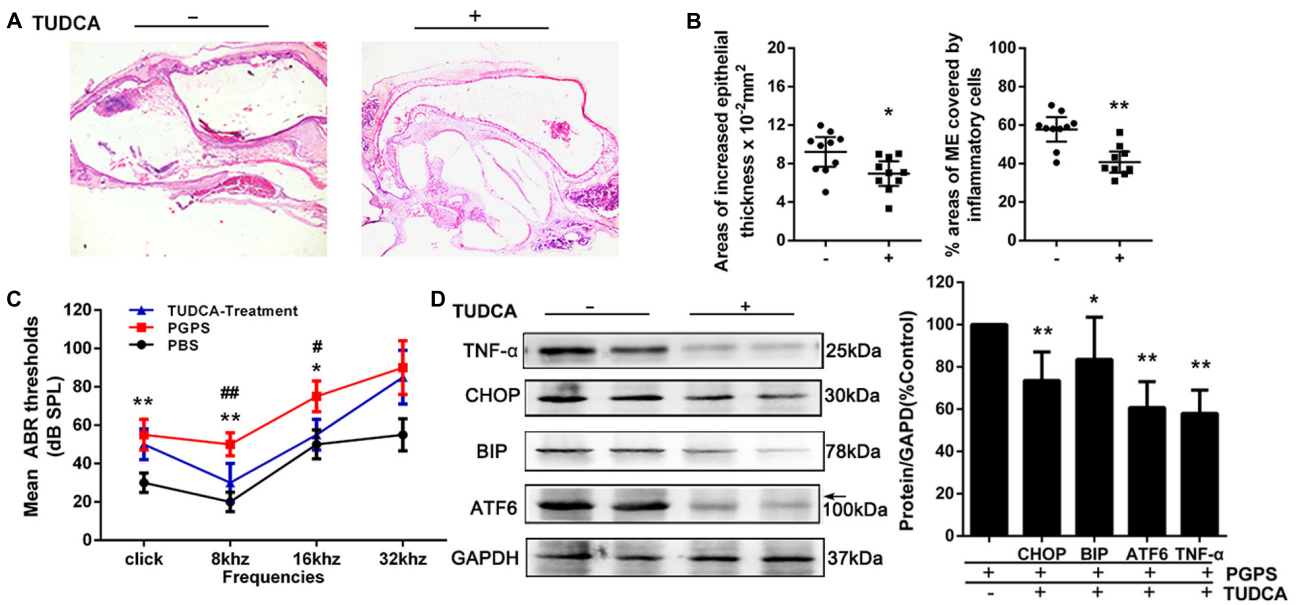

FIGURE 4 | The treatment with the ER stress inhibitor, TUDCA, alleviates PGPS-induced inflammation in the middle ear. **(A)** Morphological observations of H&E-stained middle ears. TUDCA treatment reduced the inflammatory response. **(B)** The epithelial thickness and inflammatory areas in middle ear cavity. The area showing inflammatory cells is significantly larger, and the epithelial layer is significantly thicker, in the PGPS group than those in the TUDCA group ($n = 10$ per group). **(C)** ABR detection. There is a statistically significant difference in ABR thresholds between the three groups. The mean ABR thresholds in response to low-frequency (clicks and 8-kHz tone bursts) and high-frequency stimulation (16-kHz tone bursts) were significantly higher in the PGPS mice than in the PBS mice. The mean ABR thresholds in response to low-frequency (8-kHz tone bursts) and high-frequency stimulation (16-kHz tone bursts) were significantly lower in the TUDCA-treated mice than in the PGPS-injected mice (* indicates the comparison between the PGPS and the PBS group; # indicates the comparison between the PGPS and the TUDCA group; $n = 10$ per group). **(D)** Western blot analysis of TNF-α and ER stress-related proteins. ATF-6, BIP, CHOP, and TNF-α levels were decreased in TUDCA-treated mice ($n = 6$ per group). Data are presented as the mean ± 95% CI. $^{\#,*}P < 0.05$, $^{\#\#,**}P < 0.01$.

activation occurs rapidly, but its attenuation requires time. In this study, we hypothesized that the protein expression of ATF6 was increased by the upregulated expression of TLR2. The molecules BIP and CHOP, downstream of ATF6, are targets of the ER stress response and can effectively activate UPR pathways during ER stress (Chapman et al., 1998; Okamura et al., 2000). Based on our analysis, the expression levels of BIP and CHOP were significantly increased in the PGPS-induced group (**Figure 3**), indicating that the ER stress response is activated in OM.

Research has suggested that aberrant accumulation of ROS can induce ER stress (Volmer et al., 2013). CHOP can activate ER oxidase 1α (ERO1α) to augment the production of ROS. Thus, ER stress can induce oxidative stress, which leads to cell death. Alternatively, loss of adaptation to ER stress (Guan et al., 2017) can also increase proinflammatory gene expression via activation of NF-kB (Schmitz et al., 2018). Both of these mechanisms can contribute to the inflammatory process in OM (Aydogan et al., 2013; Balikci et al., 2014). This is consistent with previous research, which found that ER stress, inflammation, and oxidative stress are tightly integrated and each one can influence the other (Zhang et al., 2017; Chen et al., 2019; Diaz-Bulnes et al., 2019). The inflammatory response can be activated by maladaptive ER stress conditions, and inflammatory gene expression and disturbed redox homeostasis in the ER can further enhance ER stress (Zhang et al., 2017). In this study, our CellROX Green reagent staining revealed that ROS levels were increased (**Figure 3D**). Therefore, PGPS associates with increased ROS-positive cells, increased ER stress markers, and increased inflammation. Although our data cannot conclude if the increased ROS levels is the result of ER stress or the result of the PGPS-mediated responses, our data clearly show that TUDCA-mediated improvement of protein folding in the ER decreases proinflammatory gene expression. Increased ROS levels are expected to oxidize free cysteines in the ER and/or cause mixed disulfide bond formations and protein misfolding (Gao et al., 2020). Therefore, independently if ROS proceeds or follows ER stress, it is expected to increase protein misfolding in the ER, decrease adaptive responses, and increase proinflammatory programs. Our data suggest that PGPS-mediated induction of ER stress contributes to the amplitude of the inflammatory response.

Rescuing ER stress can delay proinflammatory gene expression and PGPS-induced OM (**Figure 4**).

CONCLUSION

In conclusion, our findings show that PGPS-induced OM-related ER stress plays a key role in inflammation in the middle ear. Therefore, the interaction between PGPS-induced TLR2 signaling and ER stress in OM warrants further exploration. Additionally, this study indicates that a signaling crosstalk occurs between ER stress and oxidative stress in OM, signifying the need for further studies. Together, our study raises the possibility that the inhibition of ER stress could serve as a potential therapeutic approach for the prevention of OM.

DATA AVAILABILITY STATEMENT

All datasets generated for this study are included in the article/supplementary material.

ETHICS STATEMENT

The experimental protocol was approved by the Animal Use and Care Committee of the Binzhou Medical University Hospital. Studies were conducted according to the principles set forth in the Guide for the Care and Use of Laboratory Animals (DC005846) as well as the Institute of Laboratory Animal Resources (protocol 2014-0155).

AUTHOR CONTRIBUTIONS

XZ, ToZ, and XL performed the experiments. HZ, XZ, BL, and QZ wrote the manuscript. JuaC analyzed the data. YW and JuC participated in the discussion of the project. QZ, XZ, and ZF designed the study. BL, QZ, XZ, and MH acquired funding. XZ, QZ, TiZ, BH, and MH revised the manuscript. All authors reviewed and approved the manuscript.

FUNDING

This work was supported by the National Natural Science Foundation of China (81530030, 81873697, 81500797, and 81700902), the National Institutes of Health (R01DC015111, R21DC005846, DK053307, and DK060596), the Shandong Provincial Natural Science Foundation of China (ZR2019PH062), and the Taishan Scholars Foundation.

REFERENCES

Arroyo, D. S., Soria, J. A., Gaviglio, E. A., Garcia-Keller, C., Cancela, L. M., Rodriguez-Galan, M. C., et al. (2013). Toll-like receptor 2 ligands promote microglial cell death by inducing autophagy. *FASEB J.* 27, 299–312. doi: 10.1096/fj.12-214312

Aydogan, F., Tastan, E., Aydin, E., Senes, M., Akgedik, S., Berkem, R., et al. (2013). Antioxidant role of selenium in rats with experimental acute otitis media. *Indian J. Otolaryngol. Head Neck Surg.* 65, 541–547. doi: 10.1007/s12070-011-0463-8

Balikci, H. H., Karakas, M., Gurdal, M. M., Ozkul, M. H., Bayram, O., Bayram, A. A., et al. (2014). Advanced oxidation protein product level in children with chronic otitis media with effusion. *Int. J. Pediatr. Otorhinolaryngol.* 78, 551–553. doi: 10.1016/j.ijporl.2014.01.007

Botteri, G., Montori, M., Guma, A., Pizarro, J., Cedo, L., Escola-Gil, J. C., et al. (2017). VLDL and apolipoprotein CIII induce ER stress and inflammation and attenuate insulin signalling via Toll-like receptor 2 in mouse skeletal muscle cells. *Diabetologia* 60, 2262–2273. doi: 10.1007/s00125-017-4401-5

Cao, S. S., Zimmermann, E. M., Chuang, B. M., Song, B., Nwokoye, A., Wilkinson, J. E., et al. (2013). The unfolded protein response and chemical chaperones reduce protein misfolding and colitis in mice. *Gastroenterology* 144, 989–1000. doi: 10.1053/j.gastro.2013.01.023

Chapman, R., Sidrauski, C., and Walter, P. (1998). Intracellular signaling from the endoplasmic reticulum to the nucleus. *Annu. Rev. Cell Dev. Biol.* 14, 459–485. doi: 10.1016/s0955-0674(00)00219-2

Chen, S., Chen, Y., Chen, Y., and Yao, Z. (2019). InP/ZnS quantum dots cause inflammatory response in macrophages through endoplasmic reticulum stress and oxidative stress. *Int. J. Nanomedicine* 14, 9577–9586. doi: 10.2147/IJN.S218748

Diaz-Bulnes, P., Saiz, M. L., Lopez-Larrea, C., and Rodriguez, R. M. (2019). Crosstalk between hypoxia and er stress response: a key regulator of macrophage polarization. *Front. Immunol.* 10:2951. doi: 10.3389/fimmu.2019.02951

Dziarski, R., Wang, Q., Miyake, K., Kirschning, C. J., and Gupta, D. (2001). MD-2 enables Toll-like receptor 2 (TLR2)-mediated responses to lipopolysaccharide and enhances TLR2-mediated responses to Gram-positive and Gram-negative bacteria and their cell wall components. *J. Immunol.* 166, 1938–1944. doi: 10.4049/jimmunol.166.3.1938

Farabaugh, K. T., Krokowski, D., Guan, B. J., Gao, Z., Gao, X. H., Wu, J., et al. (2020). PACT-mediated PKR activation acts as a hyperosmotic stress intensity sensor weakening osmoadaptation and enhancing inflammation. *eLife* 9:e52241. doi: 10.7554/eLife.52241

Farsakoglu, Y., Palomino-Segura, M., Latino, I., Zanaga, S., Chatziandreou, N., Pizzagalli, D. U., et al. (2019). Influenza vaccination induces NK-cell-mediated type-II IFN response that regulates humoral immunity in an IL-6-dependent manner. *Cell Rep.* 26, 2307.e5–2315.e5. doi: 10.1016/j.celrep.2019.01.104

Gao, X., Cao, Q., Cheng, Y., Zhao, D., Wang, Z., Yang, H., et al. (2018). Chronic stress promotes colitis by disturbing the gut microbiota and triggering immune system response. *Proc. Natl. Acad. Sci. U.S.A.* 115, E2960–E2969. doi: 10.1073/pnas.1806622115

Gao, X., Li, L., Parisien, M., Wu, J., Bederman, I., Gao, Z., et al. (2020). Discovery of a redox thiol switch: implications for cellular energy metabolism. *Mol. Cell Proteomics* 19, 852–870. doi: 10.1074/mcp.RA119.001910

Gould, J. M., and Matz, P. S. (2010). Otitis media. *Pediatr. Rev.* 31, 102–116.

Guan, B. J., Van Hoef, V., Jobava, R., Elroy-Stein, O., Valasek, L. S., Cargnello, M., et al. (2017). A unique ISR program determines cellular responses to chronic stress. *Mol. Cell.* 68, 885.e6–900.e6. doi: 10.1016/j.molcel.2017.11.007

Han, F., Yu, H., Tian, C., Li, S., Jacobs, M. R., Benedict-Alderfer, C., et al. (2009). Role for Toll-like receptor 2 in the immune response to Streptococcus pneumoniae infection in mouse otitis media. *Infect. Immun.* 77, 3100–3108. doi: 10.1128/IAI.00204-09

Han, F., Yu, H., Zheng, T., Ma, X., Zhao, X., Li, P., et al. (2013). Otoprotective effects of erythropoietin on Cdh23erl/erl mice. *Neuroscience* 237, 1–6. doi: 10.1016/j.neuroscience.2013.01.052

Hang, A., and Brietzke, S. E. (2012). Otitis media: epidemiology and management. *Infect. Disord. Drug Targets* 12, 261–266.

Hasnain, S. Z., Lourie, R., Das, I., Chen, A. C., and Mcguckin, M. A. (2012). The interplay between endoplasmic reticulum stress and inflammation. *Immunol. Cell Biol.* 90, 260–270. doi: 10.1038/icb.2011.112

Huang, Y., Wang, Z., Jin, C., Wang, L., Zhang, X., Xu, W., et al. (2016). TLR2 promotes macrophage recruitment and Streptococcus pneumoniae clearance during mouse otitis media. *Pediatr. Res.* 80, 886–893. doi: 10.1038/pr.2016.154

Kawai, T., and Akira, S. (2010). The role of pattern-recognition receptors in innate immunity: update on Toll-like receptors. *Nat. Immunol.* 11, 373–384. doi: 10.1038/ni.1863

Kielian, T., Esen, N., and Bearden, E. D. (2005). Toll-like receptor 2 (TLR2) is pivotal for recognition of *S. aureus* peptidoglycan but not intact bacteria by microglia. *Glia* 49, 567–576. doi: 10.1002/glia.20144

Komori, M., Nakamura, Y., Ping, J., Feng, L., Toyama, K., Kim, Y., et al. (2011). Pneumococcal peptidoglycan-polysaccharides regulate Toll-like receptor 2 in the mouse middle ear epithelial cells. *Pediatr. Res.* 69, 101–105. doi: 10.1203/PDR.0b013e3182055237

Krysko, D. V., Kaczmarek, A., Krysko, O., Heyndrickx, L., Woznicki, J., Bogaert, P., et al. (2011). TLR-2 and TLR-9 are sensors of apoptosis in a mouse model of doxorubicin-induced acute inflammation. *Cell Death Differ.* 18, 1316–1325. doi: 10.1038/cdd.2011.4

Livak, K. J., and Schmittgen, T. D. (2001). Analysis of relative gene expression data using real-time quantitative PCR and the 2(-Delta Delta C(T)) Method. *Methods* 25, 402–408. doi: 10.1006/meth.2001.1262

Lukens, J. R., Gurung, P., Vogel, P., Johnson, G. R., Carter, R. A., Mcgoldrick, D. J., et al. (2014). Dietary modulation of the microbiome affects autoinflammatory disease. *Nature* 516, 246–249. doi: 10.1038/nature13788

Masters, S. L., Simon, A., Aksentijevich, I., and Kastner, D. L. (2009). Horror autoinflammaticus: the molecular pathophysiology of autoinflammatory disease (*). *Annu. Rev. Immunol.* 27, 621–668. doi: 10.1146/annurev.immunol.25.022106.141627

Menu, P., Mayor, A., Zhou, R., Tardivel, A., Ichijo, H., Mori, K., et al. (2012). ER stress activates the NLRP3 inflammasome via an UPR-independent pathway. *Cell Death Dis.* 3:e261. doi: 10.1038/cddis.2011.132

Mittal, R., Robalino, G., Gerring, R., Chan, B., Yan, D., Grati, M., et al. (2014). Immunity genes and susceptibility to otitis media: a comprehensive review. *J. Genet. Genomics* 41, 567–581. doi: 10.1016/j.jgg.2014.10.003

Nokso-Koivisto, J., Chonmaitree, T., Jennings, K., Matalon, R., Block, S., and Patel, J. A. (2014). Polymorphisms of immunity genes and susceptibility to otitis media in children. *PLoS One* 9:e93930. doi: 10.1371/journal.pone.0093930

Okamura, K., Kimata, Y., Higashio, H., Tsuru, A., and Kohno, K. (2000). Dissociation of Kar2p/BiP from an ER sensory molecule, Ire1p, triggers the unfolded protein response in yeast. *Biochem. Biophys. Res. Commun.* 279, 445–450. doi: 10.1006/bbrc.2000.3987

Qiu, Q., Zheng, Z., Chang, L., Zhao, Y. S., Tan, C., Dandekar, A., et al. (2013). Toll-like receptor-mediated IRE1alpha activation as a therapeutic target for inflammatory arthritis. *EMBO J.* 32, 2477–2490. doi: 10.1038/emboj.2013.183

Schmitz, M. L., Shaban, M. S., Albert, B. V., Gokcen, A., and Kracht, M. (2018). The crosstalk of endoplasmic reticulum (ER) stress pathways with NF-kappaB: complex mechanisms relevant for cancer, inflammation and infection. *Biomedicines* 6:58. doi: 10.3390/biomedicines6020058

Singh, M., Fowlkes, V., Handy, I., Patel, C. V., and Patel, R. C. (2009). Essential role of PACT-mediated PKR activation in tunicamycin-induced apoptosis. *J. Mol. Biol.* 385, 457–468. doi: 10.1016/j.jmb.2008.10.068

van der Poll, T., Keogh, C. V., Guirao, X., Buurman, W. A., Kopf, M., and Lowry, S. F. (1997). Interleukin-6 gene-deficient mice show impaired defense against pneumococcal pneumonia. *J. Infect. Dis.* 176, 439–444. doi: 10.1086/514062

Venekamp, R. P., Sanders, S., Glasziou, P. P., Del Mar, C. B., and Rovers, M. M. (2013). Antibiotics for acute otitis media in children. *Cochrane Database Syst. Rev.* 1:Cd000219.

Volmer, R., van der Ploeg, K., and Ron, D. (2013). Membrane lipid saturation activates endoplasmic reticulum unfolded protein response transducers through their transmembrane domains. *Proc. Natl. Acad. Sci. U.S.A.* 110, 4628–4633. doi: 10.1073/pnas.1217611110

Wang, M., and Kaufman, R. J. (2014). The impact of the endoplasmic reticulum protein-folding environment on cancer development. *Nat. Rev. Cancer* 14, 581–597. doi: 10.1038/nrc3800

Wang, M., and Kaufman, R. J. (2016). Protein misfolding in the endoplasmic reticulum as a conduit to human disease. *Nature* 529, 326–335. doi: 10.1038/nature17041

Wu, B. J., Ong, K. L., Shrestha, S., Chen, K., Tabet, F., Barter, P. J., et al. (2014). Inhibition of arthritis in the Lewis rat by apolipoprotein A-I and reconstituted high-density lipoproteins. *Arterioscler. Thromb. Vasc. Biol.* 34, 543–551. doi: 10.1161/ATVBAHA.113.302832

Yoshimura, A., Lien, E., Ingalls, R. R., Tuomanen, E., Dziarski, R., and Golenbock, D. (1999). Cutting edge: recognition of Gram-positive bacterial cell wall components by the innate immune system occurs via Toll-like receptor 2. *J. Immunol.* 163, 1–5.

Zhang, C., Syed, T. W., Liu, R., and Yu, J. (2017). Role of endoplasmic reticulum stress, autophagy, and inflammation in cardiovascular disease. *Front. Cardiovasc. Med.* 4:29. doi: 10.3389/fcvm.2017.00029

Zhang, K., and Kaufman, R. J. (2008). From endoplasmic-reticulum stress to the inflammatory response. *Nature* 454, 455–462. doi: 10.1038/nature07203

Zhang, K., Shen, X., Wu, J., Sakaki, K., Saunders, T., Rutkowski, D. T., et al. (2006). Endoplasmic reticulum stress activates cleavage of CREBH to induce a systemic inflammatory response. *Cell* 124, 587–599. doi: 10.1016/j.cell.2005.11.040

Zhang, X., Zheng, T., Sang, L., Apisa, L., Zhao, H., Fu, F., et al. (2015). Otitis media induced by peptidoglycan-polysaccharide (PGPS) in TLR2-deficient (Tlr2(-/-)) mice for developing drug therapy. *Infect. Genet. Evol.* 35, 194–203. doi: 10.1016/j.meegid.2015.08.019

Zheng, Q. Y., Tong, Y. C., Alagramam, K. N., and Yu, H. (2007). Tympanometry assessment of 61 inbred strains of mice. *Hear. Res.* 231, 23–31. doi: 10.1016/j.heares.2007.05.011

Conflict of Interest: The authors declare that the research was conducted in the absence of any commercial or financial relationships that could be construed as a potential conflict of interest.

frontiers in Genetics

ORIGINAL RESEARCH
published: 09 August 2021
doi: 10.3389/fgene.2021.508750

Hearing Loss in Id1$^{-/-}$; Id3$^{+/-}$ and Id1$^{+/-}$; Id3$^{-/-}$ Mice Is Associated With a High Incidence of Middle Ear Infection (Otitis Media)

*Qingyin Zheng[1,2], Tihua Zheng[1,3], Aizhen Zhang[2], Bin Yan[3], Bo Li[3], Zhaoqiang Zhang[2] and Yan Zhang[1]**

[1]Department of Otolaryngology – Head and Neck Surgery, Second Affiliated Hospital of Xi'an Jiaotong University School of Medicine, Xi'an, China, [2]School of Medicine, Case Western Reserve University, Cleveland, OH, United States, [3]College of Special Education, Hearing and Speech Rehabilitation Institute, Binzhou Medical University, Yantai, China

OPEN ACCESS

Edited by:
Regie Santos-Cortez,
University of Colorado, United States

Reviewed by:
Olivia J. Veatch,
University of Kansas Medical Center, United States
Arwa Kurabi,
University of California, San Diego, United States
Norma De Oliveira Penido,
Federal University of São Paulo, Brazil

***Correspondence:**
Yan Zhang
zhangyanlian@sina.com

Specialty section:
This article was submitted to Genetics of Common and Rare Diseases, a section of the journal Frontiers in Genetics

Received: 31 October 2019
Accepted: 06 July 2021
Published: 09 August 2021

Citation:
Zheng Q, Zheng T, Zhang A, Li B, Zhang Z and Zhang Y (2021) Hearing Loss in Id1$^{-/-}$; Id3$^{+/-}$ and Id1$^{+/-}$; Id3$^{-/-}$ Mice Is Associated With a High Incidence of Middle Ear Infection (Otitis Media). Front. Genet. 12:508750. doi: 10.3389/fgene.2021.508750

Inhibitors of differentiation/DNA binding (Id) proteins are crucial for inner ear development, but whether Id mutations affect middle ear function remains unknown. In this study, we obtained Id1$^{-/-}$; Id3$^{+/-}$ mice and Id1$^{+/-}$; Id3$^{-/-}$ mice and carefully examined their middle ear morphology and auditory function. Our study revealed a high incidence (>50%) of middle ear infection in the compound mutant mice. These mutant mice demonstrated hearing impairment starting around 30 days of age, as the mutant mice presented elevated auditory brainstem response (ABR) thresholds compared to those of the littermate controls. The distortion product of otoacoustic emission (DPOAE) was also used to evaluate the conductive function of the middle ear, and we found much lower DPOAE amplitudes in the mutant mice, suggesting sound transduction in the mutant middle ear is compromised. This is the first study of the middle ears of Id compound mutant mice, and high incidence of middle ear infection determined by otoscopy and histological analysis of middle ear suggests that Id1/Id3 compound mutant mice are a novel model for human otitis media (OM).

Keywords: otitis media, mouse model, hearing loss, inflammation, genetic predisposition

INTRODUCTION

Inhibitors of differentiation/DNA binding (Id) proteins are major inhibitors of helix–loop–helix (HLH) transcription factors. The Id genes encode four related transcription factors: Id1, Id2, Id3, and Id4. Id transcription factors contain a helix-loop-helix region similar to that of the basic helix–loop–helix (bHLH) transcription factors, can form heterodimers with some of them and lose their binding to DNA. However, due to the lack of basic DNA-binding regions, these heterodimers cannot bind to DNA. Consequently, Id transcription factors negatively regulate the DNA binding capacity of bHLH proteins (Benezra et al., 1990; Wong et al., 2004). In other words, Id transcription factors usually hinder cell differentiation, especially the differentiation of dendritic cells, which plays a rather important role in immunity to infectious agents (Spits et al., 2000; Kee, 2009).

Inhibitors of differentiation/DNA binding proteins regulate different kinds of cellular processes, including cellular growth, differentiation, migration, senescence, and tumorigenesis (Sikder et al., 2003; Wong et al., 2004; Wu et al., 2018). Id1, Id2, and Id3 are expressed in the otic vesicle of mouse embryos (Jen et al., 1997). The importance of these three Id genes as differentiation regulators was also illustrated by their key role in the regulation of expression of Math1 and hair cell differentiation in the developing cochlea (Jones et al., 2006). Ids expression profiles in the normal mature middle ear has not been reported. However, a previous study by Lin et al. (2002) showed that Id1 and Id3 are unregulated in the middle ears of rats following pneumococcal infection, which indicates that Id1 and Id3 may be involved in middle ear diseases such as otitis media (OM). The main objective of this study was to clarify the correlation between the two Id genes with OM.

The most common middle ear problems include cholesteatoma, tympanic membrane (TM) perforation, middle ear infection, and otosclerosis. Among these diseases, middle ear infection, or OM, is the most common, as most children younger than 3 years will have at least one episode of OM (McCaig et al., 2002; O'Brien et al., 2009). Acute OM is the most common cause of meningitis, whereas neglected chronic OM can lead to permanent hearing loss (Pont and Mazon, 2017). Previous studies have shown that genetic lesions lead to a high incidence of OM in mutant animals such as Jeff mice, Sh3pxd2b mice, and Enpp1asj mice (Hardisty-Hughes et al., 2006; Yang et al., 2011; Tian et al., 2016). Animal models with OM susceptible to a defined genetic lesion will be important to reveal the pathogenesis and underlying genetic pathways linked to OM.

Individual null mutants for Id1, Id2, and Id3 have been generated and reported to have very few abnormalities, and none associated with hearing deficit (Yan et al., 1997; Lyden et al., 1999; Yokota et al., 1999). Id1 and Id3 double-knockout mice are commonly used as animal models to study the role of Id1 and Id3 in mammalian development (Zhao et al., 2011). Unfortunately, complete loss of these genes leads to aggregation of dilated and irregularly shaped blood vessels and brain hemorrhage by E12.5, and no embryos survived beyond E13.5 (Lyden et al., 1999; Fraidenraich et al., 2004). Because of the upregulated expression of Id1 and Id3 in middle ears after the acute episode of pneumococcal otitis media has been resolved, the two genes are presumed to be involved in the development of otitis media (Lin et al., 2002). In this study, the auditory brainstem response (ABR) and middle ear morphology in $Id1^{-/-}$; $Id3^{+/-}$ and $Id1^{+/-}$; $Id3^{-/-}$ mice were carefully examined. OM and associated elevated hearing thresholds were found in the majority of the mutant mice. Our data suggest that Id1/Id3 mice are valuable models for the study of OM pathogenesis and associated genetic factors.

MATERIALS AND METHODS

Mice and Animal Care

Our Id1 and Id3 single-knockout mice were generous gifts from Dr. Robert Benezra. $Id1^{-/-}$; $Id3^{+/-}$ or $Id1^{+/-}$; $Id3^{-/-}$ mice were generated by intercrossing double heterozygous mice. Littermate mice with $Id1^{+/-}$; $Id3^{+/-}$, $Id1^{+/+}$; $Id3^{+/-}$, $Id1^{+/-}$; $Id3^{+/+}$ or $Id1^{+/+}$; $Id3^{+/+}$ genotypes were generated incidentally during breeding. We used littermate mice with $Id1^{+/+}$; $Id3^{+/+}$ genotype as wild-type controls. Mice of the other three genotypes were excluded because they did not show significant hearing loss (data not shown). No gender difference was found during the experiment. Both male and female mice from the same litter were included as the experimental and control groups. A total of 101, $Id1^{-/-}$; $Id3^{+/-}$ mice, 28 $Id1^{+/-}$; $Id3^{-/-}$ mice and 30 wild-type mice were used in this study. ABR test was performed at four time points: P30 (P: postnatal, same meaning as below), P60, P90, and P120. After ABR test, distortion product of otoacoustic emission (DPOAE) measurement was performed at two time points: P30 and P60. After ABR and DPOAE test at P30, otoscopic examination was carried out and then some of the mice were euthanized to conduct Hematoxylin-Eosin (H&E) staining. Only the data of the right ear were counted in the analysis of the experimental results. Specific details on the use of mice can be found in the **Supplementary Figure 1**. The experimental protocols were approved by the Case Western Reserve University Animal Care and Use Committee and were in agreement with the National Institutes of Health Guide for the Care and Use of Laboratory Animals. Studies were conducted according to the principles set forth in the Guide for the Care and Use of Laboratory Animals (DC005846) as well as the Institute of Laboratory Animal Resources (protocol 2014-0155).

Mice Genotyping

Genomic DNA was obtained from mouse tail tips. PCR analyses were performed with primers specific for the wild-type and targeted alleles. Primer sequences for Id1 were ID1F1 (wild-type oligonucleotide; 5'-TCCTGCAGCATGTAATCGAC-3'), ID1F2 (mutant oligonucleotide; 5'-GACACCCACTGGAAAGGACA-3'), and ID1R1 (common oligonucleotide; 5'-GAGACCCACTGGAAAGGACA-3'). Primers sequences for Id3 were ID3F1 (wild-type oligonucleotide; 5'-CTTGGGACCCTGGGACTCT-3'), ID3F2 (mutant oligonucleotide; 5'-GGGGAACTTCCTGACTAGGG-3'), and ID3R1 (common oligonucleotide; 5'-TAATCAGGGCAGCAGAGCTT-3'). The amplified PCR products were analyzed on 2% agarose gels to separate the wild-type (344 bp for ID1 and 350 bp for ID3) and targeted allele (540 bp for ID1 and 500 bp for ID3) fragments.

Auditory Brainstem Response, Distortion Product Otoacoustic Emission Tests, and Otoscopic Examination

Auditory brainstem response threshold analyses were carried out using equipment from Intelligent Hearing Systems (Miami, FL, United States) as previously described (Zheng et al., 1999). Prior to examination, mice were anesthetized with 2, 2 and 2-tribromoethanol (Avertin; 0.5 mg/g body mass), and their body temperature was kept at 37–38°C by placing them on a heating pad in a soundproof chamber during testing. Specific auditory stimuli (broadband click and pure-tone burst stimuli of 8, 16, and 32 kHz) from ER2 and high-frequency transducers were delivered through plastic tubes to the ear canals. Evoked brainstem responses were amplified and averaged, and their wave patterns were displayed on a computer screen. Auditory

thresholds were obtained for each stimulus by varying the SPL in 10 dB steps and, finally, a 5 dB step up and down to identify the lowest level at which an ABR pattern could be recognized.

The DPOAE test was performed using SmartOAE 4.50 USBez software (Intelligent Hearing Systems) and an Etymotic 10B+ OAE probe (Etymotic Research, Elk Grove Village, IL) fitted with a high-frequency transducer (Intelligent Hearing Systems) that produced two pure tones, F1 and F2, respectively. The methods and process followed those described in a previous paper (Zhang et al., 2012).

After the ABR and DPOAE tests, otoscopy was performed on both ears to determine the condition of TM, including presence of middle ear fluid, inflammation, or infection.

Histological Analysis of Middle Ear

Ten Id1/Id3 heterozygous ($Id1^{-/-}$; $Id3^{+/-}$ and $Id1^{+/-}$; $Id3^{-/-}$) and 10 wild-type mice (129Sv/C57BL6) aged 30 days of age were euthanized and decapitated. Both bullae, including the middle and inner ear (IE), were rapidly removed. The bullae were then fixed in 4% PFA, decalcified with 10% EDTA solution, dehydrated and embedded in paraffin. The paraffin block was serially sectioned at 5-μm thicknesses and stained with H&E for light microscopic examination.

Statistical Analysis

The data are presented as mean ± SEM. The difference between groups was determined using a one-way or two-way ANOVA or unpaired student *t*-test when applicable using GraphPad Prism software.

RESULTS

ABR Thresholds and DPOAE in the $Id1^{-/-}$; $Id3^{+/-}$ and $Id1^{+/-}$; $Id3^{-/-}$ Mice Indicated Hearing Loss in a Majority of Mice

Auditory brainstem response tests were carried out and analyzed with equipment from Intelligent Hearing Systems using previously described methods and equipment (Zheng et al., 1999). Mice with ABR threshold values above 55 (for click stimuli), 40 (for 8 kHz), 35 (for 16 kHz), or 60 (for 32 kHz) dB SPL were considered hearing impaired (Zheng et al., 1999). Of the 101 $Id1^{-/-}$; $Id3^{+/-}$ mice observed, 89.1% (90/101) had high ABR thresholds for at least one stimulus frequency (click, 8, 16, and 32 kHz) in at least one ear, with 82.2% (83/101) for the right ears and 81.2% (82/101) for the left ears. Of the 28 $Id1^{+/-}$; $Id3^{-/-}$ mice observed, 100% (28/28) had high ABR thresholds for at least one stimulus frequency (click, 8, 16, and 32 kHz) in at least one ear, with 92.9% (26/28) for the right ears and 92.9% (26/28) for the left ears.

A comparison of ABR thresholds in the right ears was made between wild-type, $Id1^{-/-}$; $Id3^{+/-}$ and $Id1^{+/-}$; $Id3^{-/-}$ mice at P30 and P60, respectively. The results indicated that, at P30, the mean ABR thresholds at any stimulus frequency in the $Id1^{-/-}$; $Id3^{+/-}$ (n = 41) and $Id1^{+/-}$; $Id3^{-/-}$ (n = 14) mice were significantly higher than those of the controls (n = 21; click ABR threshold: Wild-type vs. $Id1^{-/-}$; $Id3^{+/-}$, $p < 0.0001$; Wild-type vs. $Id1^{+/-}$; $Id3^{-/-}$, $p < 0.0001$; 8 kHz ABR threshold: Wild-type vs. $Id1^{-/-}$; $Id3^{+/-}$, $p < 0.0001$; Wild-type vs. $Id1^{+/-}$; $Id3^{-/-}$, $p < 0.0001$; 16 kHz ABR threshold: Wild-type vs. $Id1^{-/-}$; $Id3^{+/-}$, $p = 0.0060$; Wild-type vs. $Id1^{+/-}$; $Id3^{-/-}$, $p = 0.0057$; 32 kHz ABR threshold: Wild-type vs. $Id1^{-/-}$; $Id3^{+/-}$, $p < 0.0001$; Wild-type vs. $Id1^{+/-}$; $Id3^{-/-}$, $p = 0.0183$; **Figure 1**). At P60, ABR thresholds at all stimulus frequencies in the $Id1^{+/-}$; $Id3^{-/-}$ (n = 14) mice were significantly higher than those of the wild-type controls (n = 21; click ABR threshold: Wild-type vs. $Id1^{+/-}$; $Id3^{-/-}$, $p = 0.0010$; 8 kHz ABR threshold: Wild-type vs. $Id1^{+/-}$; $Id3^{-/-}$, $p = 0.0001$; 16 kHz ABR threshold: Wild-type vs. $Id1^{+/-}$; $Id3^{-/-}$, $p = 0.0058$; 32 kHz ABR threshold: Wild-type vs. $Id1^{+/-}$; $Id3^{-/-}$, $p = 0.0119$), and ABR thresholds for click and 8 k Hz in $Id1^{-/-}$; $Id3^{+/-}$ mice (n = 35) were significantly higher than those of the wild-type controls (n = 21; click ABR threshold: Wild-type vs. $Id1^{-/-}$; $Id3^{+/-}$, $p = 0.0386$; 8 kHz ABR threshold: Wild-type vs. $Id1^{+/-}$; $Id3^{-/-}$, $p = 0.0451$; **Figure 1**).

A time-course observation of the ABR thresholds in the right ears of Id1/Id3 compound mutant mice and wild-type

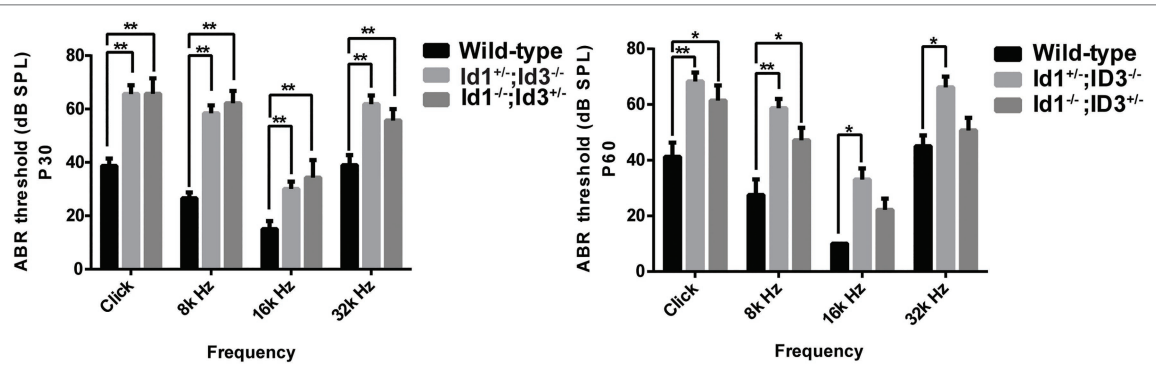

FIGURE 1 | Comparison of the mean auditory brainstem response (ABR) thresholds of right ears from age-matched littermate control mice, $Id1^{-/-}$; $Id3^{+/-}$ and $Id1^{+/-}$; $Id3^{-/-}$ mice at ages P30 and P60. The results indicated that at P30, the mean ABR thresholds at any stimulus frequencies in the $Id1^{-/-}$; $Id3^{+/-}$ (n = 41) and $Id1^{+/-}$; $Id3^{-/-}$ (n = 14) mice were significantly higher than those of the controls (n = 21; $p < 0.01$). At P60, ABR thresholds at all stimulus frequencies in the $Id1^{-/-}$; $Id3^{+/-}$ mice (n = 35) were significantly higher than those of the controls (n = 8; $p < 0.01$), and ABR thresholds at Click and 8 k Hz in the $Id1^{+/-}$; $Id3^{-/-}$ mice (n = 14) were significantly higher than those of the controls ($p < 0.05$). The error bar indicates SD from the mean of each group. *$p < 0.05$; **$p < 0.01$.

mice is shown in **Figure 2**. We divided the mice in each group into four subgroups by approximately 1-month increments in age. The results showed that the mean ABR thresholds of Id1$^{-/-}$; Id3$^{+/-}$ mice (n = 41, 35, 31, and 17 in each subgroup, respectively) and Id1$^{+/-}$; Id3$^{-/-}$ mice (n = 14, 14, 7, and 6, respectively) were elevated at various time points at all stimulus frequencies. According to the criteria (stated above) for defining hearing loss in mice, Id1/Id3 compound mutant mice present as hearing loss since 30 days at all stimulus frequencies (**Figure 2**).

The DPOAE amplitudes were generated from cochlear and recorded in the external auditory canal. DPOAE amplitudes can be influenced by the condition of middle ear. We analyzed the DPOAE amplitudes of right ears from age-matched wild-type mice, Id1$^{-/-}$; Id3$^{+/-}$ and Id1$^{+/-}$; Id3$^{-/-}$ mice at ages of P30 and P60. The results demonstrated that at P30, the DPOAE amplitudes of Id1$^{-/-}$; Id3$^{+/-}$ (n = 12) and Id1$^{+/-}$; Id3$^{-/-}$ mice (n = 9) at dominant frequencies 7,692, 10,152, 13,390, and 17,672 were significantly lower than those of wild-type mice (n = 13; DPOAE amplitude at 7,692: Wild-type vs. Id1$^{-/-}$; Id3$^{+/-}$, $p < 0.0001$; Wild-type vs. Id1$^{+/-}$; Id3$^{-/-}$, $p < 0.0001$; DPOAE amplitude at 10,152: Wild-type vs. Id1$^{-/-}$; Id3$^{+/-}$, $p < 0.0001$; Wild-type vs. Id1$^{+/-}$; Id3$^{-/-}$, $p < 0.0001$; DPOAE amplitude at 13,390: Wild-type vs. Id1$^{-/-}$; Id3$^{+/-}$, $p < 0.0001$; Wild-type vs. Id1$^{+/-}$; Id3$^{-/-}$, $p < 0.0001$; DPOAE amplitude at 17,672: Wild-type vs. Id1$^{-/-}$; Id3$^{+/-}$, $p < 0.0001$; Wild-type vs. Id1$^{+/-}$; Id3$^{-/-}$, $p < 0.0001$). At P60, the DPOAE amplitudes of Id1$^{-/-}$; Id3$^{+/-}$ mice (n = 12) at frequencies 13,390, 17,672 were significantly lower than those of wild-type mice (n = 3; DPOAE amplitude at 13,390: Wild-type vs. Id1$^{-/-}$; Id3$^{+/-}$, $p = 0.0344$; DPOAE amplitude at 17,672: Wild-type vs. Id1$^{-/-}$; Id3$^{+/-}$, $p = 0.0009$); DPOAE amplitudes of Id1$^{+/-}$; Id3$^{-/-}$ mice (n = 6) at dominant frequencies 7,692, 10,152, 13,390, and 17,672 were significantly lower than those of wild-type mice (DPOAE amplitude at 7,692: Wild-type vs. Id1$^{+/-}$; Id3$^{-/-}$, $p = 0.0137$; DPOAE amplitude at 10,152: Wild-type vs. Id1$^{+/-}$; Id3$^{-/-}$, $p = 0.0112$; DPOAE amplitude at 13,390: Wild-type vs. Id1$^{+/-}$; Id3$^{-/-}$, $p = 0.0057$; DPOAE amplitude at 17,672: Wild-type vs. Id1$^{+/-}$; Id3$^{-/-}$, $p < 0.0001$; **Figure 3**).

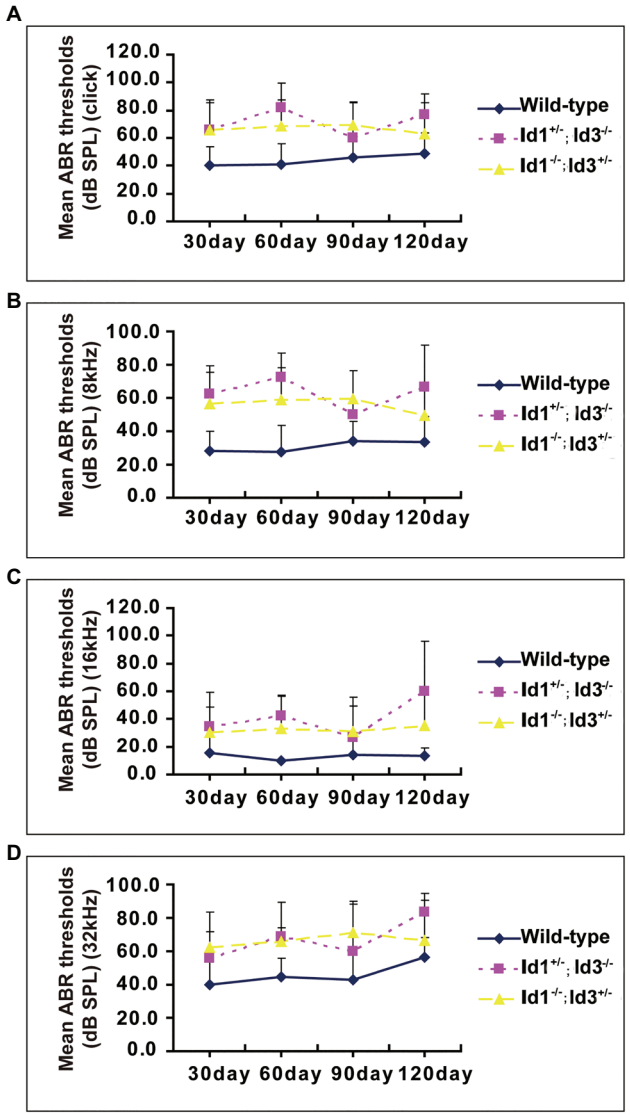

FIGURE 2 | A time-course observation of the ABR thresholds in the right ears of Id1$^{-/-}$; Id3$^{+/-}$ and Id1$^{+/-}$; Id3$^{-/-}$ mice and littermate control mice. All mice of ages from P30 to P120 and the individual ABR thresholds at all stimulus frequencies of click **(A)**, 8 **(B)**, 16 **(C)**, and 32 kHz **(D)** were variable, but the overall tendency was relatively stable at each stimulus frequency compared with the ABR thresholds of the control mice. The error bars indicate SD from the mean at each time point for each mouse group.

Otitis Media in Id1$^{-/-}$; Id3$^{+/-}$ and Id1$^{+/-}$; Id3$^{-/-}$ Mice

A total of 41 Id1$^{-/-}$; Id3$^{+/-}$ mice, 14 Id1$^{+/-}$; Id3$^{-/-}$ mice and 21 wild-type mice, aged 30 days, were randomly chosen to be screened for otitis media. Otoscopic examination of the Id1$^{-/-}$; Id3$^{+/-}$ mice and Id1$^{+/-}$; Id3$^{-/-}$ mice revealed that 51 and 71% were affected with middle ear fluid, inflammation in the TM and opacification of the TM, respectively. **Figure 4** shows representative anatomical images under otoscopy of the ears in Id1$^{-/-}$; Id3$^{+/-}$ and Id1$^{+/-}$; Id3$^{-/-}$ mice. To reveal the middle ear histopathology of Id1$^{-/-}$; Id3$^{+/-}$ and Id1$^{+/-}$; Id3$^{-/-}$ mice, the morphology of the middle ears was analyzed using H&E staining. Histological examination showed obvious inflammatory infiltrates in the tympanic cavity of Id1$^{-/-}$; Id3$^{+/-}$ and Id1$^{+/-}$; Id3$^{-/-}$ mice. Different degrees of effusion appeared in the middle ear cavities of the mutant mice and representative image of Id1$^{+/-}$; Id3$^{-/-}$ mice was shown (**Figure 5**). A high-magnification view of the tissue showed that inflammatory cells of the effusion content were mainly composed of polymorphonuclear cells. Fibrous proliferation also appeared in the middle ear space in some mice. The middle ear mucosa of Id1$^{-/-}$; Id3$^{+/-}$ and Id1$^{+/-}$; Id3$^{-/-}$ mice generally thickened. The middle ear mucosa of Id1$^{+/-}$; Id3$^{-/-}$ mice was significantly thicker than the wild-type mice ($p = 0.0101$).

DISCUSSION

In this investigation, we found that middle ear function is affected in Id1 and Id3 mutant mice due to OM, which leads

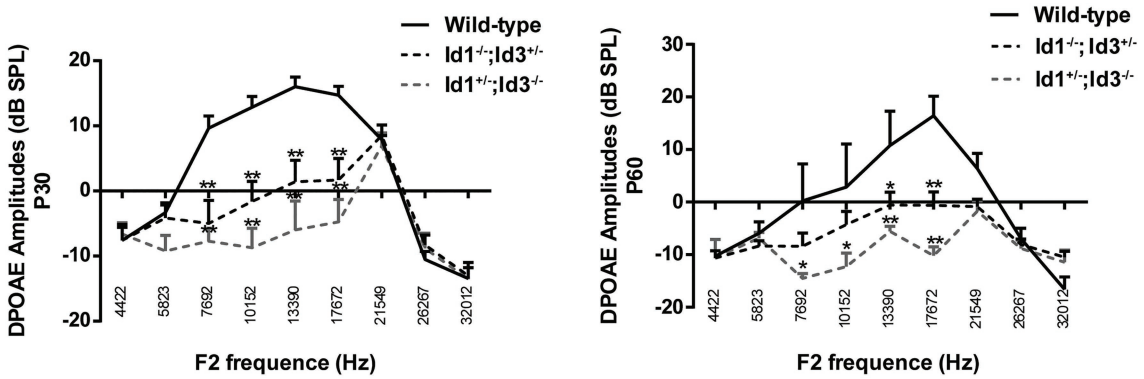

FIGURE 3 | Comparison of the distortion product of otoacoustic emission (DPOAE) amplitudes of right ears from age-matched littermate control mice, $Id1^{-/-}$; $Id3^{+/-}$ and $Id1^{+/-}$; $Id3^{-/-}$ mice at ages P30 and P60. The results indicated that at P30, the DPOAE amplitudes of $Id1^{-/-}$; $Id3^{+/-}$ (n = 12) and $Id1^{+/-}$; $Id3^{-/-}$ mice (n = 9) were significantly lower than those of the control mice (n = 13) at dominant frequencies. At P60, the DPOAE amplitudes at dominant frequencies in the $Id1^{-/-}$; $Id3^{+/-}$ mice (n = 35) were significantly lower than those of the controls (n = 8), and the DPOAE amplitudes at two frequencies in $Id1^{+/-}$; $Id3^{-/-}$ mice were significantly lower than those of the controls (n = 14). The error bar indicates SD from the mean or each group. *$p < 0.05$; **$p < 0.01$.

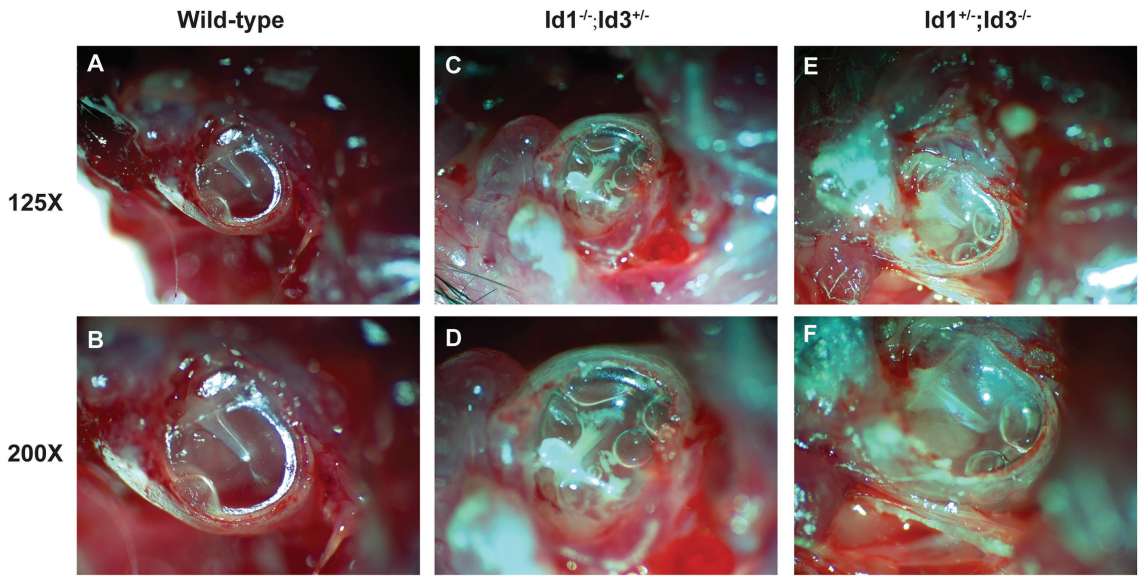

FIGURE 4 | Otoscopic examination of the middle ear in $Id1^{-/-}$; $Id3^{+/-}$ and $Id1^{+/-}$; $Id3^{-/-}$ mice. Compared with the middle ear cavities (MECs) of littermate control mice **(A,B)**, the MECs of $Id1^{-/-}$; $Id3^{+/-}$ mice **(C,D)** and $Id1^{+/-}$; $Id3^{-/-}$ mice **(E,F)** were filled with effusions, and white patches were observed on the tympanic membrane (TM).

to conductive hearing loss in the affected mice. Because Id1/Id3 double-mutant embryos die at approximately E12 (Lyden et al., 1999), and Id1 and Id3 single-knockout mice have normal hearing (Yan et al., 1997; Lyden et al., 1999; Yokota et al., 1999; data not shown), Id1/Id3 heterozygous ($Id1^{-/-}$; $Id3^{+/-}$ and $Id1^{+/-}$; $Id3^{-/-}$) mice were used to study the combined effect of missing Id1/Id3 alleles.

Auditory brainstem response has been used extensively to assess mouse IE function and also offers a valid, simple physiologic test of mouse middle ear inflammation (MacArthur et al., 2006). Overall, most observed $Id1^{+/-}$; $Id3^{-/-}$ and $Id1^{-/-}$; $Id3^{+/-}$ mice had high ABR thresholds in at least one of the stimulus frequencies (click, 8, 16, and 32 kHz) in at least one ear. At P30, both $Id1^{+/-}$; $Id3^{-/-}$ and $Id1^{-/-}$; $Id3^{+/-}$ mice showed elevated ABR thresholds compared to age-matched littermate controls. However, at P60, ABR thresholds for $Id1^{-/-}$; $Id3^{+/-}$ mice at 16 and 32 kHz no longer showed significant differences compared to the controls. Moreover, at P60, the ABR thresholds of $Id1^{-/-}$; $Id3^{+/-}$ mice were lower than those of the $Id1^{+/-}$; $Id3^{-/-}$ mice for all four frequencies tested. Studies have shown that Id1/Id3 genes have redundant functions, and the loss of one gene function is compensated by another (Lowery et al., 2010). However, based on the ABR data, we can speculate that Id3 might play a slightly

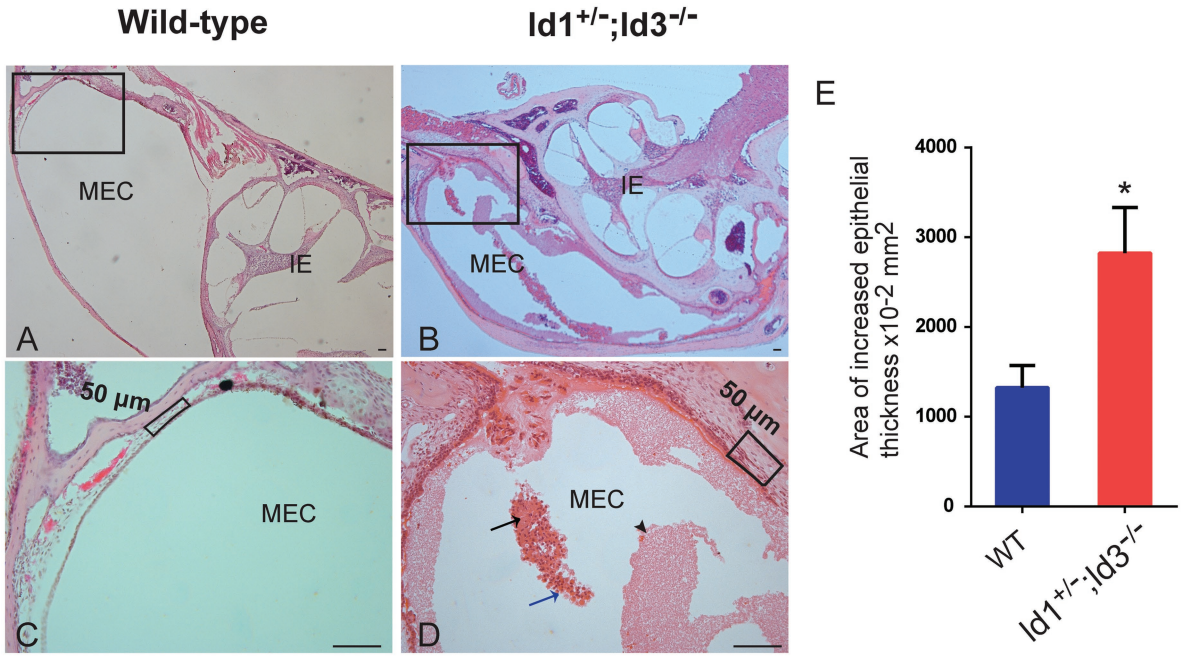

FIGURE 5 | Hematoxylin-Eosin (H&E) staining of histopathology of wild-type and Id1$^{+/-}$; Id3$^{-/-}$ mice. **(A-D)** Representative histology showed obvious inflammatory infiltrations in the MEC of Id1$^{+/-}$; Id3$^{-/-}$ mice **(B,D)** compared to the wild-type mice **(A,C)**. Scale bars: 50 μm. **(A)** The MEC and inner ear (IE) were absent of inflammations. **(C)** The boxed region of **(A)**. **(B)** Panoramic view of the histology showed various inflammations in the MEC. **(D)** At higher magnification, the boxed region in **(B)** revealed detailed view of the cell infiltrations. Exudates of fibrin and blood plasma were evident (black arrowhead). Masses of erythrocytes (black arrow) together with neutrophils (blue arrow) were also detectable in the MEC. **(E)** Comparison of the area of epithelial thickness in MEC between Wild-type mice and Id1$^{+/-}$; Id3$^{-/-}$ mice (n = 3 mice in each group). *$p < 0.05$.

greater role in middle ear function. A longitudinal tracking in our study indicated that Id1/Id3 mutant mice from P30 to P120 showed no progression of hearing loss; one explanation is that 4-month-old mice are still relatively young, and the deterioration of hearing loss in mutant mice might show up if we test the mutant mice for extended period, such as until 12 months.

Distortion product of otoacoustic emission is commonly used to evaluate outer hair cell integrity in humans and research animals. Several groups have established this method as another way to evaluate the middle ear conductance and as an indirect measure of conductive hearing loss caused by middle ear dysfunction. This is primarily due to the presence of middle ear effusion, which prevents sound transduction to the inner ear for further processing. Besides, due to lesions in the middle ear, the DPOAE energy cannot be released through the middle ear and detected in the external ear canal. We showed that Id1$^{+/-}$; Id3$^{-/-}$ and Id1$^{-/-}$; Id3$^{+/-}$ mice have much lower DP values compared to littermate controls. If this is not due to outer hair cell dysfunction, then middle ear conductance is very likely to be affected in the mutant mice.

To identify the histopathology of the Id mutant mice that leads to conductive hearing loss, we first examined the gross morphology of the TM. Transparent and balanced TM is observed in the control mice. However, in the mutant mice, bubbles are the most common observation through the TM, which is an indication of middle ear effusion. TM retraction, another common observation, is caused by negative pressure in the middle ear cavity (MEC). In some cases, we observed white patches on the TM, which is usually due to soft tissue calcification, which eventually lead to increased stiffness of the TM and decreased membrane conductance. No TM perforation or missing ossicle bone, particularly the malleus, was observed in the mutant mice. These discoveries exclude the possibility of conductive hearing loss originating from abnormal outer ear canals and TMs.

Next, HE stained inner ear and middle ear cross sections were prepared for more detailed evaluation of the middle ear and inner ear morphology. The mutant mice's inner ears did not show any abnormalities. For example, there was no hair cell, spiral ganglion neuron loss or dislocation of Reissner's membrane and no stria vascularis defect. However, different degrees of effusion were present in the middle ear cavities of the mutant mice, which is in consistent with the observation through the TM. Inflammatory cells were also present in the MEC for an extended period, primarily polymorphonuclear cells. This is a major feature of chronic middle ear inflammation. Middle ear epithelia generally thickened in most of the mutant mice, another typical feature of middle ear inflammation. Combining ABR threshold data and histological examination, we found that OM and pathology correlated well with ABR threshold data from the Id1$^{+/-}$; Id3$^{-/-}$ and Id1$^{-/-}$; /Id3$^{+/-}$ and wild-type mice. These data together suggest that Id1/Id3

mutations cause middle ear inflammation, which leads to excess effusion, mucosal thickening and the presence of inflammatory cells in the MEC and the inflammation in middle ear causes conductive hearing loss in Id1/Id3 mutant mice.

Id1 and Id3 are two members of a family of four Id proteins (designated Id1 through Id4) that act as dominant negative inhibitors of bHLH transcription factors (Benezra et al., 1990; Christy et al., 1991; Sun et al., 1991; Riechmann et al., 1994). Id1 and Id3 gene in humans are located on chromosomes 20qll (Idl), lp36.1 (Id3), and they share a very similar genomic organization of exon-intron boundaries within their coding regions (Norton et al., 1998). They are co-expressed temporally and spatially during murine neurogenesis and angiogenesis (Lyden et al., 1999). Id genes are expressed in the otic vesicle's prosensory domains and are involved in hair cell development through an unknown mechanism (Jones et al., 2006; Kamaid et al., 2010). In the larger picture, Id proteins are crucial for the proper development and function of the immune system (Pan et al., 1999; Miyazaki et al., 2014).

The function of Id proteins associated with the immune system has been well documented in several studies (Miyazaki et al., 2014; Zook and Li, 2018; Han et al., 2019). Lack of Id3 leads to impaired B-cell proliferation and immune responses (Pan et al., 1999). A recent study showed that Id1 favors the differentiation of myeloid-derived suppressor cells (MDSCs), but not dendritic cells (Papaspyridonos et al., 2015). MDSCs are a heterogeneous group of immune cells from the myeloid lineage that suppress immunity against infectious agents. These studies point the possible etiology of OM in Id1/Id3 mutant mice to impaired immune responses. It has been well recognized that a compromised immune system is one of the major contributing factors to OM. We speculate that Id1/Id3 mutations lead to an impaired immune system, which compromises the ability of the mutant mice to fight against middle ear inflammation, leading to continuous presence of effusion, epithelia hyperplasia and inflammatory cells.

Vascular endothelial growth factor (VEGF) is one of the most potent angiogenic factors under inflammatory conditions in the middle ear (Juhn et al., 2008). A previous study used clinical specimens of cholesteatoma in the middle ear to identify a transcription factor that regulate the growth of cholesteatoma. They found Id1 is an essential regulator of VEGF in the cholesteatomal matrix and perimatrix (Fukudome et al., 2013). Some studies have demonstrated that TGF-β, VEGF, or hypoxia-inducible factor (HIF) signaling plays a critical role in the pathogenesis of chronic otitis media in animal models (Tateossian et al., 2009, 2013; Cheeseman et al., 2011; Husseman et al., 2012). As the important differentiation regulators, Id proteins regulate different kinds of cellular processes. More studies need to be done to clarify the underlying mechanism of otitis media in Id1/Id3 mutant mice.

In conclusion, we have shown that the $Id1^{+/-}$; $Id3^{-/-}$ and $Id1^{-/-}$; $/Id3^{+/-}$ mice provide excellent models for studying OM. This model's susceptibility to OM may be related to the mice's weakened immune response toward infectious agents. Moreover, the individual variability observed in the $Id1^{+/-}$; $Id3^{-/-}$ and $Id1^{-/-}$; $/Id3^{+/-}$ mouse population may provide a valuable control in future explorations of this model. As such, with this mouse model, we can further elucidate causal relationships between the multiple features of OM and provide an optimal approach to minimizing hearing loss in affected individuals.

DATA AVAILABILITY STATEMENT

The datasets generated for this study are available on request to the corresponding author.

ETHICS STATEMENT

The experimental protocols were approved by the Case Western Reserve University Animal Care and Use Committee and were in agreement with the National Institutes of Health Guide for the Care and Use of Laboratory Animals.

AUTHOR CONTRIBUTIONS

YZ and QZ contributed to the study concept and design. AZ and BL organized the database. TZ performed the statistical analysis and wrote the first draft of the manuscript. BY participated in manuscript revision. All authors contribed to the article and approved the submitted version.

FUNDING

This work was supported by the National Institutes of Health (R01DC015111 and R21DC005846), the National Natural Science Foundation of China (81530030, 81873697, 81500797, and 81700902), and the Taishan Scholars Foundation.

ACKNOWLEDGMENTS

We thank Robert Benezra for providing the mouse models.

SUPPLEMENTARY MATERIAL

The Supplementary Material for this article can be found online at: https://www.frontiersin.org/articles/10.3389/fgene.2021.508750/full#supplementary-material

Supplementary Figure 1 | Sample flow chart of the experiments. A total of 101, $Id1^{-/-}$; $Id3^{+/-}$ mice, 28 $Id1^{+/-}$; $Id3^{-/-}$ mice and 30 wild-type mice were used in this study. ABR test was performed at four time points: P30, P60, P90, and P120. After ABR test, DPOAE measurement was performed at two time points: P30 and P60. After ABR and DPOAE test at P30, otoscopic examination was carried out and then some of the mice were euthanized to conduct H&E staining. *, six mice was from P60.

REFERENCES

Benezra, R., Davis, R. L., Lockshon, D., Turner, D. L., and Weintraub, H. (1990). The protein Id: a negative regulator of helix-loop-helix DNA binding proteins. *Cell* 61, 49–59. doi: 10.1016/0092-8674(90)90214-Y

Cheeseman, M. T., Tyrer, H. E., Williams, D., Hough, T. A., Pathak, P., Romero, M. R., et al. (2011). HIF-VEGF pathways are critical for chronic otitis media in Junbo and Jeff mouse mutants. *PLoS Genet.* 7:e1002336. doi: 10.1371/journal.pgen.1002336

Christy, B. A., Sanders, L. K., Lau, L. F., Copeland, N. G., Jenkins, N. A., and Nathans, D. (1991). An Id-related helix-loop-helix protein encoded by a growth factor-inducible gene. *Proc. Natl. Acad. Sci. U. S. A.* 88, 1815–1819. doi: 10.1073/pnas.88.5.1815

Fraidenraich, D., Stillwell, E., Romero, E., Wilkes, D., Manova, K., Basson, C. T., et al. (2004). Rescue of cardiac defects in id knockout embryos by injection of embryonic stem cells. *Science* 306, 247–252. doi: 10.1126/science.1102612

Fukudome, S., Wang, C., Hamajima, Y., Ye, S., Zheng, Y., Narita, N., et al. (2013). Regulation of the angiogenesis of acquired middle ear cholesteatomas by inhibitor of DNA binding transcription factor. *JAMA Otolaryngol. Head Neck. Surg.* 139, 273–278. doi: 10.1001/jamaoto.2013.1750

Han, X., Liu, H., Huang, H., Liu, X., Jia, B., Gao, G. F., et al. (2019). ID2 and ID3 are indispensable for Th1 cell differentiation during influenza virus infection in mice. *Eur. J. Immunol.* 49, 476–489. doi: 10.1002/eji.201847822

Hardisty-Hughes, R. E., Tateossian, H., Morse, S. A., Romero, M. R., Middleton, A., Tymowska-Lalanne, Z., et al. (2006). A mutation in the F-box gene, Fbxo11, causes otitis media in the Jeff mouse. *Hum. Mol. Genet.* 15, 3273–3279. doi: 10.1093/hmg/ddl403

Husseman, J., Palacios, S. D., Rivkin, A. Z., Oehl, H., and Ryan, A. F. (2012). The role of vascular endothelial growth factors and fibroblast growth factors in angiogenesis during otitis media. *Audiol. Neurootol.* 17, 148–154. doi: 10.1159/000333805

Jen, Y., Manova, K., and Benezra, R. (1997). Each member of the Id gene family exhibits a unique expression pattern in mouse gastrulation and neurogenesis. *Dev. Dyn.* 208, 92–106. doi: 10.1002/(SICI)1097-0177(199701)208:1<92::AID-AJA9>3.0.CO;2-X

Jones, J. M., Montcouquiol, M., Dabdoub, A., Woods, C., and Kelley, M. W. (2006). Inhibitors of differentiation and DNA binding (Ids) regulate Math1 and hair cell formation during the development of the organ of Corti. *J. Neurosci.* 26, 550–558. doi: 10.1523/JNEUROSCI.3859-05.2006

Juhn, S. K., Jung, M. K., Hoffman, M. D., Drew, B. R., Preciado, D. A., Sausen, N. J., et al. (2008). The role of inflammatory mediators in the pathogenesis of otitis media and sequelae. *Clin. Exp. Otorhinolaryngol.* 1, 117–138. doi: 10.3342/ceo.2008.1.3.117

Kamaid, A., Neves, J., and Giraldez, F. (2010). Id gene regulation and function in the prosensory domains of the chicken inner ear: a link between Bmp signaling and Atoh1. *J. Neurosci.* 30, 11426–11434.

Kee, B. L. (2009). E and ID proteins branch out. *Nat. Rev. Immunol.* 9, 175–184. doi: 10.1038/nri2507

Lin, J., Tsuboi, Y., Pan, W., Giebink, G. S., Adams, G. L., and Kim, Y. (2002). Analysis by cDNA microarrays of altered gene expression in middle ears of rats following pneumococcal infection. *Int. J. Pediatr. Otorhinolaryngol.* 65, 203–211. doi: 10.1016/S0165-5876(02)00130-1

Lowery, J. W., Frump, A. L., Anderson, L., Dicarlo, G. E., Jones, M. T., and De Caestecker, M. P. (2010). ID family protein expression and regulation in hypoxic pulmonary hypertension. *Am. J. Phys. Regul. Integr. Comp. Phys.* 299, R1463–R1477. doi: 10.1152/ajpregu.00866.2009

Lyden, D., Young, A. Z., Zagzag, D., Yan, W., Gerald, W., O'Reilly, R., et al. (1999). Id1 and Id3 are required for neurogenesis, angiogenesis and vascularization of tumour xenografts. *Nature* 401, 670–677. doi: 10.1038/44334

MacArthur, C. J., Hefeneider, S. H., Kempton, J. B., and Trune, D. R. (2006). C3H/HeJ mouse model for spontaneous chronic otitis media. *Laryngoscope* 116, 1071–1079. doi: 10.1097/01.mlg.0000224527.41288.c4

McCaig, L. F., Besser, R. E., and Hughes, J. M. (2002). Trends in antimicrobial prescribing rates for children and adolescents. *JAMA* 287, 3096–3102. doi: 10.1001/jama.287.23.3096

Miyazaki, M., Miyazaki, K., Chen, S., Itoi, M., Miller, M., Lu, L. F., et al. (2014). Id2 and Id3 maintain the regulatory T cell pool to suppress inflammatory disease. *Nat. Immunol.* 15, 767–776. doi: 10.1038/ni.2928

Norton, J. D., Deed, R. W., Craggs, G., and Sablitzky, F. (1998). Id helix-loop-helix proteins in cell growth and differentiation. *Trends Cell Biol.* 8, 58–65.

O'Brien, M. A., Prosser, L. A., Paradise, J. L., Ray, G. T., Kulldorff, M., Kurs-Lasky, M., et al. (2009). New vaccines against otitis media: projected benefits and cost-effectiveness. *Pediatrics* 123, 1452–1463. doi: 10.1542/peds.2008-1482

Pan, L., Sato, S., Frederick, J. P., Sun, X. H., and Zhuang, Y. (1999). Impaired immune responses and B-cell proliferation in mice lacking the Id3 gene. *Mol. Cell. Biol.* 19, 5969–5980. doi: 10.1128/MCB.19.9.5969

Papaspyridonos, M., Matei, I., Huang, Y., Do Rosario Andre, M., Brazier-Mitouart, H., Waite, J. C., et al. (2015). Id1 suppresses anti-tumour immune responses and promotes tumour progression by impairing myeloid cell maturation. *Nat. Commun.* 6:6840. doi: 10.1038/ncomms7840

Pont, E., and Mazon, M. (2017). Indications and radiological findings of acute otitis media and its complications. *Acta Otorrinolaringol. Esp.* 68, 29–37. doi: 10.1016/j.otorri.2016.02.012

Riechmann, V., Van Cruchten, I., and Sablitzky, F. (1994). The expression pattern of Id4, a novel dominant negative helix-loop-helix protein, is distinct from Id1, Id2 and Id3. *Nucleic Acids Res.* 22, 749–755. doi: 10.1093/nar/22.5.749

Sikder, H. A., Devlin, M. K., Dunlap, S., Ryu, B., and Alani, R. M. (2003). Id proteins in cell growth and tumorigenesis. *Cancer Cell* 3, 525–530. doi: 10.1016/S1535-6108(03)00141-7

Spits, H., Couwenberg, F., Bakker, A. Q., Weijer, K., and Uittenbogaart, C. H. (2000). Id2 and Id3 inhibit development of CD34(+) stem cells into predendritic cell (pre-DC)2 but not into pre-DC1. Evidence for a lymphoid origin of pre-DC2. *J. Exp. Med.* 192, 1775–1784. doi: 10.1084/jem.192.12.1775

Sun, X. H., Copeland, N. G., Jenkins, N. A., and Baltimore, D. (1991). Id proteins Id1 and Id2 selectively inhibit DNA binding by one class of helix-loop-helix proteins. *Mol. Cell. Biol.* 11, 5603–5611. doi: 10.1128/mcb.11.11.5603-5611.1991

Tateossian, H., Hardisty-Hughes, R. E., Morse, S., Romero, M. R., Hilton, H., Dean, C., et al. (2009). Regulation of TGF-beta signalling by Fbxo11, the gene mutated in the Jeff otitis media mouse mutant. *Pathogenetics* 2:5. doi: 10.1186/1755-8417-2-5

Tateossian, H., Morse, S., Parker, A., Mburu, P., Warr, N., Acevedo-Arozena, A., et al. (2013). Otitis media in the Tgif knockout mouse implicates TGFbeta signalling in chronic middle ear inflammatory disease. *Hum. Mol. Genet.* 22, 2553–2565. doi: 10.1093/hmg/ddt103

Tian, C., Harris, B. S., and Johnson, K. R. (2016). Ectopic mineralization and conductive hearing loss in Enpp1asj mutant mice, a new model for otitis media and tympanosclerosis. *PLoS One* 11:e0168159. doi: 10.1371/journal.pone.0168159

Wong, Y. C., Wang, X., and Ling, M. T. (2004). Id-1 expression and cell survival. *Apoptosis* 9, 279–289. doi: 10.1023/B:APPT.0000025804.25396.79

Wu, R. L., Sedlmeier, G., Kyjacova, L., Schmaus, A., Philipp, J., Thiele, W., et al. (2018). Hyaluronic acid-CD44 interactions promote BMP4/7-dependent Id1/3 expression in melanoma cells. *Sci. Rep.* 8:14913. doi: 10.1038/s41598-018-33337-7

Yan, W., Young, A. Z., Soares, V. C., Kelley, R., Benezra, R., and Zhuang, Y. (1997). High incidence of T-cell tumors in E2A-null mice and E2A/Id1 double-knockout mice. *Mol. Cell. Biol.* 17, 7317–7327. doi: 10.1128/MCB.17.12.7317

Yang, B., Tian, C., Zhang, Z. G., Han, F. C., Azem, R., Yu, H., et al. (2011). Sh3pxd2b mice are a model for craniofacial dysmorphology and otitis media. *PLoS One* 6:e22622. doi: 10.1371/journal.pone.0029502

Yokota, Y., Mansouri, A., Mori, S., Sugawara, S., Adachi, S., Nishikawa, S., et al. (1999). Development of peripheral lymphoid organs and natural killer cells depends on the helix-loop-helix inhibitor Id2. *Nature* 397, 702–706. doi: 10.1038/17812

Zhang, Y., Yu, H., Xu, M., Han, F., Tian, C., Kim, S., et al. (2012). Pathological features in the LmnaDhe/+ mutant mouse provide a novel model of human otitis media and laminopathies. *Am. J. Pathol.* 181, 761–774. doi: 10.1016/j.ajpath.2012.05.031

Zhao, Q., Beck, A. J., Vitale, J. M., Schneider, J. S., Gao, S., Chang, C., et al. (2011). Developmental ablation of Id1 and Id3 genes in the vasculature

leads to postnatal cardiac phenotypes. *Dev. Biol.* 349, 53–64. doi: 10.1016/j.ydbio.2010.10.004

Zheng, Q. Y., Johnson, K. R., and Erway, L. C. (1999). Assessment of hearing in 80 inbred strains of mice by ABR threshold analyses. *Hear. Res.* 130, 94–107. doi: 10.1016/S0378-5955(99)00003-9

Zook, E. C., and Li, Z. Y. (2018). Transcription factor ID2 prevents E proteins from enforcing a naïve T lymphocyte gene program during NK cell development. *Sci. Immunol.* 3:eaao2139. doi: 10.1126/sciimmunol.aao2139

Conflict of Interest: The authors declare that the research was conducted in the absence of any commercial or financial relationships that could be construed as a potential conflict of interest.

Publisher's Note: All claims expressed in this article are solely those of the authors and do not necessarily represent those of their affiliated organizations, or those of the publisher, the editors and the reviewers. Any product that may be evaluated in this article, or claim that may be made by its manufacturer, is not guaranteed or endorsed by the publisher.

Advantages of publishing in Frontiers

OPEN ACCESS
Articles are free to read for greatest visibility and readership

FAST PUBLICATION
Around 90 days from submission to decision

HIGH QUALITY PEER-REVIEW
Rigorous, collaborative, and constructive peer-review

TRANSPARENT PEER-REVIEW
Editors and reviewers acknowledged by name on published articles

Frontiers
Avenue du Tribunal-Fédéral 34
1005 Lausanne | Switzerland

Visit us: www.frontiersin.org
Contact us: frontiersin.org/about/contact

REPRODUCIBILITY OF RESEARCH
Support open data and methods to enhance research reproducibility

DIGITAL PUBLISHING
Articles designed for optimal readership across devices

FOLLOW US
@frontiersin

IMPACT METRICS
Advanced article metrics track visibility across digital media

EXTENSIVE PROMOTION
Marketing and promotion of impactful research

LOOP RESEARCH NETWORK
Our network increases your article's readership